Studies on Pyro-Oil and Pyro-Gas Derived from Lignocellulosic wastes

THESIS SUBMITTED BY

SOURAV PODDAR

DOCTOR OF PHILOSOPHY (ENGINEERING)

DEPARTMENT OF CHEMICAL ENGINEERING

FACULTY COUNCIL OF ENGINEERING AND TECHNOLOGY

JADAVPUR UNIVERSITY

KOLKATA-700032, INDIA

2016

Dedication

To my parents: words are not just expressive enough

JADAVPUR UNIVERSITY

KOLKATA-700032, INDIA

INDEX NO: 269/12/E

1. TITTLE OF THESIS: Studies on Pyro-Oil and Pyro-Gas Derived from Lignocellulosic wastes

2. NAME: Dr. RANJANA CHOWDHURY
   DESIGNATION: PROFESSOR
   INSTITUTION: DEPARTMENT OF CHEMICAL ENGINEERING
   JADAVPUR UNIVERSITY

   NAME: Dr. SUDIPTA DE
   DESIGNATION: PROFESSOR
   INSTITUTION: DEPARTMENT OF MECHANICAL ENGINEERING
   JADAVPUR UNIVERSITY

3. LIST OF PUBLICATIONS:
   Research Articles
   a. **S Poddar**, S De, R Chowdhury, "Catalytic pyrolysis of lignocellulosic bio-packaging (jute) waste – kinetics using lumped and DAE (distributed activation energy) models and pyro-oil characterization", RSC Adv., 2015, 5, 98934 - 98945. (Impact factor: 3.289)
   b. **S Poddar**, R Biswas, R Chowdhury, S De, "Analysis of tar by catalytic pyrolysis of waste jute", JAMES, 1(1), 2015, 12 - 19.

   Conference Proceedings
   a. R.Chowdhury, **S.Poddar** ,S.De,"Kinetic Modelling of Non – Catalytic Pyrolysis of Waste Jute in a Fixed Bed Pyrolyzer", APCBEE Procedia, 18-24, 9, 2014.
   b. **S Poddar**, R Biswas, R Chowdhury, S De, "Product characterization and kinetic study of co- pyrolysis of waste jute sacks and sesame oil cake", IEEE Xplore , 2014, doi: 10.1109/PESTSE.2014.6805290.
4. LIST OF PATENTS: NIL
5. LIST OF PRESENTATIONS IN NATIONAL/INTERNATIONAL/CONFERENCES/WORKSHOPS:
   a. **S Poddar,** R Biswas, R Chowdhury, S De, "Kinetic Modelling of Pyrolysis of Yellow Lime Waste of Fruit juice outlets", **International Conference on Renewable Energy and Sustainable Development, 2014.**
   b. Rima Biswas, **Sourav Poddar**, Dr. Ranjana Chowdhury, Dr. Sudipto De, "Kinetic study and characterization of product yield of Co-pyrolysis and secondary tar cracking of jute and sesame oil cake", Innovative Approaches for Food Security and Health Care for a Better Tomorrow, **Chemcon 2013.**
   c. **Sourav Poddar**, Rima Biswas, Biswarup Mondal, Dr. Ranjana Chowdhury, Dr. Sudipto De, "Primary and Secondary Semi-Batch Pyrolysis of Yellow Lime Waste of Fruit juice outlets – Experiments and Thermo – Kinetics Modelling",

Innovative Approaches for Food Security and Health Care for a Better Tomorrow, **Chemcon 2013**.

d. Rima Biswas, **Sourav Poddar**, Dr. Ranjana Chowdhury, Dr. Sudipto De, "Catalytic Pyrolysis of Waste Jute – Experiments & Kinetic Modelling", Innovative Approaches for Food Security and Health Care for a Better Tomorrow, **Chemcon 2013.**
e. B. Mondal, A. Sarkar,**S. Poddar**, R. Chowdhury, "Primary and Secondary Pyrolysis of Sesame oil cake – Experiments and kinetic Modeling", **National Seminar on Chemical Industry: In quest for clean technology & sustainable development, IICHE, 2013.**
f. **S. Poddar**, A Dey, R Chowdhury, S.De, "Transient Behaviour of a Semi – Batch pyrolyzer based on the Jute Wastes – Experiments and Modelling", International Conference on Sustainable Technologies for Energy and Environment in Process Industries and Indo-US joint International Conference on Energy and Environment, **Chemcon, 2012.**

Certificate from the supervisors

This is to certify that the thesis entitled “Studies on pyro-oil and pyro-gas derived from lignocellulosic wastes” submitted by Shri. Sourav Poddar, who got his name registered on16.02.2012 for the award of Ph.D. (Engg) degree of Jadavpur University is absolutely based upon his own work under the supervision of Dr. Ranjana Chowdhury and Dr. Sudipta De and that neither his thesis nor any part of the thesis has been submitted for any degree/diploma or any other academic award anywhere before.

1. _____
Signature of the supervisor
and date with office seal

2. _____
Signature of the supervisor
and date with office seal

Acknowledgement

I would like to take this opportunity to convey my sincere gratitude, respect and deep regards to Prof. (Dr.) Ranjana Chowdhury, Chemical Engineering Department, Jadavpur University and Prof. (Dr.) Sudipta De, Mechanical Engineering Department, Jadavpur University for their kind cooperation, able guidance, constant help and encouragement without which it would not have been possible for me to shape this thesis in the present form.

I would like to extend my sincere gratitude to the UGC-BSR, Jadavpur University funded by University Grants Commission, Government of India for their financial assistance.

My sincere thanks go to all my fellow scholars for their continuous support and help during the whole research period. I am also thankful to the Staff Members of library, office and store to the Chemical Engineering Department, Jadavpur University and Mechanical Engineering Department, Jadavpur University for their constant help throughout my work.

Above all, I am sincerely thankful to my parents and all other members of my family for their constant support and encouragement throughout the entire course of my research work.

Last but not the least, I want to thank God for showing me the correct direction.

Studies on Pyro-Oil and Pyro-Gas Derived from Lignocellulosic wastes

by

SOURAV PODDAR

Submitted to Jadavpur University

on September 28, 2016, in Partial Fulfilment of the

requirement for the Degree of

Doctor of Philosophy in Engineering

Abstract

Pyrolysis of lignocellulosic biomass stands out as one of the most promising thermochemical processes to generate energy from waste. This thesis focuses on using experimental and theoretical methods to study the pyrolysis of jute packaging waste and lime waste along with the development of kinetic and process simulation models and energy and environmental analysis. As the key experimental platform, a semi-batch pyrolyzer was first developed to study the kinetics of non-catalytic and catalytic pyrolysis of jute and lime wastes. The effects of different catalysts on the pyrolysis of waste jute and lime waste have been studied and the best performing catalysts have been selected. Reaction kinetics of catalytic and non-catalytic pyrolysis of jute and lime waste have been determined using both lumped and DAE models. For the further application in scaling –up from the first principle of mass and energy balance, a deterministic mathematical model, based on the parameters determined using lumped kinetics, has been developed and validated for a lab-scale (Φ50mm x 640mm) cylindrical semi-batch pyrolyzer using waste jute as the feedstock. To extend the scope of simultaneously using multiple feed-stocks, co-pyrolysis of jute waste and sesame oil cake have been studied. All the pyro-products, namely pyro-char, pyro-oil and pyro-gas have been analyzed using sophisticated instruments and have been observed to have great potential as energy and chemical resources. To assess the further scope for utilization of pyro-products, the parameters for lumped kinetics have also been determined for the thermal decomposition of the pyro-oil obtained at different pyrolysis temperature. The potential of the pyro-gas for the conversion to liquid fuel through Fischer Tropsch process has also been assessed for the 100 tpd pyrolysis plant. Sensitivity analysis using Response Surface Methodology (RSM) has been done using the production rates of diesel and gasoline from the FT process as the response variables and the recycle ratio of CO_2 (R_{CO_2}) and pyrolysis temperature (T) as the factors. Process simulation model using Aspen Plus ® has been developed for large scale (100 tpd) pyrolysis plant of jute waste to assess the scalability of the process. Ultimately an assessment of energy efficiency and environmental impact of the large pyrolysis plant has been made by clearly specifying the goal and scope of utilization of the pyro-products using Aspen Plus ®. The sensitivity analysis has been done to maximize CO_2 avoidance ($\mathbf{A_{CO_2}}$) and Energy Return on Energy Investment (EROEI) using RSM technique.

Thesis Supervisor: Dr. Ranjana Chowdhury

Professor of Chemical Engineering

Thesis Supervisor: Dr. Sudipta De

Professor of Mechanical Engineering

Table of Contents

Figures

.

Tables

Chapter. 1
INTRODUCTION

1. Introduction

The issues related to global warming and climate change have raised the arguments for the development of bio refining processes, particularly liquid biofuel production as a substitute for petroleum-derived transportation fuels. The most common liquid biofuels worldwide are ethanol and biodiesel, whose production has increased from 18.2 billion liters in 2000 to 115 billion liters in 2013.The biofuels contributed about 4% of global road transport fuel consumption (EMISIA 2014[1]), and their production is expected to expand tremendously by 2024 (OECD/FAO 2015[2]). Indian government has planned to achieve a target of 20% blending of fossil fuels with ethanol and biodiesel by 2017 (MNRE 2009[3]). The European Union set a binding target to have at least 10% of their transport fuels from renewable resources. Due to concerns like high food prices, competition of land for food production, acceleration of deforestation, scarcity of water resources, negative impact on biodiversity and so on (IEA Bioenergy 2008[4]) involved in the 1st generation biofuel, the interest in developing 2nd generation liquid biofuels from nonfood lignocellulosic materials has increased. Various agricultural crop residues, forest residues, dedicated energy crops, and industrial and municipal wastes are the most abundant feedstocks, and hold very high potential for large scale biofuels production. Lignocellulosic biomass is the only economically sustainable source of carbon for production of renewable liquid fuels or chemicals [1]. However, the effective utilization of lignocellulose is not always practicable due to the recalcitrance of lignocellulose to hydrolysis. Lignocelluloses are mainly composed of cellulose, hemicellulose and lignin, in addition to a small amount of pectin, starch, ash and extractives. Unlike biochemical processes the conversion through thermo-chemical routes is not restricted by the recalcitrance of lignocellulosic feedstocks. The thermochemical processes namely combustion, gasification and pyrolysis can utilize all components of lignocellulosics including lignin. Among all the thermochemical processes pyrolysis can generate all forms of fuel namely solid i.e. pyro-char, liquid i.e. pyro-oil and gas i.e. pyro-gas through a single step. The yield of solid, liquid and gaseous products from pyrolysis can be adjusted by the manipulation of pyrolysis temperature. The pyro-oil generated through pyrolysis of lignocellulosic feedstocks is considered as a second-generation bio-fuel which may be upgraded to be used in automobile sectors as well as for power generation. The pyro-gas can either be used for power generation or can be converted to green liquid fuels through Fischer-Tropsch process. The pyro-char can either be used for power generation or for soil amendment to avoid greenhouse gas(N_2O) emission. Pyrolysis also serves as the precursor process for both combustion and gasification. Understanding the versatility of pyrolysis process to address the challenges of waste management and mitigation of greenhouse gas emission, it is understandable that the conversion of Indian lignocellulosic wastes to energy sources through pyrolysis should be focused with special emphasis on the conversion and characterization of pyro-products, particularly, pyro-oil and pyro-gas.

1.1.Lignocellulosic Wastes in India

According to the report prepared by Annepu in 2012 [5], Kolkata topped the order among the Indian metro cities with respect to the amount of municipal wastes generated annually. Figure 1.1 depicts the results.

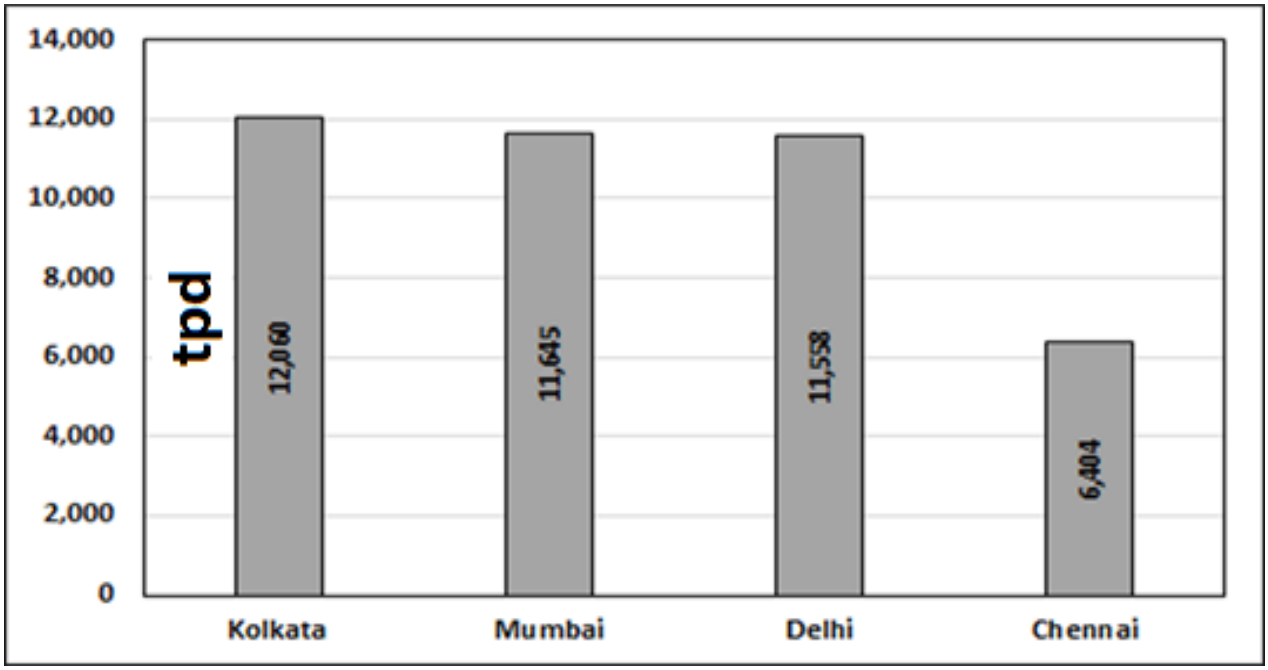

Figure 1.1. Generation rates of Municipal solid wastes in the Indian metro cities [5]

1.2. **Composition and sources of municipal wastes of West Bengal**

Different sources of municipal wastes of Kolkata are depicted in Figure. 1.2.

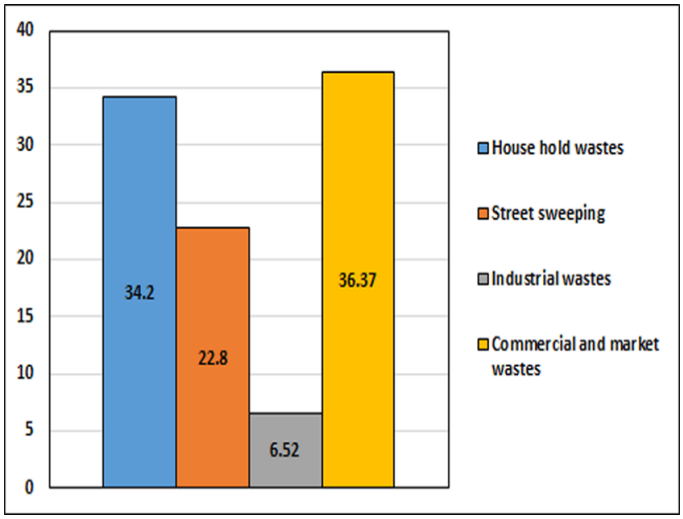

Figure 1.2. Different sources of Municipal Waste of Kolkata [6]

From the analysis of Figure 1.2, it is clear that while industrial wastes have the least share in the municipal solid wastes of Kolkata, residential and commercial sectors including markets have almost equal share of around 35% each. On the other hand, the contribution of street sweeping is as high as 22.8%.

The Figure 1.3. presents the distribution of different components in the municipal waste of Kolkata.

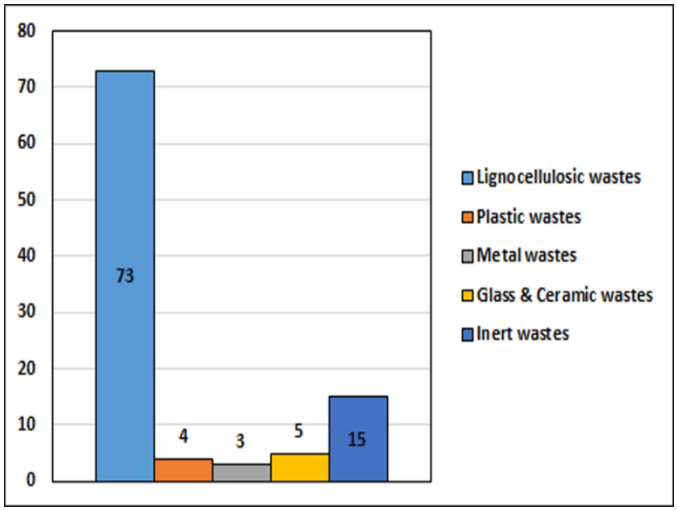

Figure 1.3. Distribution of different components in the municipal waste of Kolkata [8]

It is revealed from the Figure 1.3. that the major constituents of municipal waste are lignocellulosic in nature [7,8]. The lignocellulosic wastes are followed by inert wastes, glass and ceramics, plastic and metal wastes. This distribution is justified by the types of sources from which the wastes are generated.

The composition of lignocellulosic wastes from various sectors of city is depicted in figure. 1.4. [5]

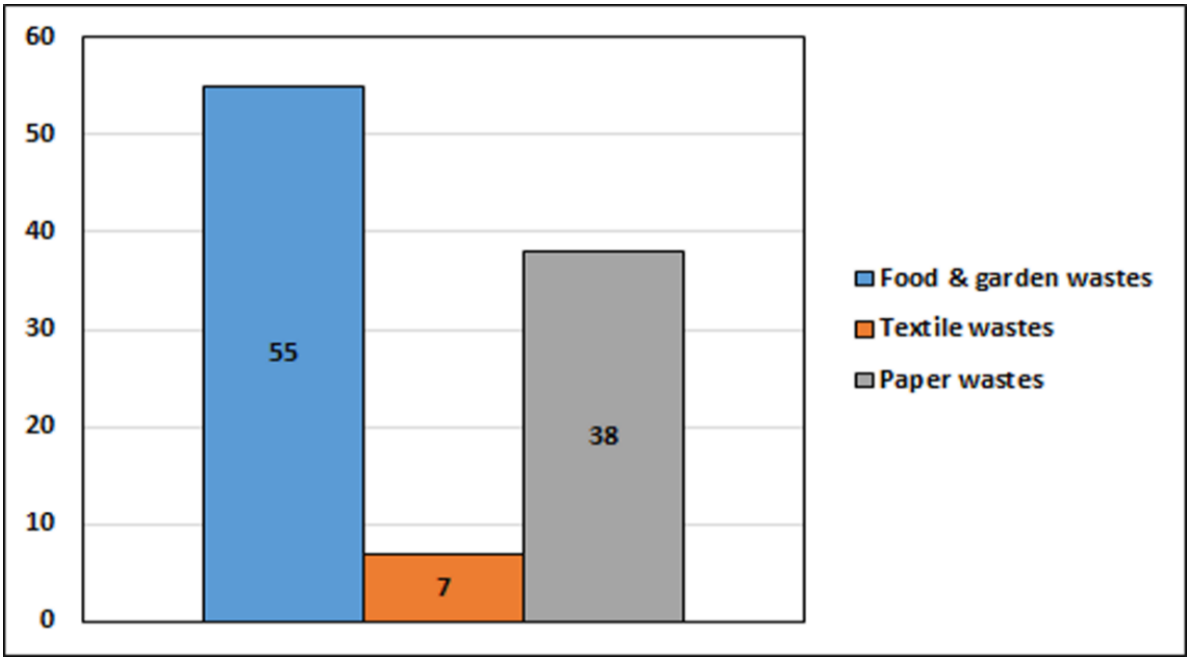

Figure. 1.4. Distribution of lignocellulosic waste of Kolkata [8]

Figure 1.4 reveals that the major part of lignocellulosic waste is food and garden wastes, followed by paper wastes and textile wastes.

Major part of the waste that is generated in all the cities is generally used for landfilling outside the cities, which at times creates stinky smell. Now according to Government of India's new policy [Dec, 2014] about 9% to 10% wastes is being processed through aerobic compositing [9-21]. No prominent route for energy generation is developed from lignocellulosic wastes.

1.3. Pyrolysis

Pyrolysis can be defined as a thermochemical process of decomposition of organic matters at elevated temperatures in absence of oxygen or any halogen compounds [22-27]. In the first step the pyrolyzing feedstock is decomposed to char, and volatiles. The condensable part of volatiles is called pyro-oil and the non-condensable part is called pyro-gas. This reaction step is known as primary pyrolysis. in the second step the components of pyro-gas react amongst

themselves to generate new products. This reaction step is known as secondary pyrolysis. the reactions of primary and secondary pyrolysis processes may be represented as follows:

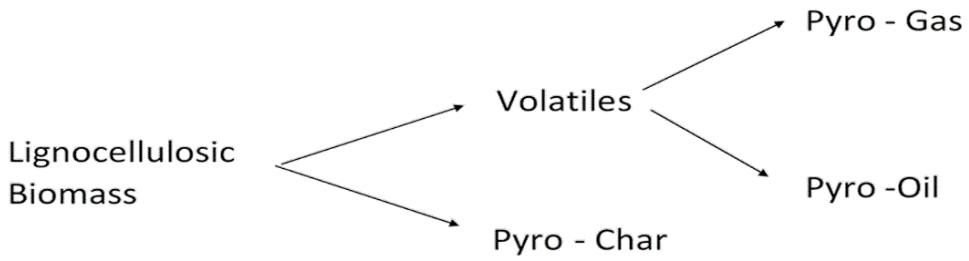

(1)

$$C + H_2O \leftrightarrow CO + H_2 \quad (2)$$

$$C + CO_2 \leftrightarrow 2CO \quad (3)$$

$$(-CH_2-) + H_2O \leftrightarrow CO + 2H_2 \quad (4)$$

$$(-CH_2-) + CO_2 \leftrightarrow 2CO + H_2 \quad (5)$$

$$CO + H_2O \leftrightarrow CO_2 + H_2 \quad (6)$$

$$CO + 3H_2O \leftrightarrow CH_4 + H_2O \quad (7)$$

1.4. Types of Pyrolysis

According to reaction conditions the pyrolysis may be categorized as follows: Fast, Flash and slow pyrolysis. [28, 29]. The detailed difference amongst the three are listed below in table.1

Table 1. Different pyrolysis processes with operating parameters and products

Pyrolysis Process	Solid Residence Time (s)	Heating Rate (K/s)	Particle Size (mm)	Temp (K)	Product Yield (%)		
					Oil	Char	Gas
Slow	450 - 550	0.1 - 1	5 -50	550 – 950	30	35	35
Fast	0.5 - 10	10 - 200	<1	850 – 1250	50	20	30
Flash	< 0.5	>1000	<0.2	1050 – 1300	75	12	13

From the table, it is clear that slow pyrolysis is widely accepted since all the conditions are more widely viable than the others and the product formation is higher than amongst the others. All these pyrolysis processes may be conducted either in non-catalytic or catalytic modes.

1.5.Pyrolysis Kinetics

Two types of models are used to analyse the kinetics of pyrolysis of lignocellulosic biomass: lumped kinetic model and distributed activation energy model.

1.5.1. Lumped kinetic model

In lumped kinetic model, the lignocellulosic biomass [30-34] is considered as a single reactant following two parallel reactions generating volatiles and char. The activation energy is assumed to be invariant with the conversion. The kinetic parameters are determined using the experimental data obtained under isothermal condition. This model is valid for primary pyrolysis where the reactions among the gaseous products are not considered.

1.5.2. Distributed activation energy model (DAEM)

The distributed activation energy model (DAEM) is a multiple reaction model, which is widely used in the pyrolysis of lignocellulosic biomass [35]. The model assumes the decomposition mechanism taking a large number of independent, parallel, first-order or nth-order reactions with different activation energies reflecting variations in the bond strengths of species. The difference in activation energies can be represented by a continuous distribution function [36]. The DAEM is not only used to describe the pyrolysis kinetics of lignocellulosic biomass and its main components, but also to describe the pyrolysis kinetics of coal [37–39] and other thermally degradable materials [40–43]. In this analysis, the activation energy is considered as

a function of conversion. The experimental data derived under non-isothermal conditions are required for the determination of the kinetic parameters. As the lignocellulosic biomass is a combination of three components, namely, cellulose, hemicellulose and lignin the pyrolysis reaction for different components takes place at different rates. Hence the DAE model can approach the reality more closely.

1.6.Uses of pyro – products

The pyro-products are categorized as solid fuel (pyro-char), liquid fuel (pyro-oil) and gaseous fuel(pyro-gas).

Pyro – char is a carbon rich product which is mainly used for soil amendment, activated carbon, co – fired power plant, carbon sequestration etc. Pyro-oil is a synthetic liquid fuel which has a potential to be used in automobile sector or can substitute diesel in oil-based power plants. The pyro-gas may be used as a direct source of energy. It may also be converted to liquid fuel through Fischer-Tropsch (FT) process through an intermediate route of syngas generation. The different scopes for the utilization of pyro-products are shown in Figure 1.5.

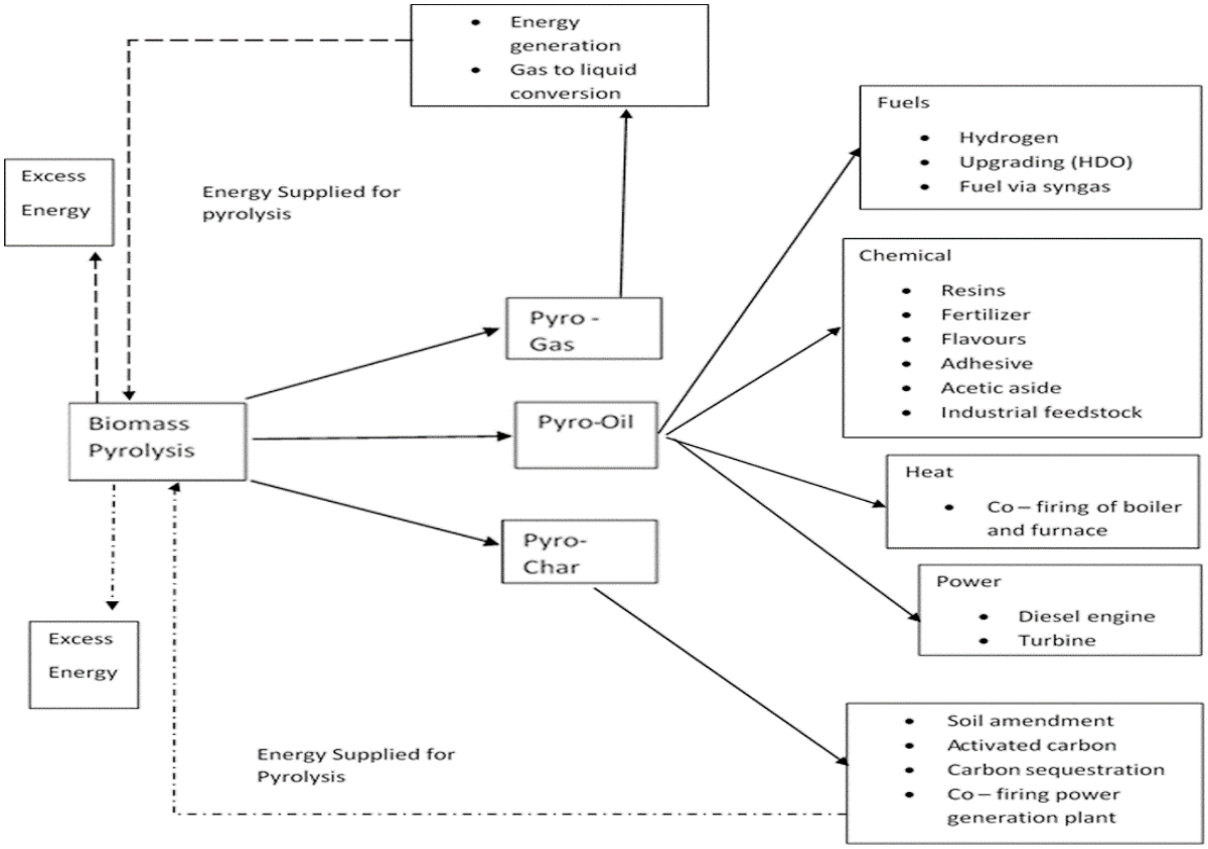

Figure. 1.5. A series of pyrolysis products and their uses

1.7.Energy and Environmental analysis

For the avoidance of unintended detrimental environmental consequences of a new technology accounting for environmental impact of the process should be done. The most appropriate methodology for this purpose is life cycle analysis (LCA) [42-44]. Similarly, the energy output-input ratio showing the net energy return from a new process is also necessary before its actual implementation. Thus, an analysis accounting both environmental impact and energy return, called energy environment analysis (EEA) following the basic principles of LCA is useful to serve the dual purpose.

References

1. EMISIA (Mission for Environment). (2014). The contribution of biofuels in transport sustainability post-2020. <http://www.ebb eu.org/studiesreports/EMISIA_Contribution_Biofuels_transport_sustainability.pdf>
2. MNRE (Ministry of New and Renewable Energy). (2009). National Policy on Biofuels. Government of India, New Delhi. <http://mnre.gov.in/file-manager/UserFiles/biofuel_policy.pdf>
3. OECD/FAO (2015). Biofuels. OECD-FAO Agricultural Outlook (2015). <http://www.fao.org/fileadmin/templates/est/COMM_MARKETS_MONITORING/Oilcrops/Documents/OECD_Reports/OECD_biofuels2015_2024.pdf>
4. IEA (International Energy Agency). (2008). Bioenergy. From 1st- to 2nd – generation biofuel technologies. An overview of current industry and RD&D activities
5. Sustainable Solid Waste Management in India, by Ranjith Kharvel Annepu, Advisor:
6. Hazra, T., Goel, S., 2009. Solid waste management in Kolkata, India: Practices and challenges, Waste Management 29, pp. 470–478.
7. Central Public Health and Environmental Engineering Organisation (CPHEEO), 2005. Manual on MSW management.
8. Kolkata Environmental Improvement Investment Programme, 2007a.
9. Gupta, S., Krishna, M., Prasad, R.K., Gupta, S., Kansal, A., 1998. Solid waste management in India: options and opportunities. Resource, Conservation and Recycling 24, pp. 137–154.
10. Gupta, P.K., Jha, A.K., Koul, S., Sharma, P., Pradhan, V., Gupta, V., Sharma, C.,Singh, N., 2007. Methane and Nitrous Oxide Emission from Bovine Manure Management Practices in India. Journal of Environmental Pollution 146 (1), pp. 219– 224.
11. Sharholy, M., Ahmad, K., Mahmood, G., Trivedi, R.C., 2006. Development of prediction models for municipal solid waste generation for Delhi city. In: Proceedings of National Conference of Advanced in Mechanical Engineering (AIME-2006), Jamia Millia Islamia, New Delhi, India, pp. 1176–1186.
12. Srivastava, P.K., Kushreshtha, K., Mohanty, C.S., Pushpangadan, P., Singh, A., 2005.
13. Stakeholder-based SWOT analysis for successful municipal solid waste management in Lucknow, India. Journal of Waste Management 25 (5), pp. 531–537.
14. Malviya, R., Chaudhary, R., Buddhi, D., 2002. Study on solid waste assessment and management – Indore city. Indian Journal of Environmental Protection 22 (8), pp. 841–846.
15. Kansal, A., 2002. Solid waste management strategies for India. Indian Journal of Environmental Protection 22 (4), pp. 444–448.
16. CPCB, 2000, Status of Solid Waste Generation, Collection, Treatment and Disposal in Metrocities, Series: CUPS/46/1999–2000.
17. CPCB, 2000. Status of Municipal Solid waste Generation, Collection,Treatment and Disposal in Class I Cities, Series: ADSORBS/31/1999–2000.
18. Reddy, S., Galab, S., 1998. An Integrated Economic and Environmental Assessment of Solid Waste Management in India – the Case of Hyderabad, India.
19. Kansal, A., Prasad, R.K., Gupta, S., 1998. Delhi municipal solid waste and environment – an appraisal. Indian Journal of Environmental Protection 18 (2), pp. 123–128.
20. Dayal, G., 1994. Solid wastes: sources, implications and management. Indian Journal of Environmental Protection 14 (9), pp. 669–677.
21. Rao, K.J., Shantaram, M.V., 1993. Physical characteristics of urban solid wastes of Hyderabad. Indian Journal of Environmental Protection 13 (10), pp. 425–721.
22. Wang Nan, Arash Tahmasebi, Jianglong Yu, Jing Xu, Feng Huang, Alisa Mameva, A C omparative study of microwave – induced pyrolysis of lignocellulosic and algal biomass, Bioresource Technol, 2015, 190, 89 – 96.
23. Torri Cristian, Daniele Fabbri, Biochar enables anaerobic digestion of aqueous phase from intermediate pyrolysis of biomass, Bioresource Technol, 2014, 172, 335 – 341.
24. Murata Kazuhisa, Yanyong Liu, Megumu Inaba, Isao Takahara, Catalytic fast pyrolysis of jatropha wastes, J. Analytical and Applied Pyrolysis, 2012, 94, 75 – 82.
25. Luo Guanqun, Fernando L.P. Resende, Fast pyrolysis of bettle – killed trees, J. Analytical and Applied Pyrolysis, 2014, 110, 100 – 107.

26. Liu Zhengang, Guanghua Han, Production of solid fuel biochar from waste biomass by low temperature pyrolysis, Fuel, 2015, 158, 159 – 165.
27. Lago Valentina, Charles Greenhalf, Cedric Briens, Franco Berruti, Mixing and operability characteristics of mechanically fluidized reactors for the pyrolysis of biomass, Powder Technology, 2015,274, 205 -212.
28. Sinha, S.; Jhalani, A.; Ravi, M.R.; Ray, A. *J. Solar Energy Soc. Ind.* 2000, *10*, 41–62.
29. Ahmad, I.; Gupta, A.K. Pyrolysis and gasification of food waste: Syngas characteristics and char gasification kinetics. *Appl. Energy* 2010, *87*, 101–108.
30. Chowdhury Ranjana, Sarkar Aparna. "Reaction Kinetics and Product Distribution of Slow Pyrolysis of Indian TextileWastes". Int J Chem Reactor Eng. 2012; 10(1).
31. White JE, Catallo WJ, Legendre BL, "Biomass pyrolysis kinetics: a comparative critical review with relevant agricultural residue case studies", J Anal Appl Pyrolysis, 2011;91,1–33.
32. Cai J, Li T, Liu R, "A critical study of the Miura–Maki integral method for the estimation of the kinetic parameters of the distributed activation energy model", Bioresour Technol, 2011,102:3894–9.
33. White JE, Catallo WJ, Legendre BL, "Biomass pyrolysis kinetics: a comparative critical review with relevant agricultural residue case studies", J Anal Appl Pyrolysis, 2011;91,1–33.
34. Cai J, Li T, Liu R, "A critical study of the Miura–Maki integral method for the estimation of the kinetic parameters of the distributed activation energy model", BioresourTechnol, 2011,102:3894–9.
35. Navarro MV, Aranda A, Garcia T, Murillo R, Mastral AM, "Application of the distributed activation energy model to blends devolatilisation", Chem Eng J, 2008, 142, 87–94.
36. Güneş M, Güneş SK., "Distributed activation energy model parameters of some Turkish coals", Energy Sources Part A, 2008, 30, 1460–72.
37. Caprariis B, Filippis P,Herce C,Verdone N, "Double-Gaussian distributed activation energy model for coal devolatilization", Energy Fuels, 2012, 26, 6153–9.
38. Dawood A, Miura K, "Pyrolysis kinetics of γ-irradiated polypropylene", Polym Degrad Stab, 2001, 73, 347–54.
39. Yan JH, Zhu HM, Jiang XG, Chi Y, Cen KF, "Analysis of volatile species kinetics during typical medical waste materials pyrolysis using a distributed activation energy model", J Hazard Mater, 2009, 162, 646–51.
40. Campbell JH, Koskinas GJ, Gregg M, "Gas evolution during oil shale pyrolysis 2. Kinetic analysis", Fuel, 1980, 57, 377–83.
41. Tiwari P, Deo M, "Detailed kinetic analysis of oil shale pyrolysis TGA data", AIChE J, 2012, 58, 505–15
42. Md Ruhul Kabir and Amit Kumar, "Development of net energy ratio and emission factor for biohydrogen production pathways", Bioresource Technology, 2011, 102, 8972–8985.
43. Kellig Roberts, Brenta Gloy, Stephen Joseph, Norman Scott and Johannes Lehmann, "Life Cycle Assessment of Biochar Systems: Estimating the Energetic, Economic, and Climate Change Potential", Environ. Sci. Technol, 2010, 44, 827–833
44. Yucheng Cao and Artur Pawłowski, "Life cycle assessment of two emerging sewage sludge-to-energy systems: Evaluating energy and greenhouse gas emissions implications", Bioresource Technology, 2013, 127, 81–91

Chapter. 2
LITERATURE REVIEW

2. Literature Review

The present status of knowledge-base on lignocellulosic feedstocks used for pyrolysis with special emphasis on jute textiles, fruit wastes and oil cakes, pyrolysis kinetics under isothermal and non-isothermal conditions, Catalytic pyrolysis of lignocellulosic feedstocks, Co-pyrolysis of lignocellulosic feedstocks. Process simulation modelling of pyrolysis using Aspen Plus and Energy and Environmental Impact, as available from the current literature, has been reviewed.

2.1. Lignocellulosic feedstocks

Production of pyro-products mainly depends on the choice of feedstocks, the types of reactors and also the temperature conditions to which it is exposed. India produces 450-500 million tons of biomass per year [1,2]. The following table shows the salient information on the pyrolysis of lignocellulosic feedstocks of India.

Table. 2.1. Different lignocellulosic feedstocks and type of reactor used for the production of pyrolysis products as per Indian community

Feedstock	Rector type	Heating condition and reaction temperature	Catalysts used	Reference
Primary wood/ Subabul wood; Rice straw; Wheat straw; Pith Coir; Soybean stalks; Mustard seed press cake (Both untreated and demineralised)	Packed bed Reactor	Both isothermal (500^{o}C) and adiabatic (Heating rate: 50^{o}C /min)	None	[3]
Primary wood/ Eucalyptus	A stainless-steel tubular Reactor	Adiabatic Heating rate: 20^{o}C/min Temperature Range- 350-600^{o}C.	Analytical grade mordenite, kaoline, silica-alumina and fly ash were used as catalysts.	[4]
Bagasse	Packed Bed Reactor	Both isothermal (500^{o}C) and adiabatic (Heating rate :50 ^{o}C /min)	None	[4]
Rice Husk; Rice straw; Millet Husk	Packed Bed Reactor	Both isothermal (500^{o}C) and adiabatic (Heating rate 60 ^{o}C /min)	None	[5]
Coconut shell	Fixed Bed Reactor	Adiabatic Heating rate :50°C/min Temperature Range- 400°C - 600°C	None	[6]

Coconut shell powder	Semi Batch Reactor	Adiabatic Heating rate :60°C/min Temperature Range- 450°C - 600°C	None	[7]
Coconut shell powder	Semi Batch Reactor	Adiabatic Heating rate -20°C/min Temperature Range: 450°C - 600°C	None	[8]
Cashew nut Shell	Fixed Bed Reactor	Adiabatic Heating rate :50°C/min Temperature Range: 400°C - 600°C	None	[9]
Ground nut Shell	Packed Bed Reactor	Both isothermal (773K) and adiabatic (Heating rate 50 K/min)	None	[10]
Corn Cob	Packed Bed Reactor	Both isothermal (773K) and adiabatic (Heating rate: 50 K/min	None	[11]
Mustard seed press cake	Fixed bed Reactor	Adiabatic Temperature range: 400 – 600^{o}C	5% NaCl, 10% NaCl, 15% NaCl	[12]
De oiled ground nut cake	Semi Batch Reactor	Adiabatic (Heating rate: 20^{o}C/min)	None	[13]
Ground nut; Sesame seed	Semi Batch Reactor	Adiabatic Heating rate: 25^{o}C/min Temperature Range :200 – 500^{o}C	None	[14]
Secondary wood from industry/ Pine wood from packing box	Packed Bed Reactor	Adiabatic Heating rate: 10^{o}C/min Temperature Range: 400-600^{o}C	None	[15-22]
Textile wastes (Cotton based varieties)	Fixed Bed Reactor	Adiabatic Heating rate: 10^{o}C/min Temperature Range: 300-900^{o}C	None	[23]
Glossy paper cup	Semi-batch Reactor	Adiabatic Heating rate: 5^{o}-15^{o} C/min Temperature Range: 30-524^{o}C	None	[24]
Paper cup waste	Semi-batch Reactor	Adiabatic Heating rate: 10^{o}-20^{o} C/min Temperature Range: 325-425^{o}C	None	[25,26]
Vegetable waste of Municipal market	Semi-batch Reactor	Adiabatic Heating rate: 10^{o}-20^{o} C/min Temperature Range: 30-700^{o}C	None	[27]
Municipal Vegetable waste	TGA Cell	Adiabatic	None	[28]

		Heating rate: 10^{o} and 40^{o} C/min Temperature Range: 523-1123K		
Jute waste	Fixed bed Reactor	Heating rate –10 - 40^{o}C/min Adiabatic condition – room temperature – 400-700^{o}C	None	[29]
Paper waste and mustard press cake	Fixed bed Reactor	Adiabatic Temperature range: 300 – 900^{o}C	None	[30]
Sesame oil cake	Fixed bed Reactor	Adiabatic Temperature range: 300 – 900^{o}C	None	[31]

From the Table 2.1, it is clear that the pyrolysis of many Indian lignocellulosic feedstocks including wood wastes, rice wastes, wheat straw, bagasse, coconut wastes, millet husks, nut shells, corn wastes, paper wastes, municipal vegetable wastes, oil seed press cakes has been studied. Most of the studies have been conducted in fixed bed or packed bed reactors operated in batch or semi-batch mode either under vacuum or nitrogen atmosphere. Data on both isothermal and adiabatic experiments using these feed stocks are available in the literature. Although most of the pyrolysis studies have been conducted under non-catalytic mode, effects of catalysts have also been investigated by some of the researchers. [4,12] The yield of pyrolysis products namely, char, pyro-oil and pyro-gas have been observed to vary in the range of 22.6 -47.2%, 6-50% and 15 -42.26% respectively. According to the literature review analytical grade mordenite, kaoline, silica-alumina and fly ash and NaCl have pronounced effect on the pyrolysis of lignocellulosic Indian biomass as observed by previous researchers [4,12]. Very little attention has however been given to utilize some of the abundant Indian lignocellulosic wastes, namely, jute waste, textile wastes and citrus fruit wastes generated from fruit juice facilities in metropolitan cities. Although a few research studies have been reported on textile wastes, jute dust etc., no information is available on the pyrolysis characteristics of waste of jute sacks extensively used for the packaging of food grains in India. Similarly, no research study has been reported on the pyrolysis of residues of citrus fruits generated during the production of fruit juice. From the prospective of dearth of information on the energy generation from jute packaging wastes and citrus fruit wastes, the research study on pyrolysis of these feed stocks can add to the database of energy generation potential of Indian lignocellulosic wastes.

The literature review, as presented in Table. 2.2, however reveals that pyrolysis of different jute and textile wastes as well as citrus fruit wastes has been investigated by researchers outside India.

Table. 2.2. International status of Studies on Pyrolysis of jute wastes, textile wastes and citrus fruit wastes

Feedstocks	Reactor	Observations	References
Jute stick	fluidized bed reactor	1. The pyrolysis of jute stick was performed at different temperatures from 300 ^{o}C to 600 ^{o}C to produce bio-oil. At 500 ^{o}C the bio-oil yield was the maximum. The yield of bio-oil increased until 500 ^{o}C and then decreased due to the secondary reforming of bio-oil vapor at higher temperatures. 2. The non-condensable gas was the mixture of mainly nitrogen, carbon monoxide (CO) and carbon dioxide (CO_2). Some of methane, ethane, propane, propene etc., were also formed in the pyrolysis reaction. The gas yield increased as temperature increased. 3. The increased temperature resulted in the lower yield of char. 4. The bio-oil was characterized. The density of the bio-oil was as high as 1.11 g/ml compared to light fuel oil at around 0.85 g/ml. The viscosity of bio-oil was found to be 2.34 cP. Since bio-oil contains some organic acids such as formic acid, acetic acid etc., it was acidic in nature and the pH and acid value were found to be around 4 and 135 mg KOH/g, respectively. The water content of bio-oil was determined and found to be 16 wt.%. The solid and ash content was found to be 0.02 and 0.03 wt.%, respectively.	Asadullah et. al[32] [2008]
Orange waste (pulp)	TGA-DSC	1. Thermal degradation was interpreted as the resultant of multiple, parallel and simultaneous reactions, related to: (i) dehydration process for temperatures ≤120 ^{o}C; (ii) pyrolytic cracking, from 125 to 450 ^{o}C, stage where the lignocellulosic components are degraded reaching a maximum the evolved gaseous products and delivery energy; and (iii) to latest stage of lignin degradation, at temperatures ≥450 ^{o}C. 2. The volatile compounds evolved from 50 to 600 ^{o}C were mainly: H_2O, CO_2 and CO, besides of a mixture organic product composed by: carboxylic acids, aldehydes or ketones (C=O), alkanes (C – C), ethers (C – O – C), alcohols (C – O – H), phenolic compounds (C – O) and aliphatic and/or unsaturated aromatic compounds (C=C).	Lopez-Velazquez et. al [33] [2013]

		3. Kinetic parameters were calculated by two kinds of model-free kinetics algorithms, Friedman (F) and Kissinger–Akahira–Sunose (KAS) methods at different heating rates (5, 10 and 15 $^{o}C\ min^{-1}$). 4. The results in terms of activation energy show the complex $E_a(\alpha)$ i.e. dependence on conversion which evidences a multi-step kinetic processes during the pyrolytic cracking of the orange waste.	
Orange waste (orange peel)	TGA-DSC	1. The orange peel degradation occurred in at least three steps associated with its three main components (hemicellulose, cellulose and lignin). 2. The volatiles compounds evolved out at 150–400 ^{o}C and the gas products were mainly CO_2, CO, and CH_4. 3. A mixture of acids, aldehydes or ketones C=O, alkanes C–C, ethers C–O–C and H_2O was also detected. 4. The results could explain the non-autocatalytic character of the reactions during the decomposition process.	Balmaseda et. al [34] [2009]
Waste wood, cardboard, textile (30% polymer and 70% cotton)	Packed bed reactor	1. Compared to TGA tests at the same programmed heating rate and final pyrolyzing temperature, the packed-bed pyrolyser produced 30–100% more char. This could be due to tar cracking and repolymerisation both inside the pyrolyzing particles and on the activated outer surface of other particles. 2. Char yield was 21–34%, tar 34–46% and gas from 23% to 43% in the range of 350–700 ^{o}C of final pyrolyzing temperature. Modelling work suggested that tar cracking in the bed is not sufficient to offset the increase in tar release as pyrolyzing temperature increases. Tar cracking ability in fuel is possibly linked to mineral contents in the fuel and needs to be explored. 3. CO and CO_2 are the major constituents (apart from tar and water) of the flue gas composition during the main pyrolysis stage which occurs between 250 and 450 ^{o}C. Noticeable release of light hydrocarbon gases and hydrogen only occurs at higher temperature levels after the bulk of the volatile matter in the fuel has been released. FG model predictions compares qualitatively well to the measured gas compositions.	Yang et. al [35] [2007]

Textile waste (cotton fabrics)	TGA	1. Thermal behaviour of textile waste was studied by thermogravimetry at different heating rates and also by semi-batch pyrolysis. 2. The onset temperature of mass loss is within 104–156 ^{o}C and the final reaction temperature is within 423–500 ^{o}C. 3. The average mass loss is 89.5%. 4. There are three DTG peaks located at the temperature ranges of 135–309, 276–394 and 374–500 ^{o}C, respectively. The first two might be associated with either with decomposition of the hemicellulose and cellulose or with different processes of cellulose decomposition. The third peak is possibly associated to a synthetic polymer. 5. At a temperature of 460 ^{o}C, the expected amount of volatiles of this waste is within 85–89%. 6. The kinetic parameters of the individual degradation processes were determined by using a parallel model. 7. The dependence on the heating rate was also established. 8. The pyrolysis rate is considered as the sum of the three reaction rates. The pyrolysis in a batch reactor at 700 ^{o}C and nitrogen flow of 60 ml/min produces 72 wt.% of oil, 13.5 wt.% of gas and 12.5 wt.% of char. 9. The kinetic parameters of the first peak do not vary with heating rate, while those of the second and the third peak increase and decrease, respectively, with an increasing heating rate, proving the existence of complex reaction mechanisms for both cases.	Miranda et. al [36]
Textile waste (combed cotton pieces)	Fixed bed reactor	1. Pyrolysis of combed cotton waste was conducted in a fixed bed reactor with the final temperatures of 450, 500, 550, and 600^{o}C. 2. Effect of the experimental conditions such as temperature, catalyst type on the formation of liquid, gas, and char products were investigated and product yields were measured. 3. The highest liquid product efficiency was achieved with 29.74% at the temperature of 550^{o}C. 4. $CaCO_3$ and Na_2CO_3 were used as catalysts. Na_2CO_3 was found to be more effective catalyst than $CaCO_3$ 5. The properties of the obtained liquid product were analyzed by high performance liquid chromatography (HPLC). Furans, ketones,	Barisci and Oncel[37] [2014]

		aldehydes, less carboxylic acids, and hydrocarbons were detected in the content of liquid product. 6. The calorific values of raw material, liquid product, and char were also determined by using IKA C 200 calorimeter. 7. The results clearly indicated that both temperature and catalyst type affect the formation of liquid product.	
Textile waste (flax and hemp natural fibres)	Fixed bed reactor	1. The research was carried on flax and hemp natural fibres, which have been manufactured into a non-woven, pre-formed matting material and subsequently treated via chemical activation and pyrolysis to produce activated carbon. 2. The influence of chemical activation process conditions using zinc chloride and phosphoric acid and the subsequent pyrolysis process conditions were investigated. 3. The results showed that an activated carbon matting with very high surface area of over 2000m^2 g^{-1} could be produced. 4. The surface area was strongly influenced by the concentration of activating agent used and the subsequent pyrolysis temperature. 5. Higher surface areas being associated with the higher concentrations of the activating agent and the lower temperatures of pyrolysis. 6. Zinc chloride produced significantly higher surface areas of the activated carbon compared to phosphoric acid activation. The pore size distribution of the carbons could be altered depending on the process conditions used.	Williams and Reed[38] [2004]
Textile waste (blue T-shirts made of 100% cotton)	TGA	1. The thermal degradation of samples of used cotton fabrics has been investigated using thermogravimetric analysis (TGA) between room temperature and 700 ^oC. 2. Experiments were carried out with about 5 mg of sample in three different atmospheres: helium, 20% oxygen in helium and 10% oxygen in helium. Three different heating rates were used at each atmosphere condition. 3. A kinetic model for the decomposition of used cotton fabrics explaining the behaviour of all the runs performed has been proposed and tested. For the pyrolysis of the cotton, the model comprises two parallel reactions. For the combustion process, one competitive reaction was added to each parallel reaction of the pyrolysis model and four combustion reactions of the different solid fractions to obtain volatiles.	Matlo et. al [39] [2006]

		4. One single set of parameters can explain all the experiments (pyrolysis, oxidative pyrolysis and combustion) at the three different heating rates used.	
Fruit wastes (mango endocarp and waste fruit peel from banana, orange and watermelon)	TGA	1. Fruit wastes of mango endocarp and waste fruits peel from banana, orange and watermelon were pyrolysed respectively and subjected to different analyses to examine their thermal behaviour, chemical functional group, elemental and proximate content. 2. The fruit wastes were dominated by volatile matter (52-67 wt.%) containing aliphatic hydrocarbons, fatty acids and lignocellulosic components that can be recovered as potential fuel or chemical feedstock via pyrolysis. 3. The wastes were also detected to have considerable amounts of fixed carbon (30-36 wt.%), thus showing potential to be pyrolysed to produce biochar for use as activated carbon or catalyst support. 4. The wastes can be pyrolysed at _ 400 ^{o}C to convert the majority of the waste content into volatiles for recovery as useful bio-oil and bio-gas, and the remaining solid mass can be recovered as bio-char. 5. The results demonstrate that the fruit wastes show exceptional promise as a feedstock for pyrolysis conversion into potentially useful products.	Lam et. al [40] , [2016]

Table 2.2 reveals that although the pyrolysis characteristics of textile wastes have been reported by a few researchers, the information on jute related wastes and citrus fruit waste is relatively scarce. Similar to the pyrolysis characteristic of Indian lignocellulosic feedstocks, maximum yield of pyro-oil is obtained around 500^{o}C. There is a general trend of increase and decrease of yields of gas and char respectively with the increase of temperature. In many cases the lumped kinetics of pyrolysis using parallel reaction scheme have been determined. Only in one case [33], distributed activation energy models namely, Friedman and Kissinger-Akahira-Sunnose models postulating the dependence of activation energy on conversion has been used. Although a few studies on jute wastes and textile wastes have been conducted in fluidized bed and fixed bed reactors, most of the studies have been done in TGA cells under adiabatic condition. The catalytic effect of Na_2Co_3 and $CaCo_3$ on the yield of pyro-oil from textile waste has been studied by a research group [37]. The usage of Na_2Co_3 has markedly increased the yield of pyro-oil. On the other hand, an investigation on pyrolysis of textile wastes ha clearly indicated the enhancement of surface area per unit volume of pyro-char of textile waste by the addition of $ZnCl_2$. The pyrolysis studies on citrus fruit wastes and jute related wastes are mainly concentrated on the trend analysis of product yields and on analysis of products. No research investigation has so far been reported on the modelling of pyrolysis reactors for these feedstocks, scope for further processing of pyrolysis products, prospect of co-pyrolysis, energy

and environmental analysis of large scale pyrolysis plants and so on. Overall, it appears that there are ample scopes for the generation of more information on the pyrolysis characteristics of both jute packaging wastes and citrus fruit wastes of India. For the assessment of the potential of commercial pyrolysis units using these feed stocks, analysis of product yield, characterization of product, determination of kinetics using both lumped and distributed activation energy models, development of mathematical model for pyrolyzer, assessment of scope of co-pyrolysis, processing of pyro products and energy and environmental analysis should be done. To decide on the strategies and methodologies for the research studies the state of the art technologies being followed for other lignocellulosic biomass have been reviewed in the following sections.

2.2. Lumped Pyrolysis kinetics

In case of analysis of experimental data using lumped model, the overall pyrolysis reaction is considered either as a single reaction or as an array of parallel reactions over the whole conversion range [9,10]. The single reaction representation is as follows:

$$Biomass \rightarrow Volatile$$

The rate equation for the volatile formation is usually represented as follows [41-43,9,10]:

According to Orfao et. al [41] [1999], Fernandez et. al [44] [2016]

$$\frac{d\alpha}{dt} = A\exp(-\frac{E}{RT}) f(\alpha) \quad (1)$$

Where, $\alpha =$ experimental conversion

$\frac{d\alpha}{dt} =$ experimental conversion rate

According to Carvalho et. al [43] [2014]

$$\frac{d\alpha_i}{dt} = k_i(1-\alpha)^{n_i} \quad (2)$$

The parallel reaction schemes used for the representation of biomass pyrolysis are as follows:

According to Sharma et. al [42] [2014],

$$biomass \xrightarrow{k_1} Gas$$
$$biomass \xrightarrow{k_2} Primary\ Tar$$
$$biomass \xrightarrow{k_3} Char$$
$$Primary\ Tar \xrightarrow{k_4} Gas$$
$$Primary\ Tar \xrightarrow{k_5} Secondary\ Tar$$
$$Secondary\ Tar \xrightarrow{k_6} Char$$

According to Bandyopadhyay et. al [9,10] [199]

$$pre-dried\ coconut\ shell \rightarrow Active\ complex$$

$$Active\ complex \xrightarrow{k_v} Volatiles$$

$$Active\ complex \xrightarrow{k_c} Char$$

$$-\frac{dW}{dt} = kW \quad (1)$$

$$\frac{dw_v}{dt} = k_v W \quad (2)$$

$$\frac{dw_c}{dt} = k_c W \quad (3)$$

For the determination of kinetics using lumped parameter model, the experimental data of batch experiments under isothermal condition are used. Although due the simplicity, the lumped kinetic parameters are often determined for the pyrolysis of biomass. Although it can represent the overall dynamics of pyrolysis of biomass, it can hardly represent the real situation where different components of biomass, namely, cellulose, hemicellulose and lignin pyrolyze at different rates. To represent the reality distributed activation energy model (DAEM) for the analysis of pyrolysis kinetics of biomass has recently been introduced.

2.3. Kinetics using distributed activation energy model (DAEM)

To incorporate the changing trend of activation energy of pyrolysis on the conversion of biomass, distributed activation energy models (DAEM) have been proposed by Friedman. From the distribution of activation energy of pyrolysis reaction, the occurrence of different types of pyrolysis reaction characterized by the presence of cellulose, hemi cellulose and lignin can be assessed. Recently, researchers [45-56] have shown interest to determine the kinetic parameters of DAEM for different pyrolyzing biomass. For this purpose, experimental data of non-isothermal condition are used. Experiments are carried out in thermogravimetric analyzer (TGA) using heating rate as a parameter. Some of the systems studied for DAEM have been detailed in Table.2.3.

Table. 2.3. DAEM for Biomass pyrolysis

Materials	Heating rate	Model	References
Wood chips	5 K/min^{-1}	Friedman	Gasparvoic et. al[45]
Cholorocoecum humicola	5 -20 K/min^{-1}	Friedman	Kirtanion et. al [46]
Lignin	5 -15 K/min^{-1}	Friedman	Mani et. al [47]
Different types of coal	20, 35, 50,75,100 K/min^{-1}	Friedman	Li et. al [48]
Kerogen	5 -20 K/min^{-1}	Friedman	Lakhmanan et. al [49]
Cellulose	5,25,50 K/min^{-1}	Friedman	Cai et. al [50]

Sub-bituminous and anthracite coal	100 K/min^{-1}	Friedman	Caprariis et. al [51]
Wood, algea, lignin, corn stalk, skin kerogen, cellulose and coal	5,25,50 K/min^{-1}	Friedman	Wu et. al [52]
Sesame oil cake	5-25 K/min^{-1}	Friedman	Sarkar et. al [30]
Posidonia oceanica (L.) and frying oil wastes	5-15 K/min^{-1}	Friedman	Zaafouri et. al[53]
agro-industrial wastes	5-15 K/min^{-1}	Coast Redfern and Sharp	Fernandez et. al[44]

2.4. Catalysts

It has been indicated by the reported literature that the usage of catalysts enhances the yield of products, particularly, the pyro-oil. Many research works [54-65] are being carried out in the field of catalytic pyrolysis of biomass in order to enhance the yield of the pyro-oil. The detailed list of catalysts, the catalyst to feed ratio are provided in the table 2.4.

Table 2.4. The list of the catalysts to feed ratio, catalysts type, feedstocks, reactor type, temperature and yields

Feedstock	Catalyst	Catalyst to feed ratio	Reference
Beech wood	MSU-S/HBEA (hexagonal) 2.MSU-S/WBEA (wormhole) 3.Al-MCM-41	0.7/1.5(wt/wt)	Kostas S. Triantafyllidis et al.(54)
hybrid poplar wood	ExxonMobil HZSM-5 catalyst	1/1(wt/wt)	Foster. A. Agblevor et al (55)
Pine wood	ZSM-5 (24)	12.0-36.0 and 1:1 (WHSV)	Lopez et al.(56)
Mixed wood	ZSM-5 (50)	1.16 (WHSV)	Horne et al.(57)
Lignocell HBS	ZSM-5 based FCC additive (10 wt% ZSM-5)	2.9–18(WHSV)	Lappas et al.(58)
Cellulose, Glucose	ZSM-5 (60)	9.9(WHSV)	Carlson et al (59)
Nannochloropsis sp. (a kind of green	HZSM-5 catalyst	(0.2/1, 0.4/1, 0.6/1, 0.8/1 1/1, wt/wt)	Pan .et.al.(60)

microalga) residue			
Barkless spruce wood	Al-MCM-41, 8MCM-41 MCM-41 with C18 Cu-Al-MCM-41 FCC -SBA-15 Al-SBA-15(20)	and 0.7/1.5	Judit Adam et.al.(61)
Wood chips of Canadian white pine	20 wt.% Na2CO3/c-Al2O3	0.5 to 1 and 2.	Nguyen et. al. (62)
Douglas fir	Zn powder	1.32 to 4.86	Bu et. Al. (63)
Wheat and barley spent grains	Activated Alumina Bed and 1:1	1:1	Sanna et. al (64)
Woody biomass	Na2CO3/γ-Al2O3 and 1:1	1:1	Imran et. al (65)

In many cases positive, catalytic effects have been observed on the pyrolysis of lignocellulosic biomass.

2.5. Co-pyrolysis

The co-pyrolysis is important from the perspective of simultaneous utilization of different lignocellulosic waste through pyrolysis. In recent times, research attention is also being given to this area [66-68,30]. Some details of reported results on co-pyrolysis of lignocellulosic feedstocks are provided in Table.2.5.

Table 2.5. Literature data on Co-pyrolysis of lignocellulosic feedstocks

Feedstock	Observations	Reference
Peanut (Arachis hypogaea) shells and cassava (Manihot esculenta) starch	Both the bio-oil yield and the water content of the liquids showed synergistic effects. A mixture composed by 75 wt.% of starch and 25 wt.% of peanut shells led to maximize the yield of the bio-oil (58.2 wt.%), On the other hand, the addition of the starch to the peanut shells led to a bio-char with less ash content. It could be more suitable for further combustion in steam boilers.	Messina et. al[66] [2015]
Energy grass and lignite	The co-pyrolysis of energy grass and lignite blend is characterized by two-stage thermal	Guan et. al[67] [2015]

	degradation processes, which is dominant by energy grass content in the first stage but lignite in the second stage. No obvious interaction between energy grass and lignite is observed during the co-pyrolysis process under the operational conditions investigated. The distributed activation energy model is applied to determine the activation energy for the pyrolysis of energy grass, lignite and their blends.	
Waste newspaper (WP) was first co-pyrolyzed with high-density polyethylene (HDPE)	Positive synergistic effects on fuel properties of co-pyrolysis oil were observed, especially demonstrating dramatically decrease in viscosity and total acid number by 75.96% and 216.04% in comparison to theoretical data.	Chen et. al[68] [2016]
Paper waste and mustard press cake	Optimization had been done by using RSM to identify the individual sets of values of independent parameters corresponding to maximum bio-oil yield (A: 9.0:1, B: 874.75 K), energy yield (A: 8.80:1, B: 812 K), and minimum oxygen content of bio-oil (A: 2.75:1, B: 883.06 K). Bio-oil obtained at maximum energy yield condition had been characterized using the Gas chromatography–mass spectrometry (GC-MS) and Fourier transform infrared spectroscopy (FTIR) spectroscopic analyses.	Sarkar and Chowdhury [30] [2016]

The reported literature reveals that copyrolysis of feedstocks usually led to enhancement of yield of bio-oil and synergistic pyrolytic behaviour has also been noticed.

2.6. Aspen Plus Modelling

Apart from carrying out experiments on the lab scale, the researchers [69-78] have also attempted to scale up the pyrolysis plant using the predictions of Aspen Plus simulator. The Table.2.6. presents some of the reported data on Aspen Plus simulation for pyrolysis process of lignocellulosic biomass.

Table. 2.6. Status of Research studies on scaling up of a pyrolysis plant of lignocellulosic biomass using Aspen Plus simulator

Reference	Observations
Gaoen and Peiqin [69] [2015]	A novel model for assessment of the conversion of biomass to valuable fuel products via fast pyrolysis using Aspen Plus has been developed. The simulation includes the pre-treatment of the biomass, the pyrolysis reactor, and a combustion reactor. Simulating each part of the process with the capacity of 2000t/d corn stover,
Hammer et. al[70] [2013]	A pyrolysis process was developed for on-site production and utilization of pyrolysis oil from equine waste at the Equine Rehabilitation Center at Morrisville State College (MSC). using equilibrium model of Aspen Plus. Results were used to size and cost 6 and 15 ODMTPD systems.

Ward et. al[71] [2014]	A computational model was developed using ASPEN PLUS software and utilised to analyse the performance of the fast pyrolysis process using municipal waste as fuels as a function of operating conditions and physical and chemical properties.
VISCONTI et. al[72] [2014]	The research group have developed kinetic-based models that are quite accurate, but computationally intensive and applicable only to specific pyrolysis installations within certain operating conditions. The work was focused on the development of an input-output model through the software Aspen Plus® that could simulate the equilibrium-based pyrolysis of a lignocellulosic biomass and, as a minimum, could predict the effects of the main process variables on the most relevant performance results.
Olcese et. al[73] [2013]	Biosourced aromatics like, BTX (benzene, toluene, xylene) and phenols) could be produced by lignin pyrolysis coupled with catalytic hydrodeoxygenation (HDO) of uncondensed pyrolysis vapors. Aspen Plus model handled (1) pyrolysis of lignin, including char, oligomers, gases and aromatic yields, (2) catalytic conversion of aromatics by the kinetic model, (3) heat exchangers, and (4) BTX vapors recovery by scrubbing with 1-methyl-naphthalene. Mass and carbon balances, heat demand, and selectivity in desired products are given for the overall process.
Ahmed et. al [74] [2015]	All the models were developed in Aspen Plus simulator based on kinetic and thermodynamic equilibrium, whereby different reactor models were used to represent processes in relevant with tar production or cracking.
Onarheim et. al [75] [2015]	A steady-state Aspen Plus simulation model has been developed that provides estimated mass and energy balances for an industrial fluidizing-bed fast pyrolysis process to produce bio-oil. The tool can be used to assess plant performance under varying process conditions using different feedstocks.
Kabir et. al[76] [2015]	A four-stage steady state simulation model was developed for pyrolysis process performance simulation using Aspen Plus software. In the first stage, the moisture content of the MGW feed was reduced. In the second stage, the MGW is decomposed according to its elemental constituents. In the third stage, condensate material was separated and, finally, the pyrolysis reactions were modelled using the Gibbs free energy minimisation approach. The MGW's ultimate and proximate analysis data were used in the Aspen Plus simulation as input parameters. The model was validated with experimentally measured data. A good agreement between simulation and experimental results was found.
Zhang et. al[77] [2013]	The economic feasibility of a facility producing monosaccharides, hydrogen and transportation fuels via fast pyrolysis and upgrading pathway was evaluated by modelling a 2000 dry metric ton biomass/day facility using Aspen Plus. .
Mobolaji et. al[78] [2015]	The techno-economic performance analysis of biofuel production and electric power generation from pine wood fast pyrolysis and bio-oil hydro processing is explored through process simulation. The researchers developed a process model of 72 MT/day and bio-oil hydro processing the effect of initial biomass moisture content on the amount of electric power generated and the effect of biomass feed composition on product yields were also reported.

From the literature review it is clear that the process simulation modelling for none of the Indian lignocellulosic biomass has been developed. The procedure is, however helpful for the decision of installation of large pyrolysis plant using the feedstock under study.

2.7. Energy and Environmental Assessment Impact

A detailed literature survey on energy and environmental assessment (EEA) of energy production systems based on biomass pyrolysis has been done in the table 2.7.

Table. 2.7. Present Status of Research Studies on Energy and Environmental Assessment of Pyrolysis Plant of Lignocellulosic Biomass

Reference	Observations
Kabir and kumar [79] [2011]	The energy and environmental outputs of producing bio-hydrogen from three different biomass feed stocks, namely, forest residue (FR), whole forest (WF) and agricultural residue (AR) through fast pyrolysis has been assessed
Zaman [80] [2010]	Three different waste treatment technologies have been analysed using LCA tool. They used SimaPro software to analyse environmental burden by different impact categories of different waste treatment technologies namely, sanitary landfill, incineration and gasification pyrolysis. They calculated energy recovery efficiency of every system.
Fan et al., [81] [2011]	The greenhouse gas emission (GHG) for energy generation from pyrolysis of forest resources, namely, the hardwood stands, hybrid poplar, short rotation forestry (SRF) willow plantations and waste wood has been investigated.
Roberts et al., [82]	They used the LCA methodology to estimate the energy and climate change impacts and the economics of biochar produced from pyrolysis of corn stover, yard waste and switchgrass. They calculated the net energy and net greenhouse gas emission from each LCA feedstock
Iribarren et al., [83] [2012]	They evaluated the environmental performance of a biofuel produced from fast pyrolysis of short rotation poplar biomass using a life cycle assessment (LCA) methodology.
Steele et al., [84] [2007]	They used the LCA methodology during the production of bio-oil from the fast pyrolysis of Southern pine (*Pinus taeda*) trees and compared with measures for residual fuel oil. They used the Aspen software to derive the input parameters and mass and energy balances. They evaluated the net energy and GHG emission using the SimaPro software.
Zhong et al., [85] [2010]	They analysed the LCA of flash pyrolysis of wood waste to study the environmental effects due to the setup of flash pyrolysis plant in locality. They calculated the net energy and GHG emission of this plant.
Cao and Pawłowski, [86] [2013]	They studied the life cycle assessment of two emerging sewage sludge-to-energy systems. According to them energy and GHG emission implications of a sludge-to-energy system based on a combination of anaerobic digestion and fast pyrolysis for energy conversion were evaluated along its life cycle, compared to a simplified system that excludes digestion process. The results demonstrated that systems can be credited with a potential of not only producing considerable net energy but also reducing GHG emissions. .

From the literature data, it is clear that the life cycle assessment (LCA) is being done for the Energy and environmental assessment of pyrolysis plant for lignocellulosic feedstocks. Very often the large-scale data to be used for LCA are generated using process simulation models of ASPEN PLUS, no such data are, however, available for Indian lignocellulosic biomass.
Overall, from the review of literature the following research gaps in the field of pyrolysis of Indian lignocellulosic biomass have been identified.

Research Gaps:

- No research studies on the pyrolysis of abundant municipal lignocellulosic biomass like jute packaging wastes, citrus fruit wastes etc, have been reported
- There is a dearth of data on reaction kinetics using both lumped and distributed models for most of the Indian lignocellulosic biomass
- Mathematical model of pyrolyzer using Indian lignocellulosic biomass is rarely reported
- There is no literature data on the catalytic pyrolysis of Indian lignocellulosic biomass
- There is no literature data on the processing of pyro-products, particularly pyro-oil and pyro-gas of Indian lignocellulosic biomass
- Limited literature is reported on the research studies on the co-pyrolysis of Indian lignocellulosic biomass
- There is no literature data on the process simulation of pyrolysis plant using ASPEN PLUS etc. for Indian lignocellulosic biomass
- There is no literature data on the energy and environmental analysis of pyrolysis plant for Indian lignocellulosic biomass using the principles of LCA

References

1. S. Murugan, Sai Gu, "Research and development activities in pyrolysis – Contributions from Indian scientific community – A review", Renewable and Sustainable Energy Reviews, 46, (2015), 282–295.
2. Dubey Anil Kumar, Chandra Pitam, Padhee Debasish, Gangil S, "Energy from cottons talks and other crop residues. ⟨https://www.icac.org/projects/Com- mon Fund/20/15chandra.pdf⟩.
3. Raveendran K, Ganesh Anuradda, Khilar KC, "Influence of mineral matter on biomass pyrolysis characteristics", Fuel, 1995, 74(12), 1812–22.
4. Gaurav Kumar, Achyut Kumar Panda, Singh RK, "Optimization of process for the production of bio-oil from eucalyptus wood", J. Fuel Chem Technol, 2010, 38(2), 162–7
5. Natarajan E, Ganapathy Sundaram E, "Pyrolysis of rice husk in a fixed bed reactor", World Acad Sci Eng Technol, 2009, 3, 467–71.
6. Das Piyali, Ganesh Anuradda, "Bio-oil from pyrolysis of cashew nutshell-a near fuel", Biomass Bioenergy, 2003, 25, 113–7.
7. Sundaram Ganapathy, Natarajan, "Pyrolysis of coconut shell: An experimental investigation", J.Eng Res, 2009, 6(2), 33–9.
8. Rout Tanmaya Kumar,Singh, "Pyrolysis of coconut shell.[M.Tech thesis report]. NIT Rourkela, 2011.
9. Swati Bandyopadhyay, Ranjana Chowdhury and Gopal Krishna Biswas, "Transient Behavior of a Coconut Shell Pyrolyzer: A Mathematical Analysis", Ind. Eng. Chem. Res., 1996, 35, 3347-3355
10. Swati Bandyopadhyay, Ranjana Chowdhury and Gopal Krishna Biswas, "Thermal Deactivation Studies of Coconut Shell Pyrolysis", The Canadian Journal of Chemical Engineering, 77, OCTOBER, 1999, 1028 -1036.
11. Powar RV, Gangil Sandip, "Study of effect of temperature on yield of bio-oil, bio-char and NCG from soybean stalk in continuous feed bio-oil reactor", Int J Renew Energy Res , 2013, 3(3), 519–22.
12. Sarkar Aparna, Chowdhury Ranjana, "Studies on catalytic pyrolysis of mustard seed press cake with NaCl", Int J Eng Sci Res Technol, 2277-9655, 2014, 3(6):90–6.

13. Sachin Kumar, Singh, “Thermogravimetric analysis of ground nut cake”, Int J Chem Eng Appl, 2012, 2(4), 268–71.

14. Pradhan Saswat Kumar, Singh, “Liquid fuel from oil seeds by pyrolysis”, [M. Tech Thesis report]; December2010

15. Prakash R, Singh R K, Murugan S, “Experimental studies on a diesel engine fuelled with wood pyrolysis oil diesel emulsions”, Int J Chem Eng Appl, 2011, 2(6), 395–9.

16. Prakash R, Singh R K, Murugan S, “Experimental investigation non diesel engine fuelled by biodiesel and its emulsions with wood pyrolysis oil”, Int J Green Energy, 2012, 9(8), 749–65.

17. Prakash R, Singh R K, Murugan S, “Comparison of performance and emission parameters of a diesel engine fuelled with biodiesel and wood pyrolysis oil emulsions”, Int Energy J, 2012, 13, 123–32.

18. Prakash R, Singh R K, Murugan S, “Experimental investigation on diesel engine fuelled with bio-oil derived from waste wood-biodiesel emulsions”, Energy, 2013, 55, 610–8.

19. Prakash R, Singh R K, Murugan S, “Use of biodiesel and wood pyrolysis oil emulsions as an alternative fuel for direct injection diesel engine”, Waste Biomass Valoriz, 2013, 4, 475–84.

20. Prakash R, Singh R K, Murugan S, “Biodiesel bio-oil emulsions as alternative fuel for diesel engine”, Int J Emerg Technol Adv Eng, 2013, 3(3), 101–5.

21. Prakash R, Singh R K, Murugan S, “Studies on behaviour of a DI diesel engine fuelled with biooil biodiesel emulsions”, Int J Oil Gas Coal Technol, 2015, 9 (1), 89–108.

22. Prakash R, Singh R K, Murugan S, “Experimental studies on a DI diesel engine fuelled with Jatropha methyl ester-wood pyrolysis oil emulsions [Ph.D. thesis report]. NITRourkela;2014.

23. Choudhry Ranajana, Sarkar Aparna, “Reaction kinetics and product distribution of slow pyrolysis of Indian textile wastes”, Int J Chem Reactor Eng 2012,10(1).

24. Sarkar Aparna, Langanaki Michael, Chouwdhry Ranajan, ‘Studies on pyrolysis of spent engine oil in a quartz load cell”, Int J Res Eng Technol, 2014, 03(06), ISSN: 23217308, 222–6.

25. Modh J K, Namjoshi SA, Channiwala SA, “Kinetics and pyrolysis of glossy paper waste”, Int J Eng Res Appl (IJERA), 2248-96222012, 2(2), 1067–74.

26. Bijayani Biswal, Sachin Kumar, Singh R K, “Production of hydrocarbon liquid by thermal pyrolysis of paper cup waste”, J Waste Manag, 2013, 1–7, Article-ID731858.

27. Singh RK, Bijayani Biswal, Kumar Sachin, “Determination of activation energy from pyrolysis of paper cup waste using thermogravimetric analysis”, Res J Recent Sci, 2277-25022013, 2, 177–82.

28. Ruby Ray, Ranjana Chowdhury and Pinaki Bhattacharya, “Studies on pyrolysis of vegetable market wastes in presence of heat transfer resistance and deactivation”, Int. J. Energy Res, 2005, 29, 811–828

29. Ruby Ray, Ranjana Chowdhury and Pinaki Bhattacharya, “Simulation and Modeling of Vegetable Market Wastes Pyrolysis Under Progressive Deactivation Condition”, The Canadian Journal of Chemical Engineering, June 2004, 566 -579.

30. Aparna Sarkar and Ranjana Chowdhury, “Co-pyrolysis of paper waste and mustard press cake in a semi-batch pyrolyzer—optimization and bio-oil characterization”, International Journal of Green Energy, 2016, VOL. 13, NO. 4, 373–382

31. Aparna Sarkar, Biswarup Mondal, and Ranjana Chowdhury, “Mathematical Modeling of a Semibatch Pyrolyser for Sesame Oil Cake”, Ind. Eng. Chem. Res., 53, 2014, 19671−19680.

32. M. Asadullah, M. Anisur Rahman, M. Mohsin Ali, M. Abdul Motin, M. Borhanus Sultan, M. Robiul Alam, M. Sahedur Rahman, “Jute stick pyrolysis for bio-oil production in fluidized bed reactor”, Bioresource Technology, 99, 2008, 44–50.

33. M.A. Lopez-Velazquez, V. Santes, J. Balmaseda, E. Torres-Garcia, “Pyrolysis of orange waste: A thermo-kinetic study”, *Journal of Analytical and Applied Pyrolysis*, 99, 2013, 170 – 177.

34. B Zapata, J Balmaseda, E Fregoso-Israel, E Torres-Garcia, “Thermo-Kinetics of orange peel in air”, Journal of Thermal Analysis and Calorimetry, 98, 2009, 309-315.

35. Yang, Y. B., Phan, A. N., Ryu, C., Sharifi, V., Swithenbank, J., “Mathematical modelling of slow pyrolysis of segregated solid wastes in a packed-bed pyrolyzer”, Fuel, 86, 2007, 169–180.

36. Miranda, R., Blanco, C. S., Bustos-Martinez, D., Vasile, C., “Pyrolysis of textile wastes I. Kinetics and yields”, J. Anal. Appl. Pyrolysis, 80, 2007, 489–495.

37. Barişçi, S., Oncel, M. S., “The Disposal of Combed Cotton Wastes by Pyrolysis”, *International Journal of Green Energy*, 11, 2014, 255–266.

38. Williams, P. T., Reed, A. R., “High grade activated carbon matting derived from the chemical activation and pyrolysis of natural fibre textile waste”, J. Anal. Appl. Pyrolysis, 71, 2004, 971–986.

39. Molto, J., Font, R., Conesa, J. A., Gullon, I. M., 2006. “Thermogravimetric analysis during the decomposition of cotton fabrics in an inert and air environment”, J. Anal. Appl. Pyrolysis 76, 2006, 124–131.

40. Su Shiung Lam, Rock Keey Liew, Xin Yi Lim, Farid Nasir Ani, Ahmad Jusoh, “Fruit waste as feedstock for recovery by pyrolysis technique”, International Biodeterioration & Biodegradation 113 (2016) 325-333.

41. J.J.M. Orfao, F.J.A. Antunes, J.L. Figueiredo, “Pyrolysis kinetics of lignocellulosic materials-three independent reactions model”, Fuel, 78, 1999, 349-358.

42. Abhishek Sharmaa, Vishnu Pareeka,, Shaobin Wanga, Zhezi Zhangb,Hong Yangb, Dongke Zhang, “A phenomenological model of the mechanisms of lignocellulosicbiomass pyrolysis processes”, Computers and Chemical Engineering 60 (2014) 231– 241.

43. Wender S. Carvalho, Tiago J. Oliveira, Cássia R. Cardoso,Carlos H. Ataíde, “Thermogravimetric analysis and analyticalpyrolysis of a variety of lignocellulosic sorghum”, Chem. Eng. Res. Des. (2014), http://dx.doi.org/10.1016/j.cherd.2014.11.010..

44. Anabel Fernandez , Alejandra Saffe , Regina Pereyra , Germán Mazza , Rosa Rodriguez, “Kinetic study of regional agro-industrial wastes pyrolysis using non-isothermal TGA analysis”, Applied Thermal Engineering, 106, 2016, 1157–1164.

45. Gasparovie, L., Labovsky, J., Markos, J., and Jelemenský, L., “Calculation of Kinetic Parameters of the Thermal Decomposition of Wood by Distributed Activation Energy Model (DAEM)”, Chem. Biochem. Eng. Q., 26 (1), 2012, 45–53.

46. Kirtania, K., Bhattacharya, S., “Application of the distributed activation energy model to the kinetic study of pyrolysis of the fresh water algae Chlorococcum humicola”, Bioresource Technology, 107, 2012, 476–481.

47. Mani, T., Murugan, P., and Mahinpey, N., “Determination of Distributed Activation Energy Model Kinetic Parameters Using Simulated Annealing Optimization Method for Nonisothermal Pyrolysis of Lignin”, Ind. Eng. Chem. Res., 48, 2009, 1464–1467.

48. Li, Z., Liu, C., Chen, Z., Qian, J., Zhao, W., Zhu, Q., “Analysis of coals and biomass pyrolysis using the distributed activation energy model”. Bioresource Technology, 100, 2009, 948–952.

49. Lakshmanan, C. C., and White, N., “A New Distributed Activation Energy Model Using Weibull Distribution for the Representation of Complex Kinetics”, Energy & Fuels, 8, 1994, 1158-1167.

50. Cai, J., Yang, S., Li, T., “Logistic distributed activation energy model – Part 2: Application to cellulose pyrolysis”, Bioresource Technology 102, 2011, 3642–3644.

51. Caprariis, B. D., Filippis, P. D., Herce, C., and Verdone, N., 2012. Double-Gaussian Distributed Activation Energy Model for Coal Devolatilization Energy Fuels, 26, 2012, 6153−6159

52. Wu, W., Cai, J., and Liu, R., 2013. Isoconversional Kinetic Analysis of Distributed Activation Energy Model Processes for Pyrolysis of Solid Fuels, Ind. Eng. Chem. Res. 52, pp. 14376−14383.

53. Kaouther Zaafouri, Aida Ben Hassen Trabelsi, Samah Krichah, Aymen Ouerghi, Abdelkarim Aydi, Carlos Alberto Claumann, Zibetti André Wüst, Silm Naoui, Latifa Bergaoui,Moktar Hamdi, "Enhancement of biofuels production by means of co-pyrolysis of Posidonia oceanica (L.) and frying oil wastes: Experimental study and process modelling", Bioresource Technology 207 (2016) 387–398.

54. Kostas S. Triantafyllidis, Eleni F. Iliopoulou , Eleni V. Antonakou , Angelos A. Lappas , Hui Wang , Thomas J. Pinnavaia, "Hydrothermally stable mesoporous aluminosilicates (MSU-S) assembled from zeolite seeds as catalysts for biomass pyrolysis", *Microporous and Mesoporous Materials,* 99 (2007) 132–139.

55. Foster. A. Agblevor, S. Beis, O. Mante, and N. Abdoulmoumine, "Fractional Catalytic Pyrolysis of Hybrid Poplar Wood", *Ind. Eng. Chem. Res.* 2010, *49,* 3533–3538.

56. Amutio, M., Lopez, G., Erkiaga, A., Artetxe, M., Olazar, M., Bilbao, J., "Vacuum Flash Pyrolysis of Pinewood Sawdust in a Conical Spouted Bed Reactor", DOI: 10.5071/19thEUBCE2011-OB11.3, 2011.

57. Patrick A. Horne, Paul T. Williams , "The effect of zeolite ZSM-5 catalyst deactivation during the upgrading of biomass-derived pyrolysis vapours", Journal of Analytical and Applied Pyrolysis , vol. 34, no. 1, pp. 65-85, 1995.

58. A.A. Lappas, M.C. Samolada, D.K. Iatridis, S.S. Voutetakis, I.A.Vasalos, "Biomass pyrolysis in a circulating fluid bed reactor for the production of fuels and chemicals", Fuel 81 (2002) 2087–2095.

59. Torren R. Carlson, Geoffrey A. Tompsett, William C. Conner, George W. Huber, "Aromatic Production from Catalytic Fast Pyrolysis of Biomass-Derived Feedstocks", Top Catal, 52, 2009, 241–252.

60. Pan Pan, Changwei Hu a, Wenyan Yang, Yuesong Li, Linlin Dong, Liangfang Zhu, Dongmei Tong, Renwei Qing, Yong Fan, "The direct pyrolysis and catalytic pyrolysis of Nannochloropsis sp. residue for renewable bio-oils", Bioresource Technology, 101, 2010, 4593–4599.

61. Judit Adam , Eleni Antonakou , Angelos Lappas , Michael Stocker , Merete H. Nilsen , Aud Bouzga , Johan E. Hustad , Gisle Oye, "In situ catalytic upgrading of biomass derived fast pyrolysis vapours in a fixed bed reactor using mesoporous materials", *Microporous and Mesoporous Materials* 96 (2006) 93–101.

62. T.S. Nguyen, M. Zabeti, L. Lefferts, G. Brem, K. Seshan, "Conversion of lignocellulosic biomass to green fuel oil over sodium based Catalysts", Bioresource Technology 142 (2013) 353–360.

63. Quan Bu, Hanwu Lei, Shoujie Ren, Lu Wang, Qin Zhang, Juming Tang, Roger Ruan, "Production of phenols and biofuels by catalytic microwave pyrolysis of lignocellulosic biomass", Bioresource Technology 108 (2012) 274–279.

64. Aimaro Sanna, Sujing Li, Rob Linforth, Katherine A. Smart, John M. Andresen, "Bio-oil and bio-char from low temperature pyrolysis of spent grains using activated alumina", Bioresource Technology 102 (2011) 10695–10703.

65. Ali Imran, Eddy A. Bramer, Kulathuiyer Seshan, Gerrit Brem, "High quality bio-oil from catalytic flash pyrolysis of lignocellulosic biomass over alumia-supported sodium carbonate", Fuel Processing Technology 127 (2014) 72 – 79.

66. L.I. Gurevich Messina, P.R. Bonelli, A.L. Cukierman, "Copyrolysis of peanut shells and cassava starch mixtures: Effect of the components proportion", Journal of Analytical and Applied Pyrolysis 113 (2015) 508–517

67. Yanjun Guan, Ying Ma, Kai Zhang, Honggang Chen, Gang Xu, Wenyi Liu, Yongping Yang, "Co-pyrolysis behaviors of energy grass and lignite", Energy Conversion and Management 93 (2015) 132–140

68. Weimin Chen, Shukai Shi, Jun Zhang, Minzhi Chen, Xiaoyan Zhou, "Co-pyrolysis of waste newspaper with high-density polyethylene: Synergistic effect and oil characterization", Energy Conversion and Management, 112, 2016, 41–48.

69. Wang Gaoen and Sun Peiqin, "A Process Modeling of Bio-oil production by Fast Pyrolysis In Aspen Plus", School of Chemical Engineering and Energy, Zhengzhou University,http://www.paper.edu.cn,2015.

70. Nicole L. Hammer, Akwasi A. Boateng, Charles A. Mullen, M. Clayton Wheeler, "Aspen Plus ® and economic modeling of equine waste utilization for localized hot water heating via fast pyrolysis", Journal of Environmental Management 128 (2013) 594 -601

71. J. Ward, M.G. Rasul, M. M. K. Bhuiya, "Energy recovery from biomass by fast pyrolysis", Procedia Engineering 90 (2014) 669 – 674

72. ALESSANDRO VISCONTI, MICHELE MICCIO and DAGMAR JUCHELKOVÁ, "Equilibrium-based simulation of lignocellulosic biomass pyrolysis via Aspen Plus®", Recent Advances in Applied Mathematics, Modelling and Simulation, 2014, 242-251, ISBN: 978-960-474-398-8.

73. R. N. Olcese, J. Francois, M. M. Bettahar, D. Petitjean, and A. Dufour, "Hydrodeoxygenation of Guaiacol, A Surrogate of Lignin Pyrolysis Vapors, Over Iron Based Catalysts: Kinetics and Modeling of the Lignin to Aromatics Integrated Process", Energy Fuels 2013, 27, 975−984

74. A.M. A Ahmed, A. Salmiaton, T. S. Y Choong, W. A. K. G. Wan Azlina, "Review of kinetic and equilibrium concepts for biomass tar modeling by using Aspen Plus", Renewable and Sustainable Energy Reviews 52 (2015) 1623–1644

75. Kristin Onarheim, Yrjö Solantausta, and Jani Lehto, "Process Simulation Development of Fast Pyrolysis of Wood Using Aspen Plus", Energy Fuels 2015, 29, 205−217

76. Mohammed J. Kabir, Ashfaque Ahmed Chowdhury and Mohammad G. Rasul, "Pyrolysis of Municipal Green Waste: A Modelling, Simulation and Experimental Analysis", *Energies* 2015, *8*, 7522-7541

77. Yanan Zhang, Tristan R. Brown, Guiping Hu, Robert C. Brown, "Techno-economic analysis of monosaccharide production via fast pyrolysis of lignocellulose", Bioresource Technology 127 (2013) 358–365

78. Mobolaji B. Shemfe, Sai Gu, Panneerselvam Ranganathan, "Techno-economic performance analysis of biofuel production and miniature electric power generation from biomass fast pyrolysis and bio-oil upgrading", Fuel 143 (2015) 361–372

79. Kabir, M. R., Kumar, A., 2011. Development of net energy ratio and emission factor for biohydrogen production pathways, Bioresource Technology, 102, pp. 8972–8985.

80. Zaman, A. U., 2010. Comparative study of municipal solid waste treatment technologies using life cycle assessment method, Int. J. Environ. Sci. Tech., 7, pp. 225-234, Spring.

81. Fan, J., Kalnes, T. N., Alward, M., 2011. Jordan Klinger, Adam Sadehvandi, David R. Shonnard, Life cycle assessment of electricity generation using fast pyrolysis bio-oil, Renewable Energy, 36, pp. 632-641.

82. Roberts, K.G., Gloy, B. A., Joseph, S., Scott, N. R., and Lehmann, J., 2010. Life Cycle Assessment of Biochar Systems: Estimating the Energetic, Economic, and Climate Change Potential, *Environ. Sci. Technol., 44,* pp. 827–833.

83. Iribarren, D., Peters, J. F., Dufour, J., 2012. Life cycle assessment of transportation fuels from biomass pyrolysis, Fuel, 97, pp. 812–821.

84. Steele, P., Puettmann, M. E., Penmetsa, V. K., Cooper, J. E., 2007. Life Cycle Assessment of Pyrolysis Bio-Oil Production, Forest Prod. J. 62, pp.326–334.

85. Zhong, Z.W., Song, B., Zaki, M. B. M., 2010. Life-cycle assessment of flash pyrolysis of wood waste, Journal of Cleaner Production18, pp. 1177-1183.

86. Yucheng Cao and Artur Pawłowski, "Life cycle assessment of two emerging sewage sludge-to-energy systems: Evaluating energy and greenhouse gas emissions implications", Bioresource Technology 127 (2013) 81–91.

Chapter. 3
AIMS AND OBJECTIVES

From the literature review, it is evident that a considerable extent of research work is being conducted on the generation of energy from lignocellulosic waste through pyrolysis process. However, the data on pyrolysis of lignocellulosic biomass, namely, waste jute, lime waste etc. of Indian origin are lacking. Based on the research gaps identified through the reviewing of the relevant literature, as discussed in Chapter 2, the following aims and the corresponding objectives have been set for the present research work.

Aim 1

To study the catalytic and the non-catalytic pyrolysis of waste jute and lime waste

- Objectives

a) To determine the thermochemical properties of jute packaging waste and lime waste by Proximate and Ultimate Analysis and also to determine the Higher Heating Values.
b) To study the kinetics of the non-catalytic pyrolysis of feedstocks
c) To study the effect of catalysts on the pyrolysis of waste jute and lime waste.
d) To characterize pyro-products.

Aim 2

To develop mathematical models to predict the transient behaviour of a semi batch pyrolyzer using waste jute.

Aim 3

To study the co – pyrolysis of the waste jute with sesame oil cake.

Aim 4

To process the pyro-oil and pyro-gas

Objectives

a) To study the kinetics of secondary pyrolysis i.e. thermal cracking of pyro -oil.
b) Assessment of conversion of pyro-gas to liquid fuel through Fischer Tropsch process using Aspen Plus ®**.**

Aim 5

Assessment of Energy and Environment Footprints of a large pyrolysis unit using LCA principle.

Objectives

a) To generate process flow data for a 100 tpd pyrolysis unit of jute waste using Aspen Plus ®
b) Assessment of Energy and Environment Footprints of a large pyrolysis unit using LCA principle.

The methodologies adopted to achieve the goal set by different aims and objectives have been adopted either by following the procedure recommended by previous researchers or by designing a new procedure. The methodologies are described as follow:

Methodology for Aim 1

(a) The pyrolysis feed stocks, namely, jute and lime wastes have been collected from the local municipal markets and fruit juice centres respectively.

(b) Proximate [D7582 – 15]and Ultimate Analysis [ASTM D5142] of the feedstocks have been conducted using a muffle furnace and a CHNSO [ASTM D5291] analyser respectively.
(c) Higher Heating Values of the feedstocks have been determined with the aid of a bomb calorimeter.
(d) The pyrolysis kinetics of collected feedstocks (jute wastes and lime wastes) have been determined by conducting both (a) isothermal experiments at different pyrolysis temperatures (523- 1173K) in a semi-batch pyrolyzer and (b) non-isothermal experiments in a thermogravimetric analyser (TGA).
(e)Experiments on catalytic pyrolysis of waste jute and lime waste have been carried out using [Aluminum Oxide [Al_2O_3], Zinc Oxide [ZnO], Sodium Chloride [NaCl], Potassium Chloride [KCl], Sodium Aluminosilicate [$NaAl(SiO_3)_2$]] in a semi – batch pyrolyzer. The ratio of catalysts to feedstocks has been maintained at 1:1.

(f) The best catalyst for each feedstock has been identified.

(g) Studies have been carried out for determination of the kinetics using experimental data under isothermal and non – isothermal conditions using the most suitable catalyst.

(h) The products, namely pyro – char, pyro -oil and pyro gas have been characterized as follows:

(i) The elemental composition, porosity, specific surface area, mineralogy and heating value of pyro-char have been determined using CHNO (ASTM D5373 -02), SEM (ASTM E 2809 -13), BET (ASTM D 5604 -96[2012]), XRD (ASTM D 3906 -03) and Bomb Calorimeter (ASTM D 2013) respectively.

(ii) The elemental composition, heating values, boiling point range and pH of pyro-oil have been determined using CHNO (ASTM D5291), Bomb Calorimeter (ASTM D240 -14), ASTM distillation (ASTM D 86) and pH meter respectively. The assessment of the pyro -oil samples for the presence of chemical bonds and compounds has been done using FTIR (ASTM D7371) and GC/MS (ASTM D 4128 -66[2012]) respectively.

(iii) The composition of pyro – gas has been determined using GC (ASTM E112).

Methodology for Aim 2

Based on primary pyrolysis kinetics determined using isothermal experiments and secondary pyrolysis kinetics data from literatures a mathematical model has been developed for a semi batch tubular pyrolyzer using waste jute. Time histories of products and reactants have been determined at each pyrolysis temperature. The model has been validated by comparing simulated predictions with the experimental results.

Methodology for Aim 3

(a) Sesame oil cake has been collected from local edible oil refineries. The proximate and ultimate analyses of sesame oil cake have been done along with the determination of higher heating values, following the same methods used in case of jute waste and lime waste. Pyrolysis kinetics data for sesame oil cake have been collected from literature.

(a) The jute waste and sesame oil cake have been mixed in the ratio 1:1.

(b) The kinetics of co-pyrolysis of jute waste-sesame oil cake mixture has been studied using lumped and distributed model for experimental data obtained under isothermal and non – isothermal condition in a semi – batch pyrolyzer and TGA respectively.

Methodology for Aim 4

(a) The secondary pyrolysis kinetics of the pyro -oil has been determined by carrying out experiments in a muffle furnace under isothermal conditions in the temperature range of 500 to 900^{o}C.

(b) Using the Aspen Plus software the production of different hydrocarbons through the conversion of pyro-gas using Fischer Tropsch synthesis has been predicted. The sensitivity analysis has been done to correlate the production rates of diesel and gasoline with the pyrolysis temperature (T) and the recycle ratio of CO_2 ($\mathbf{R_{CO_2}}$) in the Fischer Tropsch process. Further, the production rates of both the liquid fuels have been optimized using response surface methodology considering T and $\mathbf{R_{CO_2}}$ as factors.

Methodology for Aim 5

The energy and environmental footprints for large pyrolysis plants has been done using Process Simulation Software (ASPEN PLUS®) in the following way:

(a) Pyrolysis plant data for a 100 tpd capacity unit have been generated using Aspen Plus ® modelling.
(b) The following options of usage of pyro – char, pyro -oil and pyro – gas have been considered. Pyro -oil has been used in power plant located at 20 km distance from the pyrolysis plant. Pyro – gas has been utilized to supply energy of pyrolysis and drying. Pyro – char has been partially used for supplying energy of pyrolysis and drying and rest for soil amendment. Sensitivity analysis has been made to derive model equations to correlate energy return on energy investment (EROEI) and CO_2 avoidance (A_{CO_2}) with % char deposition in field and pyrolysis temperature.

Chapter. 4

MATERIAL AND METHODS

4. Material and Methods

4.1. Feedstocks

Jute wastes, sesame oil cake and lime wastes, collected from different areas of Kolkata, India have been used under the present study. The detailed descriptions are listed below in the table. 4.1.

Table. 4.1. Details of pyrolysis feedstocks

Lignocellulosic feed stock	Collection Area	Figure
Jute wastes	Local market near the research institute.	
Sesame oil cake wastes	Local oil mill	
Lime wastes	Local market near the research institute.	

4.2. Chemicals

Benzene, Acetone, Aluminium Oxide [Al_2O_3], zinc oxide [ZnO], sodium chloride [NaCl], potassium chloride [KCl], sodium aluminosilicate [$NaAl(SiO_3)_2$] procured from Merck [1], India were used.

4.3. Analytical Instruments

a) **Bomb Calorimeter:** Bomb calorimeter (Figures. 4.1.a, 4.1.b) was manufactured by S.C. Dey Company, Kolkata, India owned by Chemical Engineering Department

b) **CHNSO Analyser:** The model number of CHNSO analyser (Figure. 4.2) is Vario Micro Cube, 2400 series-II, and was manufactured by Perkin Elmer, U. S. A. owned by Chemical Engineering Department

c) **Scanning Electron Microscope (SEM):** The scanning electron microscope (SEM) (model no. JEOL – JSM 5200) (Figure. 4.3) was owned by Metallurgical and Material Engineering Department.

d) **Thermogravimetric analyser (TGA):** Pyris Diamond thermogravimetric analyser (TGA) (Figure. 4.4) was owned by Metallurgical and Material Engineering Department.

e) **X-ray Diffraction (XRD):** Manufactured by MODEL- ULTIMA-II RIGAKU MAKE (JAPAN) owned by Metallurgical and Material Engineering Department. (Figure. 4.5)

f) **Bet Analyzer (BET)**: Manufactured by Nova® e -series Quatacrome owned by CGCRI Kolkata. (Figure. 4.6)

g) **Atmospheric distillation unit:** (Figure. 4.7) Manufactured by Bhattacharya Limited, Kolkata, India. **Vacuum evaporator:** Manufactured by Bhattacharyya Company, Kolkata, India. (Figure. 4.14.c)

h) **Fourier Transform Infrared Spectrometer (FT-IR):** The FTIR (Figure. 4.8) was manufactured by Schimadzu Company (VERTEX 70). The serial no is A213748 owned by Chemical Engineering Department**.**

i) **Gas chromatography mass spectrometry (GC-MS):** Manufactured by GC-MS--Make--Varian-Model-Saturn2200 owned by Mitra SK (P) LTD. (Figure. 4.9).

j) **Muffle furnace:** A muffle furnace (Figure 1.8) was manufactured by the S.C. Dey Company, Kolkata, India used for the secondary pyrolysis. (Figure. 4.10)
Gas chromatography (GC): Manufactured by GC-Make-Varian-Model-CP3800 owned by Mitra SK (P) LTD. (Figure. 4.11)

Figure. 4.1.a. Photograph of Bomb calorimeter

Figure. 4.1.b. Photograph of Bomb

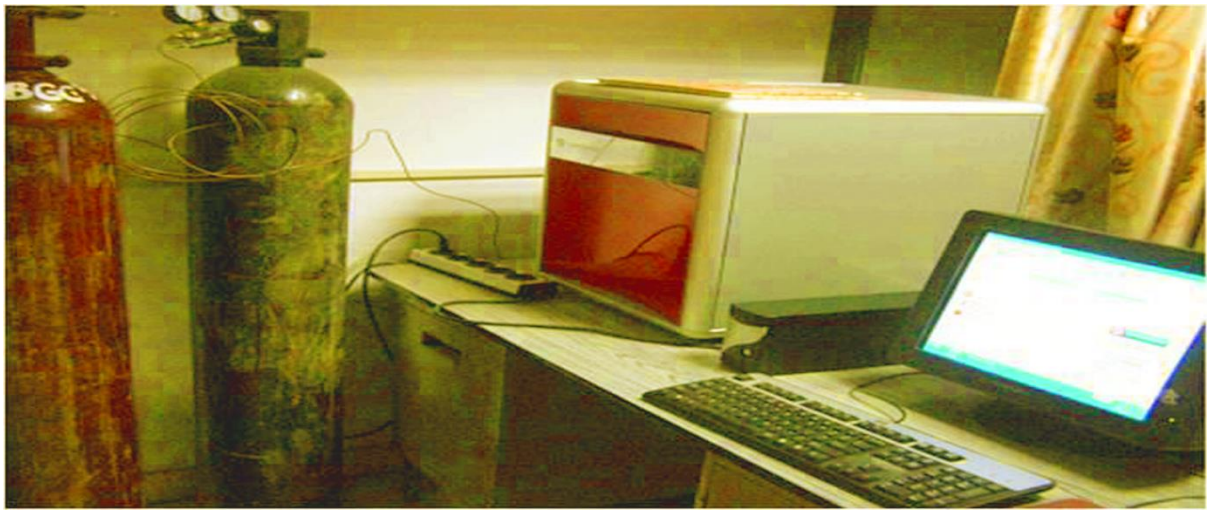

Figure. 4.2. Photograph of CHNSO Analyzer

Figure. 4.3. Photograph of SEM

Figure. 4.4. Photograph of TGA Analyzer

Figure. 4.5. Photograph of XRD

Figure. 4.6. Photograph of BET Analyzer

Figure. 4.7. Photograph of Atmospheric distillation unit

Figure. 4.8. Photograph of FTIR

Figure. 4.9. Photograph of GC-MS Analyzer

Figure 4.10. Photograph of Muffle furnace

Figure. 4.11. Photograph of GC Analyzer

4.4. Experimental Set-up

4.4.1. Experimental set-up for pyrolysis of feedstocks

Figures 4.12 and 4.13 show the experimental set up of pyrolysis of lignocellulosic feedstocks. A 50-mm diameter and 640 mm long cylindrical stainless steel fixed bed reactor was placed horizontally in a tubular furnace [2,3].

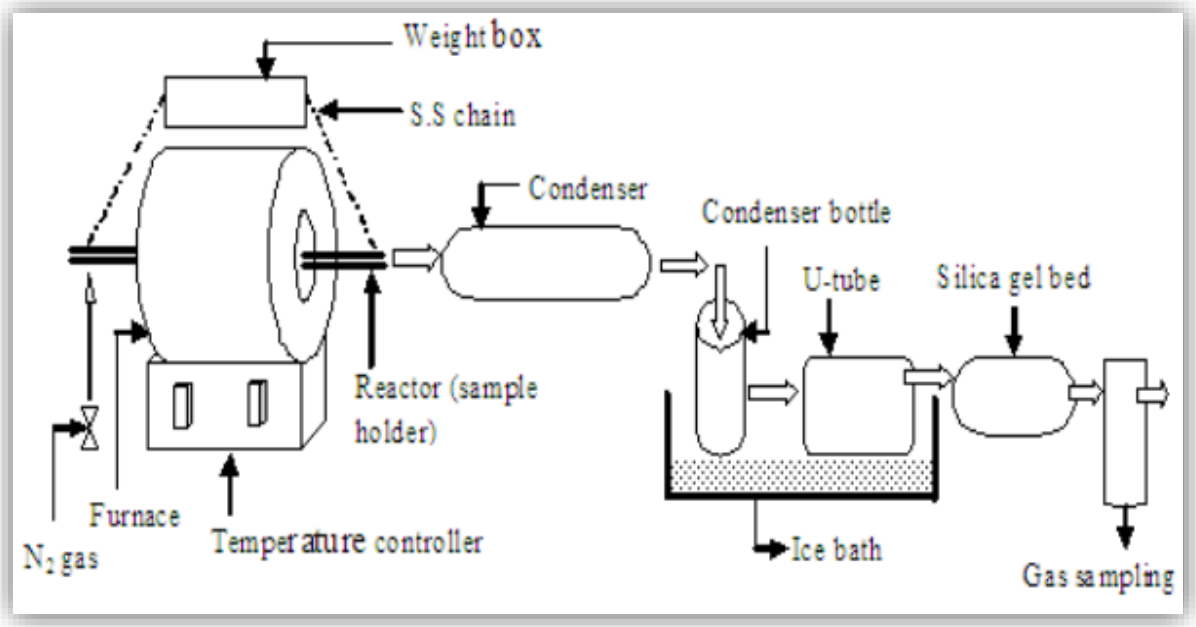

Figure 4.12. The schematic of experimental set-up of horizontal semi-batch reactor.

Figure. 4.13. Photograph of experimental set-up

Each equipment attached with the pyrolyzer have been briefly described in table.4.2.

Table. 4.2. Details of every instrument used to run the experiment

Instruments	Photograph	Specifications
1. PID Controller		Manufactured by Bhattacharya and company, Kolkata, India.

2. N_2 cylinder		Supplied by Prakash Trader India Limited, Kolkata, India. The purity of N_2 gas was 99%.
3. Weighing machine		Manufactured by S.C. Dey company, Kolkata, India

4. Tubular furnace		Manufactured by S.C. Dey company and Bhattacharya and company, Kolkata, India
5. Reactor		Manufactured by S.C. Dey company, Kolkata, India
6. Condenser		Manufactured by Sarada Chemical, Kolkata, India. Thea reactor volume is 1256 m^3.

7. Containers and U-tube	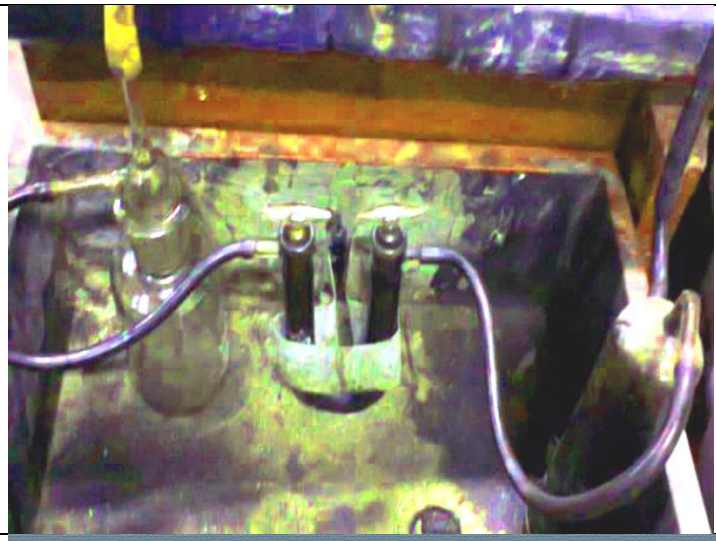	Glass apparatus were manufactured by Sarada Chemical, Kolkata, India. The basin is brought from the local market.
8. Sampling Tube		Manufactured by Sarada Chemical, Kolkata, India.
9. Constant Temperature water bath		Manufactured by S.C. Dey company, Kolkata, India

4.5. Experimental Methods

4.5.1. Pyrolysis under Isothermal condition

The pyrolysis process was carried out in three ways.: a) non-catalytic b) catalytic pyrolysis and c) co-pyrolysis

4.5.1.1. Non-catalytic: The pyrolysis reactor was hung by a S.S chain attached with a weighing machine for continuous monitoring of the residual mass of solid in the reactor. The furnace temperature was varied from 573K to 1173K for all feed stocks. Heating rate was maintained at 10^{o}C/min. Once the furnace temperature was raised to a pre-set value, pyrolyzer/reactor was inserted into the furnace. Isothermal condition was maintained throughout the entire pyrolysis period. Pyrolysis was carried out for one hour at all temperatures. Experiments were designed to investigate the effects of temperature of pyrolysis on yields of pyro – oil and char and their characteristics. Nitrogen was supplied to the pyrolyzer at a rate of 0.833 L/min throughout the experiment to sweep the volatiles produced during pyrolysis and to maintain inert atmosphere in the reactor. The volatile product stream along with nitrogen was directed to a water-cooled condenser and a series of vessels placed in an ice-bath. Finally, the gas stream was passed through a silica gel bed and was collected in a gas sampling bottle. The organic part of condensed volatiles which got dissolved in benzene was extracted in a rotary evaporator and the quantity of pyro-oil was determined.

4.5.1.1.2. Catalytic: The catalysts (Aluminium Oxide [Al_2O_3] [1], zinc oxide [ZnO] [1], sodium chloride [NaCl] [1], potassium chloride [KCl] [1], sodium aluminosilicate [$NaAl(SiO_3)_2$]) [1] were activated for 2 hrs in muffle furnace. Then the catalysts were mixed with feedstocks (jute and lime waste) in the ratio 1:10. The same experimental procedure was followed as in case of non-catalytic pyrolysis.

4.5.1.1.3. Co-pyrolysis:

The Co-pyrolysis process was carried out both in non-catalytic and catalytic routes. For both the processes the feedstocks (jute waste and sesame oil cake) were mixed in the ratio 1:1. For catalytic co-pyrolysis, the feedstocks were mixed with catalysts in the ratio 1:10. For both non-catalytic and catalytic co-pyrolysis, the experimental procedure was same as that described in the section 4.5.1.1.

4.5.2. Pyrolysis under Non-Isothermal Condition

The experiments on Pyrolysis under Non-Isothermal Condition were carried out in the Thermogravimetric analyser (TGA) The thermogravimetric analyses of different feed stocks have been performed with and without catalysts under nonisothermal conditions at specified heating rates (10 K/min, 15 K/min, 20 K/min, 25 K/min, 30 K/min) in the nitrogen atmosphere. Nitrogen atmosphere has been used and alumina has been used as the reference substance.

4.6. Extraction of pyro-oil

The condensed volatiles products (Figure 4.3.a) obtained from pyrolysis of lignocellulosic feed stock were mixed with benzene at 1:10 ratio and placed in a separating funnel (Figure 4.3.b) for 8 to 10 h to separate the aqueous and non-aqueous parts of tar content in benzene. Benzene was subsequently evaporated in a vacuum evaporator (Figure 4.3.c) to extract the pyro-oil.

a. b. c.

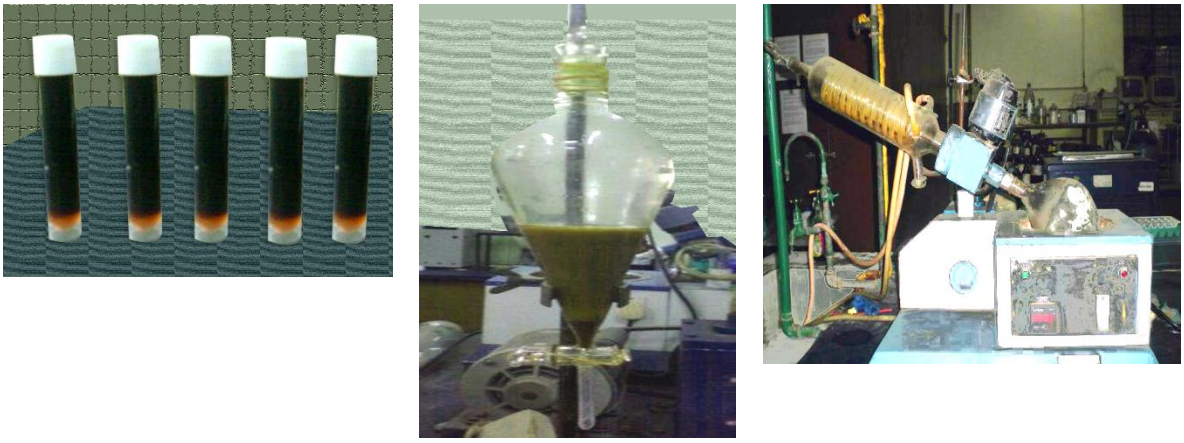

Figure.4.14. Photographs of tar product (a), separating funnel (b) and Vacuum evaporator (c)

4.7. Collection of pyro-gas

The gaseous products obtained after pyrolysis of lignocellulosic wastes were collected in Tedlar bags and were sent for analysis to Mitra SK (P) LTD. The bags were provided by CEL SCIENTIFIC CORP., Delhi, India. The photograph of Tedlar bag is shown in figure. 4.15.

Figure. 4.15. Photograph of Tedlar bag provided by CEL SCIENTIFIC CORP.

4.8. Analytical Methods

4.8.1. Proximate Analysis

ASTM D 3173 – 87[4], ASTM D 3175 – 85[5], ASTM D 3174 – 89 [6] and ASTM D 7582-15 [7] methods were used for the determination of moisture, volatile matter and ashes respectively. The determination of moisture content, volatile matter and ash content of all feed stock WERE done using the muffle furnace.

4.8.2. Ultimate Analysis (ASTM D 5291) [8]

Ultimate analyses of all feed stocks were done using CHNSO analyser to determine the elemental composition with respect to contents of carbon, hydrogen, nitrogen, sulphur and oxygen. The elemental compositions of char and pyro-oil obtained at different pyrolysis temperatures (573 to 1173K) were also done using the same method.

4.8.3. Determination of higher heating value (ASTM D 2013) [9]

The higher heating values of raw samples were determined by using bomb calorimeter (ASTM D 2015 – 85). The higher heating values of char and pyro-oil obtained at different pyrolysis temperatures (573 to 1173K) were also determined using this bomb calorimeter.

4.8.4. SEM Analysis (ASTM E 2809 -13) [10]

The Scanning electron microscope (SEM) (model no. JEOL – JSM 5200) was used to study the morphological characteristics of raw sample and char sample obtained from pyrolysis of lignocellulosic feedstock at different temperature. Micrographs with different magnification of 15KV X 100 and 15KV X 500 of raw and char sample were obtained.

4.8.5. XRD (X-ray Diffraction) (ASTM D 5758) [11]

The XRD analysis of different feedstocks and char samples were performed using the XRD analyzer. The Cu target slit 10 mm should be used for carrying out the analysis.

4.8.6. BET analysis (ASTM D 3663 -03(2015)) [12]

The surface area of the pyro-chars has been identified by BET analyzer.

4.8.7. FT-IR analysis (ASTM D 7371) [13]

Information on chemical bonds present in pyro-oil was obtained using FTIR spectroscopy. The IR spectra were obtained using the FTIR spectrometer with $4cm^{-1}$ resolution and 35 scans between 4000 and 400 cm^{-1}.

4.8.8. GC-MS analysis (ASTM D 4128-06(2012)) [14]

The compounds present in the pyro-oil were identified using Gas Chromatography mass spectroscopy (GC-MS) analyser. The gas chromatograph was fitted with a 25.0 m capillary column coated with a 0.33 μm thick film of 5% phenyl methylpolysiloxane. Helium was employed as a carrier gas at a constant flow of 1.0 mL min^{-1}. The initial oven temperature was 308K for 2.0 min and then programmed from 313 to 598K at $5^{o}Cmin^{-1}$ with an isotherm held for 48.50 min. The split ratio was maintained at 16:1 and the injection was carried out at 523K. The ion source and transfer line temperatures were 503 and 598K, respectively. Data were collected in the full-scan mode and a solvent delay of 2.0 min was used. The chromatographic peaks were identified with the help of the NBS 75 K.N data library. In addition, identification was also carried out on the basis of the fragmentation observed and taking into account the retention times of the peaks using standard compounds, whenever available.

4.8.9. Determination of boiling point of pyro-oil (ASTM D 86) [15]

The boiling points of pyro-oils obtained at different temperatures from pyrolysis of feedstocks were determined using atmospheric distillation unit.

4.8.10. GC analysis (ASTM E 112) [16]

The composition of pyro-gas obtained from pyrolysis of all lignocellulosic feedstock were determined using gas chromatography.

4.9. Computational Methods

Matlab R2014ab [17] was used for the solution of differential equations. Aspen Plus ® [18] was used for process simulation for both lab-scale and large scale pyrolysis processes. Design Expert 7.0.0 ® [19] was used for statistical modelling and optimization using Response surface methodology (RSM).

References

1. < http://www.perkinelmer.com/>
2. A Sarkar, “Studies on Pyrolysis of Spent Engine Oil and Lignocellulosic Part of Municipal Solid Waste (MSW)”, (PhD Thesis in Chemical Engineering, No. 52/10/E), 2015.
3. R. Chowdhury, A. Sarkar, “Reaction Kinetics and Product Distribution of Slow Pyrolysis of Indian Textile Wastes”, International Journal of Chemical Reactor engineering, 10, A67, 2012.
4. < http://archive.org/details/gov.law.astm.d3173.1987>
5. < http://www.astm.org/Standards/D3175>
6. < https://www.astm.org/Standards/D3176.htm>
7. < https://www.astm.org/Standards/D7582.htm>
8. < http://www.astm.org/Standards/D5291.htm>
9. < http://archive.org/details/gov.law.astm.d2013.1986>
10. < https://www.astm.org/Standards/E2809.htm>
11. < https://www.astm.org/Standards/D5758.htm>
12. < https://www.astm.org/Standards/D3663.htm>
13. < https://www.astm.org/Standards/D7371.htm>
14. < https://www.astm.org/Standards/D4128.htm>
15. < http://www.astm.org/Standards/D86>
16. < http://www.astm.org/Standards/E112>
17. <http://in.mathworks.com/products/matlab/whatsnew.html.>
18. <http://www.aspentech.com/products/engineering/aspen-plus/>
19. <https://www.statease.com/software/dx7.0.0.html>

Chapter. 5

THEORETICAL ANALYSIS

5. Theoretical Analysis

5.1. Pyrolysis Kinetics

Pyrolysis of lignocellulosic materials proceeds through complex reactions in series, parallel or combination of both. Hundreds of products and intermediates are formed. For primary pyrolysis of biomass, two types of kinetic models are developed. These are: (i) lumped kinetic model and (ii) distributed activation energy model (DAEM) Under the present study the parameters for lumped and DAE models have been determined for pyrolyzing feed-stocks, namely, waste jute and lime waste using experimental data obtained under isothermal and non-isothermal conditions respectively. Same models have been attempted for both non-catalytic and catalytic pyrolysis of waste jute and lime waste and for co-pyrolysis of waste jute and sesame oil cake. The models have been described as follows:

5.1.1. Lumped Kinetic Model

In simple lumped kinetic model [1-10] the pyrolyzing feedstock is assumed to be converted instantaneously to an active compound, which in turn is assumed to participate in two parallel reactions to generate pyrolysis products. For simplicity, all the condensable and non-condensable volatile products are lumped as volatiles and solid products are lumped as char.

In accordance with the concept of previous researchers [9,10], the reaction scheme considered for the determination of lumped kinetics is as follows:

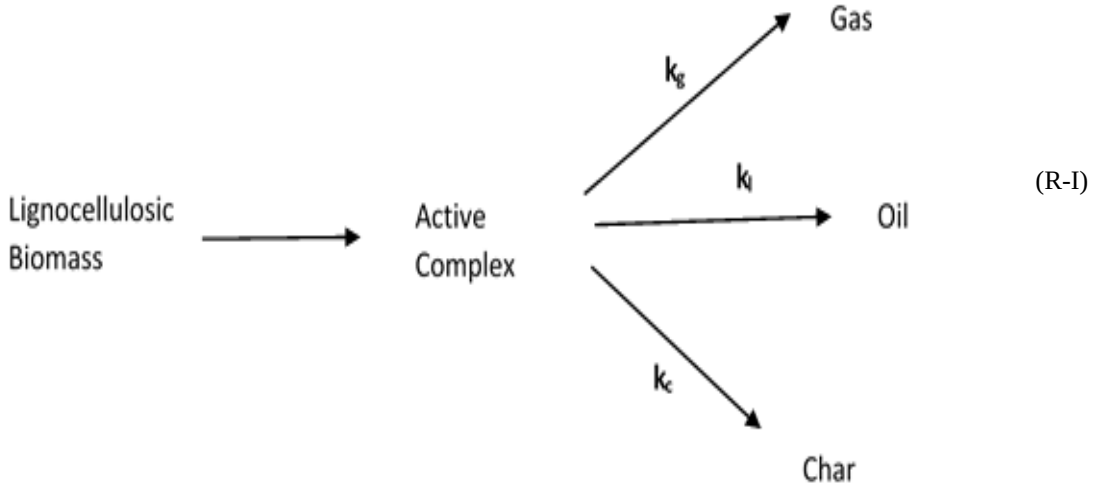

(R-I)

The model is based on the following assumptions [1,2]:

i. The first step of the scheme, i.e. the 'Active complex' formation is instantaneous. Thus, the reaction is considered to be in equilibrium.
ii. All the reactions occurring in the scheme are of first order with respect to the solid reactant.
iii. The solid residual obtained at infinite time, at any temperature in the pyrolysis zone is entirely comprised of char.
iv. Solid residue obtained at any time other than $t = \infty$ is made up of unreacted solid reactant and solid product char.
v. Absolute inert atmosphere prevails during pyrolysis.
vi. Heat and mass transfer resistance in the samples may be negligible. This may be justified by a very high specific surface area of the sample and very small size of the crucibles used.
vii. Any transport limitation within the analytical part of the system may be neglected.

The weight loss profile of the solid reactant W with time may be given by:

$$-\frac{dW}{dt} = kW \quad (1)$$

The profile of increase of weights of volatiles and char against time are given respectively by the following expressions:

$$\frac{dw_v}{dt} = k_v W \quad (2)$$

$$\frac{dw_c}{dt} = k_c W \quad (3)$$

$$\frac{dw_l}{dt} = k_l W \quad (4)$$

$$\frac{dw_g}{dt} = k_g W \quad (5)$$

From equations 1, 2 and 3,

$$k = k_v + k_c \quad (6)$$

From equation 4 and 5

$$k_v = k_l + k_g \quad (7)$$

Equations (1), (2) and (3) have been solved analytically with the following initial conditions:

$$W(t \to 0) = W_o, W_v(t \to 0) = W_{v_0}, W_c(t \to 0) = W_{c_0}, W_l(t \to 0) = W_{l_0}, \quad W_g(t \to 0) = W_{g_0} \quad (8)$$

The solutions under isothermal conditions are as follows:

$$W(t) = W_O \exp(-kt) \quad (9)$$

$$\frac{W(t)}{W_O} = \exp(-kt)$$

$$\ln[\frac{W(t)}{W_O}] = -kt$$

$$\frac{W_v(t) - W_{v_0}}{W_O} = (\frac{k_v}{k})[1 - \exp(-kt)] \quad (10)$$

$$W_c(t) - W_{c_0} = (\frac{k_c}{k}) W_O \exp(-kt) \quad (11)$$

$$\frac{W_l(t) - W_{l_0}}{W_O} = \frac{k_l}{k}[1 - \exp(-kt)] \quad (12)$$

$$\frac{W_g(t) - W_{g_0}}{W_O} = \frac{k_g}{k}[1 - \exp(-kt)] \quad (13)$$

The differentiation of solid reactant from char has been done using assumption (iii). Under isothermal condition:

$$\frac{W_c(t)-W_{c_o}}{W_v(t)-W_{v_0}}=\frac{k_cW}{k_vW}=\frac{k_c}{k_v}=\frac{W_c(t\to\infty)-W_{c_0}}{W_v(t\to\infty)-W_{V_0}} \quad (14)$$

However, according to the assumption (iii):

$$W_c(t\to\infty)=W_R(t\to\infty) \quad (15)$$

and,

$$W_v(t\to\infty)=W_0-W_R(t\to\infty) \quad (16)$$

Therefore:

$$\frac{W_c(t)-W_{c_o}}{W_v(t)-W_{v_0}}=\frac{W_R(t\to\infty)-W_{c_0}}{W_0-W_R(t\to\infty)} \quad (17)$$

Hence,

$$W_c(t)-W_{c_0}=\frac{W_R(t\to\infty)-W_{c_0}}{W_0-W_R(t\to\infty)}*[W_v(t)-W_{v_0}] \quad (18)$$

The weight of the unreacted reactant at any time t is given by:

$$W(t)=W_o-[W_V(t)-W_{v_o}]*[1+\frac{W_R(t\to\infty)-W_{c0}}{W_0-W_R(t\to\infty)}] \quad (19)$$

Determination of k, k_v, k_c, k_l and k_g

The integral method of analysis has been followed to verify the assumed order of the reactions and in turn the rate constants, k, k_v, k_c, k_l and k_g. The linearity of the plot of the logarithms of $\frac{w(t)}{w_o}$ against the pyrolysis time has been verified and the values of k have been determined from the slope at different values of pyrolysis temperature. Similarly, the validity of the 1st order kinetics of formation of volatiles and char have been verified by checking the linearity of the plots of $\frac{w_v-w_{v_o}}{w_o}$ and $\frac{w_c-w_{c_o}}{w_o}$ respectively against $[1-\exp(-kt)]$ and the values of k_v and k_c have been determined from the slopes of the plots. Similarly, the validity of the 1st order kinetics of formation of liquid and gas have been verified by checking the linearity of the plots of $\frac{w_l-w_{l_o}}{w_o}$ and $\frac{w_g-w_{g_o}}{w_o}$ respectively against $[1-\exp(-kt)]$ and the values of k_l and k_g have been determined from the slopes of the plots.

5.1.2. Temperature dependence of Rate constants

The Arrhenius equations have been attempted for the dependence of reaction rate constants on pyrolysis temperature. Therefore,

$$k=k_0\exp(-\frac{E}{RT}) \quad (20)$$

$$k_v=k_{v_o}\exp(-\frac{E}{RT}) \quad (21)$$

$$k_c=k_{c_o}\exp(-\frac{E}{RT}) \quad (22)$$

$$k_l = k_{l_o} \exp\left(-\frac{E}{RT}\right) \quad (23)$$

$$k_g = k_{g_o} \exp\left(-\frac{E}{RT}\right) \quad (24)$$

The validity of the Arrhenius type dependencies has been checked by verifying the linearity of the plots of $\ln k$, $\ln k_v$, $\ln k_c$, $\ln k_l$ and $\ln k_g$ respectively against the inverse of pyrolysis temperature. The values of A, A_v, A_c, A_l, A_g, E, E_v, E_c, E_l and E_g have been determined from the plots and through non-linear regression analysis [60].

5.2. Distributed activation energy model

The distributed activation energy model (DAEM) has been used for pyrolysis of feed-stocks under study to examine the mechanism of reactions occurring under non-isothermal conditions [11, 13-18]. Since biomass is a combination of three chemical compounds, namely cellulose, hemicellulose and lignin. An array of large number of independent parallel and series reactions characterized with different activation energies [11, 13-18] are expected to occur at different rates in the entire range of pyrolysis temperatures. Hence DAE model is particularly important for the analysis of pyrolysis kinetics of biomass under non – isothermal conditions. The main reason behind the distribution of activation energy may be due to the difference in bond strengths of components [11]. The Friedman [11] iso-conversional method has been attempted to analyze the TGA data of pyrolysis of waste jute, lime waste and co-pyrolysis feedstock. All the reactions occurring during the experiments were assumed to be of first order irreversible type with Arrhenius type temperature dependency of the rate constants [11, 12]. The Friedman iso-conversional equation is as follows:

$$\alpha_i \left(\frac{dx}{dt}\right)_{x,i} = k_{o_x} \exp(-E_x/(RT_{x,i}))\, f(x) \quad (25)$$

where,

$T = T_O + \alpha t$; $x = v/v^*$; v = volatile content; and v* = effective volatile content; i = ordinal number of a non-isothermal experiment conducted at heating rate α_i.

Using equation (25),

$$\ln\left(\alpha_i \frac{dx}{dT}\right)_{x,i} = \ln\left(k_{0_x} f(x)\right) - \frac{E_x}{RT_{x,i}} \quad (26)$$

Iso-conversion plots of $\ln\left(\alpha_i \frac{dx}{dT}\right)_{x,i}$ against (-1000/RT) at different extent of conversion have been used to determine the values of activation energies and pre-exponential factors at different conversion.

5.2.1. Distribution of activation energies

The distribution function of activation energies has also been determined by attempting a Gaussian pattern with mean activation energy E_O and standard deviation σ as follows [11]:

$$f(E) = \frac{1}{\sqrt{2\pi\sigma}} \exp\left[-\frac{(E-E_0)^2}{2\sigma}\right] \quad (27)$$

5.3. Mathematical Modelling of Pyrolyzer

The semi-batch pyrolyzer has been represented schematically in figure. 5.1.

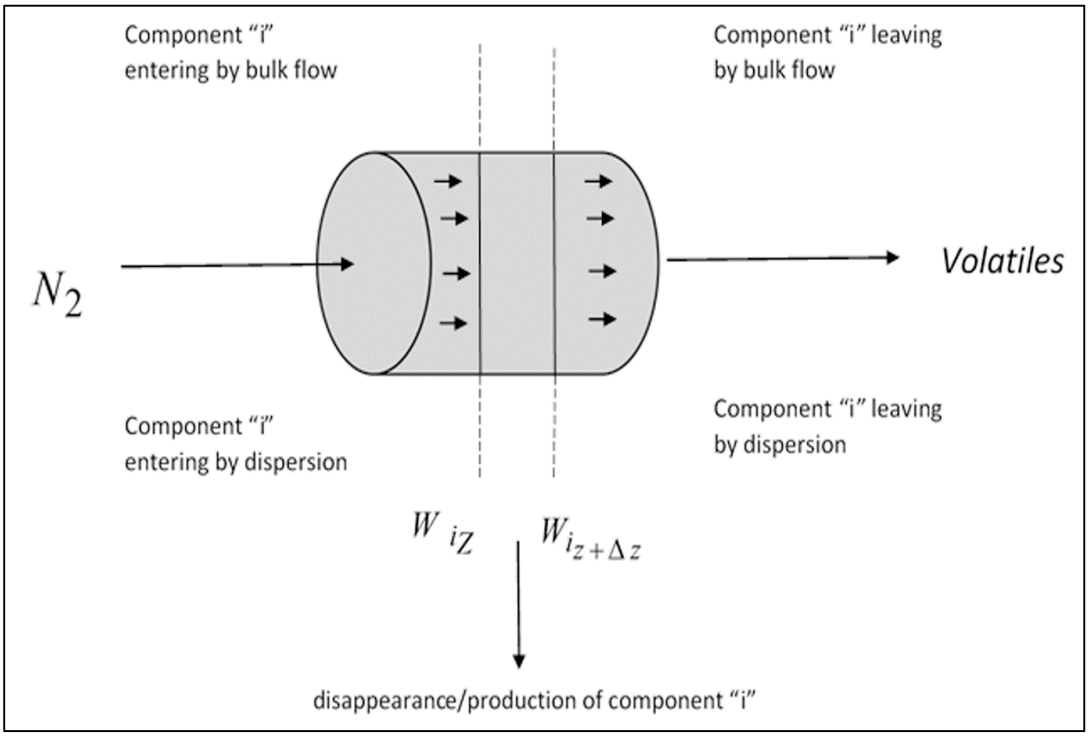

Figure 5.1. Schematic diagram of pyrolyzer

The mathematical model has been developed by taking both primary and secondary pyrolysis into account. While primary pyrolysis is a decomposition of the biomass into the lumped products namely volatiles and chars, the secondary pyrolysis signifies the decomposition of volatiles. During modelling, the decomposition of condensable volatile, namely tar is being considered and the secondary reactions among gaseous products have been neglected. The reactions considered under primary and secondary pyrolysis pathways are as follows [10]:

Primary Pyrolysis Reactions

$$Biomass \rightarrow Active - Complex \begin{matrix} \overset{k_v}{\uparrow} \rightarrow Volatiles \\ \underset{k_c}{\downarrow} \rightarrow \ Char \end{matrix} \qquad \text{(R-I)}$$

Among the condensable (pyro-oil) and non-condensable (CO, CO_2 and CH_4 etc.) volatile components, pyro-oil

generated from pyrolysis of biomass feedstocks is assumed to decompose through a homogeneous tar cracking reaction as follows:

$$Pyro-oil \rightarrow v_{CO}CO + v_{co_2}CO_2 + v_{H_2}H_2 + v_{CH_4}CH_4 + v_i Pyro-oil_{inert} \quad (28)$$

All alkanes and alkenes have been lumped as methane [19]. The secondary reactions among the gaseous components are only involved in the homogeneous tar cracking reaction. The stoichiometric coefficients, v_i, for different components have been taken from literature [20]. The rate of formation of any product, j, through cracking of pyro-oil is given as follows,

$$\dot{r}_{j.crack} = \bar{\upsilon}_j . 10^{4.98} . \exp^{(-93.37/RT_{par})} . (W_{g.tar}\rho_g) \quad (29)$$

where ($W_{g.tar}\rho_g$) is the concentration of pyro-oil in the gas phase.

The mass balance equations for unreacted feed material, char, pyro-oil and different gaseous components in the pyrolyzer have been developed with the following assumptions, [21]

1. Reactor is operated under isothermal condition
2. Cracking reaction of volatiles takes place only in the gas phase.
3. Gaseous molecules formed through cracking of volatiles do not interact among themselves.

Mass balance equations for different components under dynamic condition are as follows,

Solid phase

$$\frac{d}{dt}(1-\varepsilon)\rho_s W = -k(1-\varepsilon)\rho_s W \quad (30)$$

Char

$$\frac{d}{dt}(1-\varepsilon)\rho_s W_c = k_c(1-\varepsilon)\rho_s W \quad (31)$$

Gas phase

Material balance equations for different gaseous components are as follows,

$$\frac{\partial}{\partial t}(\varepsilon\rho W_T) = -\frac{\partial}{\partial z}(v\varepsilon\rho W_T) + \varepsilon D_T \rho \frac{\partial^2 W_T}{\partial z^2} + (k_v \rho_s W - \varepsilon\rho\, r_{crack}) \quad (32)$$

$$\frac{\partial}{\partial t}(\varepsilon\rho W_{CO}) = -\frac{\partial}{\partial z}(v\varepsilon\rho W_{CO}) + \varepsilon D_{CO} \rho \frac{\partial^2 W_{CO}}{\partial z^2} + \varepsilon\rho\, \upsilon_{CO} r_{crack}) \quad (33)$$

$$\frac{\partial}{\partial t}(\varepsilon\rho W_{CO_2}) = -\frac{\partial}{\partial z}(v\varepsilon\rho W_{CO_2}) + \varepsilon D_{CO_2} \rho \frac{\partial^2 W_{CO_2}}{\partial z^2} + \varepsilon\rho\, \upsilon_{CO_2} r_{crack}) \quad (34)$$

$$\frac{\partial}{\partial t}(\varepsilon\rho W_{CH_4}) = -\frac{\partial}{\partial z}(v\varepsilon\rho W_{CH_4}) + \varepsilon D_{CH_4} \rho \frac{\partial^2 W_{CH_4}}{\partial z^2} + \varepsilon\rho\, \upsilon_{CH_4} r_{crack}) \quad (35)$$

$$\frac{\partial}{\partial t}(\varepsilon\rho W_{H_2}) = -\frac{\partial}{\partial z}(v\varepsilon\rho W_{H_2}) + \varepsilon D_{H_2}\rho\frac{\partial^2 W_{H_2}}{\partial z^2} + \varepsilon\rho\,\upsilon_{H_2} r_{crack}) \quad (36)$$

Values of diffusivities, D_T, D_{CO}, D_{CO2}, D_{CH4}, D_{H2} have been provided in Table 2. Equation (33–37) have been solved using the following boundary conditions,

$$\text{At } t = 0 \qquad \begin{bmatrix} W = W_0 \\ W_C = 0 \\ W_V = 0 \\ W_{CO} = 0 \\ W_{CO_2} = 0 \\ W_{CH_4} = 0 \\ W_{H_2} = 0 \end{bmatrix} \qquad \text{For all Z} \quad (37)$$

$$\text{At } Z = L \qquad \begin{bmatrix} \frac{\partial W}{\partial Z} = 0 \\ \frac{\partial W_C}{\partial Z} = 0 \\ \frac{\partial W_V}{\partial Z} = 0 \\ \frac{\partial W_{CO}}{\partial Z} = 0 \\ \frac{\partial W_{CO_2}}{\partial Z} = 0 \\ \frac{\partial W_{CH_4}}{\partial Z} = 0 \\ \frac{\partial W_{H_2}}{\partial Z} = 0 \end{bmatrix} \qquad \text{for all t} \quad (38)$$

5.4. Kinetics of Secondary Cracking of pyro- oil

The reaction scheme for the secondary pyrolysis of pyro-oil may be represented below:

$$\text{Primary} - \text{pyro} - \text{oil} \rightarrow \begin{matrix} k_v \\ \uparrow \rightarrow \text{Volatiles} \\ \downarrow \rightarrow \quad \text{Soot} \\ k_c \end{matrix} \quad \text{(R-I. I)}$$

The values of k , k_v , k_c and the corresponding preexponential factors and activation energies A, A_v , A_c , E, E_v and E_c have been determined following the same procedure as that of pyrolysis of biomass.

5.5.Energy and Environmental Analysis (EEA) for the Pyrolysis of Waste Jute

To establish a new waste to energy technology on commercial scale, its potential for energy generation and its environmental impact should be assessed. Therefore, the energy and environmental analysis of the pyrolysis process of waste jute has been done under the present study on the basis of its predicted performance on large scale. For energy and environmental analysis, the performance of a large (100 tpd) pyrolysis plant of waste jute has been considered. Although the availability of jute waste in a particular locality may not always be sufficient to run a large plant of this capacity, this scale has been chosen based on the availability lignocellulosic waste biomass available in an Indian metro city like Kolkata where the total generated solid waste is 12000tpd and 73% is contributed by lignocellulosics. The standard procedure recommended by ISO 14040 (2006) [22-30] for LCA has been followed with some simplification. The structure is as follows:

1. Definition of Goal and Scope
2. Process description
3. Assessment of Impact
4. Data interpretation and parametric sensitivity

Goal and Scope

The EEA study aims at quantification and comparison of energy output and CO_2 footprints of a 100 tpd pyrolysis plant using pyrolysis temperature and percentage char deposited for soil amendment as parameters. The collected jute wastes are dried and subsequently pyrolyzed in a fixed bed pyrolyzer for the production of pyro-oil, char and gas. The pyro – products are ultimately utilized for generation of energy through different routes.

5.5.1. System Boundaries

In the scheme considered for the Energy and Environment Analysis, the following options of usage of pyro – char, pyro -oil and pyro – gas have been considered. Pyro -oil has been used in power plant located at 20 km distance from the pyrolysis plant. Pyro – gas has been utilized to supply energy of pyrolysis and drying. Pyro – char has been partially used for supplying energy of pyrolysis and drying and rest for soil amendment.

The system boundaries for the scheme are shown in Figure 5.2. The system is divided into several phases:

1. Drying of jute
2. Pyrolysis of pre-dried jute to produce pyro-oil, char and gas.
3. Utilization of a portion of char for soil amendment.
4. Utilization of gas and a portion of char for supply of energy for drying and pyrolysis.
5. Utilization of pyro – oil in a power plant based on CHP principle.

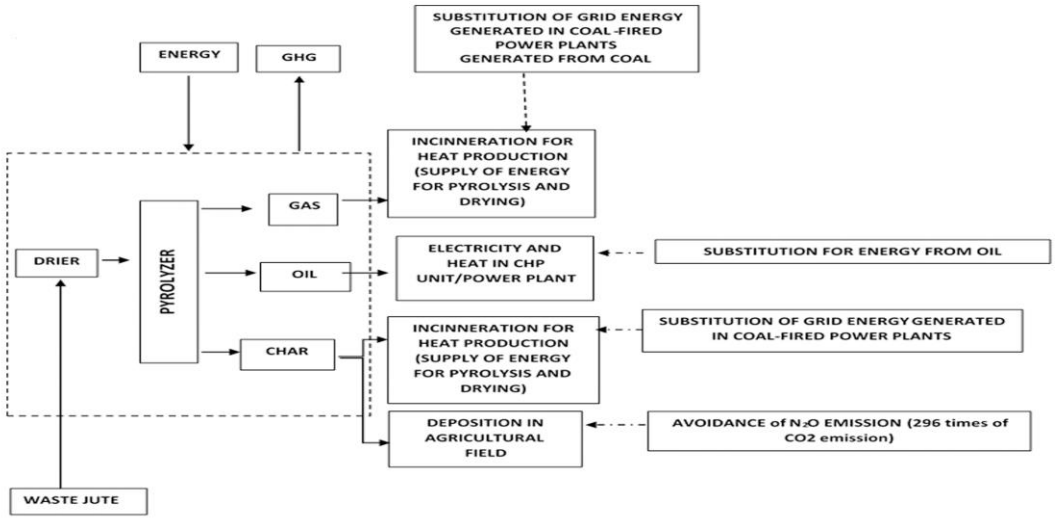

Figure 5.2. LCA system boundaries for the pyrolysis of jute

5.5.2. Process Description

For the simplification of the analysis the materials and energy involved in the installation and dismantling of the plant have not been considered. The amount of jute waste has only been considered as the inventory. The energy required for the transportation of waste from the collection point to the pyrolysis plant has also been neglected. The utilization of different pyro-products is described below:

5.5.3. Pyro – char and gas for energy generation

Energy generated through incineration of pyro-gas and a fraction of pyro-char is used to supply heat energy required for pyrolysis and drying. Since electrical energy, usually generated in coal-fired power plants in India, is to run the dryer and the pyrolyzer, the pyro-char and gas are actually replacing coal which is a potent CO_2 emitter.

5.5.4. Utilization of fraction of char for soil amendment

A portion of pyro-char has been proposed to be transported to an agricultural field situated at a distance of 20 km from the pyrolysis plant. The avoidance of N_2O emission by urea, a N-fertilizer, as a result of char deposition is evaluated using standard procedure [43,44]. The emission of CO_2 caused by transportation of bio-char has also been accounted.

5.5.5. Utilization of Bio –oil for power generation

The bio-oil obtained by the condensation of volatile products of pyrolysis i.e. pyro-oil is used for power generation.

5.5.6. Transportation of Pyro-oil to Power plant

The pyro-oil has been assumed to be utilized by substitution of diesel in a power plant, situated at a distance of 20 km from the pyrolysis unit. Therefore, both energy consumption and CO_2 emission are involved during the transportation. According to the method described by previous researchers [31,35] and following Indian convention, it has been assumed that 25t heavy duty diesel trucks are used for transportation of pyro-oil to power plant and the trucks consume 2.5kg/km and 2kg/km diesel under loaded and unloaded conditions respectively.

5.6. Simulation with *Aspen Plus* ® [55]

In the absence of real data on 100 tpd pyrolysis plant the performance of the large plant has been simulated using Aspen Plus ® [55] Software. It has been used for the calculation of the data on the utilization of different pyro-products for energy generation.

Aspen Plus ® [55] has been used for both modelling the lab-scale plants for the selection of the appropriate model through its validation by comparison with experimental data. The development of a model in *Aspen Plus* ® [55] involves the following steps:

1. Stream class specification
2. Property method selection.
3. System component specification (from databank).
4. Defining the process flowsheet (unit operation blocks and connecting material, energy and work streams)
5. Specifying feed streams (feed rate, composition and thermodynamic conditions)
6. Specifying unit operation blocks (thermodynamic condition, chemical reactions etc.)

Different equipment and their representative *Aspen Plus* ® [55] blocks along with reactions considered for the pyrolysis plant, are shown in Figure 5.3 and are described as follows:

5.6.1. Dryer

Initially the waste jute is dried in the dryer. The dryer is represented by Rstoic and Flash-dry blocks so that the moisture of the biomass can be removed. The drying process may be presented as follows:

$$Jute(wet) \rightarrow Jute(dry) + H_2O(vapour) \qquad \text{(R-II)}$$

5.6.2. Pyrolyzer

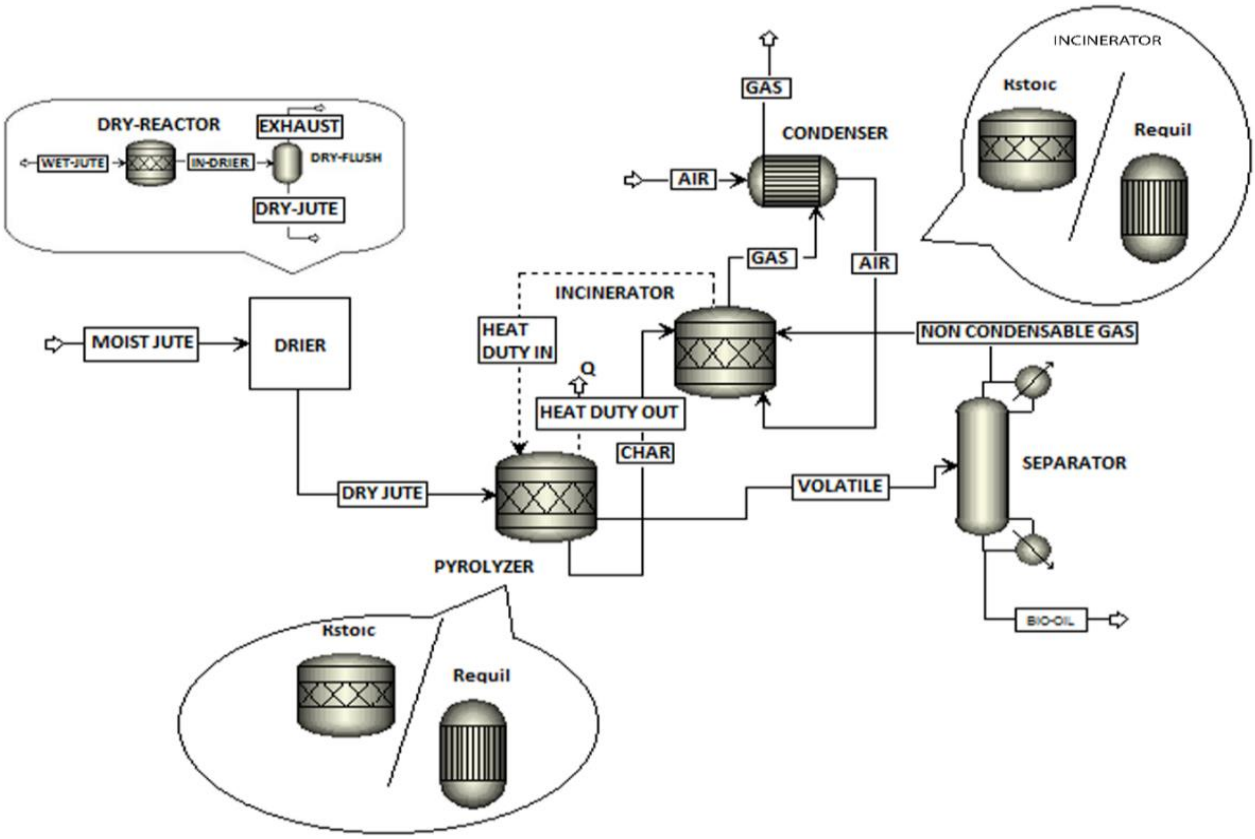

Figure 5.3. Flow sheet for the pyrolysis plant

Pyrolysis Reaction Schemes

Aspen Plus ® [55] has been used for the predication of reactor performance for the lab scale pyrolyzer and 100 tpd waste jute pyrolysis plant. During the reactor modelling, both equilibrium and stoichiometric approaches have been used. Two reaction schemes with and without accounting for secondary gaseous reactions have been used. Based on the experimental data on the yields of char and tar and the analysis of pyrolysis gas (not shown), the following representative stoichiometric equation for the chemical reaction may be written:

$$Jute \xrightarrow{k_{II}} 0.25Char + 0.26Tar + 0.39CH_4 + 0.3CO + 0.34CO_2 + 0.389H_2 \qquad \text{(R-III)}$$

According to this reaction pyrolysis of jute has been considered to be a homogeneous solid phase reaction and the pyrolysis products have been lumped as char – the solid product, and volatiles made up of tar (condensable) and gaseous products. The volatile is further assumed to crack to different gaseous components, namely, CO, CO_2, H_2, CH_4 and inert tar. Comparing the elemental composition of char and tar obtained at different temperatures with different standard compounds, Quinone ($C_6H_4O_2$) and Guaiacol ($C_7H_8O_2$) have been considered to be the closest with the former and latter respectively. In reality, pyro-oil and char are a complex combination of different hydrocarbons. However, for simplification of the model and for the facilitation of using the Aspen Plus ® [55] library, the pyro-oil and pyro-char have also been considered as guaiacol and quinone respectively by [35] during their research studies on pyrolysis of horse dung. Thus, the pyrolysis reaction reduces to

$$Jute \xrightarrow{k_{II}} 0.25\ Quinone + 0.26\ Guaiacol + 0.39\ CH_4 + 0.3\ CO + 0.34\ CO_2 + 0.389\ H_2 \qquad \text{(R-IV)}$$

Secondary reactions include the thermal cracking of guaiacol to catechol (C_6H_6O) and other secondary gaseous reactions as follows:

$$2Guaiacol \leftrightarrow 2Catechol + C_2H_4 \quad \text{(R-V)}$$
$$CO + 3H_2 \leftrightarrow CH_4 + H_2O \quad \text{(R-VI)}$$
$$CO_2 + 4H_2 \leftrightarrow CH_4 + 2H_2O \quad \text{(R-VII)}$$
$$CO + H_2O \leftrightarrow CO_2 + H_2 \quad \text{(R-VIII)}$$

Reaction Scheme-I considers only reaction R-IV and the Reaction scheme-II considers reactions R-IV to R—VIII. The pyrolyzer is represented by either Rstoic or a combination of Rstoic and Requil reactor blocks in reaction schemes I and II respectively.For lab-scale pyrolyzer model predictions have been compared with experimental data. The model giving the closest prediction for small scale reactor will be subsequently followed for 100 tpd plant.

5.6.3. Condenser

The volatile products obtained from pyrolysis are condensed by using condensing separator block in order to obtain the char (quinone) and tar (guaiacol) at 115^0C and 204^0C respectively.

Utilization of pyro-products

5.6.4. Incinerator for pyro-gas and fraction of char

The incinerator is represented by a Requil block. In the incinerator, a portion of pyro-char and the non-condensable pyro-gas generated in the pyrolyzer are combusted with 20% excess air. The main reactions are as follows:

$$CO + 0.5O_2 \leftrightarrow CO_2 \quad \text{(R-IX)}$$
$$CH_4 + 2O_2 \leftrightarrow CO_2 + 2H_2O \quad \text{(R-X)}$$
$$H_2 + 0.5O_2 \leftrightarrow H_2O \quad \text{(R-XI)}$$
$$QUINONE + 6\,O_2 \leftrightarrow 6\,CO_2 + 2\,H_2O \quad \text{(R-XII)}$$
$$C_2H_4 + 3O_2 \leftrightarrow 2CO_2 + 2H_2O \quad \text{(R-XIII)}$$

5.6.5. Utilization of Bio –oil for power generation

The bio-oil obtained by the condensation of volatile products of pyrolysis i.e. pyro-oil is used for power generation. Figures. 5.4 shows the flow sheets for CHP based power plant using *Aspen Plus* ® [55] software.

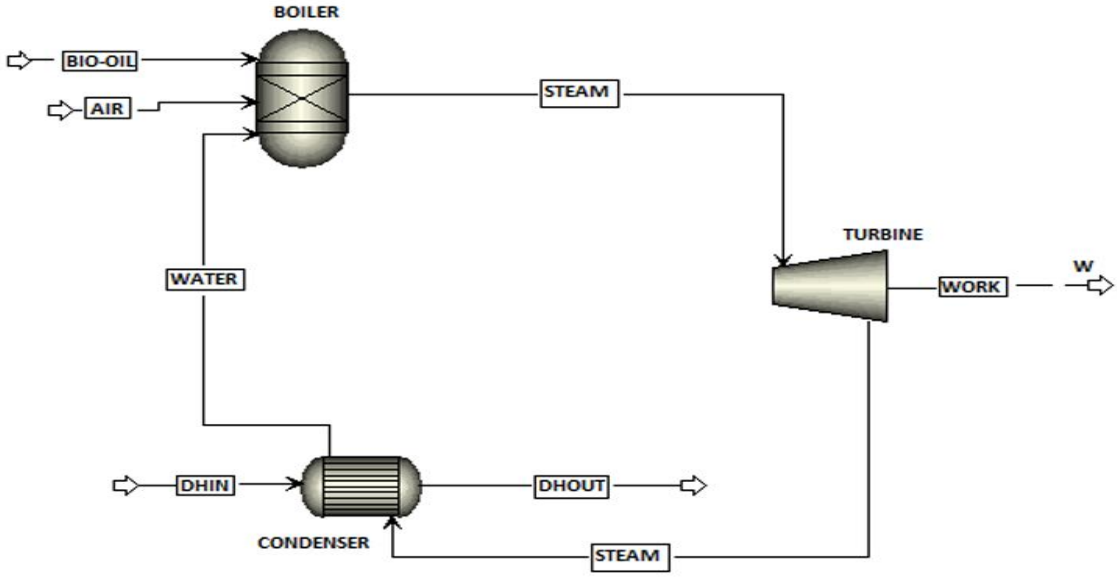

Figure 5.4. Flow sheet for CHP based power plant

The main reaction for the combustion of the bio-oil in the thermal power plant [32] is as follows:

$$Guaiacol + 8O_2 \rightarrow 7CO_2 + 4H_2O \quad \textbf{(R-XIV)}$$

$$Catechol + 7\,O_2 \rightarrow 6\,CO_2 + 3\,H_2O \quad \textbf{(R-XV)}$$

The amount of guaiacol and catechol will be determined using equations R-III and IV. The thermal power plant is assumed to run at 30% [31] efficiency for fuel to electrical energy conversion. Waste heat recovery from exhaust flue gas is assumed to be at an efficiency of 70% [34].

Aspen Plus® blocks that have been used in order to simulate the pyrolysis process are also described in Table.5.1.

Table. 5.1. Unit wise specification of process parameters and reactions of pyrolysis plant and CHP based power plant.

Unit	Aspen Process Code	Parameters	Value
Dryer		Feed Stream inlet pressure	1 bar
		Feed Stream inlet flow rate	6 tons/day, 10 tons/day, 15 tons/day
		Moisture	10% of the total flow
		Nitrogen inlet stream	50 kg/hr.
	Rstoic	Drier Temperature	100^{o}C
		Drier pressure	1 bar
		Drier reaction	Equation. R-I
	Flash2	Flash drying temp	30^{O}C

		Flash drying pressure	1 bar
Pyrolyzer	Rstoic/Requil	Pyrolyzer temperature	400^0C – 900^0C
		Pyrolyzer pressure	1 bar
		Pyrolyzer reaction (Rstoic)	Equation. R-II – R-III
		Pyrolyzer reaction (Rstoic +Requil)	Equation. R-VIII and R-III – R-VII
Heat Exchanger	HeatX	HeatX	Hot/Cold outlet temperature approaches to 180^0C
Separator	Flash2	Separator (Char Separator)	Outlet Flash Temperature: 115^0C Outlet Flash Pressure: 1 bar
	Flash2	Separator (Bio-oil Separator)	Outlet Flash Temperature: 204^0C Outlet Flash Pressure: 1 bar
Splitter	FSplit	Splitter (Char Separator)	Fraction of Char used: 2.0, 0.3, 0.4, 0.5, 0.6, 0.7
Incinerator	Rstoic/Requil	Incinerator Temperature	400^0C
		Incinerator pressure	1 bar
		Incinerator Reaction	Equation. R-IV Equation. R-V Equation. R-VI Equation. R-VII
Heat Exchanger		Feed Stream inlet pressure	1 bar
		Feed Stream inlet temperature	30^oC
		Feed Stream inlet flow rate	700 kg/hr.
		Mole frac	N_2: 0.79 O_2:0.21
	HeatX	Heat X	Hot Stream Outlet Temperature: 200^oC
Diesel Set Engine	Rstoic	Combustor	Temperature: 800^0C Pressure: 1Bar Equation. R-VIII
Thermal Power Plant Coupled with CHP			
	RGibbs	Burner (Boiler)	Temperature: 1200^oC Pressure: 1 Bar

			Calculation option: Phase equilibrium and chemical equilibrium
	HeatX	Superheated evaporator (Boiler)	Flow direction: Counter current Specification: Cold stream outlet temperature: 504 ^{0}C
	HeatX	Evaporator (Boiler)	Flow direction: Counter current Specification: Cold stream outlet vapour fraction: 1
	HeatX	Economic Evaporator (Boiler)	Flow direction: Counter current Specification: Cold stream outlet temperature: 300^{0}C
	HeatX	Air Flow rate (Boiler) In Evaporator	Temperature: 30^{0}C Pressure: 1 Bar Mass Flow rate: 100, 150, 200, 250, 300, 350 kg/hr. as the temperature of the pyrolysis changes from 400^{0}C to 900^{0}C.
	HeatX	In PHAIR (Boiler)	Temperature: 30^{0}C Pressure: 1 Bar Mass Flow rate: 100 kg/hr. Flow direction: Counter current Specification: Cold stream outlet temperature: 150^{0}C
	Compr	TURBINE	Type: Isentropic Discharge Pressure: 30 Bar
	HeatX	CONDENSER	Flow direction: Counter current Specification: Hot stream outlet temperature: 120^{0}C

5.7. Impact assessment

During the energy and environmental analysis focus has been given on the return on investment of energy, namely, energy return on energy investment (EROEI) of the 100 tpd pyrolysis plant and the consequent CO_2 avoidance (A_{CO_2}) due to utilization of pyro-products in different ways. The pyrolysis temperature (T) and % char deposited (f) in agro – field have been considered as the main independent parameters. Using the response surface methodology, EROEI and A_{CO_2} have respectively been maximized and minimized with respect to the factors T and f.

Definitions of Energy return on energy investment (EROEI) and avoidance of CO_2 (A_{CO_2}) calculated on per day basis are as follows:

$$EROEI = \frac{Energy\ delivered\ (E_D)}{Energy\ required\ to\ deliver\ that\ energy\ (E_R)} \times 100 \quad (39)$$

where,

$$E_D = Energy\ generated\ through\ utilizatio\ n\ of\ \ pyrolysis\ \ products\ (E_G) - Energy\ \ spent\ in\ the\ \ transportation\ (E_S)$$

$$E_R = Energy\ \ \sup plied\ \ by\ \ biomass\ \ (jute waste\ ) = (\ Mass\ \ of\ \ jute\ \ ) \times HHV_{\ Jute}$$

Where, $HHV = Higher\ \ Heating\ value$

$$E_G = E_{Pyrolysis + drying} + E_{Power\ Plant}$$

$$E_S = E_{Transporta\ tion\ \ of\ \ pyro-oil\ and\ \ pyro-char}$$

Total avoidance of CO_2 is possible due to (1) utilization of char and gas for the supply of energy for pyrolysis and drying and thereby replacing grid electricity which is generated in coal based power plants in India, (2) replacement of diesel oil in the power plant by pyro-oil and (3) reduction of N_2O (Equivalent CO_2) emission by the replacement of nitrogen based fertilizer by pyro-char. Conversely, the emission of CO_2 caused by transportation of pyro-oil and pyro-char from the pyrolysis plant to the power plant and agricultural field respectively has been debited. Therefore,

$$A_{CO_2} = A_{CO_2}\ (coal\ \ replacemen\ t\ by\ \ pyro - gas\ and\ \ char) + A_{CO_2}\ (diesel\ \ replacemen\ t\ by\ \ pyro - oil) + A_{CO_2}\ (Soil\ Amendment\ by\ pyro - char) - CO_2\ Emission\ \ due\ to\ transporta\ tion\ of\ \ pyro - oil\ and\ \ char \quad (40)$$

5.7.1. Calculation of Energy supplied and CO_2 emission avoided

5.7.1.1. Utilization of pyro-gas and pyro-char for the supply of energy for Pyrolysis and Drying

Data:

Coal used in power plant for grid electricity supply: Lignite:
Carbon percentage (p_1) in lignite = 71% [36]
Calorific value of lignite sub-B, = 10500 – 21000 kJ/kg [37]
Average calorific value (c1) = 15750 kJ/kg
Electrical Grid Distribution efficiency = 91% [54]

Coal-fired Power Plant efficiency = 30%

Assumption: thermal energy conversion efficiency due to incineration of gas and char is 100%

Basis 1day
Mass flow rate of CO_2 due to incineration of char and gas = m_1 kg (Aspen Plus ® [55] calculation)
Energy supplied due to incineration of char and gas = e_1 kJ (Aspen Plus ® [55] calculation)
Energy required for pyrolysis and drying = e_2 kJ (Aspen Plus ® [55] calculation)
Excess Energy left for other uses = e_1-e_2 =e_3 kJ (41)

Grid energy, supplied from power plant, replaced=e_1 KJ

Coal energy avoided (kJ) $= \frac{e_1}{0.91 \times 0.3} = H_1(say)$

Coal burning avoided (kg) $= \frac{H_1}{c_1} = H_2(say)$

Corresponding CO_2 emission avoided (kg) $= \frac{H_2 \times p_1}{12} \times 44 = H_3(say)$

Actual CO_2 emission avoided due to utilization of pyro-char and pyro-gas (kg) $= H_3 - m_1 = H_4(say)$ (35)

5.7.1.2. Utilization of pyro-oil

Data:
Molecular formula for diesel: $C_{12}H_{23}$ [38]
Molecular weight of diesel= 167
Gross calorific value of diesel: 44800 kJ/kg [38, 39]
Oil-fired Power plant efficiency: 35%
Thermal energy recovery efficiency in the CHP = 70%
CV of pyro-oil: C_2 (Experimental)
Percentage of carbon in pyro-oil=p_2 (Experimental)

5.7.1.3. Pyro-oil used in CHP Plant

Basis: 1day
Pyro-oil produced = m_2 (ASPEN calculation)
Electrical energy generated in the CHP = e_4 (Aspen Plus ® [55] calculation)
Thermal energy generated in the CHP = e_5 (Aspen Plus ® [55] calculation)

CO_2 emission due to combustion of pyro-oil in the CHP unit (kg) $= \frac{m_2 \times p_2}{12} \times 44 = H_5(say)$

Diesel burning avoided (kg) $= \frac{m_2 \times C_2}{44800} = H_6(say)$

Corresponding CO_2 emission avoided (kg) $= \frac{H_6}{167} \times 12 \times 44 = H_7(say)$

Actual CO_2 emission avoided $= H_7 - H_5 = H_8(say)$ (42)

5.7.1.4. Transportation of Pyro-oil to Power plant

Data:
Formula for diesel: $C_{12}H_{23}$ [38]
Molecular weight of diesel= 167
Gross calorific value of diesel: 44800 kJ/kg [38, 39]
Fuel consumption for transportation:

2.5 kg /km diesel for loaded truck [40,41]
2 kg /km diesel for unloaded trucks [40,41]
Number of 25t capacity trucks used for transportation of pyro-oil per day=1
Pyro-oil produced = m_2 (tonnes) (Aspen Plus ® [55] calculation)
The distance between pyrolysis unit and power plant= d (say)

Energy consumption for the forward journey (Pyro-unit to power plant) (43)
$= 2.5 \times d \times 44800 = e_6$ kJ (say)

Energy consumption for the return journey $= 2 \times d \times 44800 = e_7$ kJ (say) (44)

Total CO_2 emission that could be avoided, $= H8 - \frac{(2+2.5)\times 12\times 44}{167} \times d = H9$ Kg (say) (45)

5.7.1.5. Transportation of pyro-char to agricultural field

Similar to pyro-oil 1 truck of 25 t capacity will be sufficient for transportation of pyro char to the agricultural field, irrespective of the fraction of char being deposited and amount of char being produced in the present range of pyrolysis temperature. Since the distance between agricultural field and pyro plant is same (20 km) as that between pyro-oil power plant and the latter, therefore

Total energy consumption = $e_6 + e_7$ kJ (46)

Total CO_2 emission $= H_{10} = \frac{(2+2.5)\times 12\times 44}{167} \times d$ (47)

5.7.1.6. Avoidance of N – emission due to char deposition

Data:
Biochar deposited: 20 g biochar per kg soil [49]
Application rate of urea = 10% of soil [49]
Depth up to which urea is applied = 0.00635 m [42,44-46]
Density of soil = 1250 kg/m^3 [45,46]
N_2O emission by N-fertilizer: 1.25% of N – applied (kg N/hectare) [48]
N_2O emission avoided by biochar application: 50% [43,44]
Molecular formula of urea = CH_4N_2O
Molecular weight of urea = 60

$$\log N_{emission} = \sum_{i=1}^{n} E_i + N \times 0.0038 - 1.5160$$ [47]

where E_i = 0.15 for agricultural field [43]
N = Emission of N_2O
No of working days of pyrolysis plant per year = 300
Basis: 1 Year
Fraction of char deposited in the field = "f"
Mass of char produced per hour = m_3 kg/h (Aspen Plus®)
Annual production rate of char $= m_3 \times f \times 300 \times 24$ kg/y

Mass of soil in which biochar is deposited $= \frac{m_3 \times f \times 300 \times 24}{0.02} kg/y = m_4$ (say)

Amount of urea applied $= m_4 \times 0.1 = m_5\ kg/y$ say)

Since urea may be applied up to the depth of 0.00635m [43]

Area of soil $= \frac{m_4}{1250 \times 0.00635} m^2 = A m^2 = A \times 10^{-4} = A_1 hectare$

Since one molecule of urea contains 2 nitrogen atoms therefore,

Amount of N applied $= \frac{m_5}{60} \times 28 kg/y = m_6$ (say)

N_2O emission due fertilizer $= m_6 \times 0.0125 kg/y = m_7$ (say)

Annual N_2O emission per hectare $= \frac{m_7}{A_1} = N\, kg/y/ha$ (say)

Therefore,

$$\log N_{emission} = \sum_{i=1}^{n} E_i + N \times 0.0038 - 1.5160 \quad [47]$$

Where, $E_i = 0.15$

$$\therefore \log N_{emission} = \sum_{i=1}^{n} 0.15 + N \times 0.0038 - 1.5160 = p$$

$$\therefore N_{emission} = 10^p$$

$N_{emission}$ avoided due to biochar application $= 0.5 \times 10^p$

Equivalent CO_2 emission avoided $= \frac{0.5 \times 10^p \times 296}{300} kg/dy$ [48] (48)

5.7.1.7. Overall E_D and A_{CO_2}

Basis: 1 day;

Energy delivered (E_D) by pyro-products:

$$E_D = e_1 + e_4 + e_5 - 2(e_6 + e_7) \text{ kJ} \quad (49)$$

Total avoidance of CO_2 emission:

$$A_{CO_2} = H_4 + H_9 - H_{10} + \frac{0.5 \times 10^p \times 296}{300} \text{ kg} \quad (50)$$

5.8. Parametric Sensitivity and Optimization

The effects of parameters namely, pyrolysis temperature (T) and fraction (f) of pyro-char utilized for soil amendment on the major response variables namely, EROEI and A_{CO_2} have been correlated mathematically. The model equations have been developed with the aid of response surface methodology [57] simultaneously varying the values of f and T. The values of (T) and (f) were fixed using Box Behnken method [58,59].

The mathematical relationships between the responses (Yi) and factors, char deposition (X_1) and pyrolysis temperature (X_2) are given by,

$$Y_i = f_i(X_1, X_2) \text{ where } i = 1, 2 \quad (51)$$

$$Y_1 = EROEI$$

$$Y_1 = A_{CO_2}$$

It is assumed that the independent factors A and B are continuous and controllable by experiments with negligible errors. The generalized second order polynomial, correlating the responses with the independent factors, is of the following form:

$$y_i = \alpha_i + \sum_{j=1}^{2} \beta_{ij} X_j + \sum_{j=1}^{2} \sum_{\substack{u=1 \\ u \neq j}}^{2} \beta_{iuj} X_u X_j + \sum_{j=1}^{2} \beta_{ijj} X_j^2 \quad (52)$$

The significance of the coefficients and the adequacy of the fit are determined using Student-*t* test and Fischer F-test respectively. The values of EROEI and A_{CO_2} respectively have been maximized and minimized. The development of model equation and optimization have been done using Design -Expert Software 7.0 ® [56].

5.9. Conversion of Pyro-gas to Liquid and Gaseous Fuels through Fischer-Tropsch Process:

The conversion of pyro-gas to liquid has been studied for the 100 tpd plant using Aspen Plus ® [55]. The pyro-gas obtained from the pyrolyzer is fed to the reformer followed by shift reactor in order to obtain CO and H_2. The product of the shift reactor is fed into the FT reactor in order to obtain gasoline, bio – diesel, waxes, CO_2 and unconverted CO and H_2 and C_1 – C_4 compounds. The unconverted CO and H_2 and C_1 – C_4 compounds is fed to the power plant in order to obtain energy. The CO_2 obtained is then recycled back to the reformer and mixed with the pyro-gas to reduce its emission. The detailed flowsheet of the process is shown in figure 5.5.

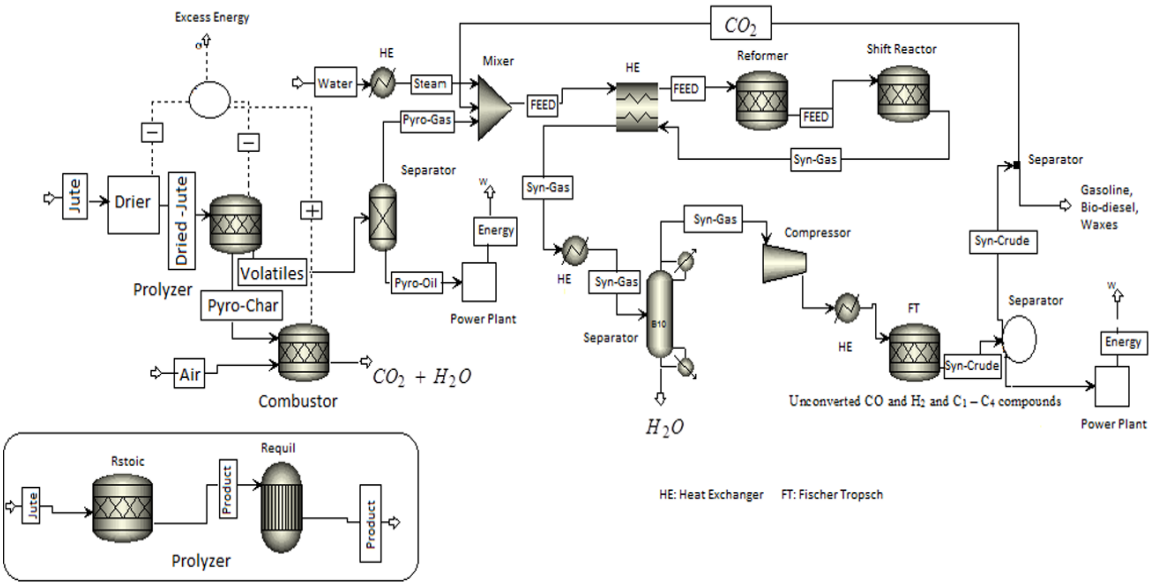

Figure 5.5. Flow sheet of pyrolysis plant integrated with FT Reactor

5.10. Syn Gas Production Unit

The syngas production unit consists of a reformer and a shift reactor. The mixture of pyro – gas and steam is fed to the reformer. The temperature of the reformer is kept 1000^0C and pressure 2 bar so that the methane, which is present in the pyro-gas will react with steam to get converted in CO and H_2 [52]. The detailed reaction is as follows:

$$Methane + H_2O \rightarrow CO + 3H_2 \quad \text{(R-XVI)}$$

The converted gas (CO and H_2) and unconverted gas which comprises of CO_2, H_2, CO and part of CH_4 is then fed to the shift rector for further conversion to CO and H_2. The reactions occurring in the reactor are as follows [52]:

$$Methane + CO_2 \rightarrow 2CO + 2H_2 \quad \text{(R-XVII)}$$

$$CO_2 + H_2 \Leftrightarrow CO + H_2O \quad \text{(R-XVIII)}$$

The final product contains CO, H_2, water vapour, CO_2, unreacted ethylene and methane, originally present in the pyro-gas. The residual CO_2 is separated and recycled to the reactor.

5.11. The Fischer Tropsch Unit

The syngas is cooled and water is removed from the gas in a flash column. The moisture-free gas is fed into the FT reactor. The catalyst that have been considered is Cobalt [53] and the ratio between the H_2 and CO_2 is considered almost 1:1. The temperature and pressure of the FT reactor are considered 240ºC and 20 bar respectively. Similar to the results obtained by previous researchers [52], the conversion of the synthetic gas is considered to be as 87% [53]. The detailed FT reactions are as follows:

$$2H_2 + C0 \rightarrow CH_4O \quad \text{(R-XIX)}$$

$$CO + 2H_2O \rightarrow CO_2 + H_2 \quad \text{(R-XX)}$$

$$4H_2 + 2CO \rightarrow C_2H_6O + H_2O \quad \text{(R-XXI)}$$

$$6H_2 + 3CO \rightarrow C_3H_8O + 2H_2O \quad \text{(R-XXII)}$$

$$8H_2 + 4CO \rightarrow C_4H_{10}O + 3H_2O \quad \text{(R-XXIII)}$$

$$10H_2 + 5CO \rightarrow C_5H_{12}O + 4H_2O \quad \text{(R-XXIV)}$$

$$12H_2 + 6CO \rightarrow C_6H_{14}O + 5H_2O \quad \text{(R-XXV)}$$

$$14H_2 + 7CO \rightarrow C_7H_{16}O + 6H_2O \quad \text{(R-XXVI)}$$

$$17H_2 + 8CO \rightarrow C_8H_{18} + 8H_2O \quad \text{(R-XXVII)}$$

$$16H_2 + 8CO \rightarrow C_8H_{18}O + 7H_2O \quad \text{(R-XXVIII)}$$

$$19H_2 + 9CO \rightarrow C_9H_{20} + 9H_2O \quad \text{(R-XXIX)}$$

$$18H_2 + 9CO \rightarrow C_9H_{20}O + 8H_2O \quad \text{(R-XXX)}$$

$$21H_2 + 10\,CO \rightarrow C_{10}H_{22} + 10H_2O \quad \text{(R-XXXI)}$$

$$20H_2 + 10CO \rightarrow C_{10}H_{22}O + 9H_2O \quad \text{(R-XXXII)}$$

$$\mathbf{23H_2 + 11\,CO \rightarrow C_{11}H_{24} + 11H_2O} \quad \text{(R-XXXIII)}$$

$$\mathbf{22H_2 + 11CO \rightarrow C_{11}H_{24}O + 10H_2O} \quad \text{(R-XXXIV)}$$

$$25H_2 + 12\,CO \rightarrow C_{12}H_{26} + 12H_2O \quad \text{(R-XXXV)}$$

$$27H_2 + 13CO \rightarrow C_{13}H_{28} + 13H_2O \quad \text{(R-XXXVI)}$$

$$29H_2 + 14CO \rightarrow C_{14}H_{30} + 14H_2O \quad \text{(R-XXXVII)}$$

$$31H_2 + 15CO \rightarrow C_{15}H_{32} + 15H_2O \quad \text{(R-XXXVIII)}$$

$$11H_2 + 5CO \rightarrow C_5H_{12} + 5H_2O \quad \text{(R-XXXIX)}$$

$$13H_2 + 6CO \rightarrow C_6H_{14} + 6H_2O \quad \text{(R-XL)}$$

$$15H_2 + 7CO \rightarrow C_7H_{16} + 7H_2O \quad \text{(R-XLI)}$$

$$33H_2 + 16CO \rightarrow C_{16}H_{34} + 16H_2O \quad \text{(R-XLII)}$$

$$35H_2 + 17CO \rightarrow C_{17}H_{36} + 17H_2O \quad \text{(R-XLIII)}$$

$$39H_2 + 19CO \rightarrow C_{19}H_{40} + 19H_2O \quad \text{(R-XLIV)}$$

$$41H_2 + 20CO \rightarrow C_{20}H_{42} + 20H_2O \quad \text{(R-XLV)}$$

$$43H_2 + 21CO \rightarrow C_{21}H_{44} + 21H_2O \quad \text{(R-XLVI)}$$

$$45H_2 + 22CO \rightarrow C_{22}H_{46} + 22H_2O \quad \text{(R-XLVII)}$$

$$47H_2 + 23CO \rightarrow C_{23}H_{48} + 23H_2O \quad \text{(R-XLVIII)}$$

$$51H_2 + 25CO \rightarrow C_{25}H_{52} + 25H_2O \quad \text{(R-XLIX)}$$

$$53H_2 + 26CO \rightarrow C_{26}H_{54} + 26H_2O \quad \text{(R-L)}$$

$$55H_2 + 27CO \rightarrow C_{27}H_{56} + 27H_2O \quad \text{(R-LI)}$$

$$57H_2 + 28CO \rightarrow C_{28}H_{58} + 28H_2O \quad \text{(R-LII)}$$

$$59H_2 + 29CO \rightarrow C_{29}H_{60} + 29H_2O \quad \text{(R-LIII)}$$

$$61H_2 + 30CO \rightarrow C_{30}H_{62} + 30H_2O \quad \text{(R-LIV)}$$

$$65H_2 + 32CO \rightarrow C_{32}H_{66} + 32H_2O \quad \text{(R-LV)}$$

$$73H_2 + 36CO \rightarrow C_{36}H_{74} + 36H_2O \quad \text{(R-LVI)}$$

$$7H_2 + 3CO \rightarrow C_3H_8 + 3H_2O \quad \text{(R-LVII)}$$

$$9H_2 + 4CO \rightarrow C_4H_{10} + 4H_2O \quad \text{(R-LVIII)}$$

The final products are gasoline (C_5- C_{11}), bio-diesel (C_{12}- C_{18}) and waxes (C_{20}-C_{60}), CO_2 and unconverted CO and H_2 and C_1 and C_4 compounds. The unconverted CO and H_2 and C_1 -C_4 compounds are sent to the power plant for energy generation. The CO_2 obtained is fed back to reformer to make the process emission free. The detailed process conditions are provided in Table- 5.2.

Table 5.2: Unit wise specification of process parameters and reactions of pyrolysis plant and gas to liquid conversion plant

Unit	Aspen Process Code	Parameters	Value
Syn-Gas Production Unit			
		Water Temperature	30^0C
		Water Flow rate	14.833/15.38/18.41/21.45/22.5/22.73 kmol/h
Heater	Heater	Heater Pressure	2 Bar
		Vap Frac	1

Mixer	Mixer	Mixer Pressure	2 Bar
Heat Exchanger	MHeatX	Hot stream Feed inlet	Gas
		Hot stream Feed Temperature	700^0C
		Cold stream feed inlet	Syn-Gas1
Reformer	Requil	Reformer Pressure	2 Bar
		Reformer Temperature	1000^0C
		Reformer Reaction	R- XVII
Heater	Heater	Pressure	5 Bar
		Temperature	927^0C
Shift Reactor	Requil	Shift Reactor Pressure	2 Bar
		Shift Reactor Temperature	650^0C
		Shift Reactor Reaction	R- XVII -R- XVIII
		The mole ratio of CO and H_2	23.23: 36.14
FT Reactor Unit			
Heater	Heater	Temperature	500^0C
		Pressure	1 Bar
Separator	Sep	Mixed	
		Split Fraction of H_2O	1
Compressor	Compr	Type	Isentropic
		Outlet Discharge Pressure	20 Bar
FT Reactor	Rstoic	FT Reactor Pressure	20 Bar
		FT Reactor Temperature	240^0C
		FT Reactor Reactions	R- XIX - R- LV
		The ratio of H_2 and CO_2	1:1
Separator	Sep	Mixed	
		Split Fraction of H_2O	1
		Split Fraction of Methane	1
		Split Fraction of CO	1

		Split Fraction of C_2H_4	1
		Split Fraction of CH_4O	1
Separator	Sep	Mixed	
		Split Fraction of CO_2	1
Thermal Power Plant Coupled with CHP (unconverted product and $C_1 - C_4$)			
	RGibbs	Burner (Boiler)	Temperature: 1200°C Pressure: 1 Bar Calculation option: Phase equilibrium and chemical equilibrium
	HeatX	Superheated evaporator (Boiler)	Flow direction: Counter current Specification: Cold stream outlet temperature: 504 ^{0}C
	HeatX	Evaporator (Boiler)	Flow direction: Counter current Specification: Cold stream outlet vapour fraction: 1
	HeatX	Economic Evaporator (Boiler)	Flow direction: Counter current Specification: Cold stream outlet temperature: 300^{0}C
	HeatX	Air Flow rate (Boiler) In Evaporator	Temperature: 30^{0}C Pressure: 1 Bar Mass Flow rate: 10000, 11000, 12000, 13000, 14000, 15000 kg/hr. as the temperature of the pyrolysis changes from 400^{0}C to 900^{0}C.
	HeatX	In PHAIR (Boiler)	Temperature: 30^{0}C Pressure: 1 Bar Mass Flow rate: 100 kg/hr. Flow direction: Counter current Specification: Cold stream outlet temperature: 150^{0}C
	Compr	TURBINE	Type: Isentropic Discharge Pressure: 30 Bar
	HeatX	CONDENSER	Flow direction: Counter current Specification: Hot stream outlet temperature: 120^{0}C

5.12. Parametric Sensitivity

The yields of gasoline and diesel have been correlated individually to the factors, namely, pyrolysis temperature (T) and recycle ratio (R_{CO_2}) of CO_2 by response

surface methodology [57] using the same procedure described in section 5.8. The optimum values of T and R_{CO_2} have also been determined.

References

1. Ruby Ray, Pinaki Bhattacharya and Ranjana Chowdhury.” Simulation and Modeling of Vegetable Market Wastes Pyrolysis Under Progressive Deactivation Condition”. The Canadian Journal of Chemical Engineering, 2004, 82, 566-579.
2. Ruby Ray, Ranjana Chowdhury and Pinaki Bhattacharya.” Studies on pyrolysis of vegetable market wastes in presence of heat transfer resistance and deactivation” .Int. J. Energy Res, 2005, 29, 811–828.
3. Raja S. Antony, Smart D. S. Robinson, Pillai B. C. and Lee Robert C. Lindon, “Parametric studies on pyrolysis of pungam oil cake in electrically heated fluidized bed reactor”, Research Journal of Chemical Science, Volume 1, Issue 1, 70-80, 2011.
4. Asadullah, M., Rahman, M.N., Ali, M.N., Motin, M.A., Sultan, M.B., Alam, M.R., Rahman, M.S “Jute stick pyrolysis for bio-oil production in fluidized bed reactor”, Bioresource Technology, 99, 44 – 50, 2008.
5. Mohammad Rofiqul Islam, MD. Nurun Nabi and Mohammad Nurul Islam, “The fuel properties of pyrolytic oils derived from carbonaceous solid wastes in Bangladesh”, Jurnal Teknologi, Volume 38, Issue A, 75–89, Jun. 2003.
6. Basak Burcu Uzun, Ayse Eren Putun, Ersan Putun, “Fast pyrolysis of soybean cake: Product yield and compositions”, Bioresource Technology, Volume 97, Issue 4, 569-576, 2006.
7. Oztem Onay and O. Mote Kockar, “Slow, fast and flash pyrolysis of rapeseed”, Renewable Energy, Volume 18, Issue 15, 2417-2433, 2003.
8. S. Yorgun, S. Sensoz, O. M. Kockar, “Flash pyrolysis of sunflower oilcake for production of liquid fuels”, Journal of Analytical and Applied Pyrolysis, Volume 60, Issue 1, 1-12, 2001.
9. R. Chowdhury, A. Sarkar, “Reaction Kinetics and Product Distribution of Slow Pyrolysis of Indian Textile Wastes”, International Journal of Chemical Reactor engineering, 10, A67, 2012.
10. A Sarkar, “Studies on Pyrolysis of Spent Engine Oil and Lignocellulosic Part of Municipal Solid Waste (MSW)”, (PhD Thesis in Chemical Engineering, No. 52/10/E), 2015.
11. Wu, W.; Cai, J.; Liu, R. “Isoconversional Kinetic Analysis of Distributed Activation Energy Model Processes for Pyrolysis of Solid Fuels”, Ind. Eng. Chem. Res., 52, 14376−14383, 2013.
12. Aparna Sarkar, Biswarup Mondal and Ranjana Chowdhury, “Mathematical Modeling of a Semi-Batch Pyrolyser for Sesame Oil Cake”, Ind Eng Chem Res, 2014, 53, 19671-19680.
13. Anthony, D. B.; Howard, J. B. “Coal devolatilization and hydrogasification”, AIChE J, 22, 625−656, 1976.
14. Gasparovic, L.; Labovsky, J.; Markos, J.; Jelemensky, L, “Calculation of kinetic parameters of the thermal decomposition of wood by distributed activation energy model (DAEM),” Chem. Biochem. Eng. Q., 26, 45−53, 2012.
15. Mani, T.; Murugan, P.; Mahinpey, N, “Determination of distributed activation energy model kinetic parameters using simulated annealing optimization method for nonisothermal pyrolysis of lignin”, Ind. Eng. Chem. Res., 48, 1464−1467, 2009.
16. Li, Z. Q.; Liu, C. L.; Chen, Z. C.; Qian, J.; Zhao, W.; Zhu, Q. Y, “Analysis of coals and biomass pyrolysis using the distributed activation energy model”, Bioresour. Technol., 100, 948−952, 2009.
17. Cai, J. M.; Yang, S. Y.; Li, T, “Logistic distributed activation energy model. Part 2: Application to cellulose pyrolysis”, Bioresour. Technol., 102, 3642−3644, 2011.
18. Cai, J.; Chen, Y, “Iterative linear integral isoconversional method: Theory and application”, Bioresour. Technol., 103, 309−312, 2012.
19. Lehmann, J., Pereira da Silva, J., Steiner, C., Nehls, T., Zech, W., Glaser, B., 2003. “Nutrient availability and leaching in an archaeological Anthrosol and a Ferralsol of the Central Amazonbasin: fertilizer, manure and charcoal amendments. Plant Soil,249 (2), pp. 343–357.

20. CPCB, 2000, Status of Solid Waste Generation, Collection, Treatment and Disposal in Metro cities, Series: CUPS/46/1999–2000.
21. Kansal, A., 2002. Solid waste management strategies for India. Indian Journal of Environmental Protection 22 (4), pp. 444–448.
22. Das L.M, Gulati R, Gupta P.K. "A comparative evaluation of the performance characteristics of a spark ignition engine using hydrogen and compressed natural gas as alternative fuels", *Int. J. Hydrog. Energy,* 2000, *25*, 783.
23. Blanco Lopez M.C, Blanco C.G, Martinez-Alonso, A. Toscon. J.M.D. "Composition of gases released during olive stones pyrolysis", *J. Anal. Appl. Pyrolysis,* 2002, *65*, 313.
24. Minkova V, Razvigorova M, Bjornbom E, Zanzi R, Budinova T, Petrov N. "Performance analysis of a fixed-bed biomass gasifier using high-temperature air", *Fuel Proc. Technol.,* 2001, *70*, 53.
25. Lei Wang, Richard Templer and Richard "Environmental sustainability of bioethanol production from waste papers: sensitivity to the system boundary", J. Murphy. Energy Environ. Sci., 2012, 5, 8281.
26. Dezhen Chen, Lijie Yin, Huan Wang, Pinjing He. "Reprint of: Pyrolysis technologies for municipal solid waste: A review", Waste Management, 2015,37, 116.
27. G. Doka, "Life Cycle Inventories of Waste Treatment Services, Swiss Centre for Life Cycle Inventories", Dŭbendorf, 2009.
28. N. Jungbluth, "Life cycle inventories of Bioenergy, Swiss Centre for Life Cycle Inventories", Dŭbendorf, 2007.
29. ISO 14041, Environmental Management-Life Cycle Assessment- Goal and Scope Definition and Inventory Analysis, 1998.
30. R. Hischier, "Life Cycle Inventories of Packaging and Graphical Papers, Swiss Centre for Life Cycle Inventories", Dŭbendorf, 2007.
31. R. Heijungs, J. Guinée, R. Kleijn and V. Rovers, "Bias in Normalization: Causes, Consequences, Detection and Remedies", Int. J. Life Cycle Assess, 2007, 12, 211.
32. A.Magnusson, H., Process simulation in Aspen Plus of an Integrated Ethanol and CHP Plant, UMEA UNIVERSITET (Master Thesis in Energy Engineering, EN0601), 2014.
33. B. Yucheng Cao and Artur Pawtowsk, "Life cycle assessment of two emerging sewage sludge-to-energy systems: Evaluating energy and greenhouse gas emissions implications", Bioresource Technology, 2013, 127, 81.
34. Rafael Luque, J. Angel Men_endez, Ana Arenillas and Jaume Cot. "Microwave-assisted pyrolysis of biomass feedstocks: the way forward?", Energy Environ. Sci., 2012, 5, 5481.
35. Nicole L. Hammer, Akwasi A. Boateng, Charles A. Mullen, M. Clayton Wheeler, "Aspen Plus® and economic modeling of equine waste utilization for localized hot water heating via fast pyrolysis", Journal of Environmental Management, 2013, 128, 594.
36. Mittal, M. L. Estimates of emission from coal fired thermal power plant in India, www.epa.gov/ttnchie/conference/ei20/session5/mmittal.pdf
37. Prostein, R. F and R. E. Hicks. Synthetic Fuels. McGraw Hill, 1982, New York.
38. http://www.che.utexas.edu/course/che359&384/lecture_notes
39. http://en.wikipedia.org/wiki/Energy_value_of_coal
40. Yucheng Cao and Artur Pawłowsk. Bioresource Technology, 2013, 127, 81.
41. Kabir M.R., Kumar A. Bioresour. Technol, 2011, 102, 8972–8985.
42. http://www.agriculturalproductsindia.com/fertilizers/fertilizersureafertilizer.html
43. Elke Stehfest and Lex Bouwman, "N_2O and NO emission from agricultural fields and soils under natural vegetation: summarizing available measurement data and modeling of global annual emissions", Nutrient Cycling in Agroecosystems (2006) 74: 207.
44. Minghua Zhou, Bo Zhu, Klaus Butterbach-Bahl, Tao Wang, Jessica Bergmann, Nicolas Brüggemann, Zhenhua Wang, Taikui Li, Fuhong Kuang, "Nitrate leaching, direct and indirect nitrous oxide fluxes from sloping cropland in the purple soil area, southwestern China", Environmental Pollution 162 (2012) 361.
45. http://www.ipcc-nggip.iges.or.jp/public/gp/bgp/4_5_N2O_Agricultural_Soils.pdf
46. http://convert-units.info/density/kilogram-liter/1.25
47. Jan Peter Lesschen, Gerard L. Velthof, Wim de Vries, Johannes Kros, "Differentiation of nitrous oxide emission factors for agricultural soils", Environmental Pollution 159 (2011) 3215.

48. < http://webcache.googleusercontent.com/search?q=cache:-u98ZBZwusUJ:www.ipccnggip.iges.or.jp/public/gp/bgp/4_5_N2O_Agricultural_Soils.pdf+&cd=1&hl=en&ct=clnk&gl=in>
49. Yucheng Cao, Artur Pawłowski, "Life cycle assessment of two emerging sewage sludge-to-energy systems", Bioresource Technology, 2013, 127, 81.
50. Jan Peter Lesschen, Gerard L. Velthof, Wim de Vries, Johannes Kros, "Evaluating energy and greenhouse gas emissions implications", Bioresource Technology 127 (2013) 81.
51. <http://webcache.googleusercontent.com/search?q=cache:6IP6_Ox36TYJ:www.fertilizerseurope.com/fileadmin/user_upload/publications/agriculture_publications/Energy_Efficiency__V9.pdf+&cd=1&hl=en&ct=clnk&gl=in>
52. Hanaâ Er-rbib, Chakrib Bouallbou, François Werkoff, "Production of synthetic gasoline and diesel fuel from dry reforming of methane", Energy Procedia, 29,212, 156-165.
53. Sudiro, M, Bertucco, A, "Production of synthetic gasoline and gasoil fuel by alternative processes using natural gas and coal: Process simulation and optimization", Energy, 34,2009, 2206-2214.
54. Woo-Kyu Chae, Hak-Ju Lee, Jong-Nam Won, Jung-Sung Park and Jae-Eon Kim, "Design and Field Tests of an Inverted Based Remote MicroGrid on a Korean Island", *Energies* 2015, *8*(8), 8193-8210.
55. Aspen Tech, 2001. Aspen Physical Property System 11.1. Aspen Technology, Inc.,Cambridge, MA, USA.
56. http://www.statease.com/training.html>
57. Marcos Almeida Bezerra, Ricardo Erthal Santelli, Eliane Padua Oliveira, Leonardo Silveira Villar, Luciane Amélia Escaleira, "Response surface methodology (RSM) as a tool for optimization in analytical chemistry", Talanta, 2008, 75 (5), 965 -977.
58. < http://www.weibull.com/hotwire/issue130/hottopics130.htm>
59. Box, G. and Behnken, D., "Some New Three. Level Designs for the Study of Quantitative. Variables", Technometrics, 2, 1960, 455 – 475
60. Chatterjee, S. et al., ―Regression Analysis by Example, 2nd Ed., Wiley and Sons, Inc., 1977, 200-202

Chapter. 6

RESULTS AND DISCUSSION

6. Results and Discussion

6.1. Characterization of pyrolysis feed stocks

6.1.1. Results of proximate and ultimate analyses

The higher heating values and the results of proximate and ultimate analyses of all pyrolysis feed stocks under study have been provided in Table.1.

Table.6.1. Proximate and Ultimate analyses, Heating Values and Bulk Density of the feed stocks

Properties	Jute Wastes	Sesame Oil Cake	Lime Wastes
Moisture (w%)	10.025	7.41	9.2
Volatile Matter (w%)	77.15	85.72	78.3
Ash (w%)	2.59	3.8	2.00
Fixed Carbon (w%)	10.235	3.07	10.5
C% (w/w)	49.79	45.19	46.42
H% (w/w)	6.02	7.55	8.00
O% (w/w)	41.37	39.27	44.56
N% (w/w)	0.19	7.26	0.44
Cl% (w/w)	0.05	0.08	0.08
S% (w/w)	0.05	0.721	0.5
Heating value (MJ /kg)	18.7	19.78	22.56
Bulk Density (kg/m^3)	110	460	1050

6.2. Kinetics of non-catalytic pyrolysis

6.2.1 Lumped Kinetics

6.2.1.1. Experimental time histories

As described in the section 5.1.1, the lumped kinetics [3,11,12] of pyrolysis of all feedstocks namely waste jute and lime waste have been determined using integral method of analysis. Time histories of weight fractions of residue, volatiles and char obtained during the batch mode experiments in the semi -batch pyrolyzer have been used for this purpose.

6.2.1.1.1. Use of jute waste and lime waste as pyrolysis feedstock

Figures 6.1 represent the profiles of residual weight fractions of jute wastes and lime waste with respect to pyrolysis time using the experimental data obtained from the semi-batch pyrolyzer using approximately 100g of each sample in the temperature range of 573 to 1173K. The corresponding data used for the plots are provided in TableA.1 in the Appendix. Figures 6.2 show the profiles of volatile weight fraction obtained through pyrolysis of jute wastes and lime waste with respect to pyrolysis time. Figures 6.3 show the profiles of char fraction obtained through pyrolysis of jute wastes [4,5,6] and lime waste [7,8] with respect to pyrolysis time. The corresponding values used for the plots are provided in the Table A.2. and A.3. respectively.

From the analysis of the figures it is evident that the pyrolysis of both feedstocks begins at 673K. Below this temperature the reactions do not occur at a detectable rate. From the plots, it can be predicted that at each temperature, a saturation level of residues, volatile weight fraction and char weight fraction is obtained at 60 minutes or earlier. In previous research articles, it has been reported that the constituent molecules, namely, cellulose, hemicellulose and lignin of lignocellulosic biomass have different pyrolysis characteristics [1,2]. While the pyrolysis of hemicellulose and cellulose occurs at 220 – 315 ^oC and 315 – 400 ^oC respectively, that of lignin occurs in a very wide range of temperature from 160 – 900 ^oC [3].

a)

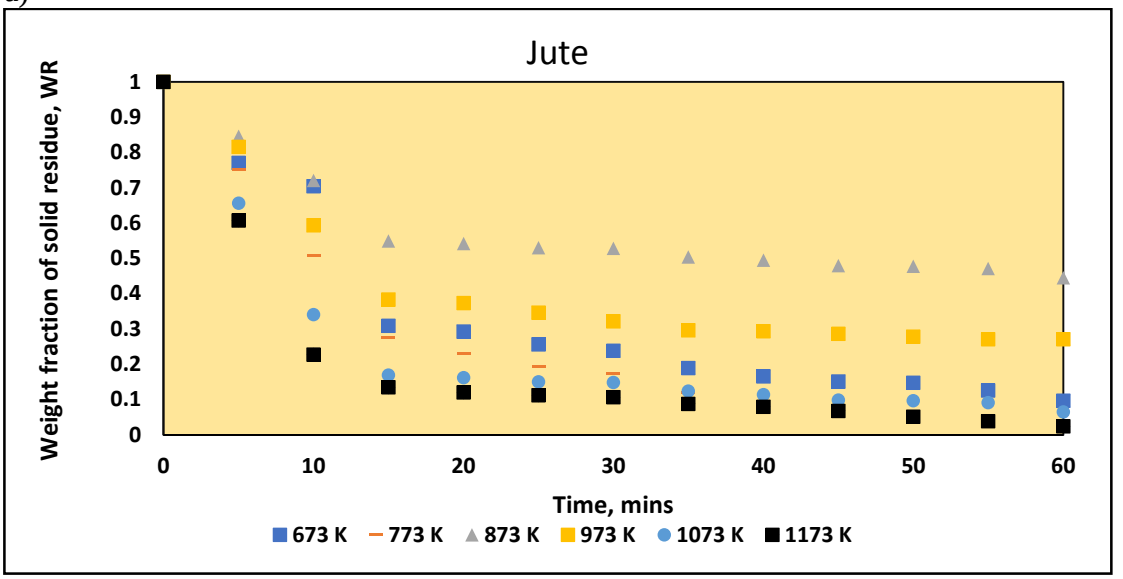

b)

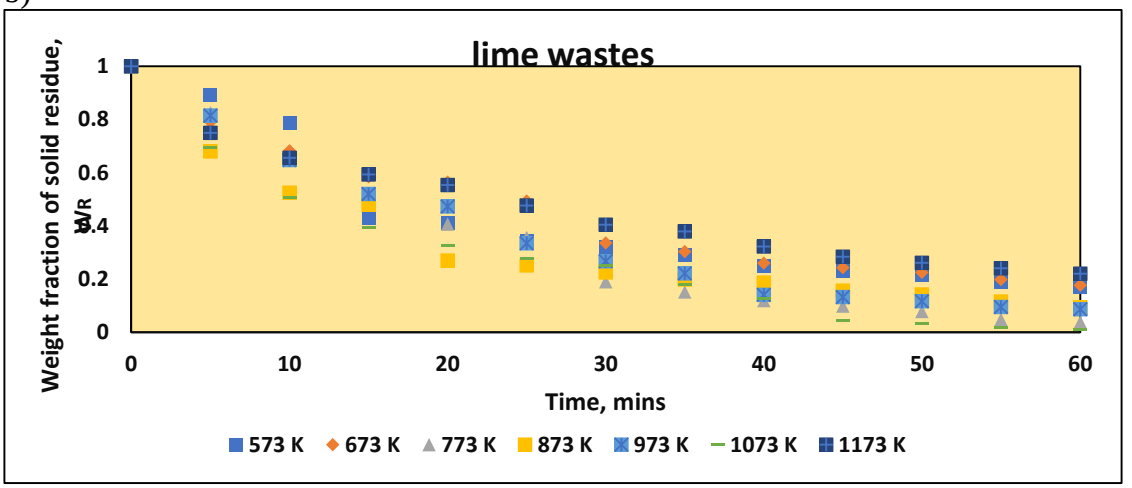

Figure 6.1. Time histories of weight fraction of residue of (a) jute wastes (b) lime waste using pyrolysis temperature as parameter.

a)

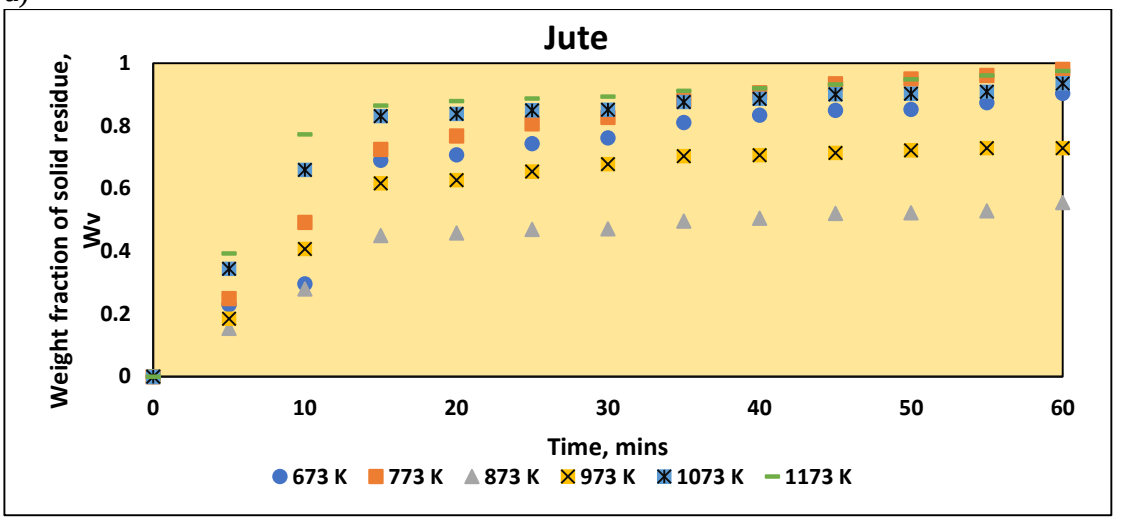

b)

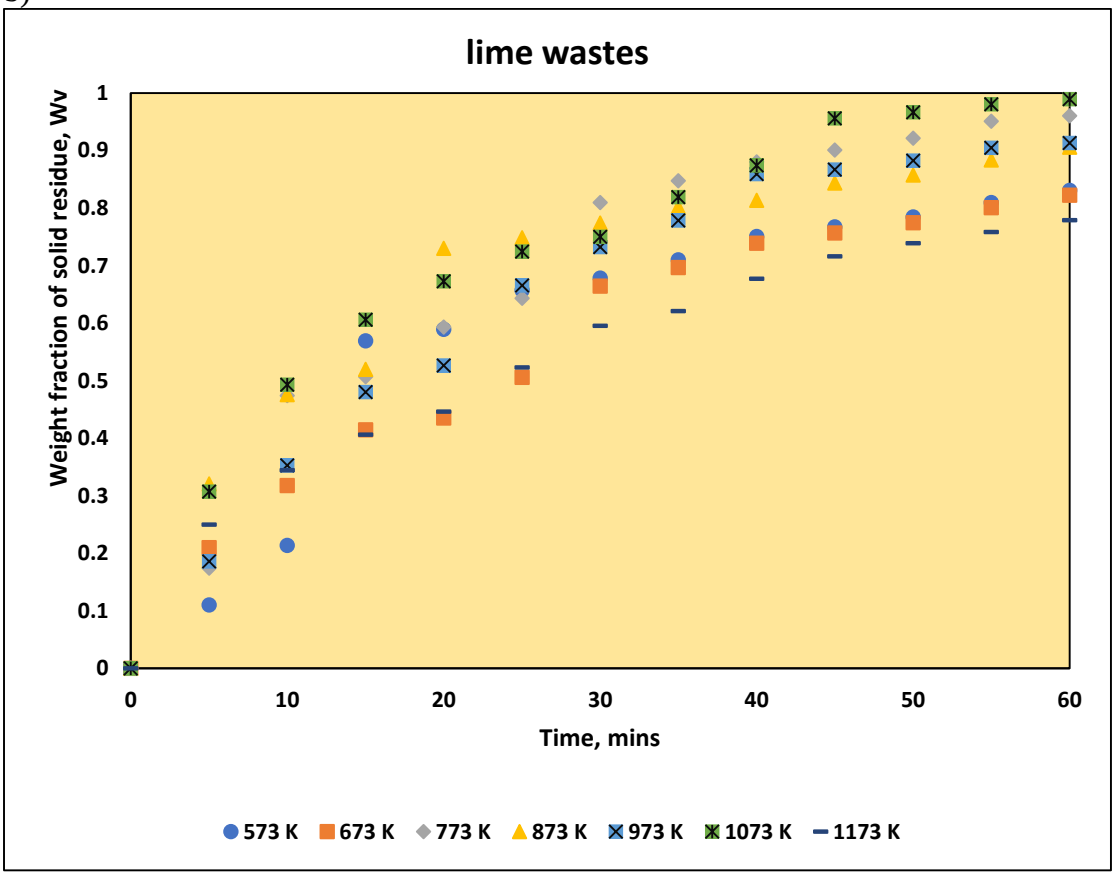

Figure 6.2. Time Histories of volatile weight fraction using pyrolysis temperature as parameter: (a) jute wastes (b) lime waste

a)

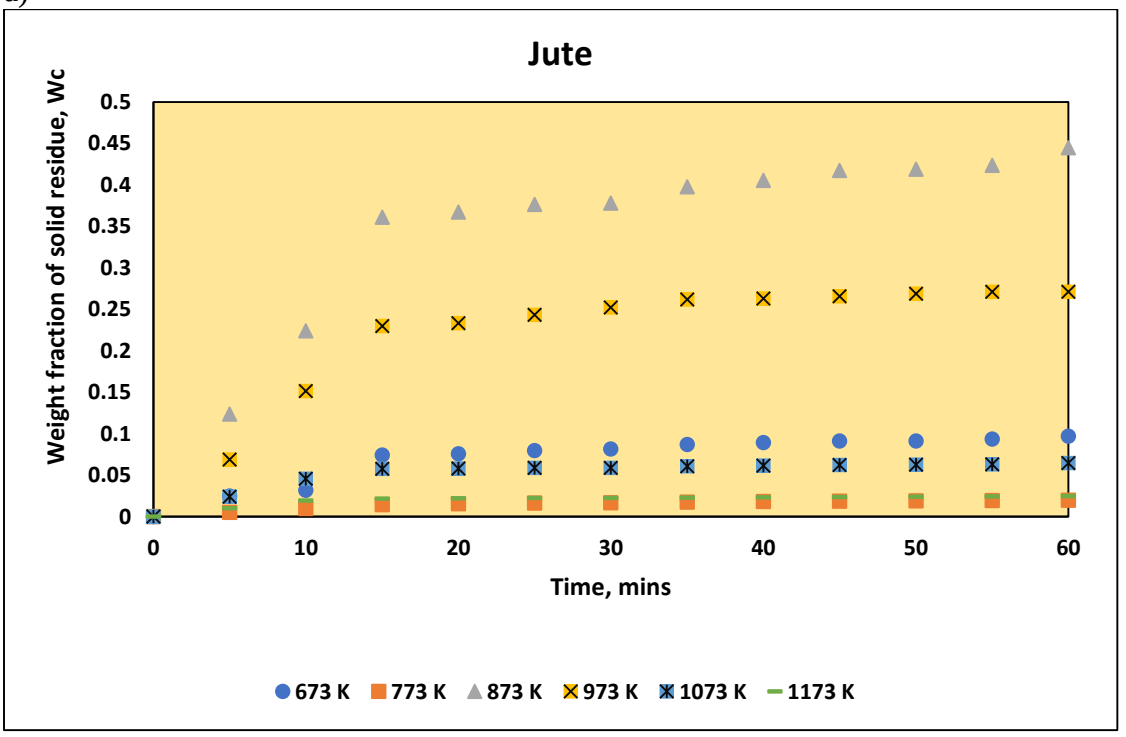

b)

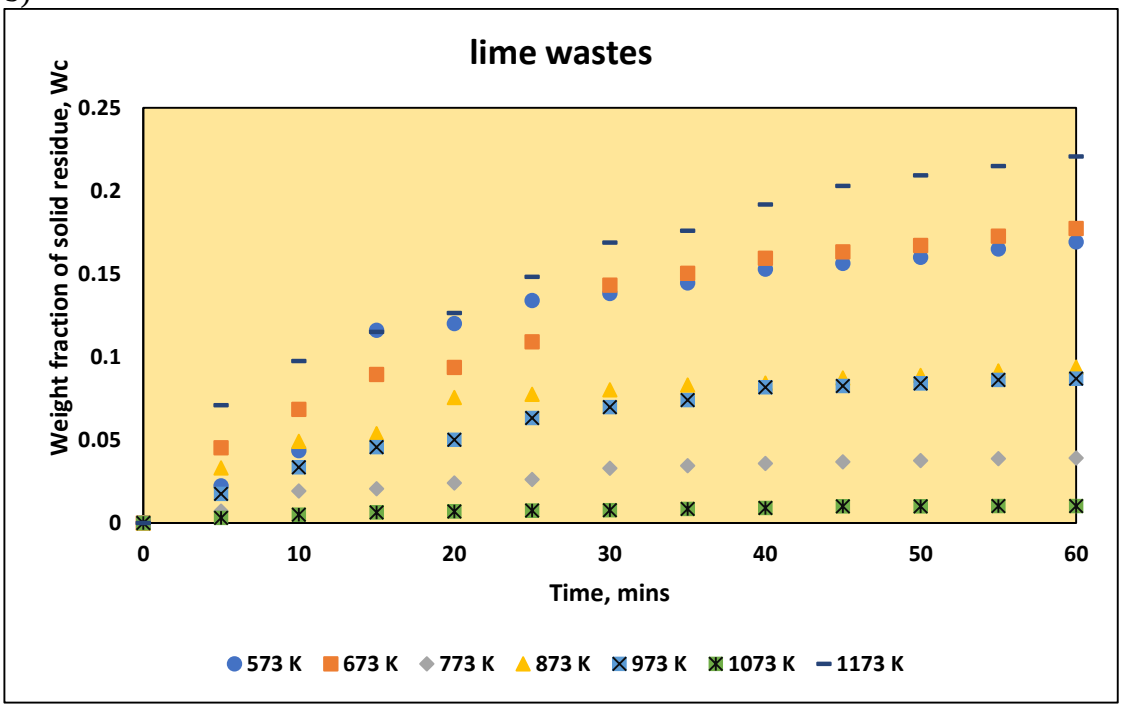

Figure 6.3. Time Histories of char weight fraction using pyrolysis temperature as parameter: (a) jute wastes (b) lime waste

6.2.1.2. Parameters of lumped kinetic Model

In Figures 6.4 and 6.5., experimental values of $\mathbf{ln}\left(\frac{w_o}{w}\right)$ have been plotted against time and those of $\frac{w_v}{w_o}$, $\frac{w_c}{w_o}$, $\frac{w_l}{w_o}$ **and** $\frac{w_g}{w_o}$ have been plotted against $\mathbf{(1-exp[-k*t])/k}$ for pyrolysis of jute wastes and lime wastes respectively. The corresponding data used for the plots have been provided in Tables A4. – A8. in the appendix. From the close inspection of the figures, it is clearly evident that linear plots have obtained for both feedstocks establishing the validity of 1st order kinetics [3, 9-12]. The rate constants for pyrolysis have been determined from the slope of the linear plot as well as from the regression equations ($R^2 = 1$) at different temperature. The results of statistical "t-test" [14] and "f-test" [13] shown in each figure (Figures 6.4-6.5) suggest the perfect agreement between the regressed and experimental data.

a) 673K

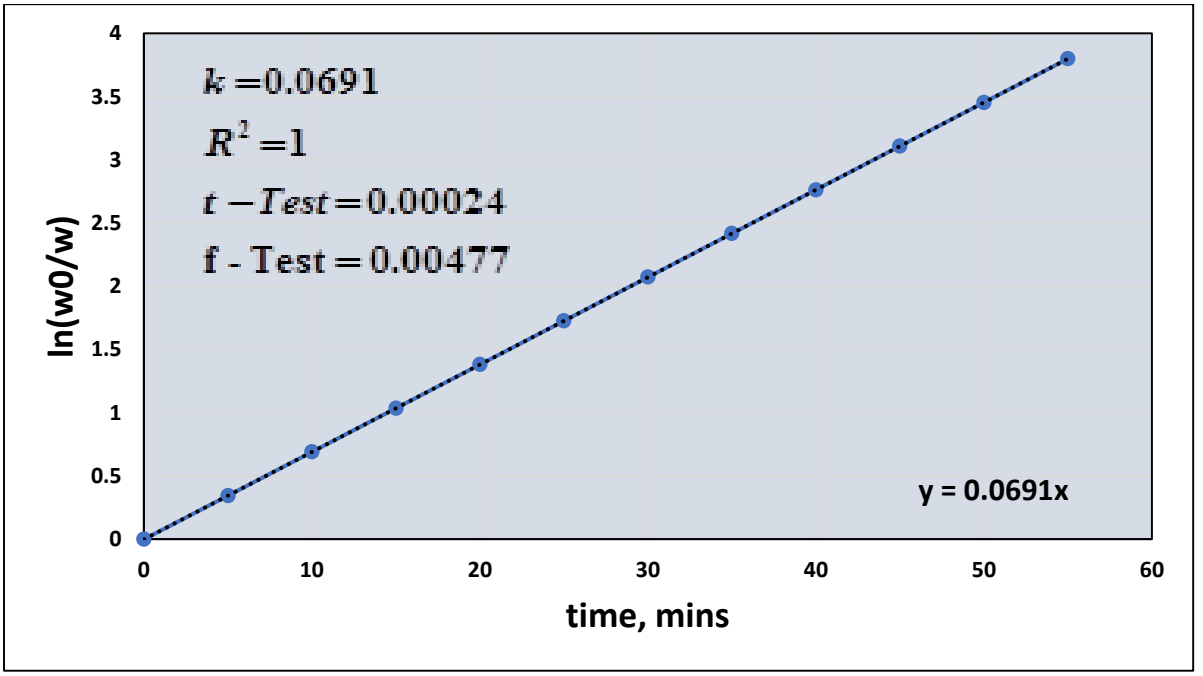
k =0.0691
R² =1
t – Test =0.00024
f - Test = 0.00477
y = 0.0691x
ln(w0/w)
time, mins
0
0.5
1
1.5
2
2.5
3
3.5
4
0
10
20
30
40
50
60

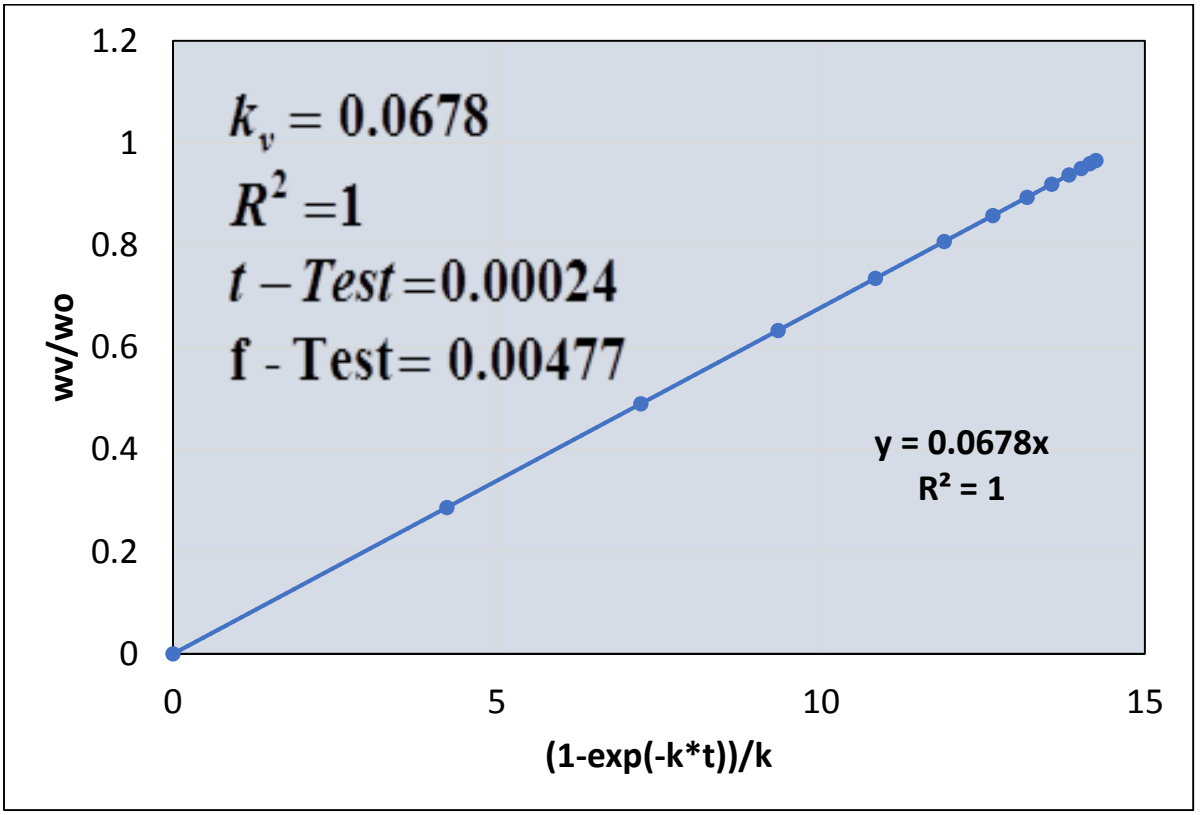
k_v = 0.0678
R² =1
t – Test =0.00024
f - Test= 0.00477
y = 0.0678x
R² = 1
wv/wo
(1-exp(-k*t))/k
0
0.2
0.4
0.6
0.8
1
1.2
0
5
10
15

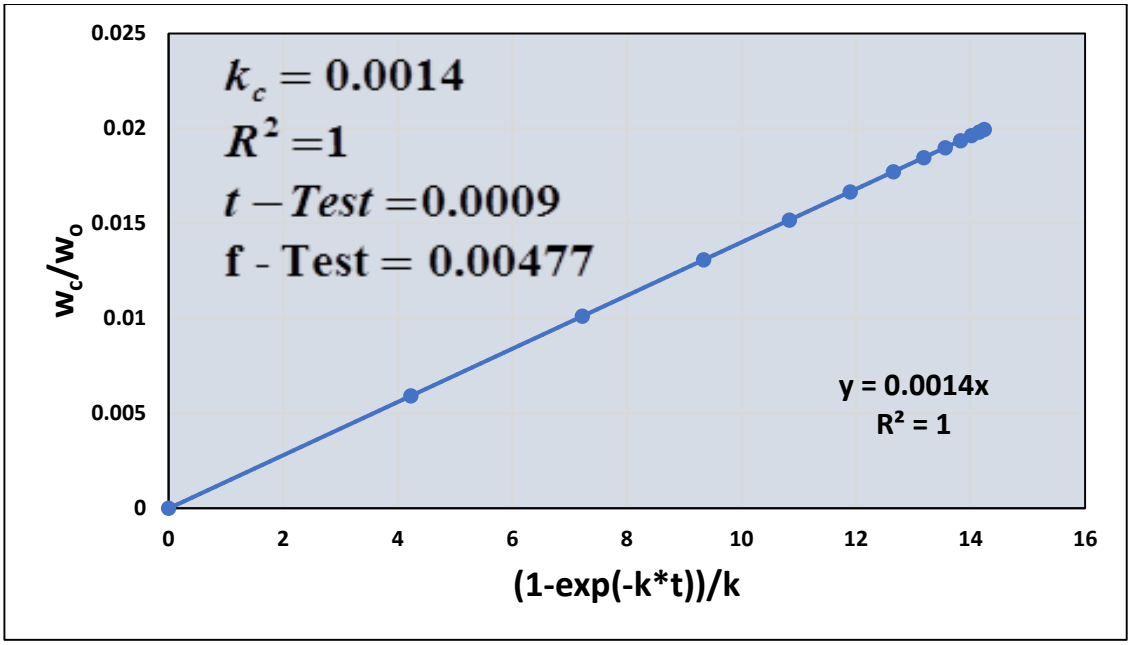
$k_c = 0.0014$
$R^2 = 1$
$t - Test = 0.0009$
f - Test = 0.00477
y = 0.0014x
R² = 1
w_c/w_o
(1-exp(-k*t))/k
0.025
0.02
0.015
0.01
0.005
0
0 2 4 6 8 10 12 14 16

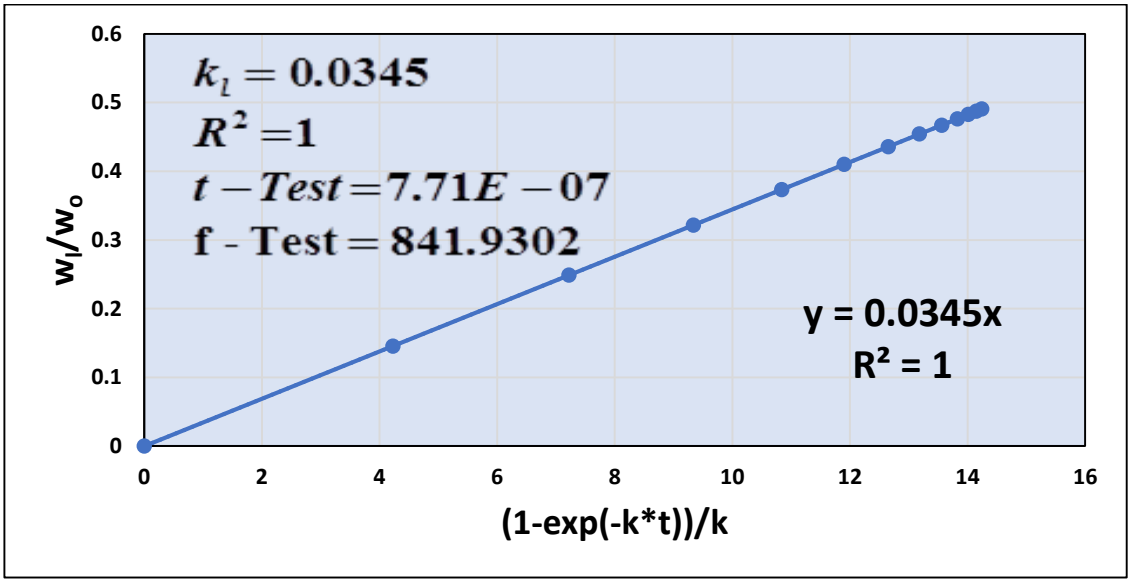
$k_l = 0.0345$
$R^2 = 1$
$t - Test = 7.71E-07$
f - Test = 841.9302
y = 0.0345x
R² = 1
w_l/w_o
(1-exp(-k*t))/k
0.6
0.5
0.4
0.3
0.2
0.1
0
0 2 4 6 8 10 12 14 16

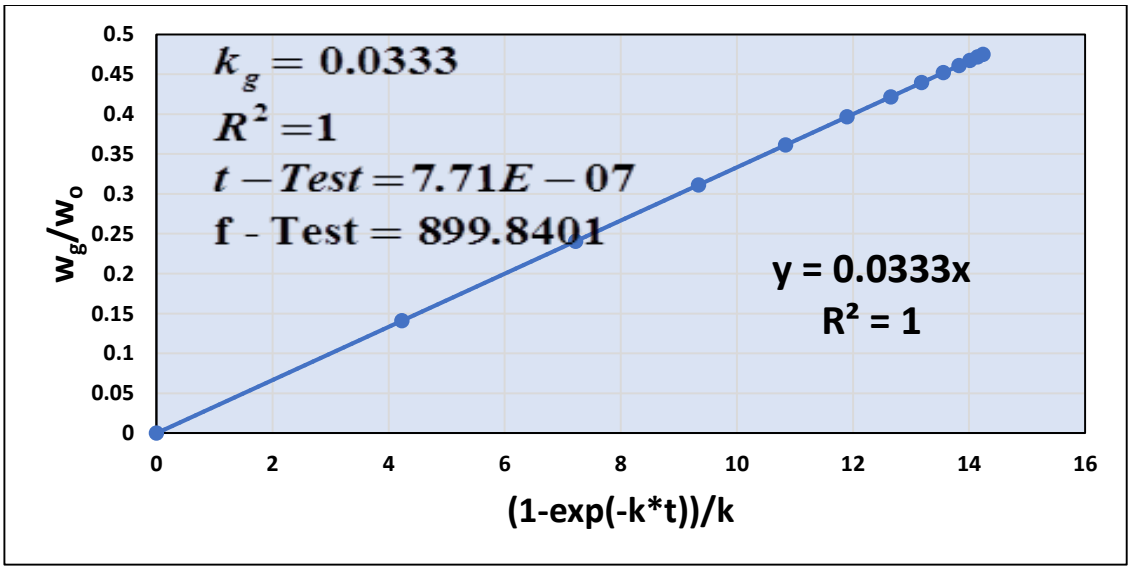
$k_g = 0.0333$
$R^2 = 1$
$t - Test = 7.71E-07$
f - Test = 899.8401
y = 0.0333x
R² = 1
w_g/w_o
(1-exp(-k*t))/k
0.5
0.45
0.4
0.35
0.3
0.25
0.2
0.15
0.1
0.05
0
0 2 4 6 8 10 12 14 16

b) 773K

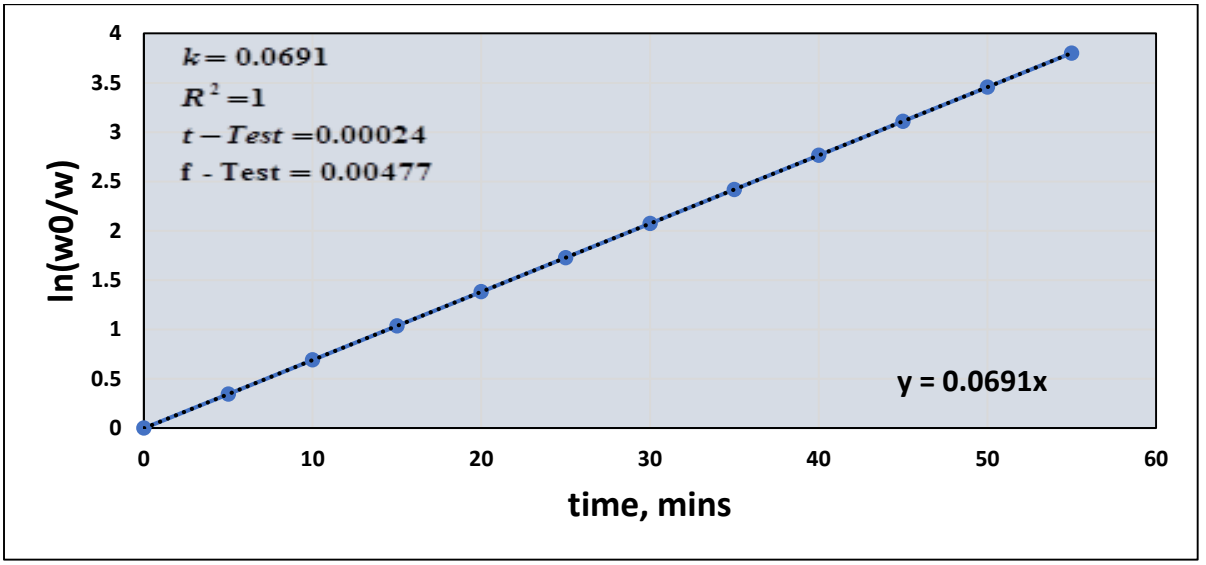
k = 0.0691
R² = 1
t – Test = 0.00024
f - Test = 0.00477
y = 0.0691x
ln(w0/w)
time, mins

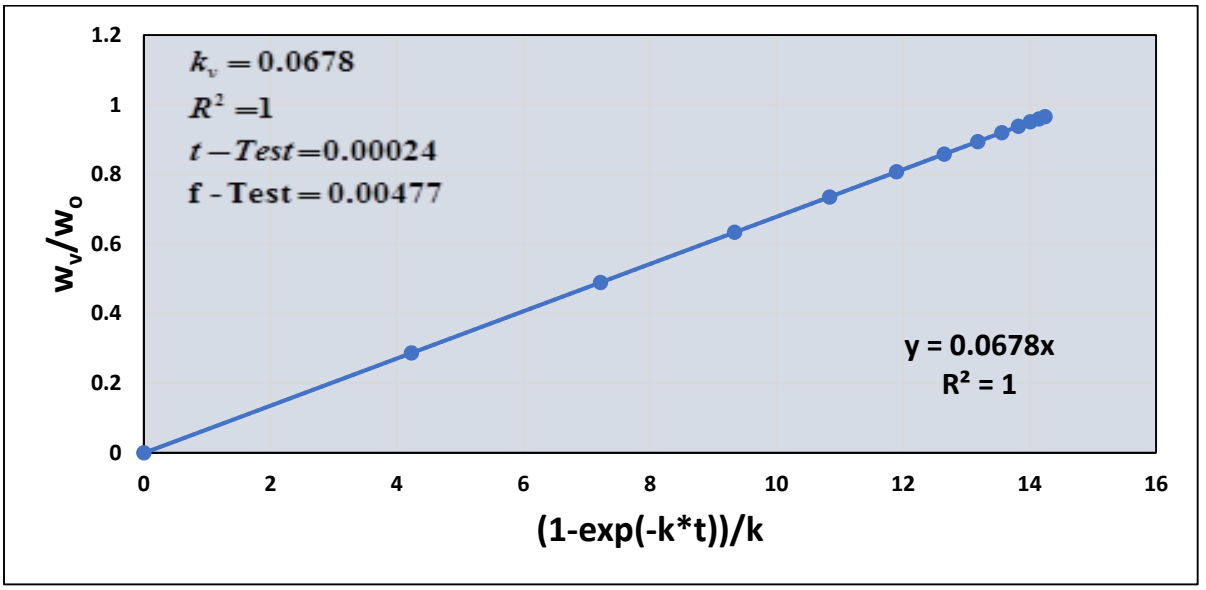
k_v = 0.0678
R² = 1
t – Test = 0.00024
f - Test = 0.00477
y = 0.0678x
R² = 1
w_v/w_o
(1-exp(-k*t))/k

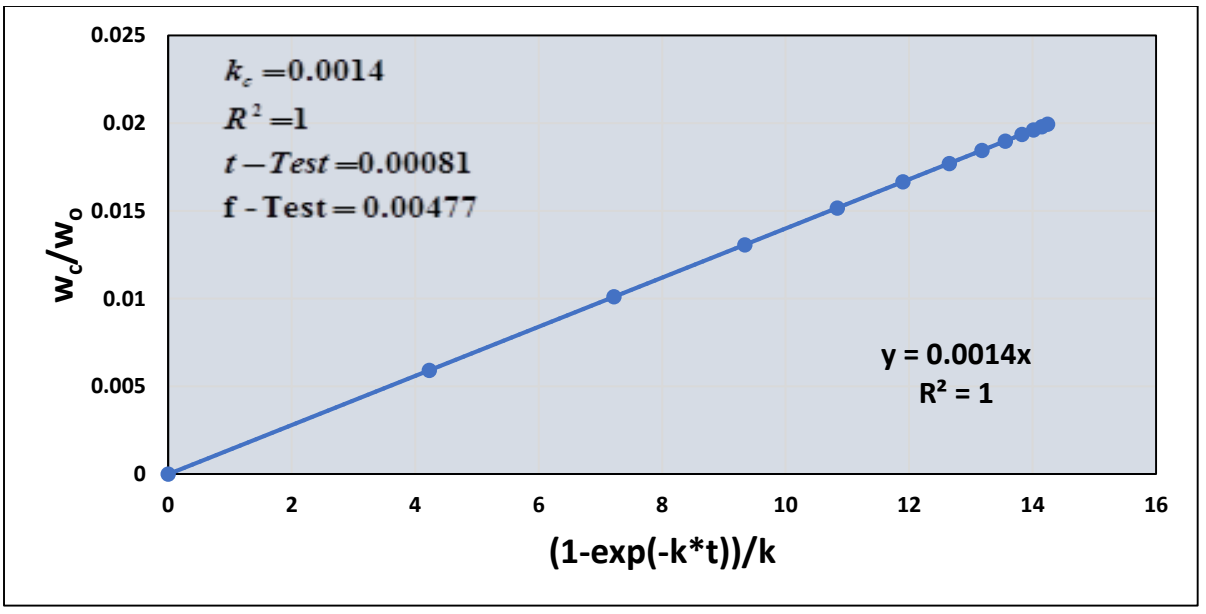
k_c = 0.0014
R² = 1
t – Test = 0.00081
f - Test = 0.00477
y = 0.0014x
R² = 1
w_c/w_o
(1-exp(-k*t))/k

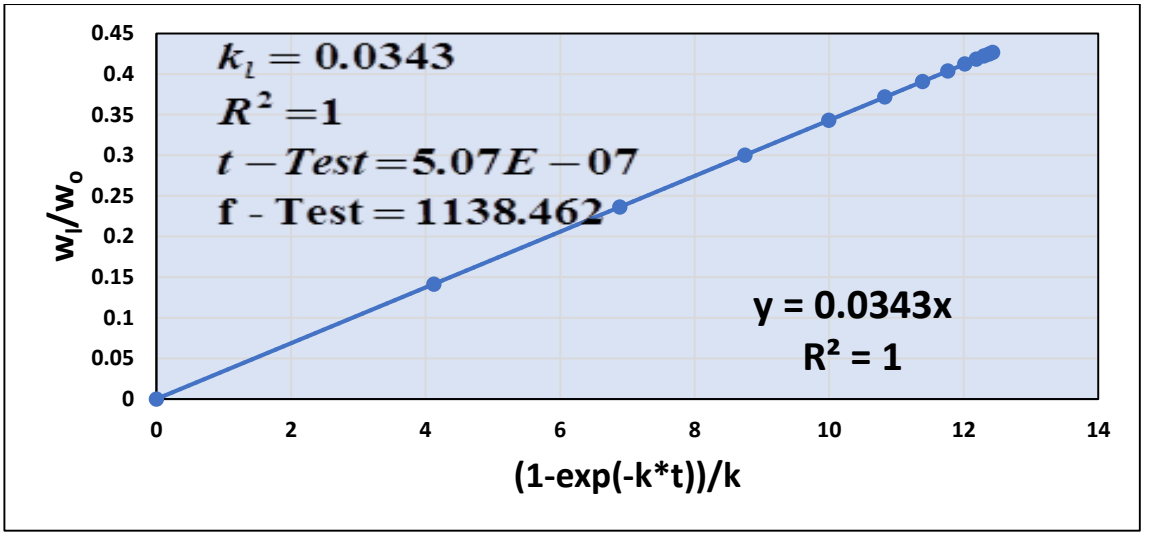
$k_l = 0.0343$
$R^2 = 1$
$t - Test = 5.07E - 07$
f - Test = 1138.462
y = 0.0343x
R² = 1
w_l/w_o
(1-exp(-k*t))/k

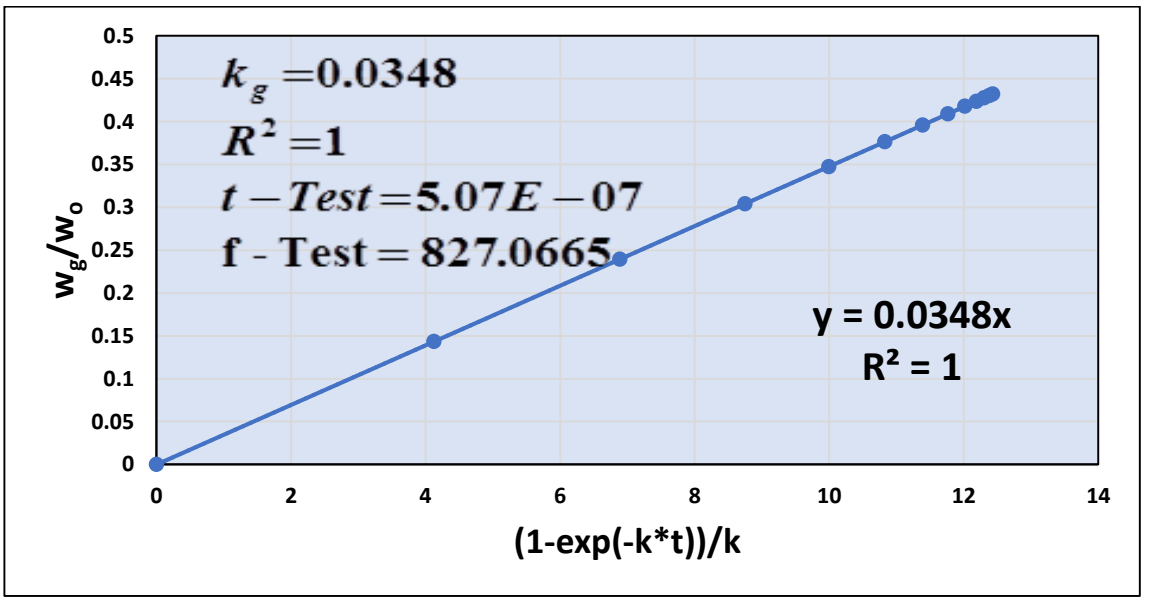
$k_g = 0.0348$
$R^2 = 1$
$t - Test = 5.07E - 07$
f - Test = 827.0665
y = 0.0348x
R² = 1
w_g/w_o
(1-exp(-k*t))/k

c) 873K

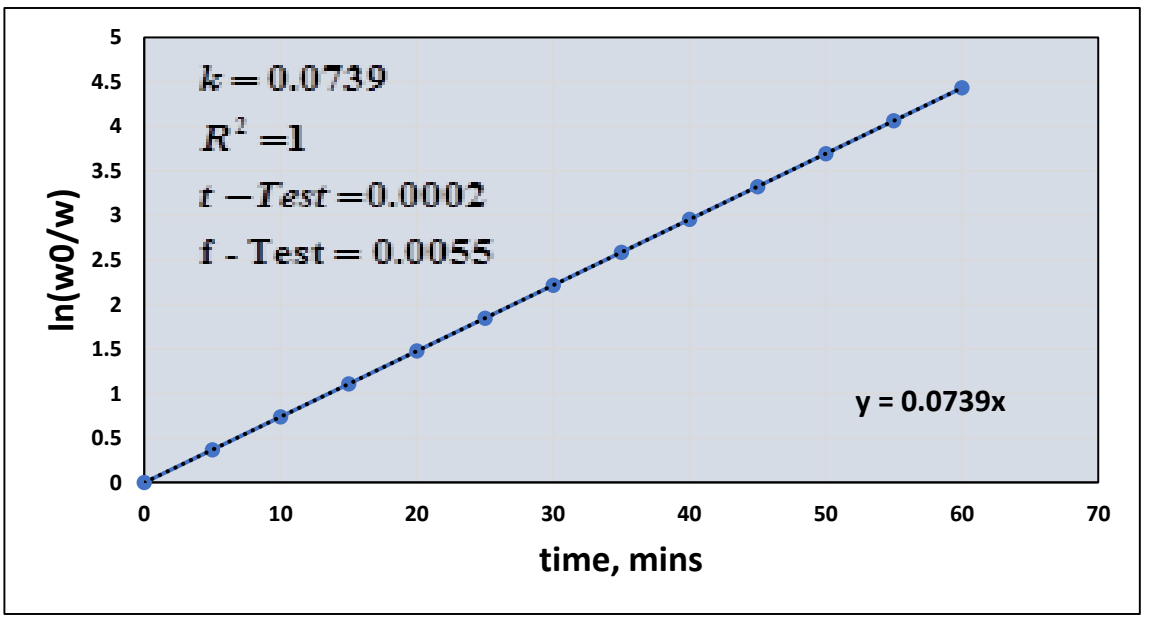
$k = 0.0739$
$R^2 = 1$
$t - Test = 0.0002$
f - Test = 0.0055
y = 0.0739x
ln(w0/w)
time, mins

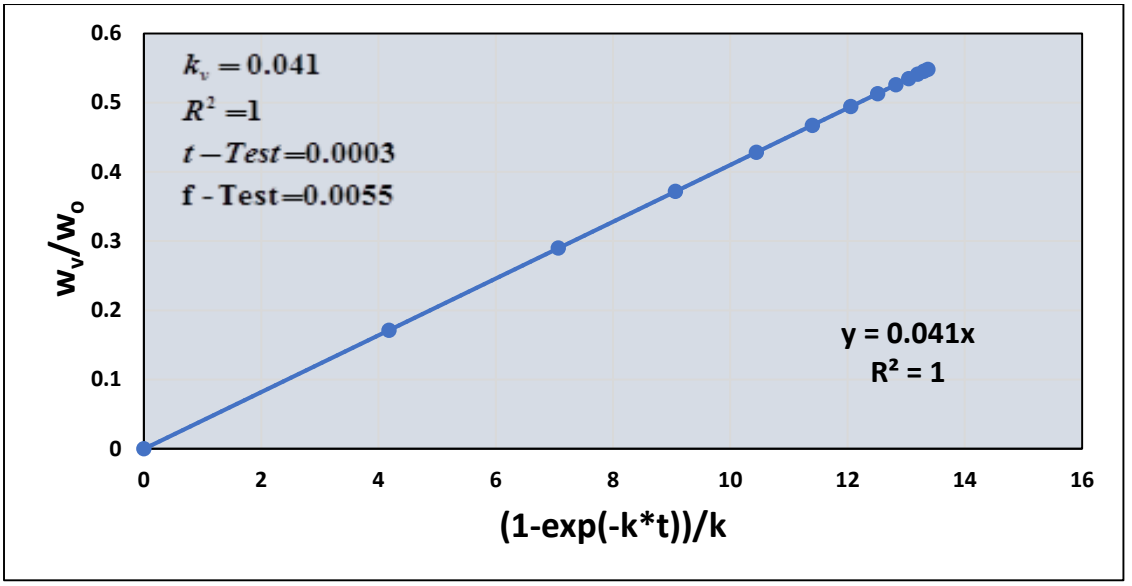
$k_v = 0.041$
$R^2 = 1$
$t - Test = 0.0003$
f - Test=0.0055
y = 0.041x
R² = 1
w_v/w_o
(1-exp(-k*t))/k

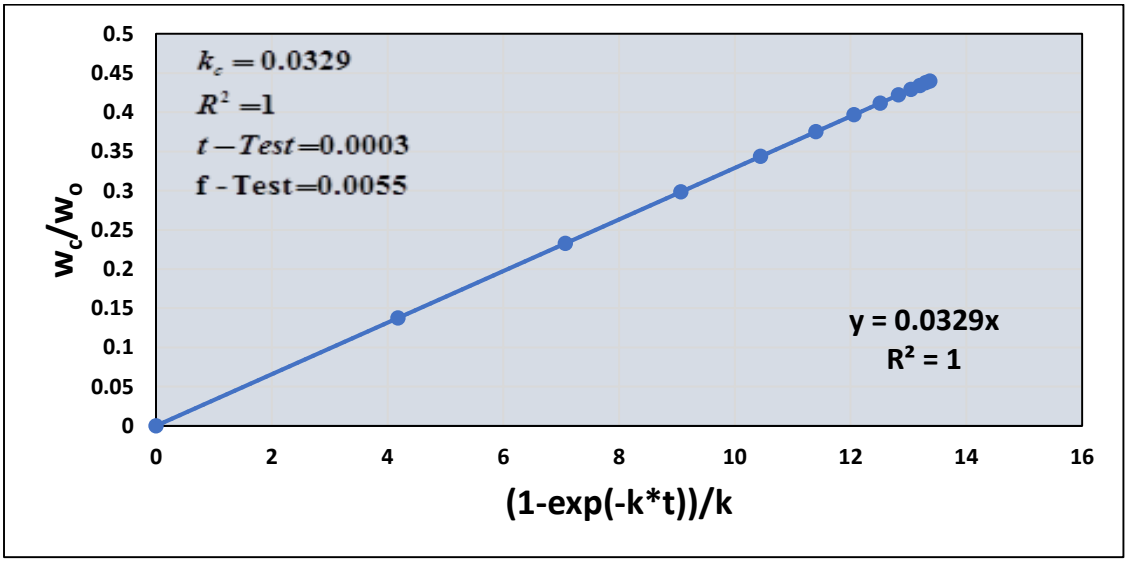
$k_c = 0.0329$
$R^2 = 1$
$t - Test = 0.0003$
f - Test=0.0055
y = 0.0329x
R² = 1
w_c/w_o
(1-exp(-k*t))/k

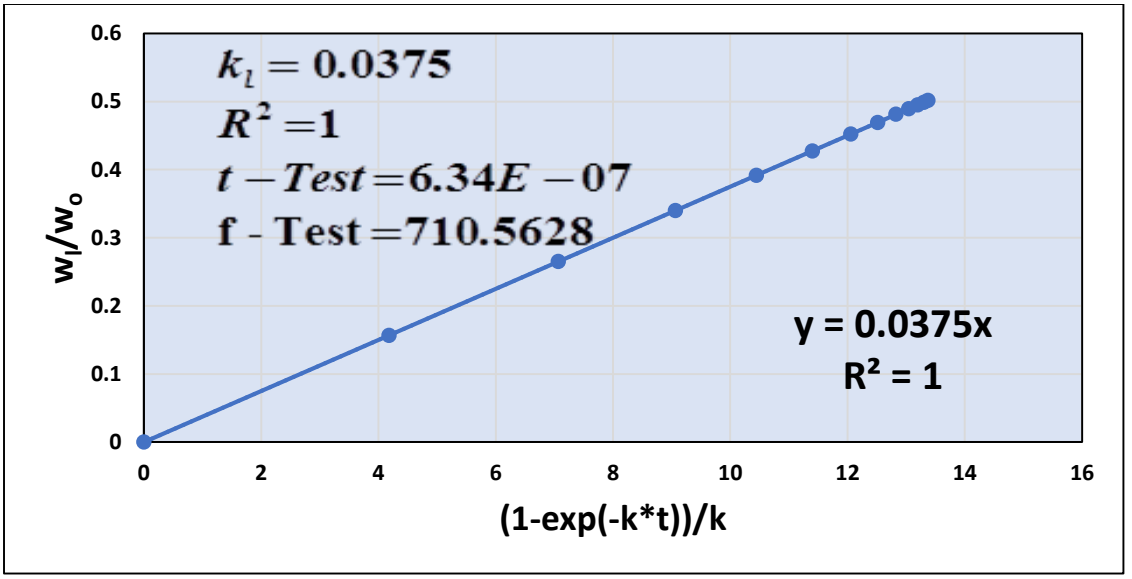
$k_l = 0.0375$
$R^2 = 1$
$t - Test = 6.34E - 07$
f - Test =710.5628
y = 0.0375x
R² = 1
w_l/w_o
(1-exp(-k*t))/k

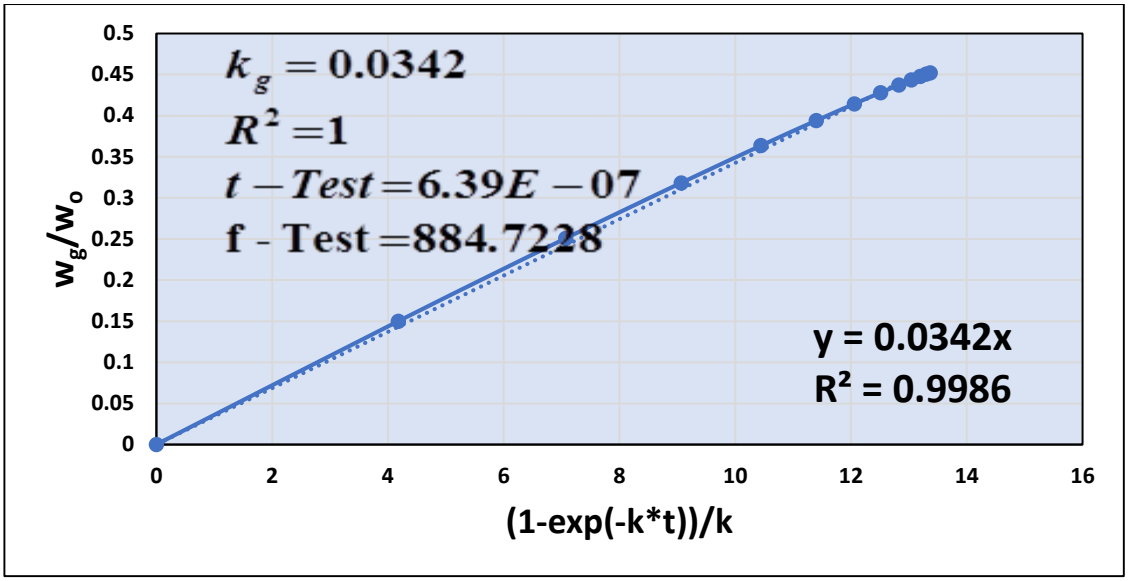
$k_g = 0.0342$
$R^2 = 1$
$t - Test = 6.39E - 07$
f - Test = 884.7228
y = 0.0342x
R² = 0.9986
w_g/w_o
(1-exp(-k*t))/k

d) 973 K

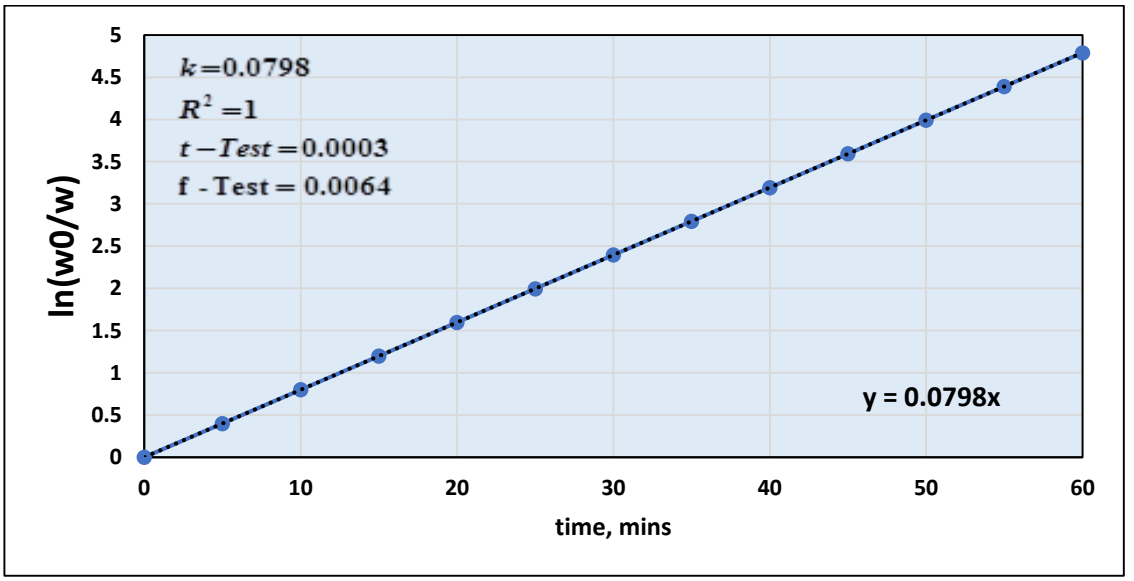
$k = 0.0798$
$R^2 = 1$
$t - Test = 0.0003$
f - Test = 0.0064
y = 0.0798x
ln(w0/w)
time, mins

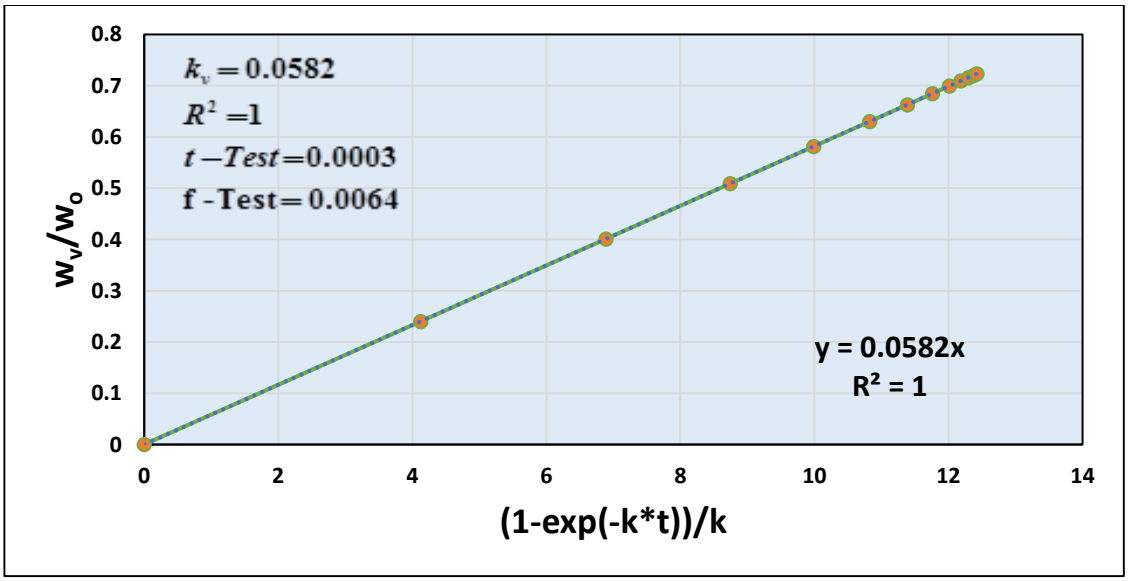
$k_v = 0.0582$
$R^2 = 1$
$t - Test = 0.0003$
f - Test = 0.0064
y = 0.0582x
R² = 1
w_v/w_o
(1-exp(-k*t))/k

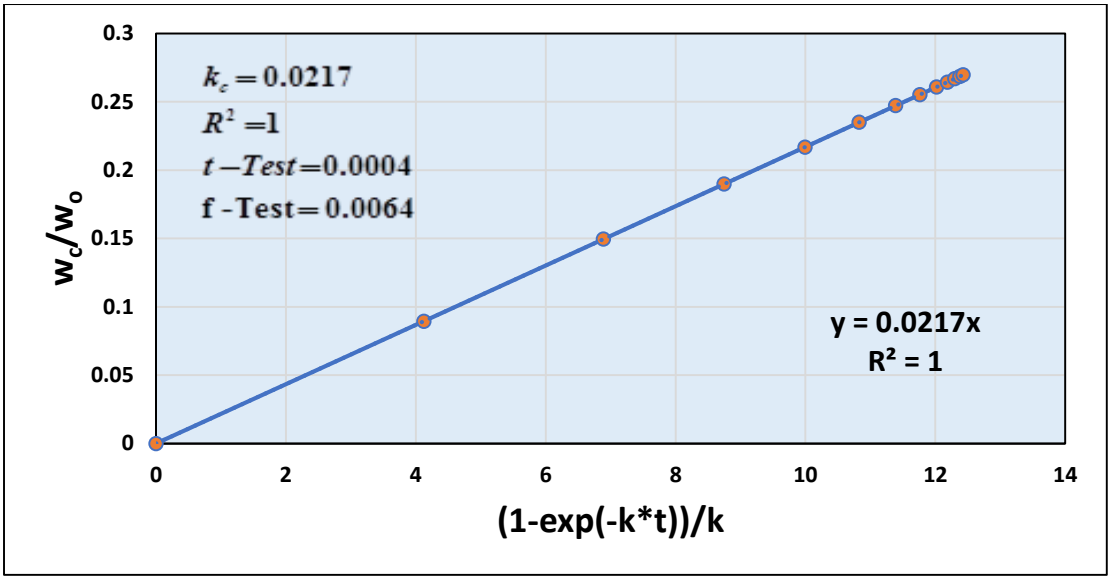
$k_c = 0.0217$
$R^2 = 1$
$t - Test = 0.0004$
f - Test = 0.0064
y = 0.0217x
R² = 1
w_c/w_o
(1-exp(-k*t))/k

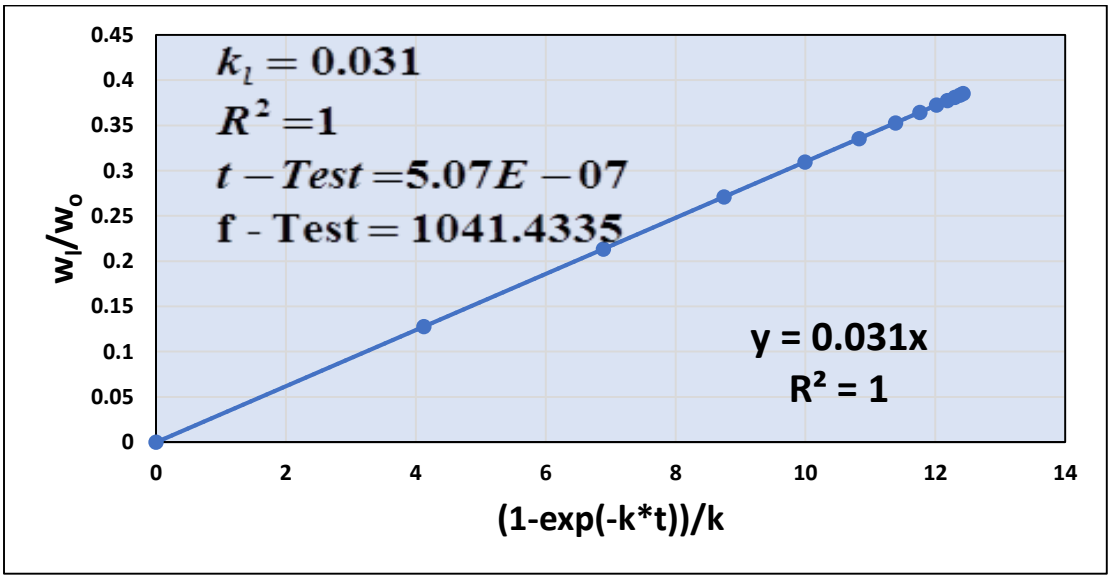
$k_l = 0.031$
$R^2 = 1$
$t - Test = 5.07E - 07$
f - Test = 1041.4335
y = 0.031x
R² = 1
w_l/w_o
(1-exp(-k*t))/k

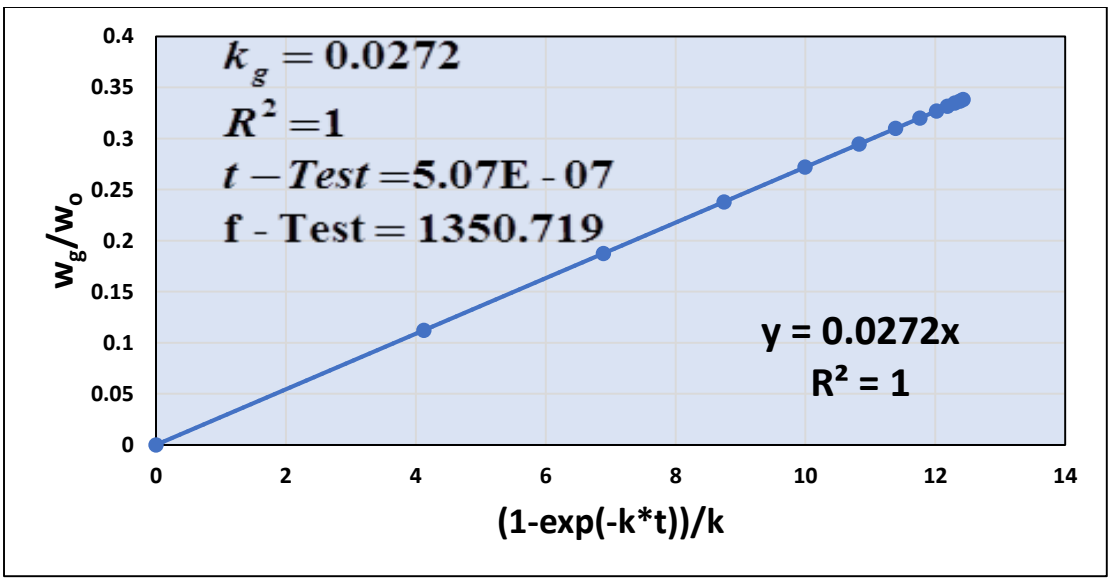
$k_g = 0.0272$
$R^2 = 1$
$t - Test = 5.07E - 07$
f - Test = 1350.719
y = 0.0272x
R² = 1
w_g/w_o
(1-exp(-k*t))/k

e) 1073 K

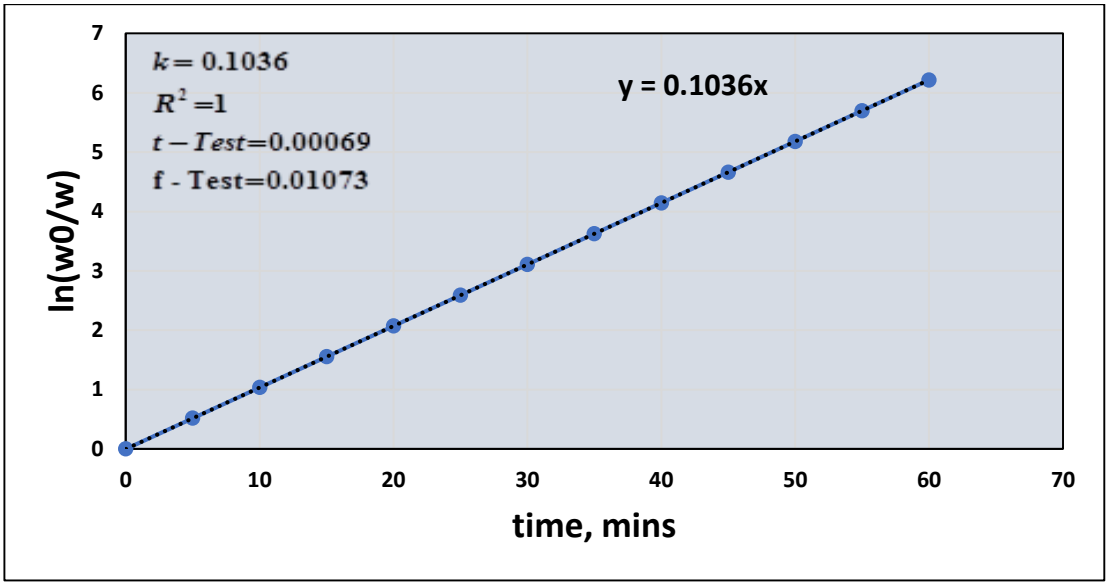
k = 0.1036
R² = 1
t − Test = 0.00069
f - Test = 0.01073
y = 0.1036x
ln(w0/w)
time, mins

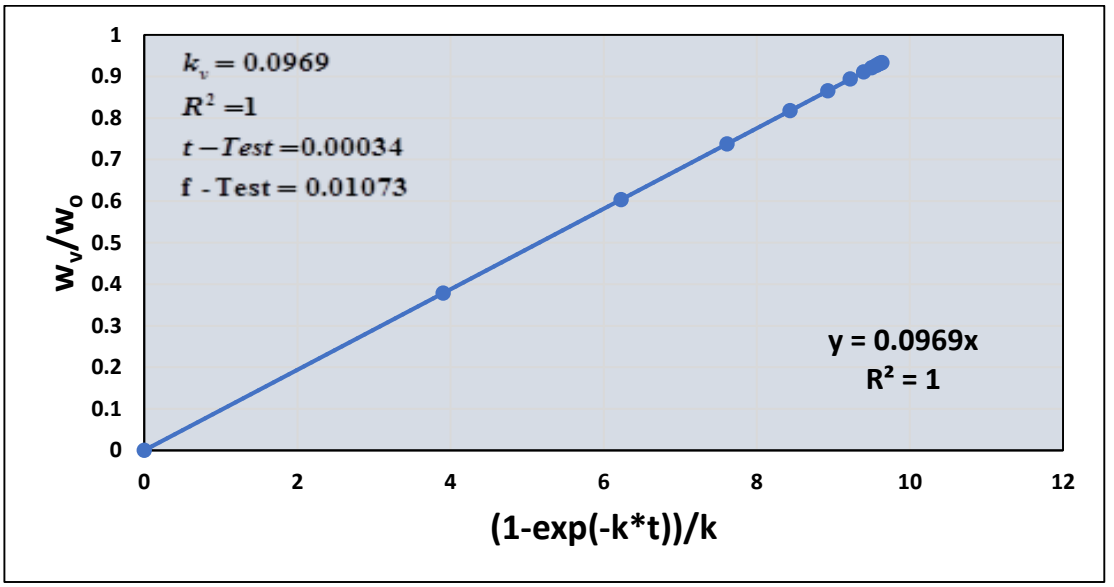
k_v = 0.0969
R² = 1
t − Test = 0.00034
f - Test = 0.01073
y = 0.0969x
R² = 1
w_v/w_o
(1-exp(-k*t))/k

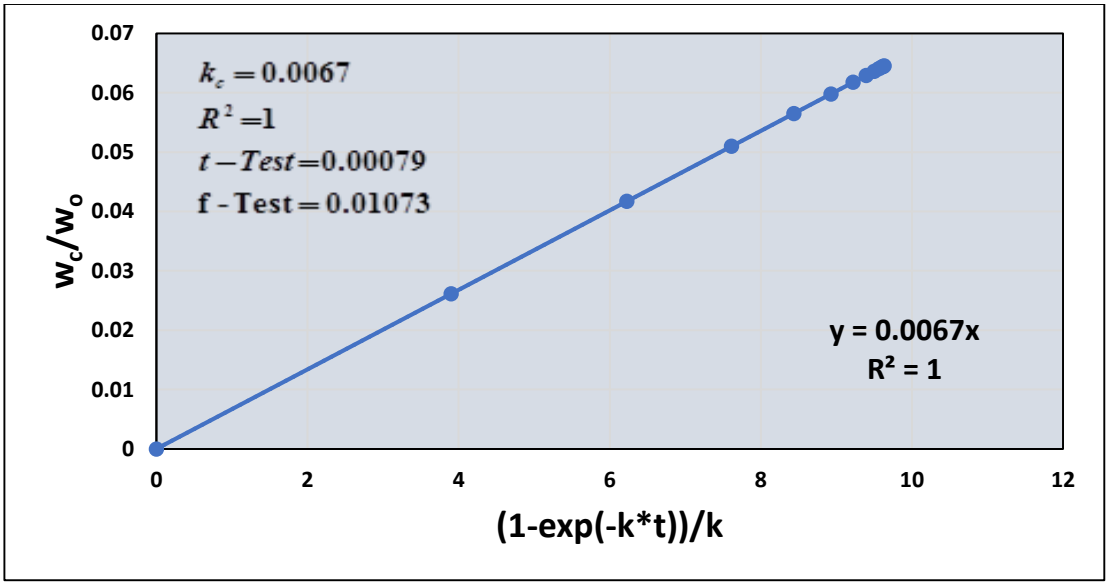
k_c = 0.0067
R² = 1
t − Test = 0.00079
f - Test = 0.01073
y = 0.0067x
R² = 1
w_c/w_o
(1-exp(-k*t))/k

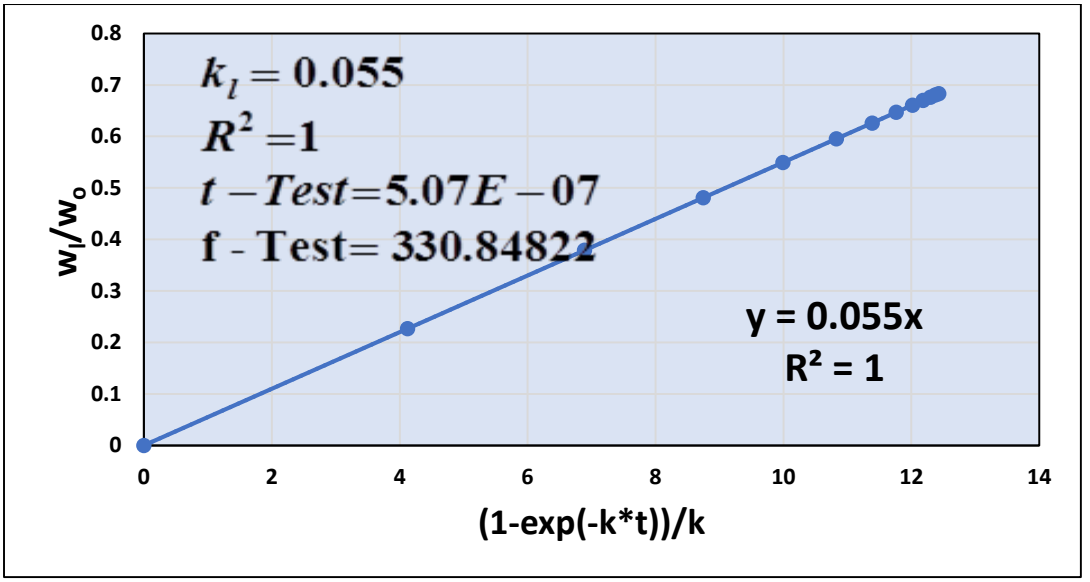
$k_l = 0.055$
$R^2 = 1$
$t - Test = 5.07E - 07$
f - Test= 330.84822
y = 0.055x
R² = 1
w_l/w_o
(1-exp(-k*t))/k

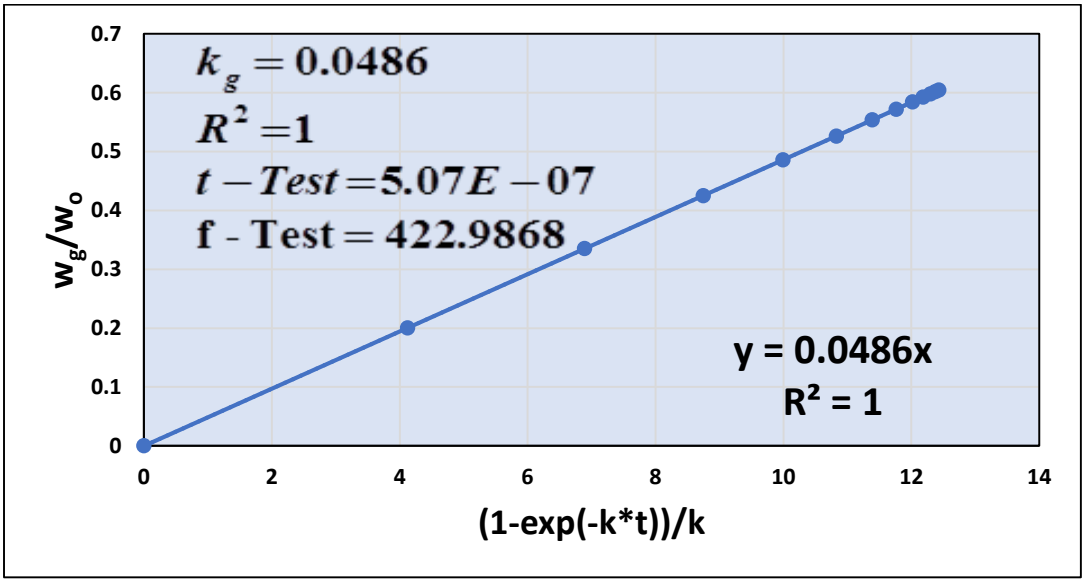
$k_g = 0.0486$
$R^2 = 1$
$t - Test = 5.07E - 07$
f - Test = 422.9868
y = 0.0486x
R² = 1
w_g/w_o
(1-exp(-k*t))/k

f) 1173K

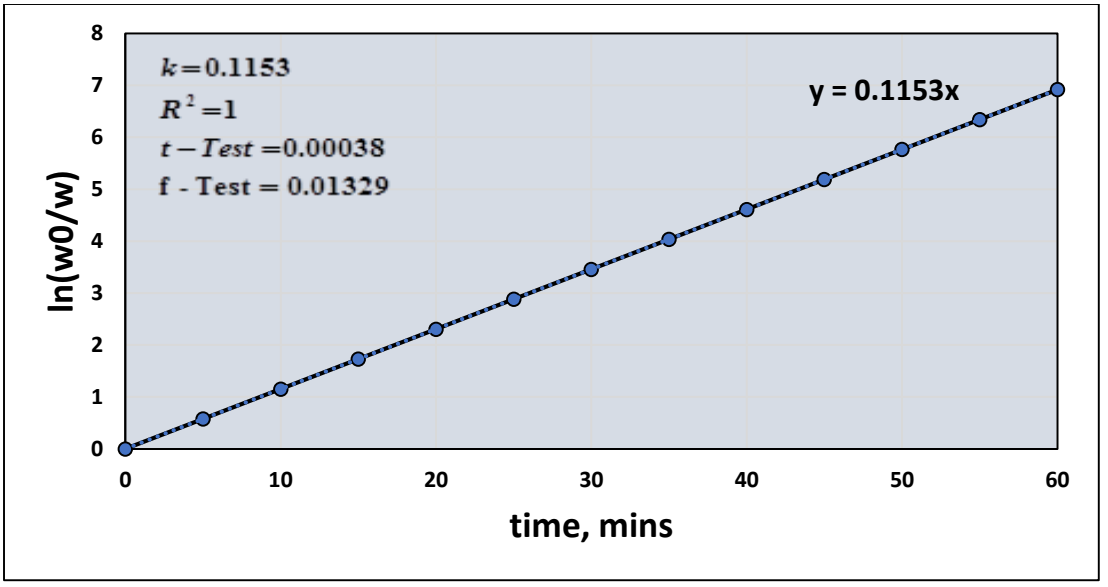
$k = 0.1153$
$R^2 = 1$
$t - Test = 0.00038$
f - Test = 0.01329
y = 0.1153x
ln(w0/w)
time, mins

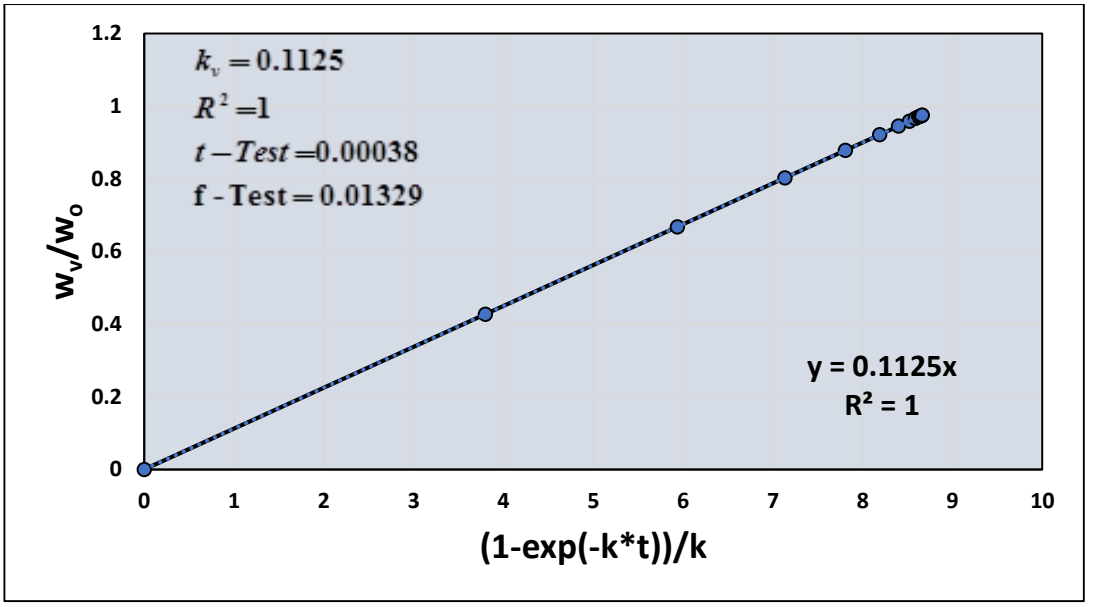
$k_v = 0.1125$
$R^2 = 1$
$t - Test = 0.00038$
f - Test = 0.01329
y = 0.1125x
R² = 1
w_v/w_o
(1-exp(-k*t))/k

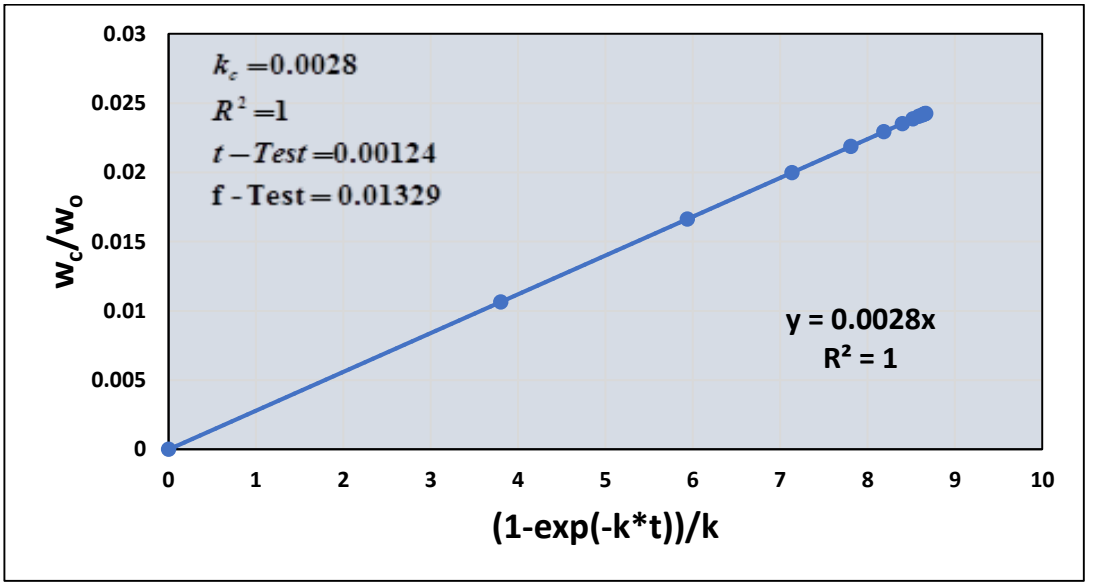
$k_c = 0.0028$
$R^2 = 1$
$t - Test = 0.00124$
f - Test = 0.01329
y = 0.0028x
R² = 1
w_c/w_o
(1-exp(-k*t))/k

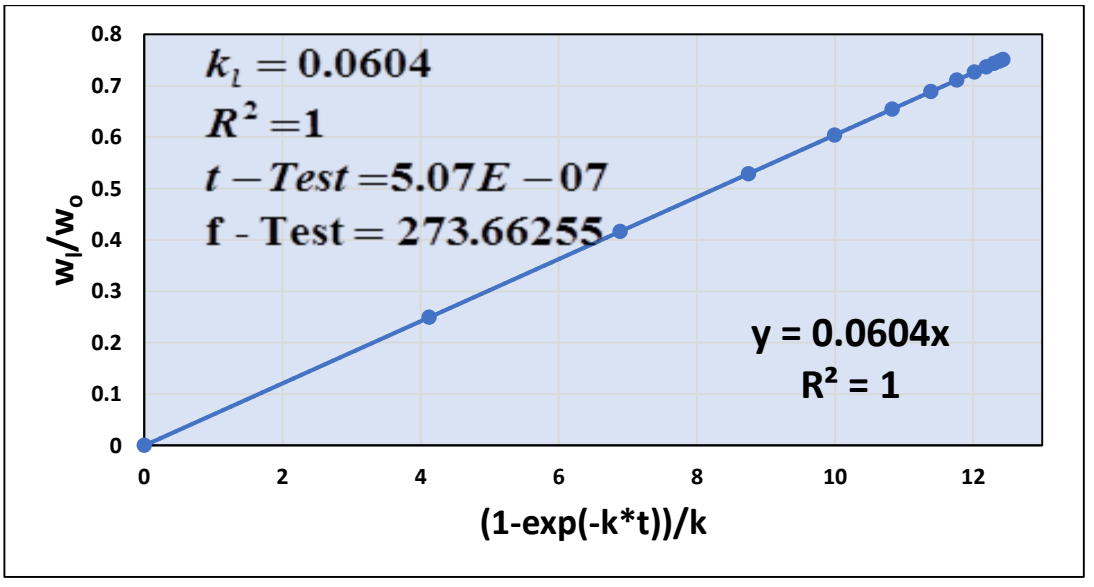
$k_l = 0.0604$
$R^2 = 1$
$t - Test = 5.07E-07$
f - Test = 273.66255
y = 0.0604x
R² = 1
w_l/w_o
(1-exp(-k*t))/k

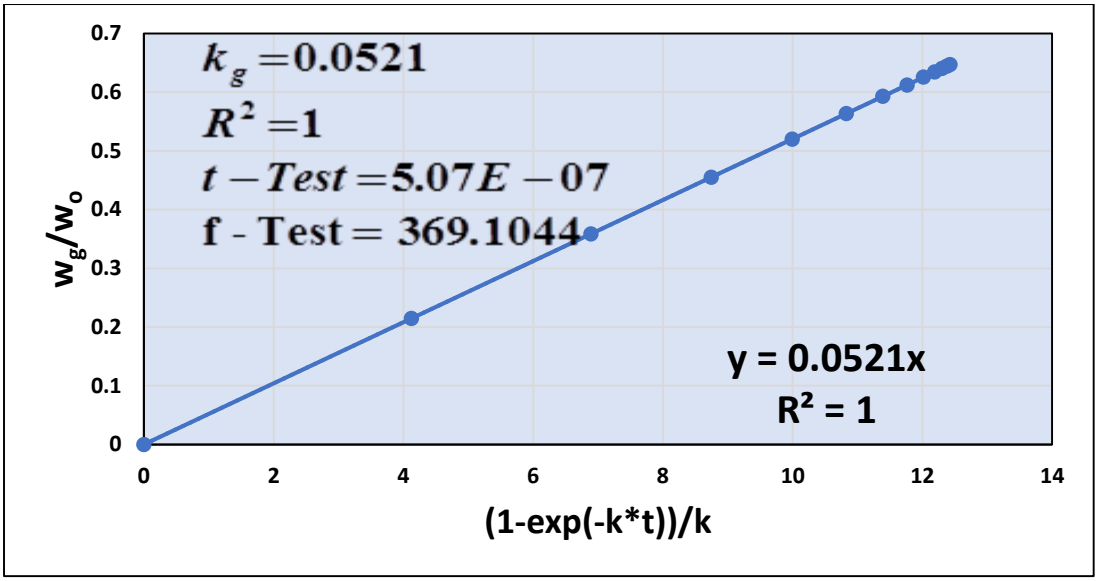

Figure 6.4. Plots of $\ln\left[\frac{w_o}{w}\right]$ vs time and $\frac{w_v}{w_0}$, $\frac{w_c}{w_0}$, $\frac{w_l}{w_0}$ and $\frac{w_g}{w_0}$ vs $(1-\exp[-k*t])/k$ at different temperature of jute wastes

a) 573 K

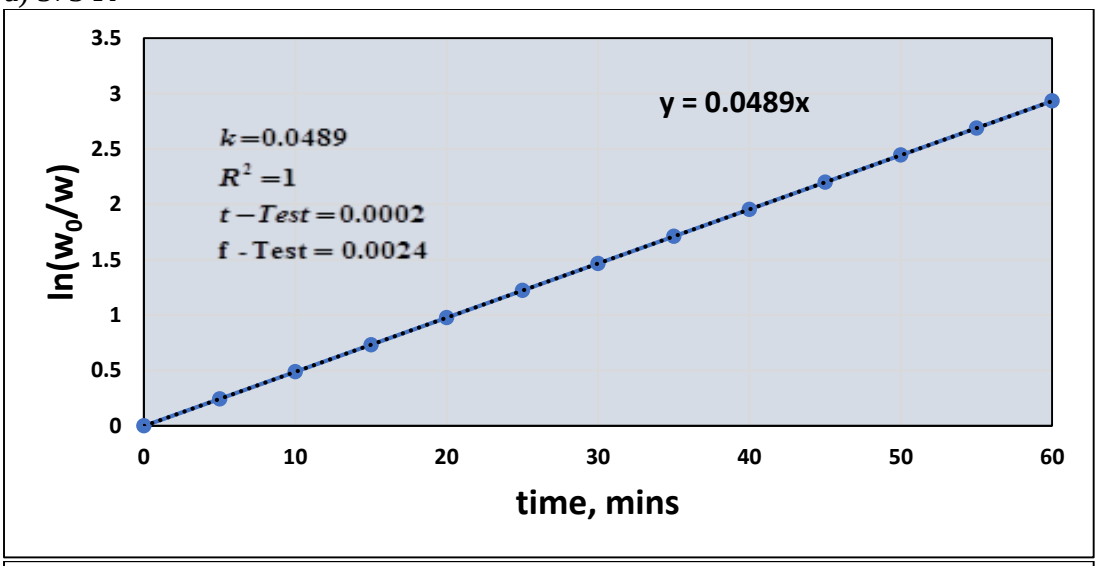

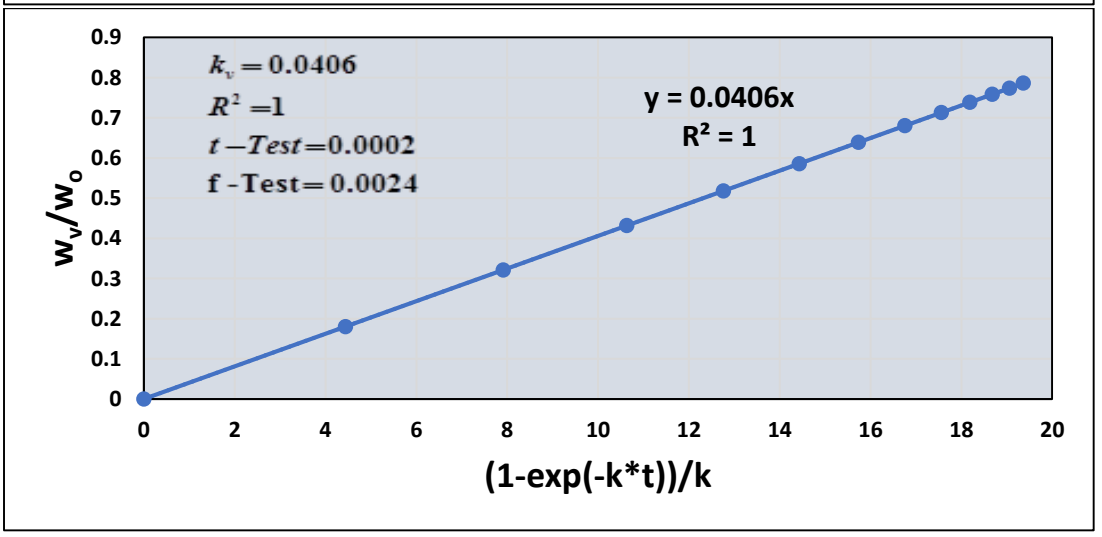

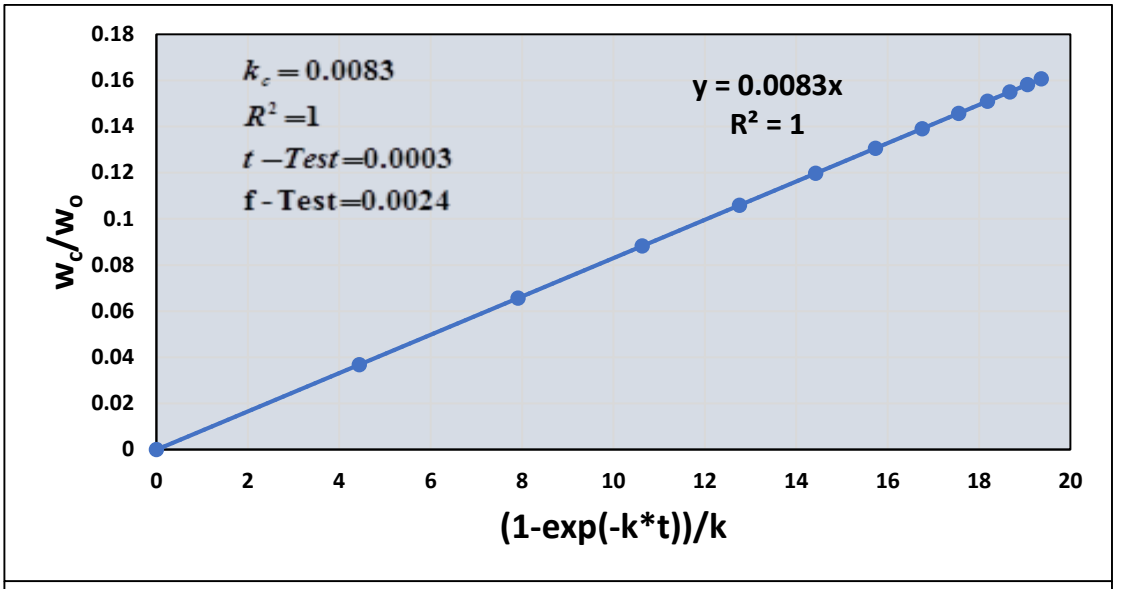
$k_c = 0.0083$
$R^2 = 1$
$t - Test = 0.0003$
f - Test=0.0024
y = 0.0083x
R² = 1
w_c/w_o
(1-exp(-k*t))/k

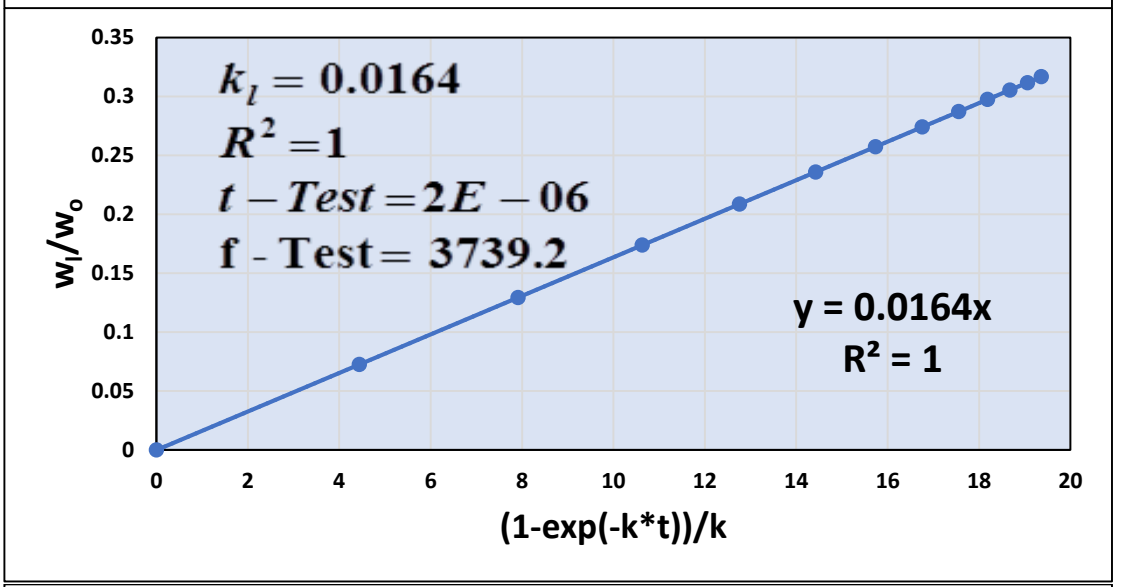
$k_l = 0.0164$
$R^2 = 1$
$t - Test = 2E - 06$
f - Test= 3739.2
y = 0.0164x
R² = 1
w_l/w_o
(1-exp(-k*t))/k

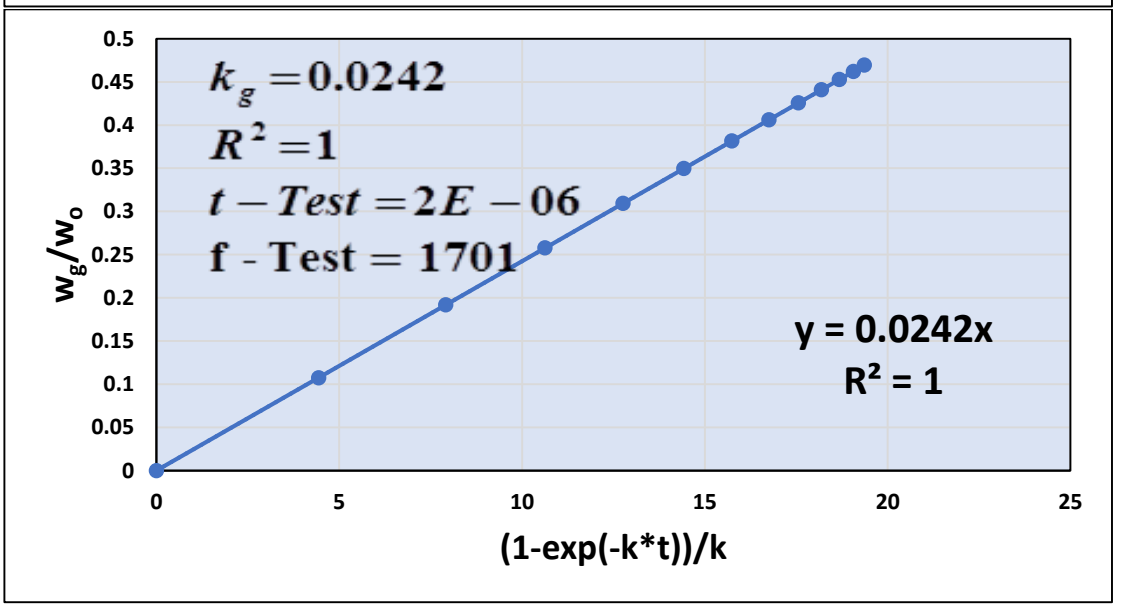
$k_g = 0.0242$
$R^2 = 1$
$t - Test = 2E - 06$
f - Test = 1701
y = 0.0242x
R² = 1
w_g/w_o
(1-exp(-k*t))/k

b) 673 K

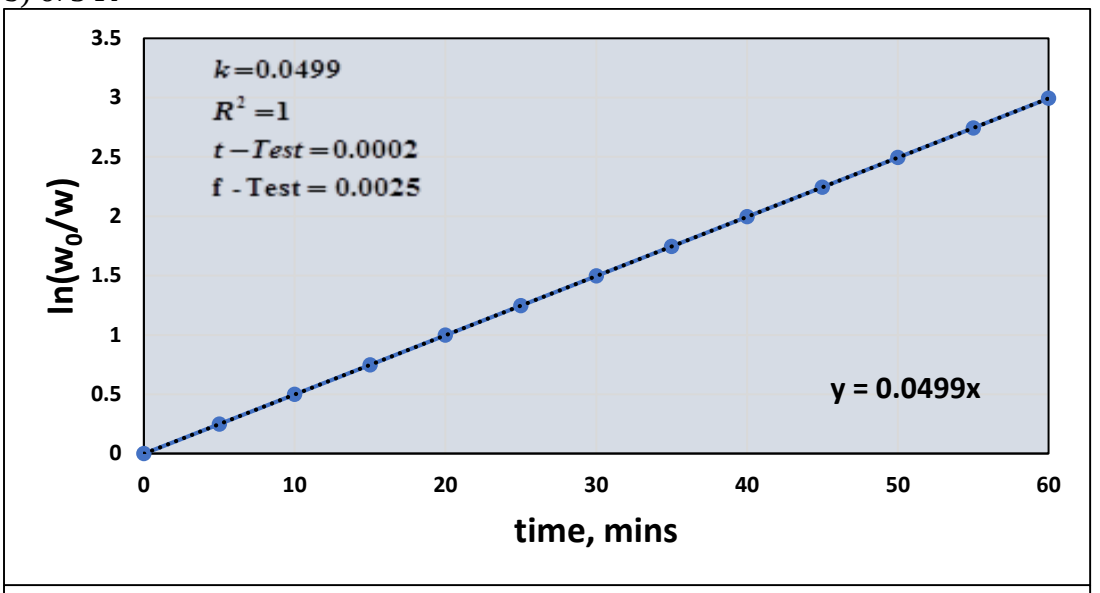
k=0.0499
R² =1
t−Test=0.0002
f -Test= 0.0025
y = 0.0499x
ln(w0/w)
time, mins

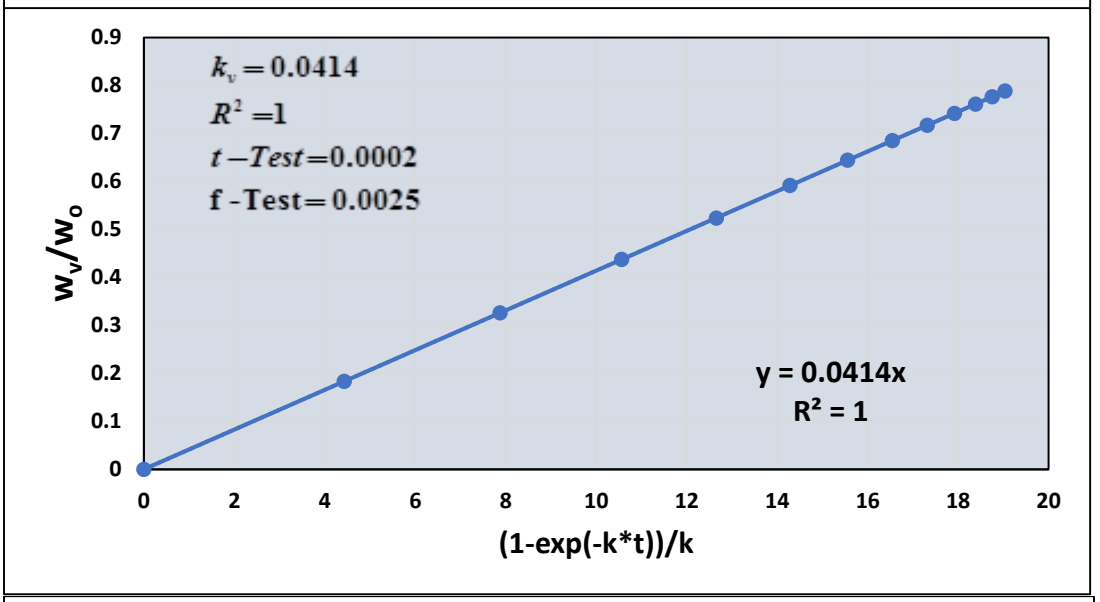
kv = 0.0414
R² =1
t−Test=0.0002
f -Test= 0.0025
y = 0.0414x
R² = 1
wv/wo
(1-exp(-k*t))/k

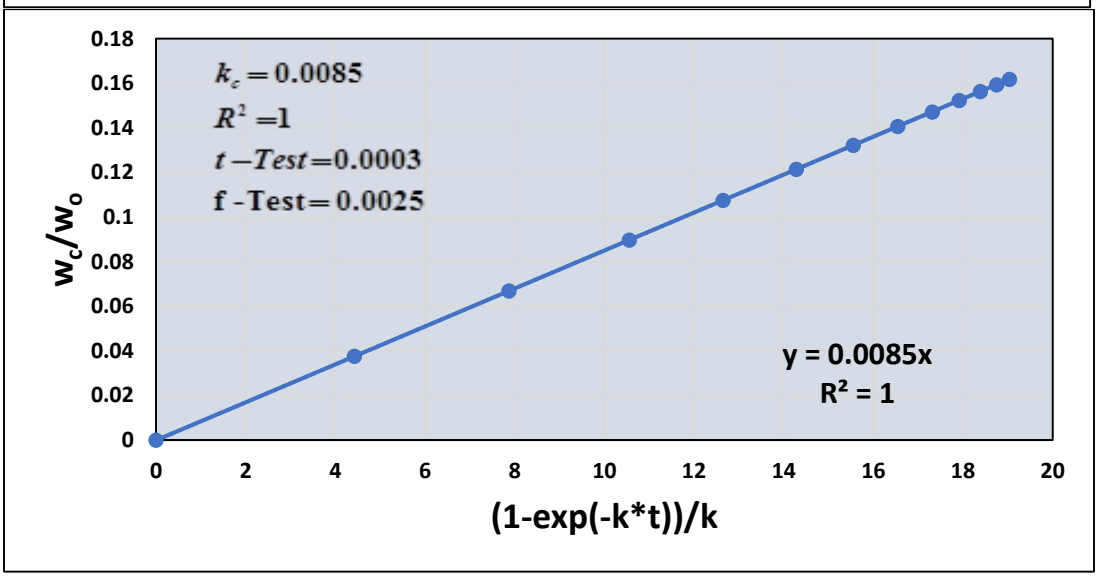
kc = 0.0085
R² =1
t−Test=0.0003
f -Test= 0.0025
y = 0.0085x
R² = 1
wc/wo
(1-exp(-k*t))/k

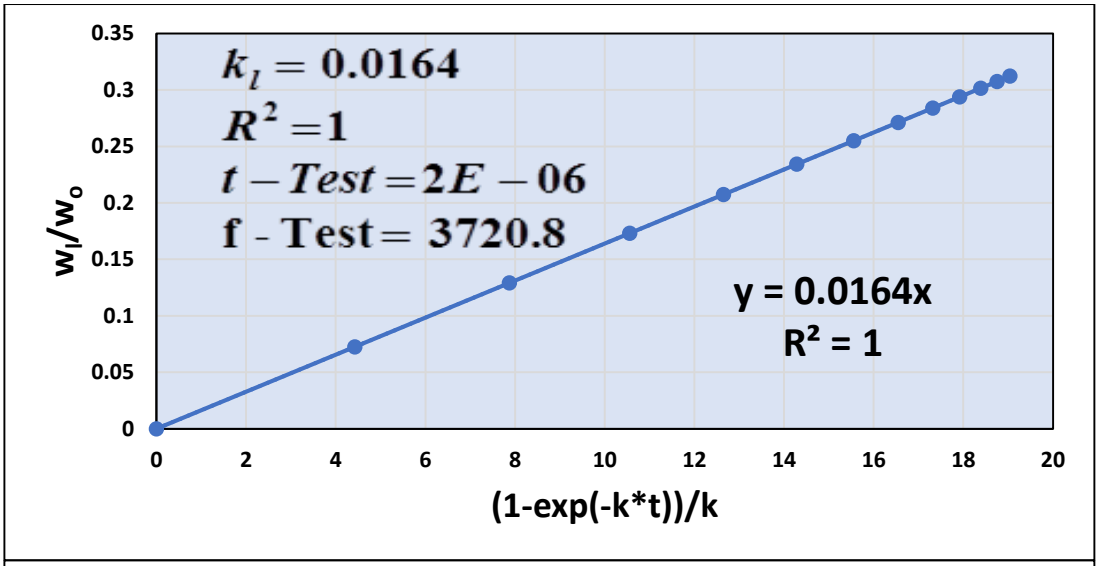
$k_l = 0.0164$
$R^2 = 1$
$t - Test = 2E - 06$
f - Test = 3720.8
y = 0.0164x
R² = 1
w_l/w_o
(1-exp(-k*t))/k

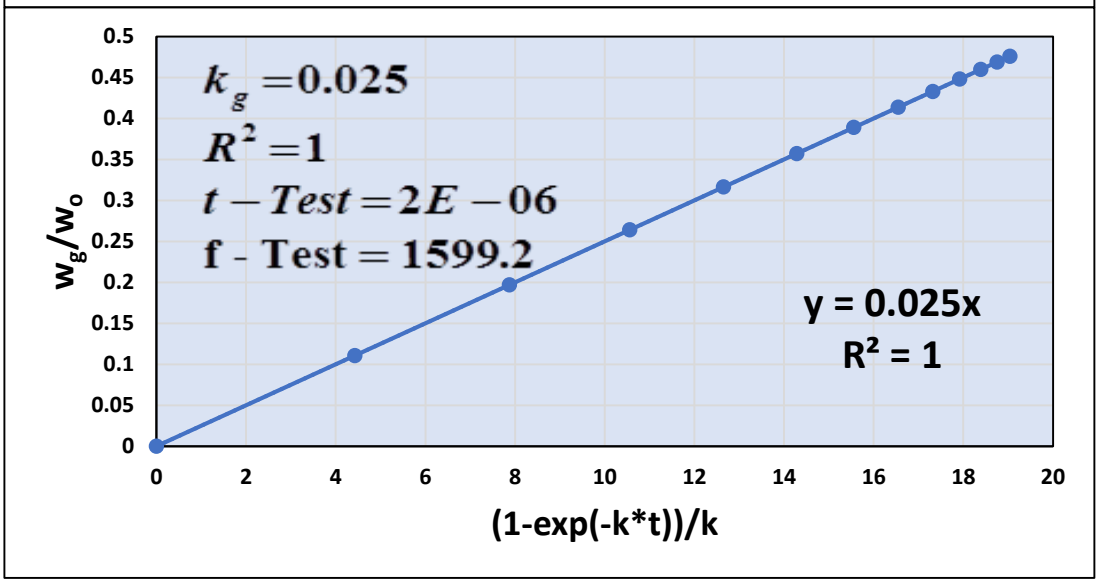
$k_g = 0.025$
$R^2 = 1$
$t - Test = 2E - 06$
f - Test = 1599.2
y = 0.025x
R² = 1
w_g/w_o
(1-exp(-k*t))/k

c) 773 K

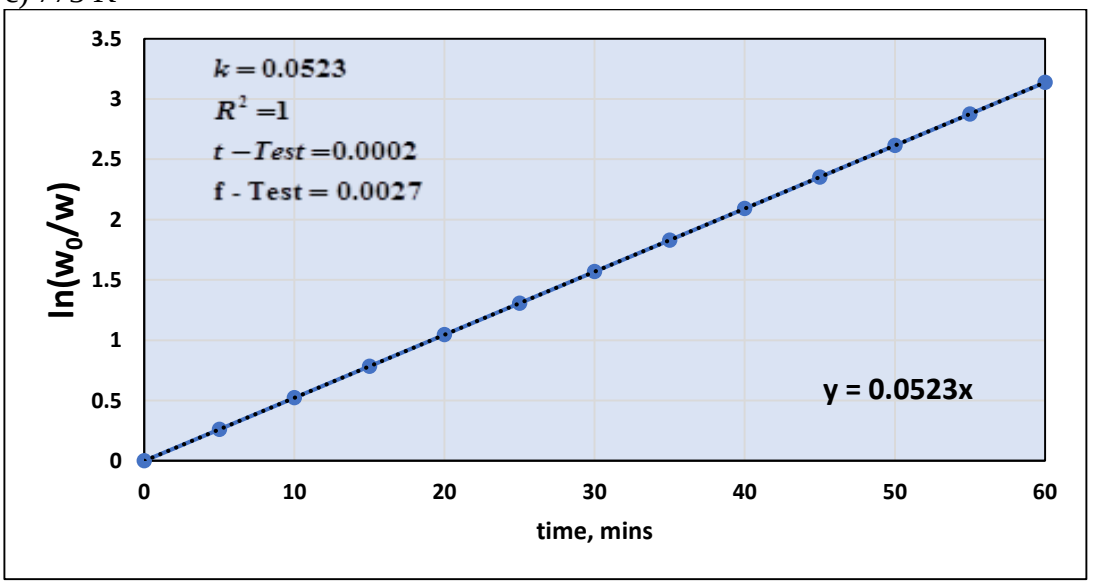
$k = 0.0523$
$R^2 = 1$
$t - Test = 0.0002$
f - Test = 0.0027
y = 0.0523x
$\ln(w_0/w)$
time, mins

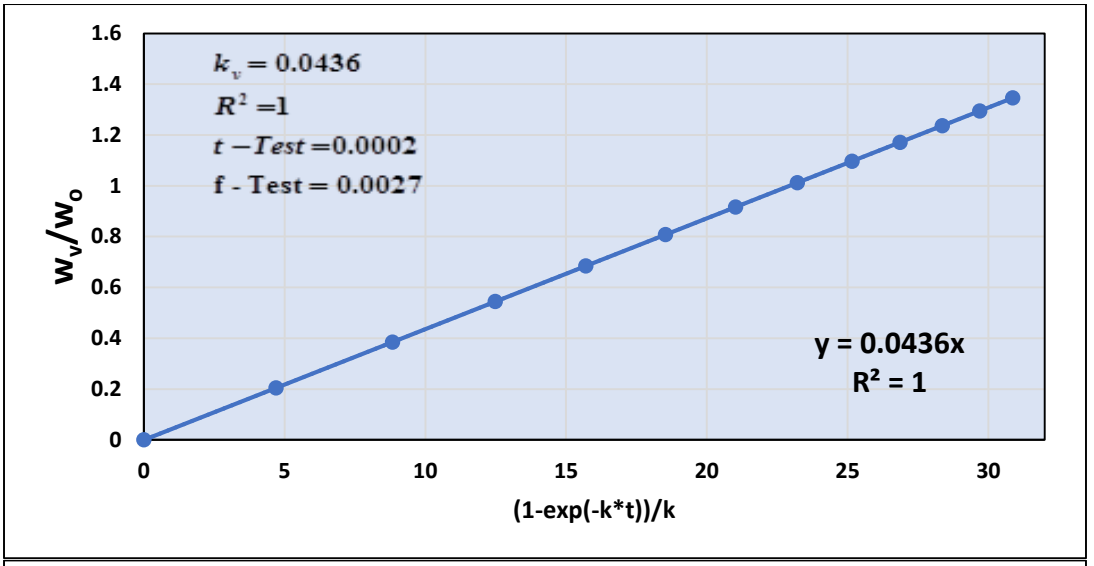
$k_v = 0.0436$
$R^2 = 1$
$t - Test = 0.0002$
f - Test = 0.0027
y = 0.0436x
R² = 1
w_v/w_o
(1-exp(-k*t))/k

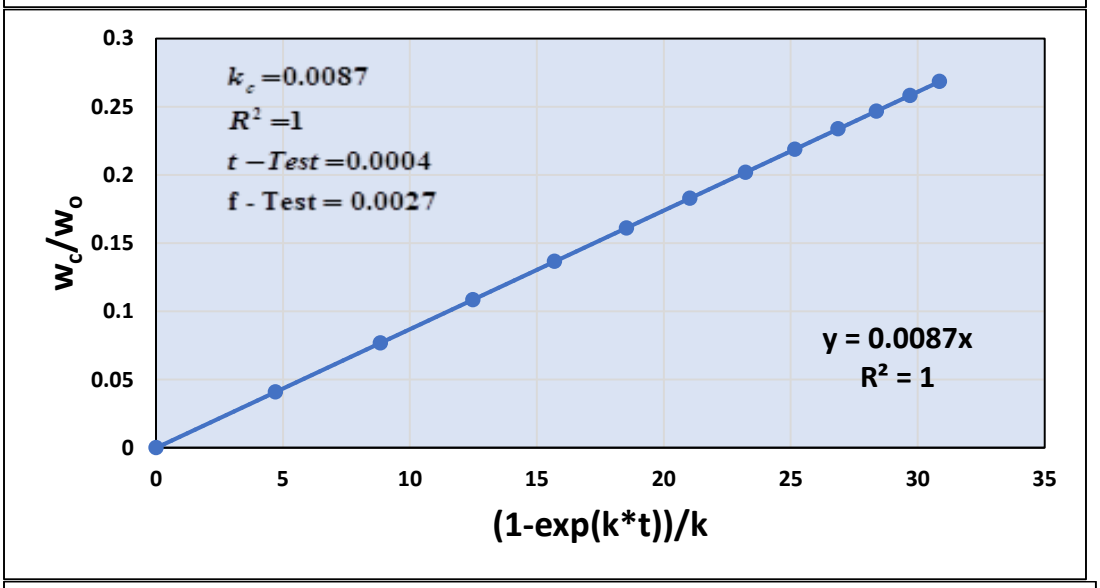
$k_c = 0.0087$
$R^2 = 1$
$t - Test = 0.0004$
f - Test = 0.0027
y = 0.0087x
R² = 1
w_c/w_o
(1-exp(k*t))/k

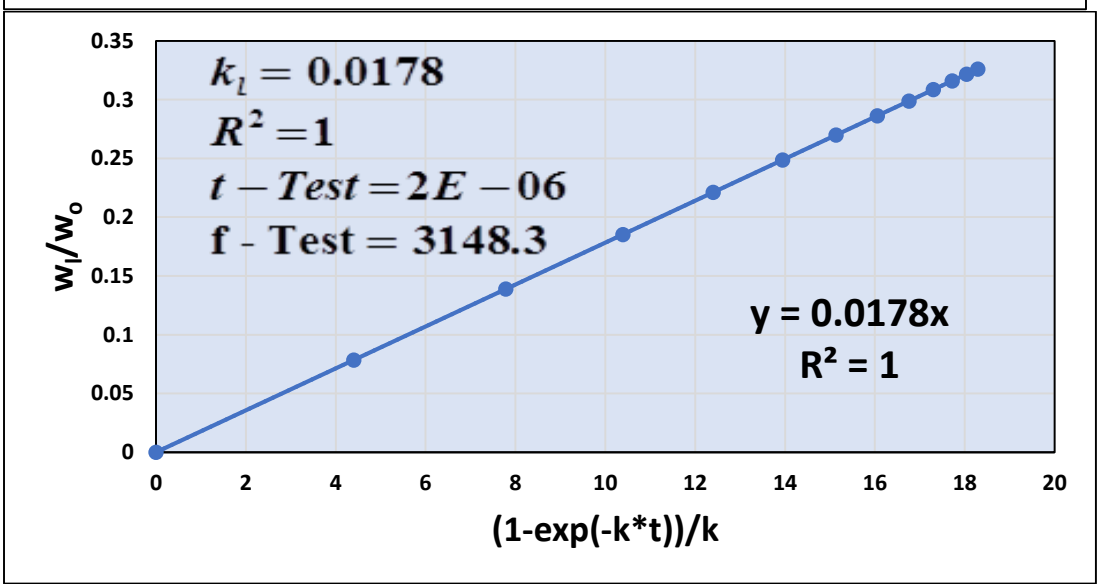
$k_l = 0.0178$
$R^2 = 1$
$t - Test = 2E - 06$
f - Test = 3148.3
y = 0.0178x
R² = 1
w_l/w_o
(1-exp(-k*t))/k

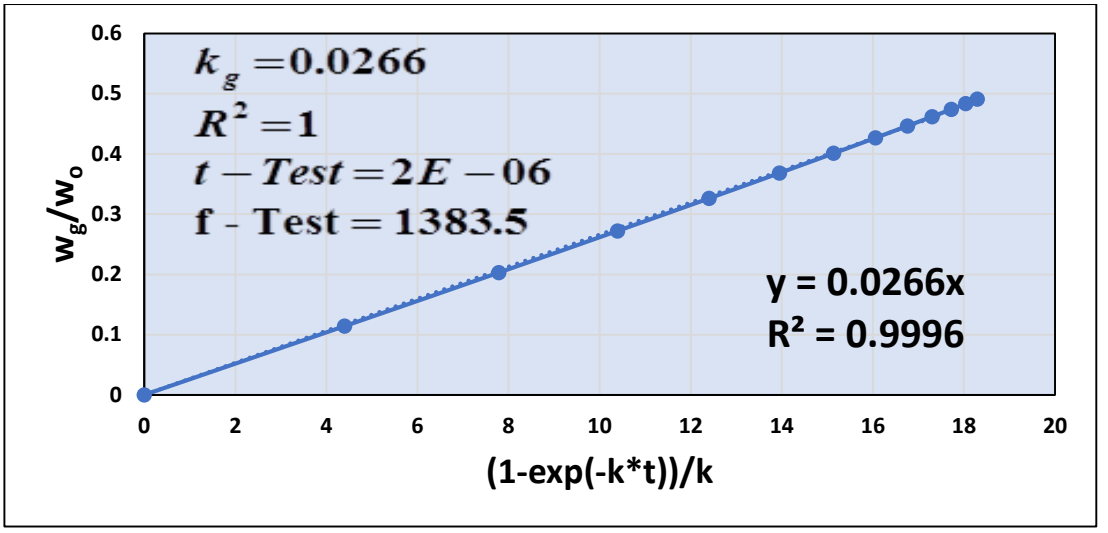
$k_g = 0.0266$
$R^2 = 1$
$t - Test = 2E - 06$
f - Test = 1383.5
y = 0.0266x
R² = 0.9996
w_g/w_o
(1-exp(-k*t))/k

d) 873K

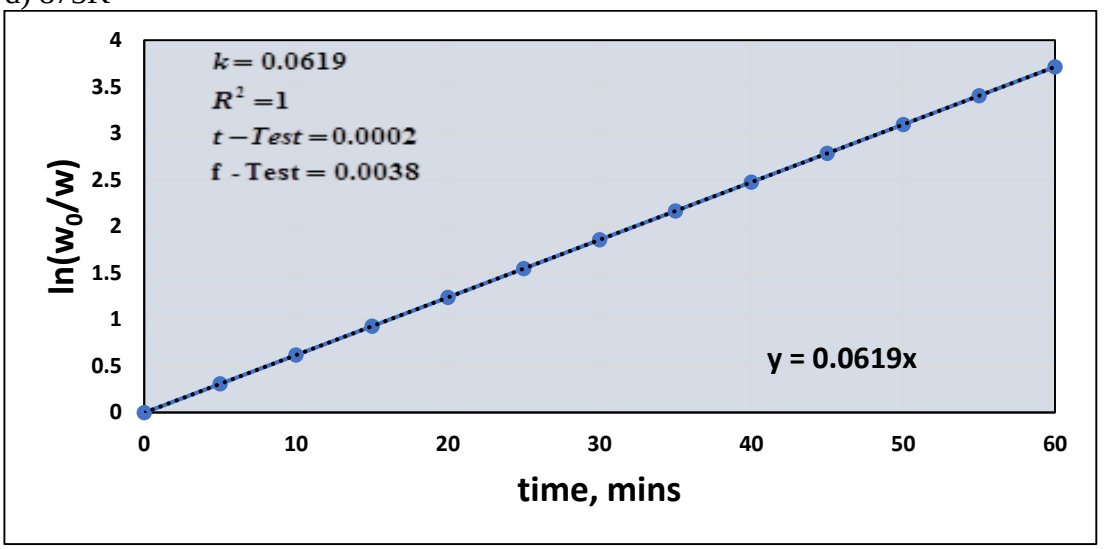
$k = 0.0619$
$R^2 = 1$
$t - Test = 0.0002$
f - Test = 0.0038
y = 0.0619x
ln(w0/w)
time, mins

d) 873 K

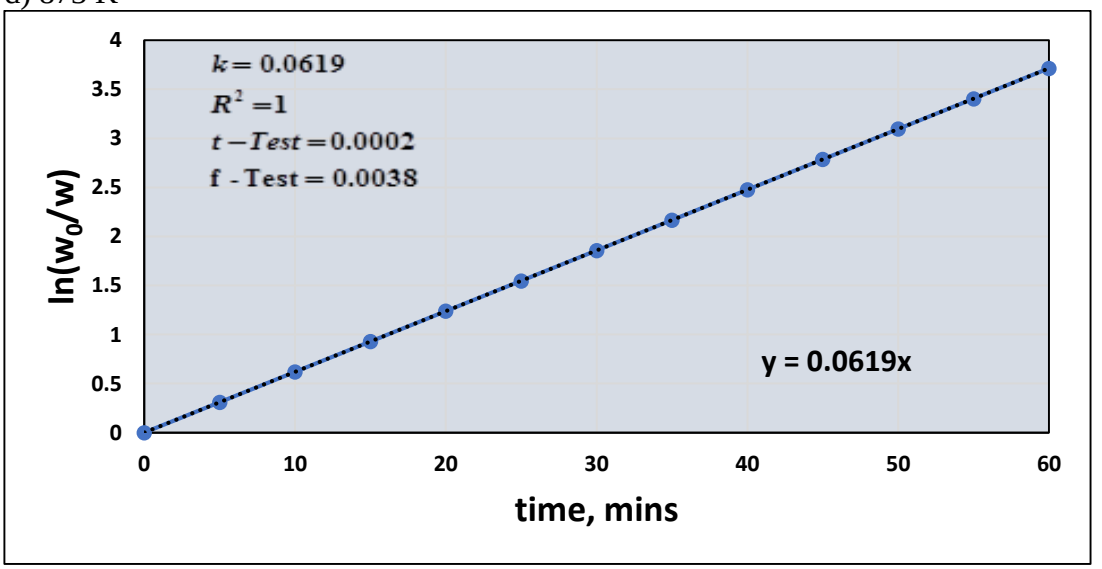
$k = 0.0619$
$R^2 = 1$
$t - Test = 0.0002$
f - Test = 0.0038
y = 0.0619x
ln(w0/w)
time, mins

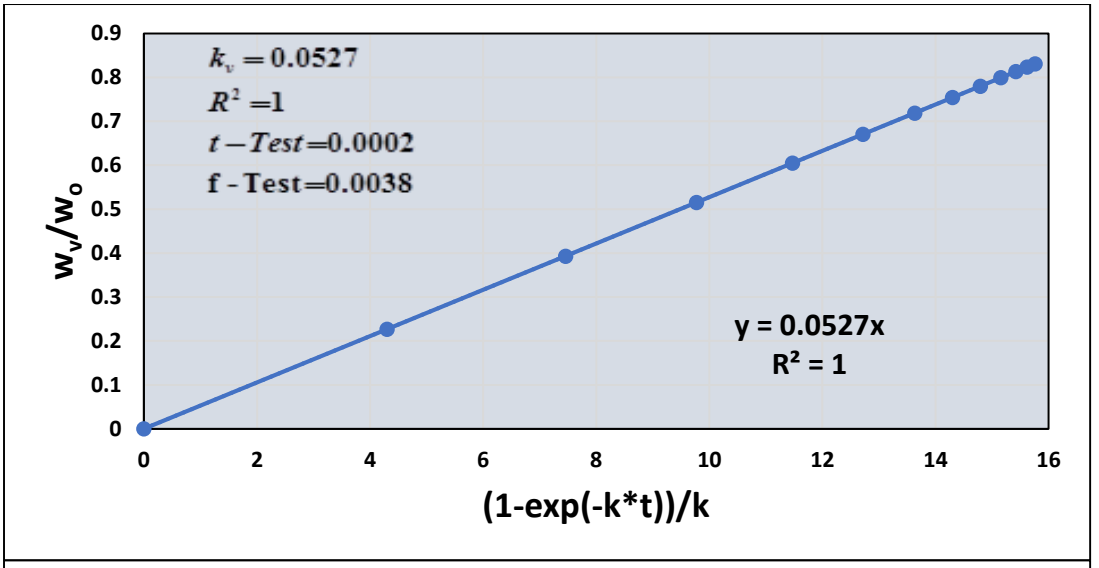
$k_v = 0.0527$
$R^2 = 1$
$t - Test = 0.0002$
f - Test = 0.0038
y = 0.0527x
R² = 1
w_v/w_o
(1-exp(-k*t))/k

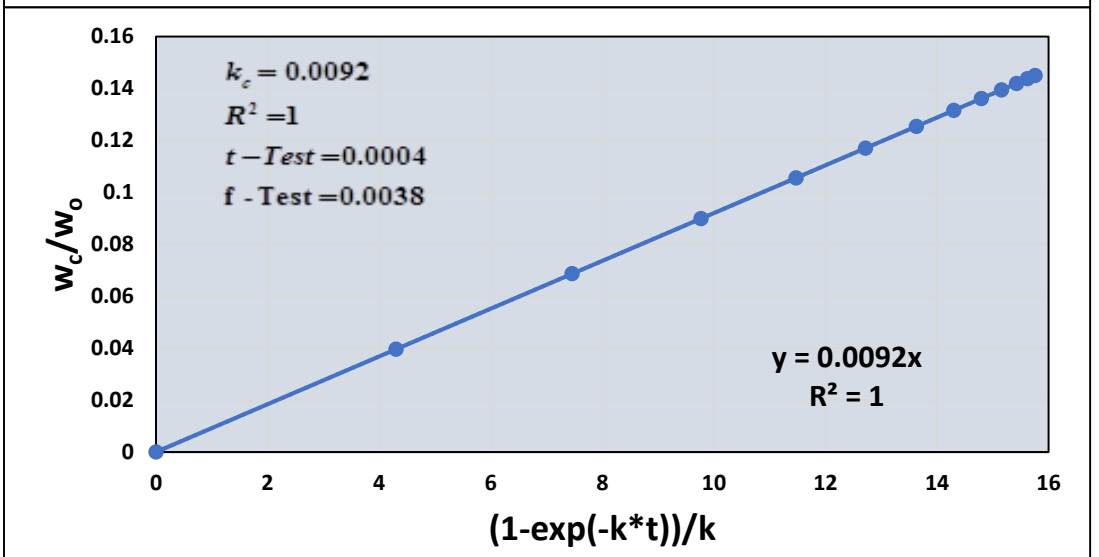
$k_c = 0.0092$
$R^2 = 1$
$t - Test = 0.0004$
f - Test = 0.0038
y = 0.0092x
R² = 1
w_c/w_o
(1-exp(-k*t))/k

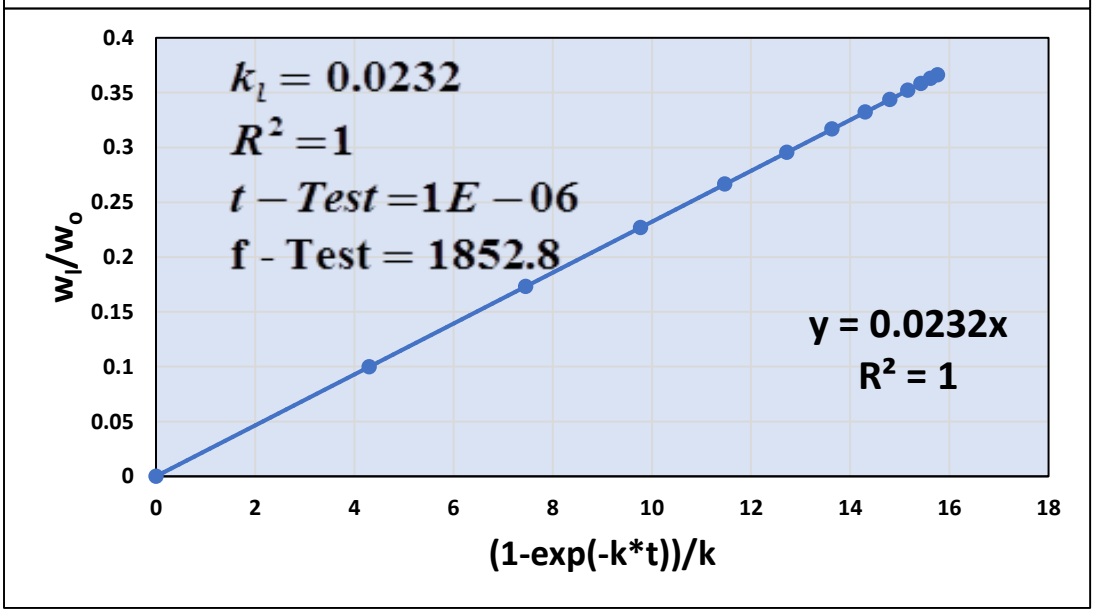
$k_l = 0.0232$
$R^2 = 1$
$t - Test = 1E-06$
f - Test = 1852.8
y = 0.0232x
R² = 1
w_l/w_o
(1-exp(-k*t))/k

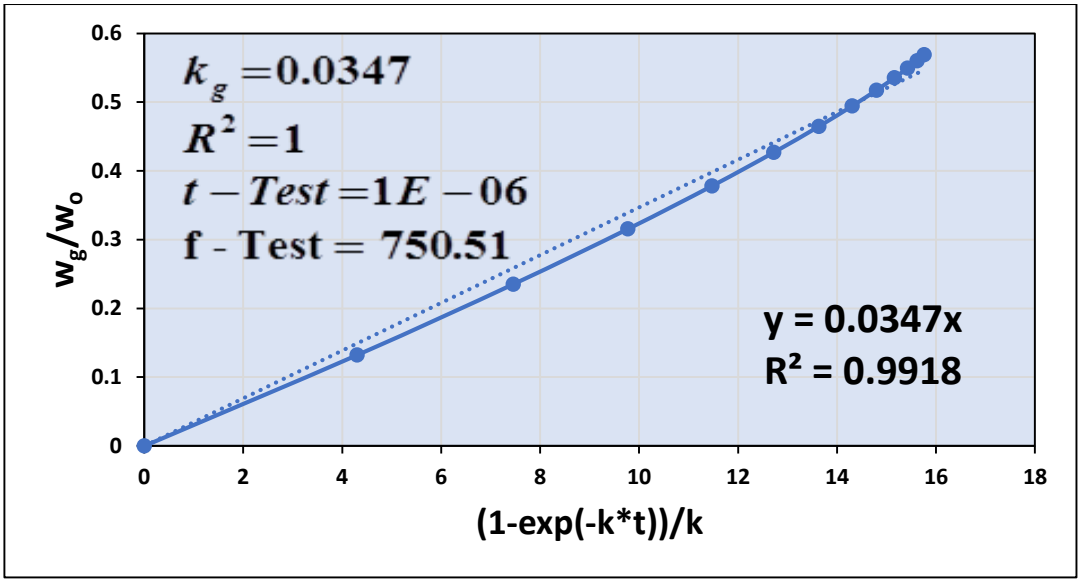
$k_g = 0.0347$
$R^2 = 1$
$t - Test = 1E-06$
f - Test = 750.51
y = 0.0347x
R² = 0.9918
w_g/w_o
(1-exp(-k*t))/k

e) 973K

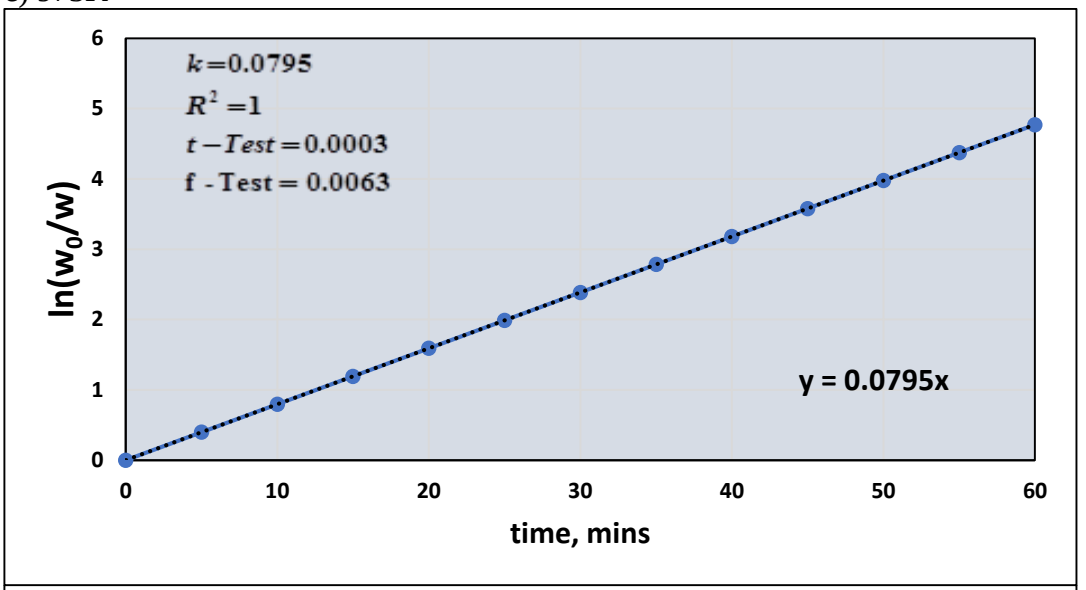
$k = 0.0795$
$R^2 = 1$
$t - Test = 0.0003$
f - Test = 0.0063
y = 0.0795x
ln(w0/w)
time, mins

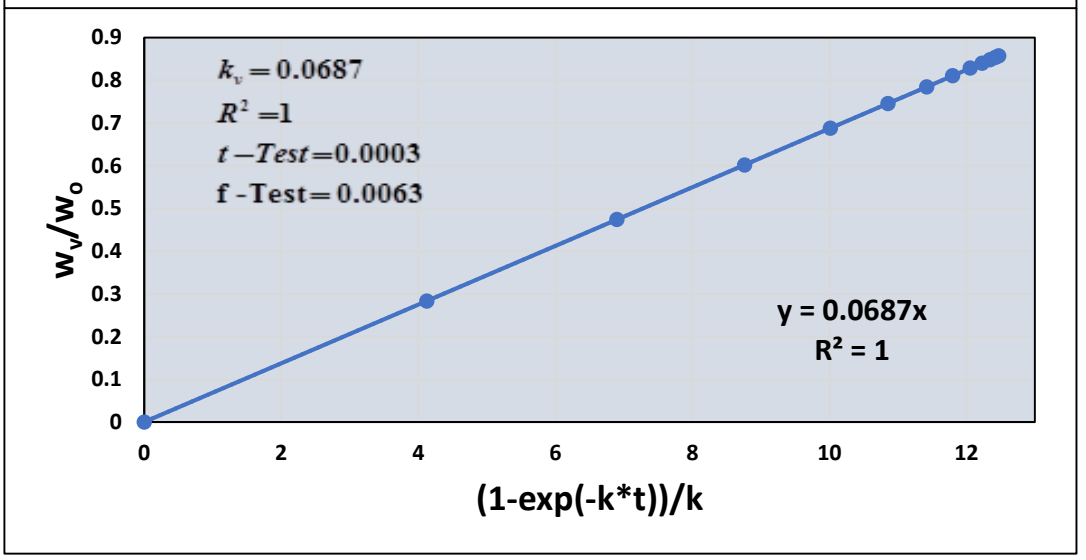
$k_v = 0.0687$
$R^2 = 1$
$t - Test = 0.0003$
f - Test = 0.0063
y = 0.0687x
R² = 1
w_v/w_o
(1-exp(-k*t))/k

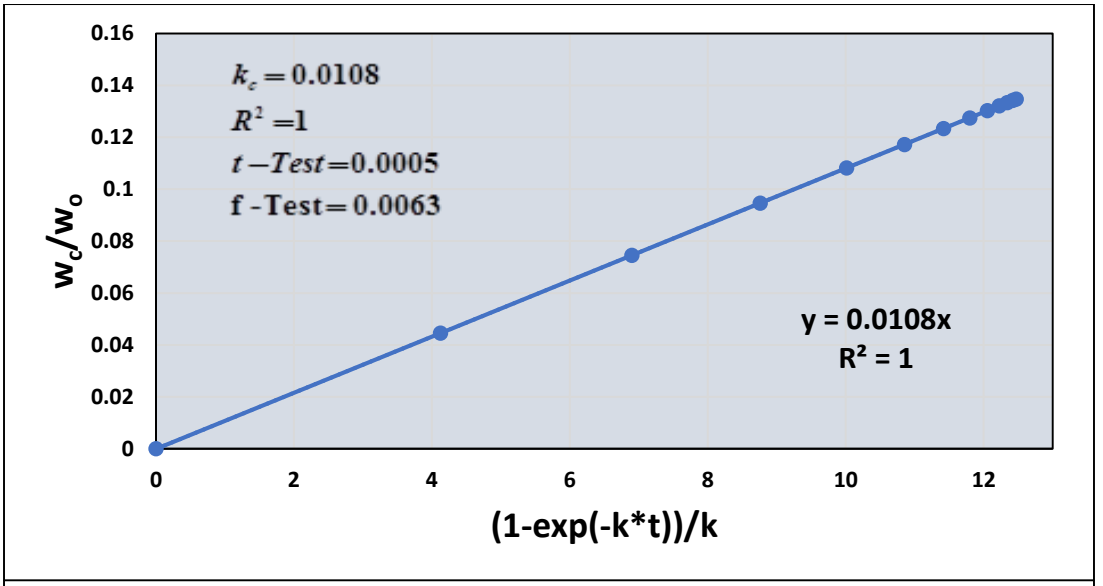
$k_c = 0.0108$
$R^2 = 1$
$t - Test = 0.0005$
f - Test = 0.0063
y = 0.0108x
R² = 1
w_c/w_o
(1-exp(-k*t))/k

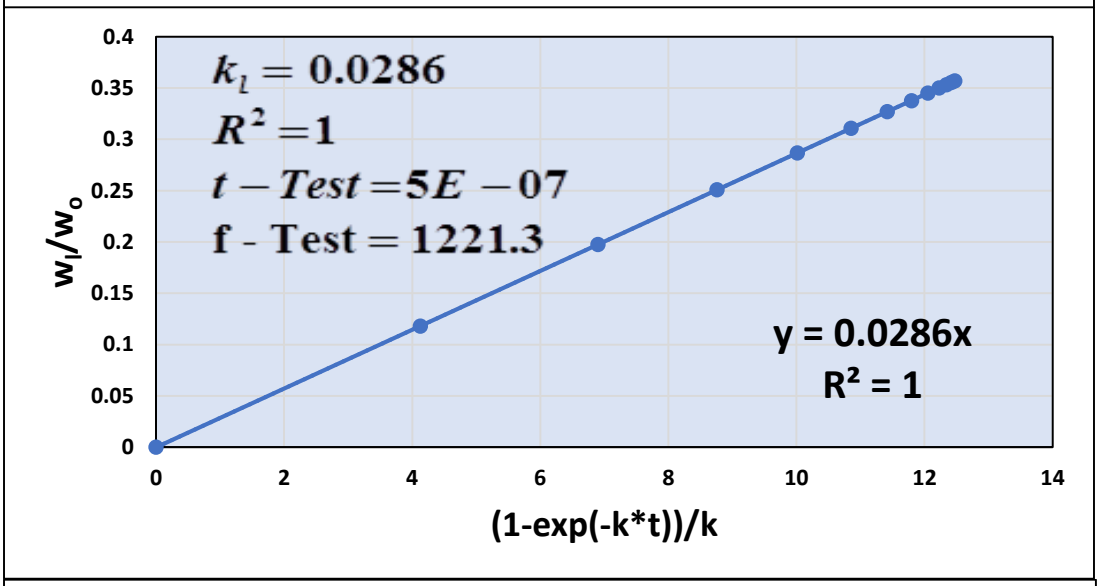
$k_l = 0.0286$
$R^2 = 1$
$t - Test = 5E-07$
f - Test = 1221.3
y = 0.0286x
R² = 1
w_l/w_o
(1-exp(-k*t))/k

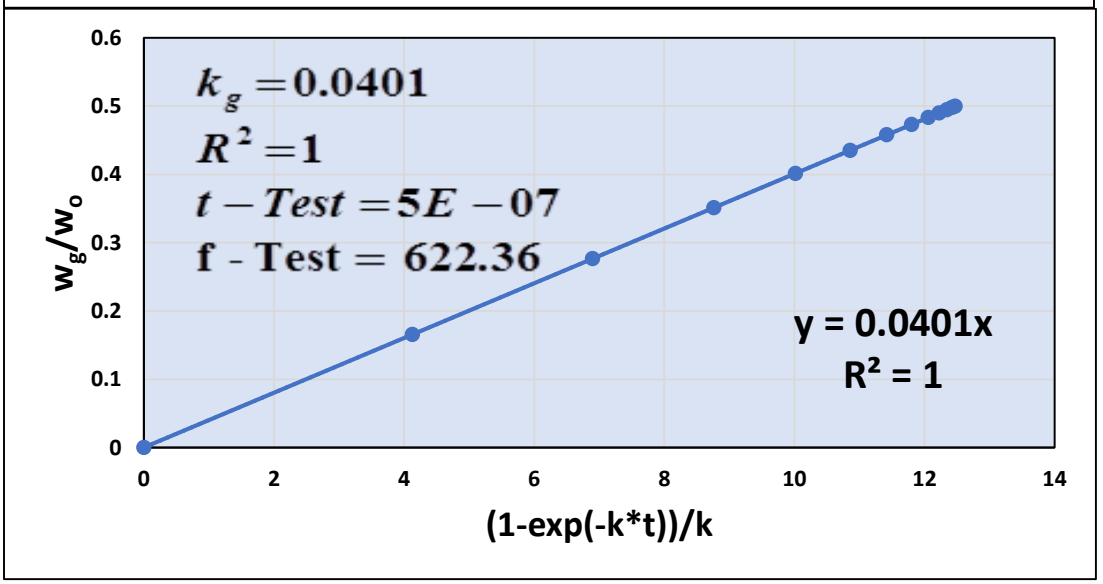
$k_g = 0.0401$
$R^2 = 1$
$t - Test = 5E-07$
f - Test = 622.36
y = 0.0401x
R² = 1
w_g/w_o
(1-exp(-k*t))/k

f) 1073 K

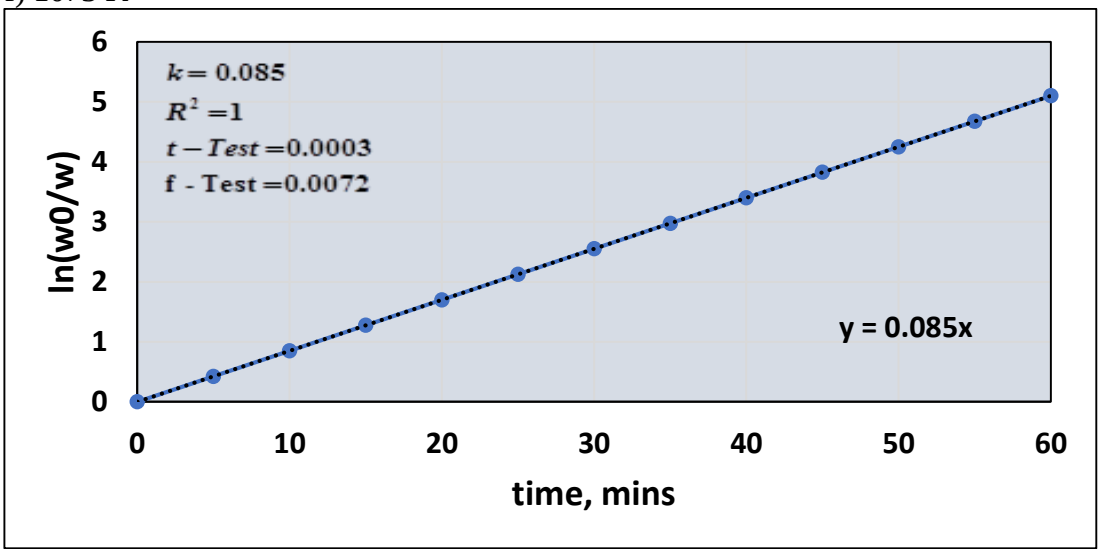
k = 0.085
R² = 1
t − Test = 0.0003
f - Test = 0.0072
y = 0.085x
ln(w0/w)
time, mins

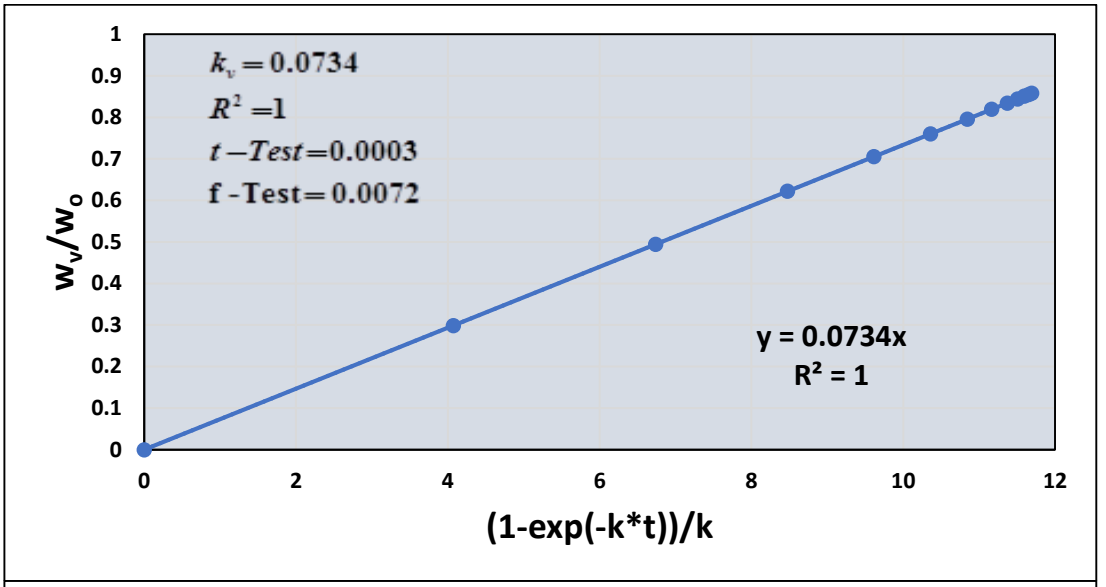
k_v = 0.0734
R² = 1
t − Test = 0.0003
f - Test = 0.0072
y = 0.0734x
R² = 1
w_v/w_o
(1-exp(-k*t))/k

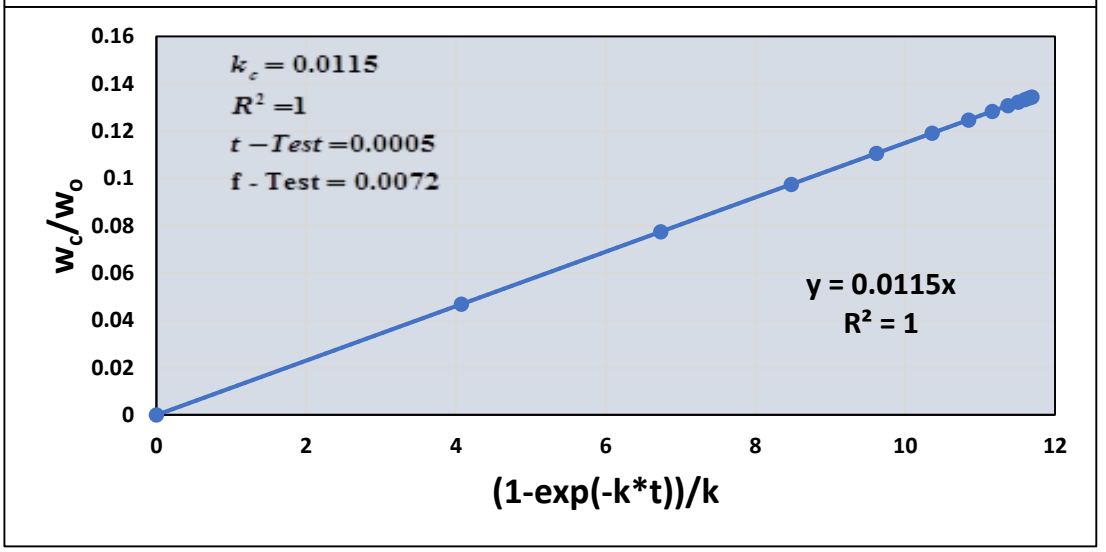
k_c = 0.0115
R² = 1
t − Test = 0.0005
f - Test = 0.0072
y = 0.0115x
R² = 1
w_c/w_o
(1-exp(-k*t))/k

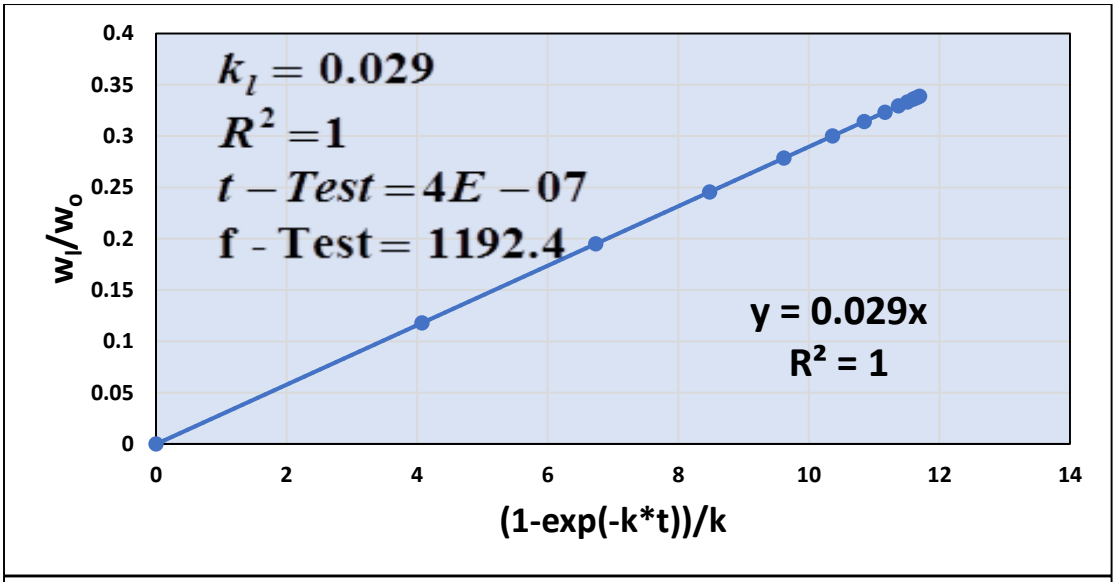
$k_l = 0.029$
$R^2 = 1$
$t - Test = 4E - 07$
f - Test = 1192.4
y = 0.029x
R² = 1
w_l/w_o
(1-exp(-k*t))/k

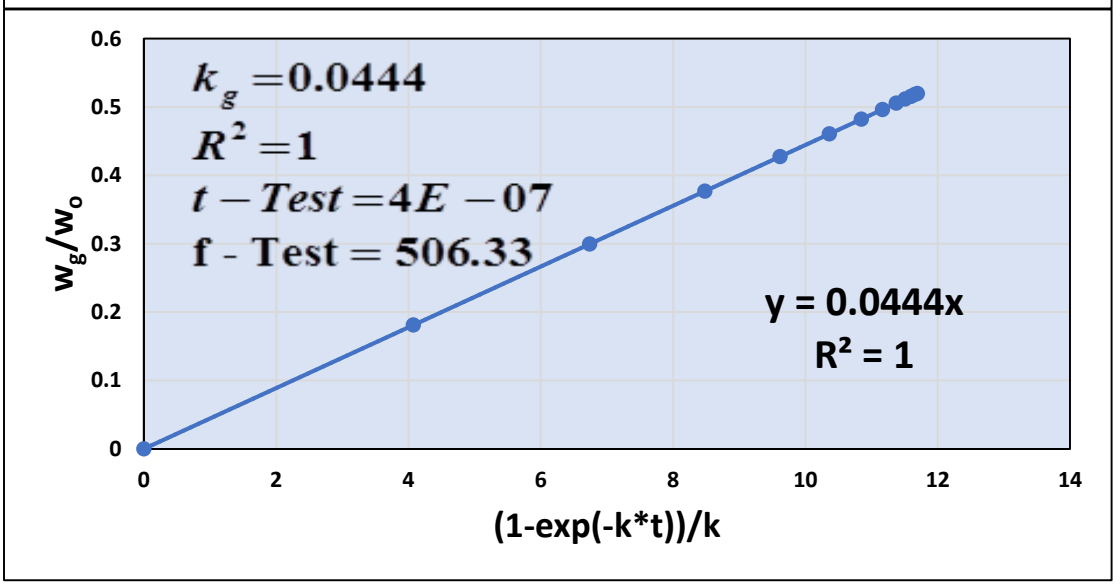
$k_g = 0.0444$
$R^2 = 1$
$t - Test = 4E - 07$
f - Test = 506.33
y = 0.0444x
R² = 1
w_g/w_o
(1-exp(-k*t))/k

g) 1173K

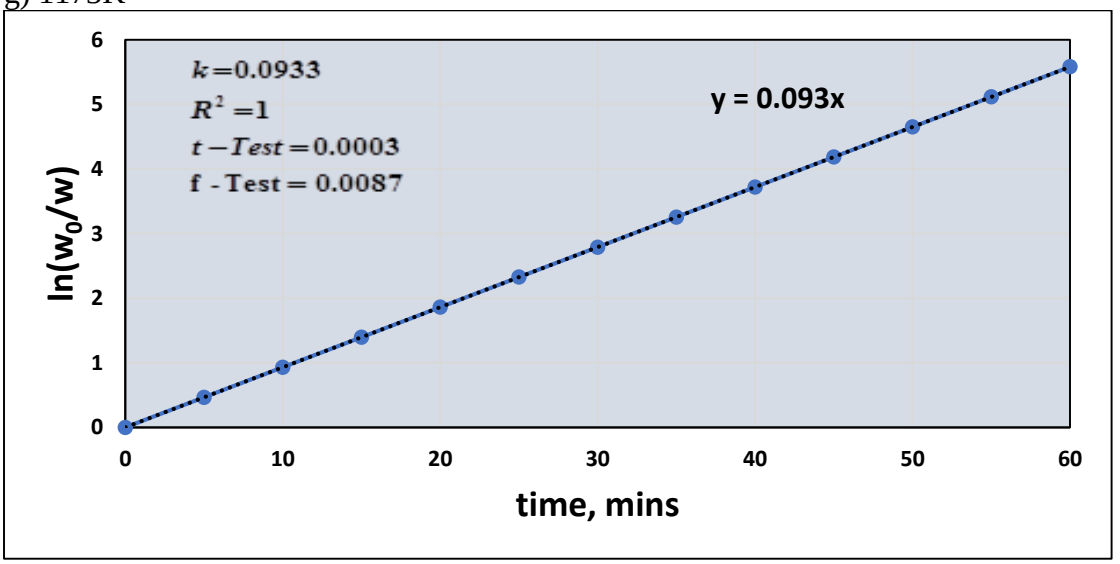
$k = 0.0933$
$R^2 = 1$
$t - Test = 0.0003$
f - Test = 0.0087
y = 0.093x
$\ln(w_0/w)$
time, mins

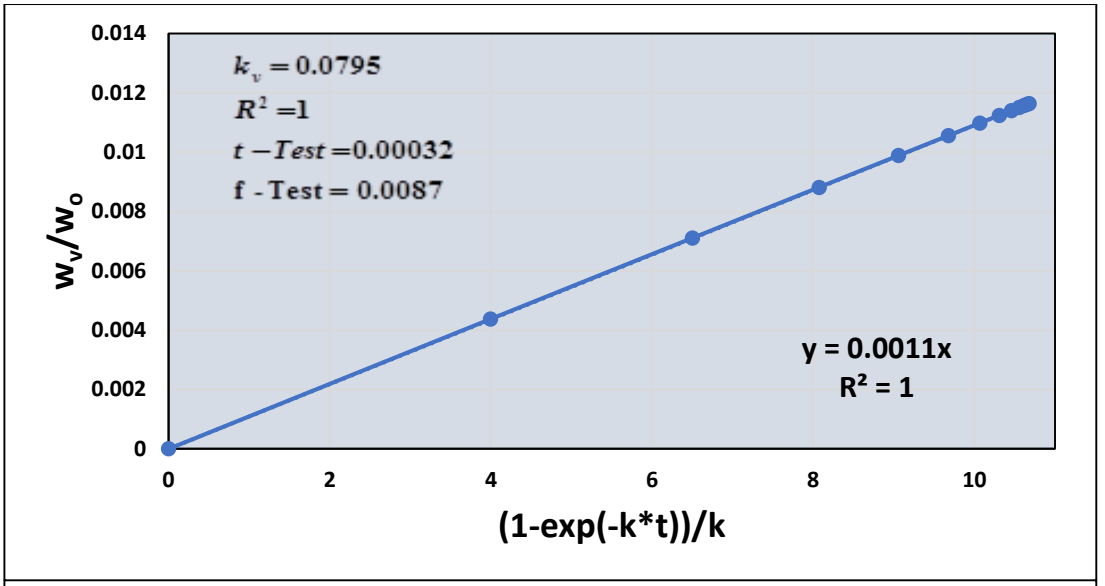
$k_v = 0.0795$
$R^2 = 1$
$t - Test = 0.00032$
f - Test = 0.0087
y = 0.0011x
R² = 1
w_v/w_o
(1-exp(-k*t))/k

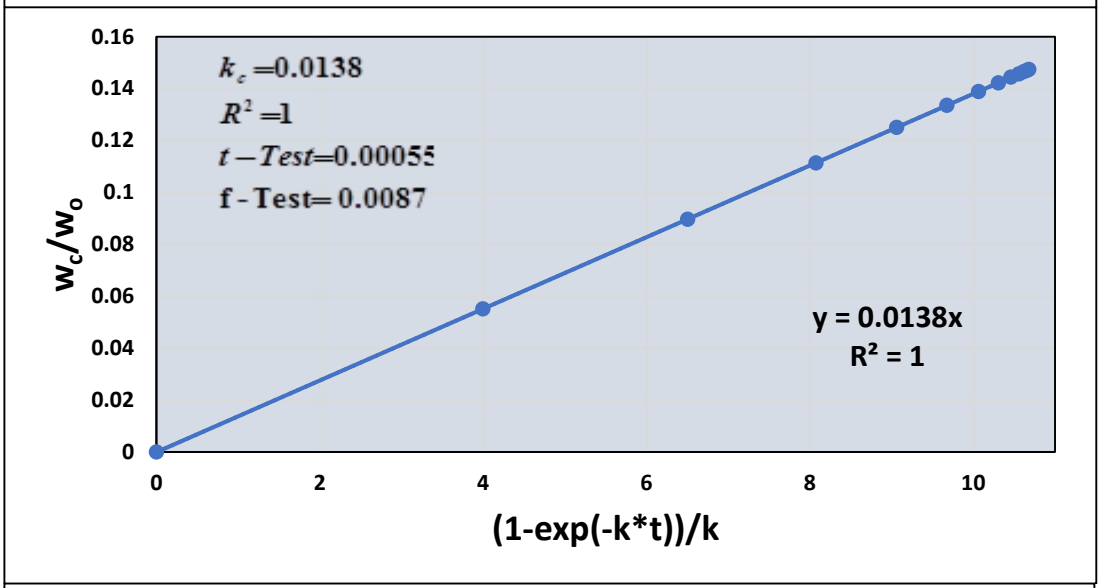
$k_c = 0.0138$
$R^2 = 1$
$t - Test = 0.00055$
f - Test= 0.0087
y = 0.0138x
R² = 1
w_c/w_o
(1-exp(-k*t))/k

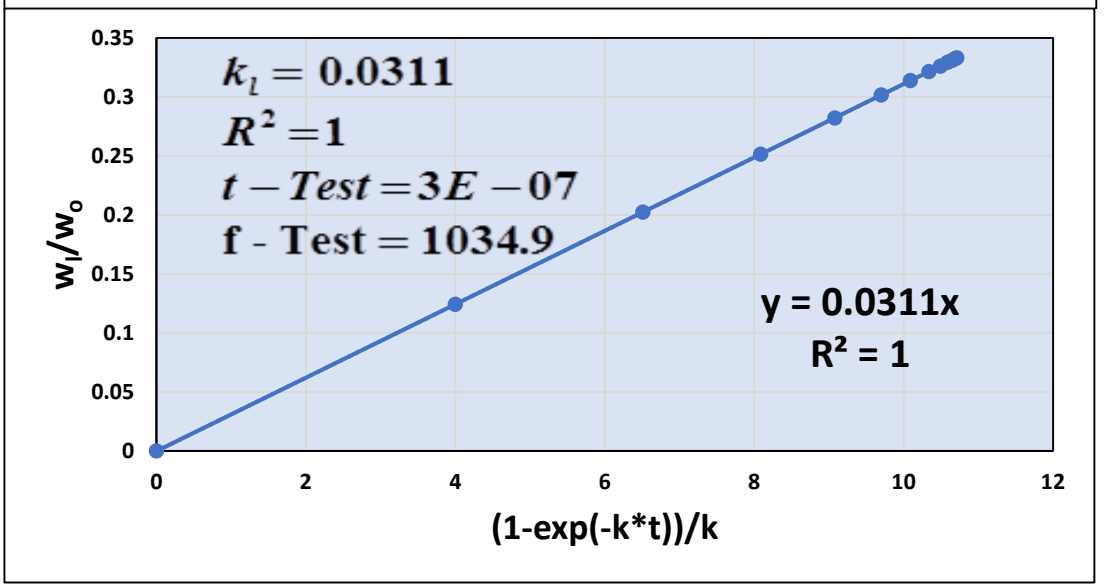
$k_l = 0.0311$
$R^2 = 1$
$t - Test = 3E - 07$
f - Test = 1034.9
y = 0.0311x
R² = 1
w_l/w_o
(1-exp(-k*t))/k

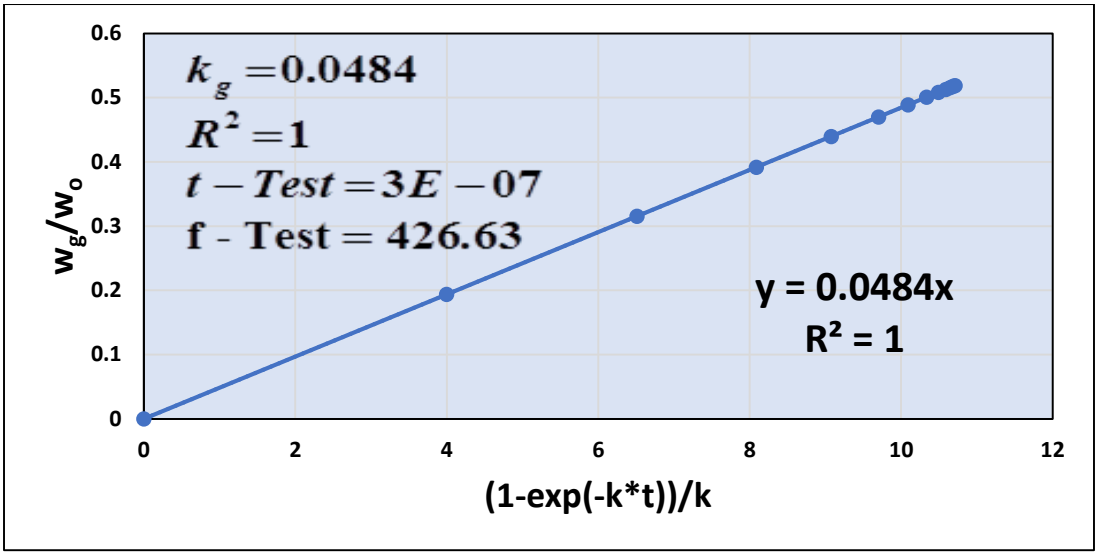

Figure 6.5. Plots of $\ln\left[\frac{w_o}{w}\right]$ vs time and $\frac{w_v}{w_o}$, $\frac{w_c}{w_o}$, $\frac{w_l}{w_o}$ and $\frac{w_g}{w_o}$ vs $(1-\exp[-k*t])/k$ at different temperature of lime waste

Values of k for jute wastes and lime waste have been in reported in Table 6.2. It is clearly seen that with the increase in temperature the values of k show an increasing trend for both the feedstocks. Similarly, the values for k_v, k_c, k_l and k_g for jute and lime waste have been reported in the table 6.3., 6.4., 6.5. and 6.6. respectively [9-12,15].

Table 6.2. Values of "k" at different temperature of jute wastes and lime waste

T (K)	Jute wastes	Lime wastes
573K	-	0.0489
673K	0.0691	0.0499
773K	0.0691	0.0523
873K	0.0739	0.0619
973K	0.0798	0.0795
1073K	0.1036	0.085
1173K	0.1153	0.0933

Table 6.3. Values of "k_v" at different temperature of jute wastes and lime waste

T (K)	Jute wastes	Lime wastes
573K	-	0.0406
673K	0.066	0.0414
773K	0.0678	0.0436
873K	0.041	0.0527
973K	0.0582	0.0687
1073K	0.0969	0.0734
1173K	0.1125	0.0795

Table 6.4. Values of "k_c" at different temperature of jute wastes and lime waste

T (K)	Jute wastes	Lime wastes
573K	-	0.0083
673K	0.001	0.0085
773K	0.0014	0.0087
873K	0.0329	0.0092
973K	0.0217	0.0108
1073K	0.0067	0.0115
1173K	0.0028	0.0138

Table.6.5. Values of "k_l" at different temperature of jute wastes and lime waste

T (K)	Jute wastes	Lime wastes
573K	-	0.0164
673K	0.0345	0.0164
773K	0.0343	0.0178
873K	0.0375	0.0232
973K	0.031	0.0286
1073K	0.055	0.029
1173K	0.0604	0.0311

Table.6.6. Values of "k_g" at different temperature of jute wastes and lime waste

T (K)	Jute wastes	Lime wastes
573K	-	0.0242
673K	0.0333	0.025
773K	0.0348	0.0266
873K	0.0342	0.0347
973K	0.0272	0.0401
1073K	0.0486	0.0444
1173K	0.0521	0.0484

6.2.1.3. Temperature dependence of rate constant

In figures 6.6 and 6.7. the logarithms of rate constant k, k_v, k_c, k_l and k_g have been plotted against the reciprocal of pyrolysis temperature for pyrolysis of jute waste and lime waste respectively. The linear nature of the plots in all cases proves the validity of Arrhenius equations to correlate the dependence of rate constants on reaction temperature. The values of activation energies (E, E_V, E_C, E_l, E_g) [15] and pre-exponential factors (A, A_V, A_c, A_l, A_g) [15] have also been determined from the Arrhenius plots and have been tabulated in table 6.7. The corresponding values used for the plots are provided in the Table 6.2., 6.3., 6.4. 6.5. and 6.6 respectively.

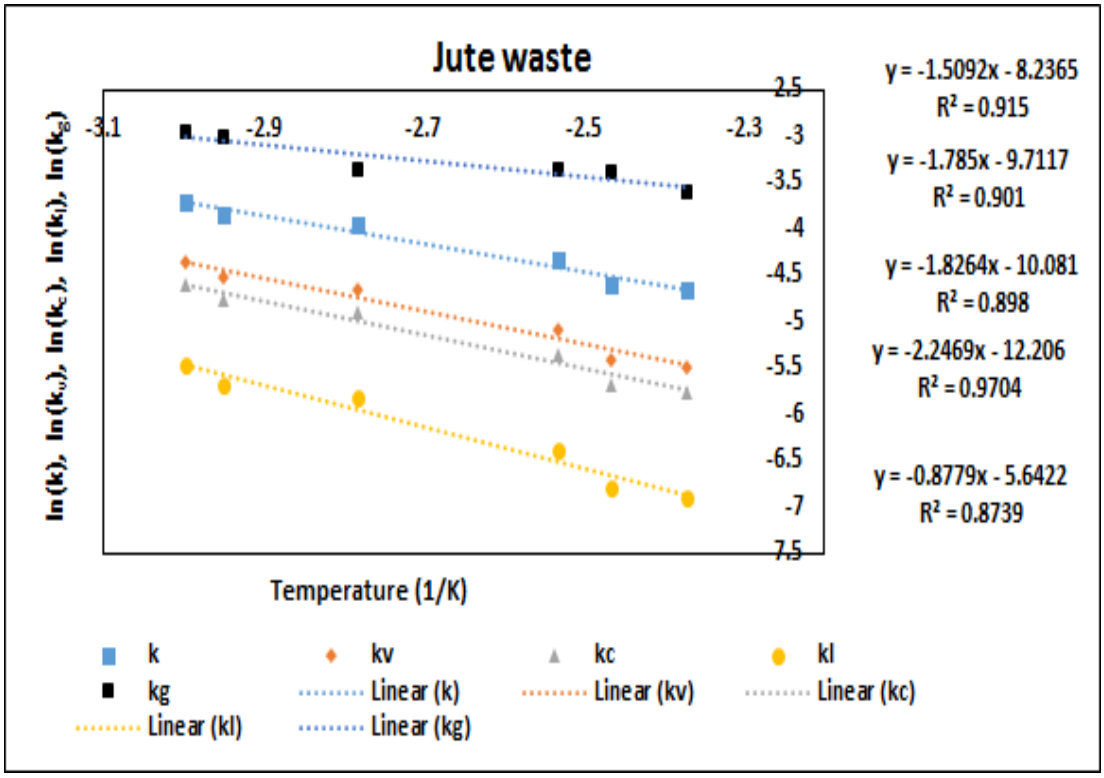

Figure 6.6. Calculated Rate Constants for weight loss of jute waste, Volatile formation, char formation, liquid formation and gas formation as per Arrhenius law in logarithmic scale against reciprocal of temperature for jute waste (k), volatile formation (k_v), char formation (k_c) and liquid formation (k_l) and gas formation (k_g) respectively.

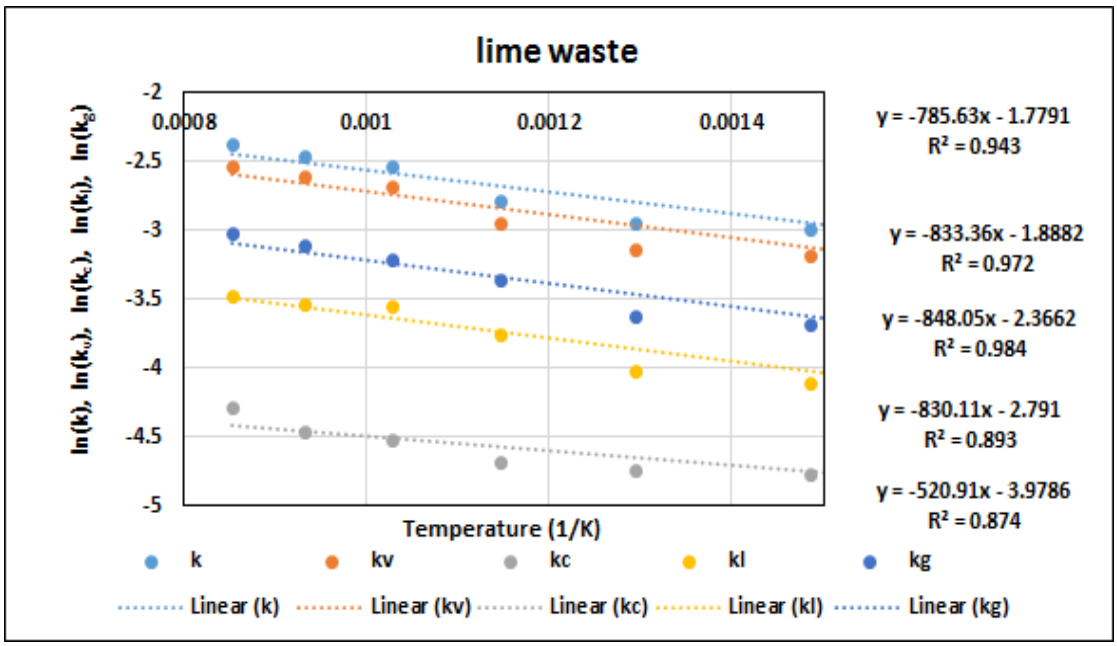

Figure 6.7. Calculated Rate Constants for weight loss of lime waste, Volatile formation, char formation, liquid formation and gas formation as per Arrhenius law in logarithmic scale against reciprocal of temperature for lime waste (k), volatile formation (k_v), char formation (k_c) and liquid formation (k_l) and gas formation (k_g) respectively.

Table 6.7. Calculated Activation Energies and Frequency Factors as per Arrhenius Law for jute wastes and lime waste

Sl. No.	Feed Stocks	Reaction rate constant	Activation Energy (kJ/mol)	Frequency factor (min^{-1})	Correlation Coefficient
1	Jute	k	9.153714 (E)	0.216103 (A)	0.915
		k_v	7.201587 (E_V)	0.163327 (A_V)	0.901
		k_c	24.74246 (E_C)	0.156609 (A_C)	0.898
		k_l	6.809831 (E_l)	0.102192 (A_l)	0.9704
		k_g	4.9228.3 (E_g)	0.072679 (A_g)	0.8739
2	Lime wastes	k	6.6918 (E)	0.1717 (A)	0.943
		k_v	6.9285 (E_V)	0.1522 (A_V)	0.972
		k_c	4.3308 (E_C)	0.0187 (A_C)	0.984
		k_l	7.050688 (E_l)	0.093837 (A_l)	0.893
		k_g	6.901535 (E_g)	0.06136 (A_g)	0.874

6.2.2. Distributed Activation Energy Model (DAEM)

6.2. 2.1 TGA Plots

Figures. 6.8 and 6.9. show respectively the time trajectories of % (w/w) of solid residue for waste jute and lime wastes remaining during TGA under nonisothermal conditions using heating rate (10 K min^{-1}, 15 K min^{-1}, 20 K min^{-1}, 25 K min^{-1}, 30 K min^{-1}) as a parameter.

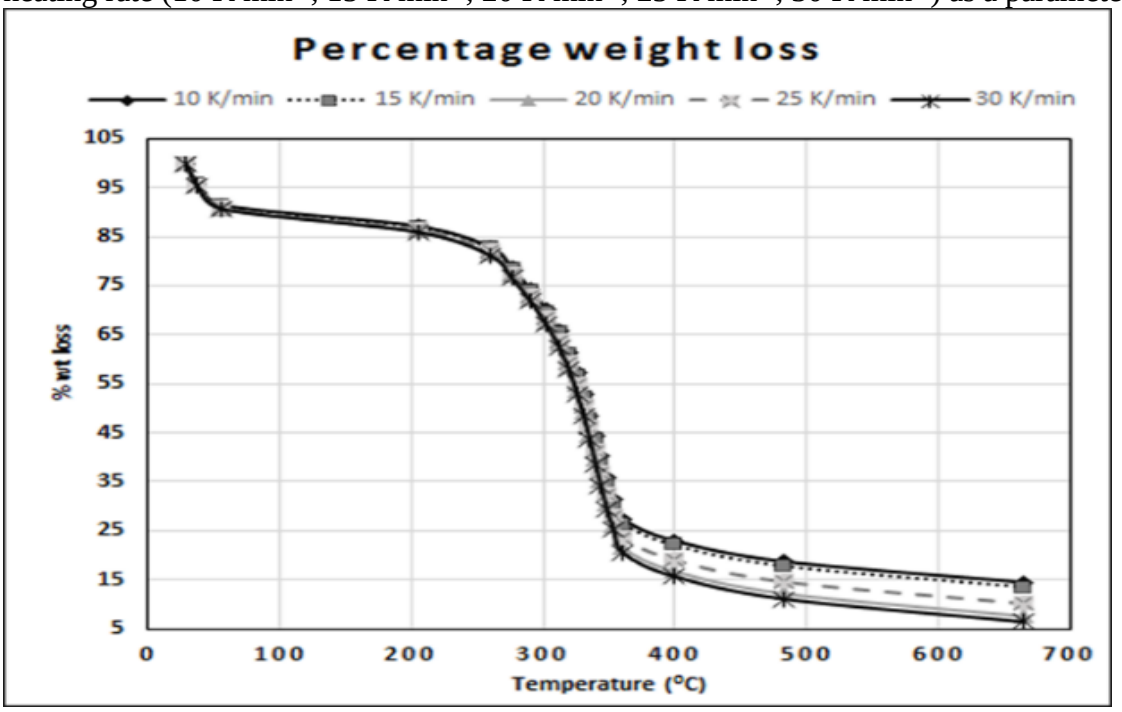

Figure 6.8 Percentage of weight residue of jute waste in the temperature range of 30–900 ^{0}C at different heating rates (TGA plot).

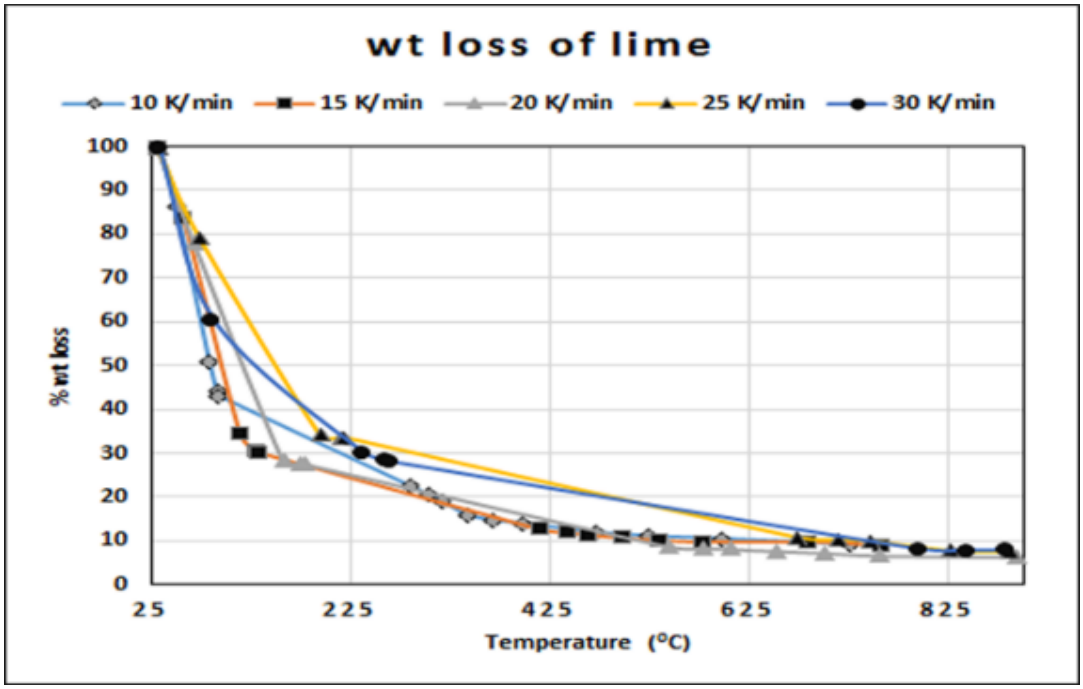

Figure 6.9. Percentage of weight residue of lime wastes in the temperature range of 30–900 ^{0}C at different heating rates (TGA plot).

From the analysis of the plots it is clearly evident that distinct patterns of weight loss are followed in different temperature ranges for both the feedstocks. While for waste jute the trajectory may be divided into four zones, namely 30–100 ^{o}C, 100–275 ^{o}C, 275–350 ^{o}C and 350–700 ^{o}C, for lime waste the temperature zones are 25–100 ^{o}C, 100–275 ^{o}C, 275–775 ^{o}C and 775-900 ^{o}C. The presence of several types of components following different pyrolyzing characteristics is probably reflected by these patterns. While the cellulosic and hemi-cellulosic components of jute are thermally decomposed at less severity of temperature, the lignin present in jute is expected to react at higher temperatures corresponding to higher conversion levels. The difference in the temperature zone above 275^{o}C may be due to the difference in their compositions with respect to cellulose, hemicellulose and lignin. The wide span of pyrolysis pattern above 275 ^{o}C may be explained by no lignin content of the biomass. The single pyrolysis pattern from 275 ^{o}C – 775^{o}C may be due to the thermal decomposition of cellulose and hemicellulose in that zone.

6.2.2.1.1. Isoconversion Plots

In Figures 6.10. and 6.11. logarithm of $[\alpha i(dx/dT)_{x,i}]$ has been plotted against $(-1000/RT_i)$ for pyrolysis of waste jute and lime waste respectively.. A set of straight lines have been obtained at different values for conversion for both the feedstocks validating the Friedman model [30] with the assumptions of 1st order kinetics and Arrhenius type temperature dependence of rate constants for the pyrolytic reactions. From the detailed analysis of the figures it is revealed that parallel lines are obtained in the conversion ranges of 0.2 to 0. 8 and 0.05 to 0.7 for waste jute and lime waste respectively. The parallel nature of straight lines indicates a close distribution of activation energies. On the other hand, the non-parallel relationship at lower (<0.2 for jute and <0.05 for lime waste) and higher (>0.8 for jute and 0.7 for lime waste) ranges of conversion clearly indicates the probability of occurrence of pyrolysis reactions, distinctly different from those occurring at the widely spread intermediate (0.2–0.8 for jute and 0.05 – 0.7 for lime) conversion levels. Further investigation is required for this purpose. It is expected that the conversion below 0.2 and 0.05 for jute waste and lime waste respectively represents mostly the removal of moisture and commencement of primary pyrolysis of hemicelluloses and cellulose.

On the other hand, at high conversion levels (>0.8 for jute waste and >0.7 for lime waste) the pyrolysis of recalcitrant components like lignin following a pattern, distinctly different from the primary and secondary pyrolysis of cellulosic components in the intermediate conversion ranges, is dominant.

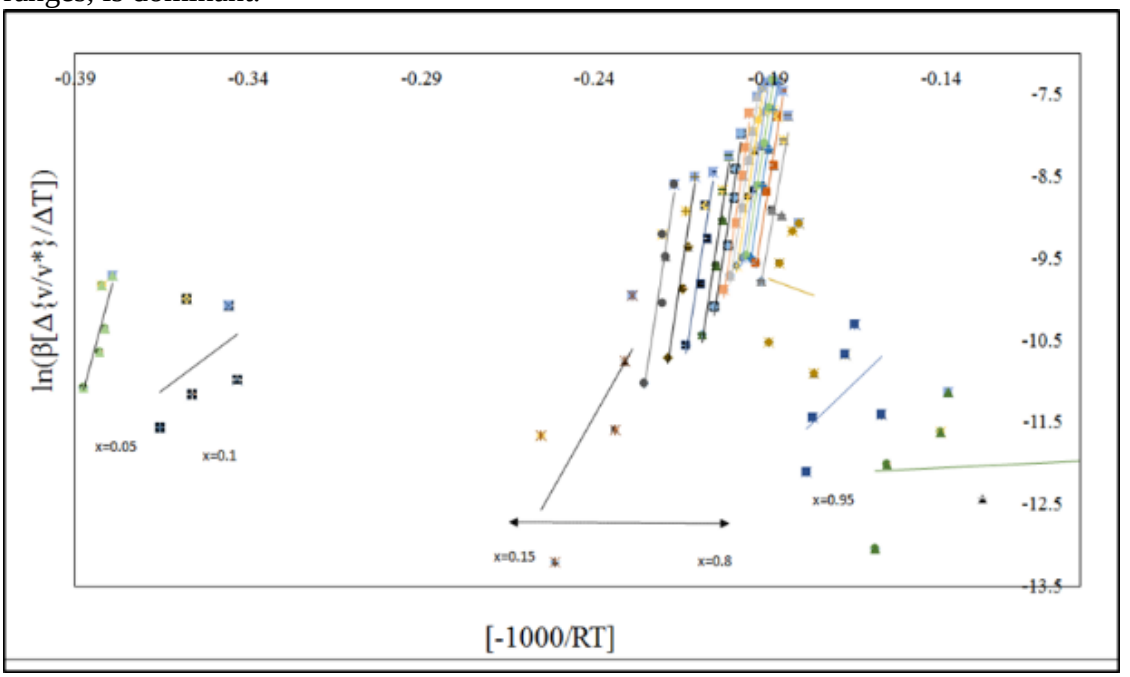

Figure 6.10. Plot of ln[αi(dx/dT) $_{x,\,i}$**] *vs.* (-1000/RT$_i$) at different conversion values from 0.05 to 0.95 for all the heating rates (5-25 K min^{-1}) of jute wastes.**

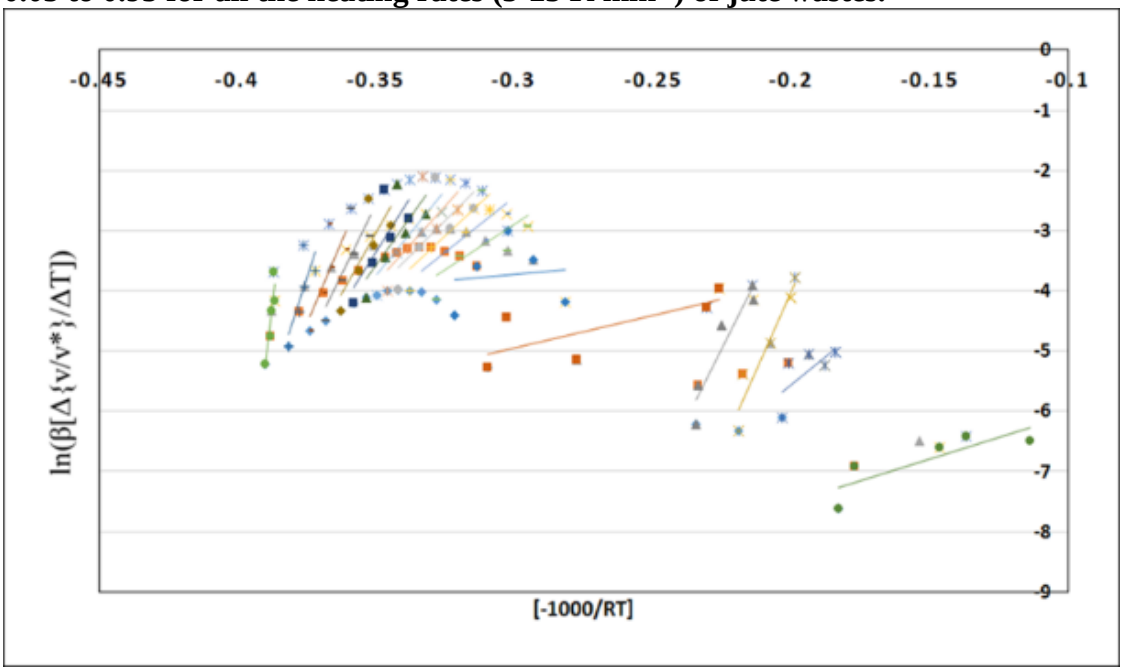

Figure 6.11. Plot of ln[αi(dx/dT) $_{x,\,i}$**] vs. (-1000/RT$_i$) at different conversion values from 0.05 to 0.95 for all the heating rates (5-30 K min^{-1}) of lime wastes.**

6.2.2.1.2. Dependence of activation energies and frequency factor on conversion

In Figures 6.12 -6.13. activation energies and ln[A**f(x)*], as obtained from the iso-conversion plots, have been graphed against conversion for jute and lime wastes respectively. The patterns

of the plots for waste jute are similar to those reported by Wu et al. [16] during the pyrolysis of biomass feedstocks.
However, the resemblance is nominal in case of lime waste. This may be due to very low lignin content and citrus nature of lime waste unlike most of the biomass usually studied [17-29].

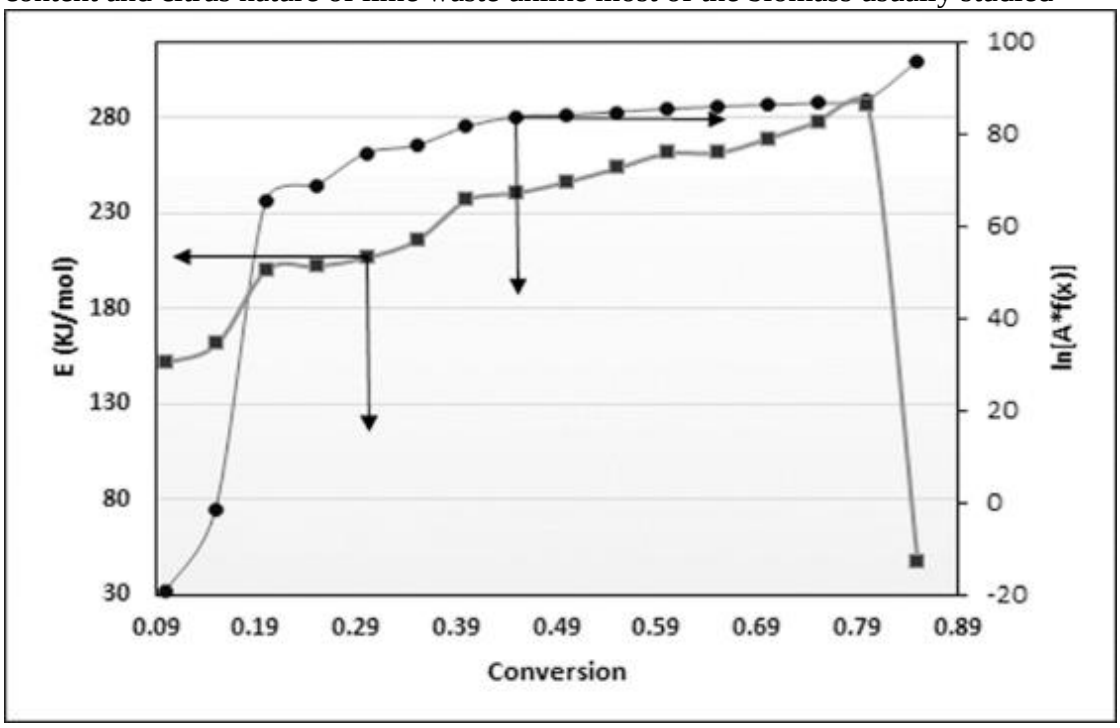

Figure 6.12. Plot of E and ln[A*$f(x)$] vs. conversion for non-catalytic pyrolysis of jute waste

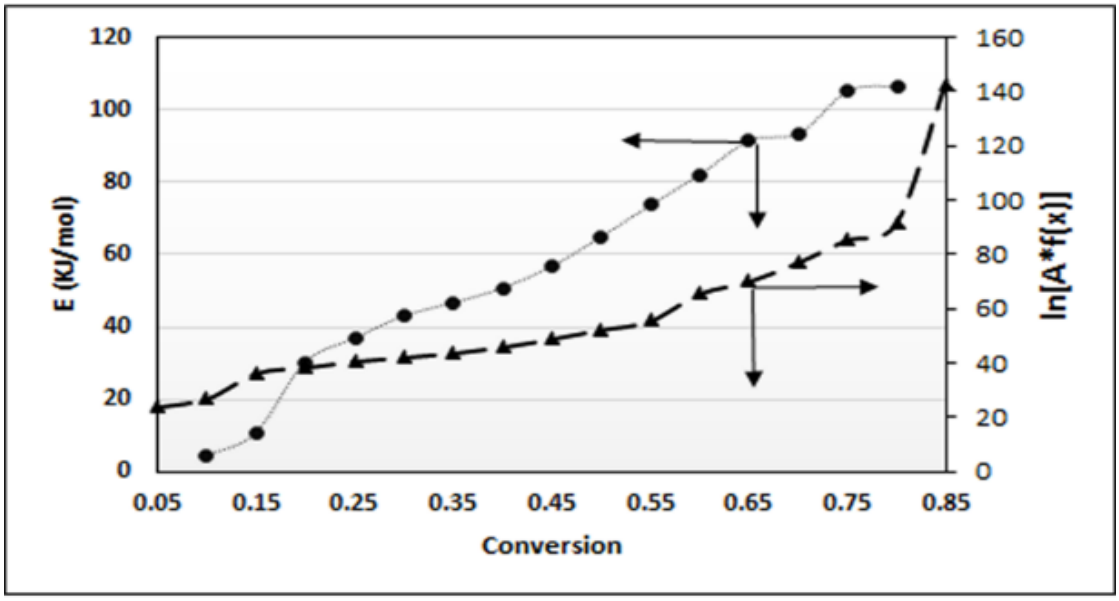

Figure 6.13 Plot of E and ln[A*$f(x)$] vs. conversion for non-catalytic pyrolysis of lime waste

6.2.2.1.3. Distribution of activation energy

In Figures 6.14-6.15, *f(E)* has been plotted against E respectively for jute wastes and lime wastes. The analysis of the figure 6.14. reveals that *f(E) versus E* follows almost a Gaussian distribution [31] in the conversion range of 0.2 -0.8 for jute waste where the relationship between E and conversion is linear. Similar observation has been reported for pyrolysis of other biomasses. [17-29] Figure 6.15 reveals that no such Gaussian relationship is obtained between

f(E) and E for lime waste. The low lignin content and citrus nature of lime waste may be responsible for this non-Gaussian distribution of f(E) on E. The mean values of average activation energy are 276.56 kJ mol^{-1} and 83.71 kJ mol^{-1} for jute and lime wastes respectively. When compared to the activation energies of lumped kinetics no parity is observed with those obtained through DAE modelling for both the feedstocks. Since the pyrolysis is actually a complex combination of reactions causing decomposition of different constituent molecules of a biomass, it is understandable that DAEM kinetics should represent the reality more closely.

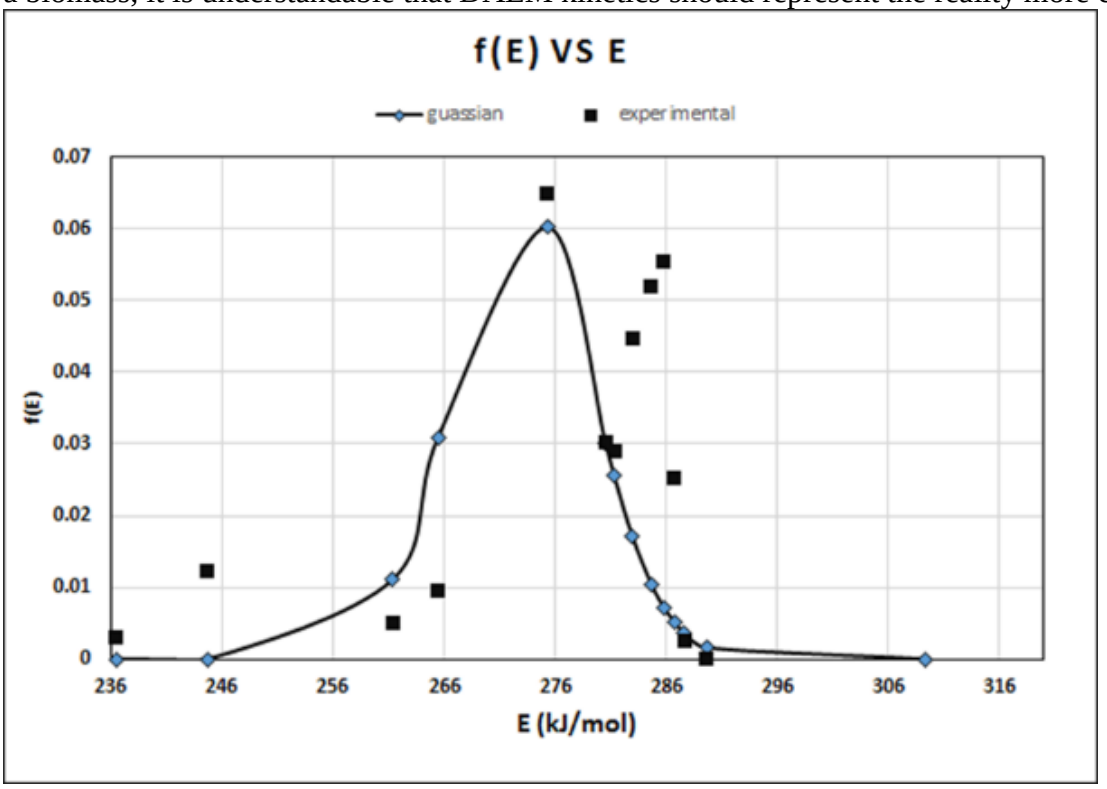

Figure 6.14. Plot of *f(E) vs.* E obtained from Friedman differential isoconversion method for pyrolysis of jute waste.

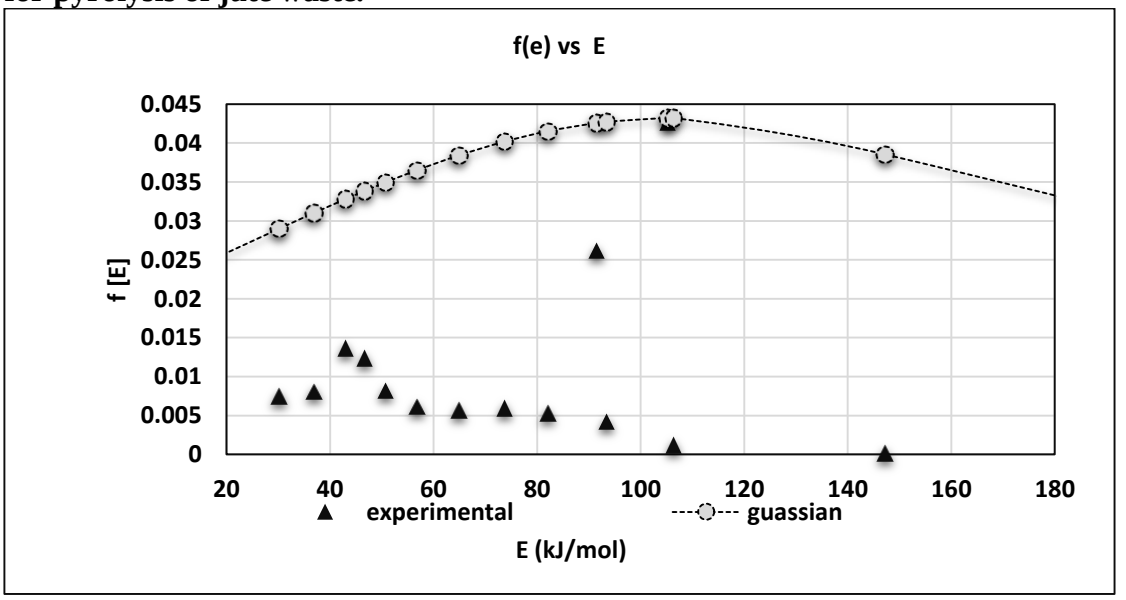

Figure 6.15. Plot of *f(E) vs.* E obtained from Friedman differential isoconversion method for pyrolysis of lime waste.

6.3. Results of pyrolyzer model

Using model predictions of concentration of tar, CO2, CO, H_2 and CH_4 against dimensionless axial position (z) and reaction time (t), surface plots (3D) and 2D plots have been generated for jute waste [15,32,33]. Figures 6.16. show the simulated surface plots for the variation of pyro-oil with respect to time and axial position. Similarly figures 6.15-6.18. represent the plots for CO, H_2, CO_2 and CH_4 respectively. All plots shown in figures 6.17 -6.20 predict the trends of pyrolysis temperature at 973K. The predicted trends of variation of concentration of condensable and non-condensable gaseous components of pyrolysis products of jute waste with respect to time and axial position are being discussed. It is evident that the maximum fraction of reactive tar in the gaseous phase is 31% whereas of CO, H_2, CO_2 and CH_4 are 2%, 0.1%, 11% and 1.75% respectively.

6.3.1 pyro-oil

Figure 6.16 (3D plot and 2D plot) reveals that at each grid point (z=1; 0.75; 0.50; 0.25), concentration of tar obtained from pyrolysis of jute waste, increases sharply with reaction time up to 1200s at 973K. The maximum predicted mass fraction of tar, W_T, in gas phase at 973K after a time interval of 1200 s are 0.31, 0.2, 0.1 and 0.05 at dimensionless axial length, z=1, 0.75, 0.50 and 0.25 respectively. As time progresses beyond 1200s mass of tar subsequently declines almost exponentially and reaches zero level at 3600s. The pattern signifies the generation of tar during the initial period (up to 1200s) of pyrolysis and the decomposition and conversion of tar through homogeneous and heterogeneous reactions beyond this period at each axial grid position. (MATLAB PROGRAMME are given in Appendix A.9) As the pyrolyzer is operated in semi-batch mode, the amount of unreacted biomass gets diminished and hence the amount of tar decreases afterwards.

6.3.2. CO

The surface plot for the variation of mass fraction of "CO" in the gas phase against time and temperature at 973K is shown in Figure 6.17. It is evident that similar to tar, there exists an increasing trend of "CO" up to a reaction time of 1200 s beyond which the concentration decreases. This trend is also supported by the 2D plot, obtained by graphing the same parameter against reaction time using axial position as a parameter at 973K. The weight fraction of "CO" is always very low and the maximum value is 2%.

6.3.3. H_2

Surface plots and 2D plots for weight fractions of "H_2" in the void space of thermally degrading waste jute sample, are shown in Figures 6.18 for pyrolysis temperatures of 973K. Similar to the trend obtained for weight fraction of "CO", the maximum weight fraction of "H_2" at 973K, indicating the feasibility of tar cracking reaction at higher pyrolysis temperature. The maximum weight fractions of "H_2" for 973K are obtained at 1200s. The maximum weight fraction of "H_2" at 973K is $3.6X10^{-5}$.

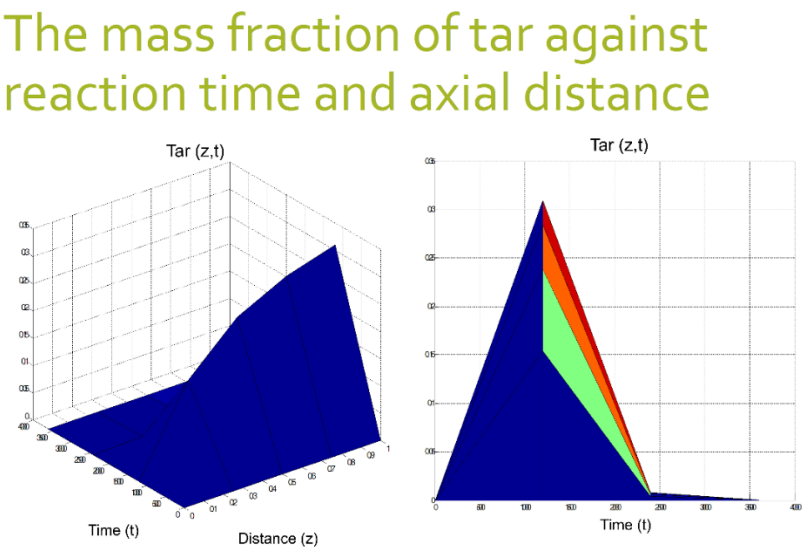

Figure 6.16. 3d and 2d plot of mass fraction of pyro-oil in gas phase of jute waste at 973K.

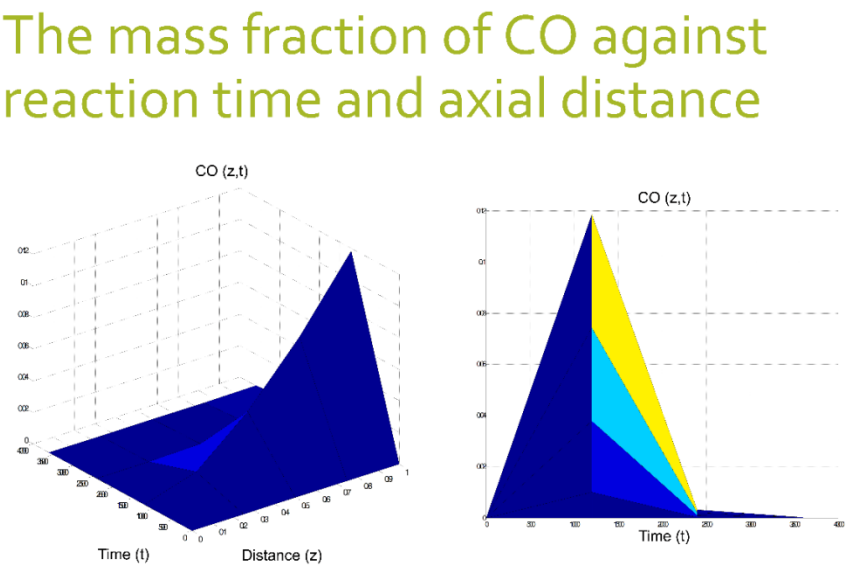

Figure 6.17. 3d and 2d plot of mass fraction of CO in gas phase of jute waste at 973K.

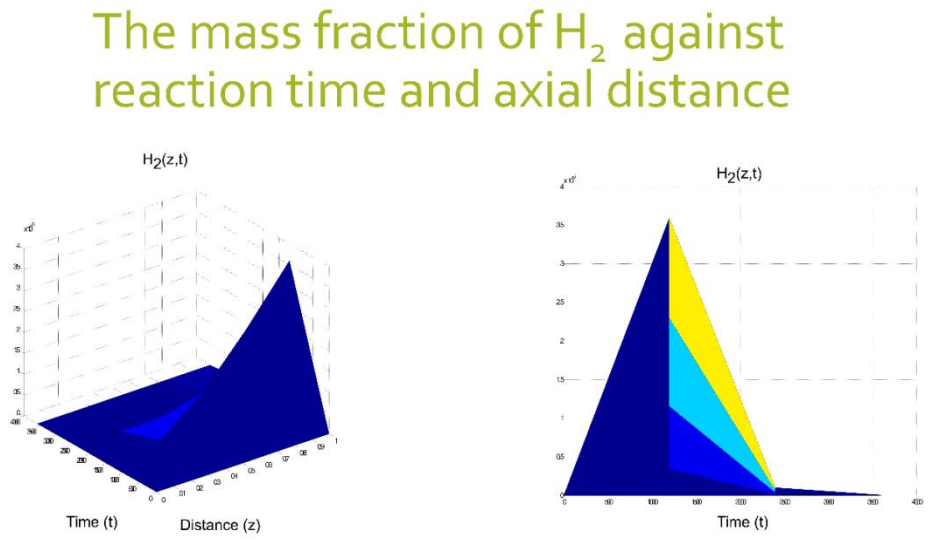

Figure 6.18. 3d and 2d plot of mass fraction of H_2 in gas phase of jute waste at 973K.

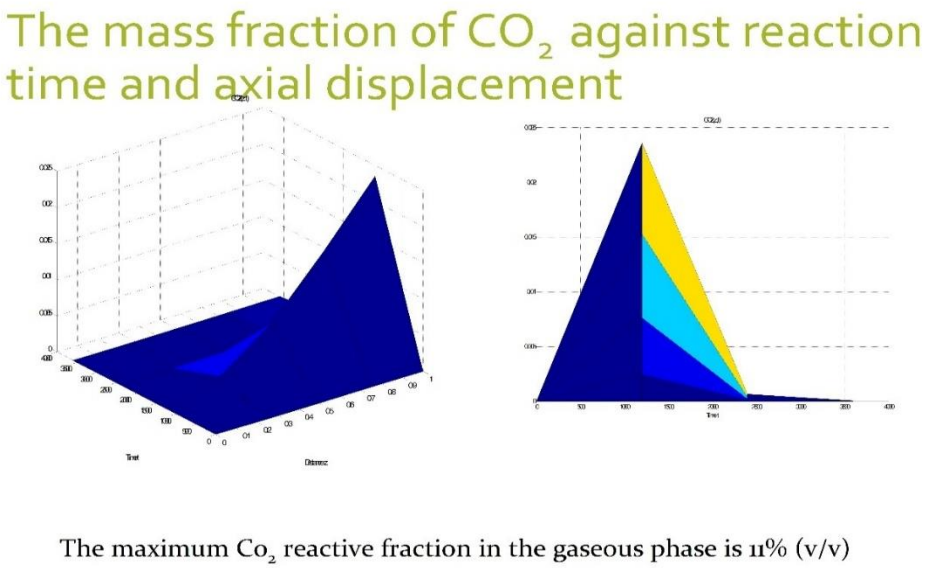

Figure 6.19. 3d and 2d plot of mass fraction of CO_2 in gas phase of jute waste at 973K.

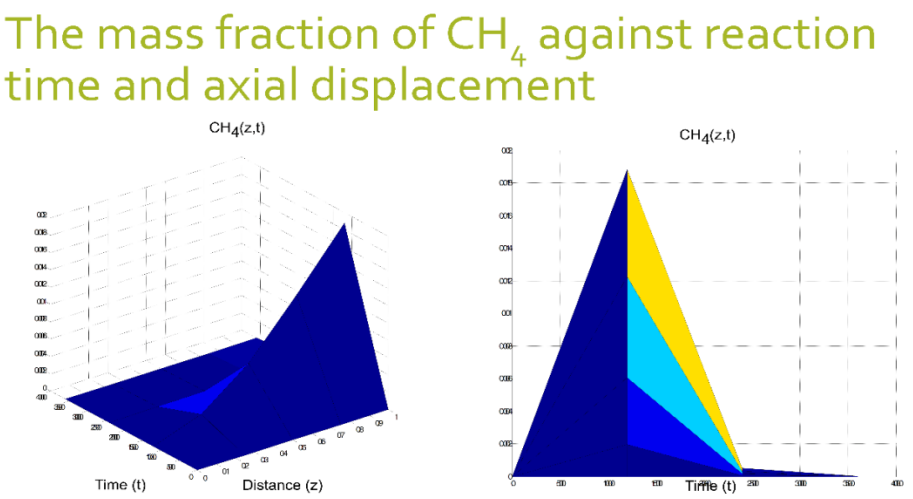

Figure 6.20. 3d and 2d plot of mass fraction of CH_4 in gas phase of jute waste at 973K.

6.3.4 CO_2

Surface plots of variation of weight fractions of "CO_2" as a function of time and axial position are shown in Figure 6.19 for 973K. At 973K the maximum weight fraction obtained for "CO_2" is 0.024.

6.3.5. CH_4

Surface plots of variation of weight fractions of "CH_4" as a function of time and axial position are shown in Figure 6.20 for 973K. At 973K the maximum weight fraction obtained for "CH_4" is 0.0175.

6.3.6. Validation of model

6.3.6.1. Tar (condensable part)

In Figure 6.21 the simulated and experimental values of exit concentration of pyro-oil of jute waste obtained in the temperature range of 400 (673K) to 900^0C (1173K) have been plotted. The agreement between simulated and experimental values at the pyrolyzer exit is commendable. Thus, the applicability of mathematical model for the present system is validated.

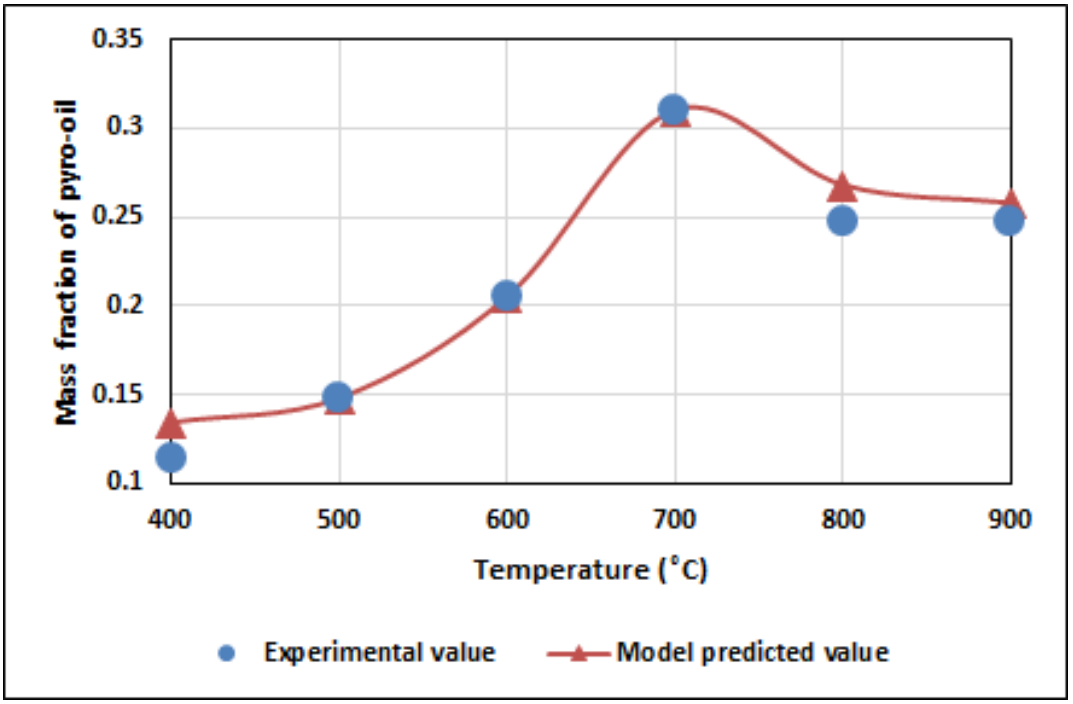

Figure 6.21. Comparison of simulated and experimental values of exit concentration of tar against pyrolysis temperatures (at Z=1)

6.4. Catalytic pyrolysis

6.4.1. Lumped kinetics

6.4.1.1. Experimental time histories

As described in the section 5.1.1, the lumped kinetics [3,11,12] of catalytic pyrolysis of all feedstocks namely, jute waste and lime waste have been determined using integral method of analysis.

6.4.1.2 Jute waste

Figure 6.22 represent the profiles of residual weight fraction of pyrolysis of jute wastes in presence of a) alumina b) ZnO c) KCl d) NaCl and e) sodium aluminosilicate [34-38] respectively with respect to pyrolysis time in the temperature range of 573K to 1173 K. The corresponding data are provided in the Table A.10.a. in the appendix. Similarly, the figures 6.23. and 6.24. represent respectively the time histories of weight fractions of volatile and char generated during the pyrolysis of jute wastes in presence of a) alumina b) ZnO c) KCl d) NaCl and e) sodium aluminosilicate with respect to pyrolysis time in the temperature range of 573K to 1173 K.

a)

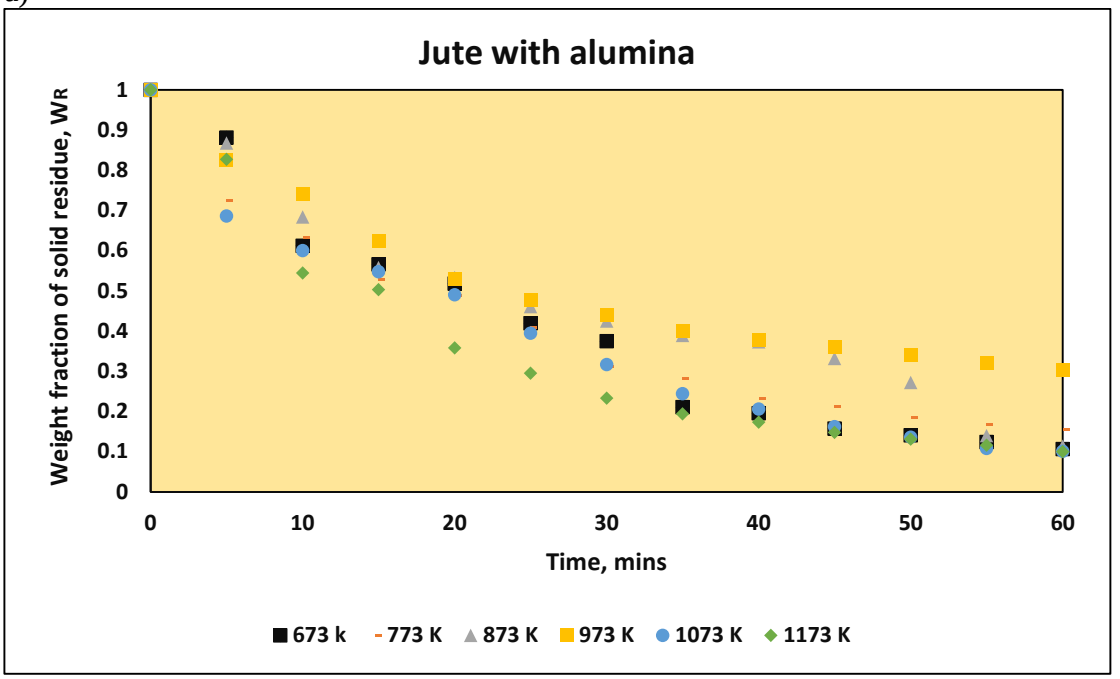
Jute with alumina
Weight fraction of solid residue, WR
1
0.9
0.8
0.7
0.6
0.5
0.4
0.3
0.2
0.1
0
0
10
20
30
40
50
60
Time, mins
673 k
773 K
873 K
973 K
1073 K
1173 K

b)

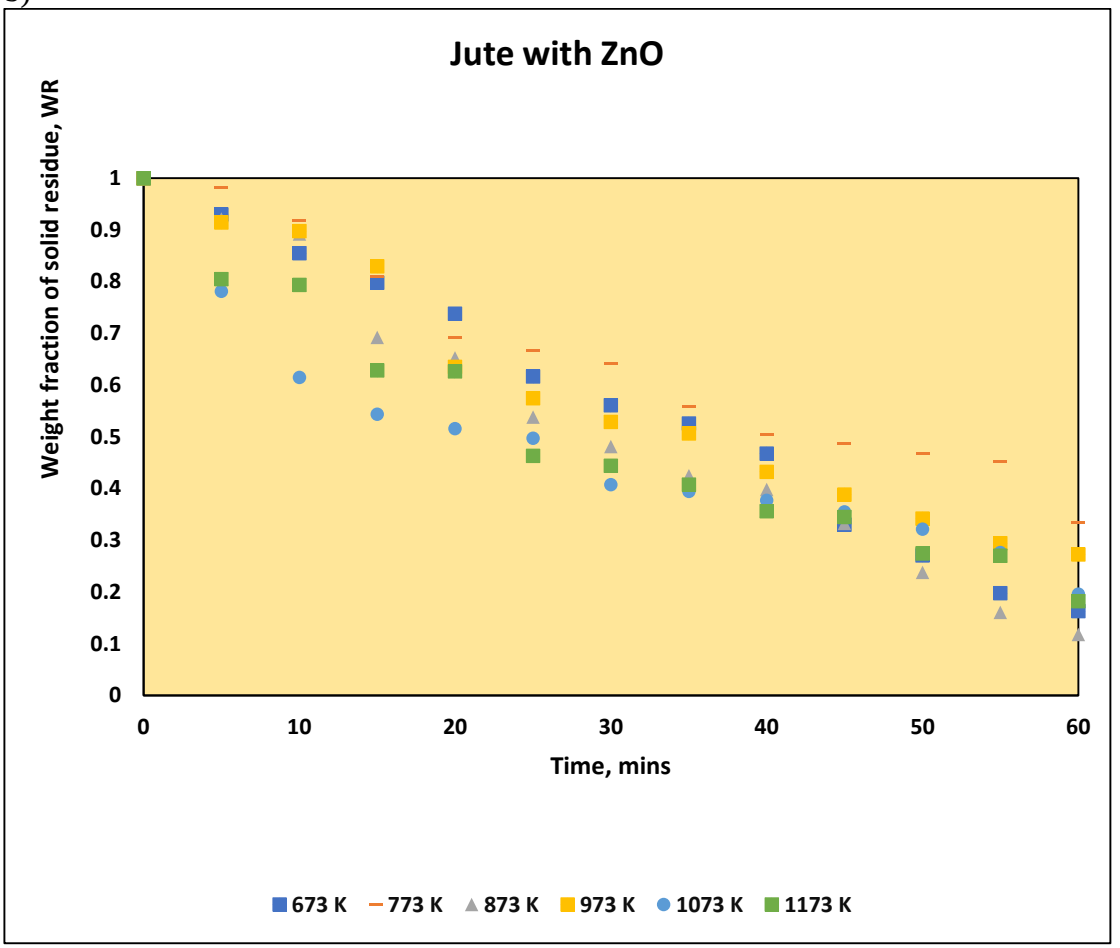
Jute with ZnO
Weight fraction of solid residue, WR
1
0.9
0.8
0.7
0.6
0.5
0.4
0.3
0.2
0.1
0
0
10
20
30
40
50
60
Time, mins
673 K
773 K
873 K
973 K
1073 K
1173 K

.

c)

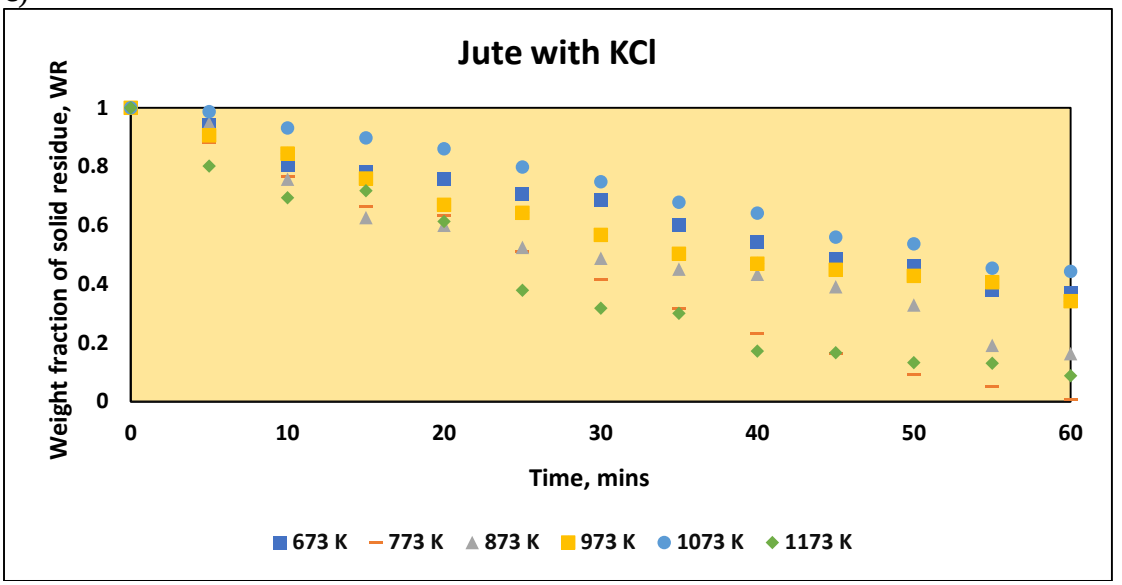

d)

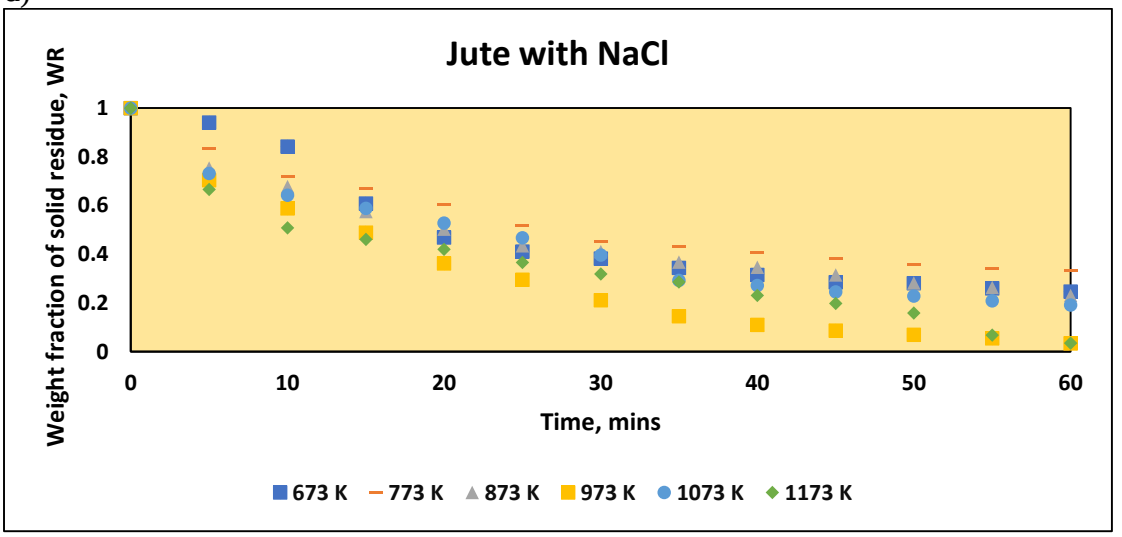

e)

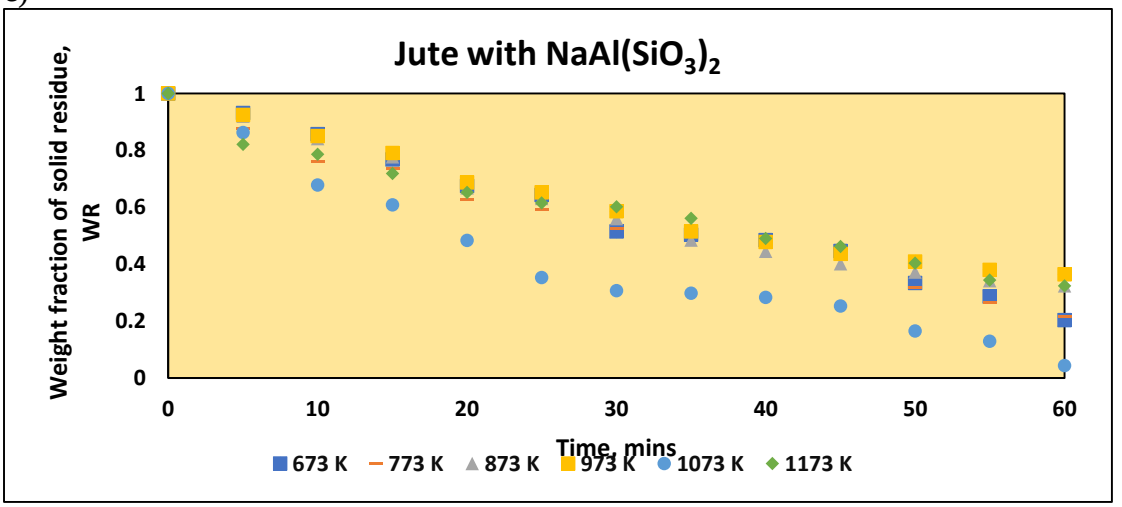

Figure 6.22. Time histories of weight fraction of residue of (a) jute with alumina (b) jute with ZnO (c) jute with KCl (d) jute with NaCl and (e) jute with Aluminosilicate using pyrolysis temperature as parameter.

a)

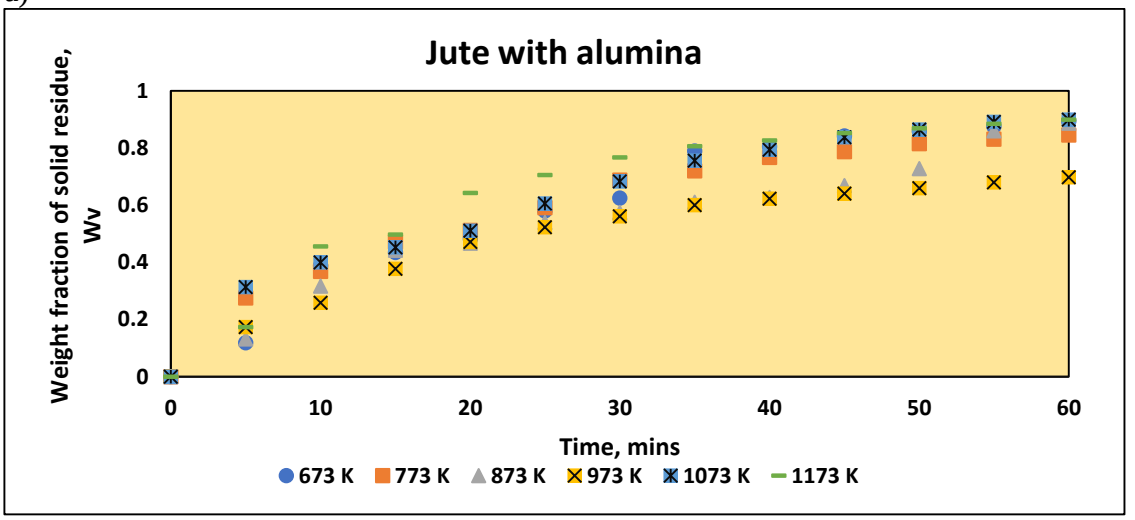
Jute with alumina
Weight fraction of solid residue, Wv
1
0.8
0.6
0.4
0.2
0
0
10
20
30
40
50
60
Time, mins
673 K
773 K
873 K
973 K
1073 K
1173 K

b)

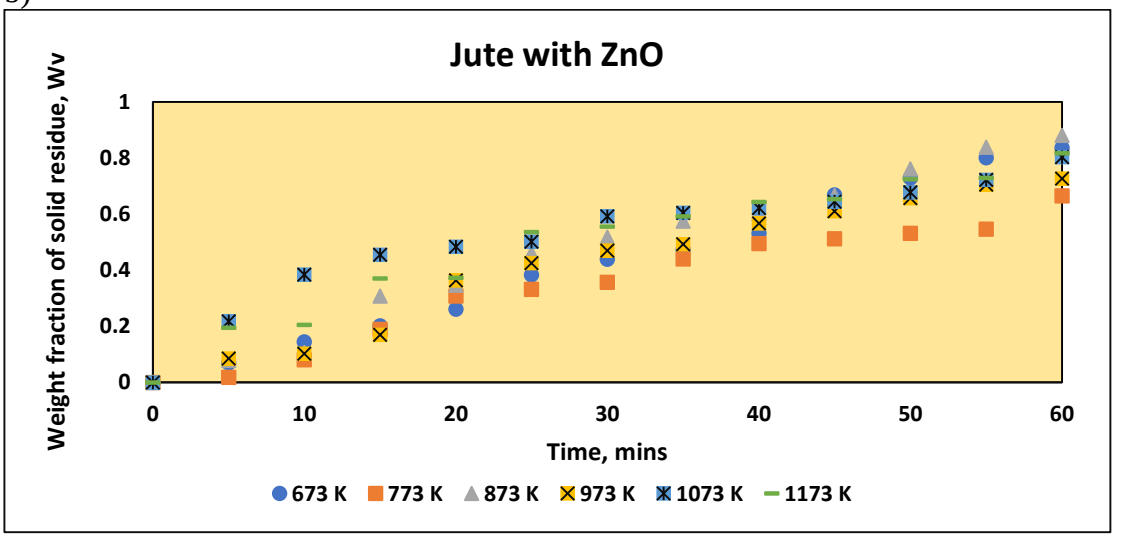
Jute with ZnO
Weight fraction of solid residue, Wv
1
0.8
0.6
0.4
0.2
0
0
10
20
30
40
50
60
Time, mins
673 K
773 K
873 K
973 K
1073 K
1173 K

c)

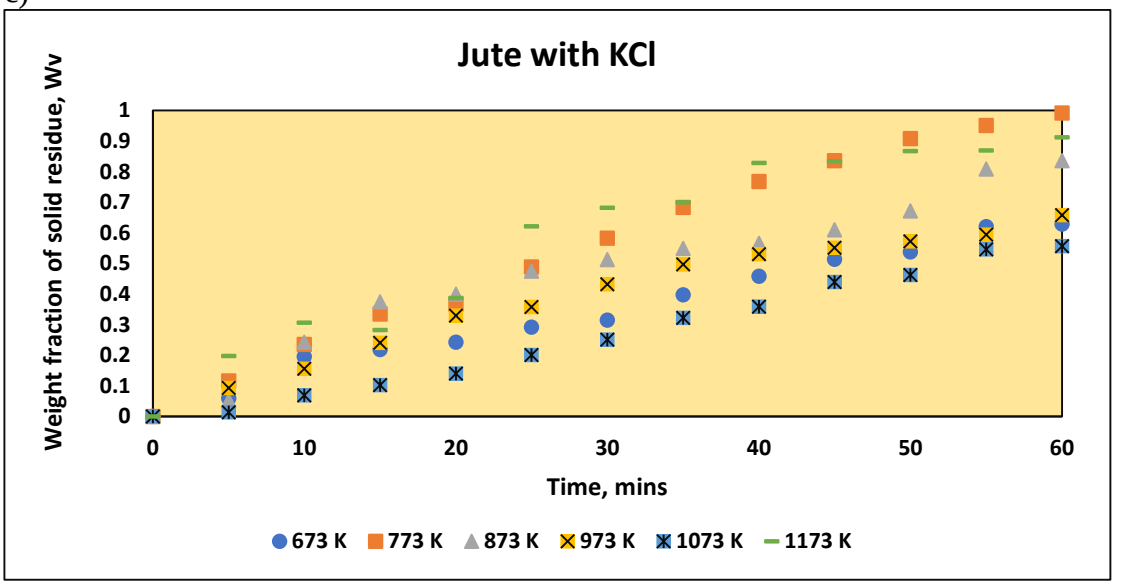
Jute with KCl
Weight fraction of solid residue, Wv
1
0.9
0.8
0.7
0.6
0.5
0.4
0.3
0.2
0.1
0
0
10
20
30
40
50
60
Time, mins
673 K
773 K
873 K
973 K
1073 K
1173 K

d)

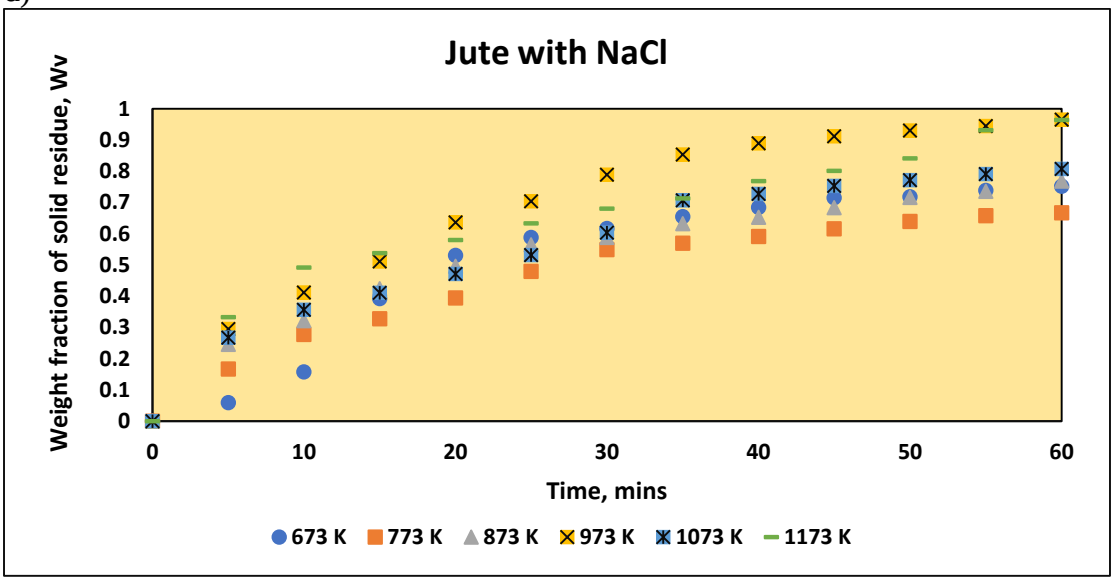

e)

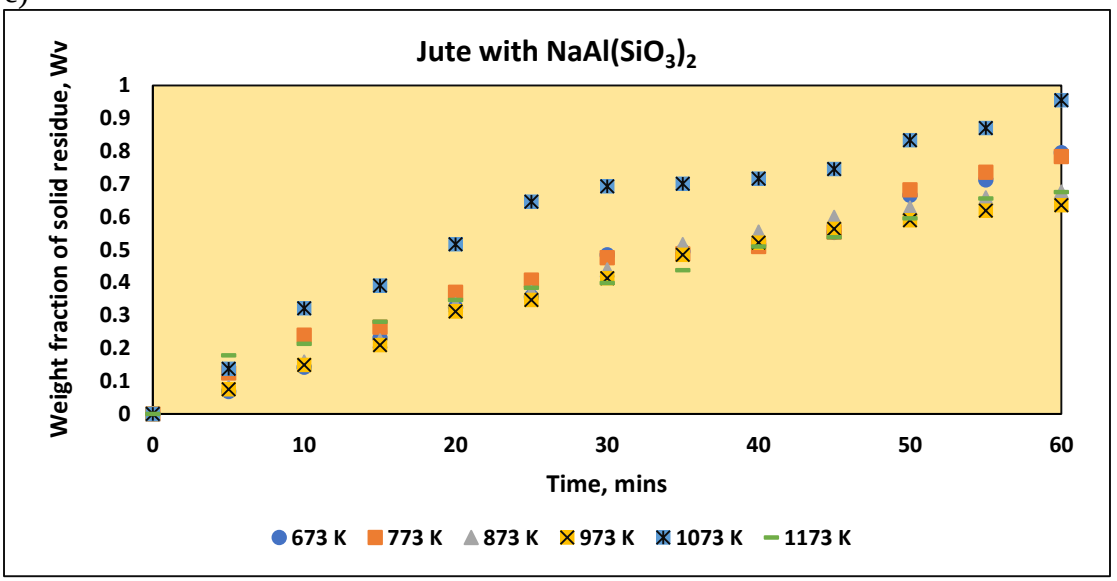

Figure 6.23. Time Histories of volatile weight fraction using pyrolysis temperature as parameter: (a) jute with alumina (b) jute with ZnO (c) jute with KCl (d) jute with NaCl and (e) jute with Aluminosilicate

The corresponding values used for the plots are provided in the Table A.11.a. and Table A.12.a. respectively in the appendix. From the analysis of the figures it is revealed that similar to non-catalytic pyrolysis, catalytic pyrolysis of jute wastes begins at 673K for all catalysts under study [34-38].

a)

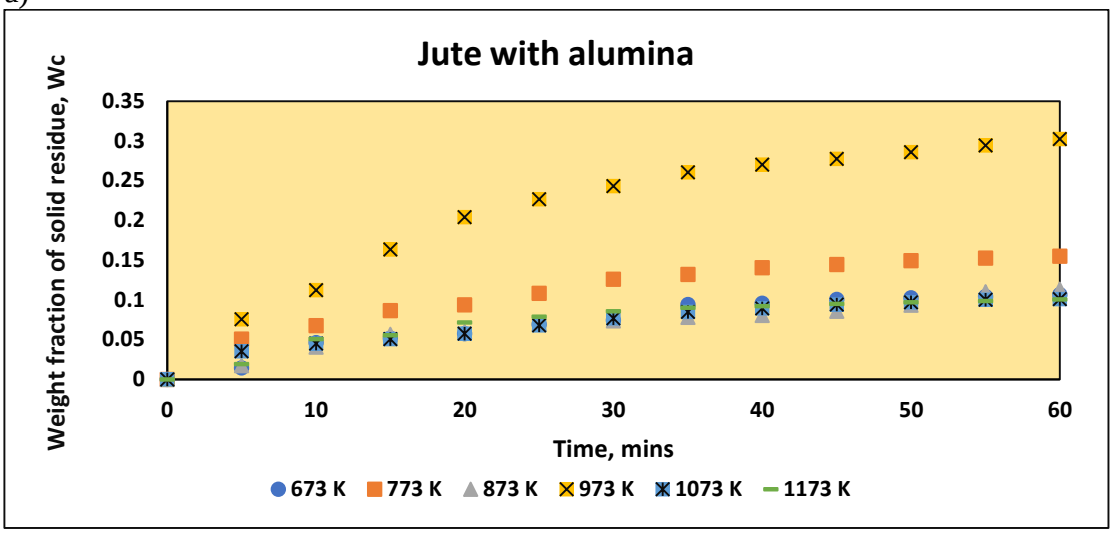
Jute with alumina
Weight fraction of solid residue, Wc
0.35
0.3
0.25
0.2
0.15
0.1
0.05
0
0
10
20
30
40
50
60
Time, mins
673 K
773 K
873 K
973 K
1073 K
1173 K

b)

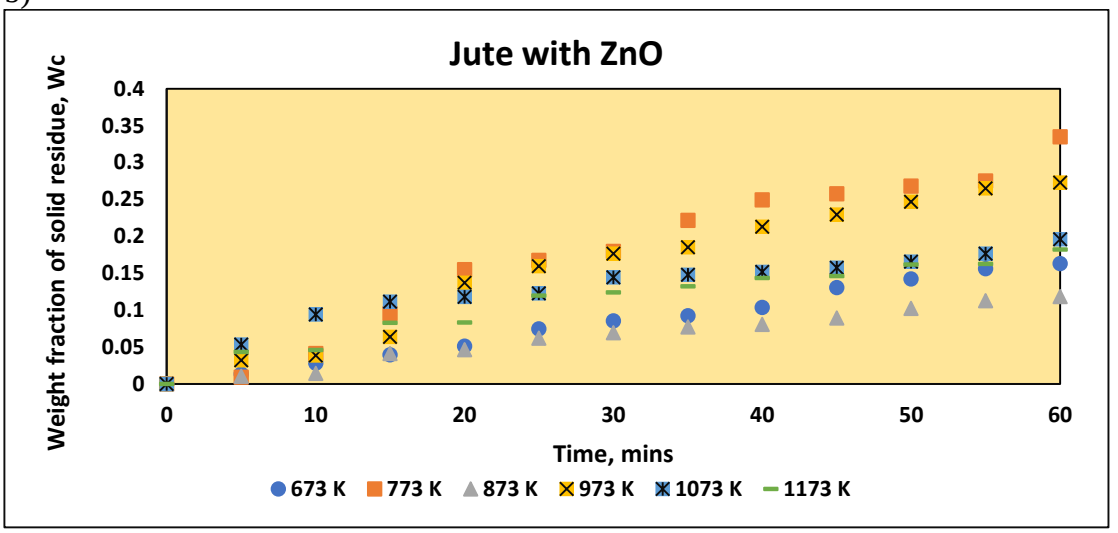
Jute with ZnO
Weight fraction of solid residue, Wc
0.4
0.35
0.3
0.25
0.2
0.15
0.1
0.05
0
0
10
20
30
40
50
60
Time, mins
673 K
773 K
873 K
973 K
1073 K
1173 K

c)

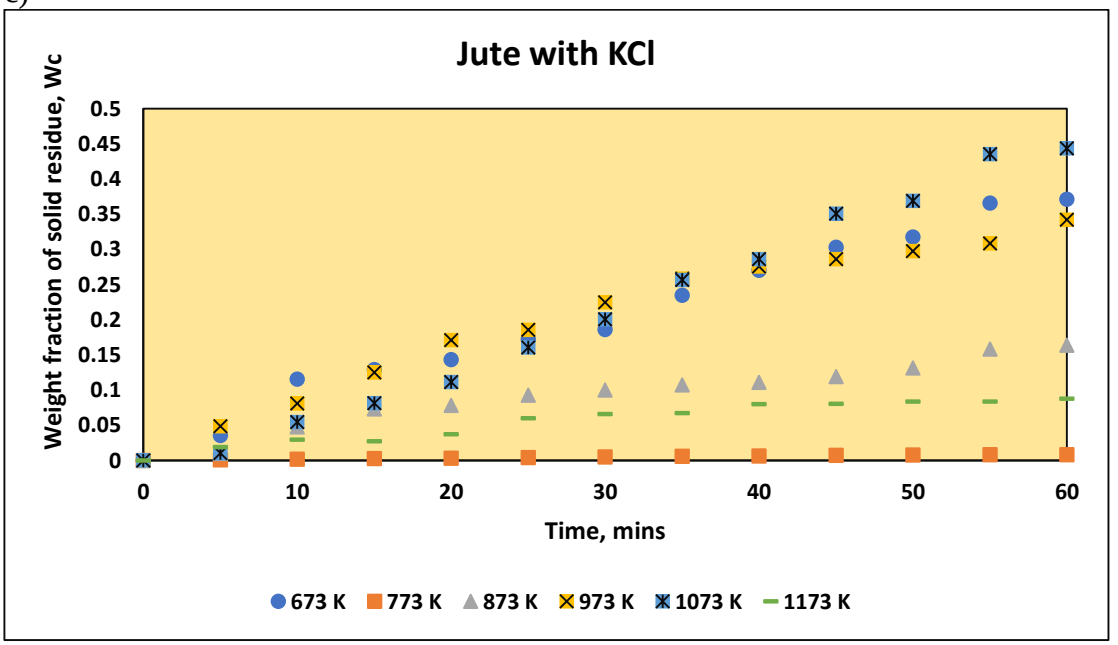
Jute with KCl
Weight fraction of solid residue, Wc
0.5
0.45
0.4
0.35
0.3
0.25
0.2
0.15
0.1
0.05
0
0
10
20
30
40
50
60
Time, mins
673 K
773 K
873 K
973 K
1073 K
1173 K

d)

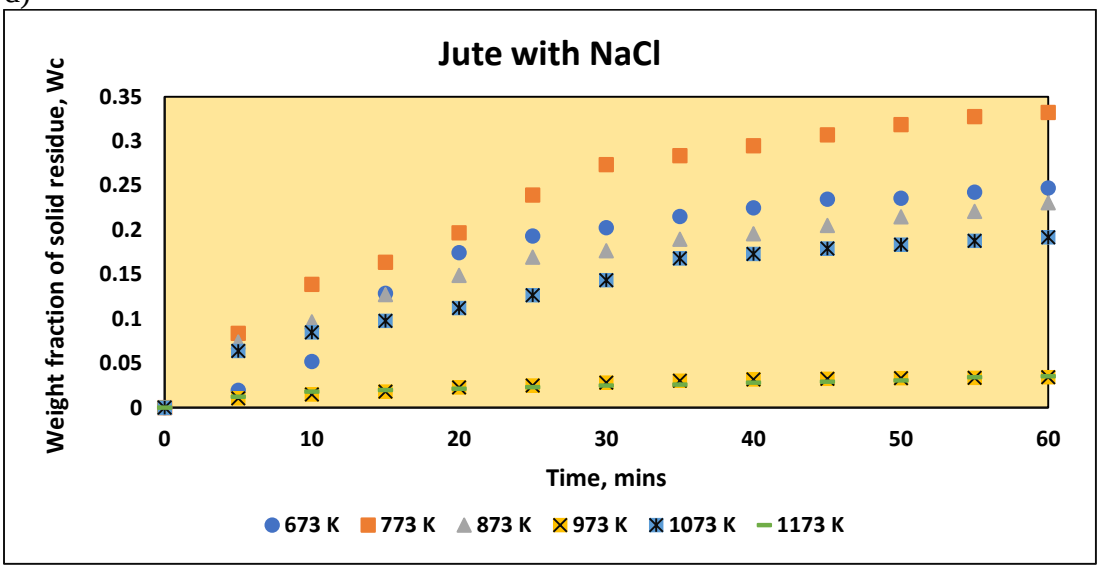

e)

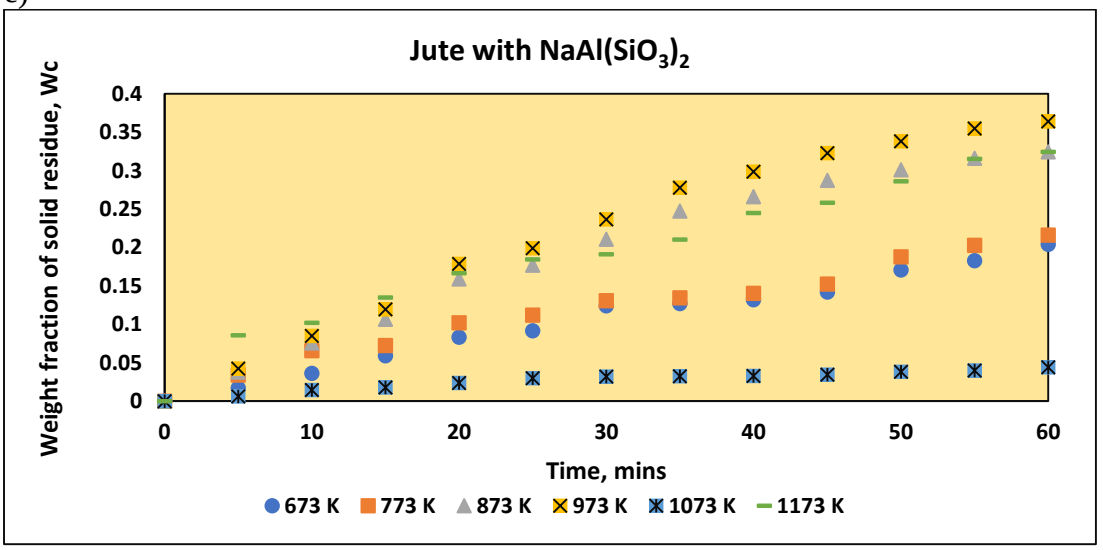

Figure 6.24. Time Histories of char weight fraction using pyrolysis temperature as parameter: (a) jute with alumina (b) jute with ZnO (c) jute with KCl (d) jute with NaCl and (e) jute with Aluminosilicate

6.4.1.2.1. Parameters of lumped kinetic Model

Experimental values of $\mathbf{ln}\left(\frac{w_o}{w}\right)$ have been plotted against time and those of $\frac{\mathbf{w_v}}{\mathbf{w_0}}$, $\frac{\mathbf{w_c}}{\mathbf{w_0}}$, $\frac{\mathbf{w_l}}{\mathbf{w_0}}$ **and** $\frac{\mathbf{w_g}}{\mathbf{w_0}}$ have been plotted against $\mathbf{(1-exp[-k*t])/k}$ for catalytic pyrolysis of jute wastes for all temperatures and catalysts under study [A.13.a – A.17.a]. Figures 6.25 -6.27 show the series of plots for 773K, 973K and 1173K respectively using all catalysts [34-38]. The linearity of the plots proves the validity of 1st order kinetics [3, 9-12] for all cases. Similar, plots have also been obtained at other temperature (not shown). The values of k', k_v' k_c' k_l' and k_g' [9-12,15] have been determined from the slopes of the respective plots and are provided in table 6.8-6.12.

a)

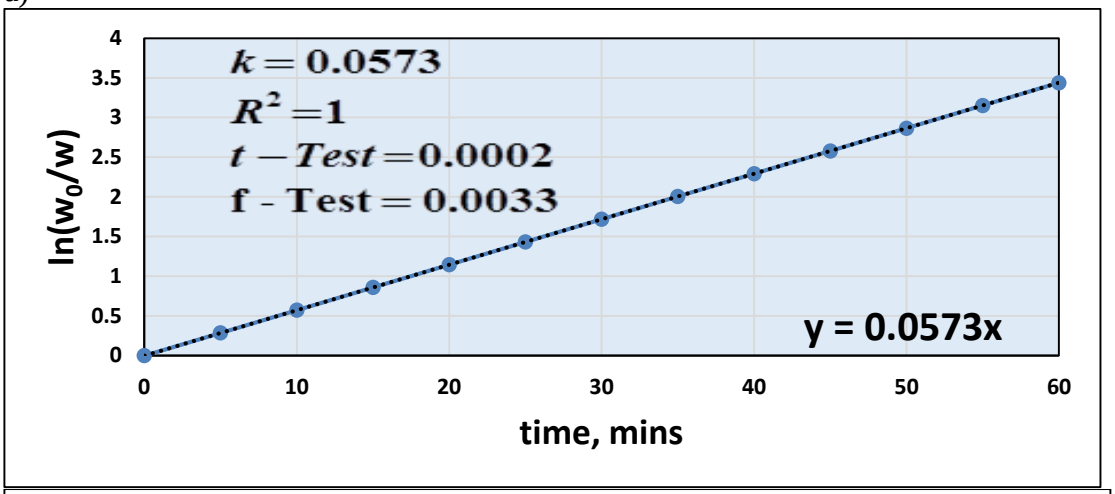
$k = 0.0573$
$R^2 = 1$
$t - Test = 0.0002$
f - Test = 0.0033
y = 0.0573x
ln(w0/w)
time, mins

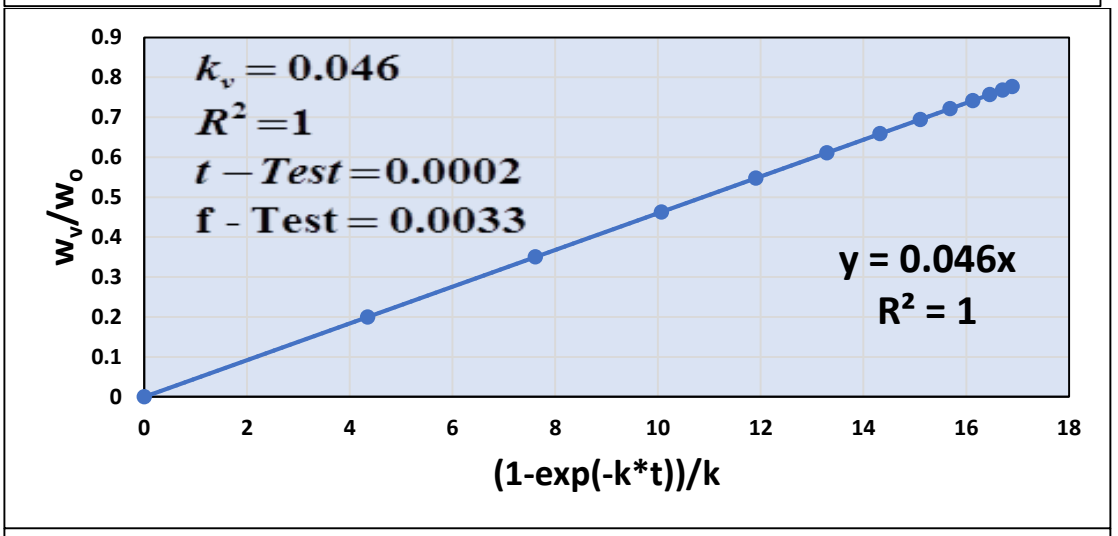
$k_v = 0.046$
$R^2 = 1$
$t - Test = 0.0002$
f - Test = 0.0033
y = 0.046x
R² = 1
wv/wo
(1-exp(-k*t))/k

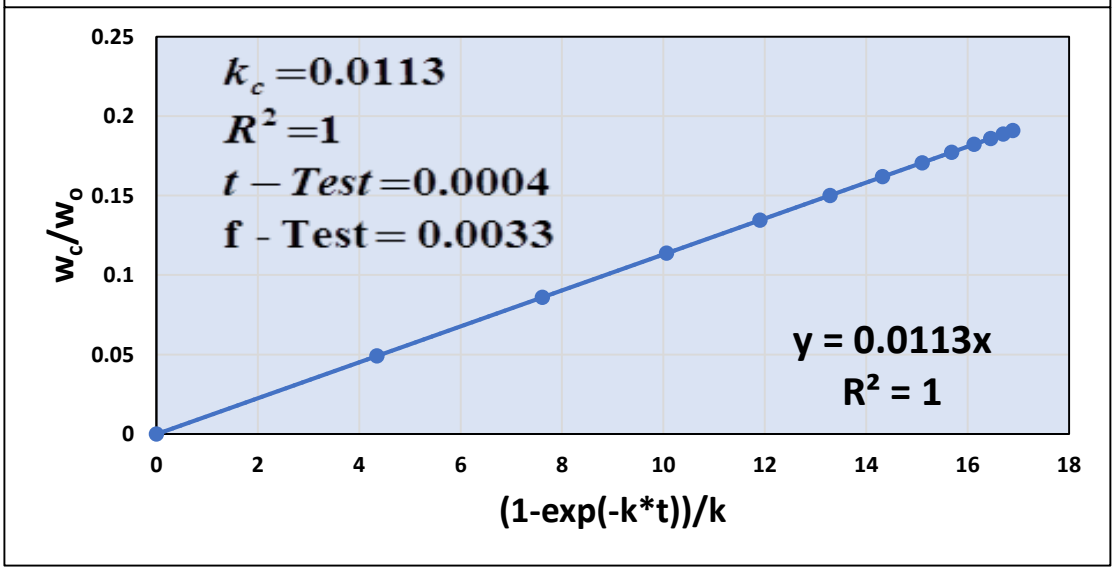
$k_c = 0.0113$
$R^2 = 1$
$t - Test = 0.0004$
f - Test = 0.0033
y = 0.0113x
R² = 1
wc/wo
(1-exp(-k*t))/k

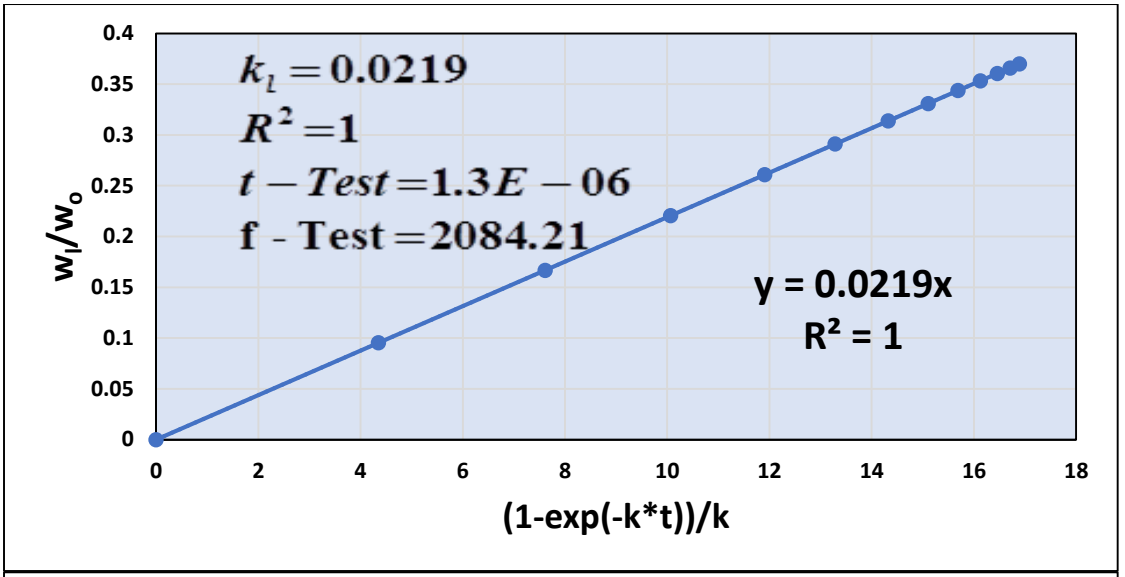
$k_l = 0.0219$
$R^2 = 1$
$t - Test = 1.3E - 06$
f - Test = 2084.21
y = 0.0219x
R² = 1
w_l/w_o
(1-exp(-k*t))/k

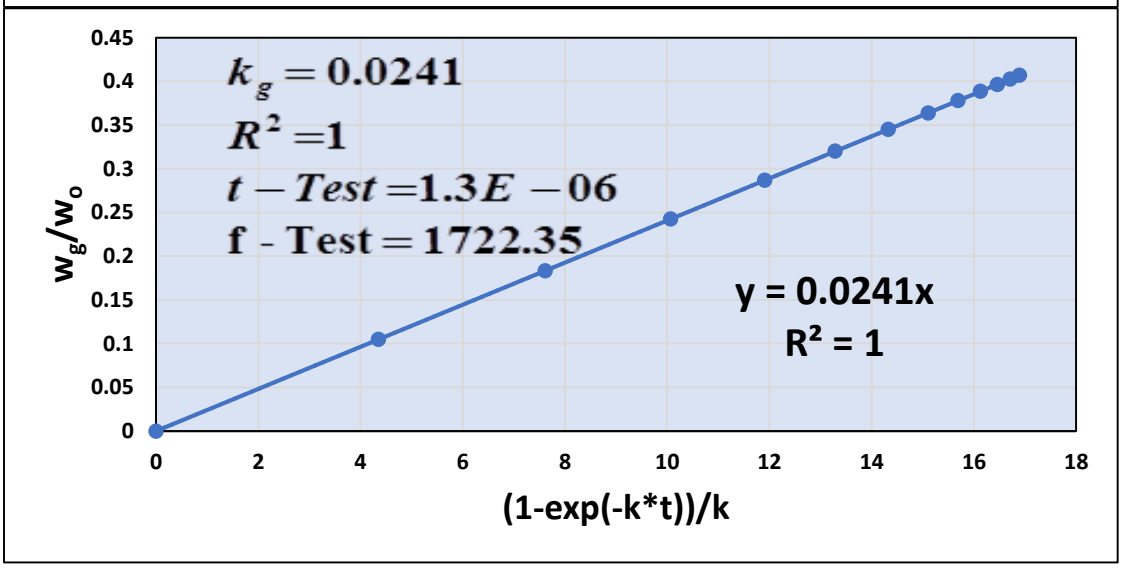
$k_g = 0.0241$
$R^2 = 1$
$t - Test = 1.3E - 06$
f - Test = 1722.35
y = 0.0241x
R² = 1
w_g/w_o
(1-exp(-k*t))/k

b)

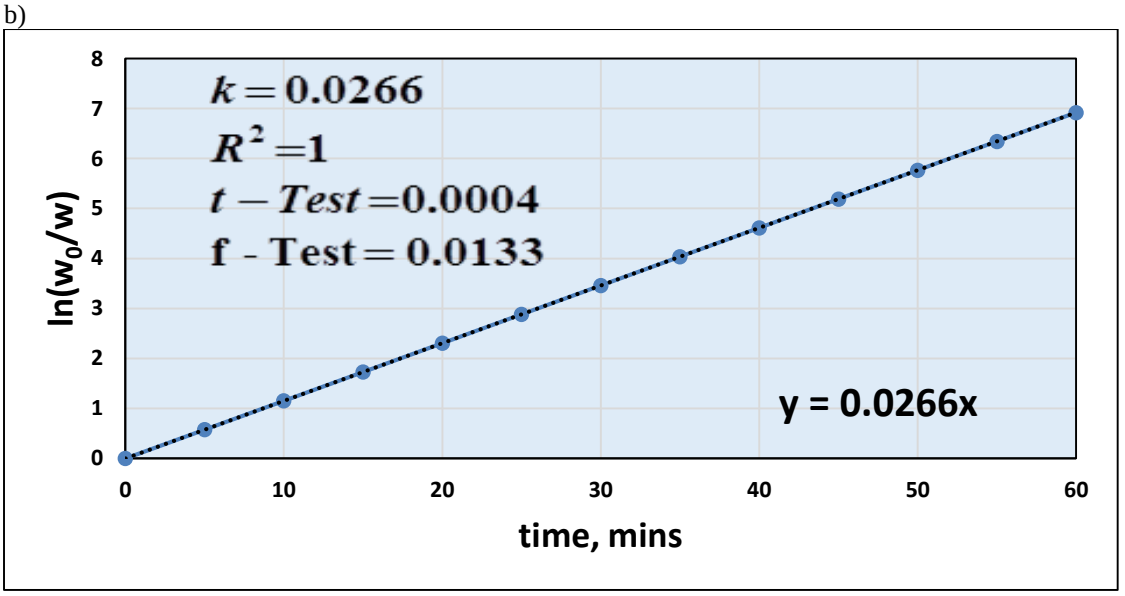
$k = 0.0266$
$R^2 = 1$
$t - Test = 0.0004$
f - Test = 0.0133
y = 0.0266x
$\ln(w_0/w)$
time, mins

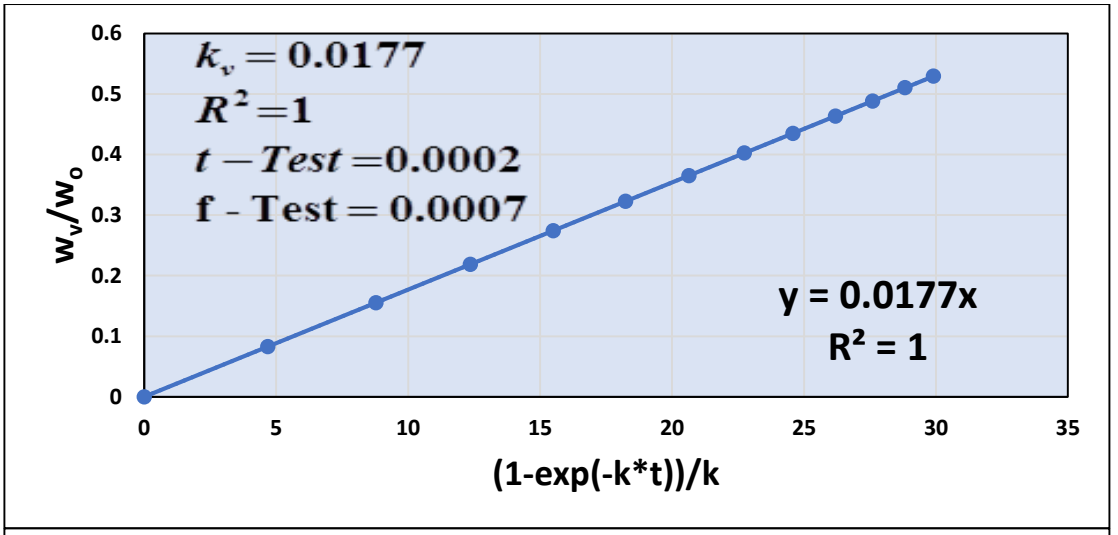
$k_v = 0.0177$
$R^2 = 1$
$t - Test = 0.0002$
f - Test = 0.0007
y = 0.0177x
R² = 1
w_v/w_o
(1-exp(-k*t))/k

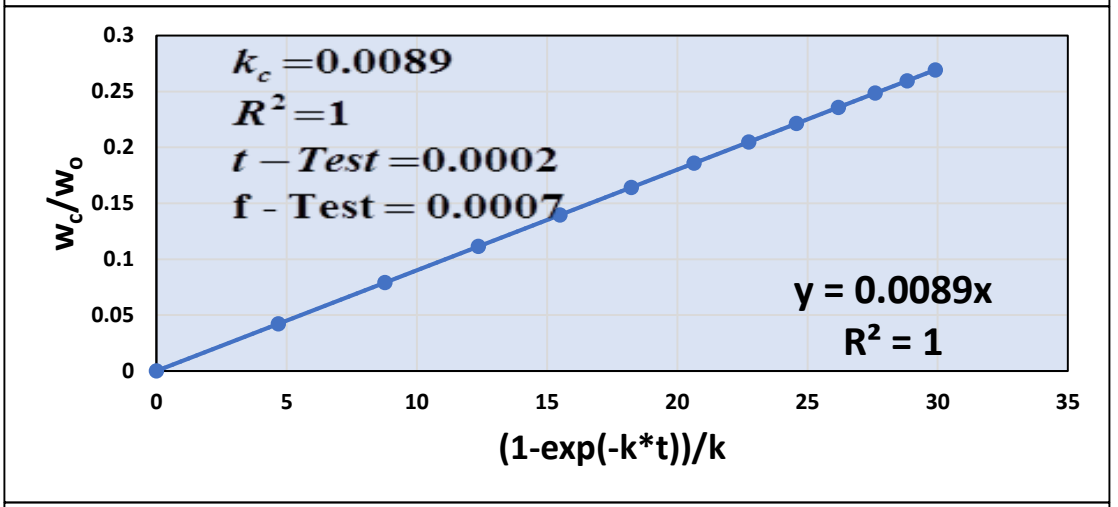
$k_c = 0.0089$
$R^2 = 1$
$t - Test = 0.0002$
f - Test = 0.0007
y = 0.0089x
R² = 1
w_c/w_o
(1-exp(-k*t))/k

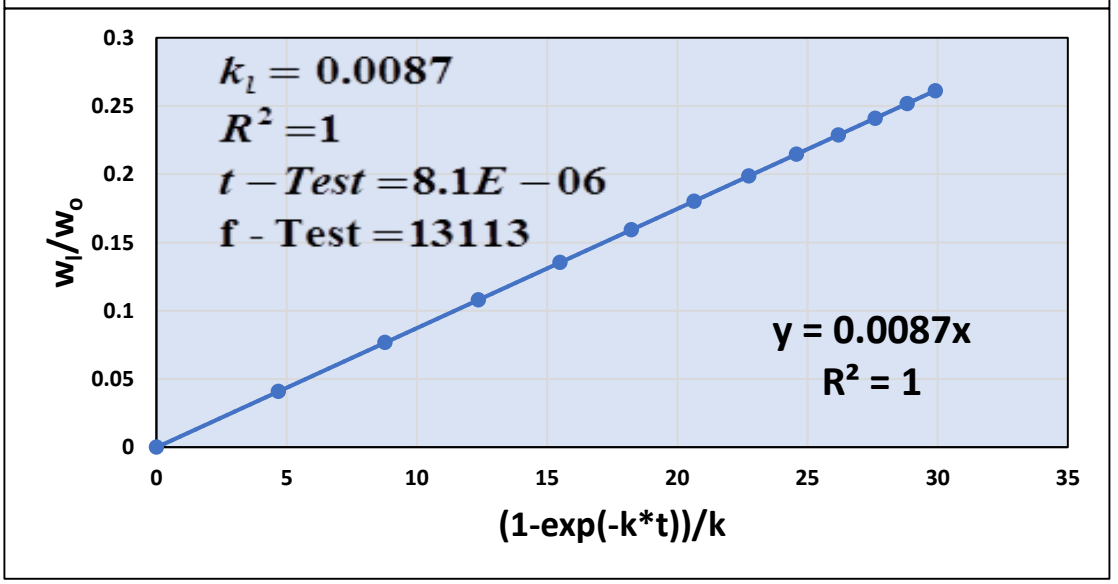
$k_l = 0.0087$
$R^2 = 1$
$t - Test = 8.1E-06$
f - Test = 13113
y = 0.0087x
R² = 1
w_l/w_o
(1-exp(-k*t))/k

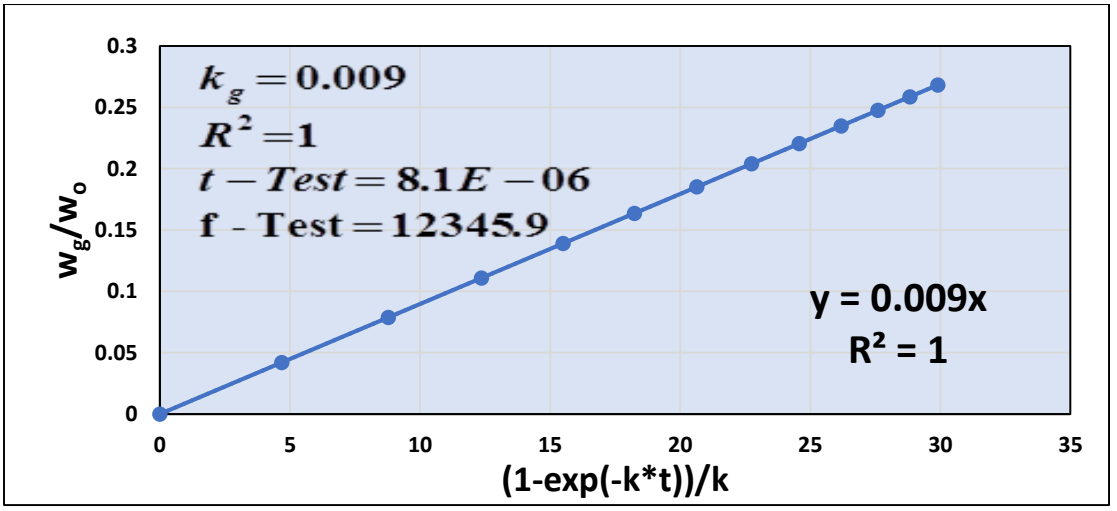
$k_g = 0.009$
$R^2 = 1$
$t - Test = 8.1E-06$
f - Test = 12345.9
y = 0.009x
R² = 1
w_g/w_o
(1-exp(-k*t))/k

c)

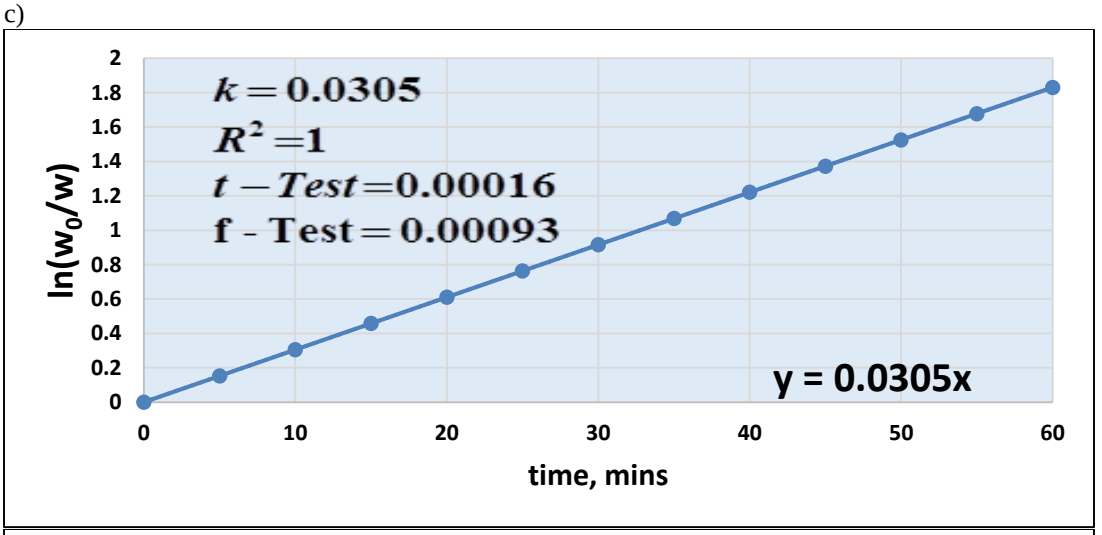
$k = 0.0305$
$R^2 = 1$
$t - Test = 0.00016$
f - Test = 0.00093
y = 0.0305x
$\ln(w_0/w)$
time, mins

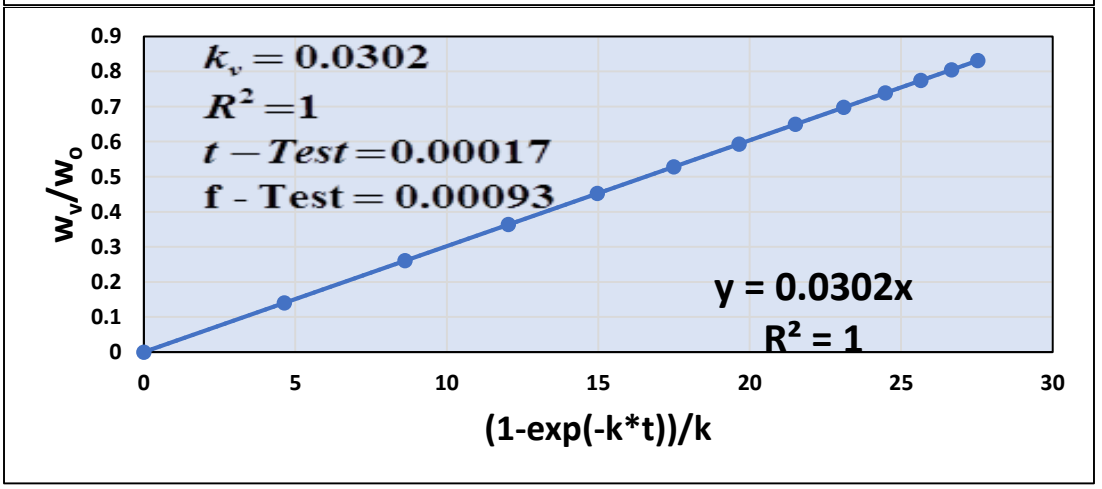
$k_v = 0.0302$
$R^2 = 1$
$t - Test = 0.00017$
f - Test = 0.00093
y = 0.0302x
R² = 1
w_v/w_o
(1-exp(-k*t))/k

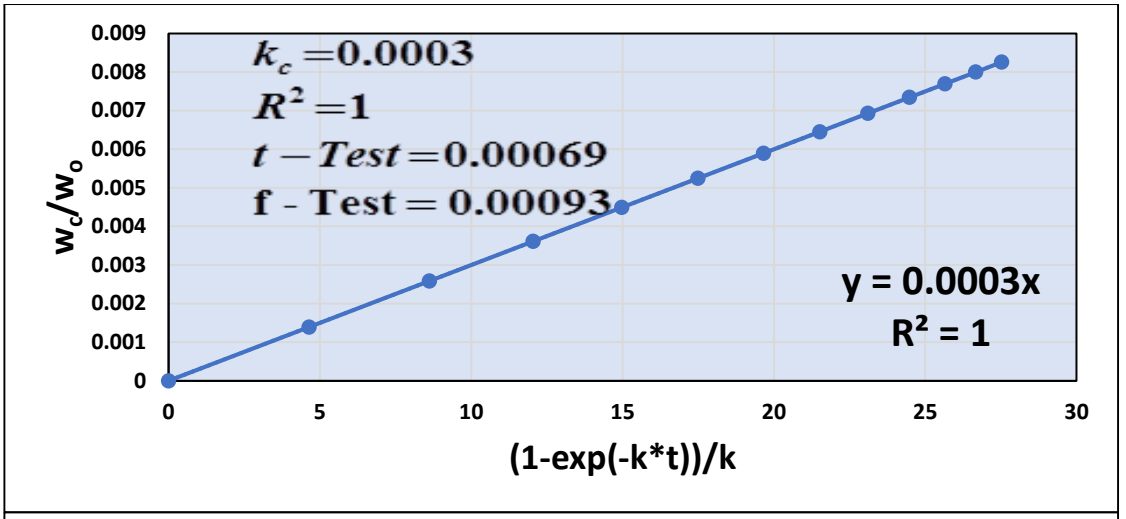
$k_c = 0.0003$
$R^2 = 1$
$t - Test = 0.00069$
f - Test = 0.00093
y = 0.0003x
R² = 1
w_c/w_o
(1-exp(-k*t))/k

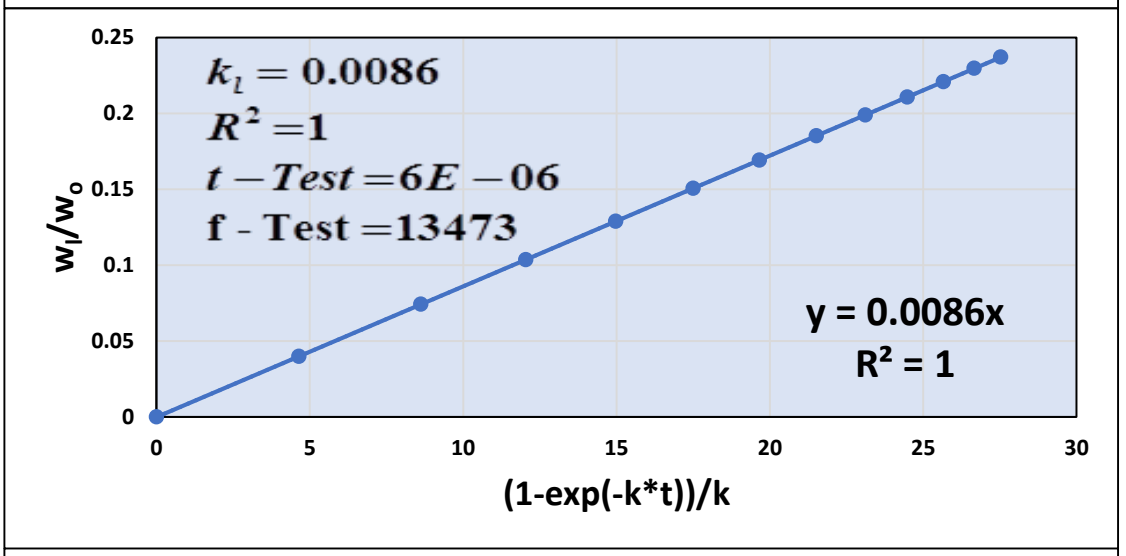
$k_l = 0.0086$
$R^2 = 1$
$t - Test = 6E-06$
f - Test = 13473
y = 0.0086x
R² = 1
w_l/w_o
(1-exp(-k*t))/k

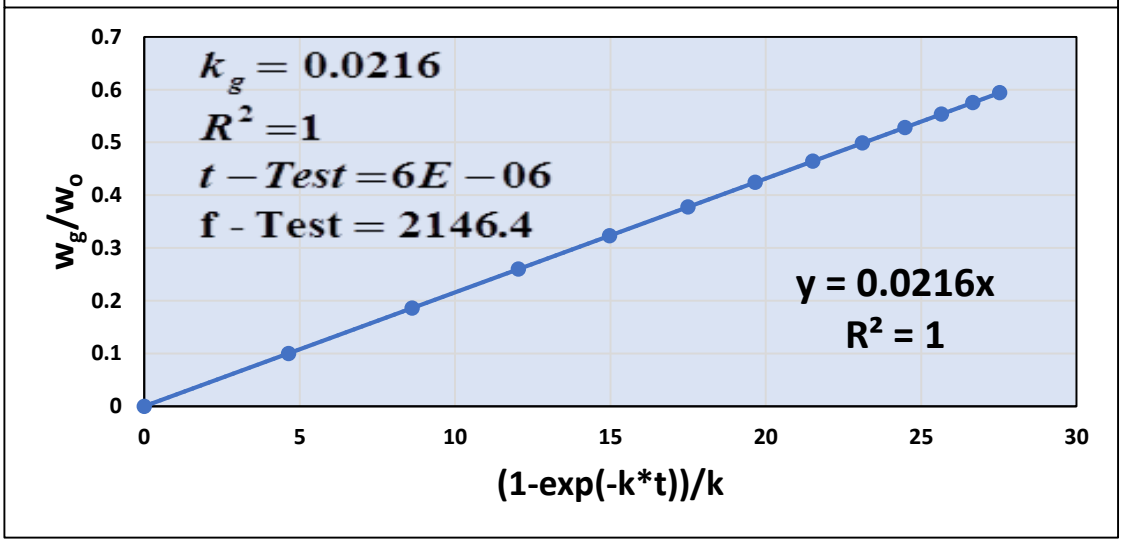
$k_g = 0.0216$
$R^2 = 1$
$t - Test = 6E-06$
f - Test = 2146.4
y = 0.0216x
R² = 1
w_g/w_o
(1-exp(-k*t))/k

d)

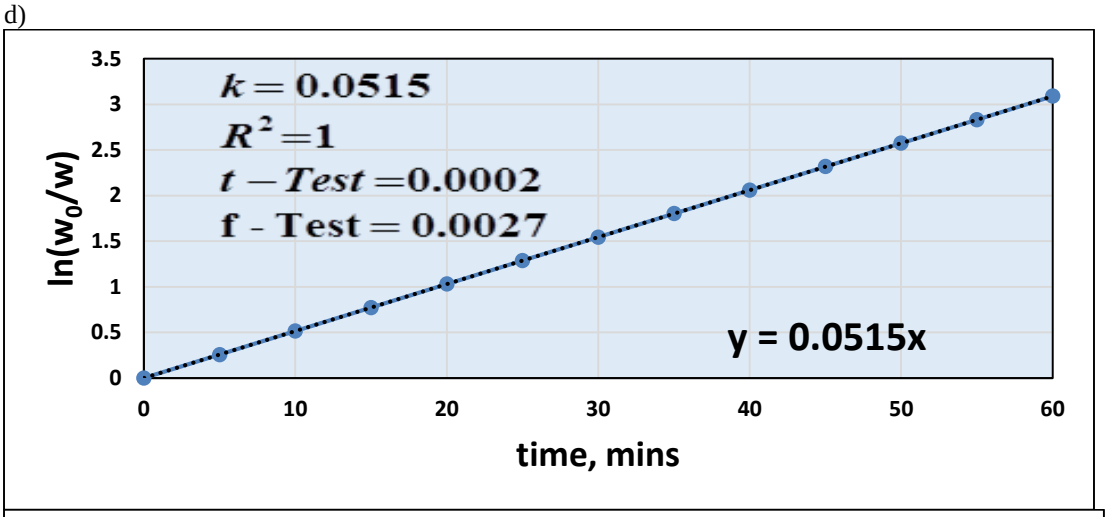
$k = 0.0515$
$R^2 = 1$
$t - Test = 0.0002$
f - Test = 0.0027
y = 0.0515x
ln(w0/w)
time, mins

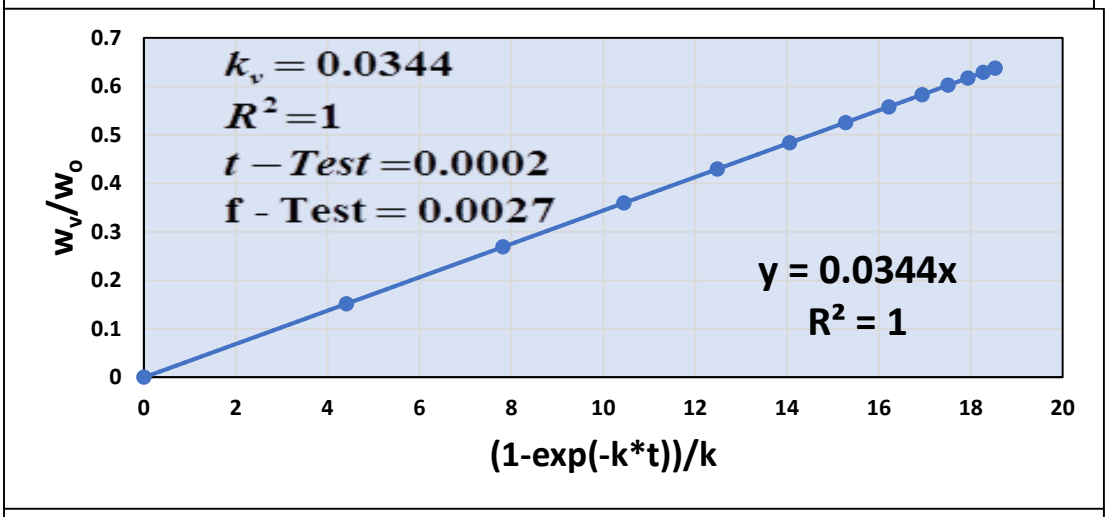
$k_v = 0.0344$
$R^2 = 1$
$t - Test = 0.0002$
f - Test = 0.0027
y = 0.0344x
R² = 1
wv/wo
(1-exp(-k*t))/k

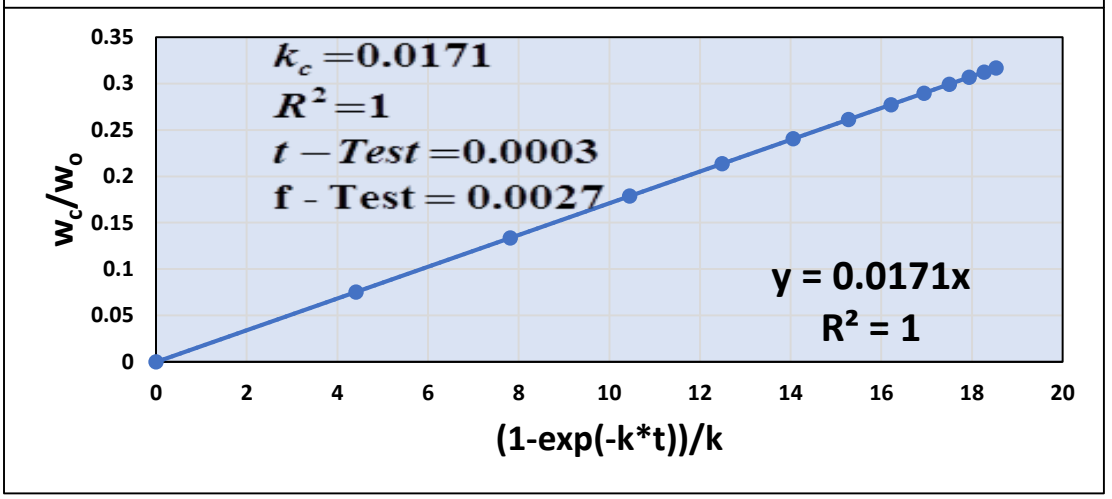
$k_c = 0.0171$
$R^2 = 1$
$t - Test = 0.0003$
f - Test = 0.0027
y = 0.0171x
R² = 1
wc/wo
(1-exp(-k*t))/k

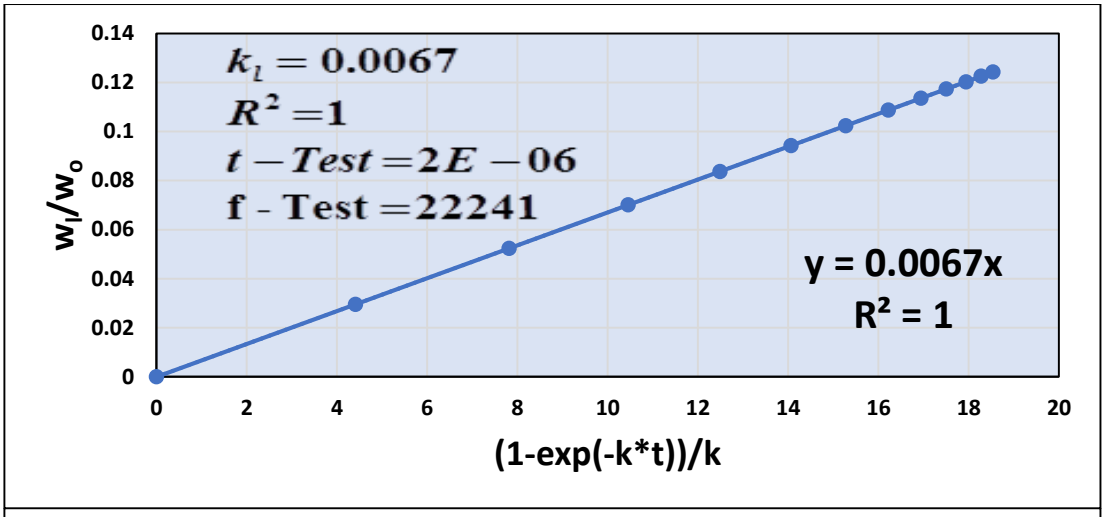
$k_l = 0.0067$
$R^2 = 1$
$t - Test = 2E - 06$
f - Test = 22241
y = 0.0067x
R² = 1
w_l/w_o
(1-exp(-k*t))/k

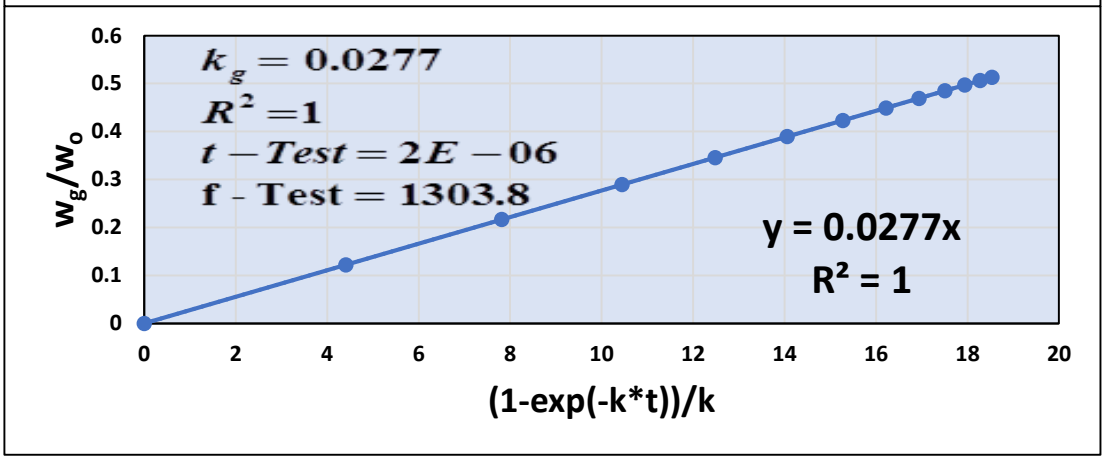
$k_g = 0.0277$
$R^2 = 1$
$t - Test = 2E - 06$
f - Test = 1303.8
y = 0.0277x
R² = 1
w_g/w_o
(1-exp(-k*t))/k

e)

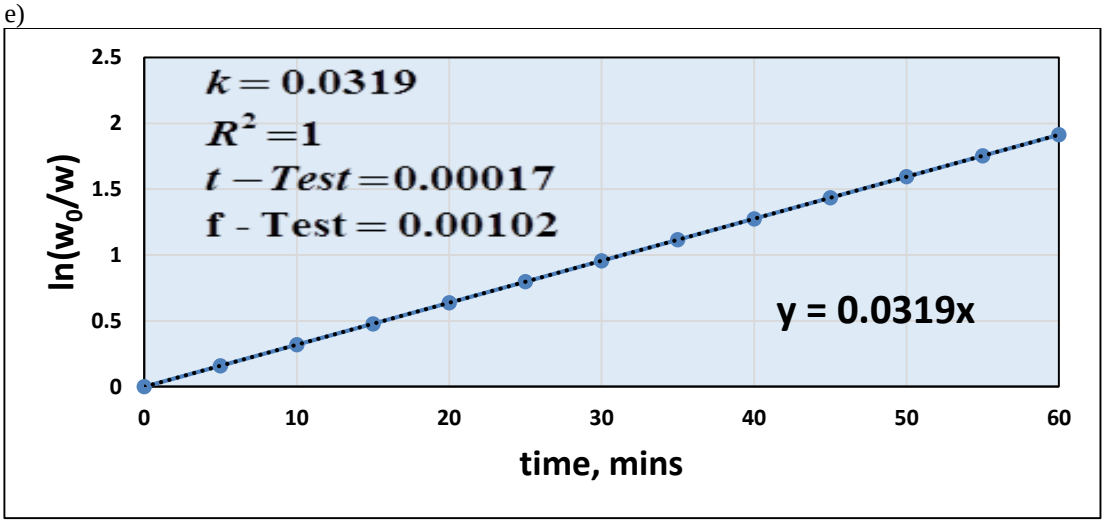
$k = 0.0319$
$R^2 = 1$
$t - Test = 0.00017$
f - Test = 0.00102
y = 0.0319x
ln(w₀/w)
time, mins

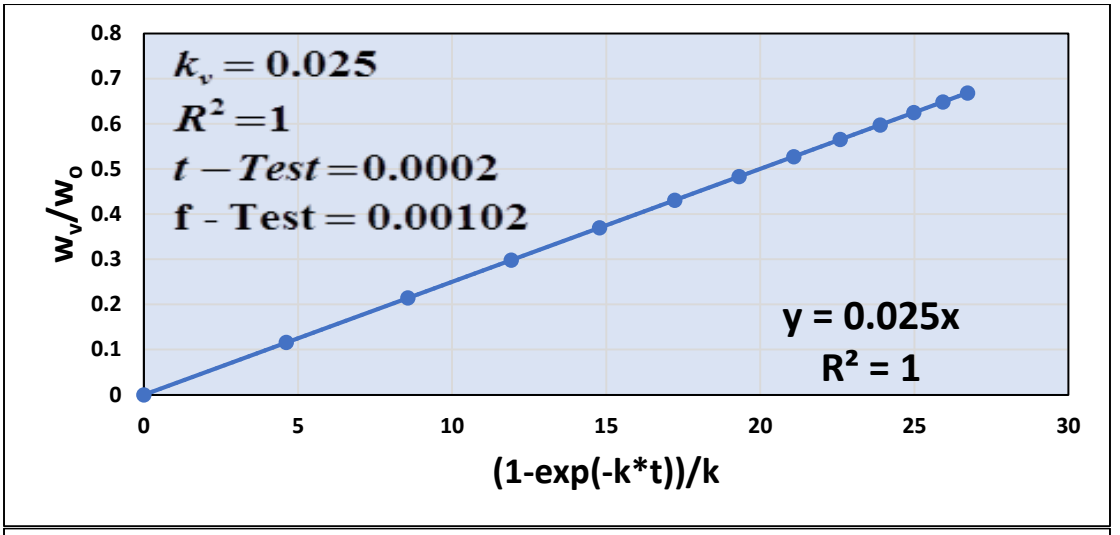
$k_v = 0.025$
$R^2 = 1$
$t - Test = 0.0002$
f - Test = 0.00102
y = 0.025x
R² = 1
w_v/w_o
(1-exp(-k*t))/k

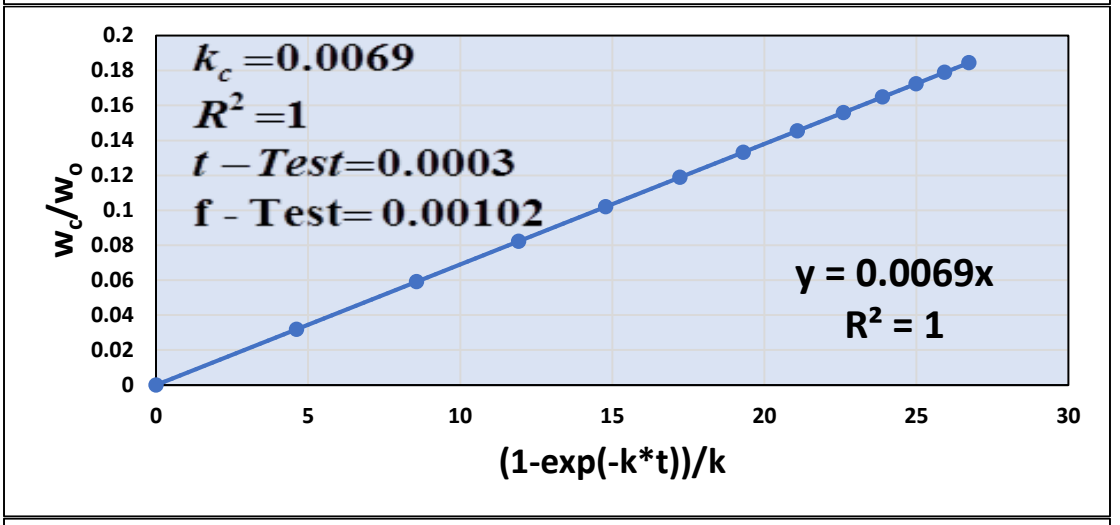
$k_c = 0.0069$
$R^2 = 1$
$t - Test = 0.0003$
f - Test= 0.00102
y = 0.0069x
R² = 1
w_c/w_o
(1-exp(-k*t))/k

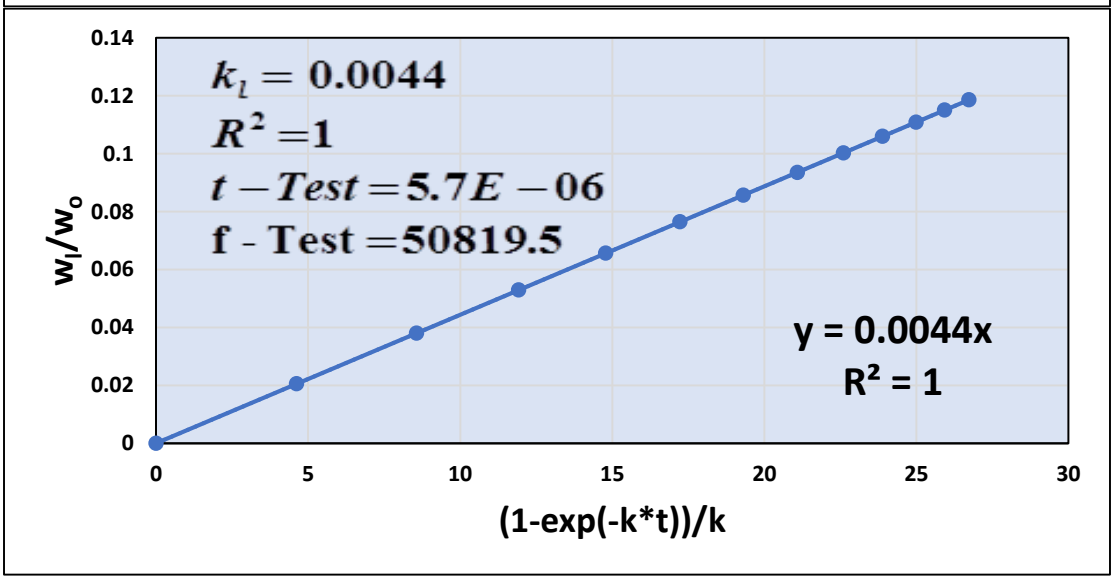
$k_l = 0.0044$
$R^2 = 1$
$t - Test = 5.7E-06$
f - Test =50819.5
y = 0.0044x
R² = 1
w_l/w_o
(1-exp(-k*t))/k

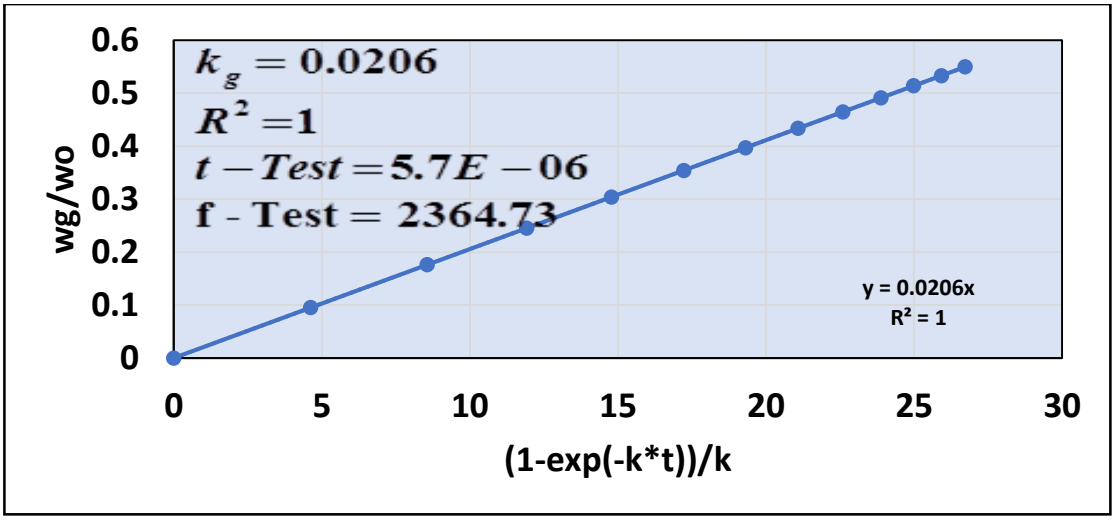

Figure 6.25. Plots of $\ln\left[\frac{w_o}{w}\right]$ vs time and $\frac{w_v}{w_0}$, $\frac{w_c}{w_0}$, $\frac{w_l}{w_0}$ and $\frac{w_g}{w_0}$ vs $(1-\exp[-k*t])/k$ at 773K (a) jute with alumina (b) jute with ZnO (c) jute with KCl (d) jute with NaCl and (e) jute with Aluminosilicate

a)

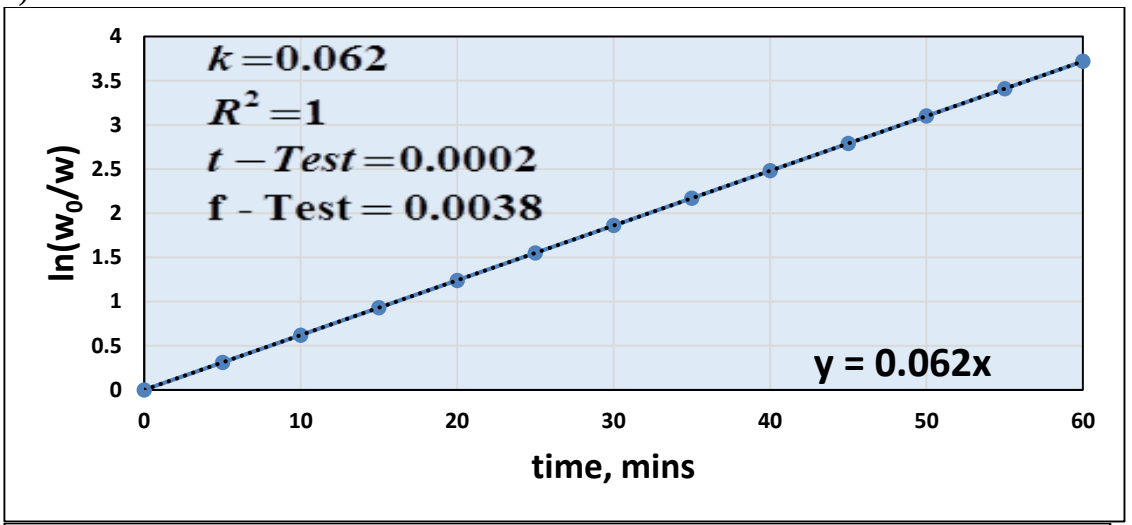

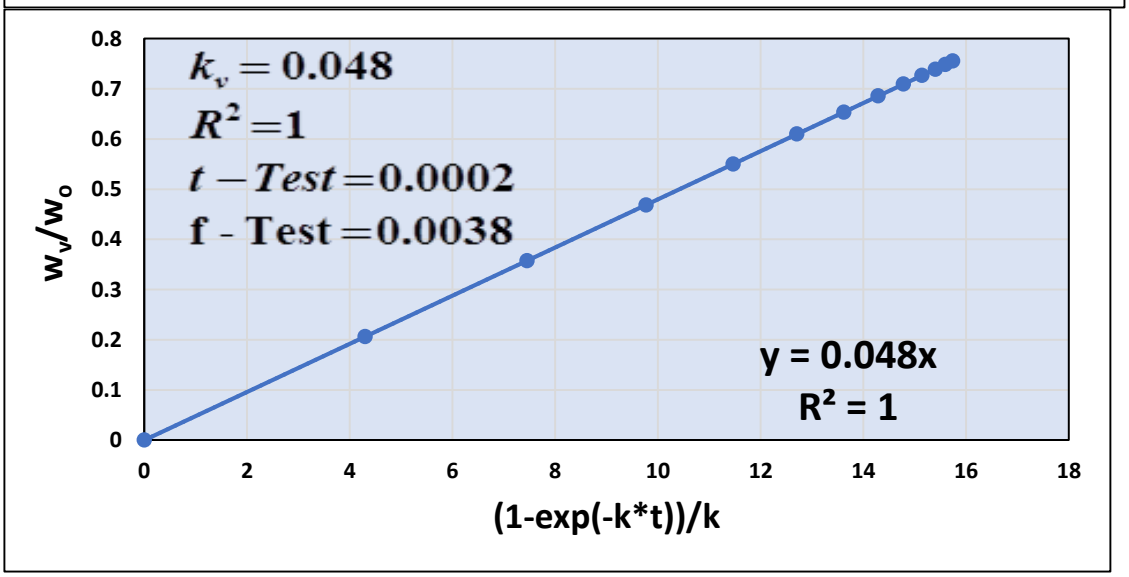

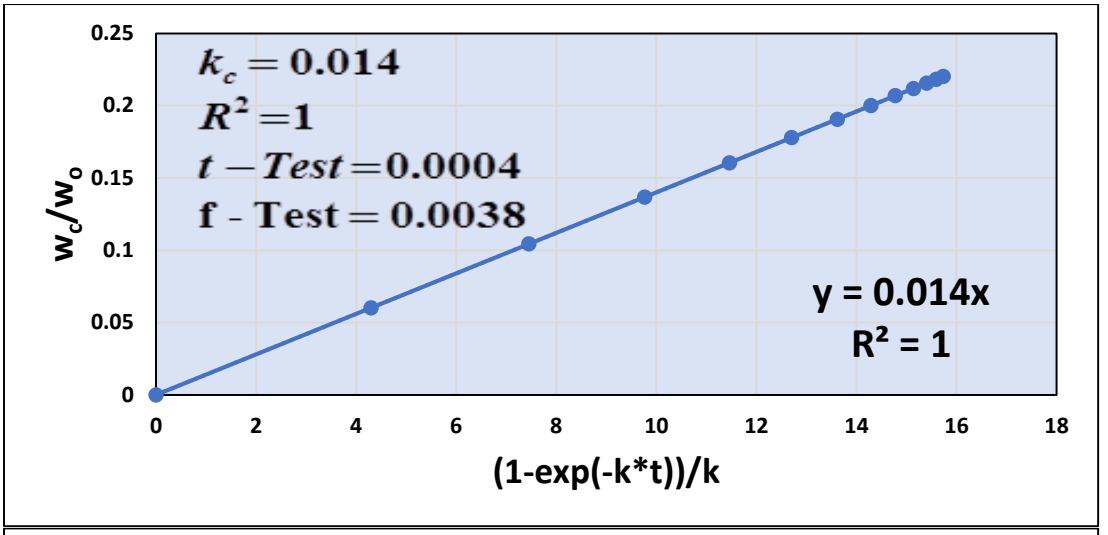
$k_c = 0.014$
$R^2 = 1$
$t - Test = 0.0004$
f - Test = 0.0038
y = 0.014x
R² = 1
w_c/w_o
(1-exp(-k*t))/k

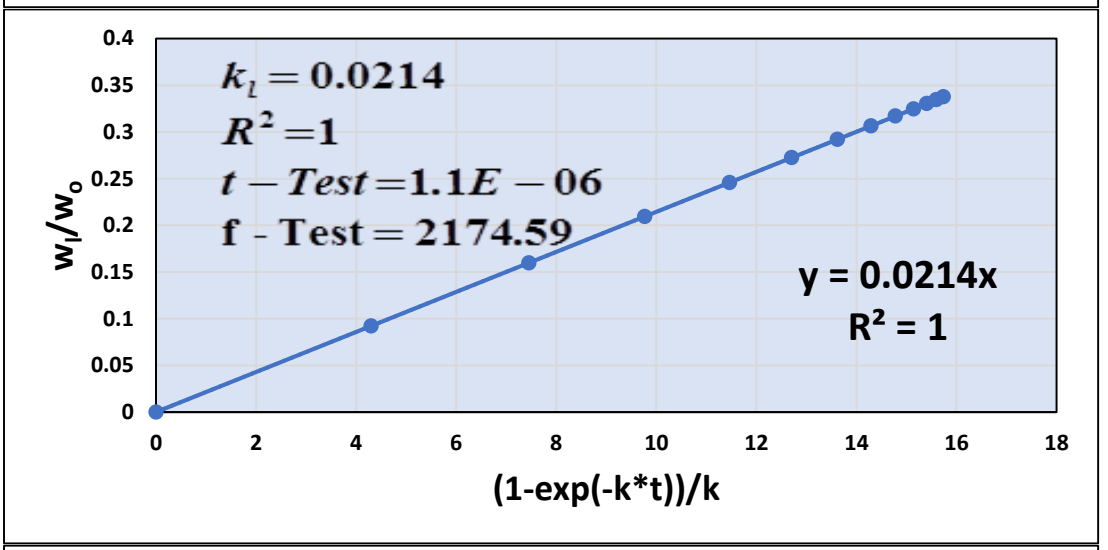
$k_l = 0.0214$
$R^2 = 1$
$t - Test = 1.1E-06$
f - Test = 2174.59
y = 0.0214x
R² = 1
w_l/w_o
(1-exp(-k*t))/k

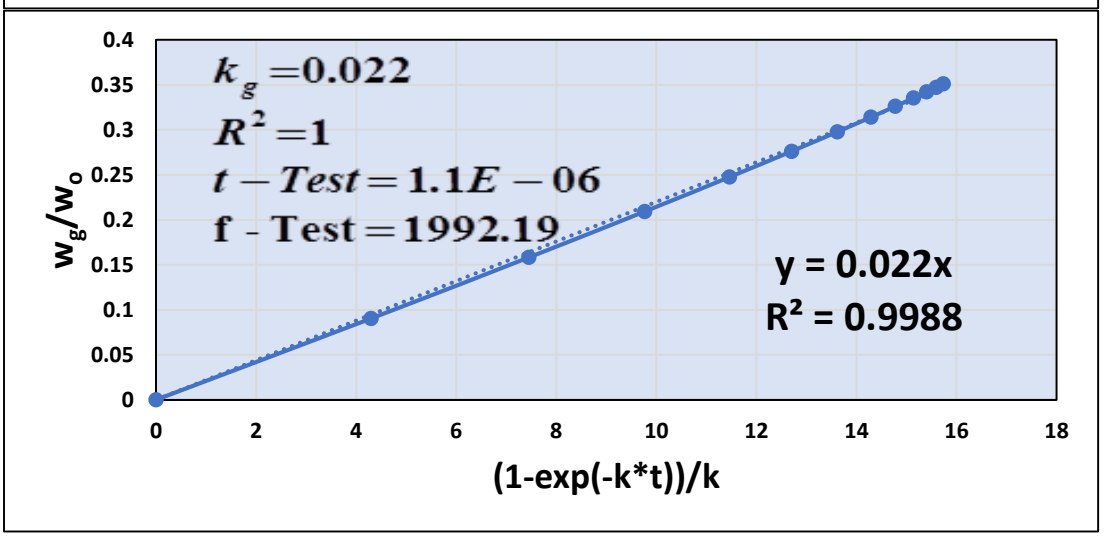
$k_g = 0.022$
$R^2 = 1$
$t - Test = 1.1E-06$
f - Test = 1992.19
y = 0.022x
R² = 0.9988
w_g/w_o
(1-exp(-k*t))/k

b)

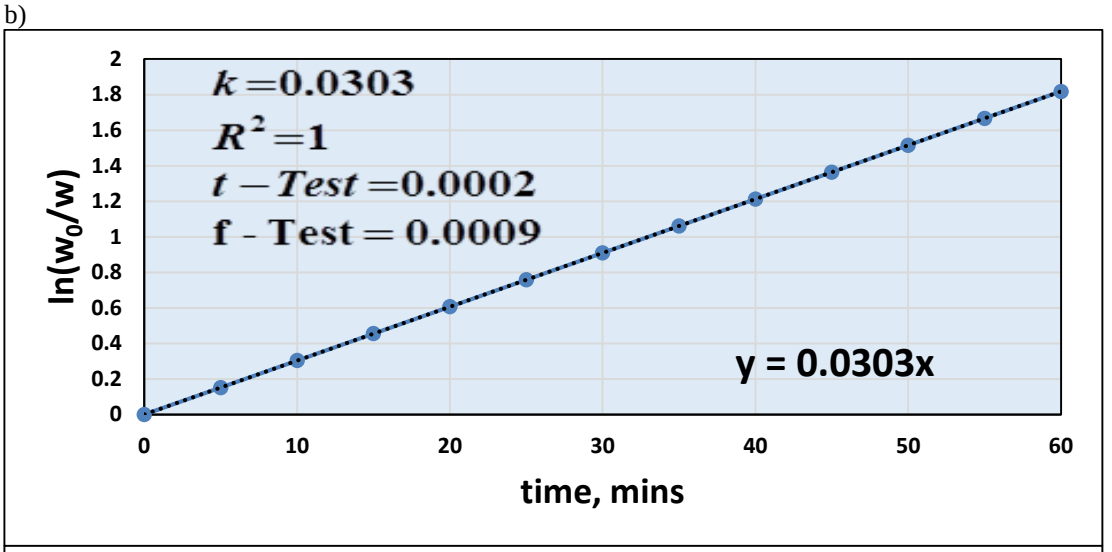
k =0.0303
R² =1
t – Test =0.0002
f - Test = 0.0009
y = 0.0303x
ln(w0/w)
time, mins

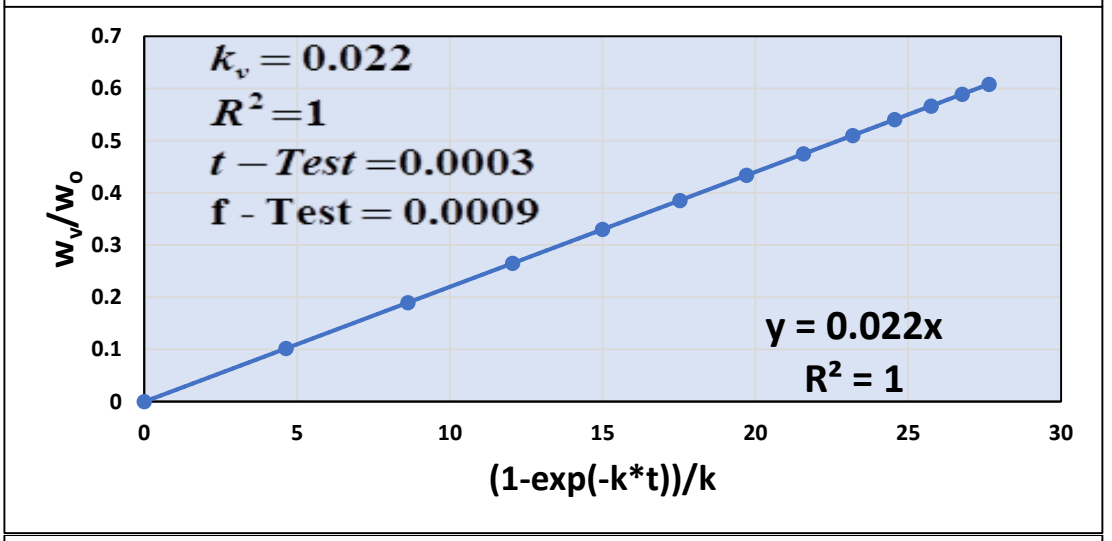
kv = 0.022
R² =1
t – Test =0.0003
f - Test = 0.0009
y = 0.022x
R² = 1
wv/wo
(1-exp(-k*t))/k

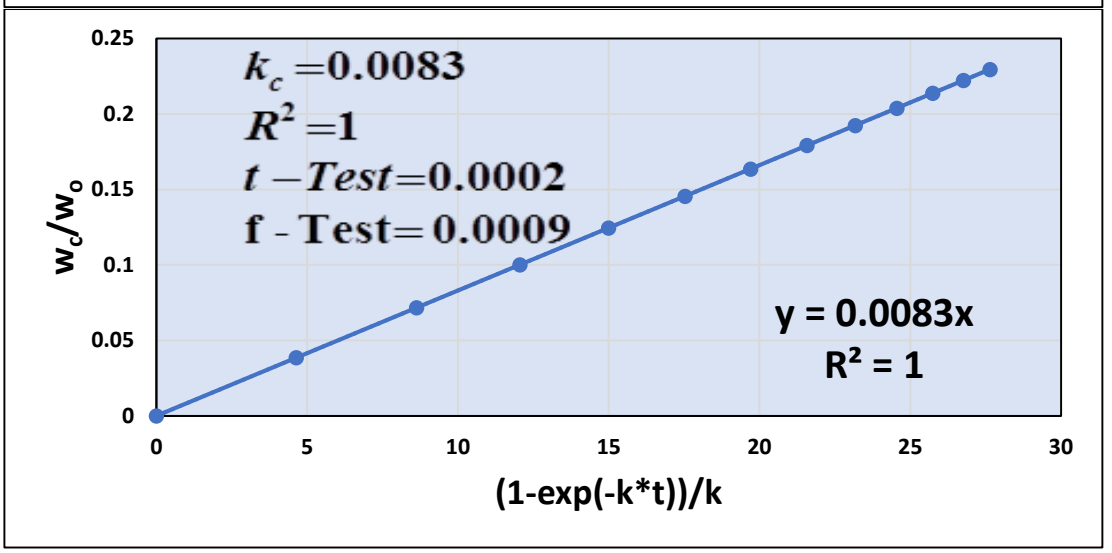
kc =0.0083
R² =1
t – Test=0.0002
f - Test= 0.0009
y = 0.0083x
R² = 1
wc/wo
(1-exp(-k*t))/k

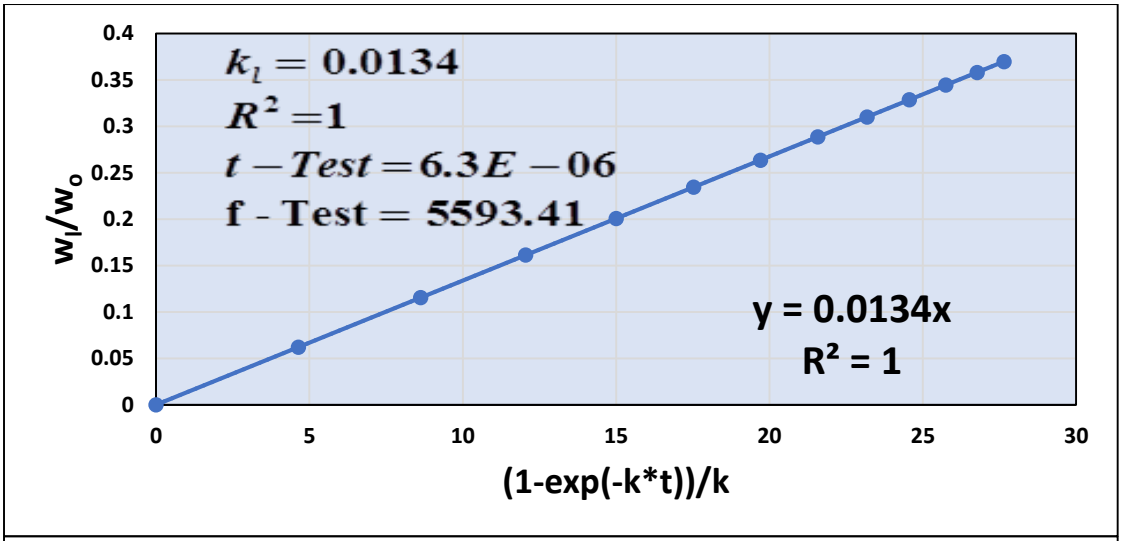
$k_l = 0.0134$
$R^2 = 1$
$t - Test = 6.3E - 06$
f - Test = 5593.41
y = 0.0134x
R² = 1
w_l/w_o
(1-exp(-k*t))/k

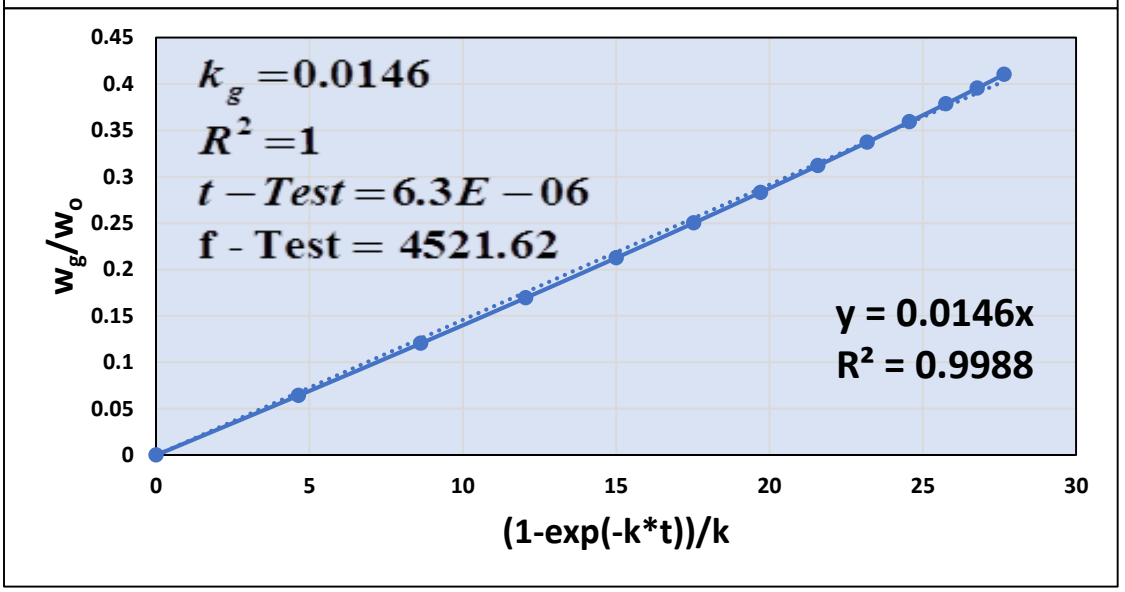
$k_g = 0.0146$
$R^2 = 1$
$t - Test = 6.3E - 06$
f - Test = 4521.62
y = 0.0146x
R² = 0.9988
w_g/w_o
(1-exp(-k*t))/k

c)

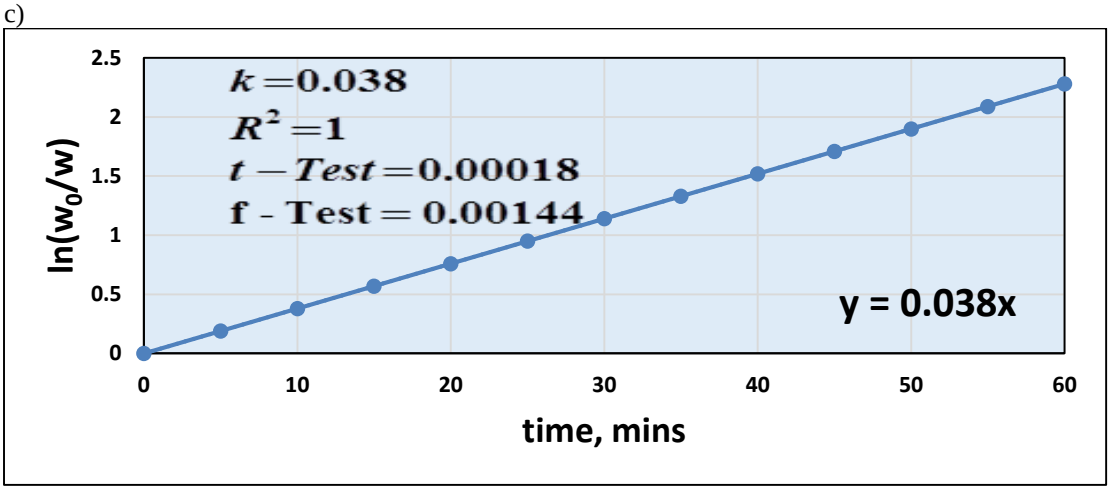
$k = 0.038$
$R^2 = 1$
$t - Test = 0.00018$
f - Test = 0.00144
y = 0.038x
$\ln(w_0/w)$
time, mins

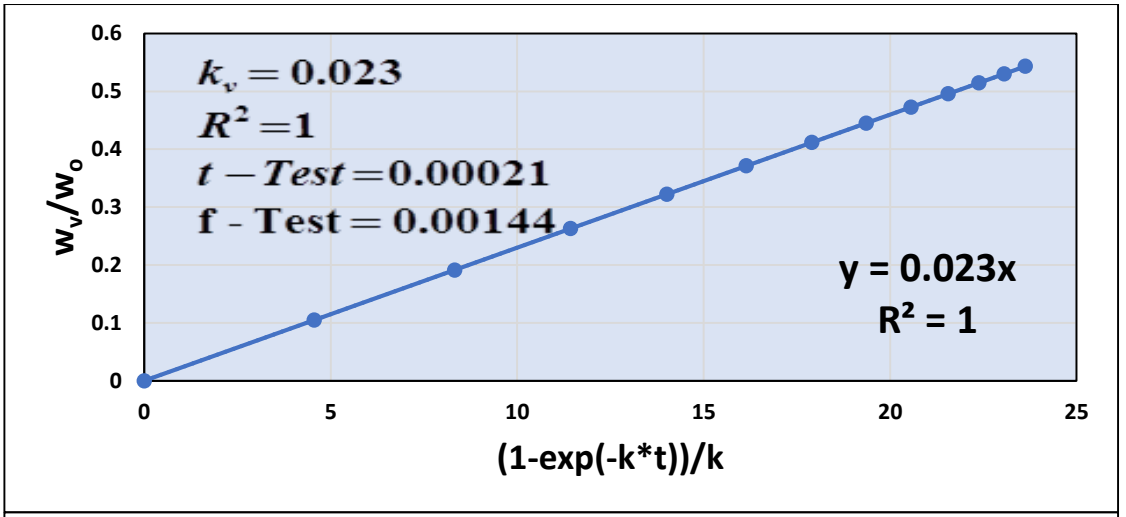
$k_v = 0.023$
$R^2 = 1$
$t - Test = 0.00021$
f - Test = 0.00144
y = 0.023x
R² = 1
w_v/w_o
(1-exp(-k*t))/k

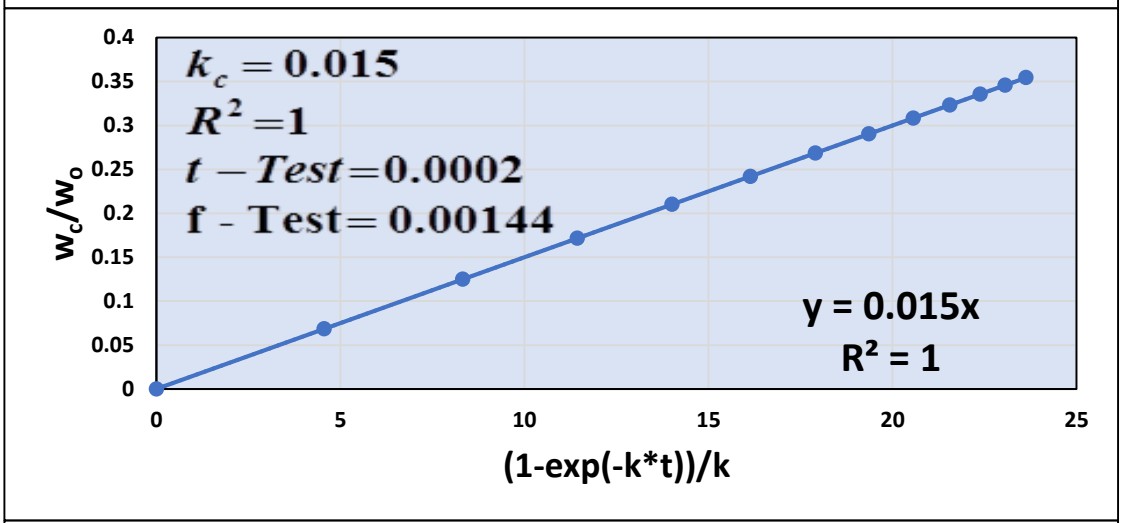
$k_c = 0.015$
$R^2 = 1$
$t - Test = 0.0002$
f - Test = 0.00144
y = 0.015x
R² = 1
w_c/w_o
(1-exp(-k*t))/k

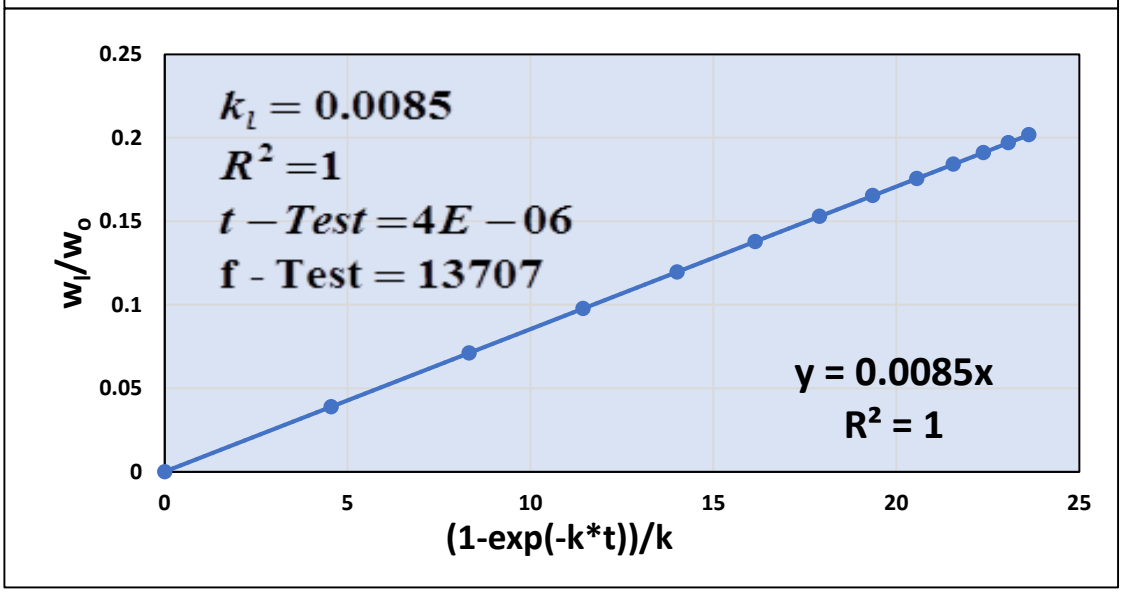
$k_l = 0.0085$
$R^2 = 1$
$t - Test = 4E-06$
f - Test = 13707
y = 0.0085x
R² = 1
w_l/w_o
(1-exp(-k*t))/k

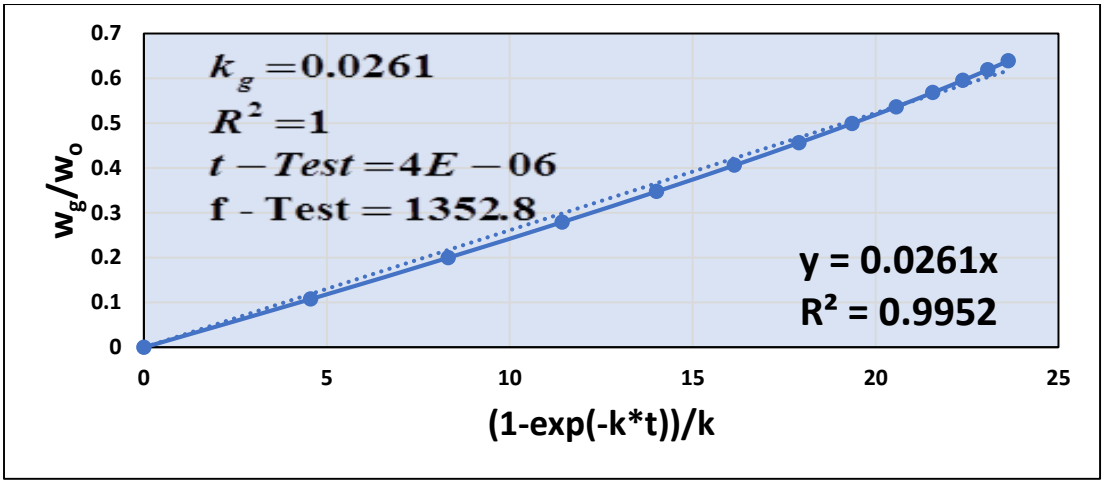
$k_g = 0.0261$
$R^2 = 1$
$t - Test = 4E-06$
f - Test = 1352.8
y = 0.0261x
R² = 0.9952
w_g/w_o
(1-exp(-k*t))/k

d)

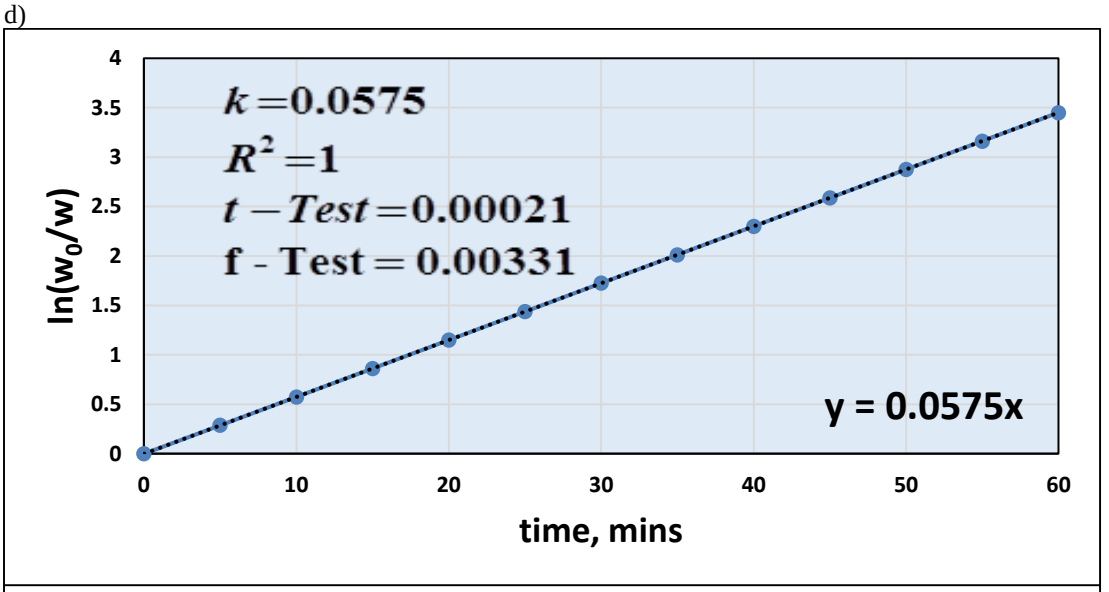
$k = 0.0575$
$R^2 = 1$
$t - Test = 0.00021$
f - Test = 0.00331
y = 0.0575x
$\ln(w_0/w)$
time, mins

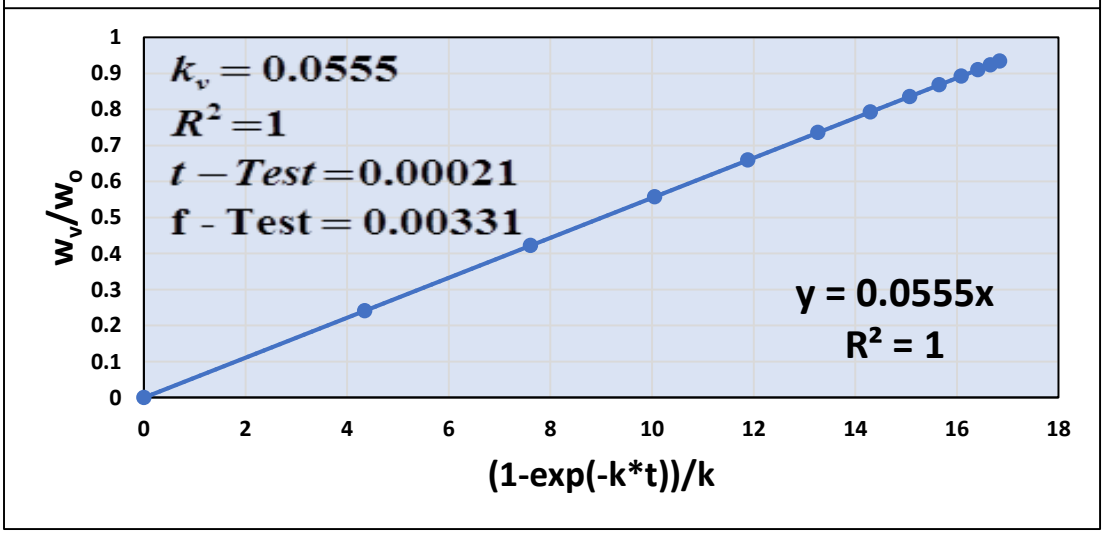
$k_v = 0.0555$
$R^2 = 1$
$t - Test = 0.00021$
f - Test = 0.00331
y = 0.0555x
R² = 1
w_v/w_o
(1-exp(-k*t))/k

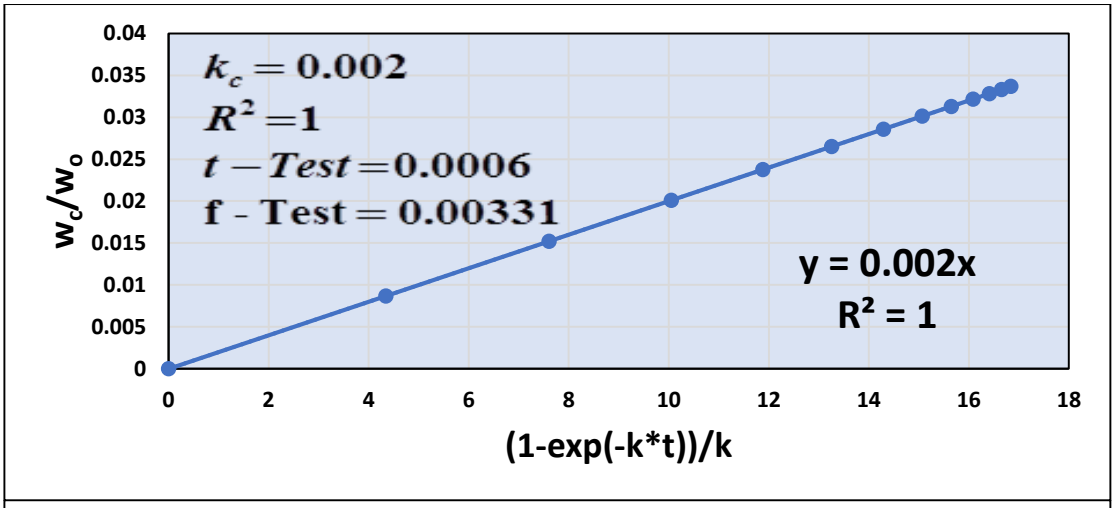
$k_c = 0.002$
$R^2 = 1$
$t - Test = 0.0006$
f - Test = 0.00331
y = 0.002x
R² = 1
w_c/w_o
(1-exp(-k*t))/k

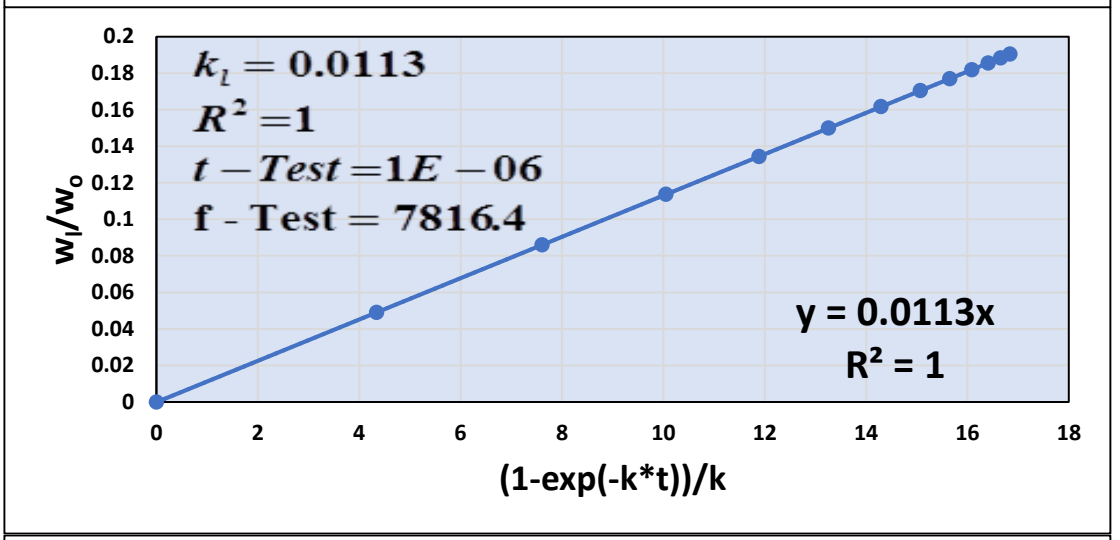
$k_l = 0.0113$
$R^2 = 1$
$t - Test = 1E-06$
f - Test = 7816.4
y = 0.0113x
R² = 1
w_l/w_o
(1-exp(-k*t))/k

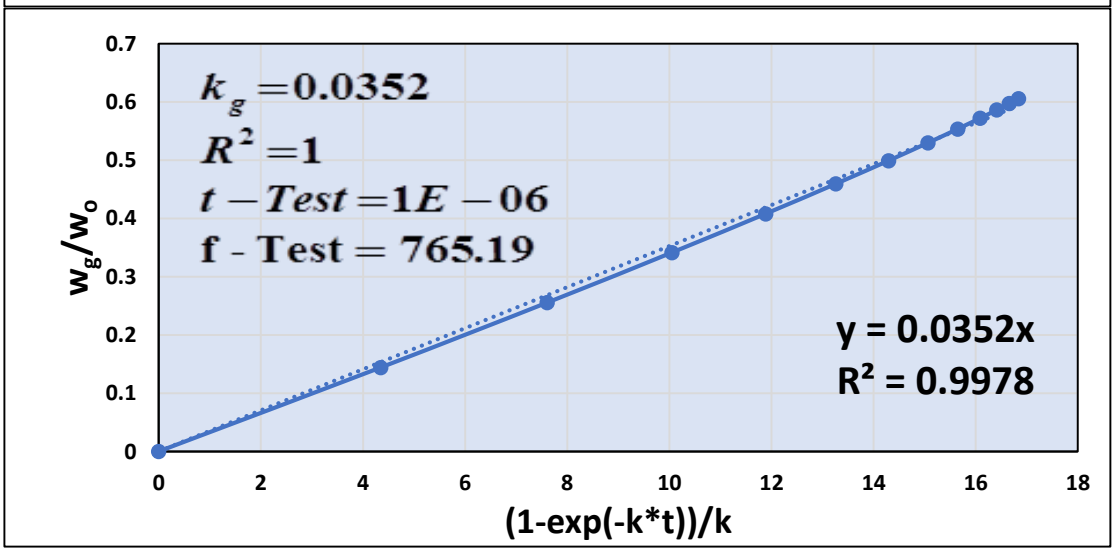
$k_g = 0.0352$
$R^2 = 1$
$t - Test = 1E-06$
f - Test = 765.19
y = 0.0352x
R² = 0.9978
w_g/w_o
(1-exp(-k*t))/k

e)

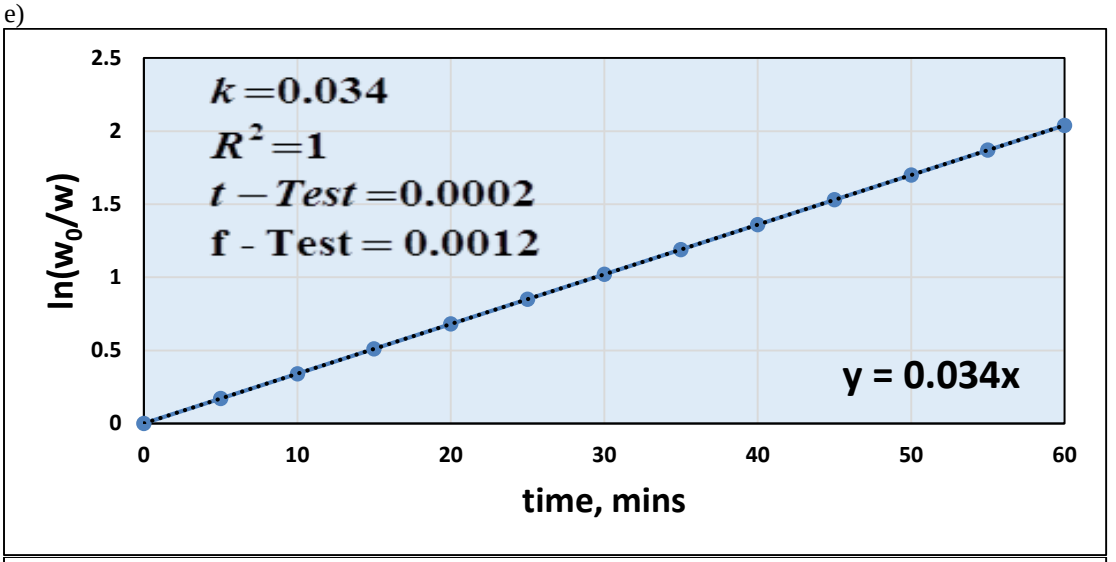
k =0.034
R² =1
t – Test =0.0002
f - Test = 0.0012
y = 0.034x
ln(w0/w)
time, mins

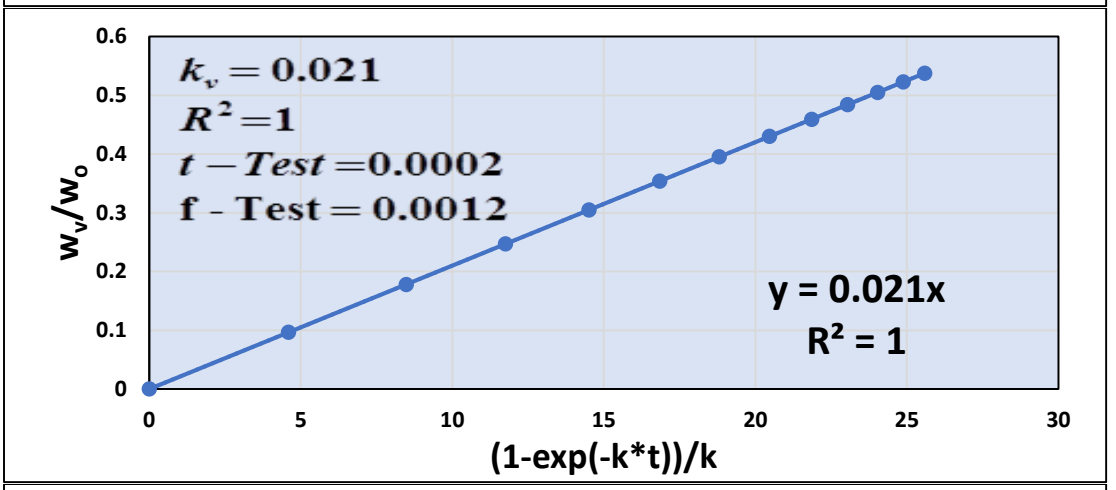
kv = 0.021
R² =1
t – Test =0.0002
f - Test = 0.0012
y = 0.021x
R² = 1
wv/wo
(1-exp(-k*t))/k

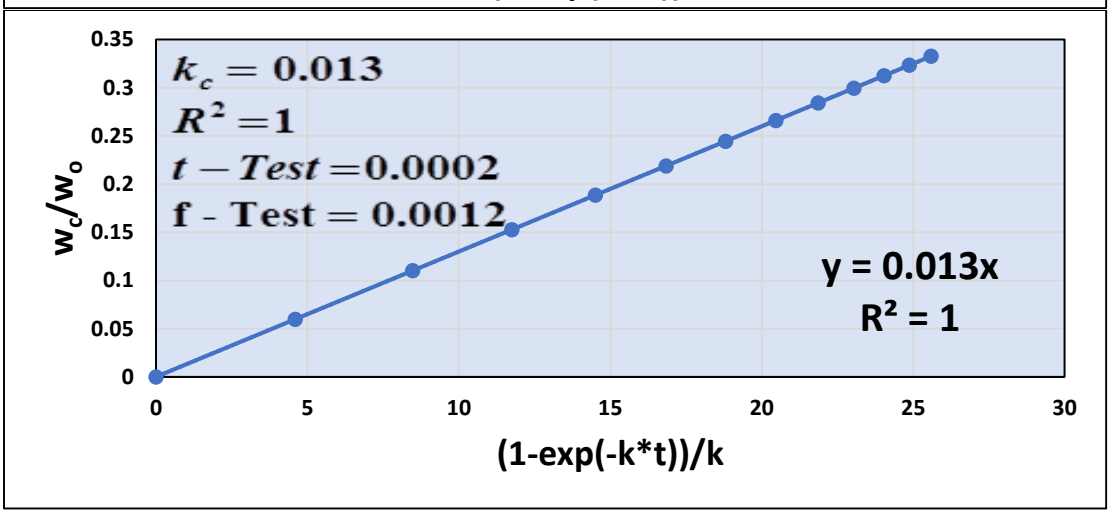
kc = 0.013
R² =1
t – Test =0.0002
f - Test = 0.0012
y = 0.013x
R² = 1
wc/wo
(1-exp(-k*t))/k

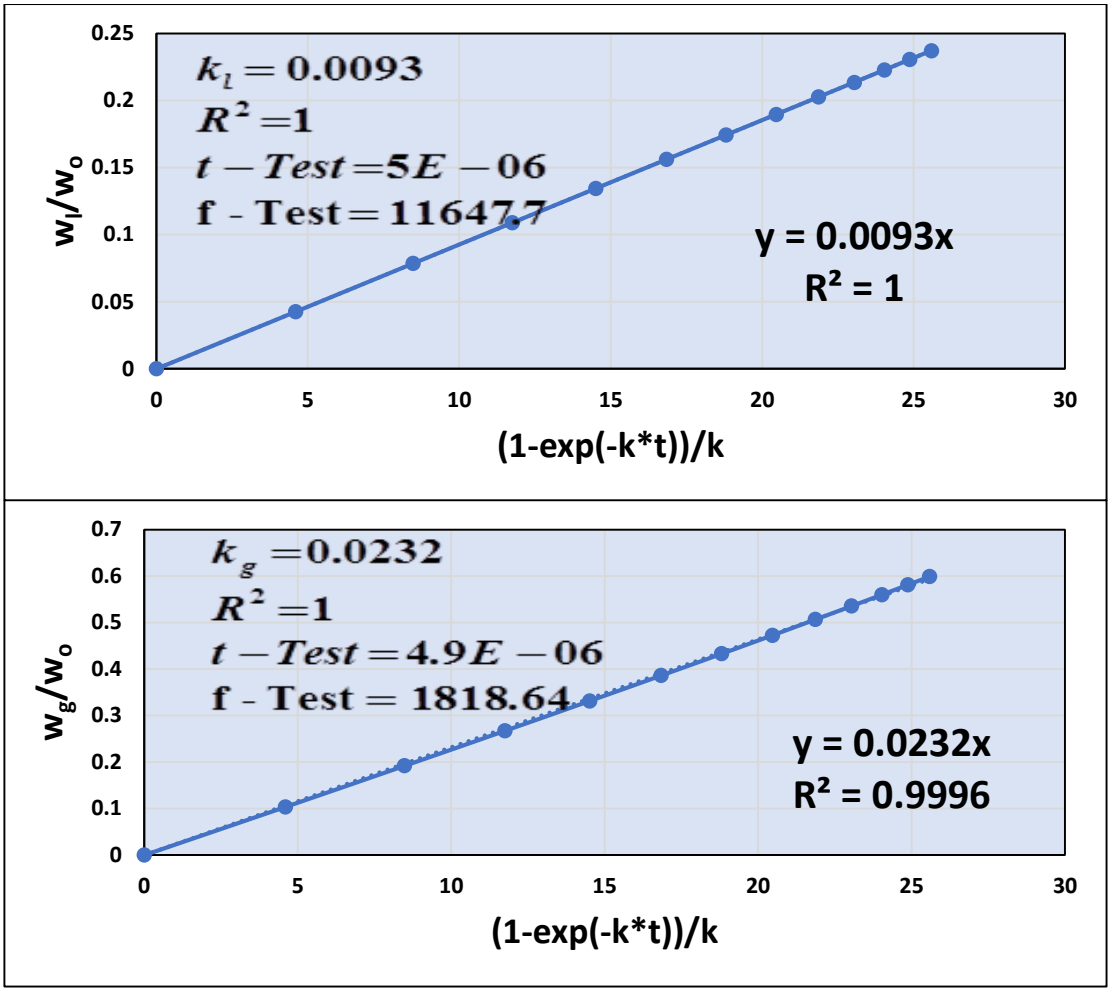

Figure 6.26. Plots of $\ln\left[\frac{w_o}{w}\right]$ vs time and $\frac{w_v}{w_0}$, $\frac{w_c}{w_0}$, $\frac{w_l}{w_0}$ and $\frac{w_g}{w_0}$ vs $(1-\exp[-k*t])/k$ at 973K (a) jute with alumina (b) jute with ZnO (c) jute with KCl (d) jute with NaCl and (e) jute with Aluminosilicate

a)

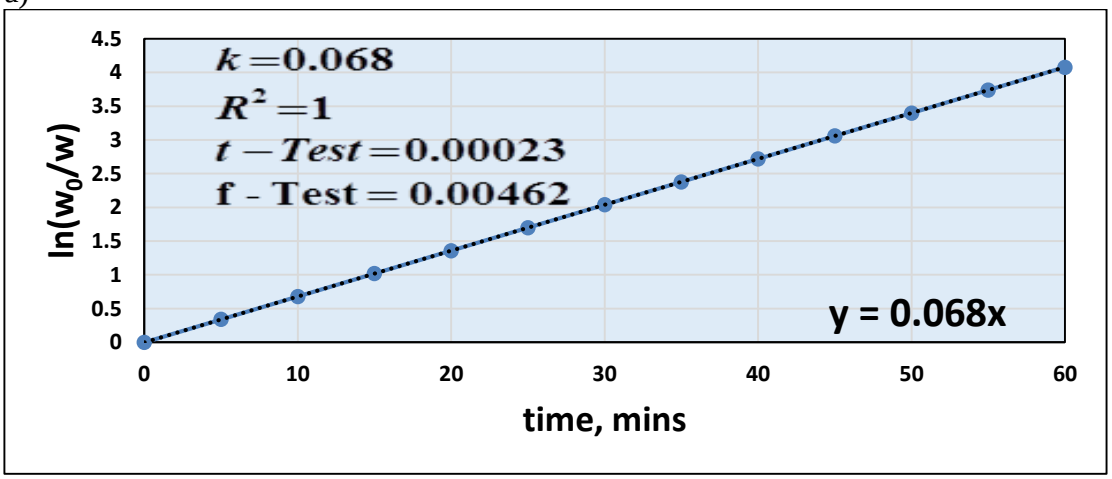

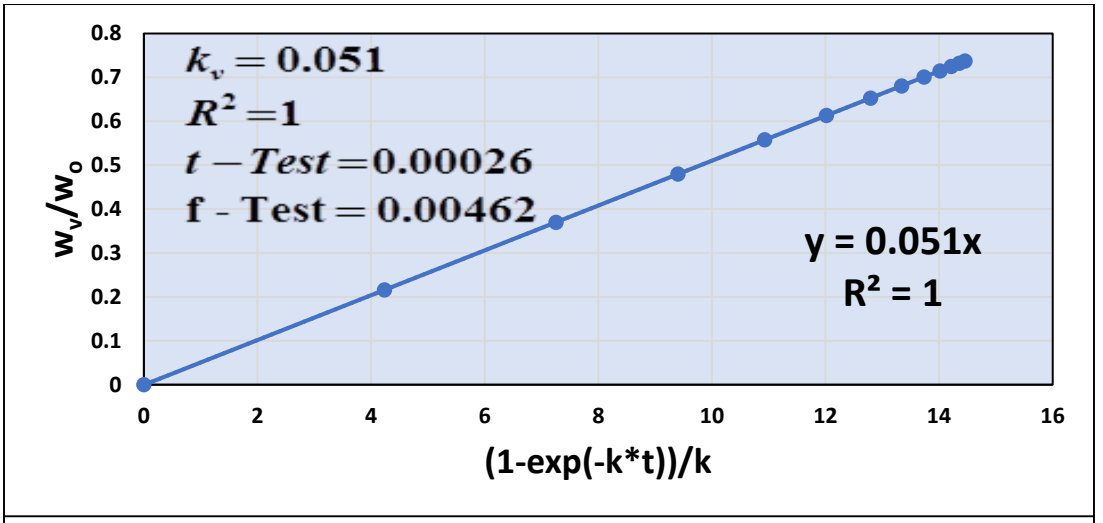
$k_v = 0.051$
$R^2 = 1$
$t - Test = 0.00026$
f - Test = 0.00462
y = 0.051x
R² = 1
w_v/w_o
(1-exp(-k*t))/k

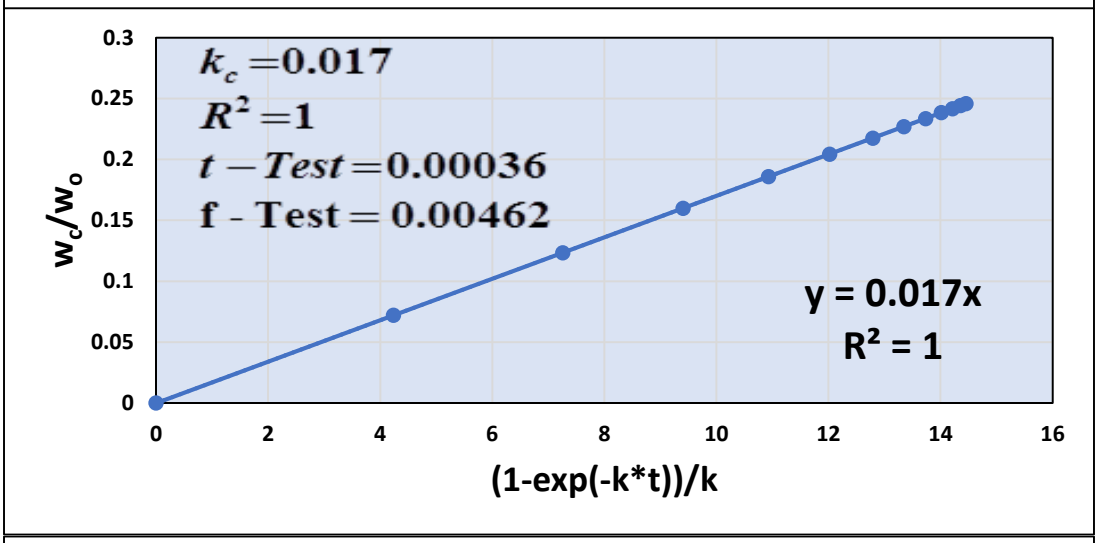
$k_c = 0.017$
$R^2 = 1$
$t - Test = 0.00036$
f - Test = 0.00462
y = 0.017x
R² = 1
w_c/w_o
(1-exp(-k*t))/k

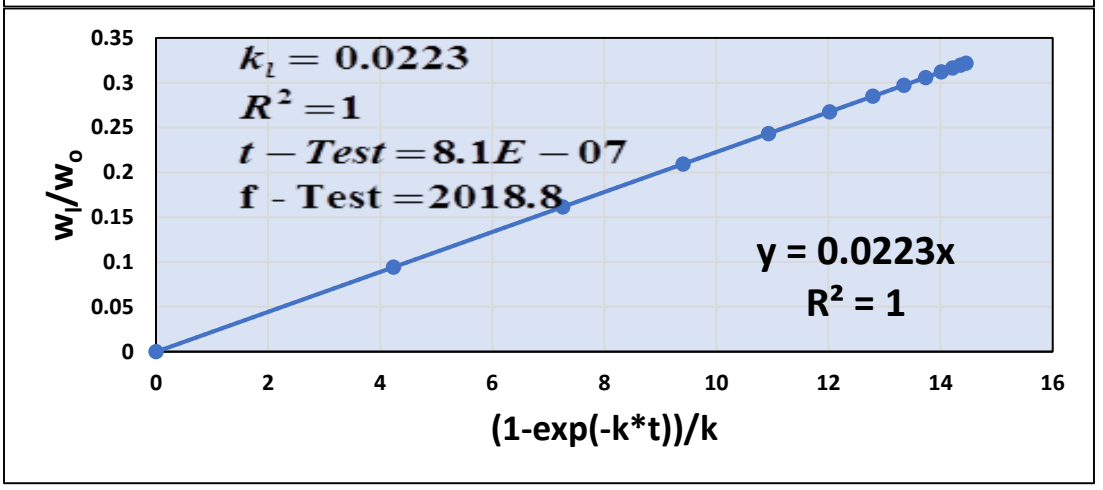
$k_l = 0.0223$
$R^2 = 1$
$t - Test = 8.1E-07$
f - Test = 2018.8
y = 0.0223x
R² = 1
w_l/w_o
(1-exp(-k*t))/k

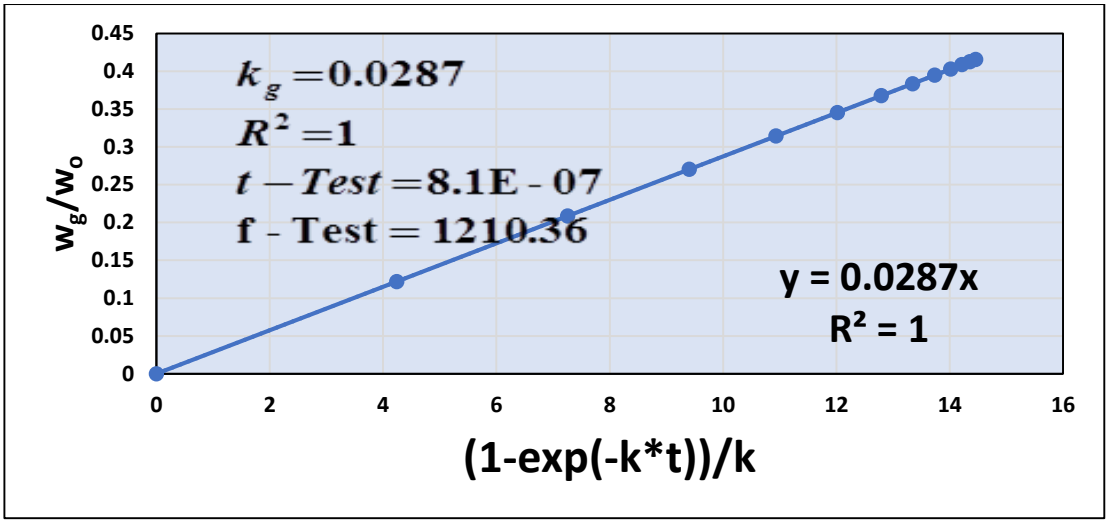
$k_g = 0.0287$
$R^2 = 1$
$t - Test = 8.1E-07$
f - Test = 1210.36
y = 0.0287x
R² = 1
w_g/w_o
(1-exp(-k*t))/k

b)

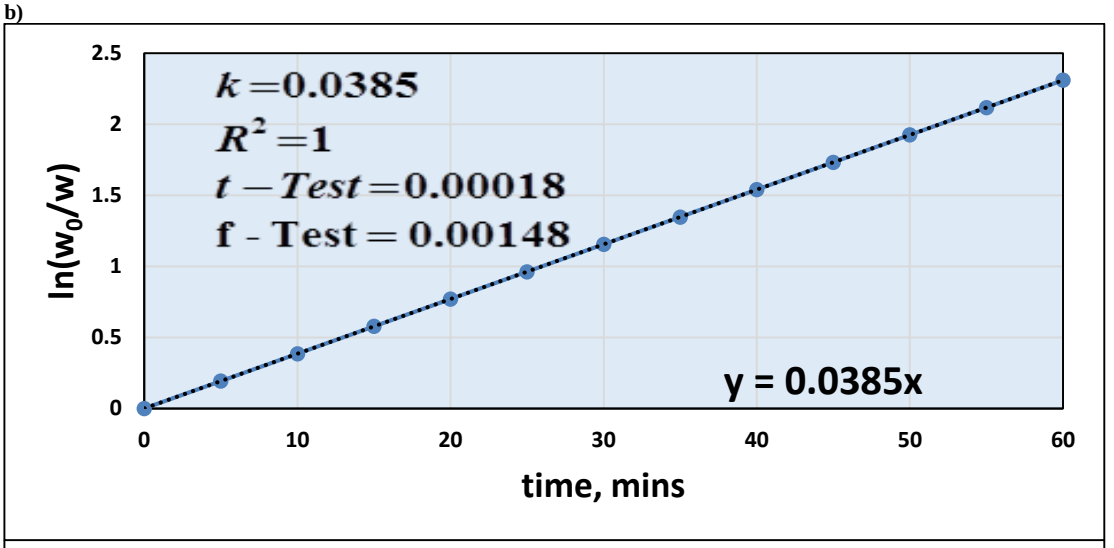
$k = 0.0385$
$R^2 = 1$
$t - Test = 0.00018$
f - Test = 0.00148
y = 0.0385x
$\ln(w_0/w)$
time, mins

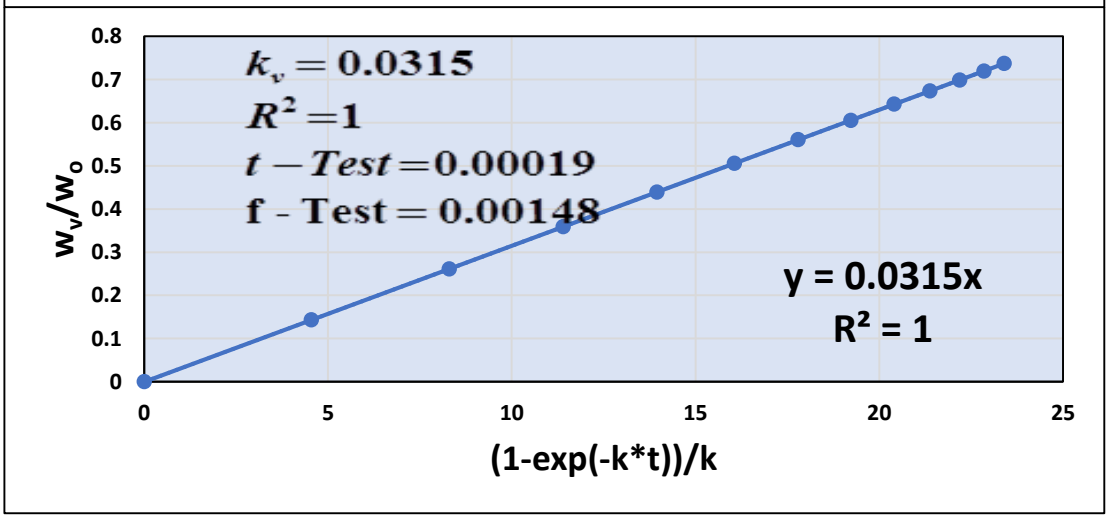
$k_v = 0.0315$
$R^2 = 1$
$t - Test = 0.00019$
f - Test = 0.00148
y = 0.0315x
R² = 1
w_v/w_o
(1-exp(-k*t))/k

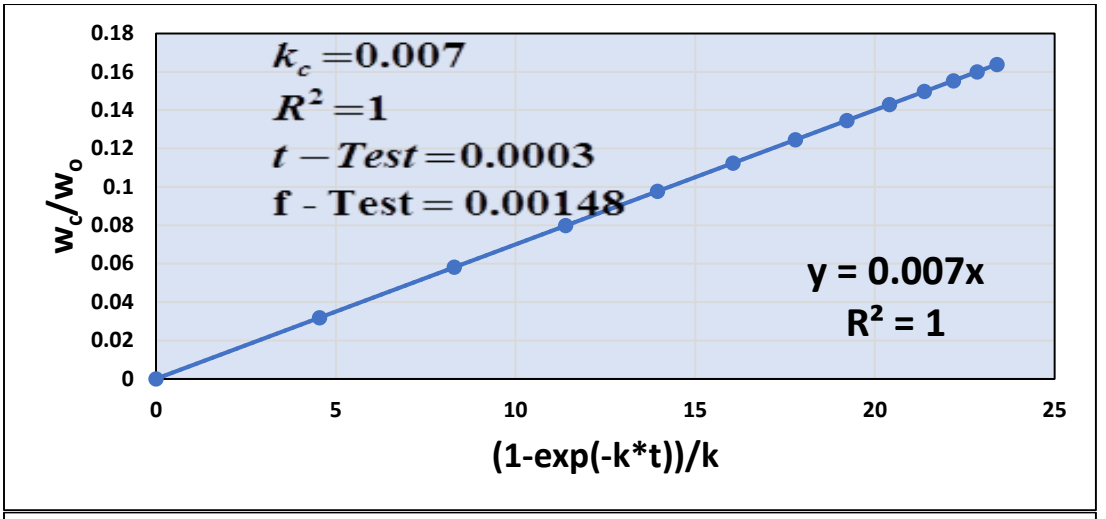
$k_c = 0.007$
$R^2 = 1$
$t - Test = 0.0003$
f - Test = 0.00148
y = 0.007x
R² = 1
w_c/w_o
(1-exp(-k*t))/k

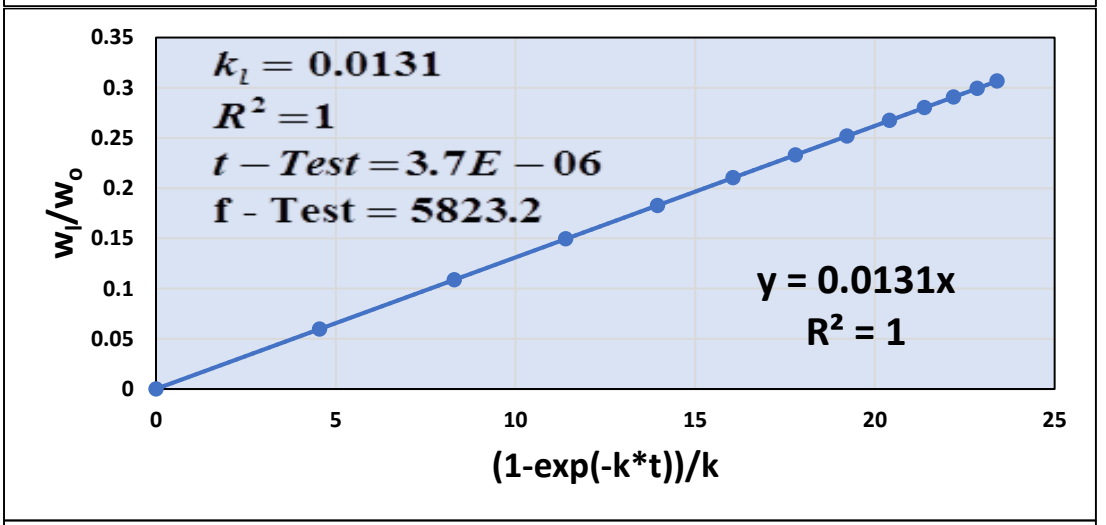
$k_l = 0.0131$
$R^2 = 1$
$t - Test = 3.7E-06$
f - Test = 5823.2
y = 0.0131x
R² = 1
w_l/w_o
(1-exp(-k*t))/k

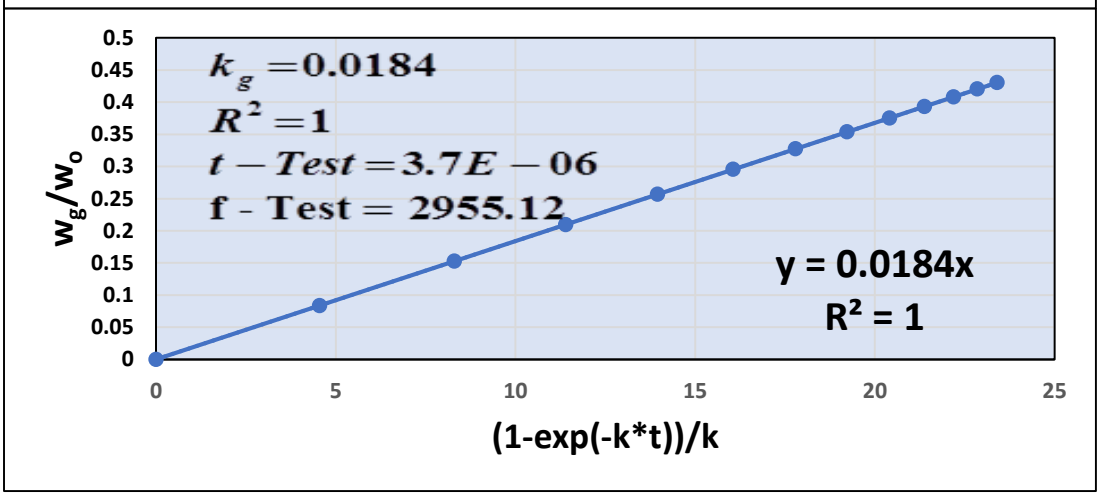
$k_g = 0.0184$
$R^2 = 1$
$t - Test = 3.7E-06$
f - Test = 2955.12
y = 0.0184x
R² = 1
w_g/w_o
(1-exp(-k*t))/k

c)

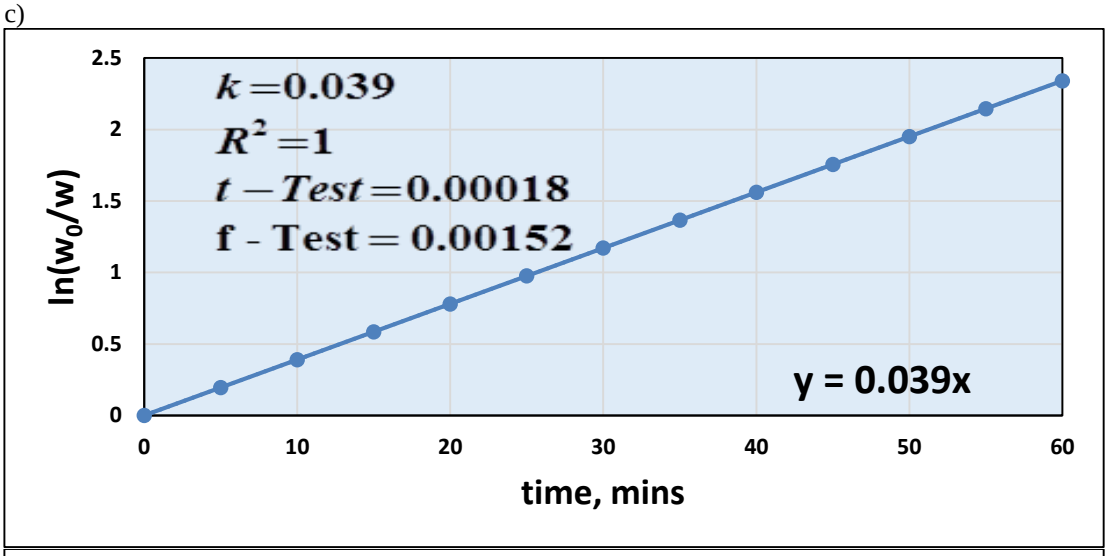
k =0.039
R² =1
t – Test =0.00018
f - Test = 0.00152
y = 0.039x
ln(w0/w)
time, mins

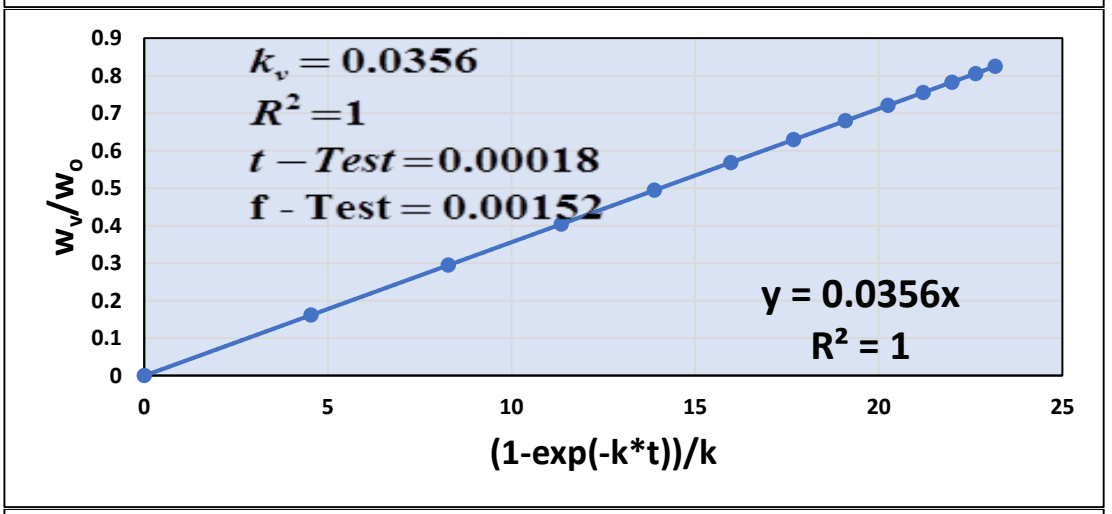
kv = 0.0356
R² =1
t – Test =0.00018
f - Test = 0.00152
y = 0.0356x
R² = 1
wv/wo
(1-exp(-k*t))/k

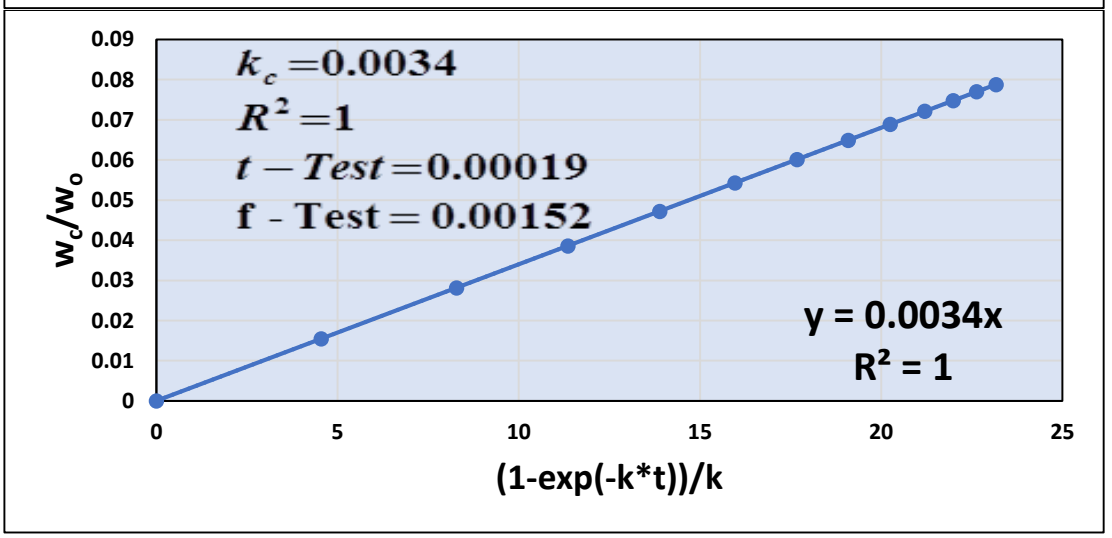
kc =0.0034
R² =1
t – Test =0.00019
f - Test = 0.00152
y = 0.0034x
R² = 1
wc/wo
(1-exp(-k*t))/k

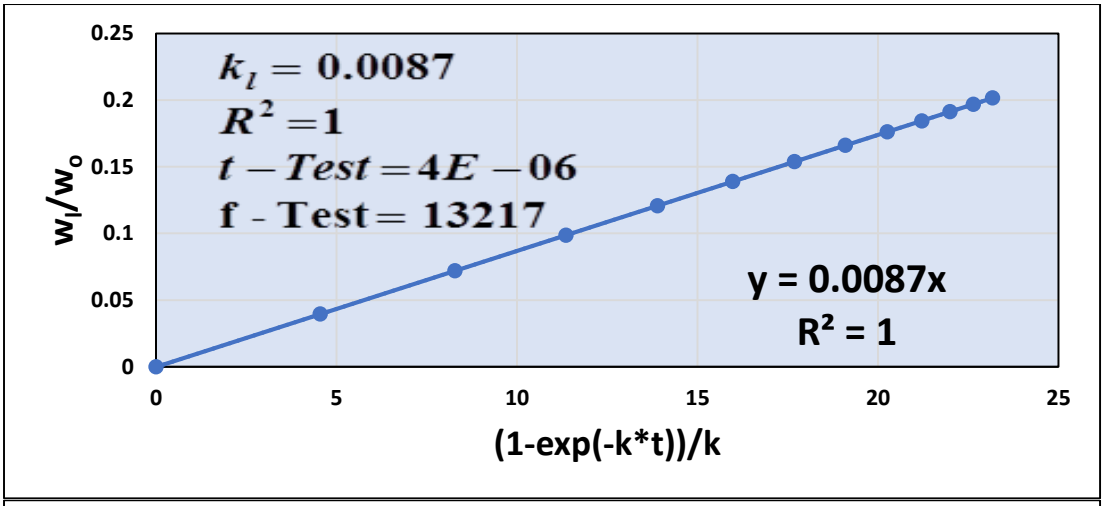
$k_l = 0.0087$
$R^2 = 1$
$t - Test = 4E - 06$
f - Test = 13217
y = 0.0087x
R² = 1
w_l/w_o
(1-exp(-k*t))/k

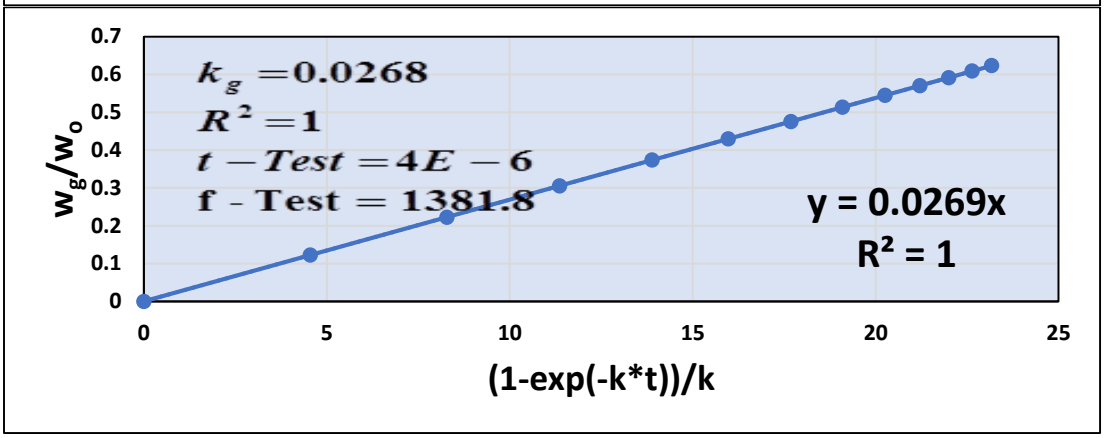
$k_g = 0.0268$
$R^2 = 1$
$t - Test = 4E - 6$
f - Test = 1381.8
y = 0.0269x
R² = 1
w_g/w_o
(1-exp(-k*t))/k

d)

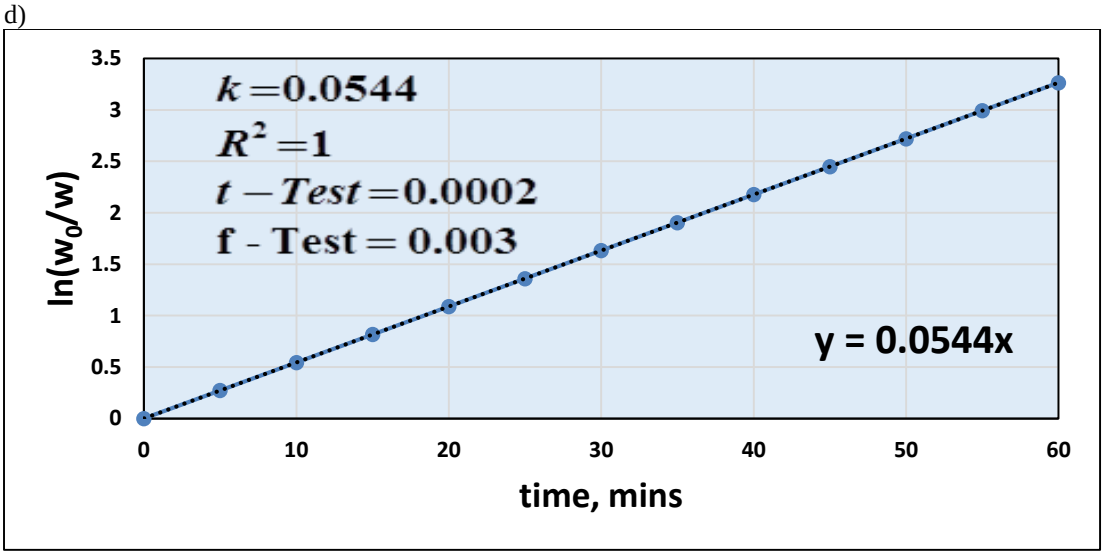
$k = 0.0544$
$R^2 = 1$
$t - Test = 0.0002$
f - Test = 0.003
y = 0.0544x
$\ln(w_0/w)$
time, mins

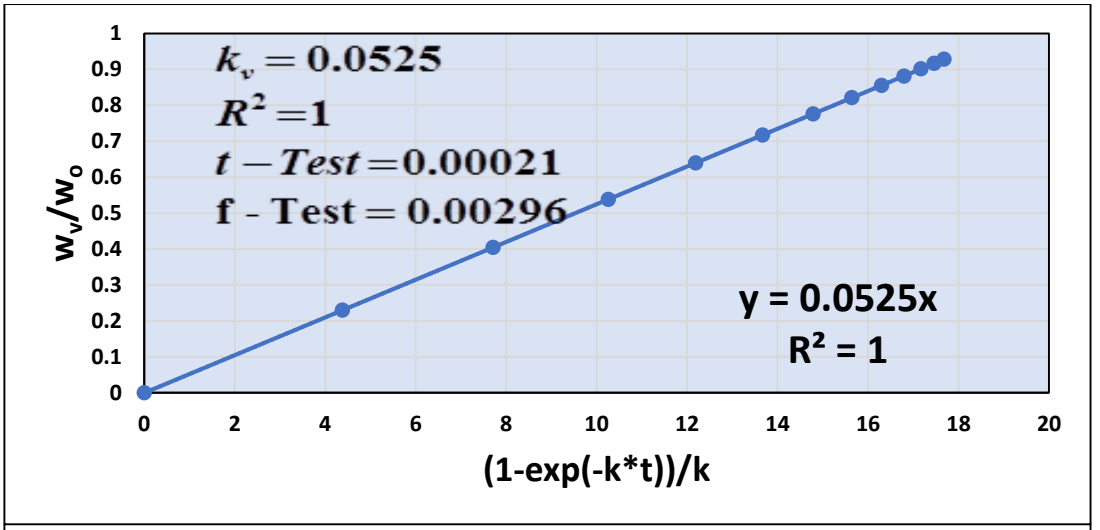
$k_v = 0.0525$
$R^2 = 1$
$t - Test = 0.00021$
f - Test = 0.00296
y = 0.0525x
R² = 1
w_v/w_o
(1-exp(-k*t))/k

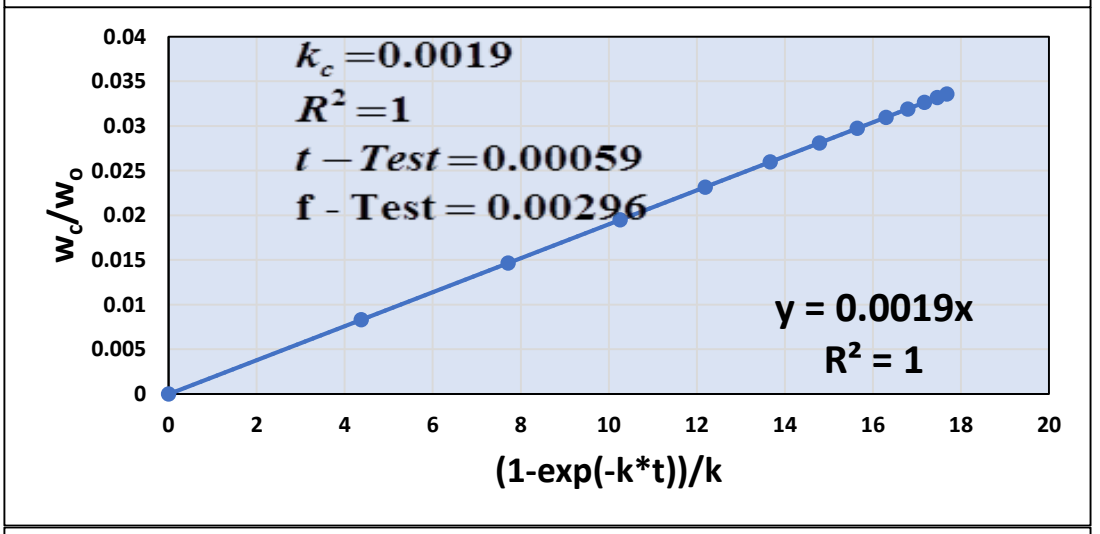
$k_c = 0.0019$
$R^2 = 1$
$t - Test = 0.00059$
f - Test = 0.00296
y = 0.0019x
R² = 1
w_c/w_o
(1-exp(-k*t))/k

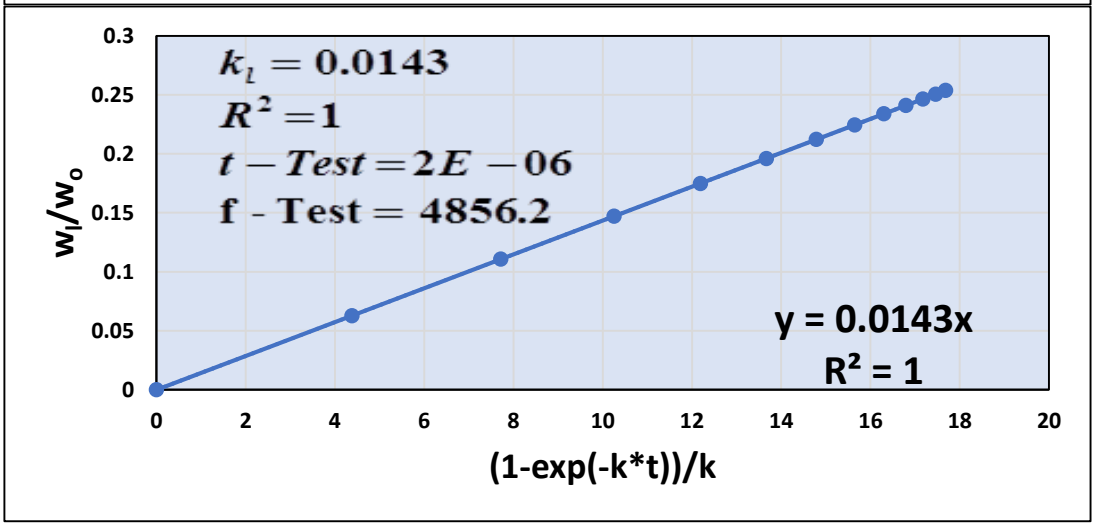
$k_l = 0.0143$
$R^2 = 1$
$t - Test = 2E-06$
f - Test = 4856.2
y = 0.0143x
R² = 1
w_l/w_o
(1-exp(-k*t))/k

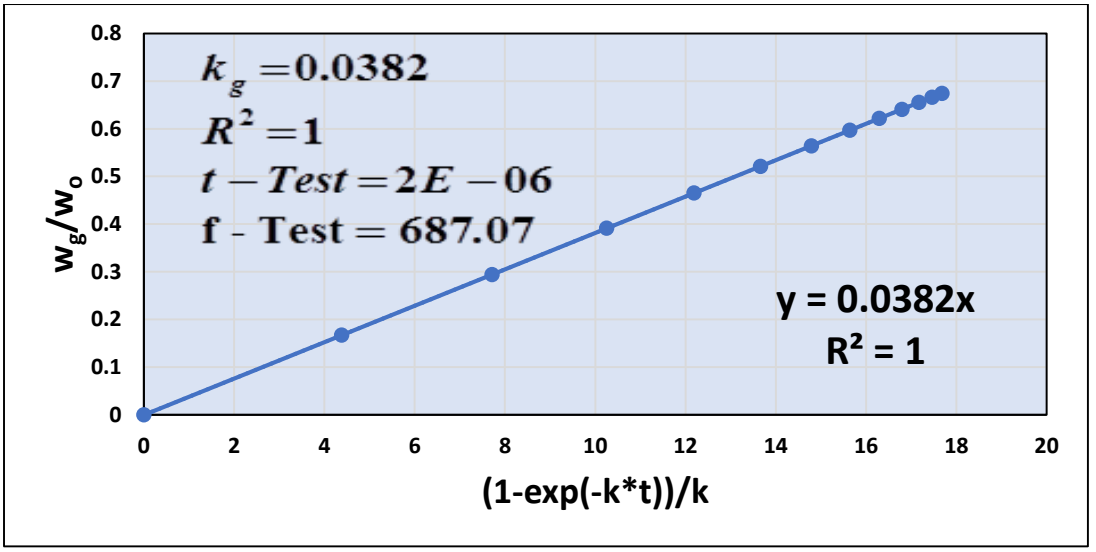
$k_g = 0.0382$
$R^2 = 1$
$t - Test = 2E - 06$
f - Test = 687.07
y = 0.0382x
R² = 1
w_g/w_o
(1-exp(-k*t))/k

e)

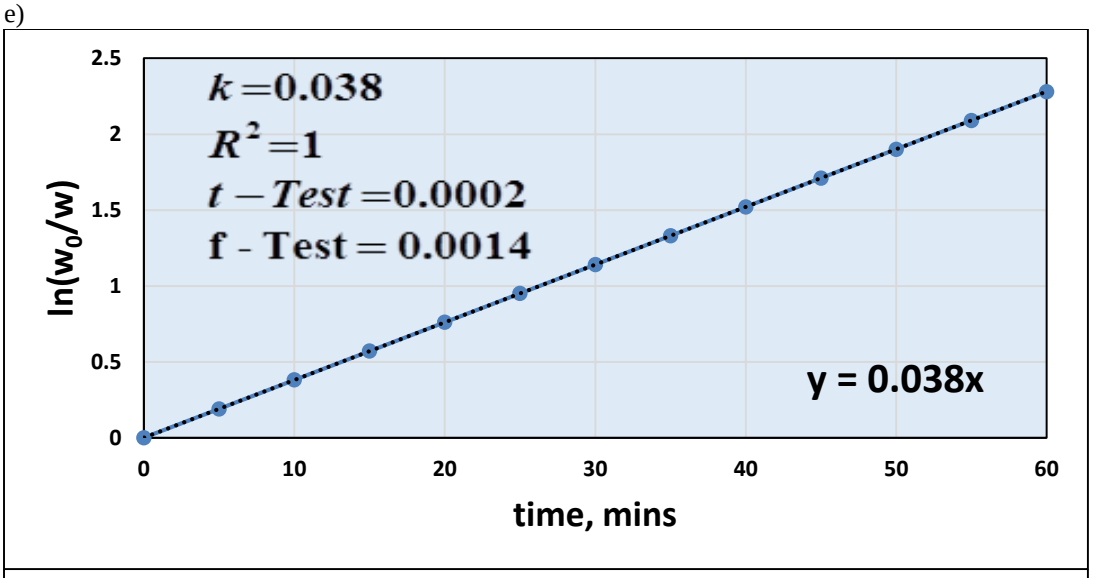
$k = 0.038$
$R^2 = 1$
$t - Test = 0.0002$
f - Test = 0.0014
y = 0.038x
$\ln(w_0/w)$
time, mins

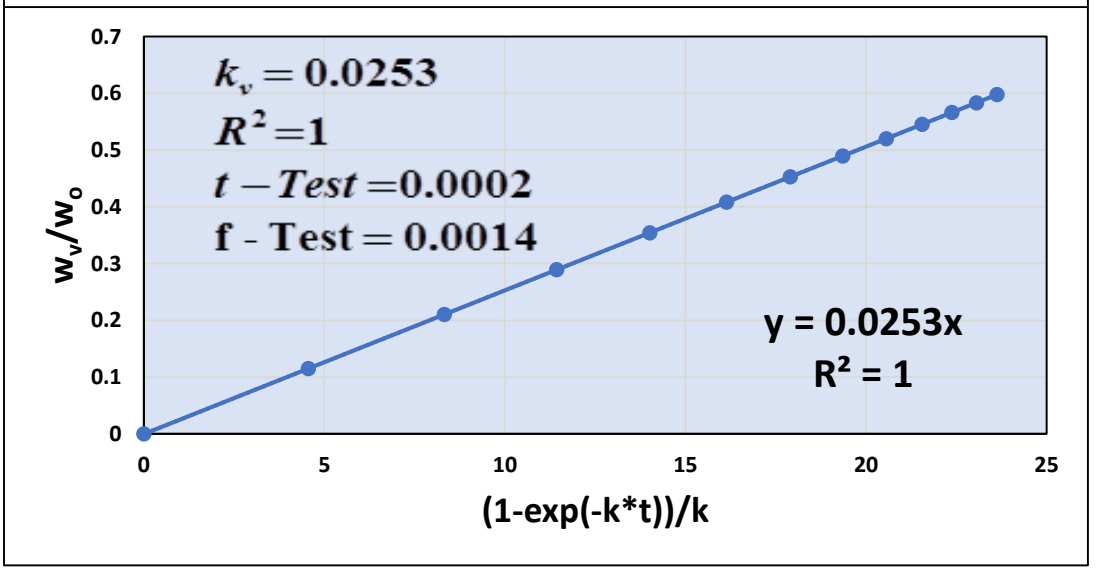
$k_v = 0.0253$
$R^2 = 1$
$t - Test = 0.0002$
f - Test = 0.0014
y = 0.0253x
R² = 1
w_v/w_o
(1-exp(-k*t))/k

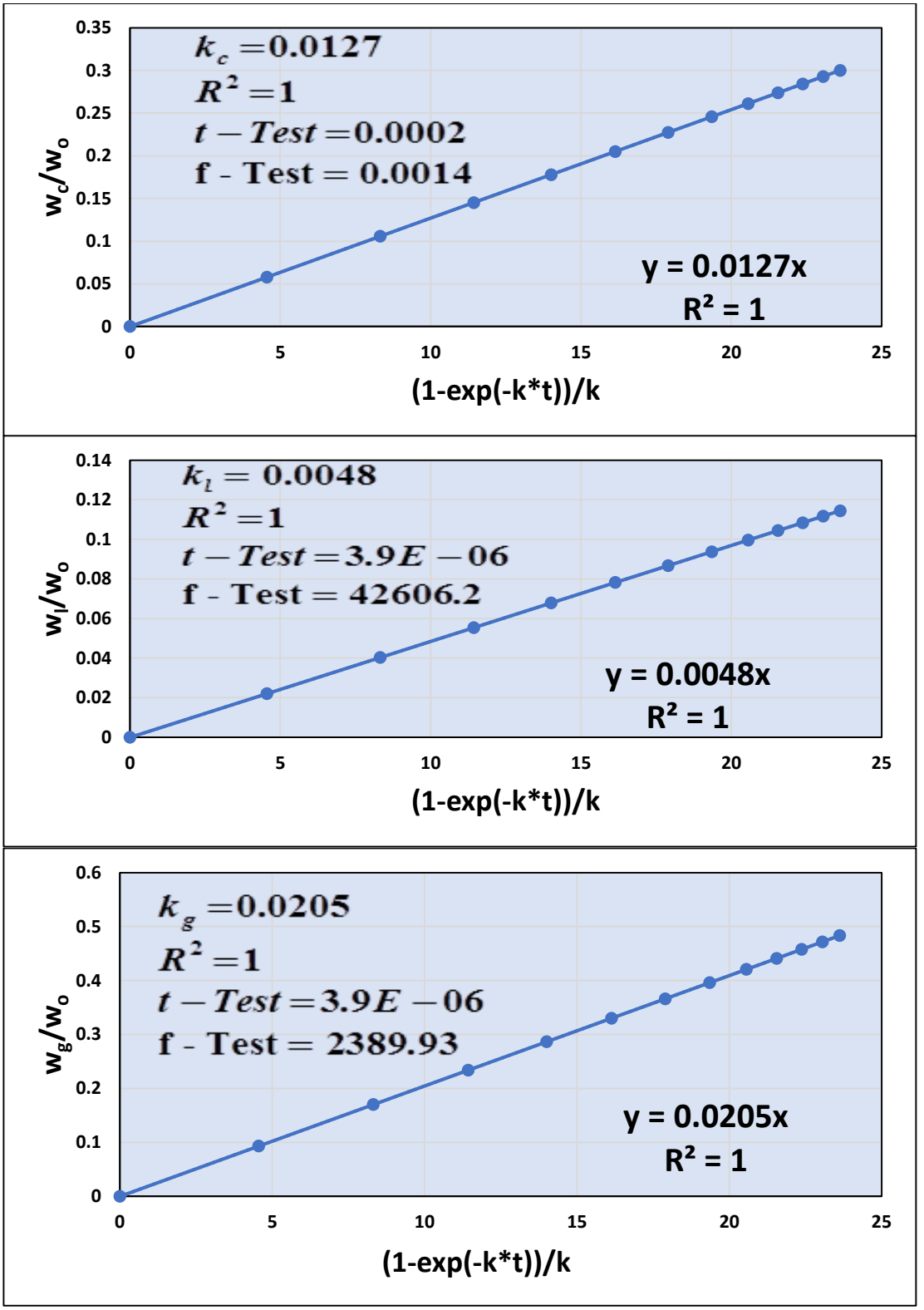

Figure 6.27. Plots of $\ln\left[\frac{w_o}{w}\right]$ vs time and $\frac{w_v}{w_o}$, $\frac{w_c}{w_o}$, $\frac{w_l}{w_o}$ and $\frac{w_g}{w_o}$ vs $(1-\exp[-k*t])/k$ at 1173K (a) jute with alumina (b) jute with ZnO (c) jute with KCl (d) jute with NaCl and (e) jute with Aluminosilicate

Table 6.8. Values of "k'" of catalytic pyrolysis of jute waste at different temperature

T (K)	Jute wastes with alumina	Jute wastes with ZnO	Jute wastes with KCl	Jute wastes with NaCl	Jute wastes with Aluminosilicate
673K	0.044	0.0253	0.03	0.0425	0.027
773K	0.0573	0.0267	0.0305	0.0515	0.0319
873K	0.058	0.0281	0.032	0.056	0.034
973K	0.062	0.0303	0.038	0.0575	0.034
1073K	0.064	0.0303	0.034	0.0575	0.034
1173K	0.068	0.0385	0.039	0.0544	0.038

Table 6.9. Values of "k_v'" of catalytic pyrolysis of jute waste at different temperature

T (K)	Jute wastes with alumina	Jute wastes with ZnO	Jute wastes with KCl	Jute wastes with NaCl	Jute wastes with Aluminosilicate
673K	0.0398	0.0212	0.0187	0.032	0.0215
773K	0.046	0.0177	0.0302	0.0344	0.025
873K	0.047	0.0248	0.027	0.0431	0.023
973K	0.048	0.022	0.023	0.0555	0.021
1073K	0.049	0.022	0.0225	0.0555	0.0213
1173K	0.051	0.0315	0.0356	0.0525	0.0253

Table 6.10. Values of "k_c'" of catalytic pyrolysis of jute waste at different temperature

T (K)	Jute wastes with alumina	Jute wastes with ZnO	Jute wastes with KCl	Jute wastes with NaCl	Jute wastes with Aluminosilicate
673K	0.0047	0.0041	0.011	0.0105	0.0055
773K	0.011	0.0089	0.0003	0.0171	0.0069
873K	0.012	0.0033	0.023	0.0129	0.0109
973K	0.014	0.0083	0.026	0.002	0.0122
1073K	0.015	0.0083	0.027	0.002	0.0122
1173K	0.017	0.007	0.034	0.0019	0.0123

Table 6.11. Values of "k_i'" of catalytic pyrolysis of jute waste at different temperature

T (K)	Jute wastes with alumina	Jute wastes with ZnO	Jute wastes with KCl	Jute wastes with NaCl	Jute wastes with Aluminosilicate
673K	0.0153	0.0063	0.0026	0.0071	0.0031
773K	0.0219	0.0087	0.0086	0.0067	0.0044
873K	0.0248	0.0118	0.0069	0.0092	0.0038
973K	0.0214	0.0134	0.0085	0.0113	0.0093
1073K	0.0228	0.0093	0.0037	0.0158	0.0038
1173K	0.0223	0.0131	0.0087	0.0143	0.0048

Table 6.12. Values of "k_g'" of catalytic pyrolysis of jute waste at different temperature

T (K)	Jute wastes with alumina	Jute wastes with ZnO	Jute wastes with KCl	Jute wastes with NaCl	Jute wastes with Aluminosilicate
673K	0.0245	0.0149	0.0161	0.0249	0.0184
773K	0.0241	0.009	0.0216	0.0277	0.0206
873K	0.0224	0.0133	0.0206	0.0359	0.0198
973K	0.022	0.0146	0.0261	0.0352	0.0232
1073K	0.0262	0.0127	0.0188	0.0397	0.0175
1173K	0.0287	0.0189	0.0269	0.0387	0.0205

6.4.1.2.2. Temperature dependence of rate constant

Using the values of rate constants k', k_v', k_c', k_l' and k_g' Arrhenius plots (shown in the Appendix A.18.a.) have been made following the same method as used in case of non-catalytic pyrolysis of jute. The Arrhenius type dependence of rate constants on temperature has been established from the linearity of the plots. The values of activation energies and pre-exponential factors for catalytic pyrolysis using all catalysts under study have been determined from the Arrhenius plots and through non-linear regression analysis and are tabulated in table 6.13.

Table 6.13. Calculated Activation Energies and Frequency Factors as per Arrhenius Law for catalytic pyrolysis of jute wastes

Sl. No.	Feed Stocks	Reaction rate constant	Activation Energy (kJ/mol)	Frequency factor (min^{-1})	Correlation Coefficient
1	Jute + alumina	k'	3.5337 (***E'***)	0.0545 (***A'***)	0.967
		k_v'	4.1361 (***E**V*'**)	0.0447 (***A**V*'**)	0.968
		k_c'	13.309 (***E**C*'**)	0.1330 (***A**C*'**)	0.962
		k_l'	1.489869 (***E**l*'**)	0.03002 (***A**l*'**)	0.815
		k_g'	4.089906 (***E**g*'**)	0.036806(***A**g*'**)	0.896
2	Jute+ ZnO	k'	4.833 (***E'***)	0.0566 (***A'***)	0.872
		k_v'	8.129 (***E**V*'**)	0.5038 (***A**V*'**)	0.959
		k_c'	14.392 (***E**C*'**)	0.5071 (***A**C*'**)	0.945
		k_l'	3.578179(***E**l*'**)	0.022005(***A**l*'**)	0.935
		k_g'	8.157032(***E**g*'**)	0.030367(***A**g*'**)	0.9516
3	Jute+ KCl	k'	5.9087 (***E'***)	0.1236 (***A'***)	0.963
			6.5688 (***E**V*'**)	0.1065 (***A**V*'**)	0.961

		k_v'	13.5018 (E_C')	0.0189 (A_C')	0.940
		k_c'	4.707719(E_l')	0.040312(A_l')	0.901
		k_l'	8.318988(E_g')	0.01815(A_g')	0.856
		k_g'			
4	Jute+ NaCl	k'	5.0881 (***E'***)	0.1159 (A')	0.905
		k_v'	3.0703 (E_V')	0.0704 (A_V')	0.889
		k_c'	16.769 (E_C')	0.1072 (A_C')	0.899
		k_l'	6.375258(E_l')	0.078519(A_l')	0.9119
		k_g'	11.58639(E_g')	0.048709(A_g')	0.9406
5	Jute+ $NaAl(SiO_3)_2$	k'	7.84737 (***E'***)	0.0524 (A')	0.945
		k_v'	5.5672 (E_V')	0.0241 (A_V')	0.926
		k_c'	21.617 (E_C')	0.0458 (A_C')	0.894
		k_l'	6.153133(E_l')	0.021647(A_l')	0.838
		k_g'	5.853638(E_g')	0.010016(A_g')	0.8909

6.4.1.2.3. Comparison of Activation energies and pre-exponential factor of catalytic and non-catalytic pyrolysis of jute wastes.

The lumped kinetic parameters determined using the data of isothermal experiments have been shown in Table 6.12. From the analysis of the table, it is evident that the lowering of activation energy occurs with the use of all catalysts and it is maximum for alumina with respect to the overall pyrolysis reaction. Thus, alumina is selected as the best performing catalyst for the pyrolysis of jute waste.

6.4.1.3. lime wastes

Figure 6.28 represent the profiles of residual weight fraction of pyrolysis of lime wastes in presence of a) alumina b) ZnO c) KCl d) NaCl and e) sodium aluminosilicate [34-38] respectively with respect to pyrolysis time in the temperature range of 573K to 1173 K. The corresponding data are provided in the Table A.10.b. in the appendix. Similarly, the figures 6.29. and 6.30. represent respectively the time histories of weight fractions of volatile and char generated during the pyrolysis of lime wastes [7,8] in presence of a) alumina b) ZnO c) KCl d) NaCl and e) sodium aluminosilicate [34-38] with respect to pyrolysis time in the temperature range of 573K to 1173 K. The corresponding values used for the plots are provided in the Table A.11.b. and Table A.12.b. respectively in the appendix. From the analysis of the figures it is revealed that similar to non-catalytic pyrolysis, catalytic pyrolysis of lime wastes begins at 673K for all catalysts under study.

a)

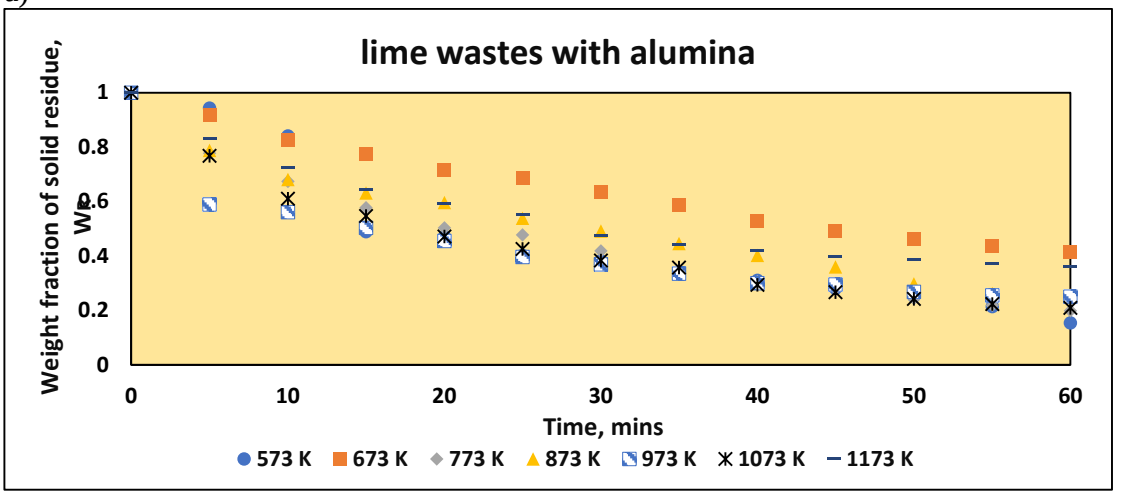
lime wastes with alumina
Weight fraction of solid residue, WR
1
0.8
0.6
0.4
0.2
0
0
10
20
30
40
50
60
Time, mins
573 K
673 K
773 K
873 K
973 K
1073 K
1173 K

b)

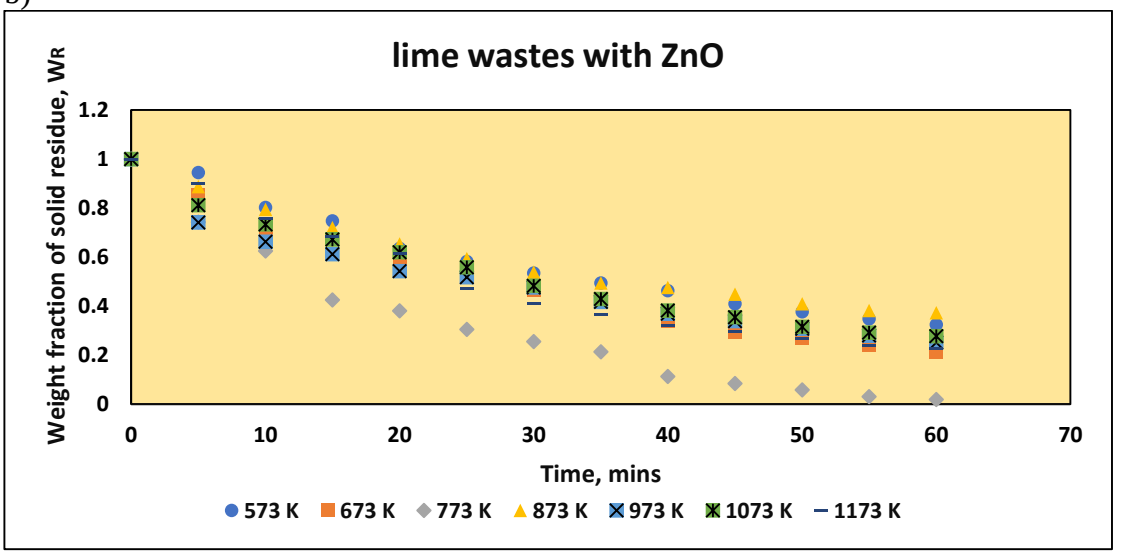
lime wastes with ZnO
Weight fraction of solid residue, WR
1.2
1
0.8
0.6
0.4
0.2
0
0
10
20
30
40
50
60
70
Time, mins
573 K
673 K
773 K
873 K
973 K
1073 K
1173 K

c)

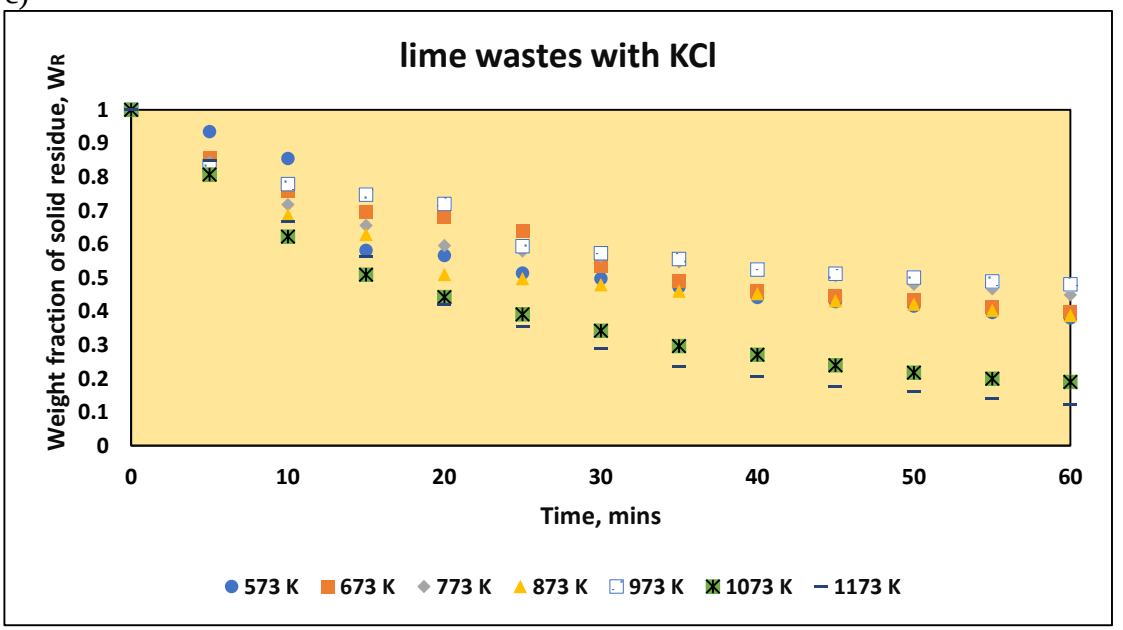
lime wastes with KCl
Weight fraction of solid residue, WR
1
0.9
0.8
0.7
0.6
0.5
0.4
0.3
0.2
0.1
0
0
10
20
30
40
50
60
Time, mins
573 K
673 K
773 K
873 K
973 K
1073 K
1173 K

d)

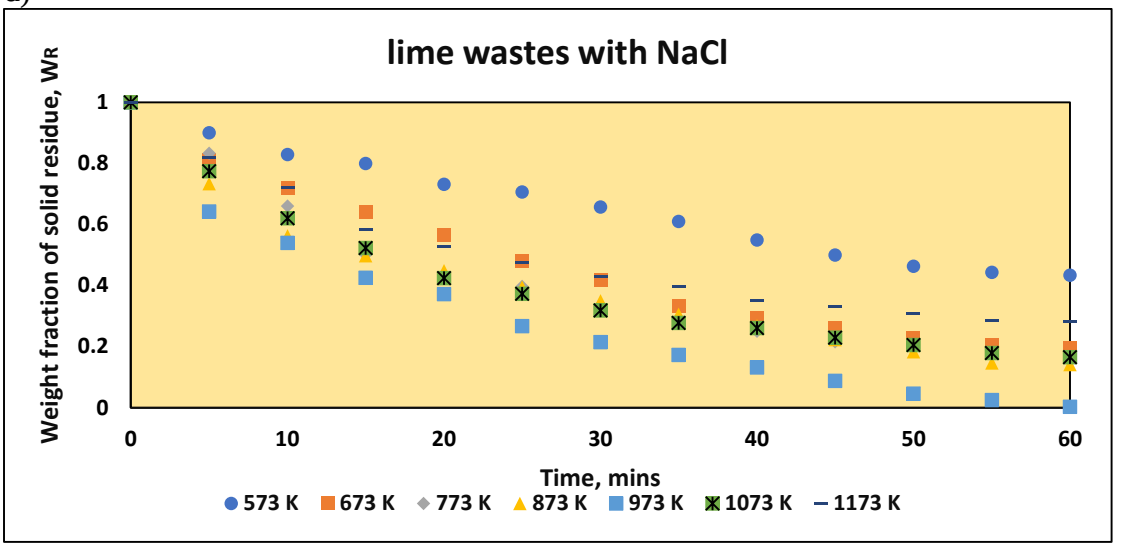

e)

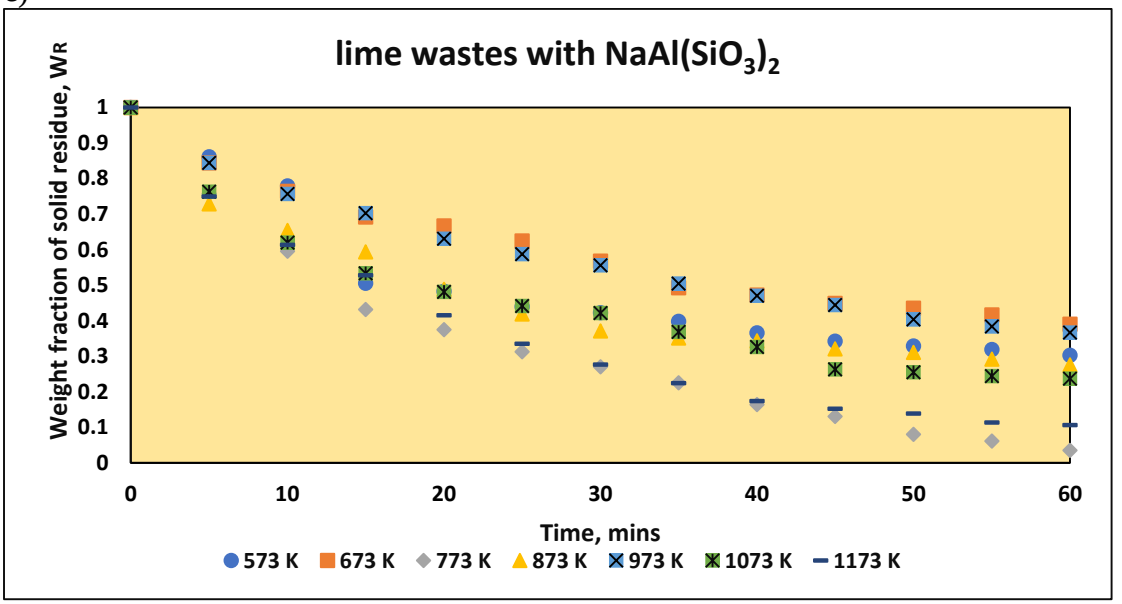

Figure 6.28. Time histories of weight fraction of residue of (a) lime waste with alumina (b) lime waste with ZnO (c) lime waste with KCl (d) lime waste with NaCl and (e) lime waste with Aluminosilicate using pyrolysis temperature as parameter.

a)

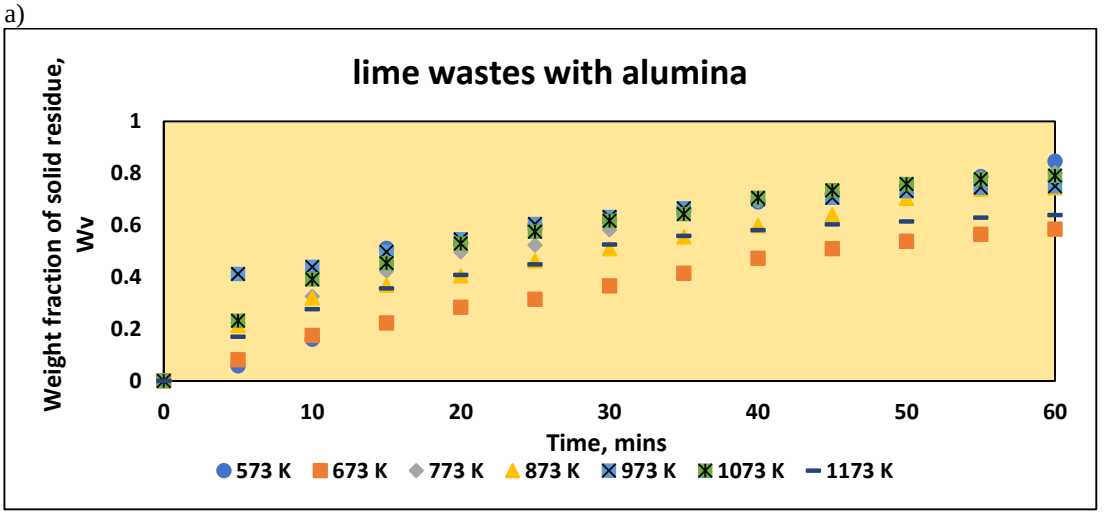
lime wastes with alumina
Weight fraction of solid residue, Wv
1
0.8
0.6
0.4
0.2
0
0
10
20
30
40
50
60
Time, mins
573 K
673 K
773 K
873 K
973 K
1073 K
1173 K

b)

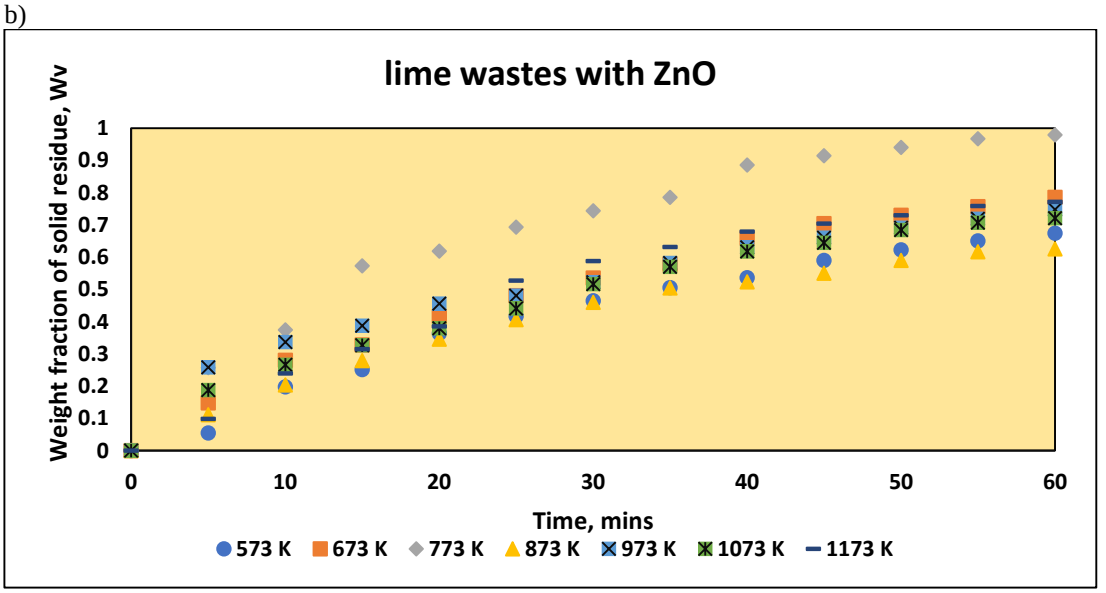
lime wastes with ZnO
Weight fraction of solid residue, Wv
1
0.9
0.8
0.7
0.6
0.5
0.4
0.3
0.2
0.1
0
0
10
20
30
40
50
60
Time, mins
573 K
673 K
773 K
873 K
973 K
1073 K
1173 K

c)

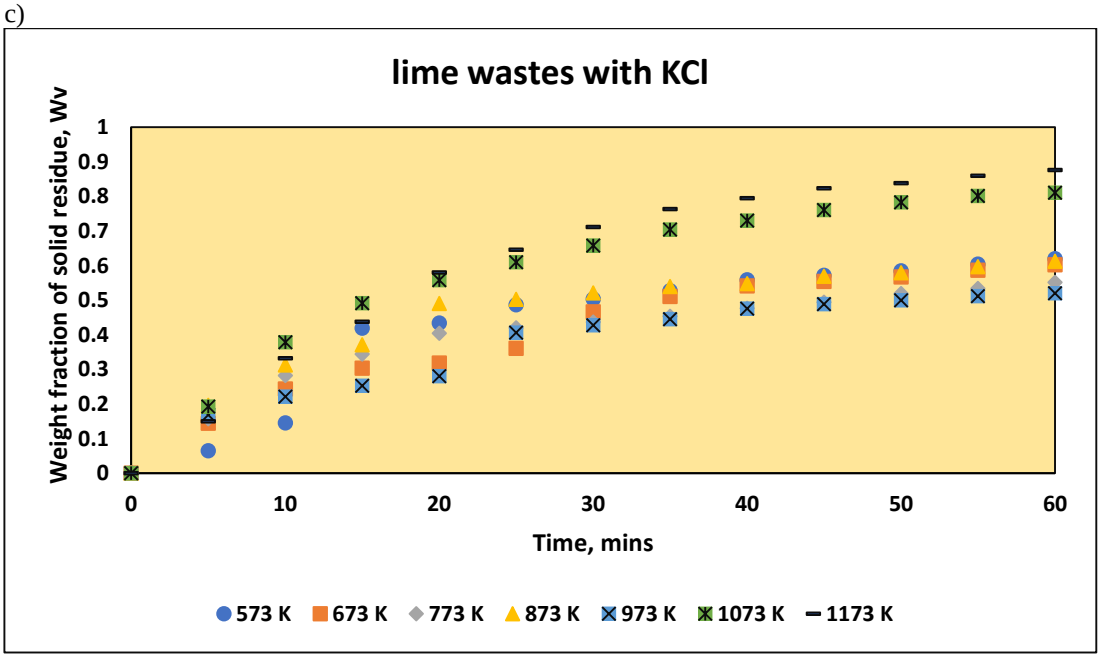
lime wastes with KCl
Weight fraction of solid residue, Wv
1
0.9
0.8
0.7
0.6
0.5
0.4
0.3
0.2
0.1
0
0
10
20
30
40
50
60
Time, mins
573 K
673 K
773 K
873 K
973 K
1073 K
1173 K

d)

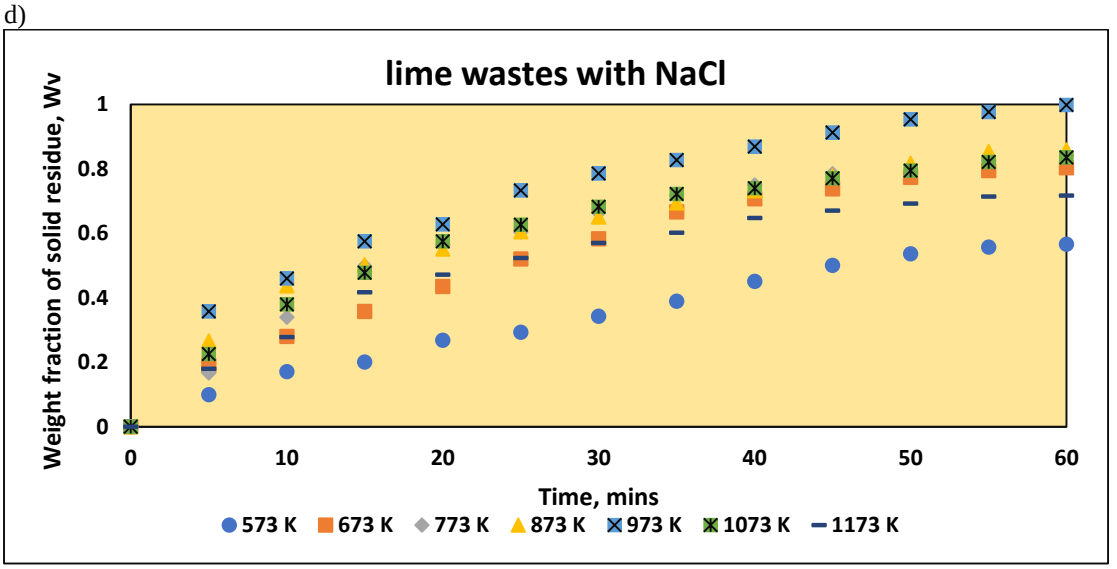

e)

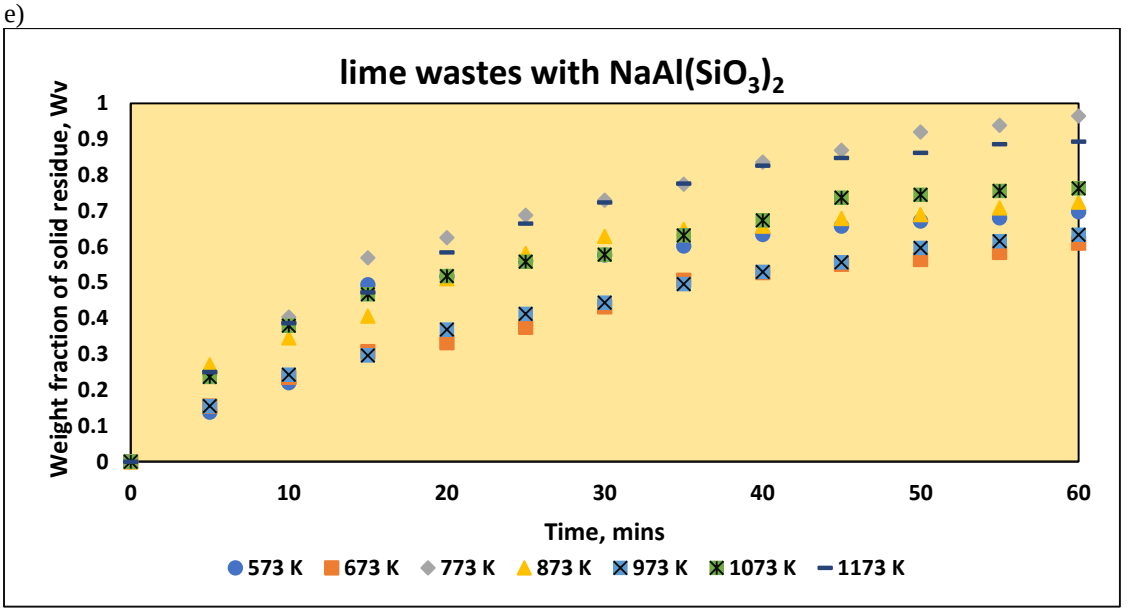

Figure 6.29. Time Histories of volatile weight fraction using pyrolysis temperature as parameter: (a) lime waste with alumina (b) lime waste with ZnO (c) lime waste with KCl (d) lime waste with NaCl and (e) lime waste with Aluminosilicate

a)

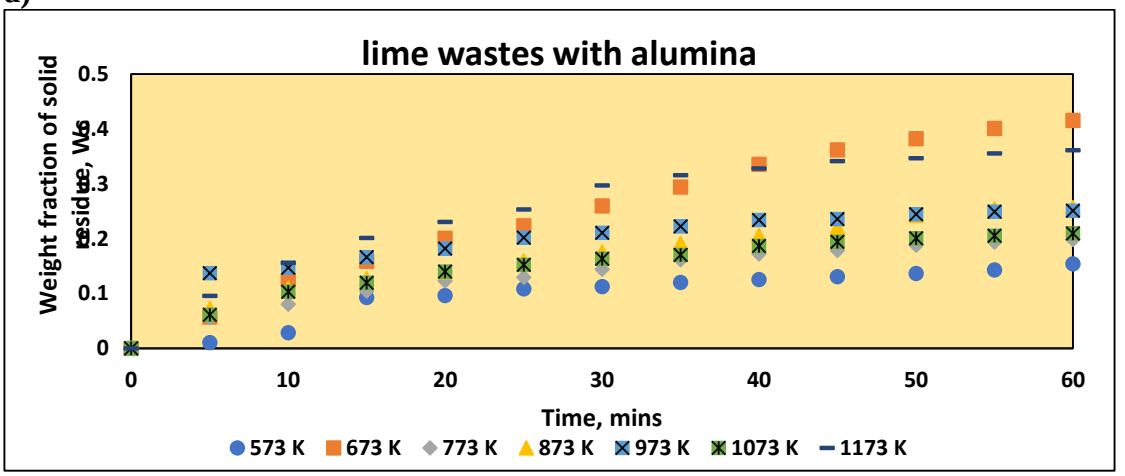
lime wastes with alumina
Weight fraction of solid residue, Wc
0.5
0.4
0.3
0.2
0.1
0
0
10
20
30
40
50
60
Time, mins
573 K
673 K
773 K
873 K
973 K
1073 K
1173 K

b)

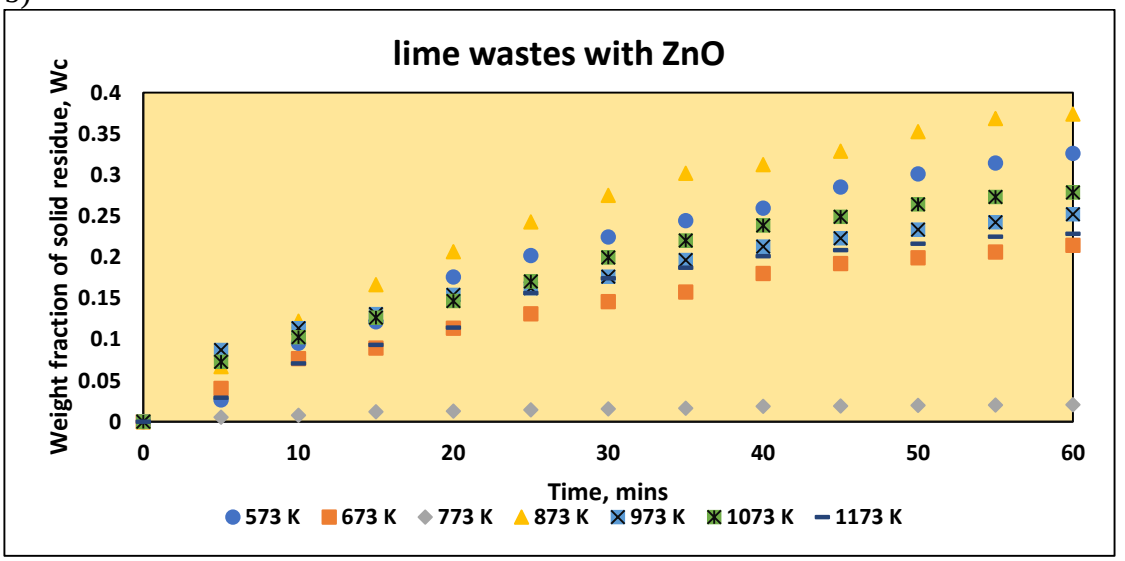
lime wastes with ZnO
Weight fraction of solid residue, Wc
0.4
0.35
0.3
0.25
0.2
0.15
0.1
0.05
0
0
10
20
30
40
50
60
Time, mins
573 K
673 K
773 K
873 K
973 K
1073 K
1173 K

c)

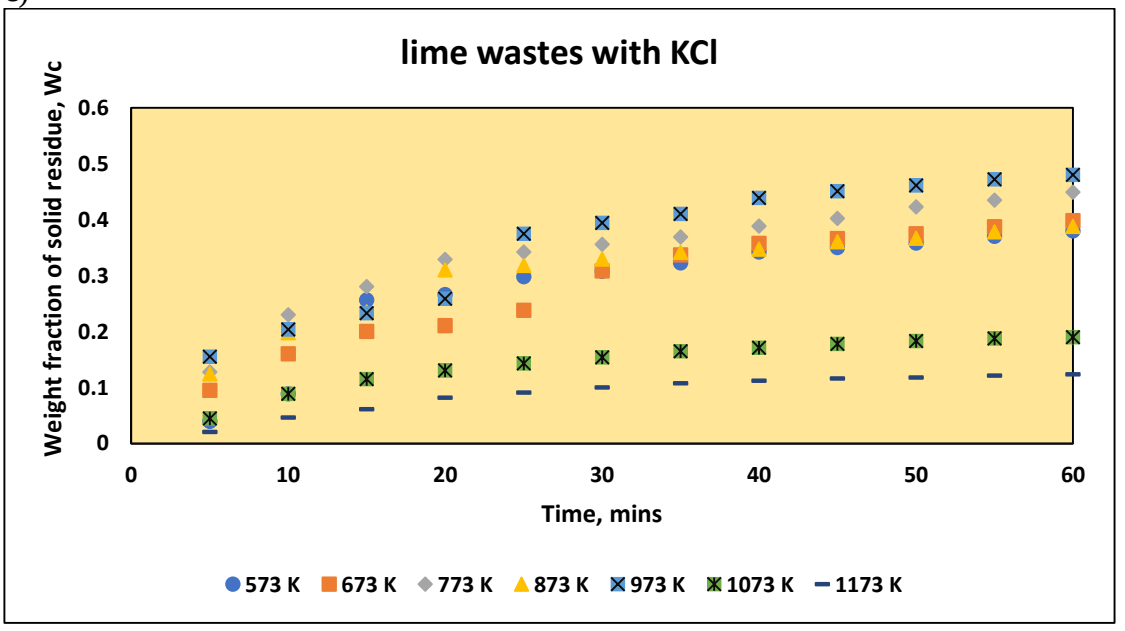
lime wastes with KCl
Weight fraction of solid residue, Wc
0.6
0.5
0.4
0.3
0.2
0.1
0
0
10
20
30
40
50
60
Time, mins
573 K
673 K
773 K
873 K
973 K
1073 K
1173 K

d)

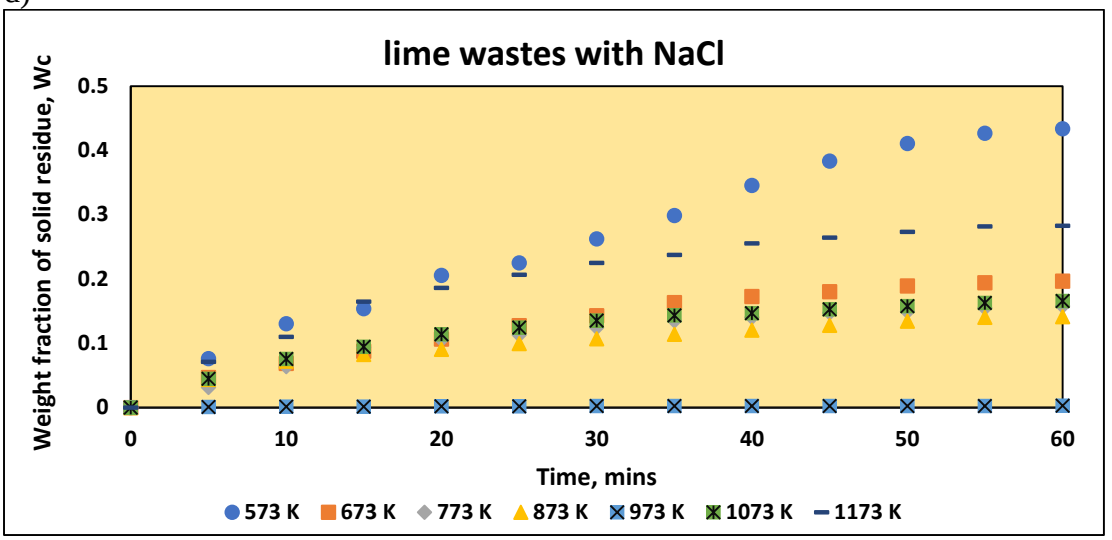

e)

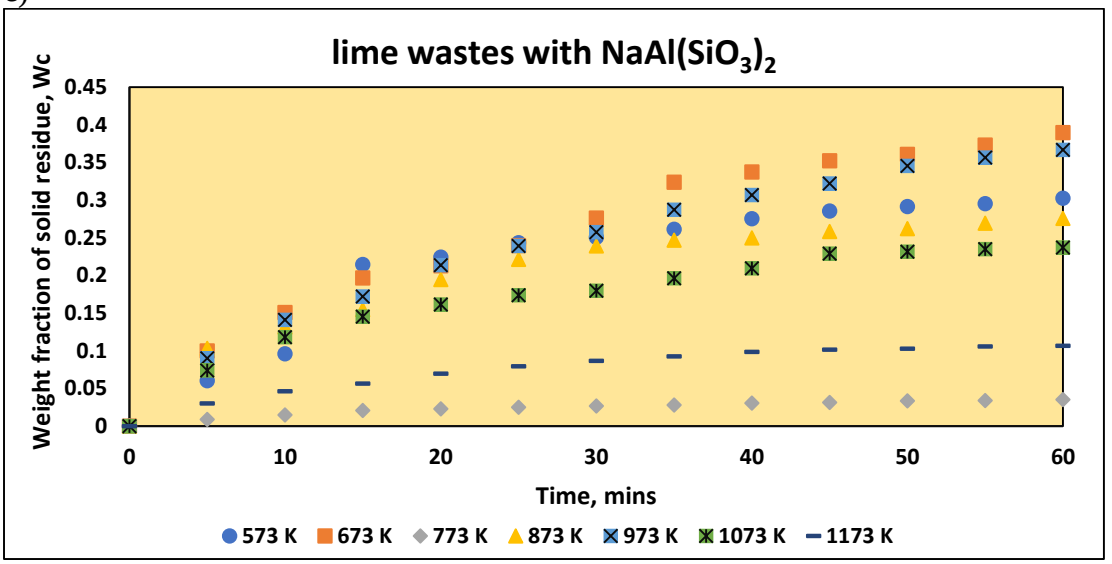

Figure 6.30. Time Histories of char weight fraction using pyrolysis temperature as parameter: (a) lime waste with alumina (b) lime waste with ZnO (c) lime waste with KCl (d) lime waste with NaCl and (e) lime waste with Aluminosilicate

6.4.1.3.1. Parameters of lumped kinetic Model

Experimental values of $\ln\left(\frac{w_o}{w}\right)$ have been plotted against time and those of $\frac{w_v}{w_o}$, $\frac{w_c}{w_o}$, $\frac{w_l}{w_o}$ **and** $\frac{w_g}{w_o}$ have been plotted against $(1-\exp[-k*t])/k$ for catalytic pyrolysis of lime wastes for all temperatures and catalysts under study [A.13.b -A.17.b]. . Figures 6.31 -6.33 show the series of plots for 773K, 973K and 1173K respectively using all catalysts. The linearity of the plots proves the validity of 1st order kinetics [3, 9-12] for all cases. Similar, plots have also been

obtained at other temperature (not shown). The values of k', k_v', k_c', k_l' and k_g' [9-12,15] have been determined from the slopes of the respective plots and are provided in table 6.14-6.18.

a)

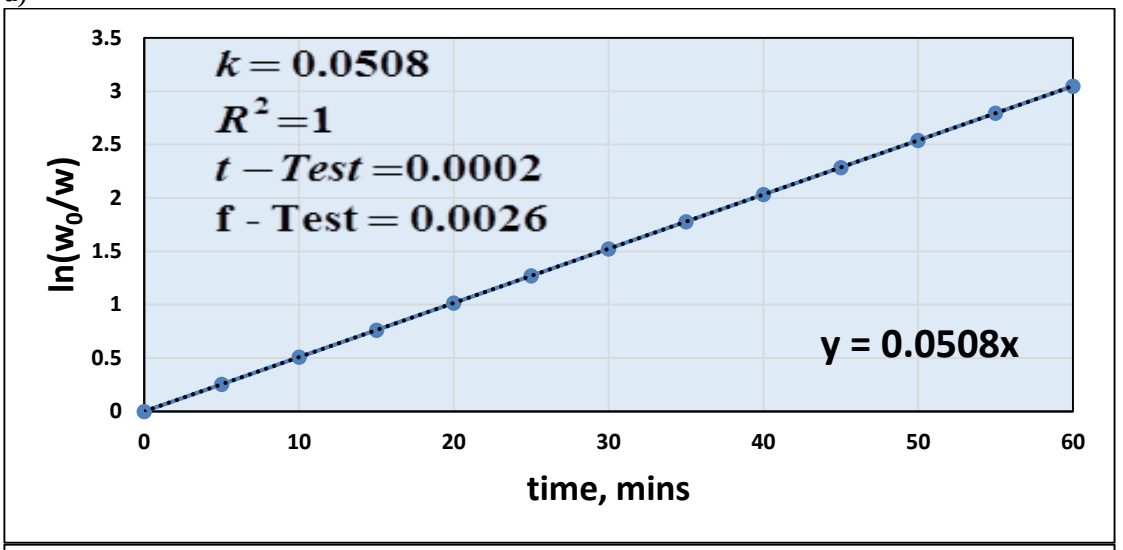

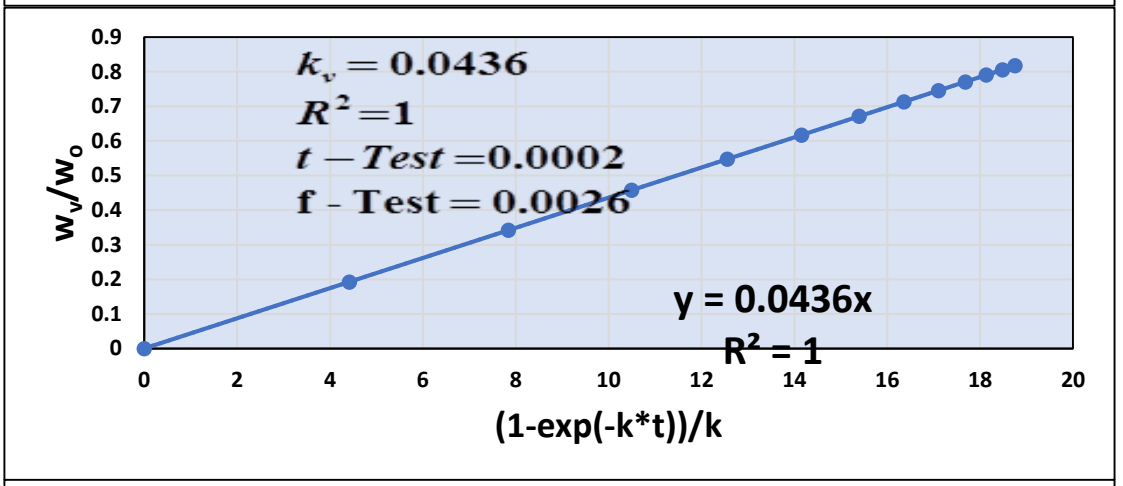

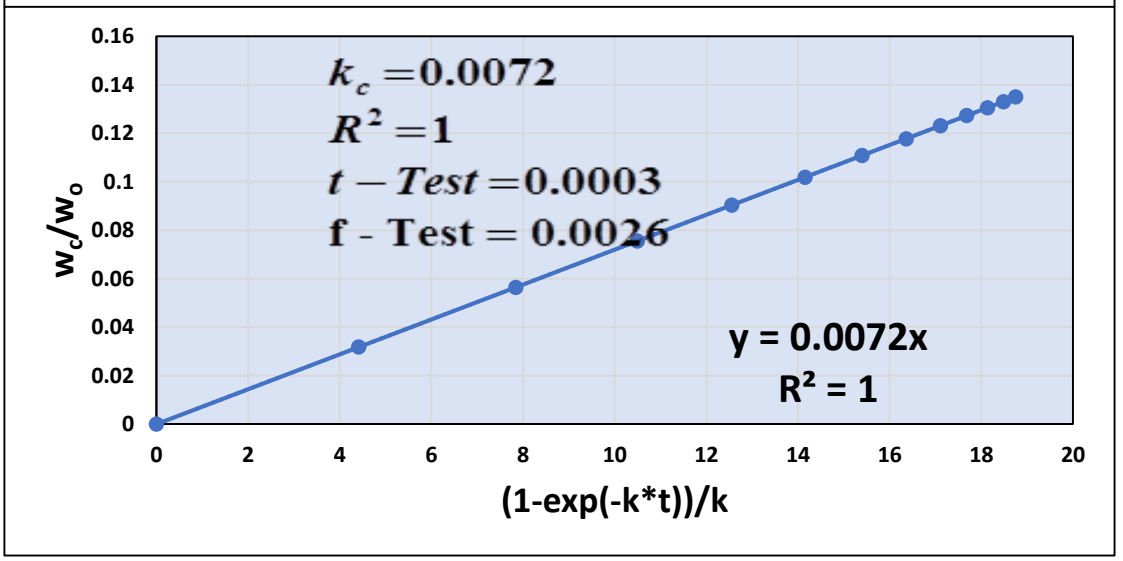

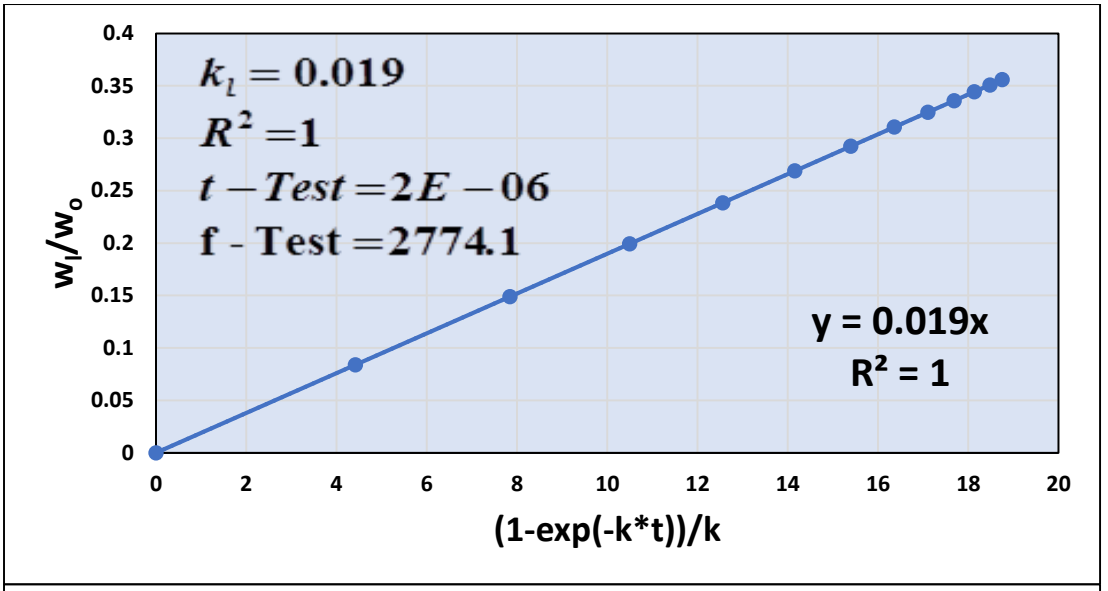
$k_l = 0.019$
$R^2 = 1$
$t - Test = 2E - 06$
f - Test = 2774.1
y = 0.019x
R² = 1
w_l/w_o
(1-exp(-k*t))/k

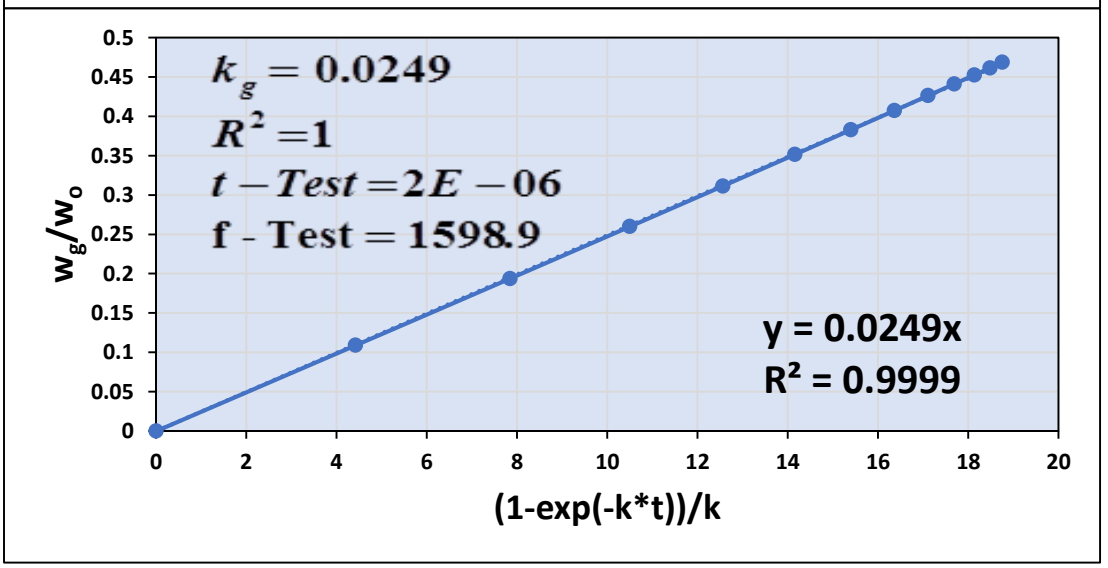
$k_g = 0.0249$
$R^2 = 1$
$t - Test = 2E - 06$
f - Test = 1598.9
y = 0.0249x
R² = 0.9999
w_g/w_o
(1-exp(-k*t))/k

b)

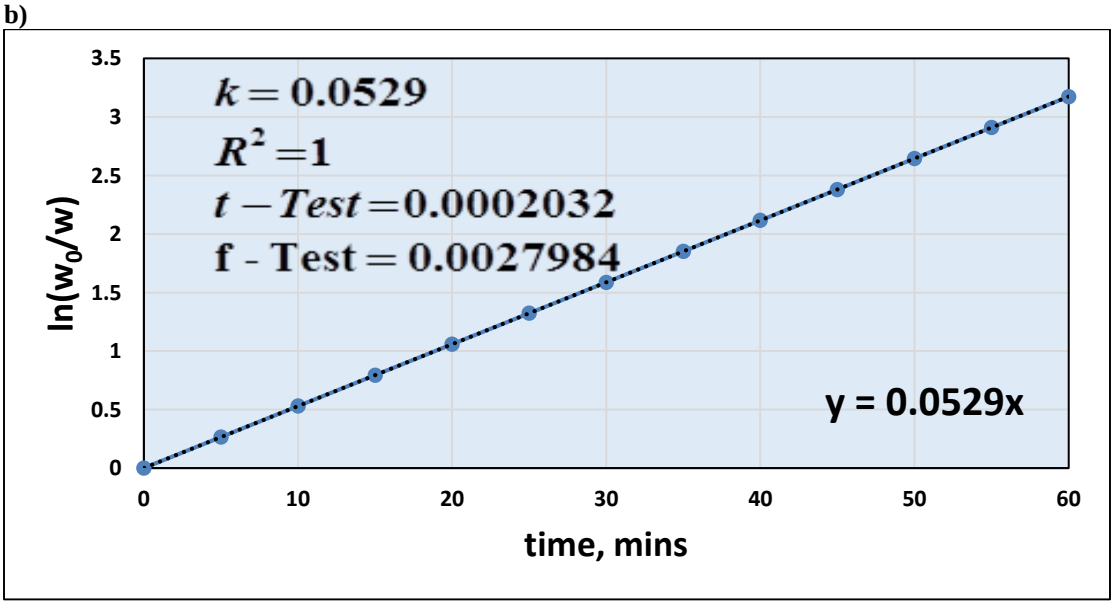
$k = 0.0529$
$R^2 = 1$
$t - Test = 0.0002032$
f - Test = 0.0027984
y = 0.0529x
$\ln(w_0/w)$
time, mins

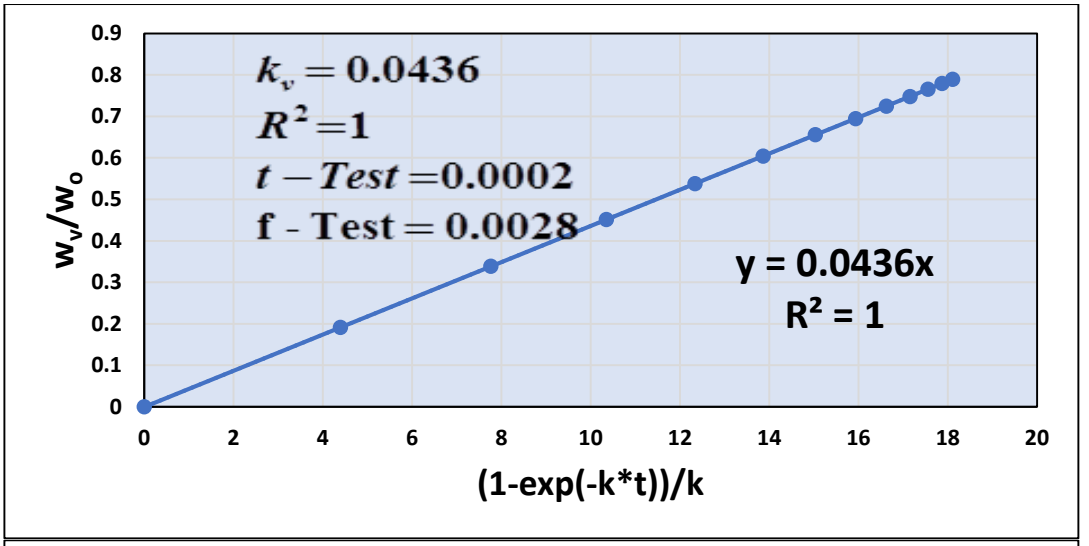
$k_v = 0.0436$
$R^2 = 1$
$t - Test = 0.0002$
f - Test = 0.0028
y = 0.0436x
R² = 1
w_v/w_o
(1-exp(-k*t))/k

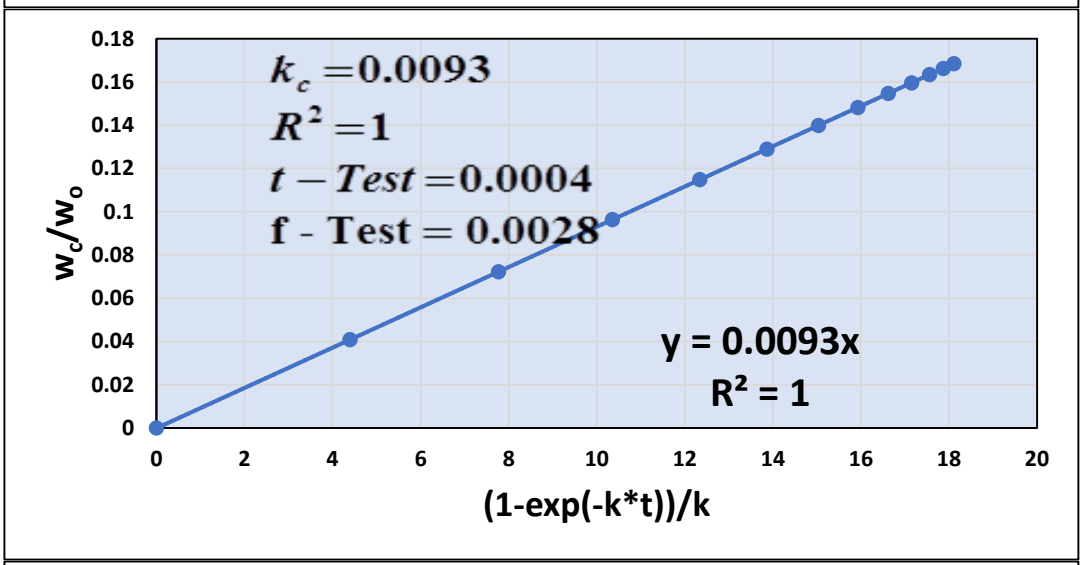
$k_c = 0.0093$
$R^2 = 1$
$t - Test = 0.0004$
f - Test = 0.0028
y = 0.0093x
R² = 1
w_c/w_o
(1-exp(-k*t))/k

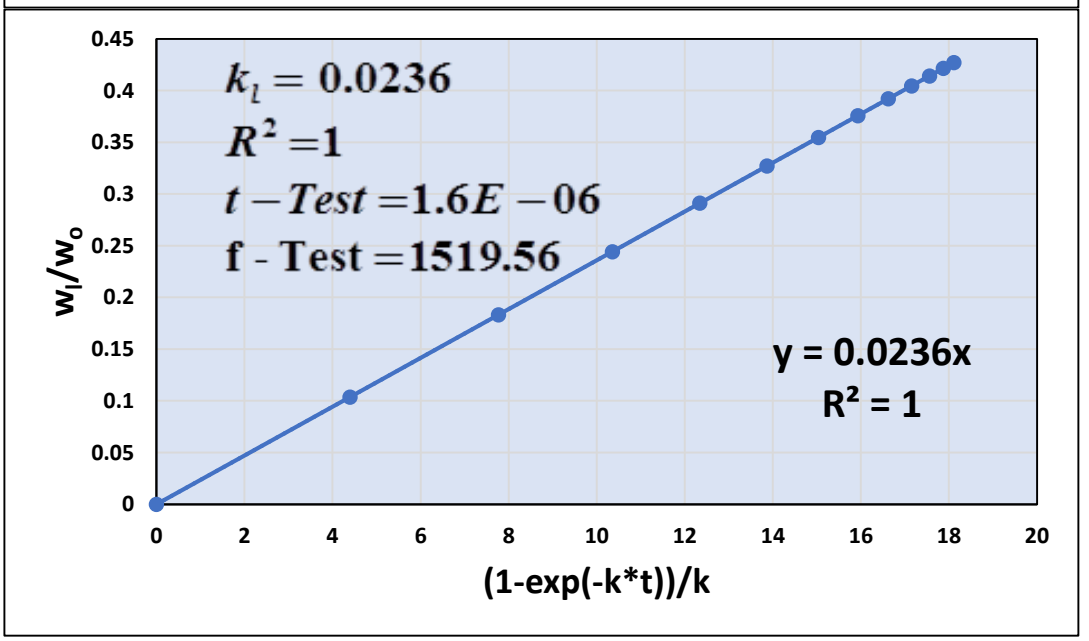
$k_l = 0.0236$
$R^2 = 1$
$t - Test = 1.6E-06$
f - Test = 1519.56
y = 0.0236x
R² = 1
w_l/w_o
(1-exp(-k*t))/k

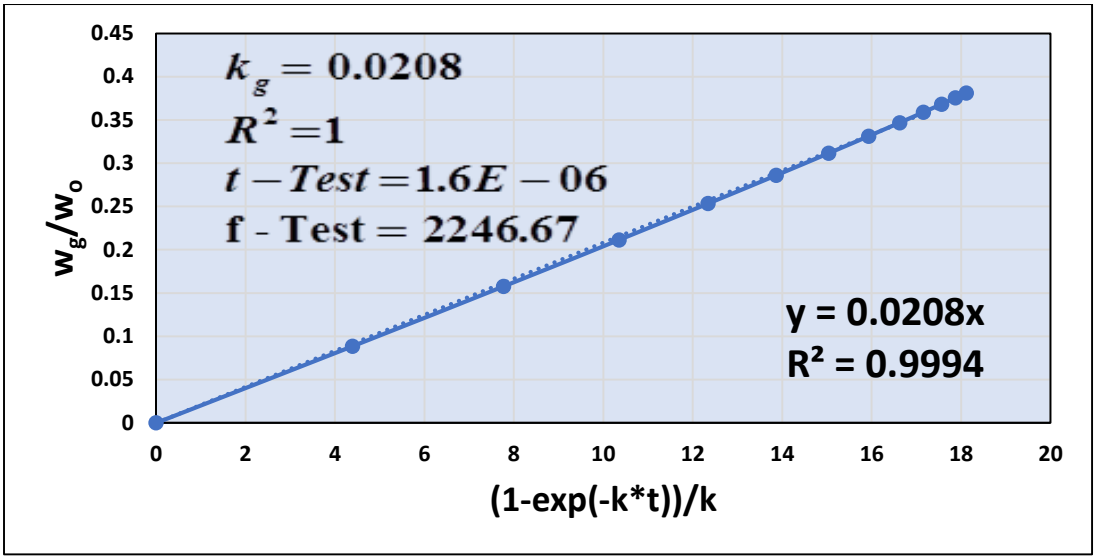
$k_g = 0.0208$
$R^2 = 1$
$t - Test = 1.6E - 06$
f - Test = 2246.67
y = 0.0208x
R² = 0.9994
w_g/w_o
(1-exp(-k*t))/k

c)

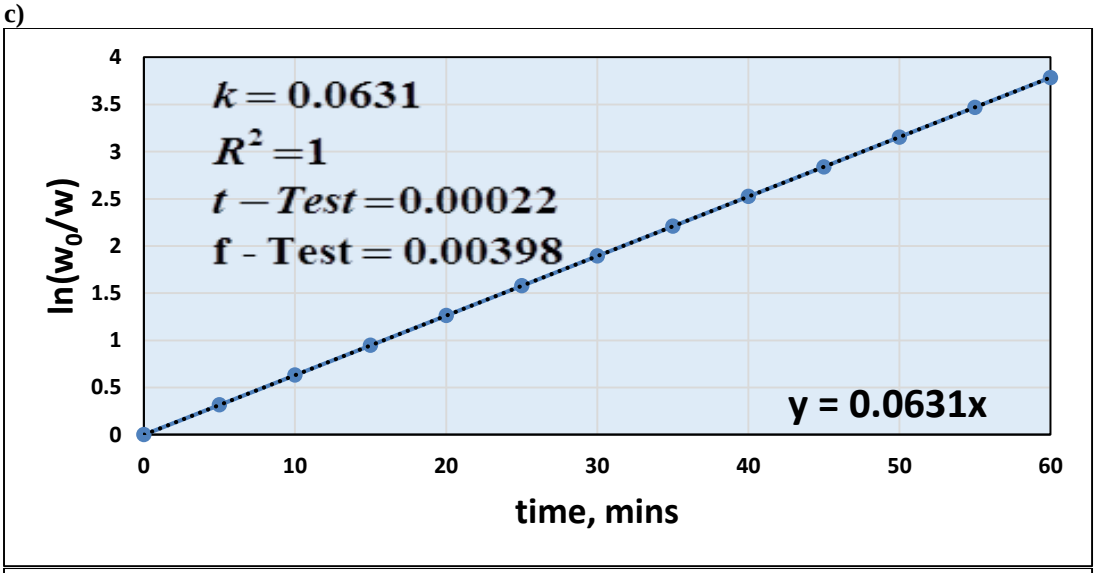
$k = 0.0631$
$R^2 = 1$
$t - Test = 0.00022$
f - Test = 0.00398
y = 0.0631x
$\ln(w_0/w)$
time, mins

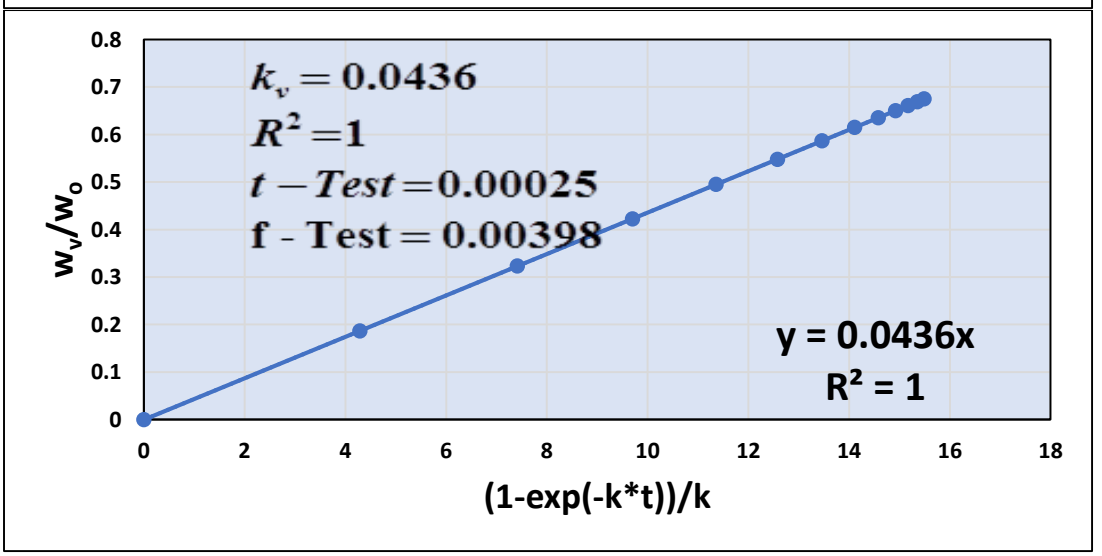
$k_v = 0.0436$
$R^2 = 1$
$t - Test = 0.00025$
f - Test = 0.00398
y = 0.0436x
R² = 1
w_v/w_o
(1-exp(-k*t))/k

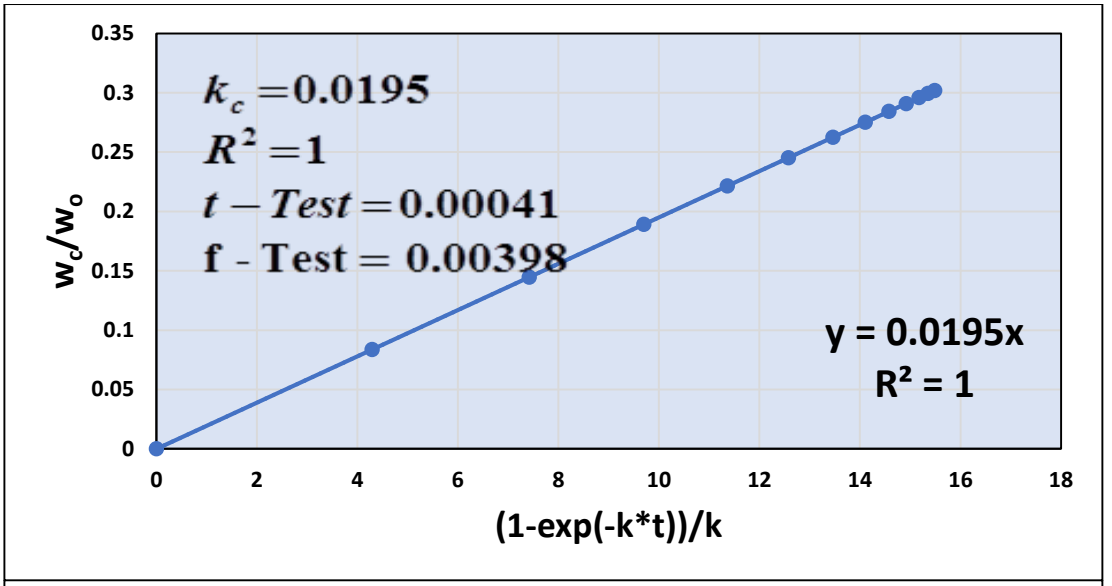
$k_c = 0.0195$
$R^2 = 1$
$t - Test = 0.00041$
f - Test = 0.00398
y = 0.0195x
R² = 1
w_c/w_o
(1-exp(-k*t))/k

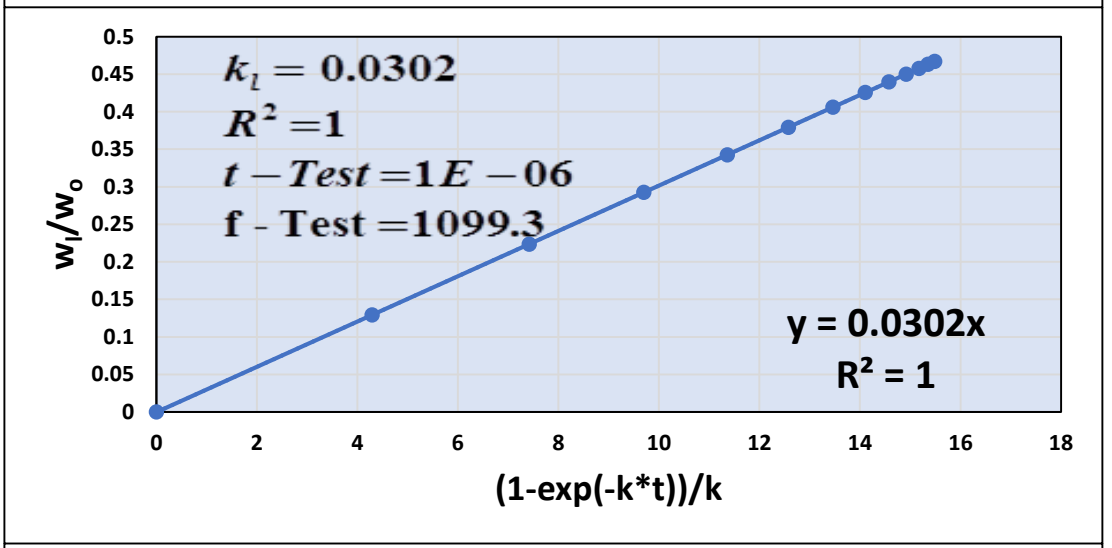
$k_l = 0.0302$
$R^2 = 1$
$t - Test = 1E-06$
f - Test = 1099.3
y = 0.0302x
R² = 1
w_l/w_o
(1-exp(-k*t))/k

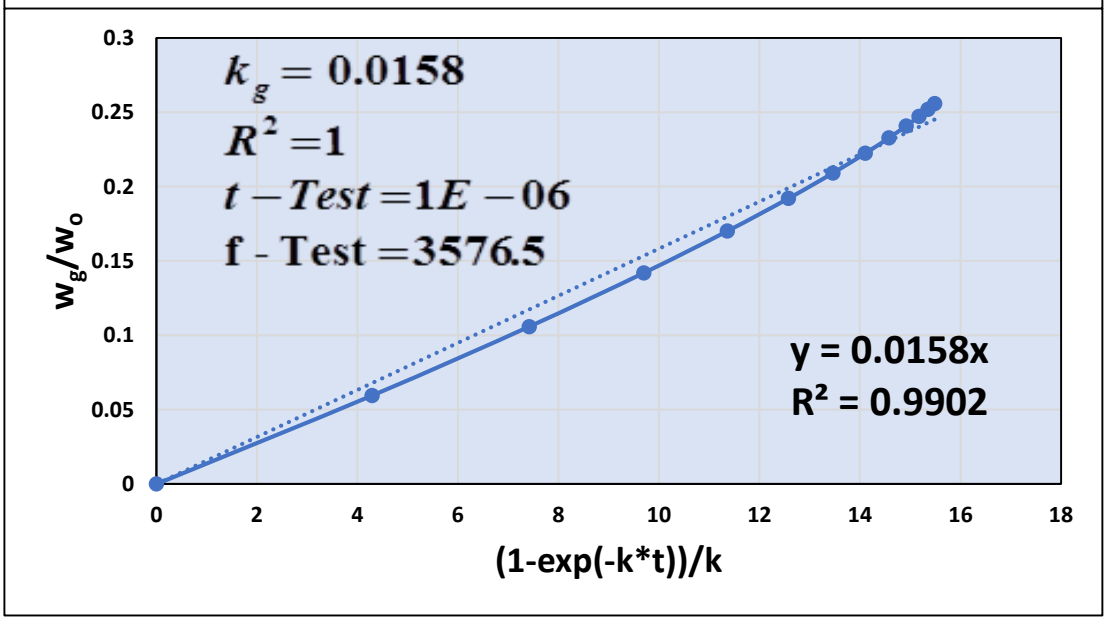
$k_g = 0.0158$
$R^2 = 1$
$t - Test = 1E-06$
f - Test = 3576.5
y = 0.0158x
R² = 0.9902
w_g/w_o
(1-exp(-k*t))/k

d)

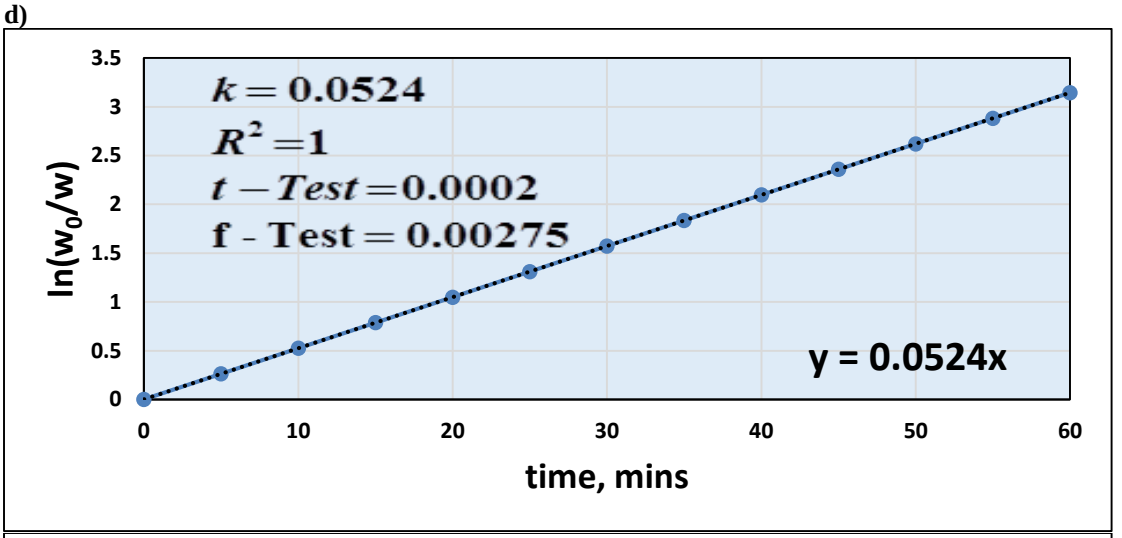
$k = 0.0524$
$R^2 = 1$
$t - Test = 0.0002$
f - Test = 0.00275
y = 0.0524x
ln(w0/w)
time, mins

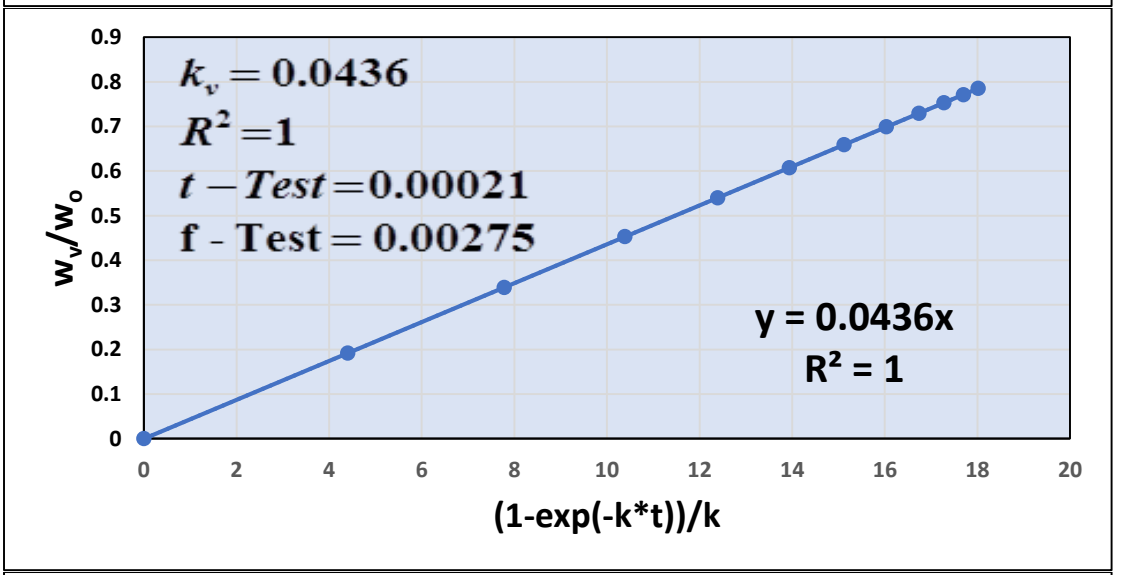
$k_v = 0.0436$
$R^2 = 1$
$t - Test = 0.00021$
f - Test = 0.00275
y = 0.0436x
R² = 1
wv/wo
(1-exp(-k*t))/k

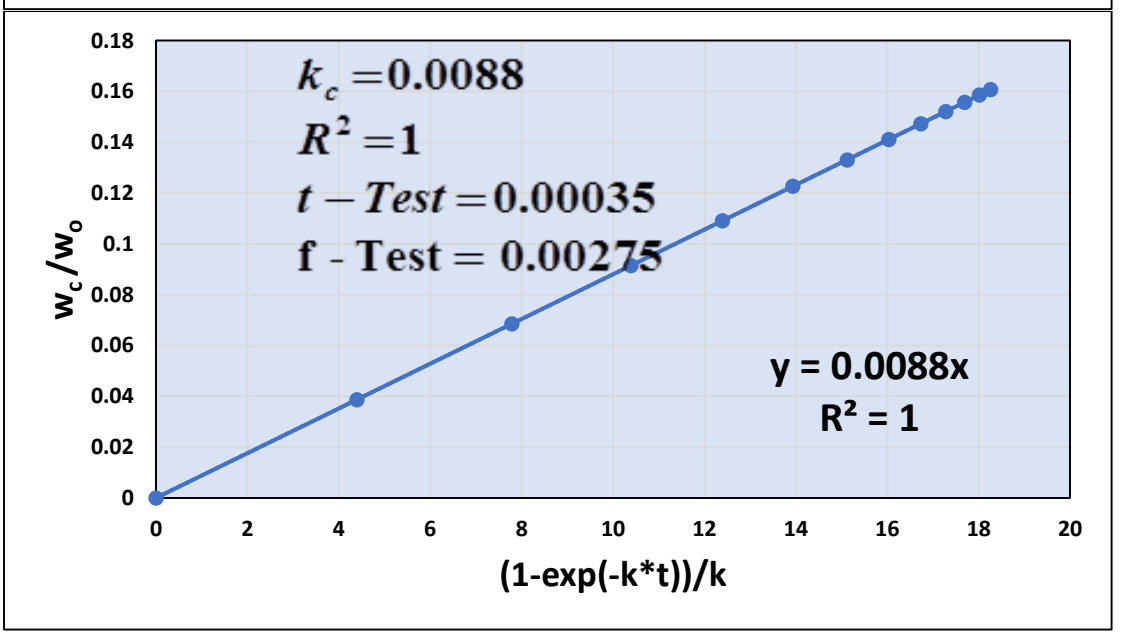
$k_c = 0.0088$
$R^2 = 1$
$t - Test = 0.00035$
f - Test = 0.00275
y = 0.0088x
R² = 1
wc/wo
(1-exp(-k*t))/k

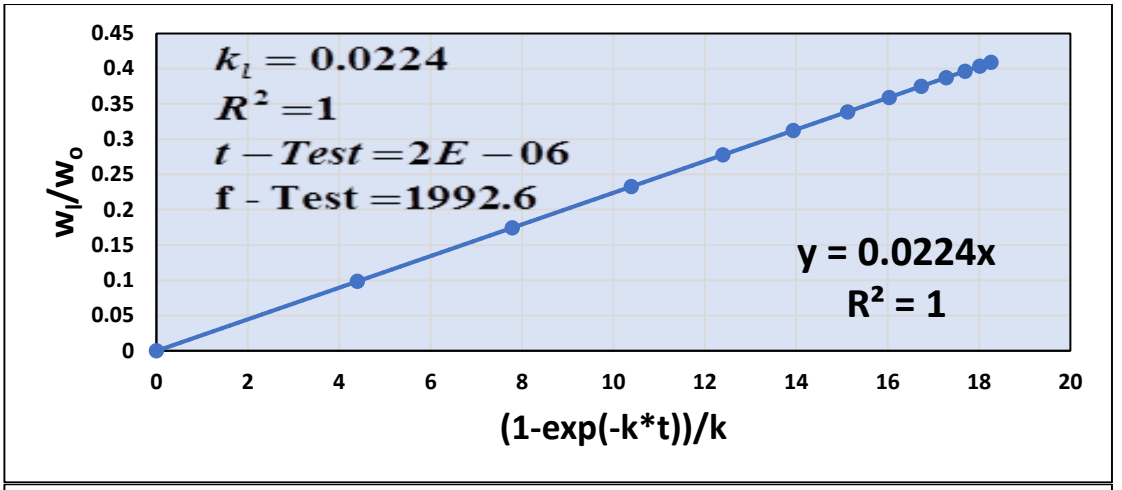
$k_l = 0.0224$
$R^2 = 1$
$t - Test = 2E - 06$
f - Test = 1992.6
y = 0.0224x
R² = 1
w_l/w_o
(1-exp(-k*t))/k

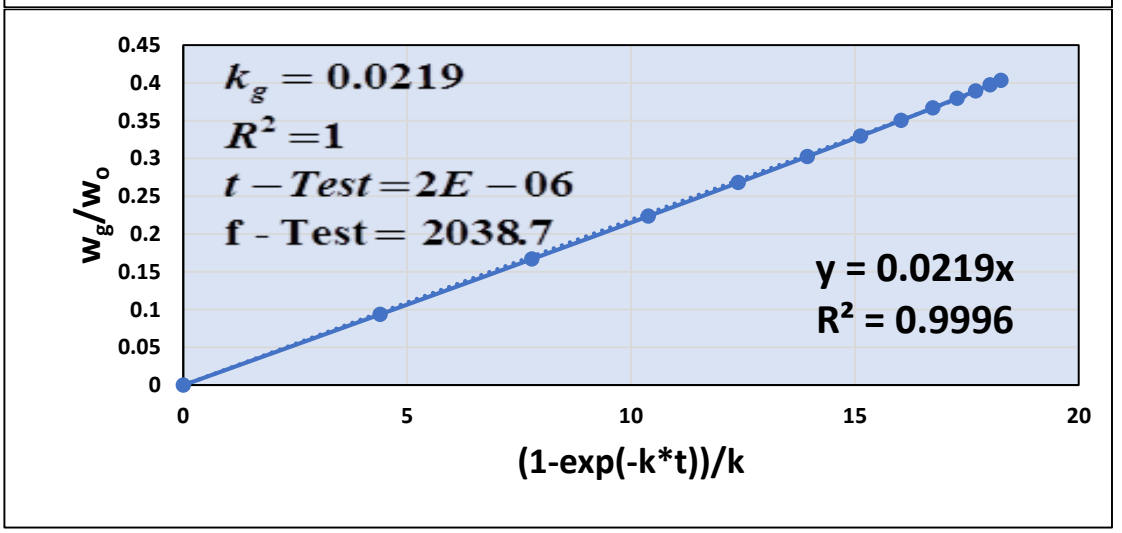
$k_g = 0.0219$
$R^2 = 1$
$t - Test = 2E - 06$
f - Test = 2038.7
y = 0.0219x
R² = 0.9996
w_g/w_o
(1-exp(-k*t))/k

e)

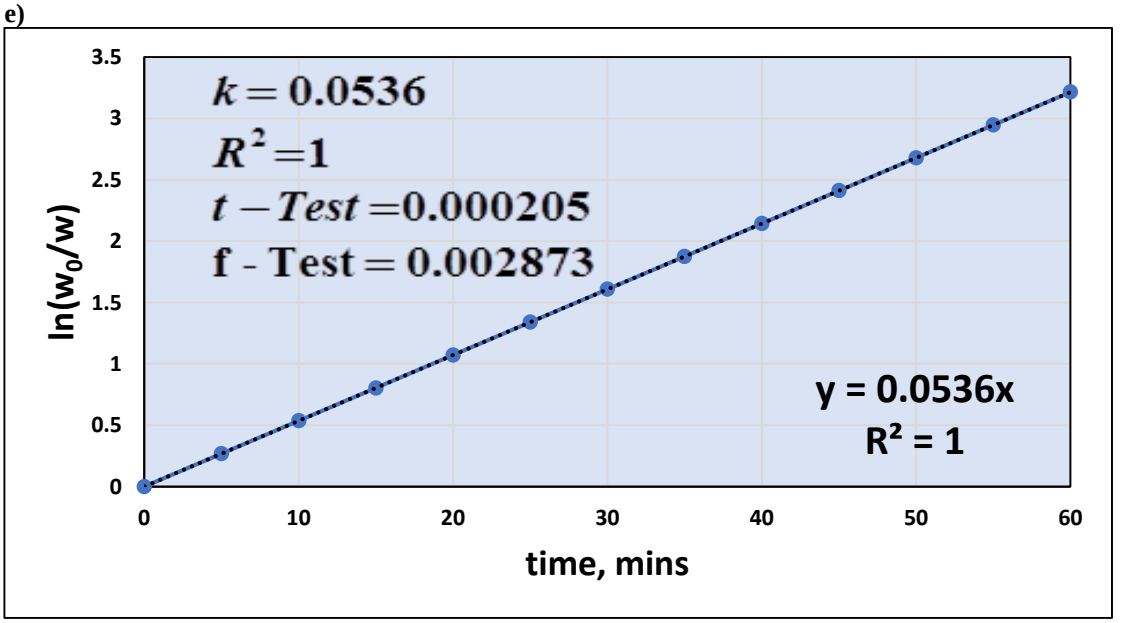
$k = 0.0536$
$R^2 = 1$
$t - Test = 0.000205$
f - Test = 0.002873
y = 0.0536x
R² = 1
$\ln(w_0/w)$
time, mins

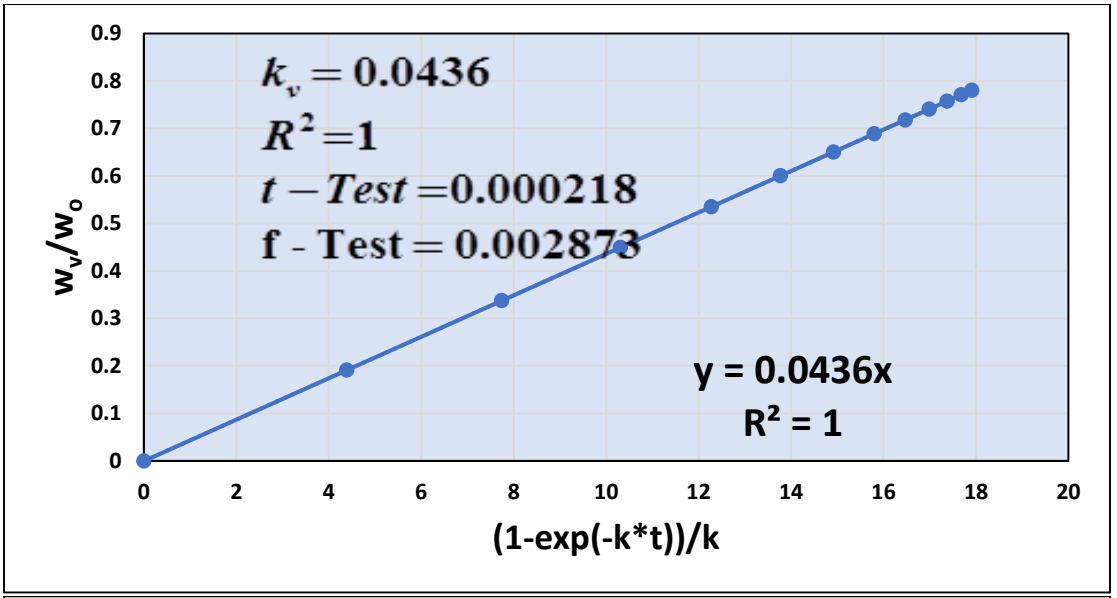
$k_v = 0.0436$
$R^2 = 1$
$t - Test = 0.000218$
f - Test = 0.002873
y = 0.0436x
R² = 1
w_v/w_o
(1-exp(-k*t))/k

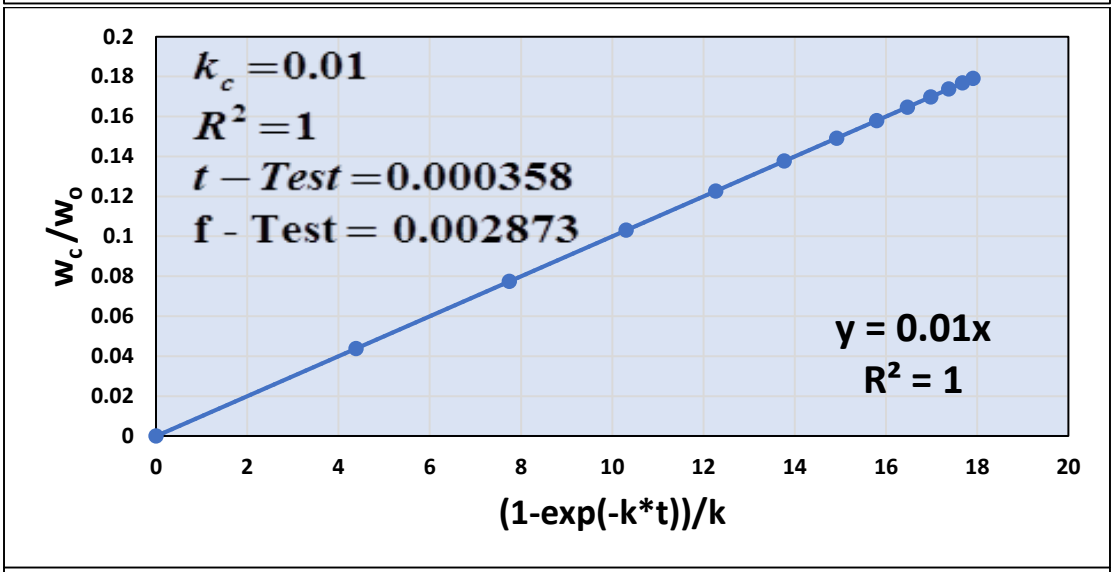
$k_c = 0.01$
$R^2 = 1$
$t - Test = 0.000358$
f - Test = 0.002873
y = 0.01x
R² = 1
w_c/w_o
(1-exp(-k*t))/k

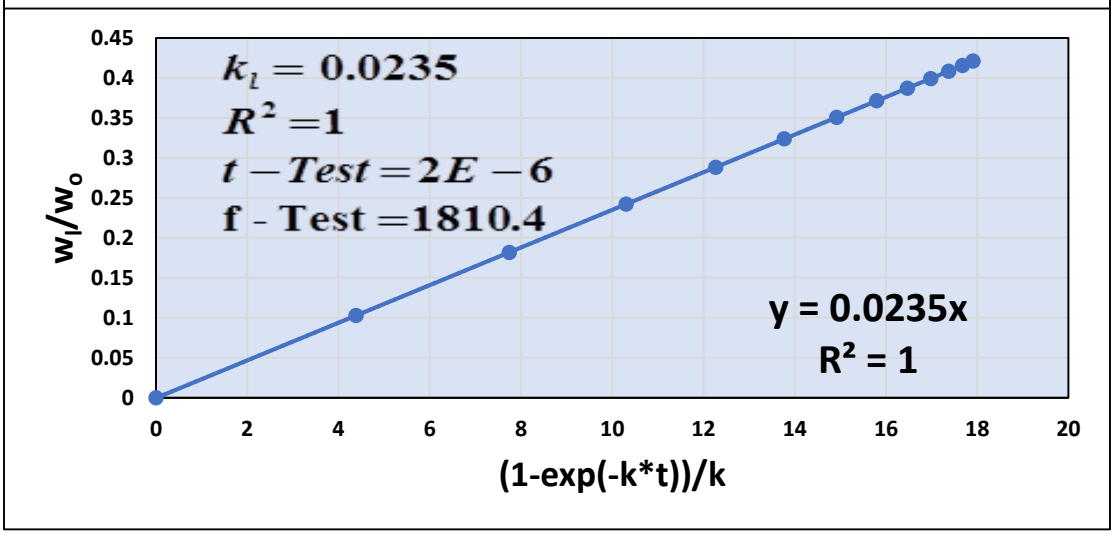
$k_l = 0.0235$
$R^2 = 1$
$t - Test = 2E-6$
f - Test = 1810.4
y = 0.0235x
R² = 1
w_l/w_o
(1-exp(-k*t))/k

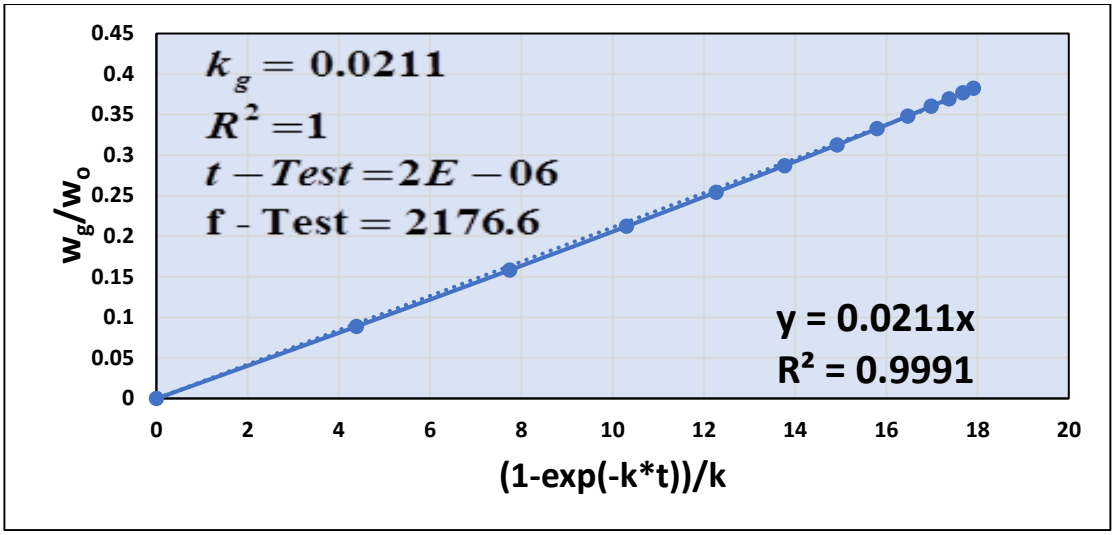

Figure 6.31. Plots of $\ln\left[\frac{w_o}{w}\right]$ vs time and $\frac{w_v}{w_0}$, $\frac{w_c}{w_0}$, $\frac{w_l}{w_0}$ and $\frac{w_g}{w_0}$ vs $(1-\exp[-k*t])/k$ at 773K (a) lime waste with alumina (b) lime waste with ZnO (c) lime waste with KCl (d) lime waste with NaCl and (e) lime waste with Aluminosilicate

a)

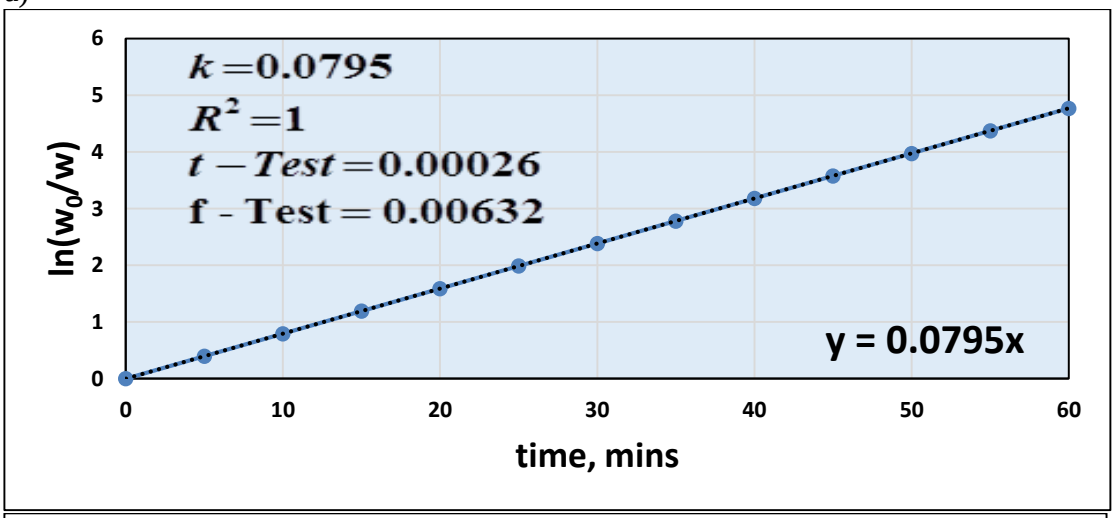

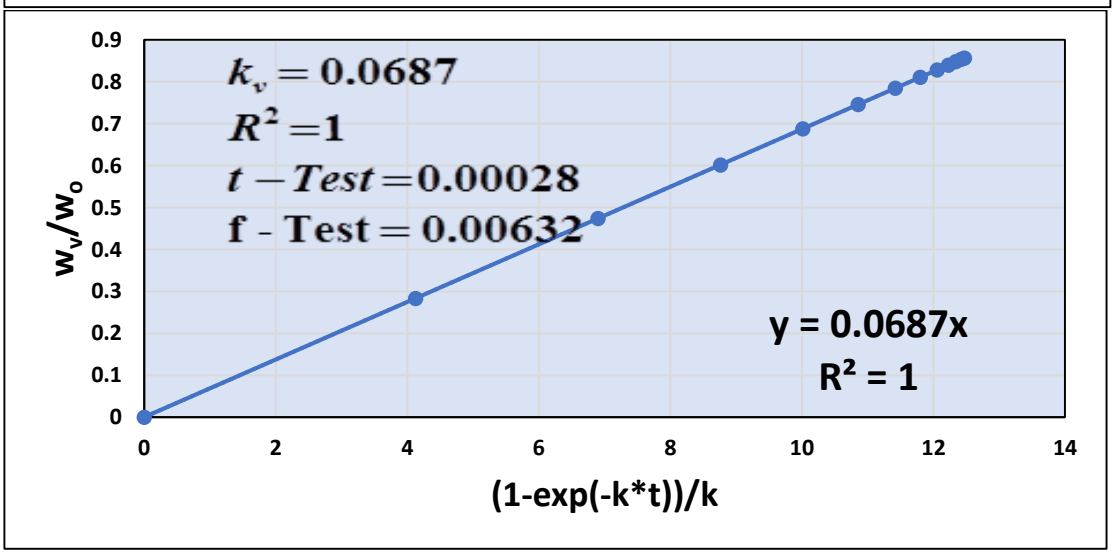

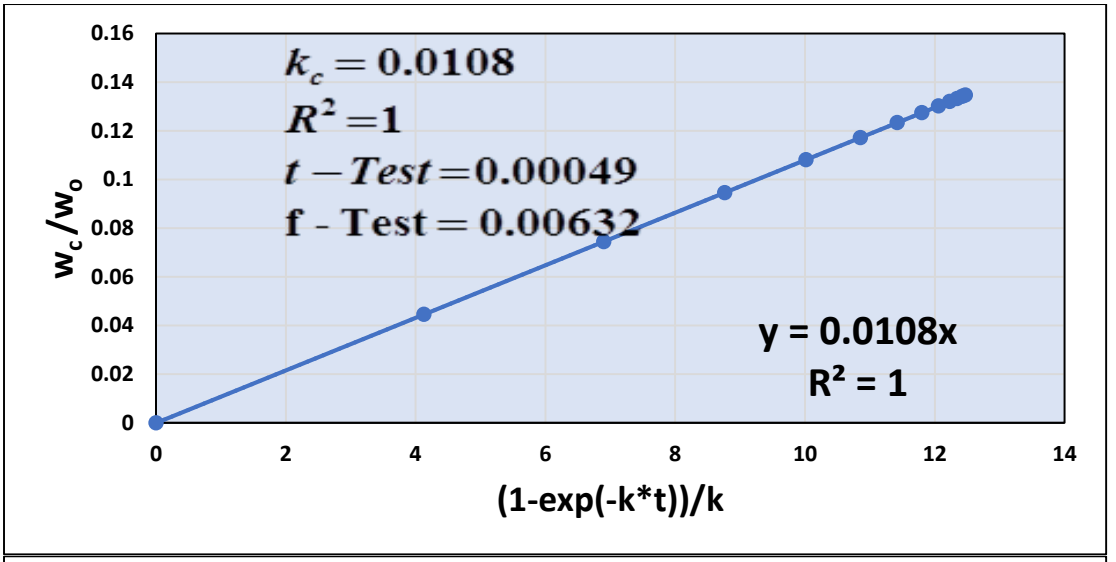
$k_c = 0.0108$
$R^2 = 1$
$t - Test = 0.00049$
f - Test = 0.00632
y = 0.0108x
R² = 1
w_c/w_o
(1-exp(-k*t))/k

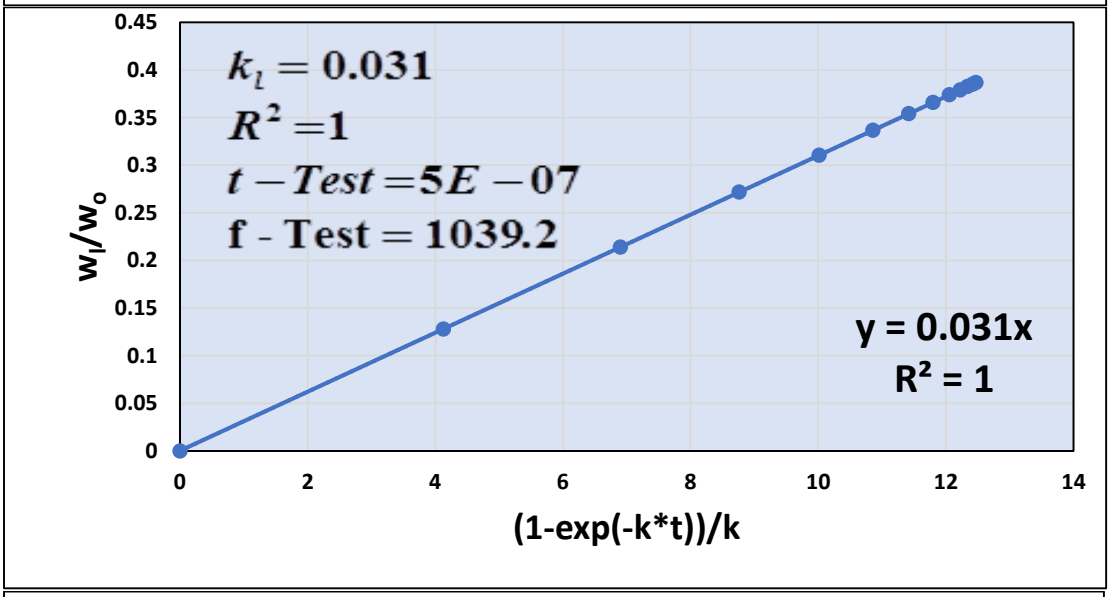
$k_l = 0.031$
$R^2 = 1$
$t - Test = 5E-07$
f - Test = 1039.2
y = 0.031x
R² = 1
w_l/w_o
(1-exp(-k*t))/k

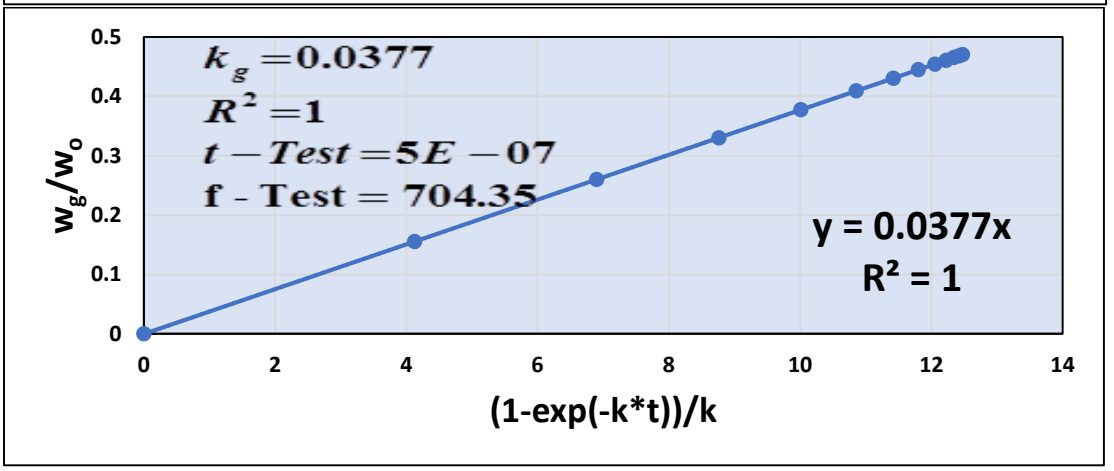
$k_g = 0.0377$
$R^2 = 1$
$t - Test = 5E-07$
f - Test = 704.35
y = 0.0377x
R² = 1
w_g/w_o
(1-exp(-k*t))/k

b)

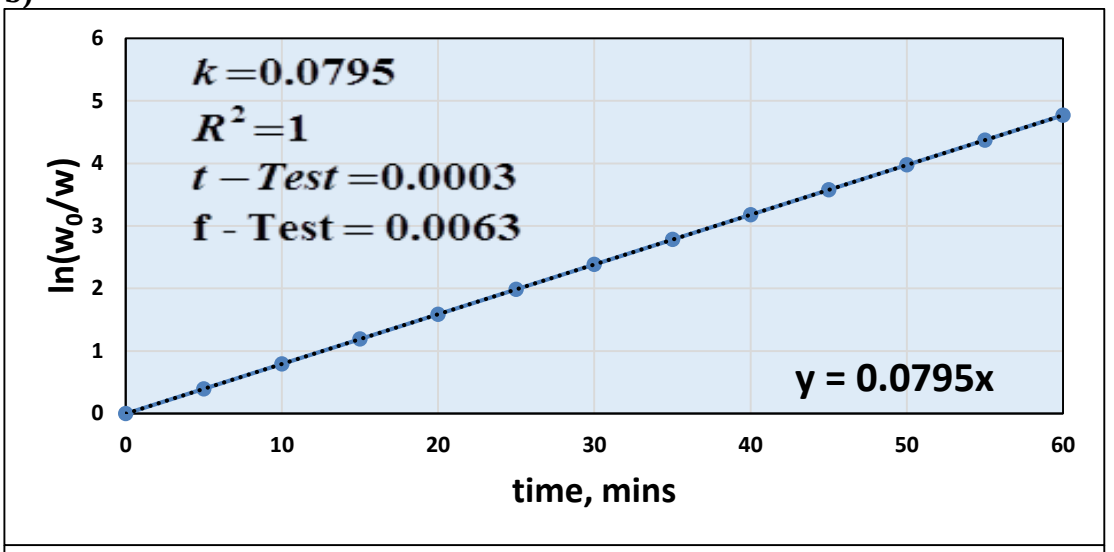
$k = 0.0795$
$R^2 = 1$
$t - Test = 0.0003$
f - Test = 0.0063
y = 0.0795x
ln(w0/w)
time, mins

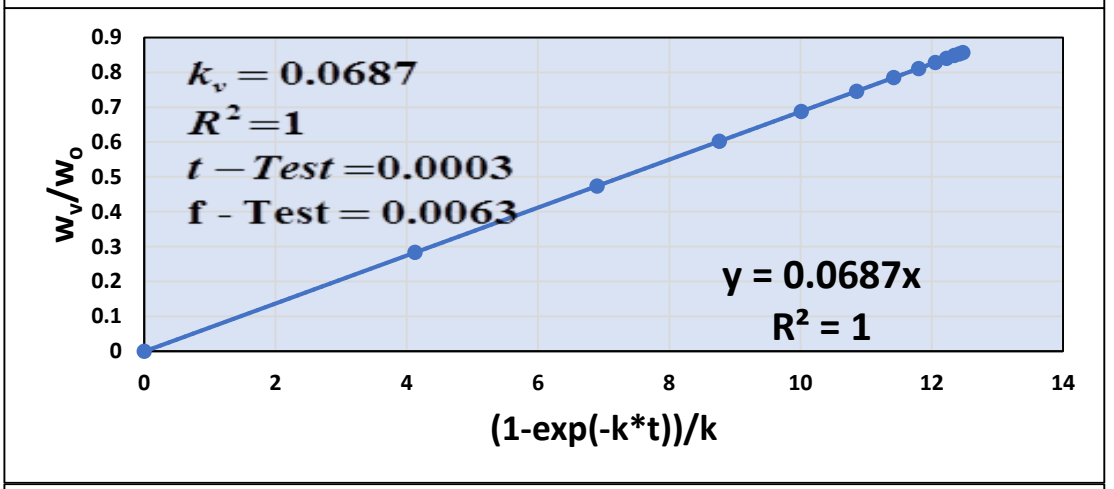
$k_v = 0.0687$
$R^2 = 1$
$t - Test = 0.0003$
f - Test = 0.0063
y = 0.0687x
R² = 1
wv/wo
(1-exp(-k*t))/k

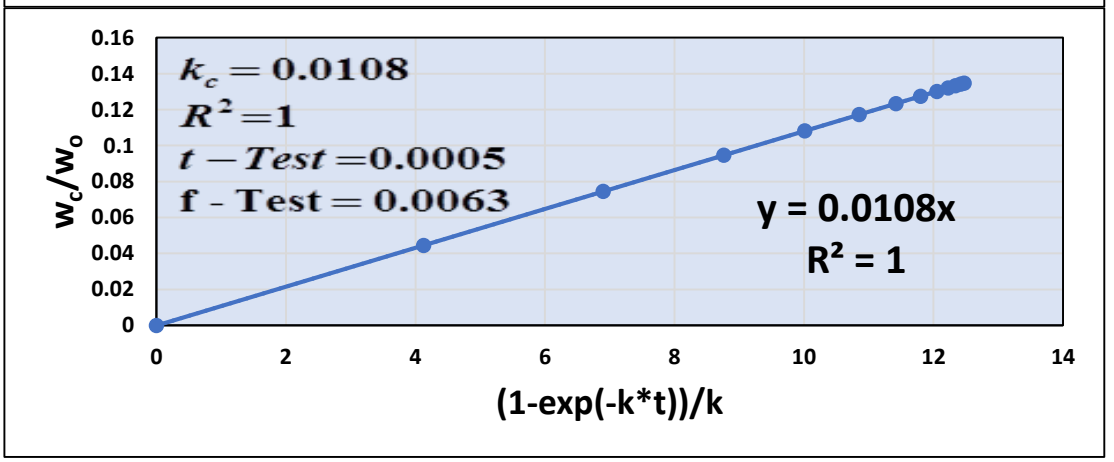
$k_c = 0.0108$
$R^2 = 1$
$t - Test = 0.0005$
f - Test = 0.0063
y = 0.0108x
R² = 1
wc/wo
(1-exp(-k*t))/k

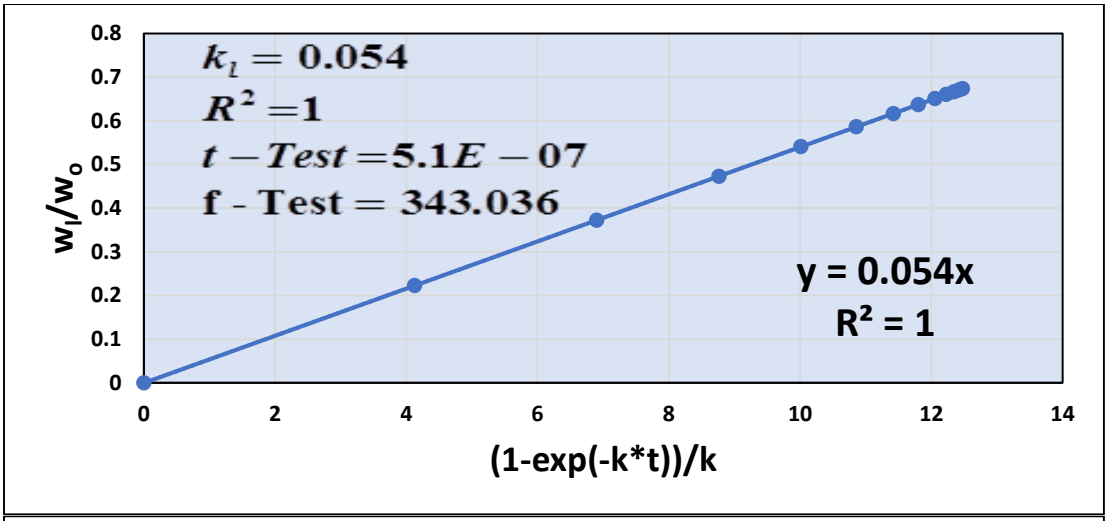
$k_l = 0.054$
$R^2 = 1$
$t - Test = 5.1E-07$
f - Test = 343.036
y = 0.054x
R² = 1
w_l/w_o
(1-exp(-k*t))/k

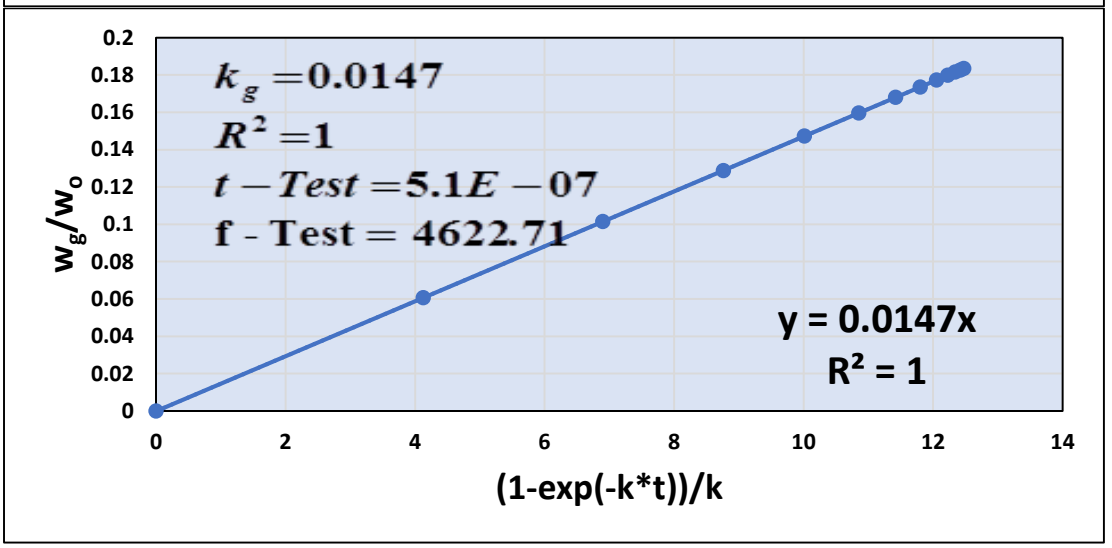
$k_g = 0.0147$
$R^2 = 1$
$t - Test = 5.1E-07$
f - Test = 4622.71
y = 0.0147x
R² = 1
w_g/w_o
(1-exp(-k*t))/k

c)

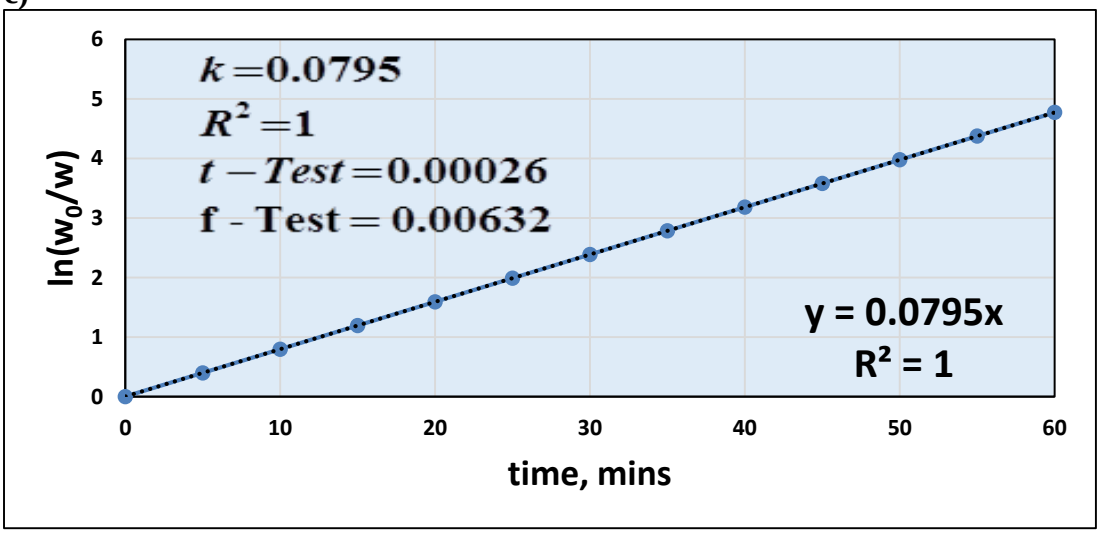
$k = 0.0795$
$R^2 = 1$
$t - Test = 0.00026$
f - Test = 0.00632
y = 0.0795x
R² = 1
$\ln(w_0/w)$
time, mins

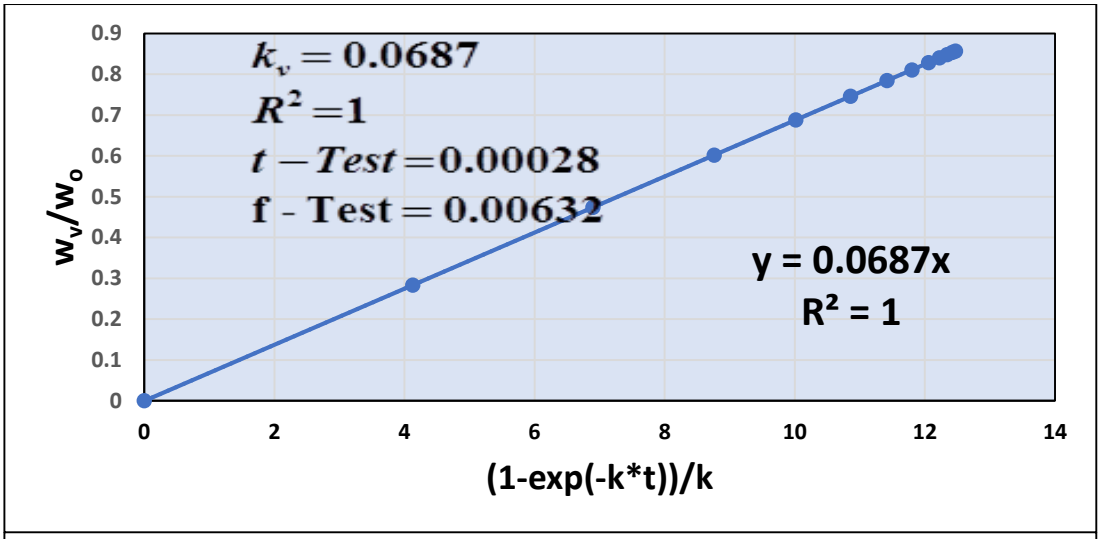
$k_v = 0.0687$
$R^2 = 1$
$t - Test = 0.00028$
f - Test = 0.00632
y = 0.0687x
R² = 1
w_v/w_o
(1-exp(-k*t))/k

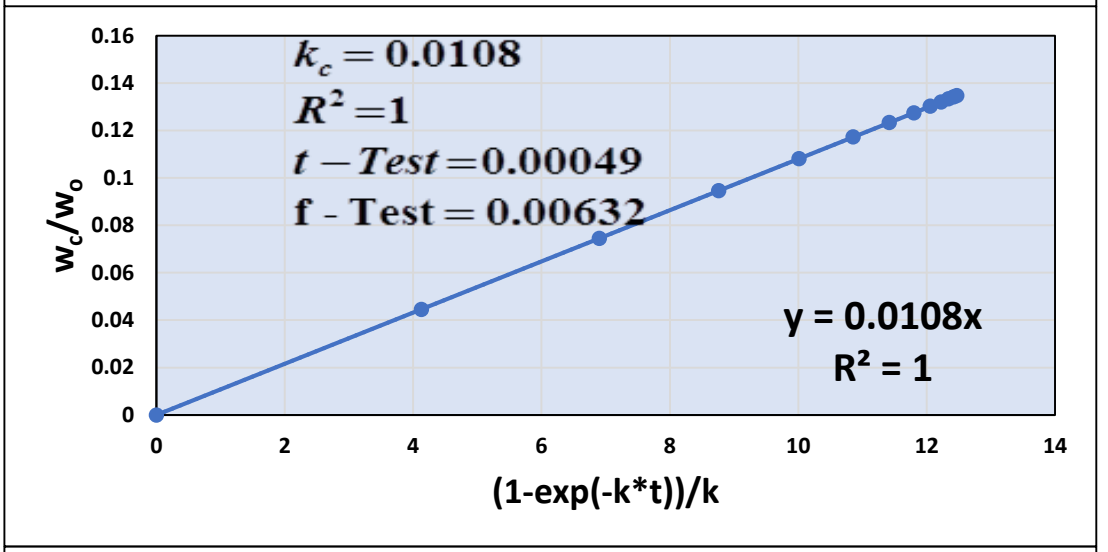
$k_c = 0.0108$
$R^2 = 1$
$t - Test = 0.00049$
f - Test = 0.00632
y = 0.0108x
R² = 1
w_c/w_o
(1-exp(-k*t))/k

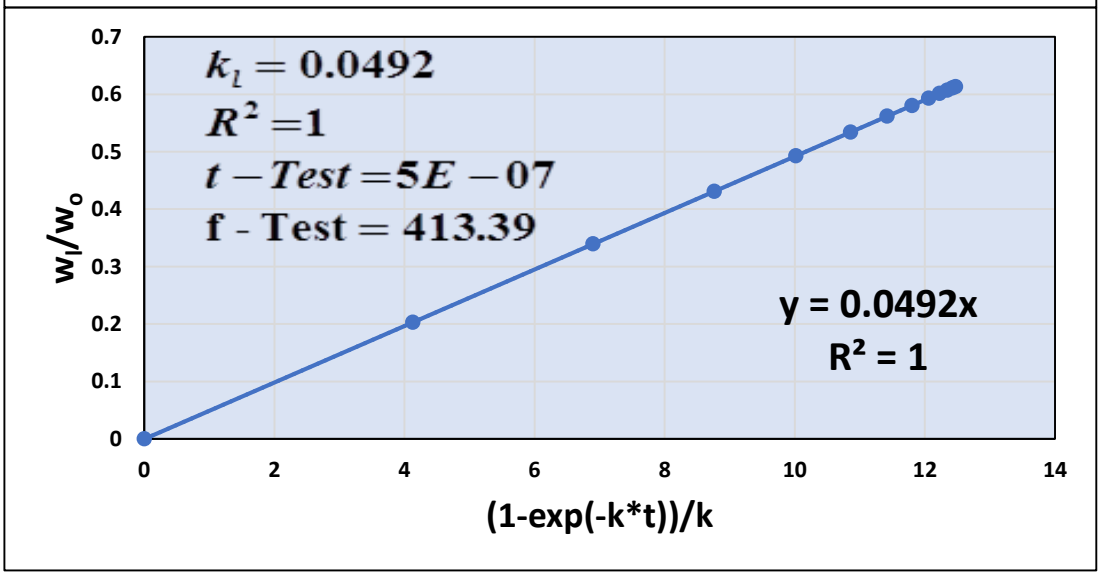
$k_l = 0.0492$
$R^2 = 1$
$t - Test = 5E-07$
f - Test = 413.39
y = 0.0492x
R² = 1
w_l/w_o
(1-exp(-k*t))/k

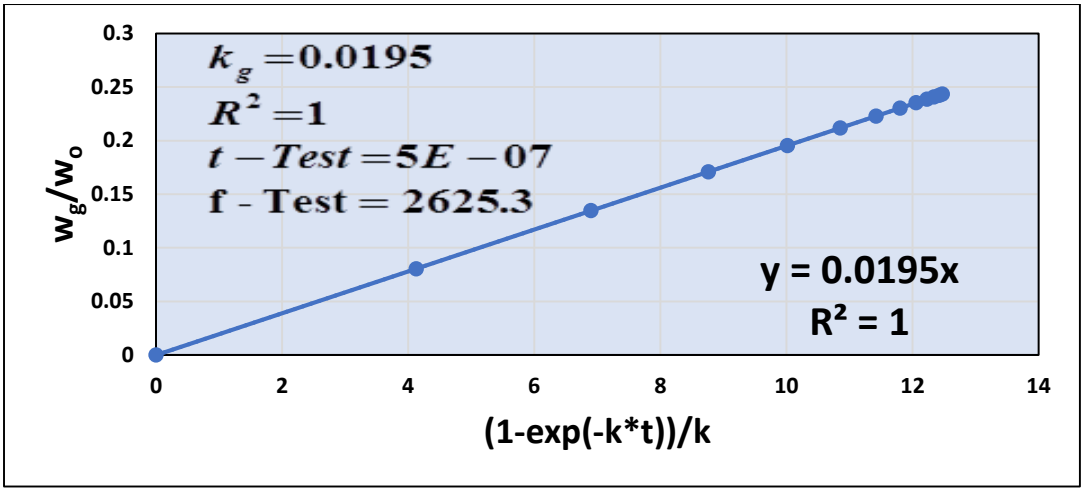
$k_g = 0.0195$
$R^2 = 1$
$t - Test = 5E - 07$
f - Test = 2625.3
y = 0.0195x
R² = 1
w_g/w_o
(1-exp(-k*t))/k

d)

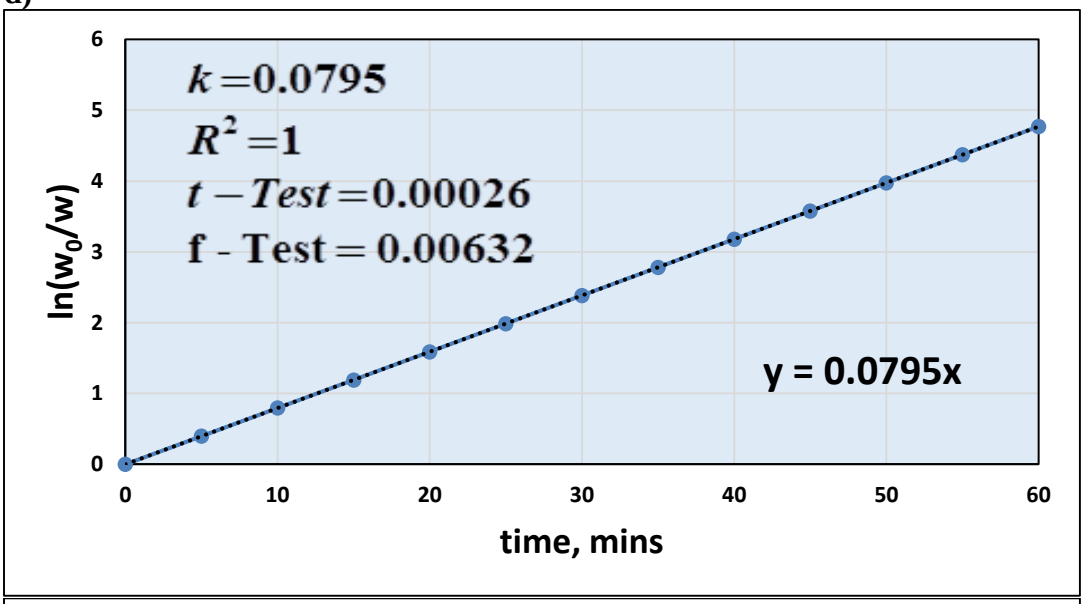
$k = 0.0795$
$R^2 = 1$
$t - Test = 0.00026$
f - Test = 0.00632
y = 0.0795x
$\ln(w_0/w)$
time, mins

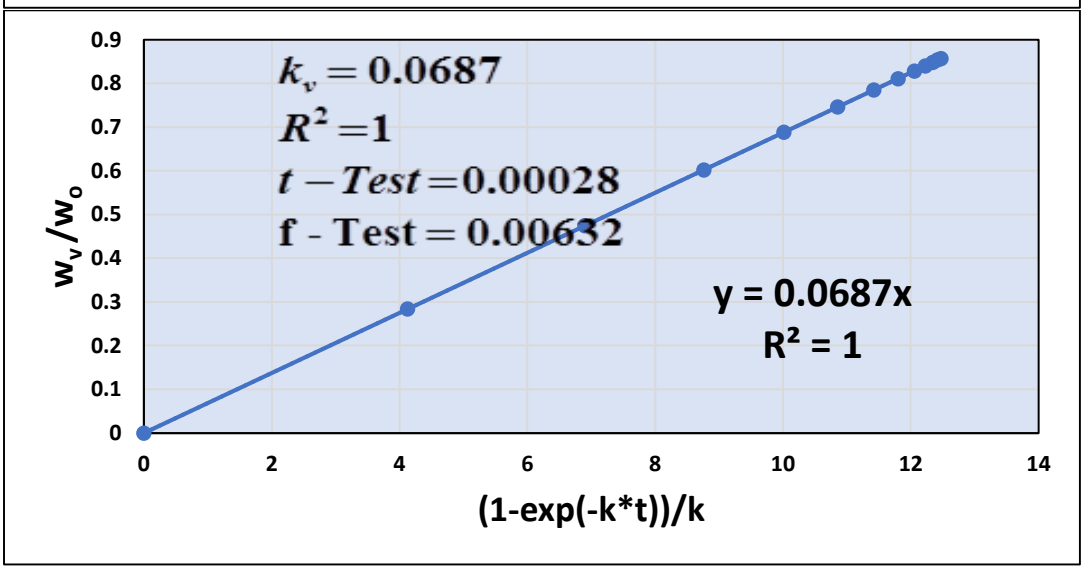
$k_v = 0.0687$
$R^2 = 1$
$t - Test = 0.00028$
f - Test = 0.00632
y = 0.0687x
R² = 1
w_v/w_o
(1-exp(-k*t))/k

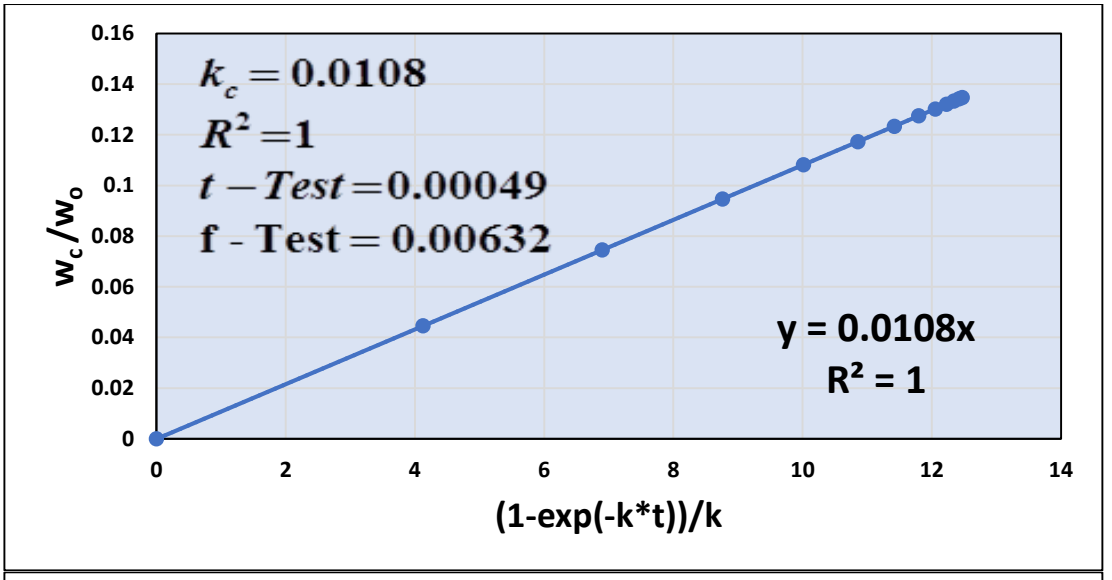
$k_c = 0.0108$
$R^2 = 1$
$t - Test = 0.00049$
f - Test = 0.00632
y = 0.0108x
R² = 1
w_c/w_o
(1-exp(-k*t))/k

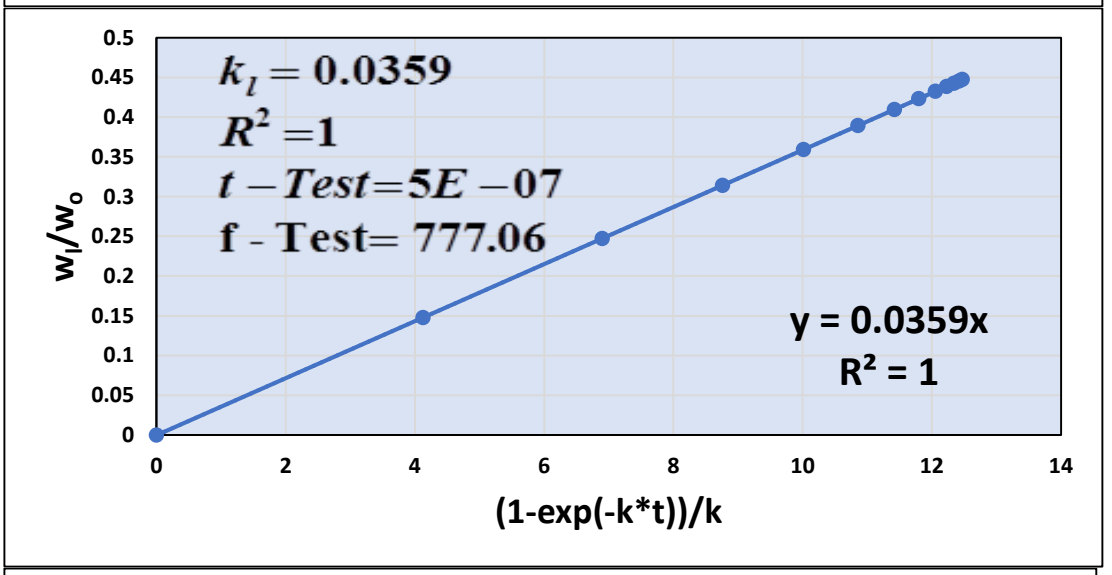
$k_l = 0.0359$
$R^2 = 1$
$t - Test = 5E-07$
f - Test= 777.06
y = 0.0359x
R² = 1
w_l/w_o
(1-exp(-k*t))/k

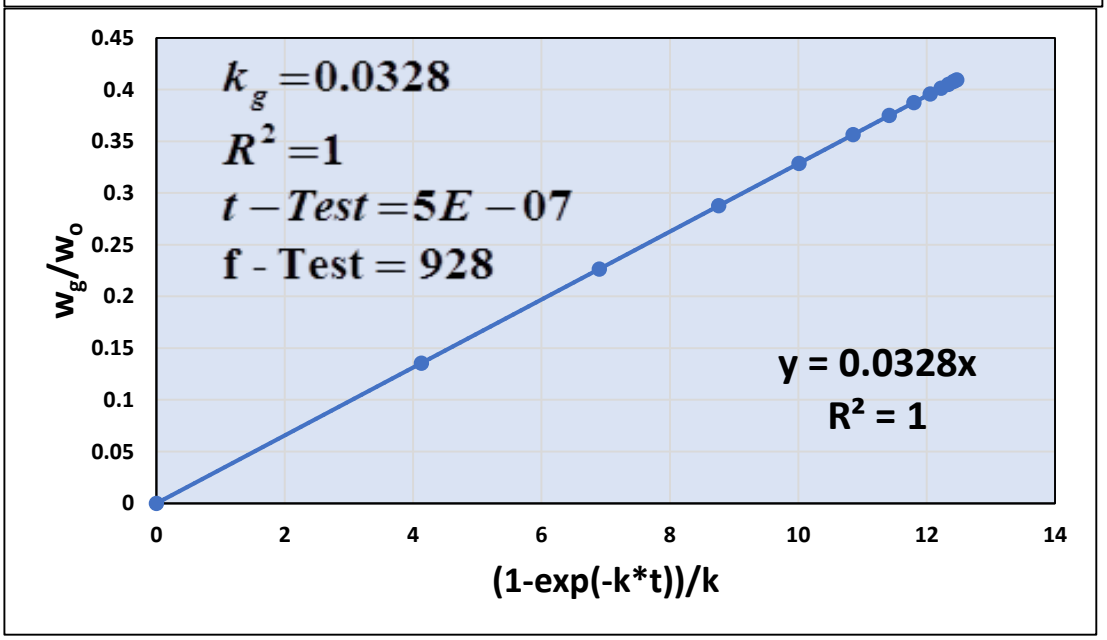
$k_g = 0.0328$
$R^2 = 1$
$t - Test = 5E-07$
f - Test = 928
y = 0.0328x
R² = 1
w_g/w_o
(1-exp(-k*t))/k

e)

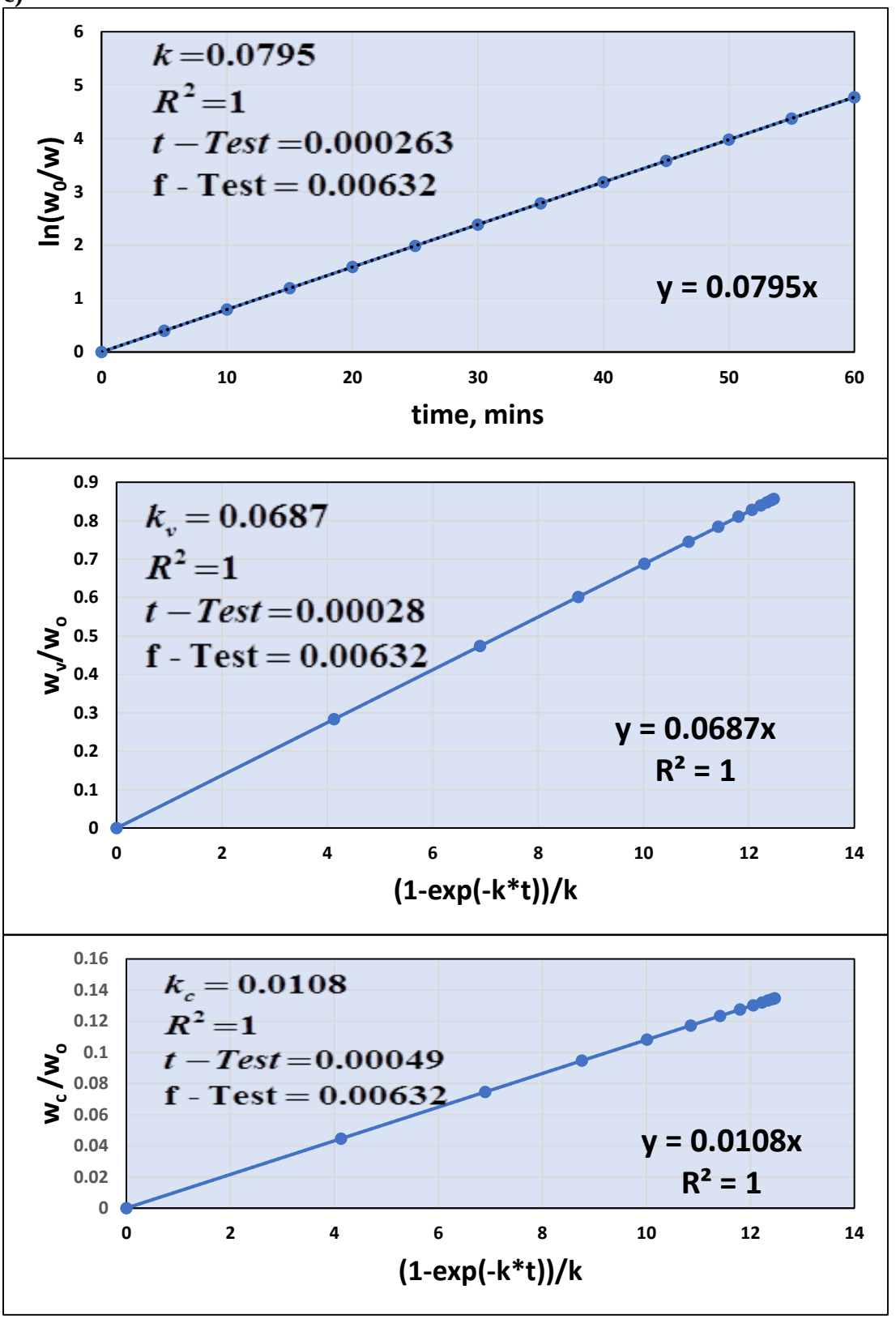
k =0.0795
R² =1
t – Test =0.000263
f - Test = 0.00632
y = 0.0795x
ln(w0/w)
time, mins
k_v = 0.0687
R² =1
t – Test =0.00028
f - Test = 0.00632
y = 0.0687x
R² = 1
wv/wo
(1-exp(-k*t))/k
k_c = 0.0108
R² =1
t – Test =0.00049
f - Test = 0.00632
y = 0.0108x
R² = 1
wc/wo
(1-exp(-k*t))/k

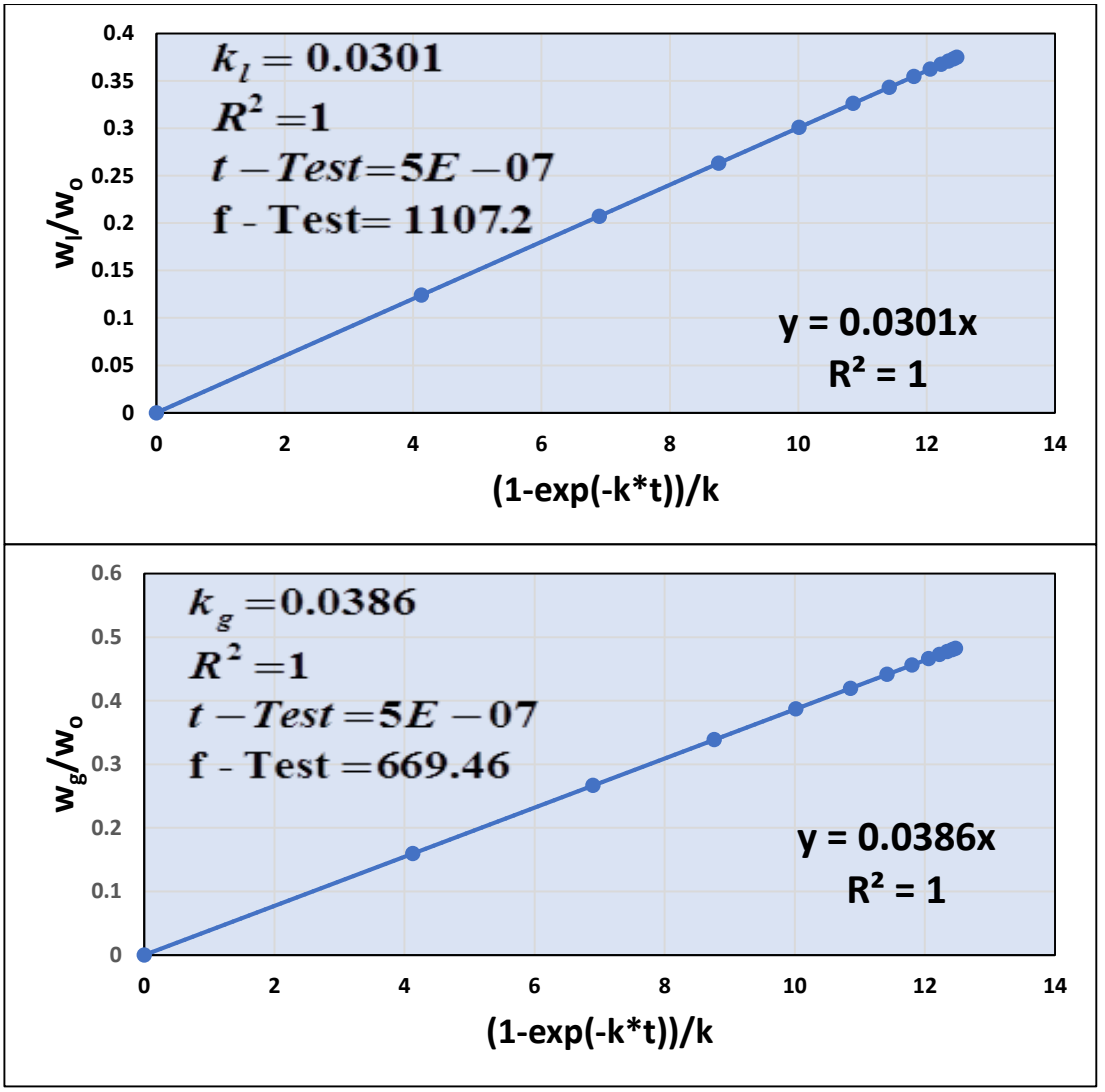

Figure 6.32. Plots of $\ln\left[\frac{w_o}{w}\right]$ vs time and $\frac{w_v}{w_o}$, $\frac{w_c}{w_o}$, $\frac{w_l}{w_o}$ and $\frac{w_g}{w_o}$ vs $(1-\exp[-k*t])/k$ at 973K (a) lime waste with alumina (b) lime waste with ZnO (c) lime waste with KCl (d) lime waste with NaCl and (e) lime waste with Aluminosilicate

a)

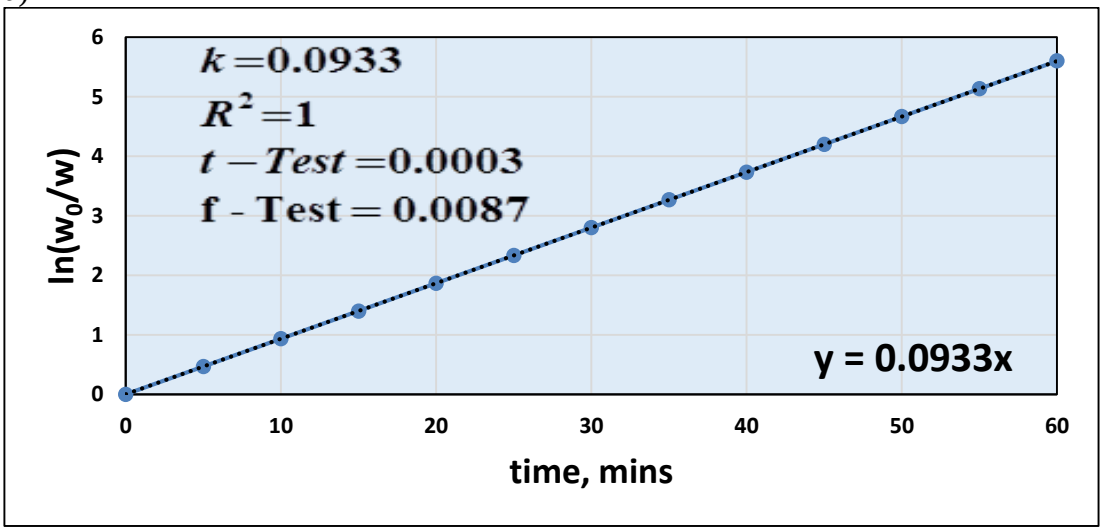

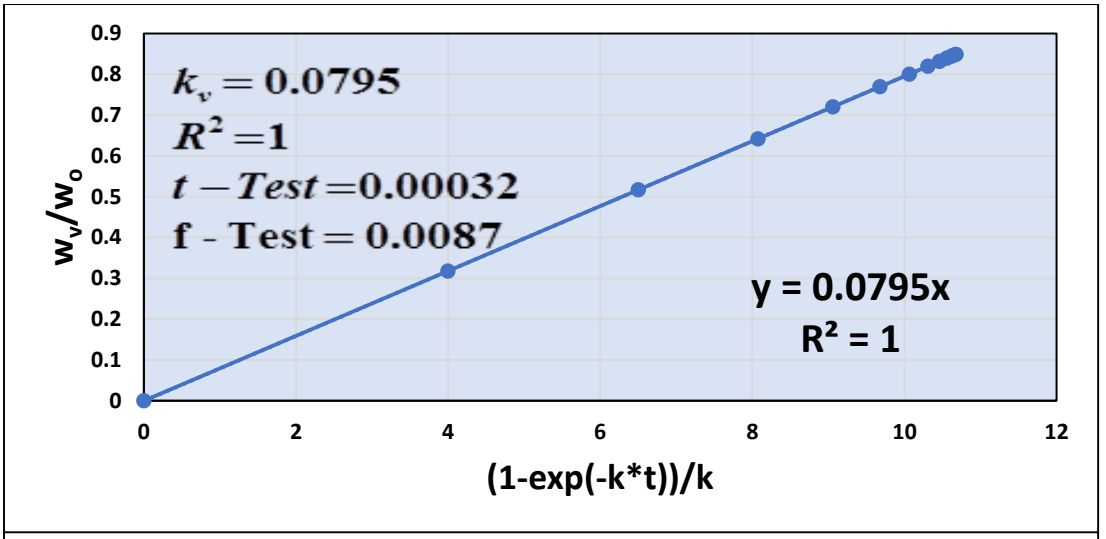
$k_v = 0.0795$
$R^2 = 1$
$t - Test = 0.00032$
f - Test = 0.0087
y = 0.0795x
R² = 1
w_v/w_o
(1-exp(-k*t))/k

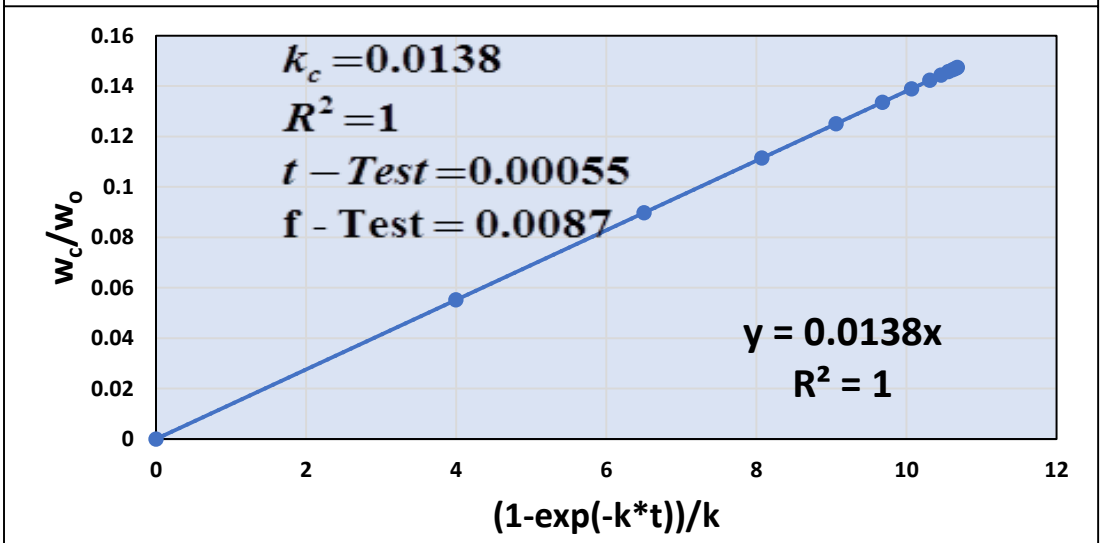
$k_c = 0.0138$
$R^2 = 1$
$t - Test = 0.00055$
f - Test = 0.0087
y = 0.0138x
R² = 1
w_c/w_o
(1-exp(-k*t))/k

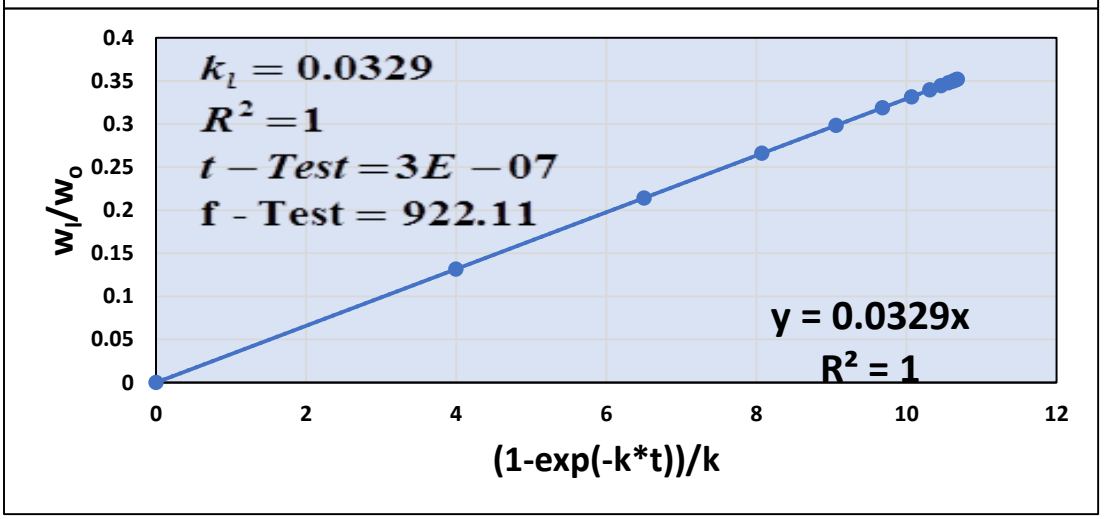
$k_l = 0.0329$
$R^2 = 1$
$t - Test = 3E-07$
f - Test = 922.11
y = 0.0329x
R² = 1
w_l/w_o
(1-exp(-k*t))/k

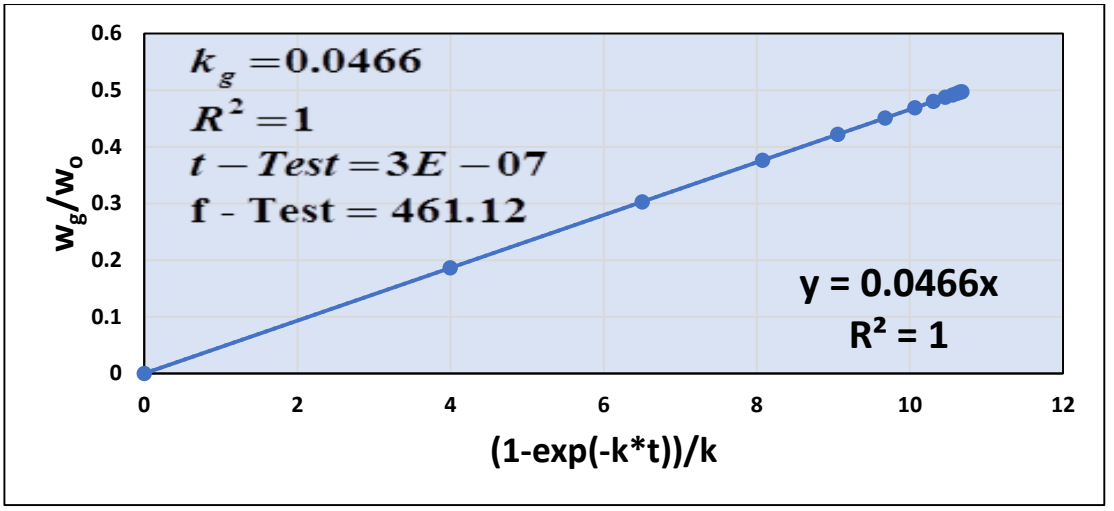
$k_g = 0.0466$
$R^2 = 1$
$t - Test = 3E-07$
f - Test = 461.12
y = 0.0466x
R² = 1
w_g/w_o
(1-exp(-k*t))/k

b)

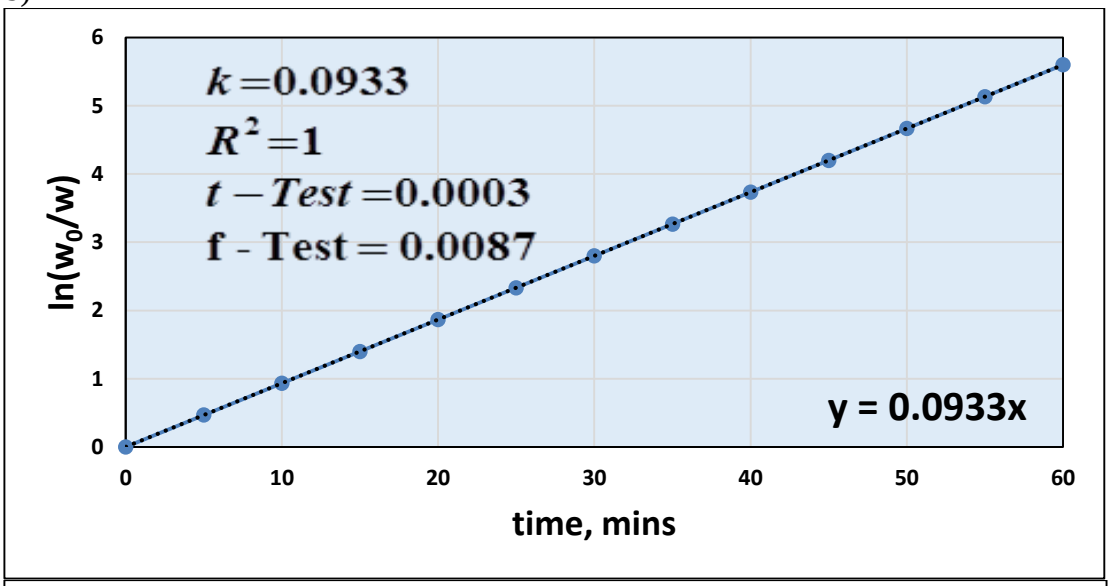
$k = 0.0933$
$R^2 = 1$
$t - Test = 0.0003$
f - Test = 0.0087
y = 0.0933x
ln(w₀/w)
time, mins

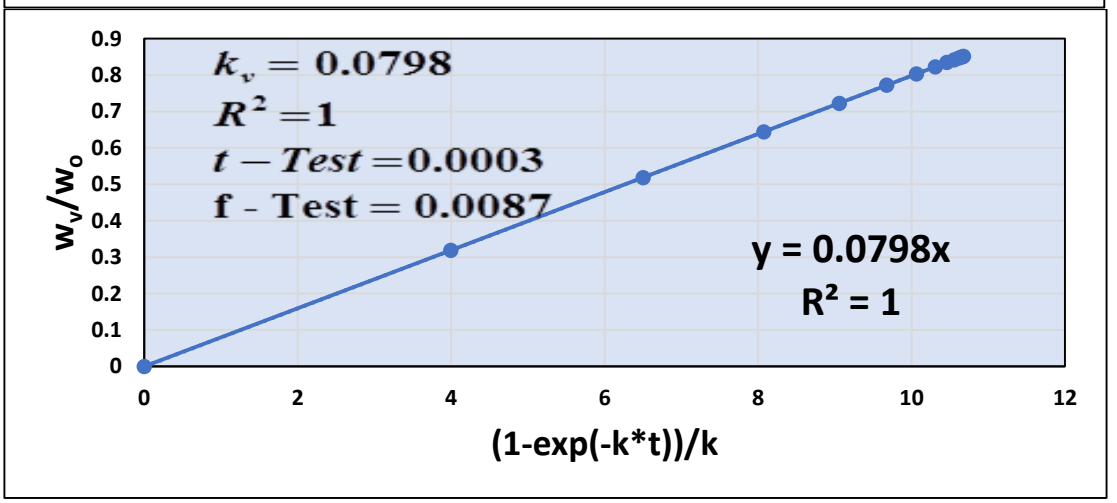
$k_v = 0.0798$
$R^2 = 1$
$t - Test = 0.0003$
f - Test = 0.0087
y = 0.0798x
R² = 1
w_v/w_o
(1-exp(-k*t))/k

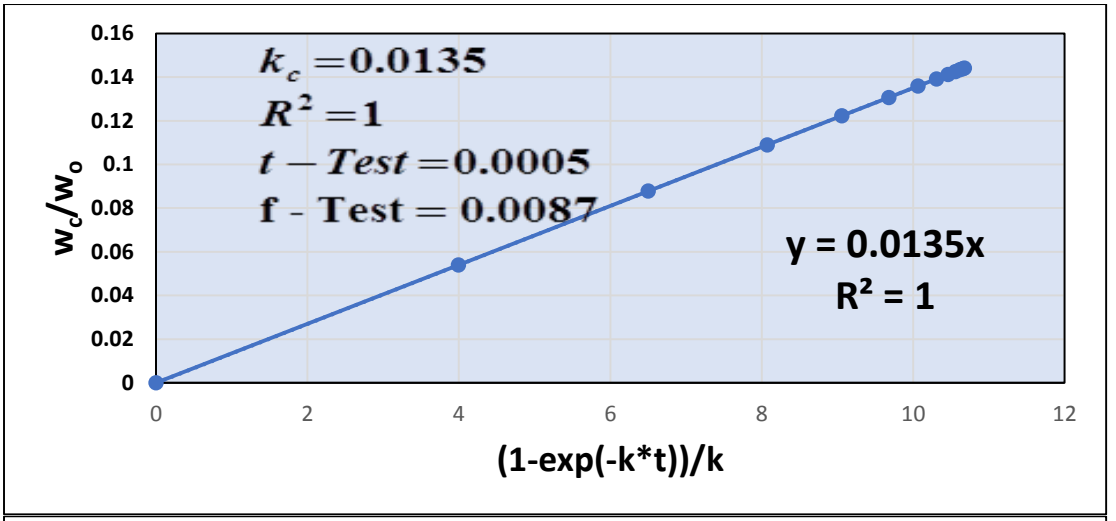
$k_c = 0.0135$
$R^2 = 1$
$t - Test = 0.0005$
f - Test = 0.0087
y = 0.0135x
R² = 1
w_c/w_o
(1-exp(-k*t))/k

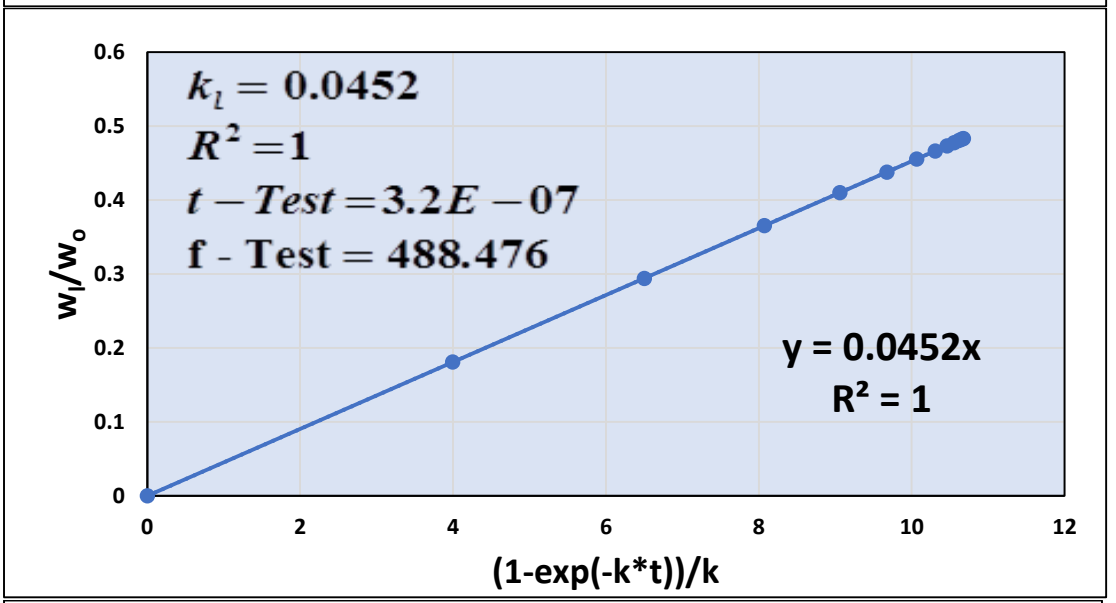
$k_l = 0.0452$
$R^2 = 1$
$t - Test = 3.2E-07$
f - Test = 488.476
y = 0.0452x
R² = 1
w_l/w_o
(1-exp(-k*t))/k

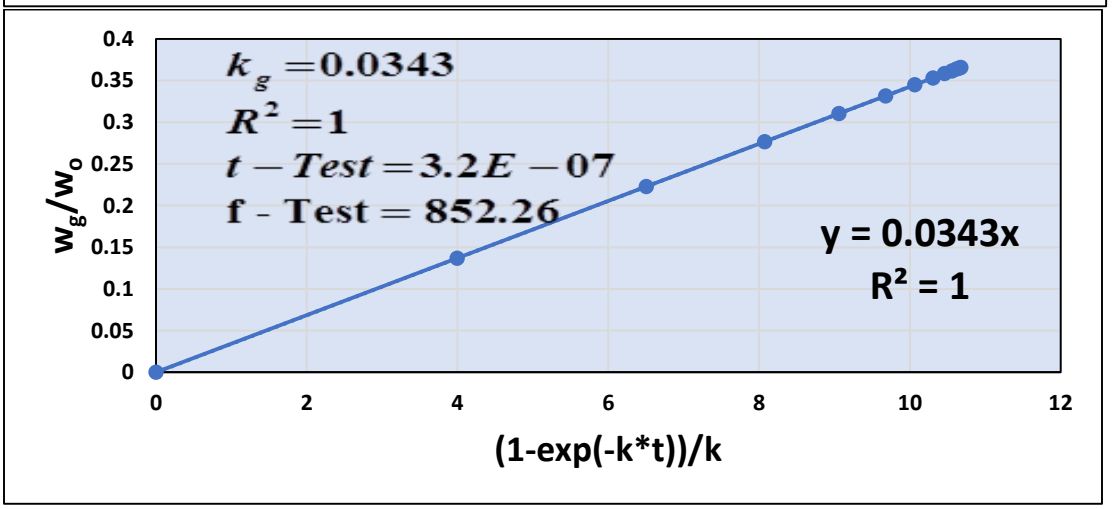
$k_g = 0.0343$
$R^2 = 1$
$t - Test = 3.2E-07$
f - Test = 852.26
y = 0.0343x
R² = 1
w_g/w_o
(1-exp(-k*t))/k

c)

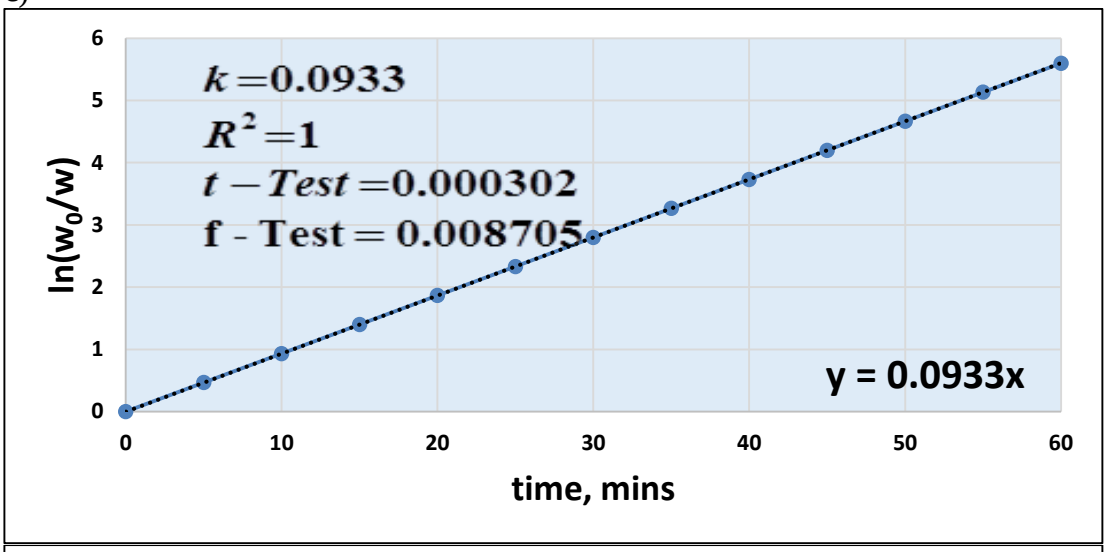
k =0.0933
R² =1
t – Test =0.000302
f - Test = 0.008705
y = 0.0933x
ln(w0/w)
time, mins

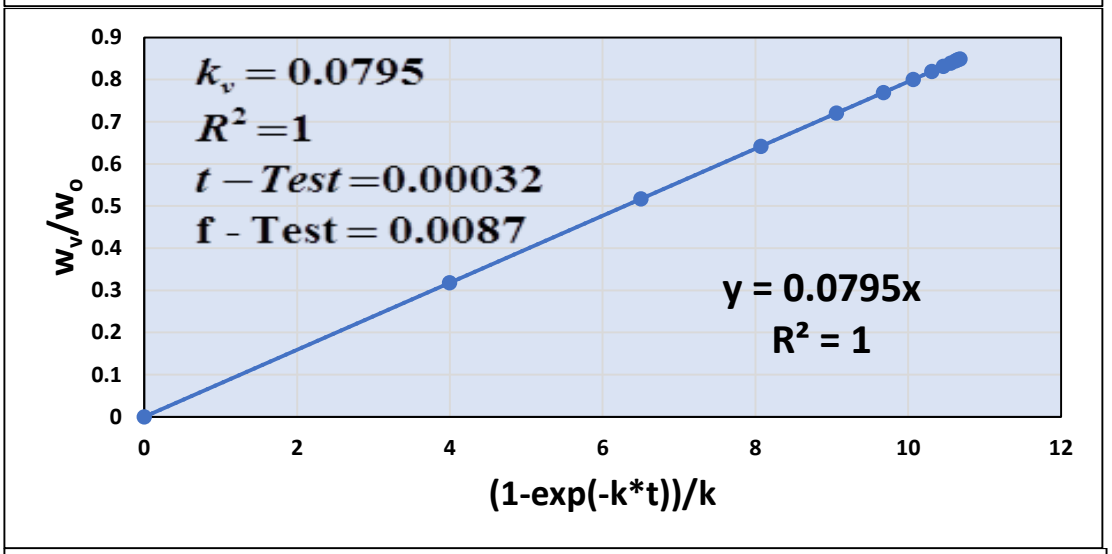
kv = 0.0795
R² =1
t – Test =0.00032
f - Test = 0.0087
y = 0.0795x
R² = 1
wv/wo
(1-exp(-k*t))/k

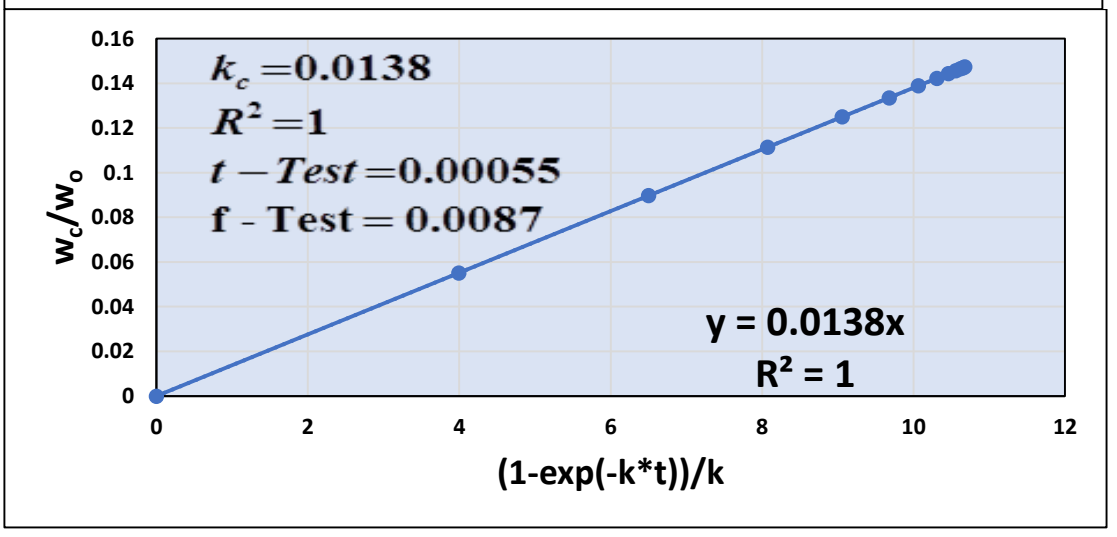
kc =0.0138
R² =1
t – Test =0.00055
f - Test = 0.0087
y = 0.0138x
R² = 1
wc/wo
(1-exp(-k*t))/k

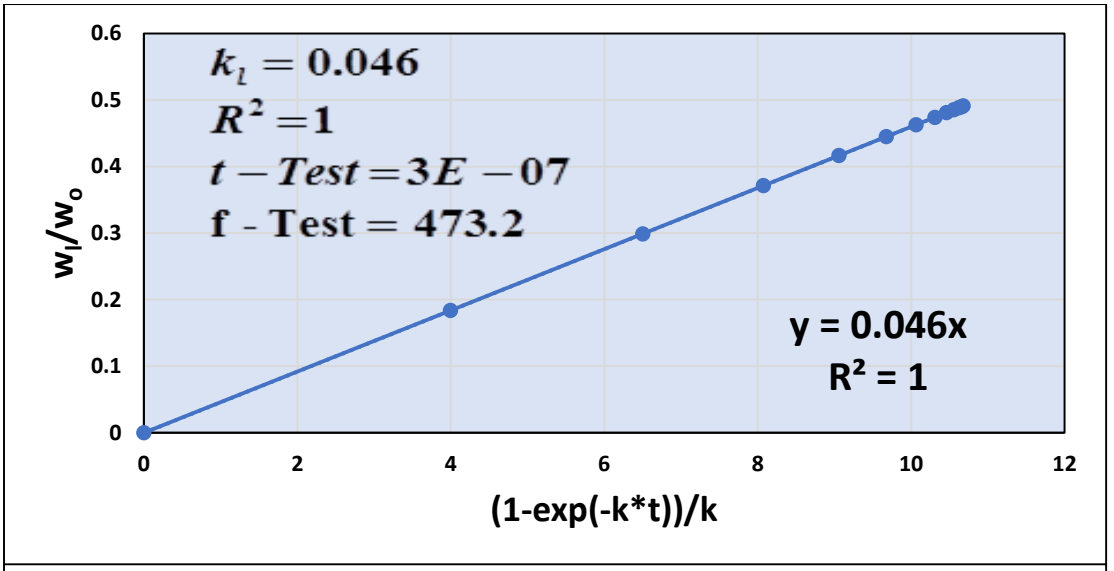
$k_l = 0.046$
$R^2 = 1$
$t - Test = 3E - 07$
f - Test = 473.2
y = 0.046x
R² = 1
w_l/w_o
(1-exp(-k*t))/k

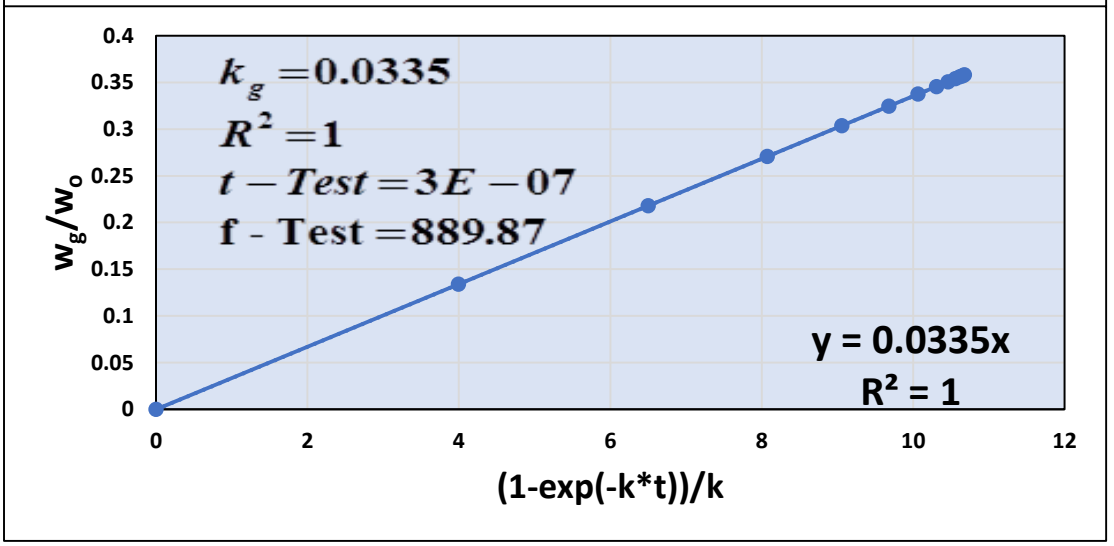
$k_g = 0.0335$
$R^2 = 1$
$t - Test = 3E - 07$
f - Test = 889.87
y = 0.0335x
R² = 1
w_g/w_o
(1-exp(-k*t))/k

d)

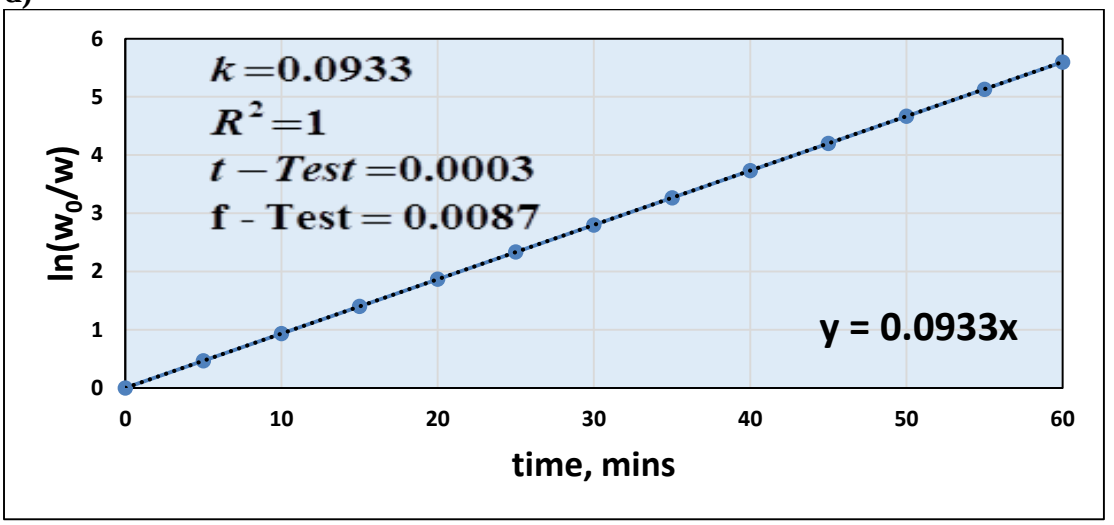
$k = 0.0933$
$R^2 = 1$
$t - Test = 0.0003$
f - Test = 0.0087
y = 0.0933x
$\ln(w_0/w)$
time, mins

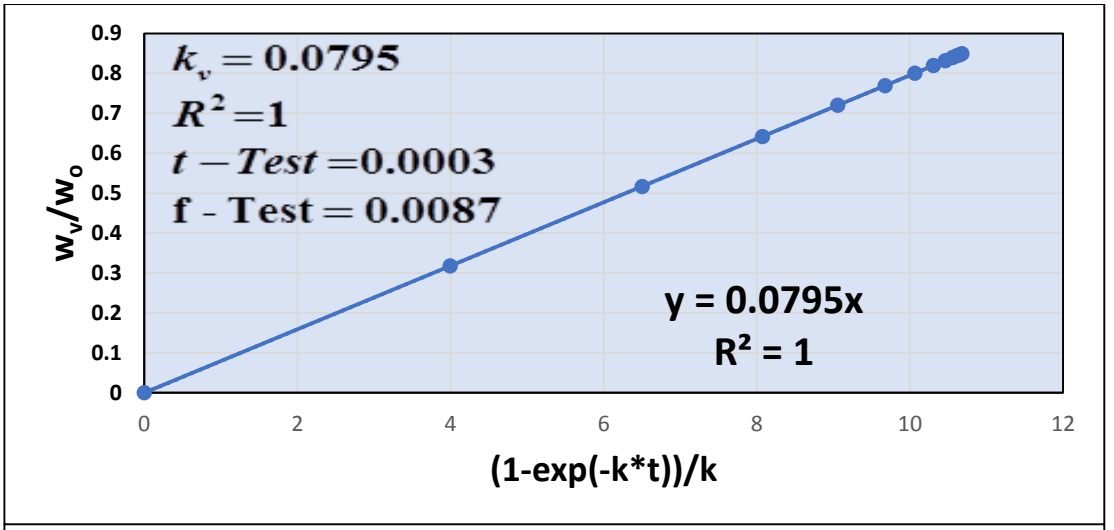
$k_v = 0.0795$
$R^2 = 1$
$t - Test = 0.0003$
f - Test = 0.0087
y = 0.0795x
R² = 1
w_v/w_o
(1-exp(-k*t))/k

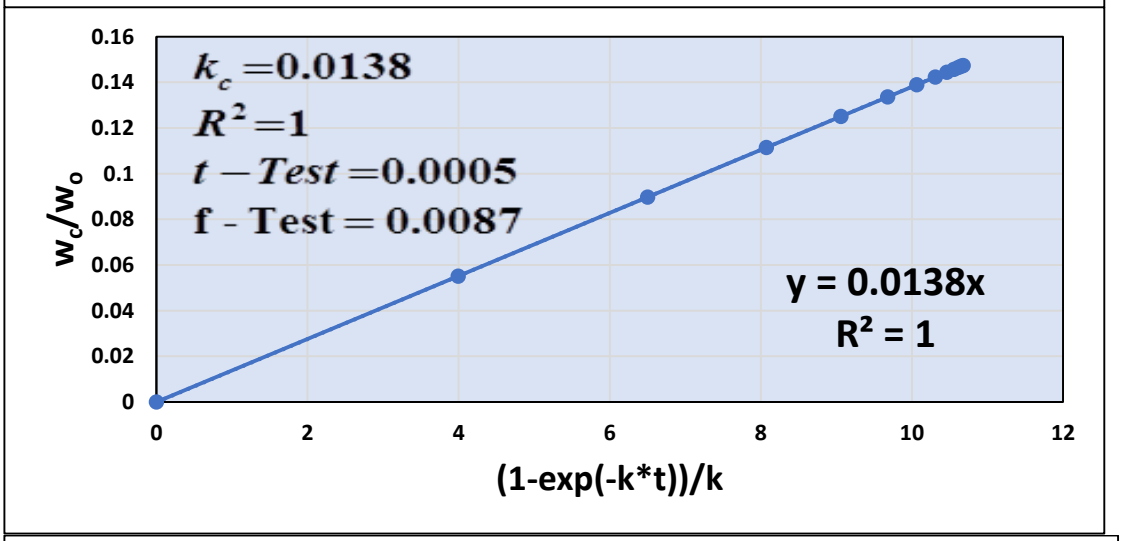
$k_c = 0.0138$
$R^2 = 1$
$t - Test = 0.0005$
f - Test = 0.0087
y = 0.0138x
R² = 1
w_c/w_o
(1-exp(-k*t))/k

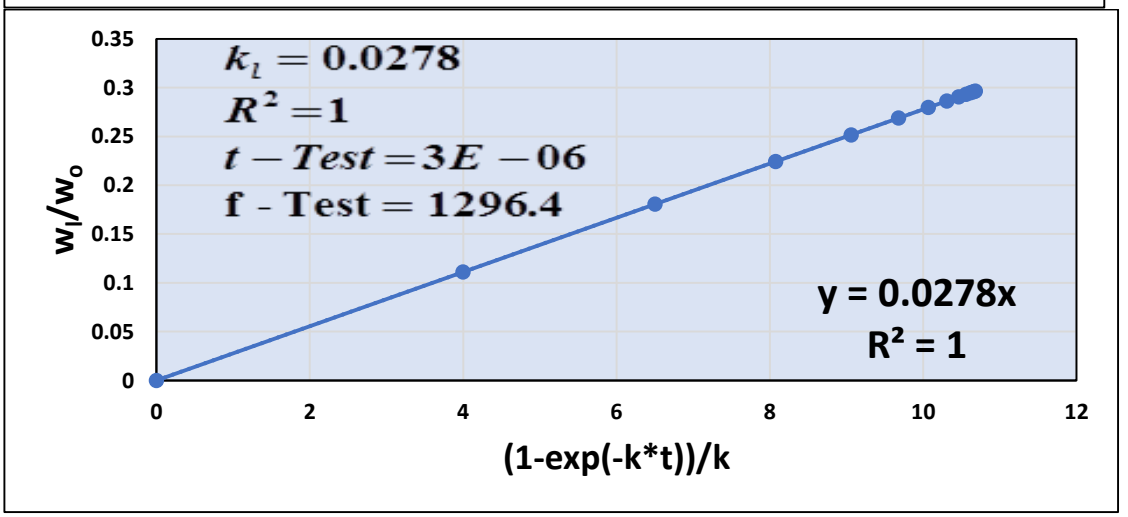
$k_l = 0.0278$
$R^2 = 1$
$t - Test = 3E - 06$
f - Test = 1296.4
y = 0.0278x
R² = 1
w_l/w_o
(1-exp(-k*t))/k

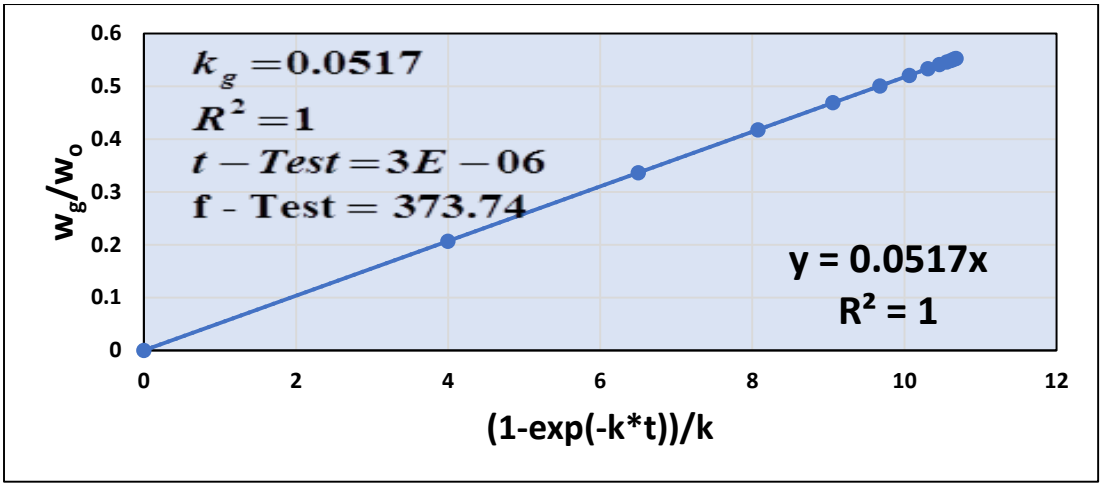
$k_g = 0.0517$
$R^2 = 1$
$t - Test = 3E-06$
f - Test = 373.74
y = 0.0517x
R² = 1
w_g/w_o
(1-exp(-k*t))/k

e)

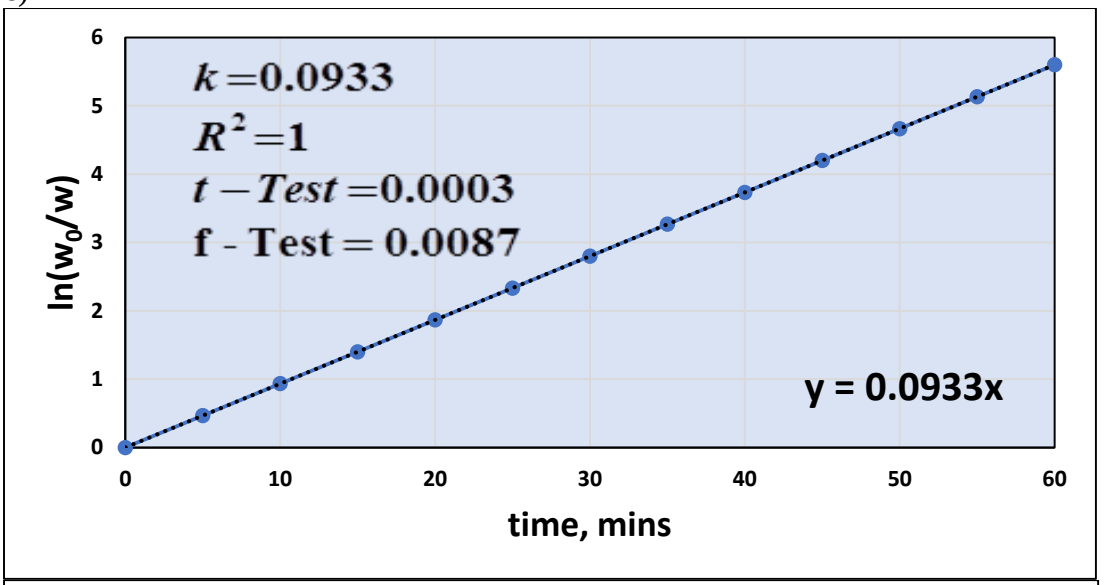
$k = 0.0933$
$R^2 = 1$
$t - Test = 0.0003$
f - Test = 0.0087
y = 0.0933x
$\ln(w_0/w)$
time, mins

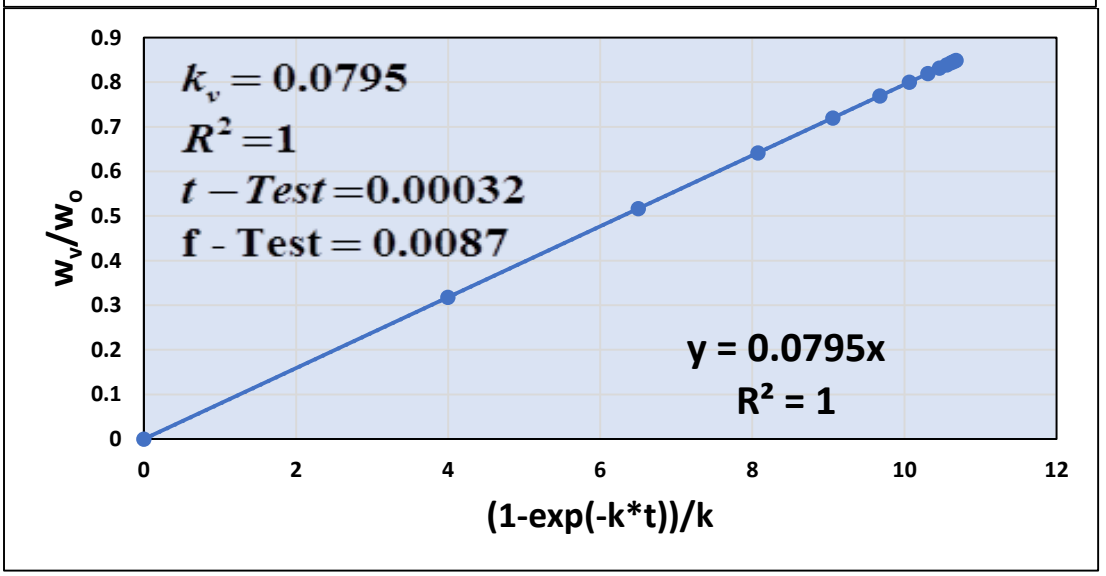
$k_v = 0.0795$
$R^2 = 1$
$t - Test = 0.00032$
f - Test = 0.0087
y = 0.0795x
R² = 1
w_v/w_o
(1-exp(-k*t))/k

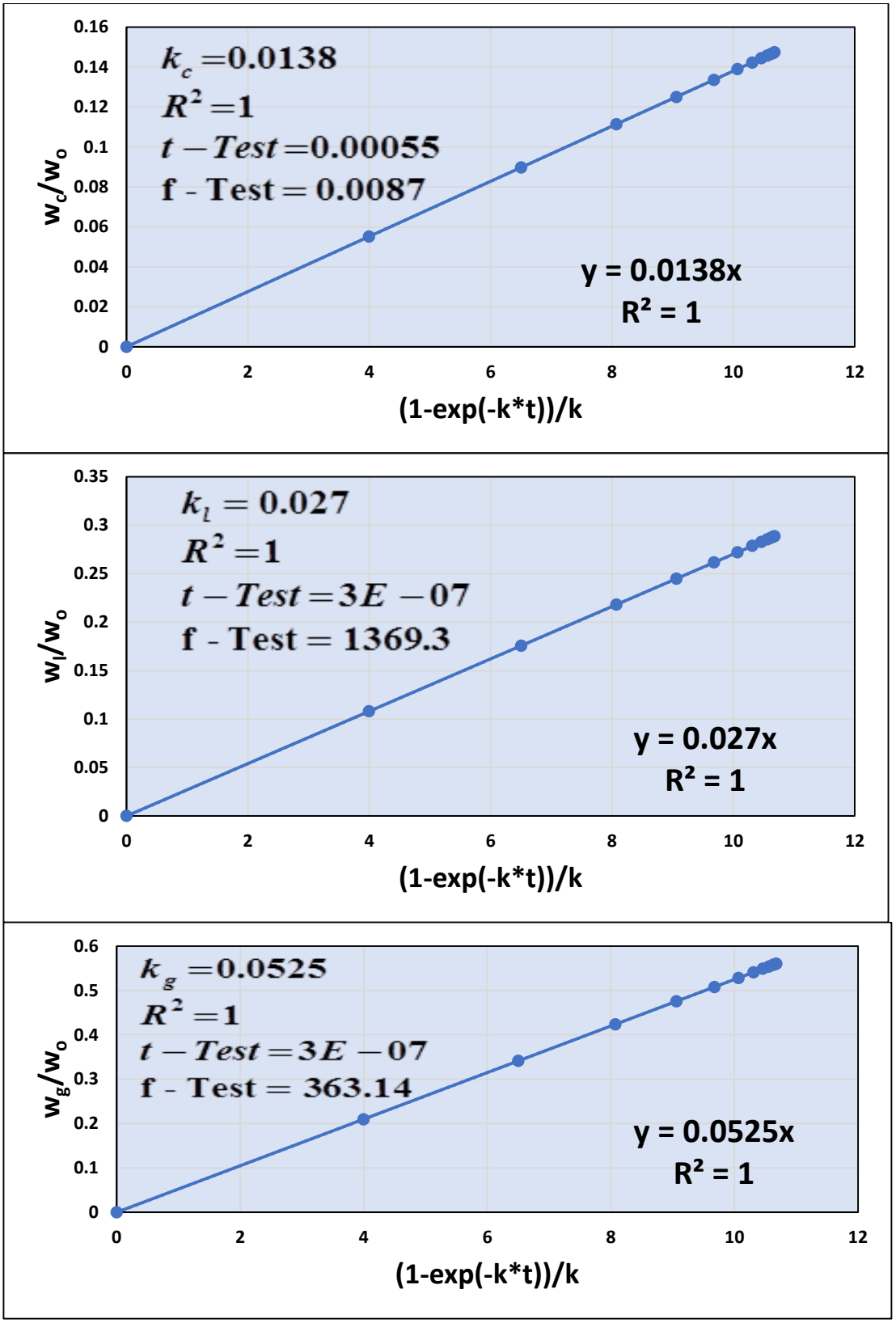

Figure 6.33. Plots of $\ln\left[\frac{w_o}{w}\right]$ vs time and $\frac{w_v}{w_o}$, $\frac{w_c}{w_o}$, $\frac{w_l}{w_o}$ and $\frac{w_g}{w_o}$ vs $(1-\exp[-k*t])/k$ at 1173K (a) lime waste with alumina (b) lime waste with ZnO (c) lime waste with KCl (d) lime waste with NaCl and (e) lime waste with Aluminosilicate

Table 6.14. Values of "k'" of catalytic pyrolysis of lime waste at different temperature

T (K)	Lime wastes with alumina	Lime wastes with ZnO	Lime wastes with KCl	Lime wastes with NaCl	Lime wastes with Aluminosilicate
573K	0.0392	0.0359	0.0465	0.0347	0.0554
673K	0.0499	0.0499	0.0499	0.0499	0.0499
773K	0.0508	0.0529	0.0631	0.0524	0.0536
873K	0.0619	0.0619	0.0619	0.0619	0.0619
973K	0.0795	0.0795	0.0795	0.0795	0.0795
1073K	0.085	0.085	0.085	0.085	0.085
1173K	0.0933	0.0933	0.0933	0.0933	0.0933

Table 6.15. Values of "k_v'" of catalytic pyrolysis of lime waste at different temperature

T (K)	Lime wastes with alumina	Lime wastes with ZnO	Lime wastes with KCl	Lime wastes with NaCl	Lime wastes with Aluminosilicate
573K	0.0331	0.0242	0.0288	0.0197	0.0386
673K	0.0414	0.0414	0.0414	0.0414	0.0414
773K	0.0436	0.0436	0.0436	0.0436	0.0436
873K	0.0527	0.0527	0.0527	0.0527	0.0527
973K	0.0687	0.0687	0.0687	0.0687	0.0687
1073K	0.0734	0.0734	0.0734	0.0734	0.0734
1173K	0.0795	0.0795	0.0795	0.0795	0.0795

Table 6.16. Values of "k_c'" of catalytic pyrolysis of lime waste at different temperature

T (K)	Lime wastes with alumina	Lime wastes with ZnO	Lime wastes with KCl	Lime wastes with NaCl	Lime wastes with Aluminosilicate
573K	0.006	0.0117	0.0177	0.0151	0.0168
673K	0.0145	0.0087	0.0187	0.0087	0.0182
773K	0.0087	0.0087	0.0087	0.0087	0.0087
873K	0.0092	0.0092	0.0092	0.0092	0.0092
973K	0.0108	0.0108	0.0108	0.0108	0.0108
1073K	0.0115	0.0115	0.0115	0.0115	0.0115
1173K	0.0138	0.0138	0.0138	0.0138	0.0138

Table 6.17. Values of "k_l'" of catalytic pyrolysis of lime waste at different temperature

T (K)	Lime wastes with alumina	Lime wastes with ZnO	Lime wastes with KCl	Lime wastes with NaCl	Lime wastes with Aluminosilicate
573K	0.013	0.0131	0.0185	0.0111	0.0175
673K	0.0167	0.0222	0.0256	0.0223	0.0171
773K	0.019	0.0236	0.0302	0.0224	0.0235
873K	0.0251	0.0347	0.0295	0.0214	0.0231
973K	0.031	0.054	0.0492	0.0354	0.031

1073K	0.032	0.0521	0.0453	0.0291	0.0268
1173K	0.0329	0.0452	0.046	0.0278	0.027

Table 6.18. Values of "k_g'" of catalytic pyrolysis of lime waste at different temperature

T (K)	Lime wastes with alumina	Lime wastes with ZnO	Lime wastes with KCl	Lime wastes with NaCl	Lime wastes with Aluminosilicate
573K	0.0201	0.0111	0.0103	0.0086	0.0211
673K	0.0247	0.0192	0.0158	0.0191	0.0243
773K	0.0249	0.0208	0.0158	0.0219	0.0211
873K	0.0332	0.02	0.023	0.0266	0.0296
973K	0.0377	0.147	0.0195	0.0328	0.0386
1073K	0.0414	0.0213	0.0281	0.0443	0.0466
1173K	0.0464	0.0343	0.0335	0.0517	0.0525

6.4.1.3.2. Temperature dependence of rate constant

Using the values of rate constants k', k_v', k_c', k_l' and k_g' [9-12, 15] Arrhenius plots (shown in the Appendix A.18.b) have been made following the same method as used in case of non-catalytic pyrolysis of lime waste. The Arrhenius type dependence of rate constants on temperature has been established from the linearity of the plots. The values of activation energies and pre-exponential factors for catalytic pyrolysis using all catalysts under study have been determined from the Arrhenius plots and through non-linear regression analysis and are tabulated in table 6.19.

Table 6.19. Calculated Activation Energies and Frequency Factors as per Arrhenius Law for catalytic pyrolysis of lime wastes

Sl. No.	Feed Stocks	Reaction rate constant	Activation Energy (kJ/mol)	Frequency factor (min^{-1})	Correlation Coefficient
1	Lime + alumina	k'	4.9343 (E')	0.1220 (A')	0.923
		k_v'	3.9715 (E_V')	0.0976 (A_V')	0.937
		k_c'	20.693 (E_C')	0.0542 (A_C')	0.968
		k_l'			
		k_g'	7.84833 (E_l')	0.098392 (A_l')	0.9471
			9.36655 (E_g')	0.089977(A_g')	0.9728
2	Lime+ ZnO	k'	4.5868 (E')	0.1357 (A')	0.967
		k_v'	5.8929 (E_V')	0.1225 (A_V')	0.985
		k_c'	1.2895 (E_C')	0.0209 (A_C')	0.989
		k_l'			

		k_g'	13.09206(E_l')	0.211845 (A_l')	0.9147
			12.23405(E_g')	0.158453(A_g')	0.945
3	Lime+ KCl	k'	6.5065 (E')	0.1718 (A')	0.941
		k_v'	8.7047 (E_V')	0.1699 (A_V')	0.932
		k_c'	1.9072 (E_C')	0.0241 (A_C')	0.947
		k_l'			
		k_g'	8.96082(E_l')	0.12207(A_l')	0.8999
			9.821328(E_g')	0.081749(A_g')	0.8995
4	Lime+ NaCl	k'	9.2035 (E')	0.2371 (A')	0.941
		k_v'	12.4292 (E_V')	0.3030 (A_V')	0.932
		k_c'	6.7576 (E_C')	0.0224 (A_C')	0.947
		k_l'			
		k_g'	15.33767(E_l')	0.08803(A_l')	0.9653
			8.256301(E_g')	0.076597(A_g')	0.899
5	Lime+ $NaAl(SiO_3)_2$	k'	8.9541 (E')	0.2290 (A')	0.981
		k_v'	10.7333 (E_V')	0.2446 (A_V')	0.983
		k_c'	2.5149 (E_C')	0.0148 (A_C')	0.988
		k_l'			
		k_g'	8.749654(E_l')	0.112478(A_l')	0.894
			5.174135(E_g')	0.049371(A_g')	0.8909

6.4.1.3.3. Comparison of Activation energies and pre-exponential factor of catalytic and non-catalytic pyrolysis of lime wastes.

The lumped kinetic parameters determined using the data of isothermal experiments have been shown in Table 6.18. From the analysis of the table, it is evident that the lowering of activation energy occurs with the use of all catalysts and it is maximum for ZnO with respect to the overall pyrolysis reaction. Thus, ZnO is selected as the best performing catalyst for the pyrolysis of lime waste.

6.4.2. Distributed Activation Energy Model (DAEM)

6.4.2.1. TGA plots

Figures. 6.34 and 6.35. show respectively the time trajectories of % (w/w) of solid residue for catalytic pyrolysis of jute and lime wastes remaining during TGA under nonisothermal conditions using heating rate (10 K min^{-1}, 15 K min^{-1}, 20 K min^{-1}, 25 K min^{-1}, 30 K min^{-1}) as a parameter. The experimental data obtained using alumina and zinc oxide respectively for jute and lime wastes have been used.

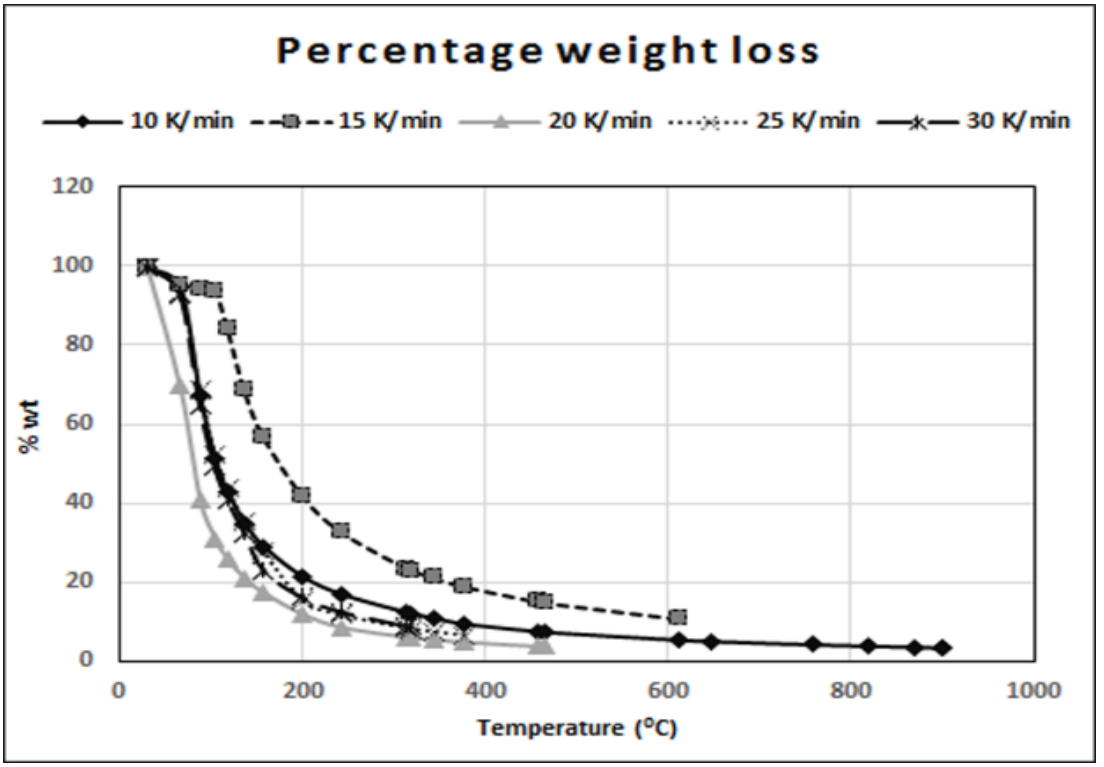

Figure 6.34. Percentage of weight residue of jute waste using catalysts in the temperature range of 30–900 ^{0}C at different heating rates (TGA plot).

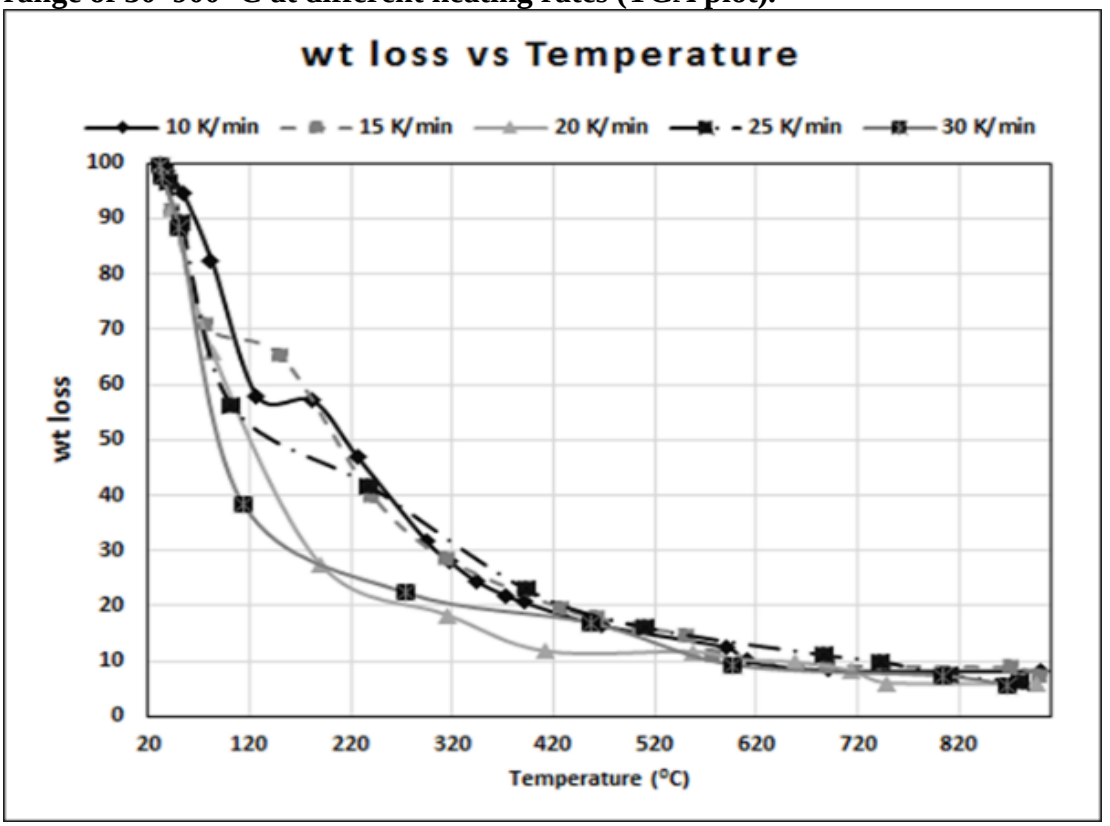

Figure 6.35. Percentage of weight residue of lime waste using catalysts in the temperature range of 30–900 ^{0}C at different heating rates (TGA plot).

From the analysis of the plots it is clearly evident that distinct patterns of weight loss are followed in different temperature ranges for both the feedstocks. While four distinct temperature zones following unique patterns of decomposition are obtained for non-catalytic

pyrolysis of jute (30–100 ^{o}C, 100–275 ^{o}C, 275–350 ^{o}C and 350–700 ^{o}C) and lime wastes (25–100 ^{o}C, 100–275 ^{o}C, 275–775 ^{o}C and 775-900 ^{o}C), two prominent temperature zones for jute waste (30–150 ^{o}C ,150–700 ^{o}C), and lime waste (25–600 ^{o}C, and 600-900^{o}C) are obtained for catalytic pyrolysis. The residual solid obtained at each temperature is much less in case of catalytic pyrolysis as compared to the non-catalytic one for both the feedstocks. Both the observations signify the pronounced catalytic effect of alumina and ZnO on the primary and secondary reactions generating condensable and non-condensable volatiles during pyrolysis of jute and lime waste respectively.

6.4.2.1.1. Isoconversion Plots

In Figures 6.36. and 6.37. logarithm of [$\alpha i(dx/dT)_{x,i}$] has been plotted against (-1000/RT$_i$) for catalytic pyrolysis of waste jute and lime waste respectively

.

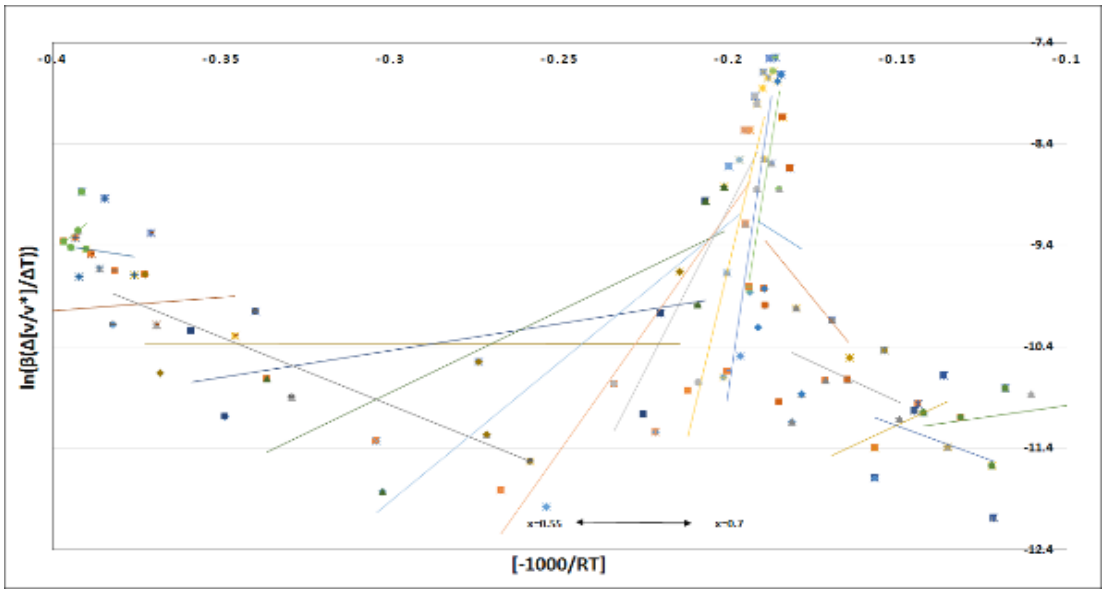

Figure 6.36. Plot of ln[$\alpha i(dx/dT)_{x,i}$] *vs.* (-1000/RT$_i$) at different conversion values from 0.05 to 0.95 for all the heating rates (5-30 K min^{-1}) of jute wastes using catalysts.

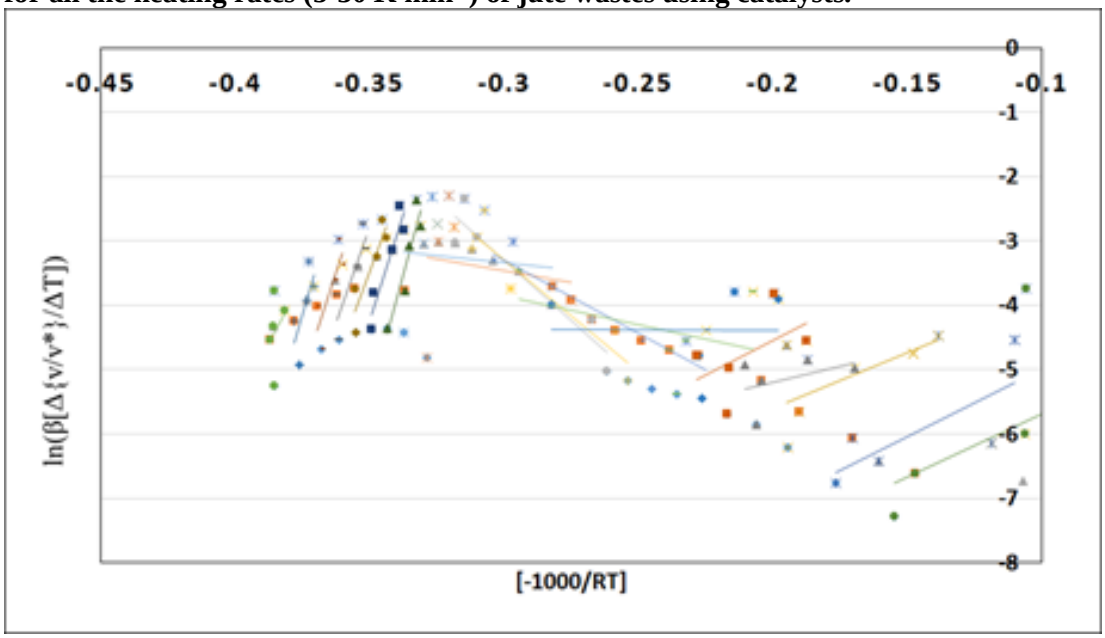

Figure 6.37. Plot of ln[$\alpha i(dx/dT)_{x,i}$] vs. (-1000/RT$_i$) at different conversion values from 0.05 to 0.95 for all the heating rates (5-30 K min^{-1}) of lime wastes using catalysts.

A set of straight lines have been obtained at different values of conversion for both the feedstocks validating the Friedman model [30] with the assumptions of 1st order kinetics and Arrhenius type temperature dependence of rate constants for the pyrolytic reactions. From the detailed analysis of the figures it is revealed that parallel lines are obtained in the conversion ranges of 0.55 to 0. 70 and 0.10 to 0.35 for catalytic pyrolysis of waste jute and lime waste respectively signifying a close distribution of activation energies. The zones are distinctly different from those obtained for non-catalytic (0.15-0.8 for jute and 0.05-0.70 for lime waste) pyrolysis. This may be justified by different catalytic effects of alumina and zinc oxide respectively on different array of pyrolytic reactions for jute and lime wastes. The exact mechanism of catalytic effects should further be investigated to reveal the real facts. As discussed in case of non-catalytic pyrolysis, the non-parallel relationship at lower (<0.55 for jute and <0.1 for lime waste) and higher (>0.7 for jute and >0.35 for lime waste) ranges of conversion clearly indicates the probability of occurrence of pyrolysis reactions, distinctly different from those occurring at the intermediate (0.55–0.7 for jute and 0.1 – 0.35 for lime) conversion levels.

6.4.2.1.2. Dependence of activation energies and frequency factor on conversion

In Figures 6.38 and 6.39. activation energies and ln[A**f(x)*], as obtained from the iso-conversion plots, have been graphed against conversion for catalytic pyrolysis of jute and lime wastes respectively. The patterns of the plots for catalytic waste jute are similar to those of reported by Wu et al. [16] during the pyrolysis of biomass feedstocks. However, as observed in case of noncatalytic pyrolysis of lime waste, the resemblance with pyrolysis of biomass is nominal even in presence of catalyst, namely zinc oxide. The dissimilarity may again be justified by low lignin content and citrus nature of lime waste compared to most of the biomass usually studied [17-29].

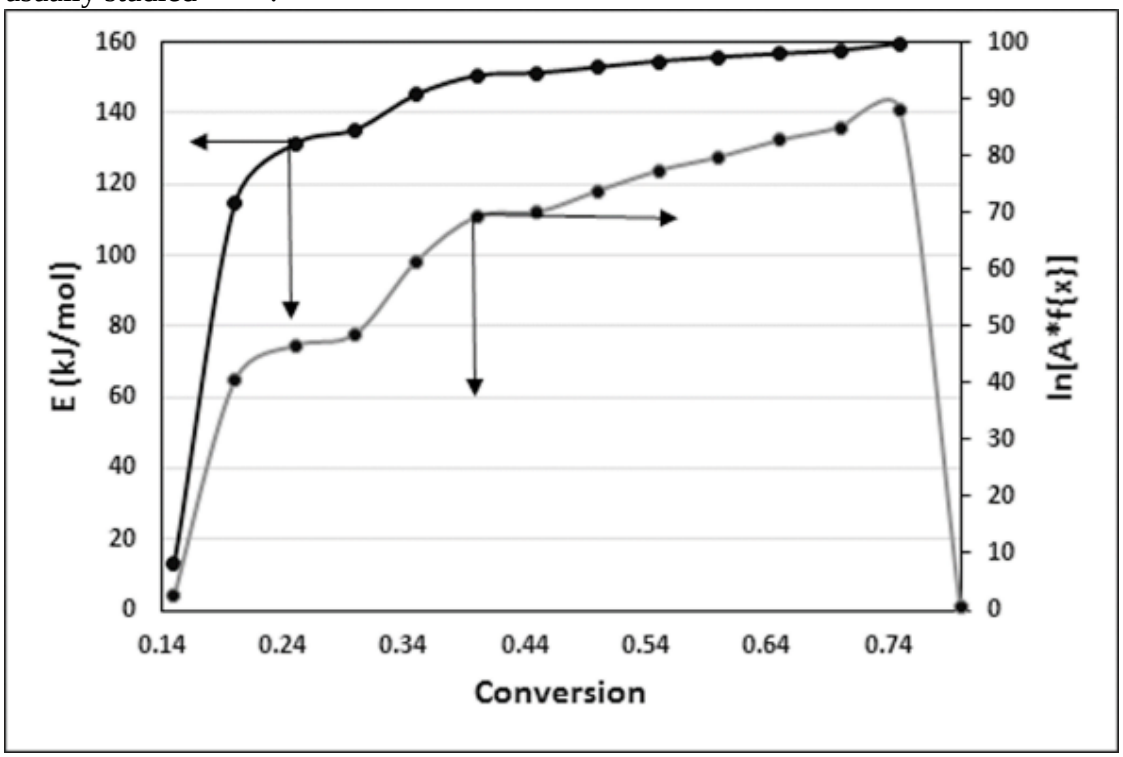

Figure 6.38. Plot of E and ln[Af(x)*] vs. conversion for catalytic pyrolysis of jute waste using catalyst Al_2O_3.**

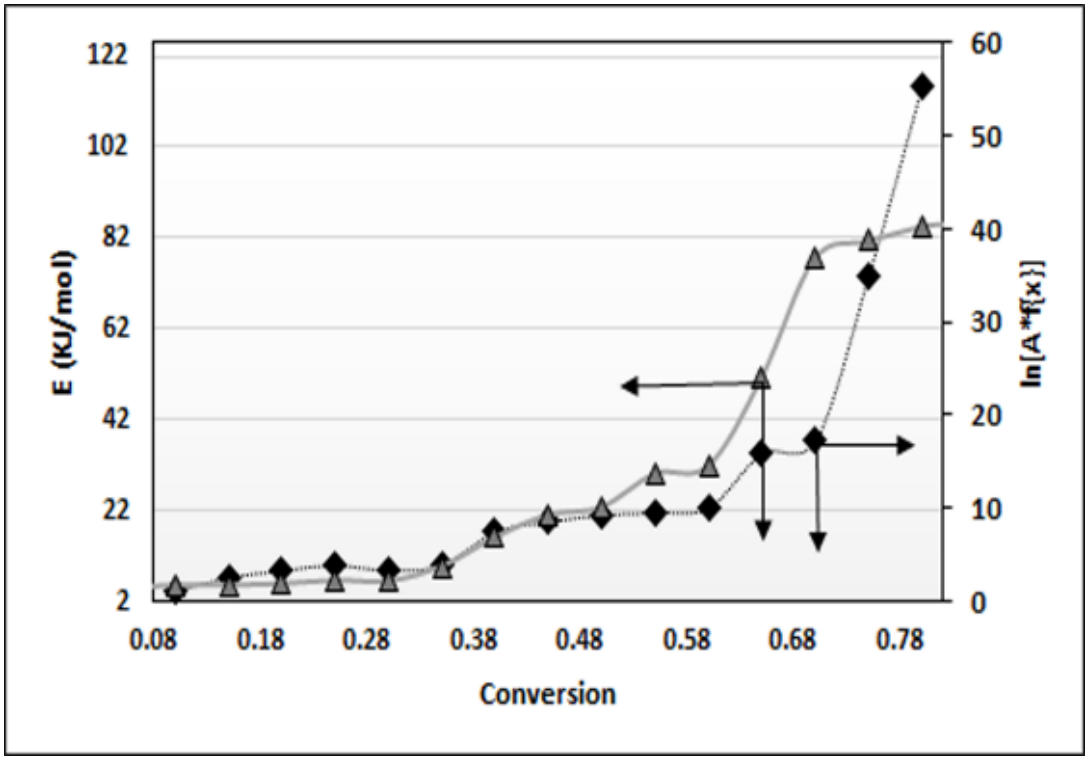

Figure 6.39. Plot of E and ln[Af(x)*] vs. conversion for catalytic pyrolysis of lime waste using ZnO as catalyst.**

6.4.2.1.3. Distribution of activation energy

In Figures 6.40-6.41, *f(E)* has been plotted against E respectively for catalytic pyrolysis of jute wastes and lime wastes.

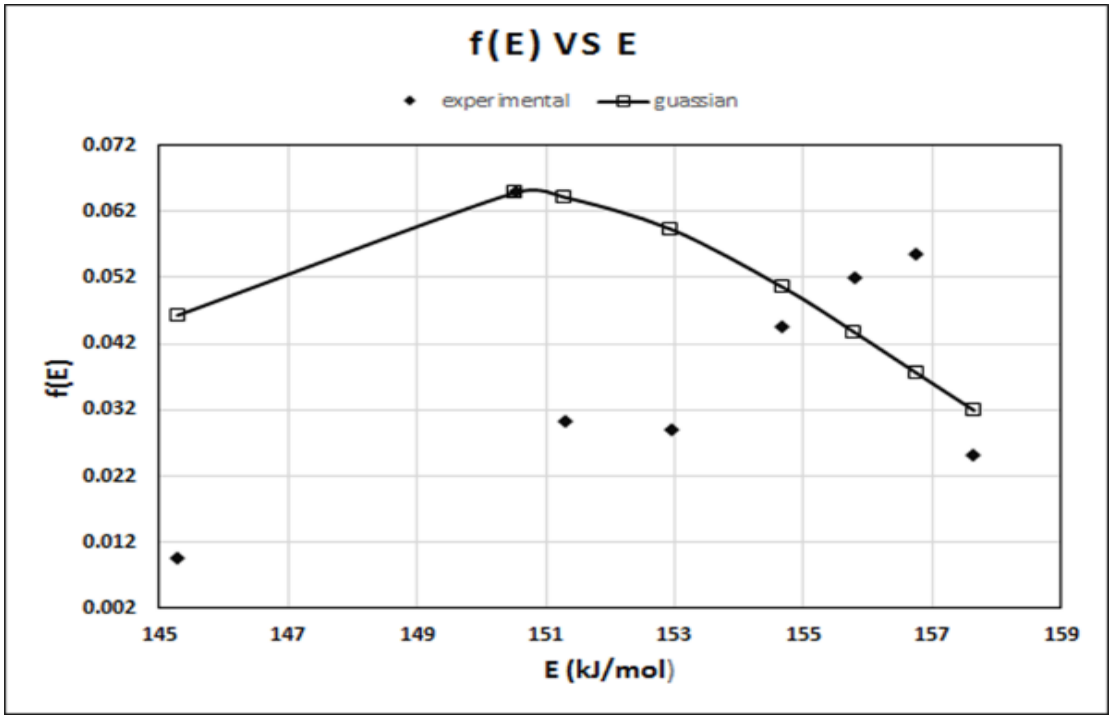

Figure 6.40. Plot of *f(E) vs.* E obtained from Friedman differential isoconversion method and Gaussian distribution for catalytic pyrolysis of jute waste.

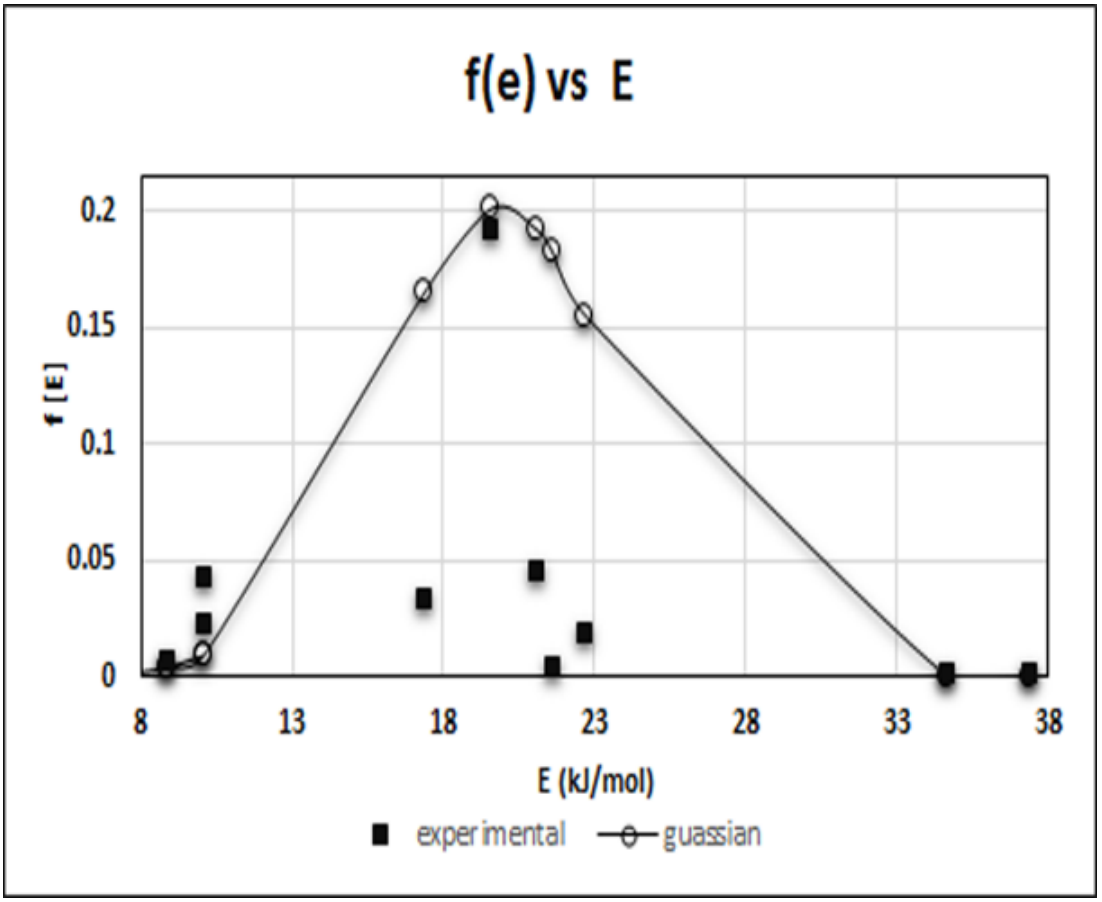

Figure 6.41. Plot of *f(E) vs.* E obtained from Friedman differential isoconversion method and Gaussian distribution for catalytic pyrolysis of lime waste.

The analysis of the figure 6.40. reveals that *f(E) versus E* follows almost a Gaussian distribution [31] in the conversion range of 0.55 -0.7 for catalytic pyrolysis of jute waste where the relationship between E and conversion is linear. Similar observation has been reported for pyrolysis of other biomasses. [17-29] Figure 6.41 reveals that no such Gaussian relationship is obtained between f(E) and E for catalytic pyrolysis of lime waste. The low lignin content and citrus nature of lime waste may be responsible for this non-Gaussian distribution of f(E) on E. The mean values of average activation energy are 150.33 kJ mol^{-1} and 51.91 kJ mol^{-1} for catalytic pyrolysis of jute and lime wastes respectively. For both the feedstocks, the values are much lower in comparison to those (276.56 kJ mol^{-1} for waste jute and 83.71 kJ mol^{-1} for lime waste) for non-catalytic pyrolysis. Lower range of E for catalytic pyrolysis reveals the positive influence of alumina and zinc oxide on pyrolysis of jute and lime wastes respectively. The values of the pre-exponential factors for both catalytic and non-catalytic pyrolysis of jute waste are in the same order, the values of catalytic one being slightly greater. No such comparison can be drawn for pyrolysis of lime waste in presence of ZnO since the values of pre-exponential factors for catalytic is lower than that of the non-catalytic one. When compared to the activation energies of lumped kinetics no parity is observed with those obtained through DAE modelling for both the feedstocks. Since the pyrolysis is actually a complex combination of reactions causing decomposition of different constituent molecules of a biomass, it is understandable that DAEM kinetics should represent the reality more closely.

6.5. co-pyrolysis of jute waste and sesame oil cake

6.5.1. lumped kinetics

6.5.1.1. Experimental time histories

Figures 6.42 a, b and c represent the time histories of weight fractions of residue, volatile and char respectively for non-catalytic and catalytic co-pyrolysis [39] of jute waste and sesame oil cake in the pyrolysis temperature range of 573K to 1173K. The corresponding data are provided in the Table A.19 in the appendix. From the analysis of the figures it is revealed that catalytic and non-catalytic co-pyrolysis of feedstocks begins at 673K, which is very similar to that of jute waste [4,5,6] and sesame oil cake [15,38].

a)

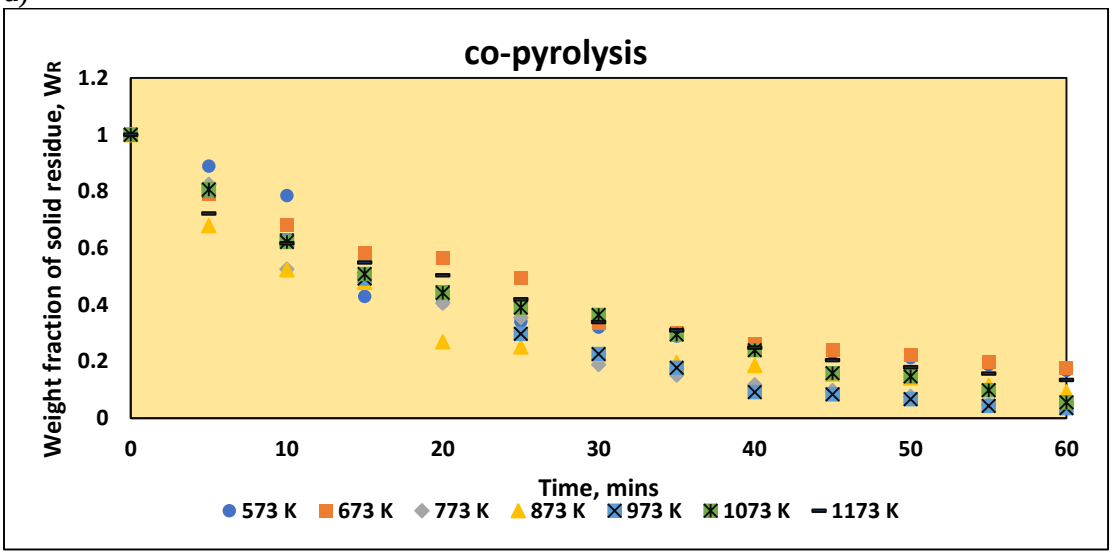

b)

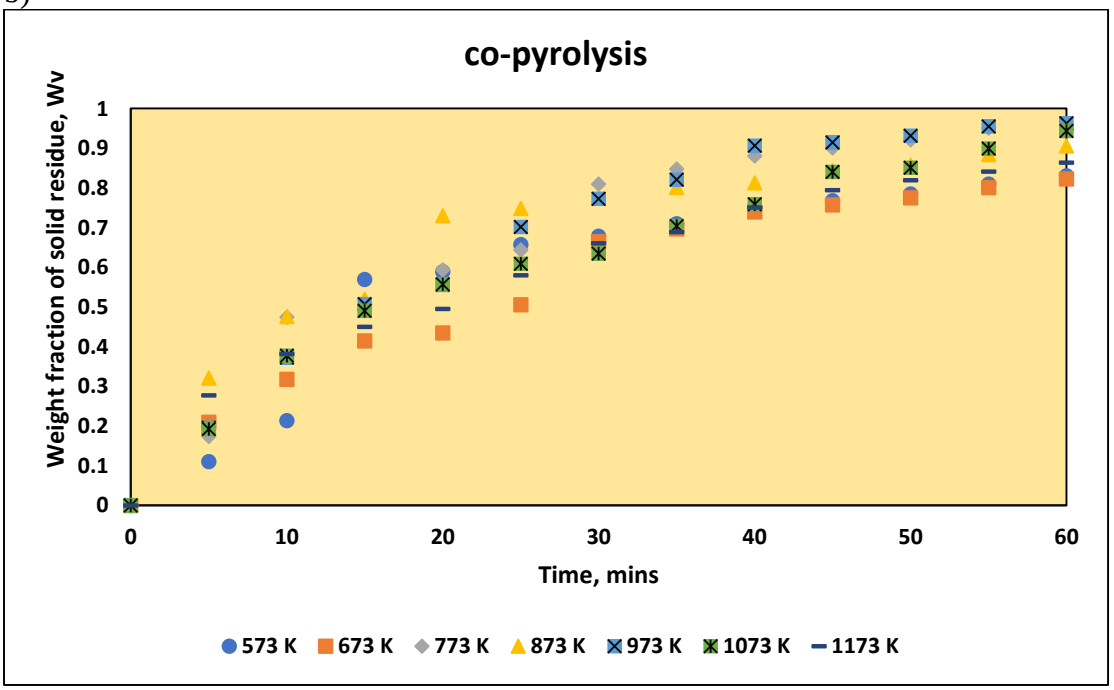

c)

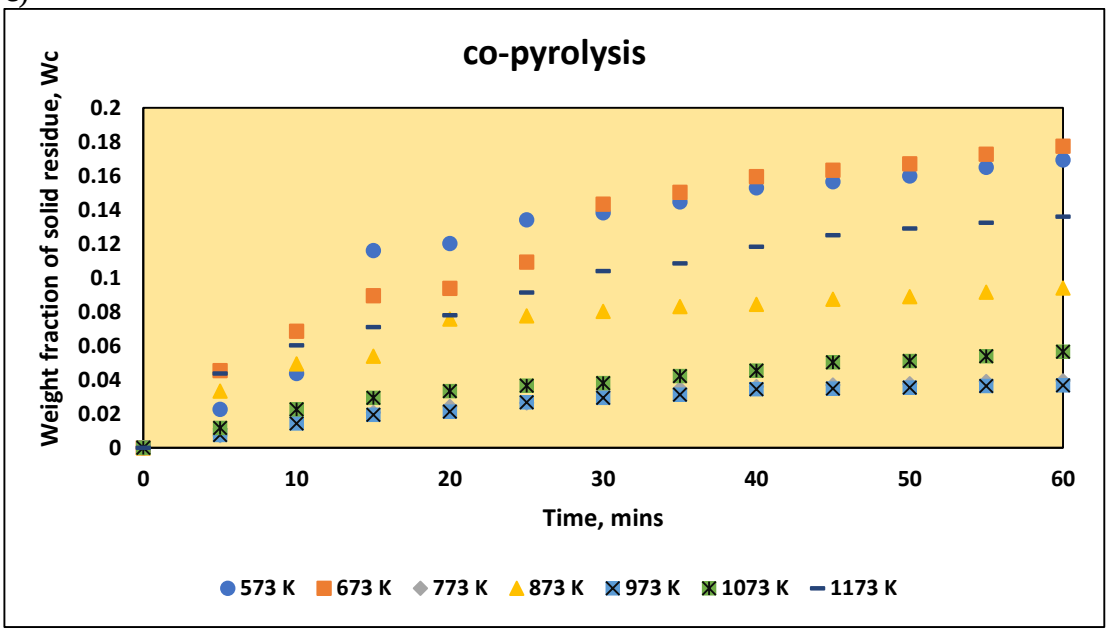

Figures 6.42. (a) Time histories of weight fraction of residue of co-pyrolysis of jute wastes and sesame oil cake (b) Time Histories of volatile weight fraction using pyrolysis temperature as parameter for co-pyrolysis of jute wastes and sesame oil cake (c) **Time Histories of char weight fraction using pyrolysis temperature as parameter: (a) co-pyrolysis of jute wastes and sesame oil cake**

6.5.1.2. Parameters of lumped kinetic Model

Experimental values of $\ln\left(\frac{w_o}{w}\right)$ have been plotted against time and those of $\frac{w_v}{w_o}$, $\frac{w_c}{w_o}$, $\frac{w_l}{w_o}$ **and** $\frac{w_g}{w_o}$ have been plotted against $(1-\exp[-k*t])/k$ for co-pyrolysis of jute wastes and sesame oil for all temperatures. Figures 6.43 -6.45 show the series of plots for 773K, 973K and 1173K respectively using all jute wastes and sesame oil cake [A20-A-24]. The linearity of the plots proves the validity of 1st order kinetics [3, 9-12] for all cases. Similar, plots have also been obtained at other temperature (not shown). The values of *k*, k_v, k_c, k_l and k_g [9-12,15] have been determined from the slopes of the respective plots and are provided in table 6.20. Figure 6.46, 6.47, 6.48 shows the variation of k, k_v, k_c of jute waste [4-6], sesame oil cake [15,38] and co-pyrolysis [39] of jute waste and sesame oil cake [38] respectively. From the figure, it appears that the values of k, k_v and k_c of co-pyrolysis [39] of jute waste and sesame oil cake is very similar to that of jute waste. This may be due to the presence of recalcitrant lignocellulosic in jute which dominates the overall trend of co-pyrolysis. Similar observation has been reported by Aparna et al during their studies on co-pyrolysis of mustard oil cake and paper waste [39].

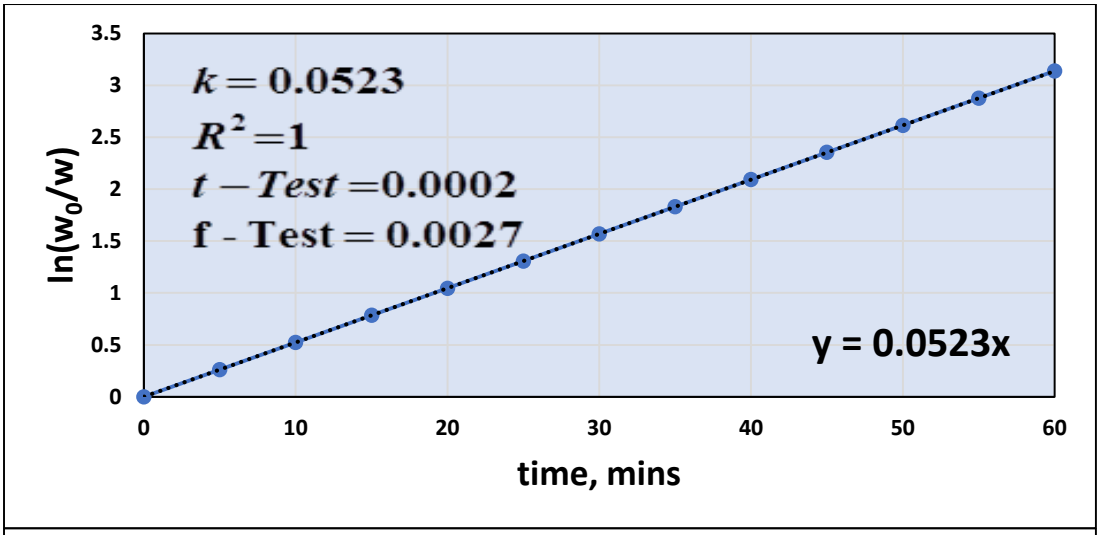
$k = 0.0523$
$R^2 = 1$
$t - Test = 0.0002$
f - Test = 0.0027
y = 0.0523x
ln(w0/w)
time, mins

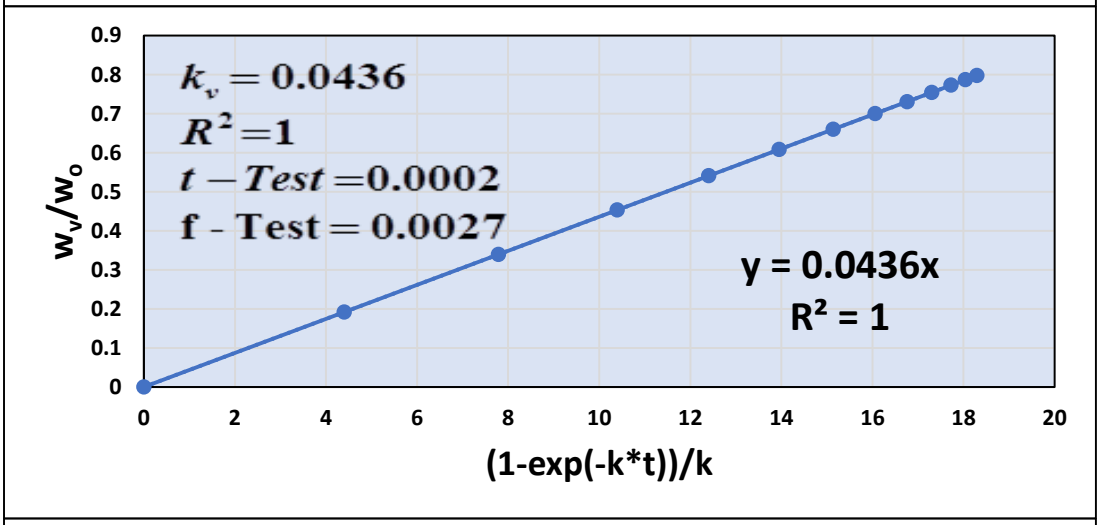
$k_v = 0.0436$
$R^2 = 1$
$t - Test = 0.0002$
f - Test = 0.0027
y = 0.0436x
R² = 1
wv/wo
(1-exp(-k*t))/k

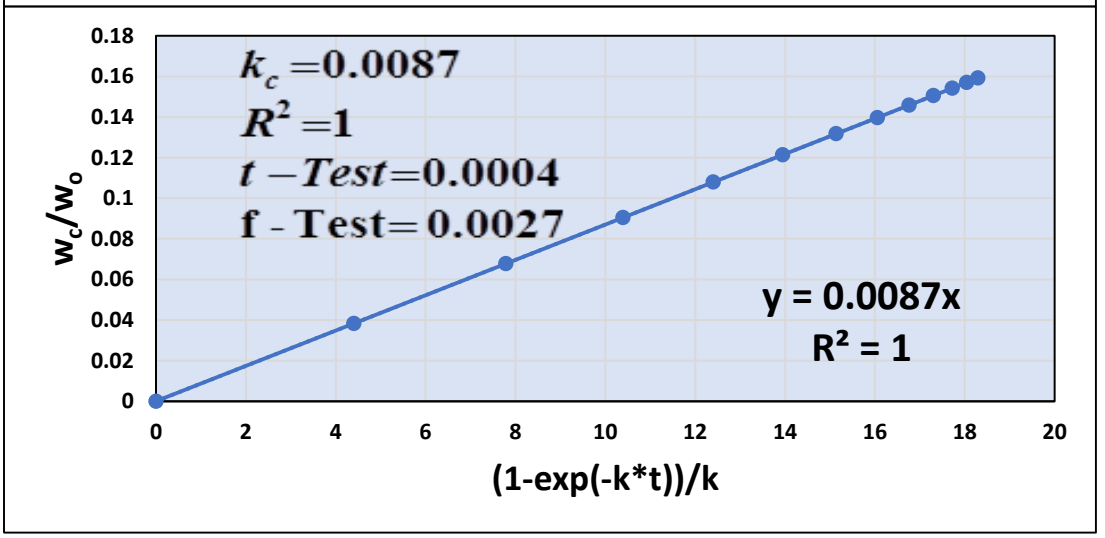
$k_c = 0.0087$
$R^2 = 1$
$t - Test = 0.0004$
f - Test = 0.0027
y = 0.0087x
R² = 1
wc/wo
(1-exp(-k*t))/k

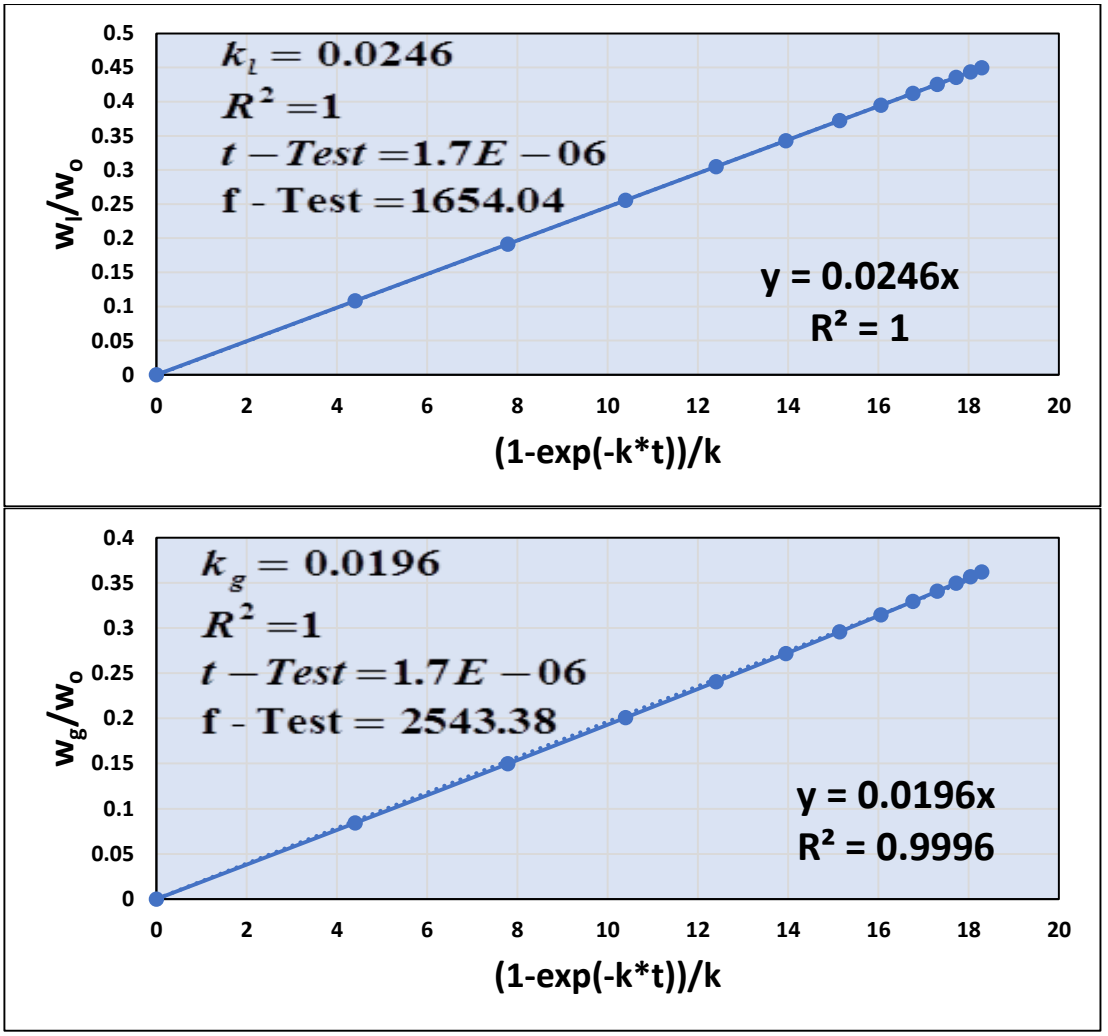

Figure 6.43. Plots of $\ln\left[\frac{w_o}{w}\right]$ vs time and $\frac{w_v}{w_0}$, $\frac{w_c}{w_0}$, $\frac{w_l}{w_0}$ and $\frac{w_g}{w_0}$ vs $(1-\exp[-k*t])/k$ at 773K of co-pyrolysis of jute wastes and sesame oil cake.

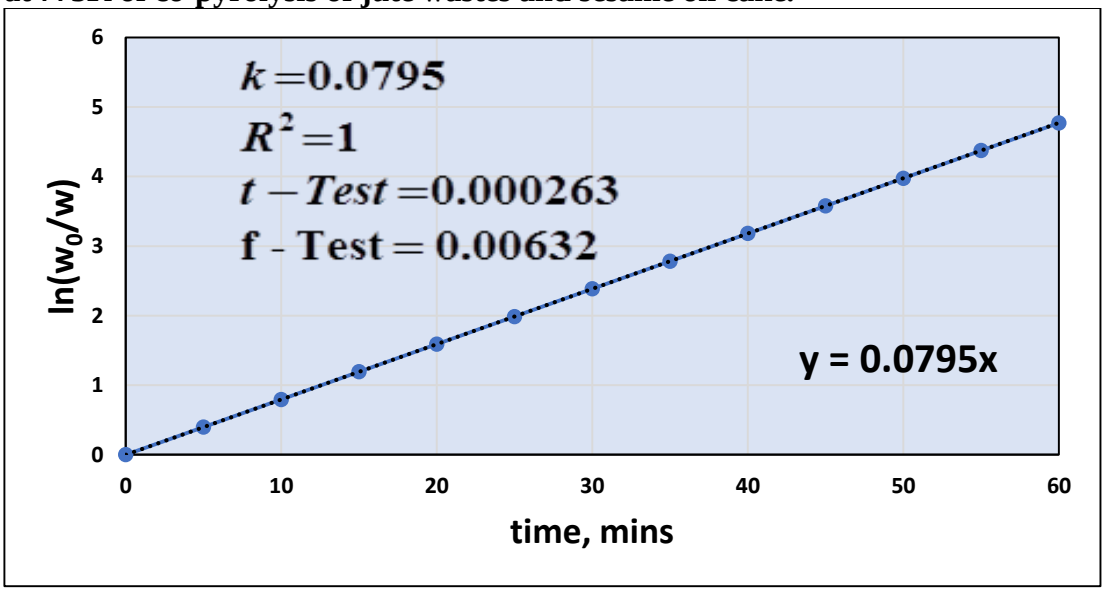

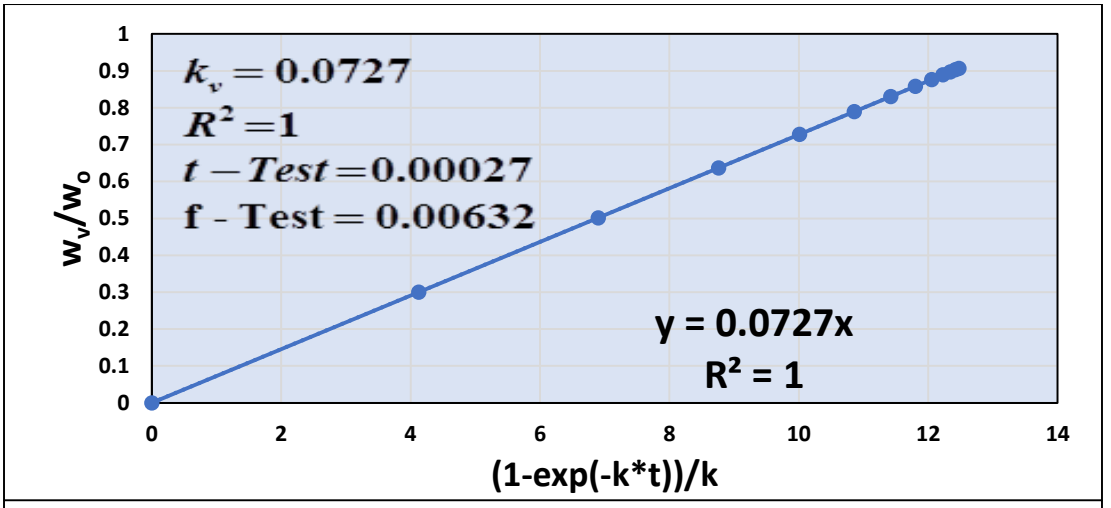
$k_v = 0.0727$
$R^2 = 1$
$t - Test = 0.00027$
f - Test = 0.00632
y = 0.0727x
R² = 1
w_v/w_o
(1-exp(-k*t))/k

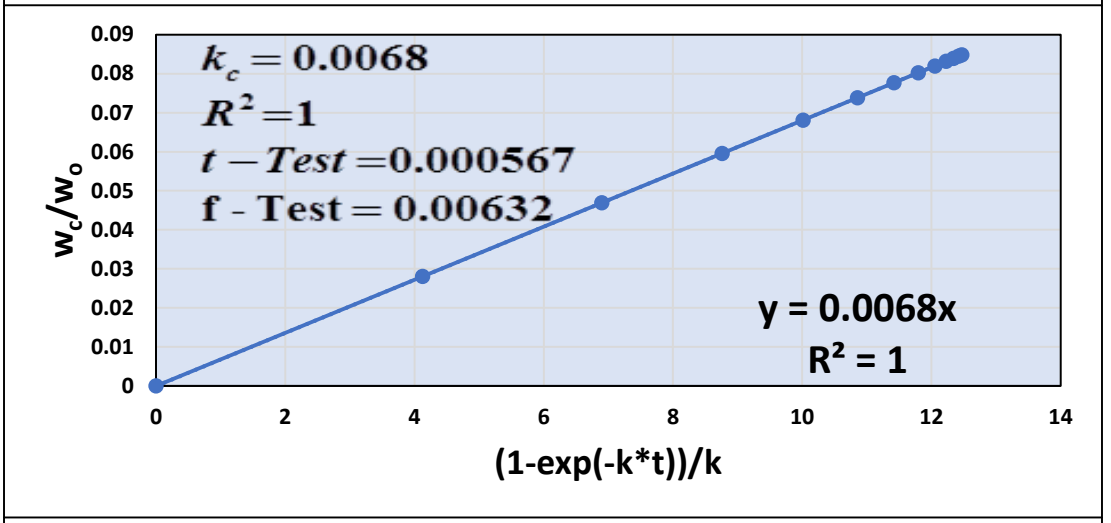
$k_c = 0.0068$
$R^2 = 1$
$t - Test = 0.000567$
f - Test = 0.00632
y = 0.0068x
R² = 1
w_c/w_o
(1-exp(-k*t))/k

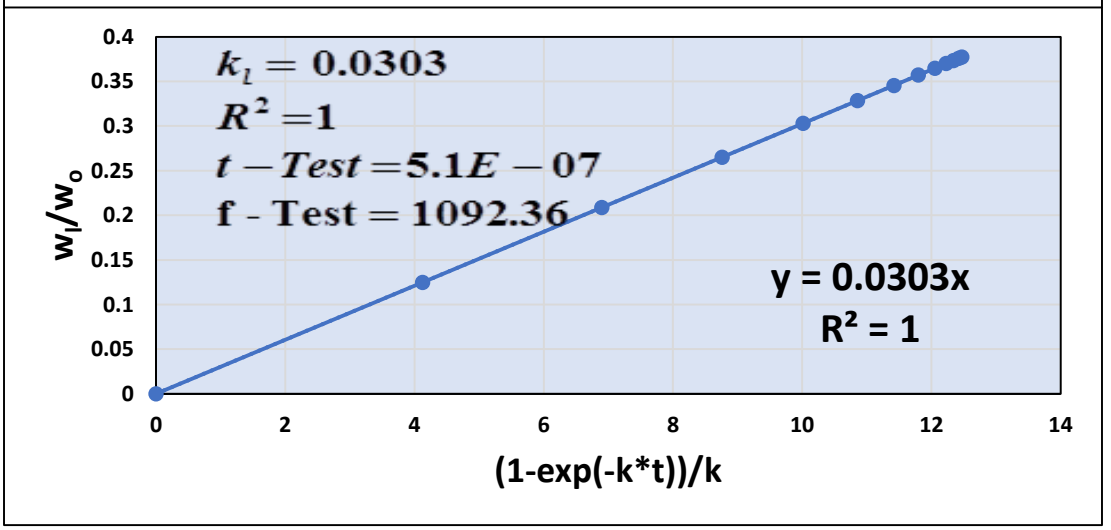
$k_l = 0.0303$
$R^2 = 1$
$t - Test = 5.1E-07$
f - Test = 1092.36
y = 0.0303x
R² = 1
w_l/w_o
(1-exp(-k*t))/k

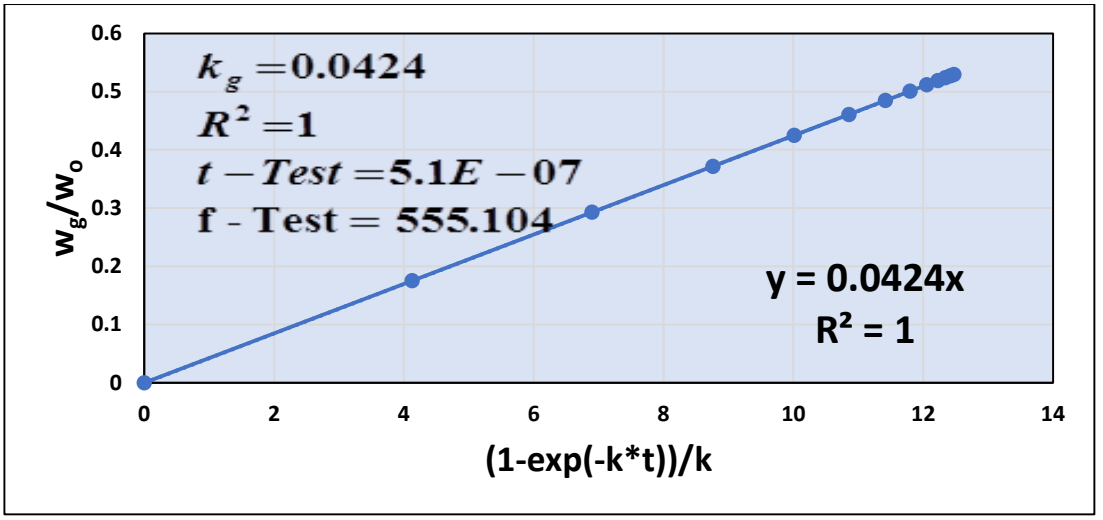

Figure 6.44. Plots of $\ln\left[\frac{w_o}{w}\right]$ vs time and $\frac{w_v}{w_0}$, $\frac{w_c}{w_0}$, $\frac{w_l}{w_0}$ and $\frac{w_g}{w_0}$ vs $(1-\exp[-k*t])/k$ at 973K of co-pyrolysis of jute wastes and sesame oil cake.

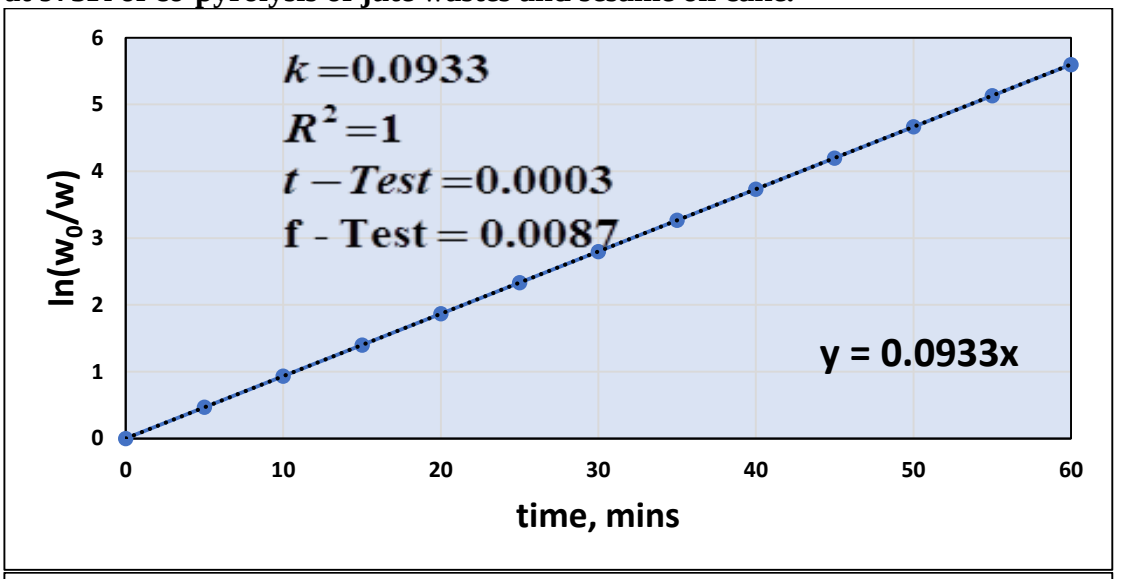

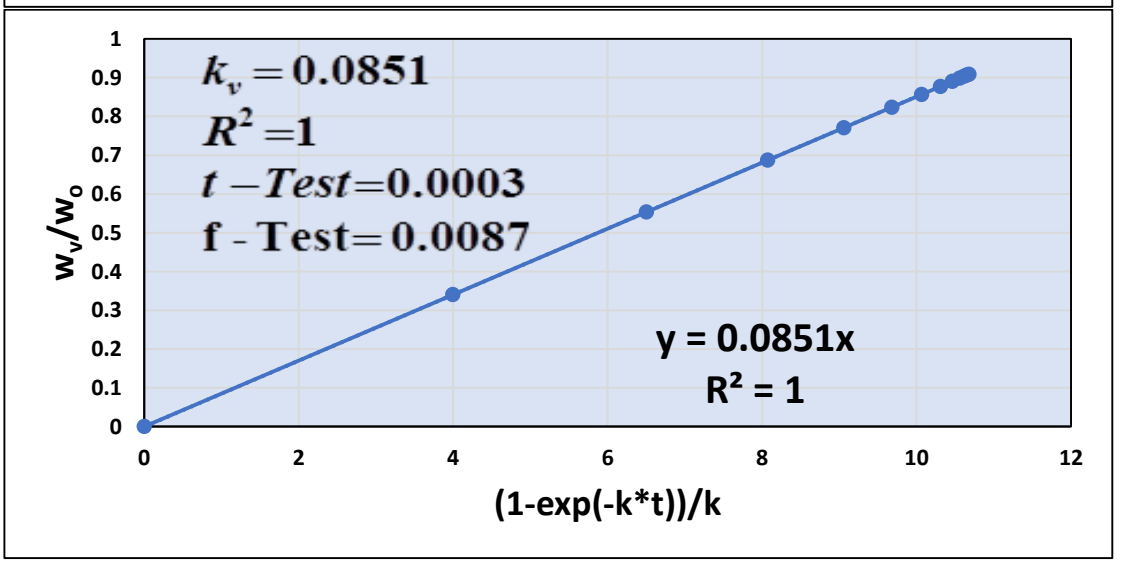

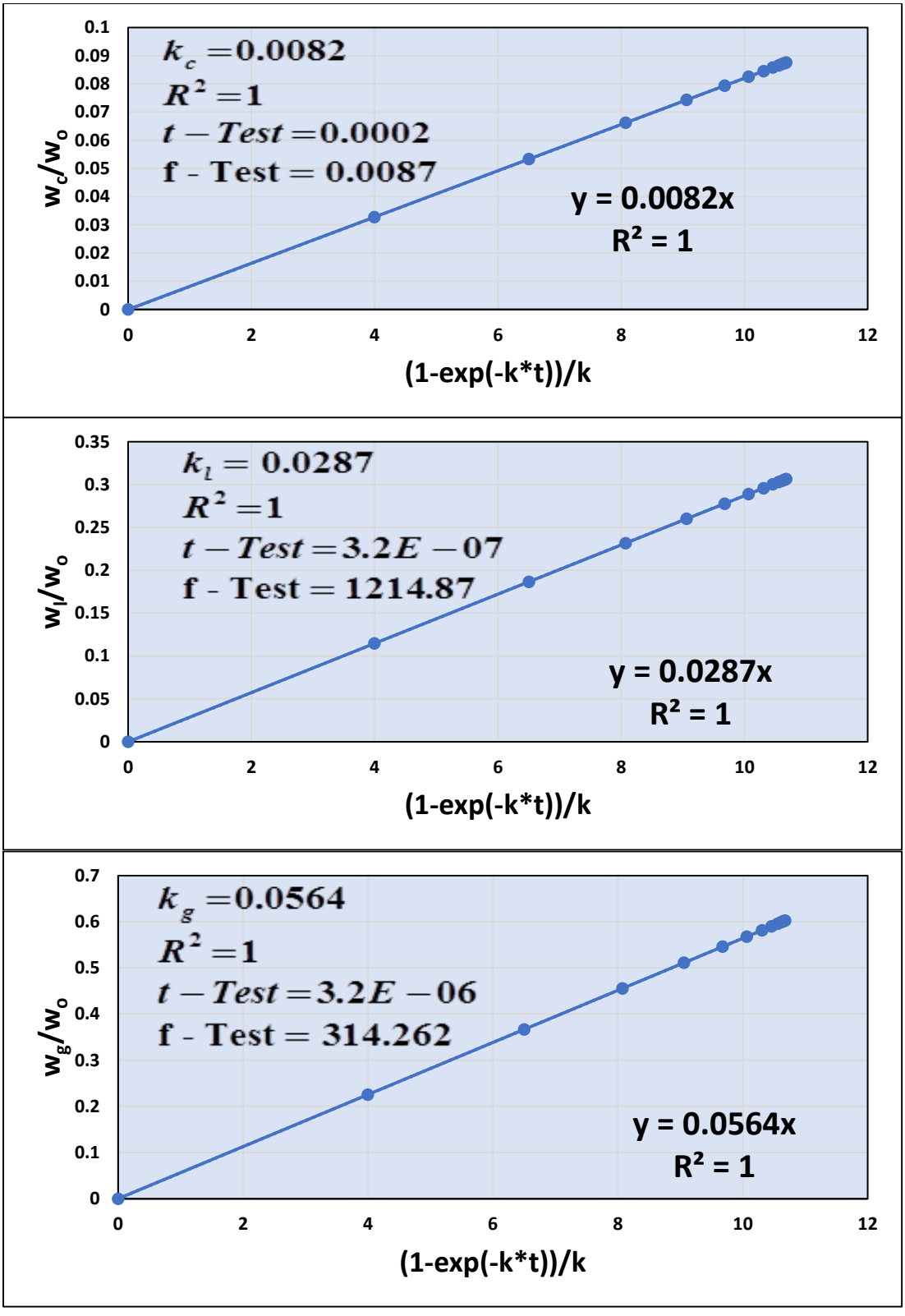

Figure 6.45. Plots of $\ln\left[\frac{w_o}{w}\right]$ vs time and $\frac{w_v}{w_o}$, $\frac{w_c}{w_o}$, $\frac{w_l}{w_o}$ and $\frac{w_g}{w_o}$ vs $(1-\exp[-k*t])/k$ at 1173K of co-pyrolysis of jute wastes and sesame oil cake.

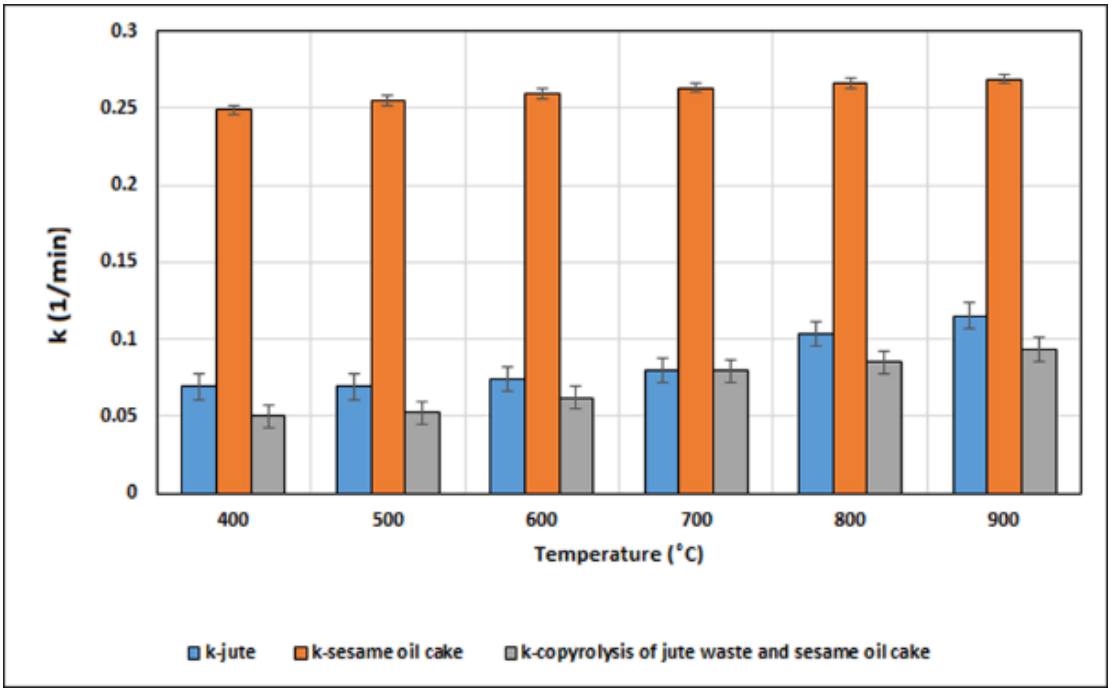

Figure 6.46 Variation of k of jute waste, sesame oil cake and co-pyrolysis of jute waste and sesame oil cake.

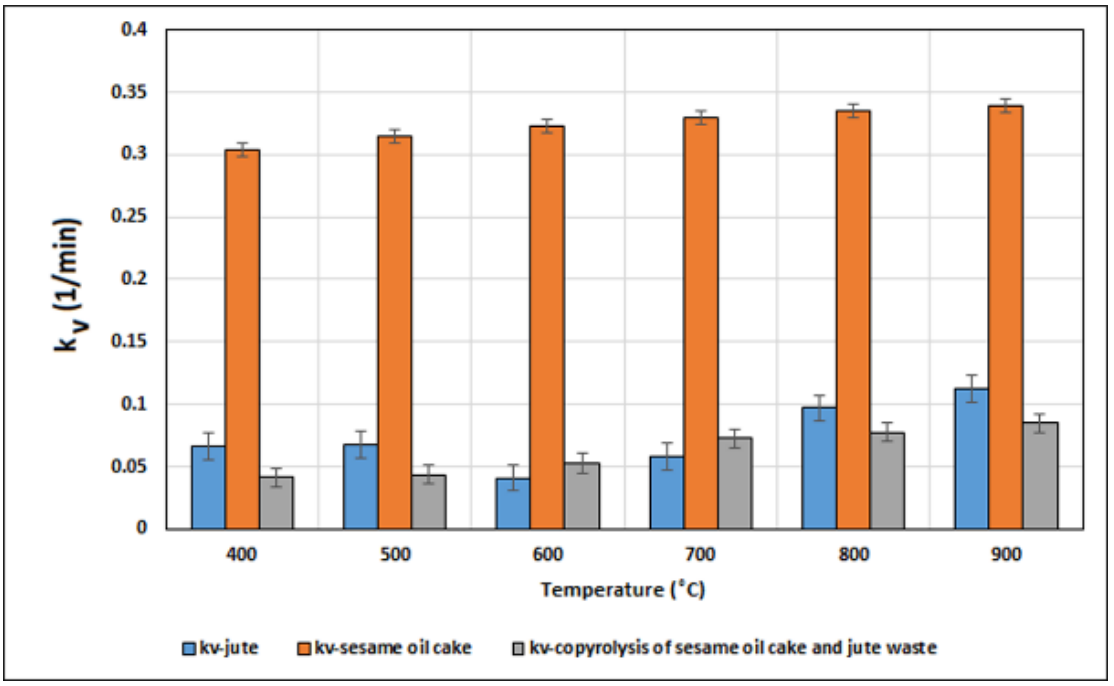

Figure 6.47 Variation of k_v of jute waste, sesame oil cake and co-pyrolysis of jute waste and sesame oil cake.

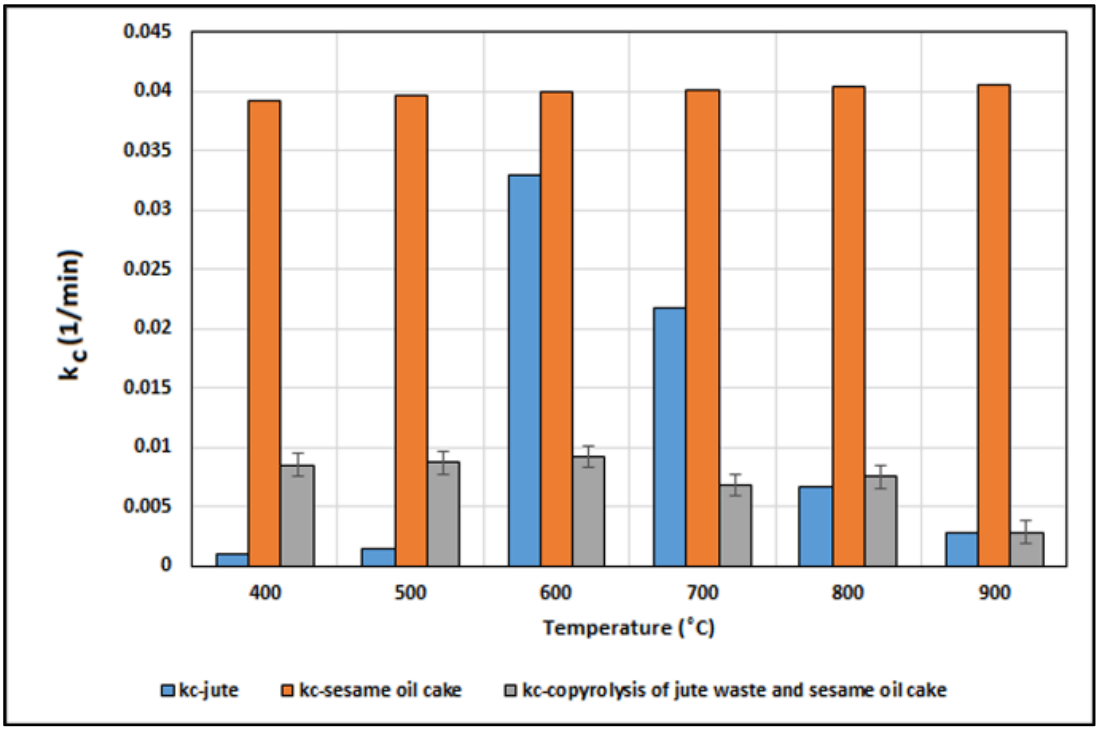

Figure 6.48 Variation of k_c of jute waste, sesame oil cake and co-pyrolysis of jute waste and sesame oil cake

Table 6.20. Values of "*k, k_v, k_c, k_l and k_g*" at different temperature for co-pyrolysis of jute wastes and sesame oil cake

T (K)	co-pyrolysis of jute wastes and sesame oil cake (*k*)	co-pyrolysis of jute wastes and sesame oil cake (k_v)	co-pyrolysis of jute wastes and sesame oil cake (k_c)	co-pyrolysis of jute wastes and sesame oil cake (k_l)	co-pyrolysis of jute wastes and sesame oil cake (k_g)
573K	0.0489	0.0406	0.0083	0.0202	0.0204
673K	0.0499	0.0414	0.0085	0.0209	0.0205
773K	0.0523	0.0436	0.0087	0.0246	0.0196
873K	0.0619	0.0527	0.0092	0.0197	0.0219
973K	0.0795	0.0727	0.0068	0.0303	0.0424
1073K	0.085	0.0775	0.0075	0.0339	0.0436
1173K	0.0082	0.0851	0.0028	0.0287	0.0564

6.5.1.3. Temperature dependence on rate constant

Using the values of rate constants *k*, k_v, k_c, k_l and k_g [9-12,15] Arrhenius plots (shown in the Appendix A.25) have been made following the same method as used in case of pyrolysis of other feedstocks. The linearity of the plots proves the validity of Arrhenius relationship [11,12,15].

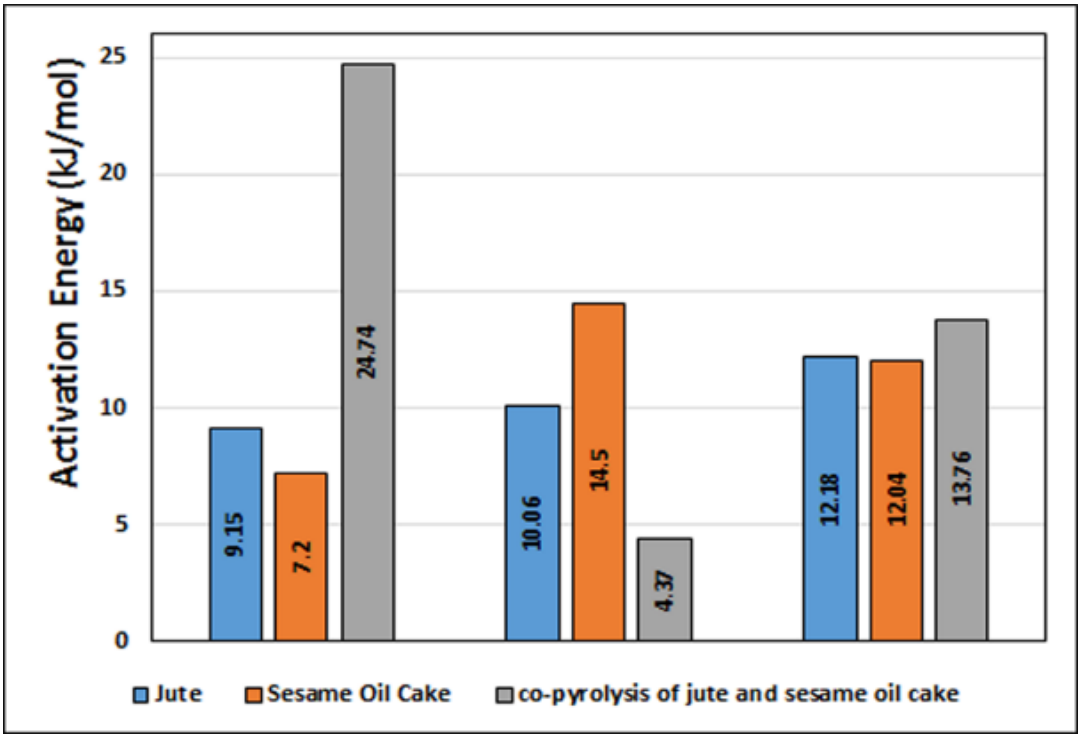

Figure 6.49. Comparison of Activation energies between pyrolysis of jute, sesame oil cake and co-pyrolysis of jute and sesame oil cake.

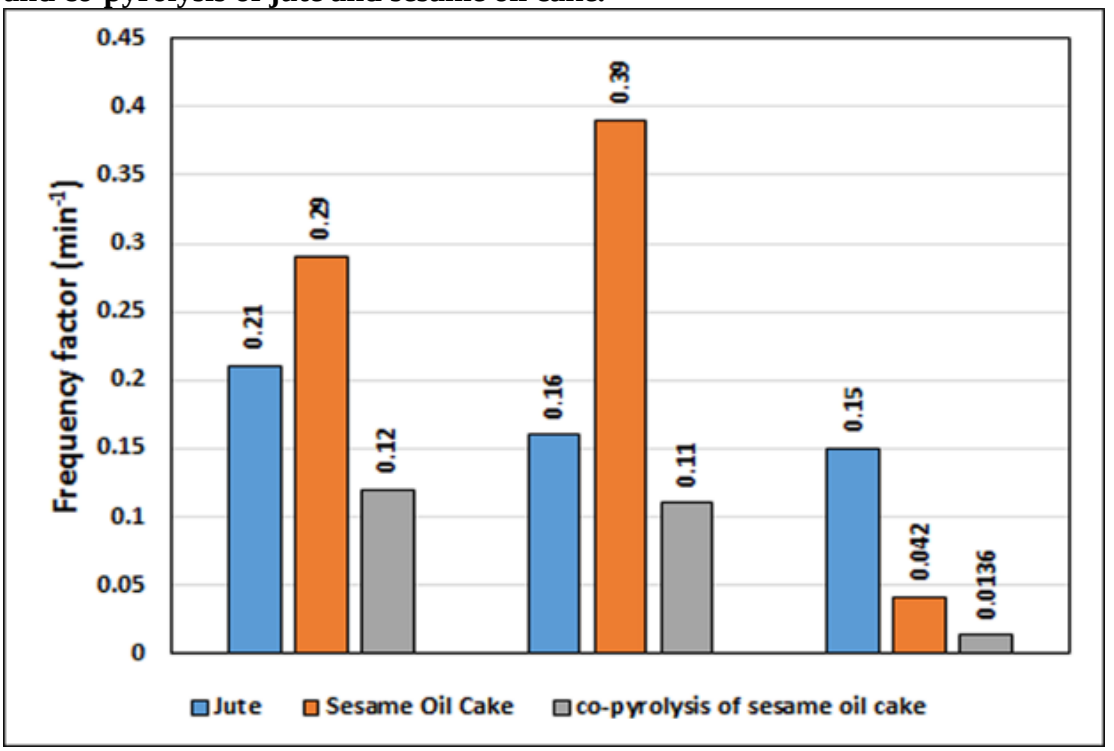

Figure 6.50. Comparison of frequency factors between pyrolysis of jute, sesame oil cake and co-pyrolysis of jute and sesame oil cake.

Figure 6.49 -6.50 represents the activation energies and frequency factors of co-pyrolysis [39] of jute and sesame oil cake [38,34-38].

6.5.2. DAEM (Distributed activation model)

6.5.2.1. TGA plots

Figures. 6.51. shows the time trajectories of % (w/w) of solid residue for non-catalytic co-pyrolysis of jute waste and sesame oil cake remaining during TGA under nonisothermal conditions using heating rate (10 K min^{-1}, 15 K min^{-1}, 20 K min^{-1}, 25 K min^{-1}, 30 K min^{-1}) as a parameter. From the analysis of the plots it is clearly evident that distinct patterns of weight loss are followed in different temperature ranges for the feedstock. A comparison can be made between jute waste, sesame oil cake and co-pyrolysis of jute waste and sesame oil cake. The temperature profiles for jute waste [1] are 30 -100°C, 100-275 °C, 275 -350 °C, 350-700 °C and for sesame oil cake [2] are 30-227 °C, 227-477 °C, 477 °C >, co-pyrolysis of jute waste and sesame oil cake are 60-220 °C, 220-430 °C, 430-840 °C, 840 °C >. From the comparison, it may be inferred that although the trend of non-isothermal co-pyrolysis is distinct from that of individual constituents, the trend is more similar to that of jute rather than sesame oil cake. The dominating behaviour of the recalcitrant lignin in jute may be responsible for such observation. The residual solid obtained is approximately 10% of the weight loss for non-catalytic co-pyrolysis.

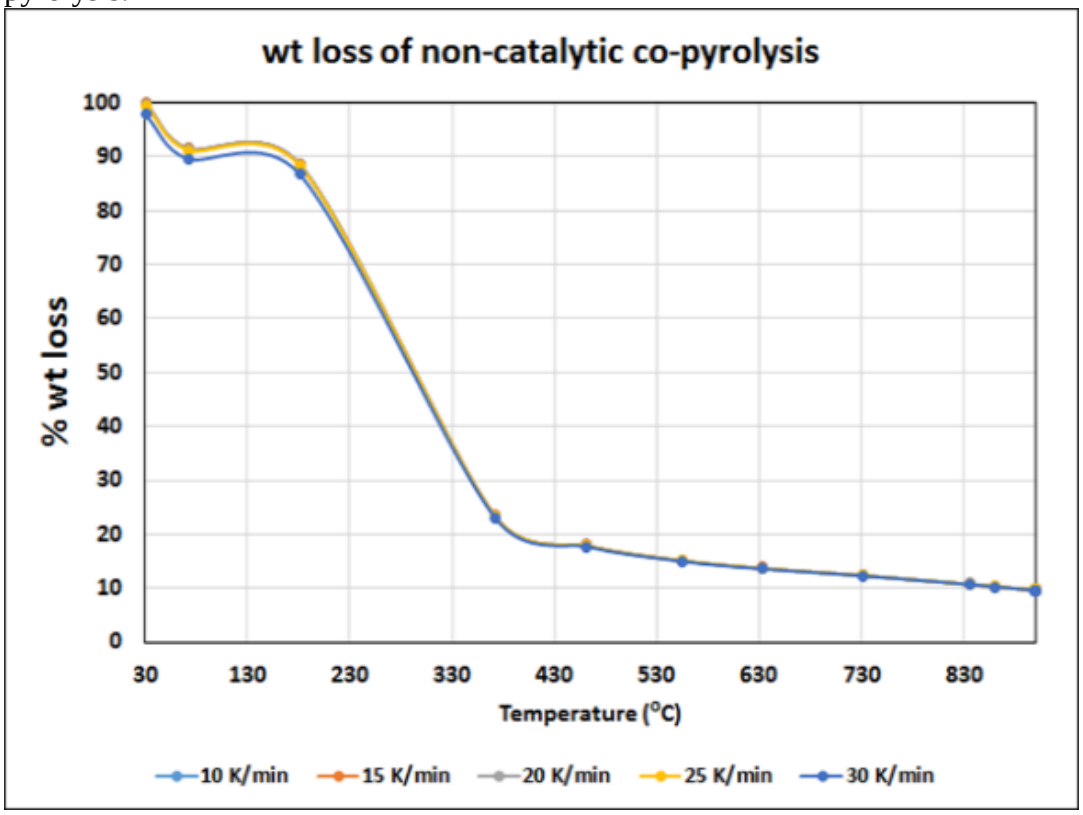

Figure 6.51. Percentage of weight residue of co-pyrolysis of jute wastes and sesame oil cake in the temperature range of 30–900 °C at different heating rates (TGA plot).

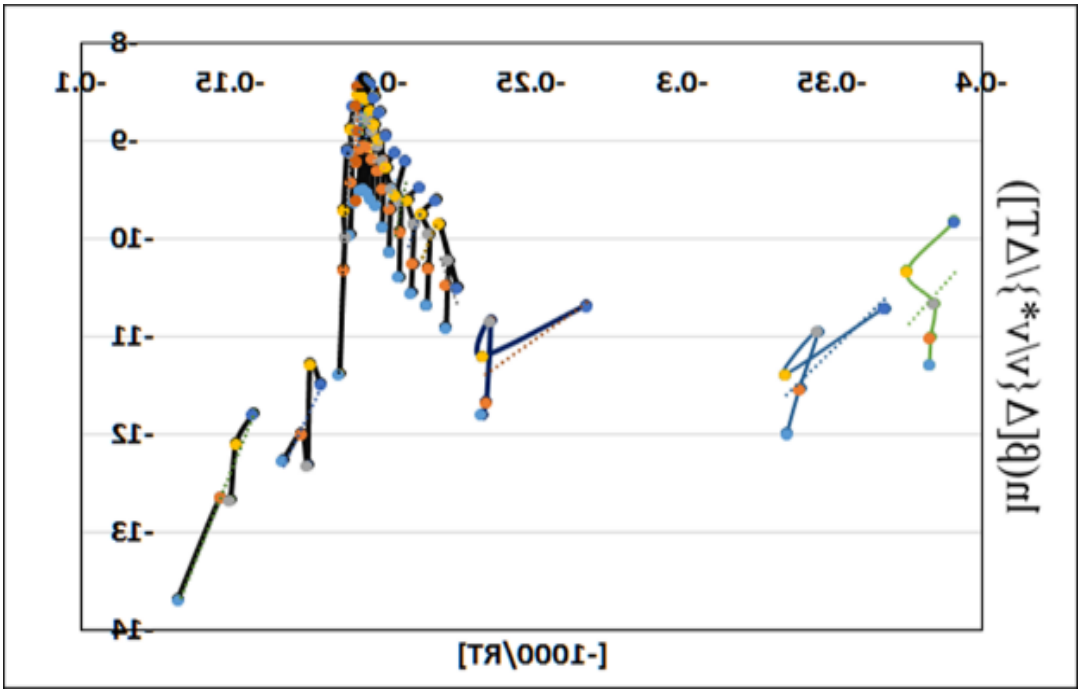

Figure 6.52. Plot of ln[αi(dx/dT) x, i] vs. (-1000/RTi) at different conversion values from 0.05 to 0.95 for all the heating rates (5-30 K min-1) of co-pyrolysis of jute wastes and sesame oil cake.

6.5.2.2. Isoconversion Plots

In Figures 6.53. logarithm of [αi(dx/dT) $_{x,\ i}$] has been plotted against (-1000/RT$_i$) for non-catalytic and catalytic co-pyrolysis of feedstock respectively. From the figure, it is revealed that parallel curves are generated. From the non-linearity of the plots it may be inferred that Friedman model [30] is not valid.

6.6. Product Yield

Pyrolysis of lignocellulosic wastes (jute wastes [4-6], lime wastes [7,8]) and co-pyrolysis [39] of jute wastes and lime wastes were carried out respectively in horizontal and vertical semi-batch pyrolyzer described in section 5.1. Three products, namely, char, tar and gas were obtained from pyrolysis of lignocellulosic wastes. The yield of each product was defined on the basis of initial mass of pyrolysis feed stock used. Thus, yield of any product, i, may be defined as

$$Y_i = \left[\frac{M_i}{M_o}\right] \times 100$$

where,

$M_i = Mass\ \ of\ \ product\ \ i$

$M_o = Initial\ \ \ mass\ \ of\ \ reactant$

The effect of pyrolysis temperature on product yield are described below:

6.6.1. Pyro-char yield of various lignocellulosic wastes

Figures 6.55-57 presents the formation of pyro-char after catalytic and non-catalytic pyrolysis for waste jute [4-6], lime waste [7-8] and co-pyrolysis [39] of jute waste and sesame oil cake [38]. From figure 6.55 it is evident that the formation of pyro-char decreases from 673K (400 ^{0}C) to 973K (700 ^{0}C) after which it remains constant in case of non-catalytic pyrolysis of waste jute. The maximum and minimum yields of pyro-char are 49% and 26% respectively. However, in the case of

catalytic pyrolysis it is evident that the formation of pyro-char decreases monotonously with the rise in temperature. It is also clear that the decrease in the formation of pyro-char from jute waste is maximum in the presence of alumina (46% to 22%) followed by KCl (34% to 24%), NaCl (45% to 23%), ZnO (44% to 34%) and sodium Aluminosilicate (44% to 32%).

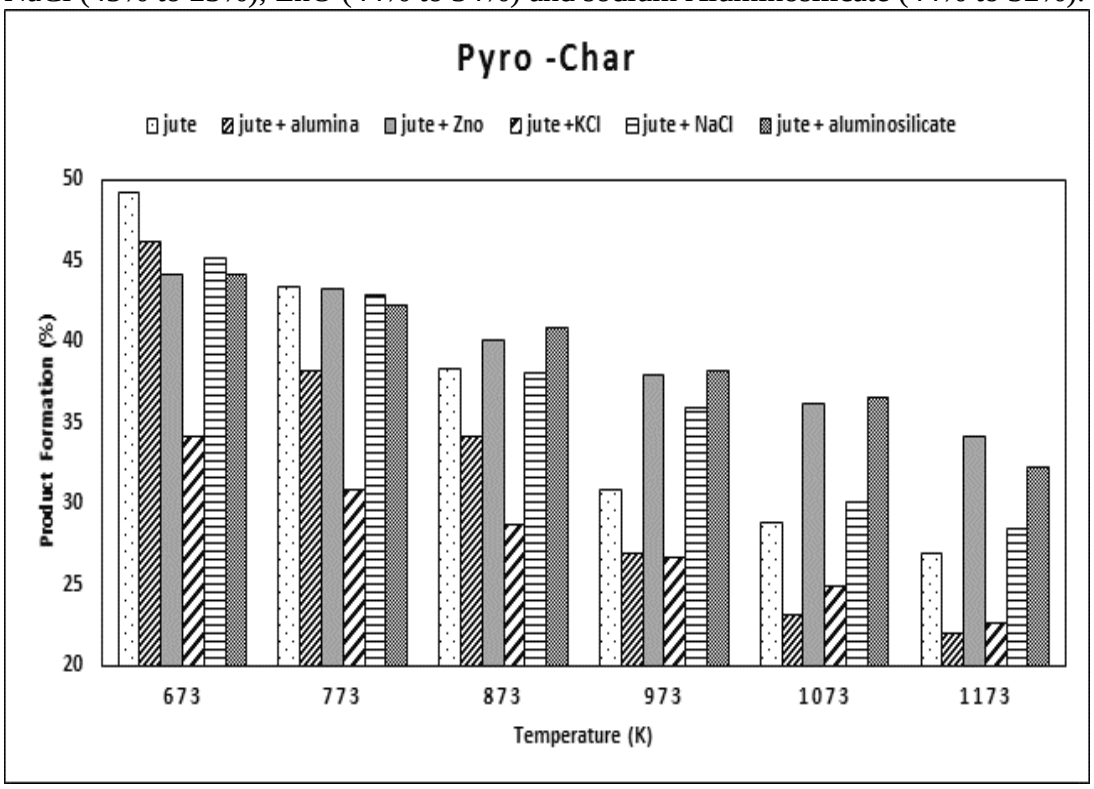

Figure 6.55. Yield of Pyro-char of jute wastes with and without catalyst at different temperature (K).

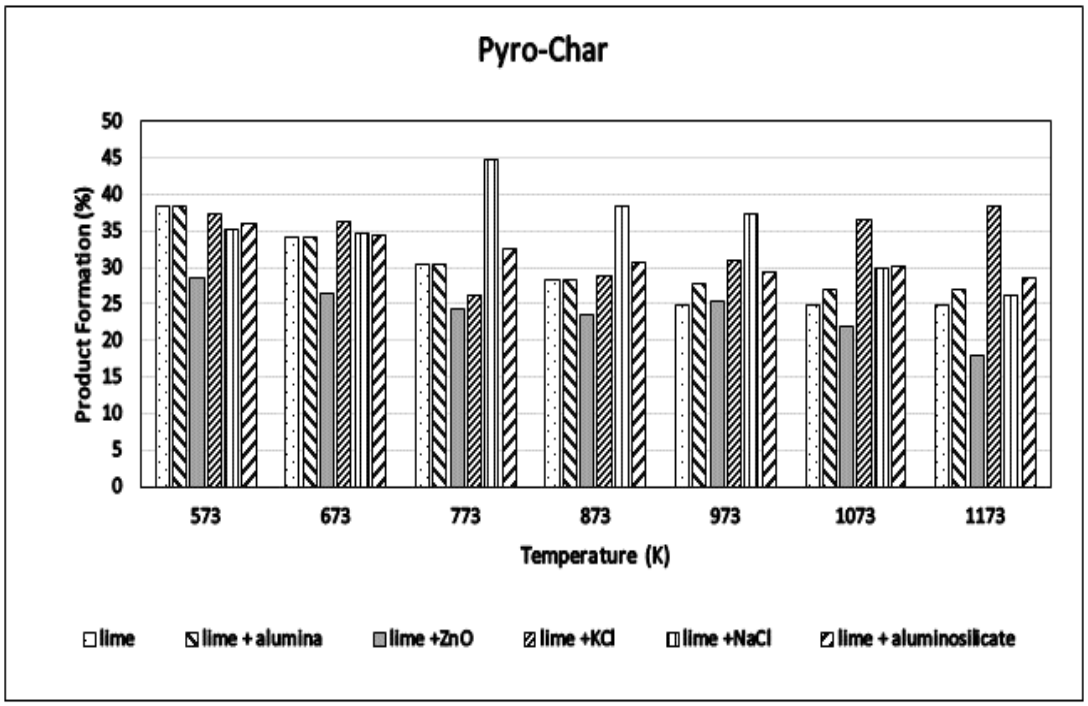

Figure 6.56. Yield of Pyro-char of lime wastes with and without catalyst at different temperature (K)

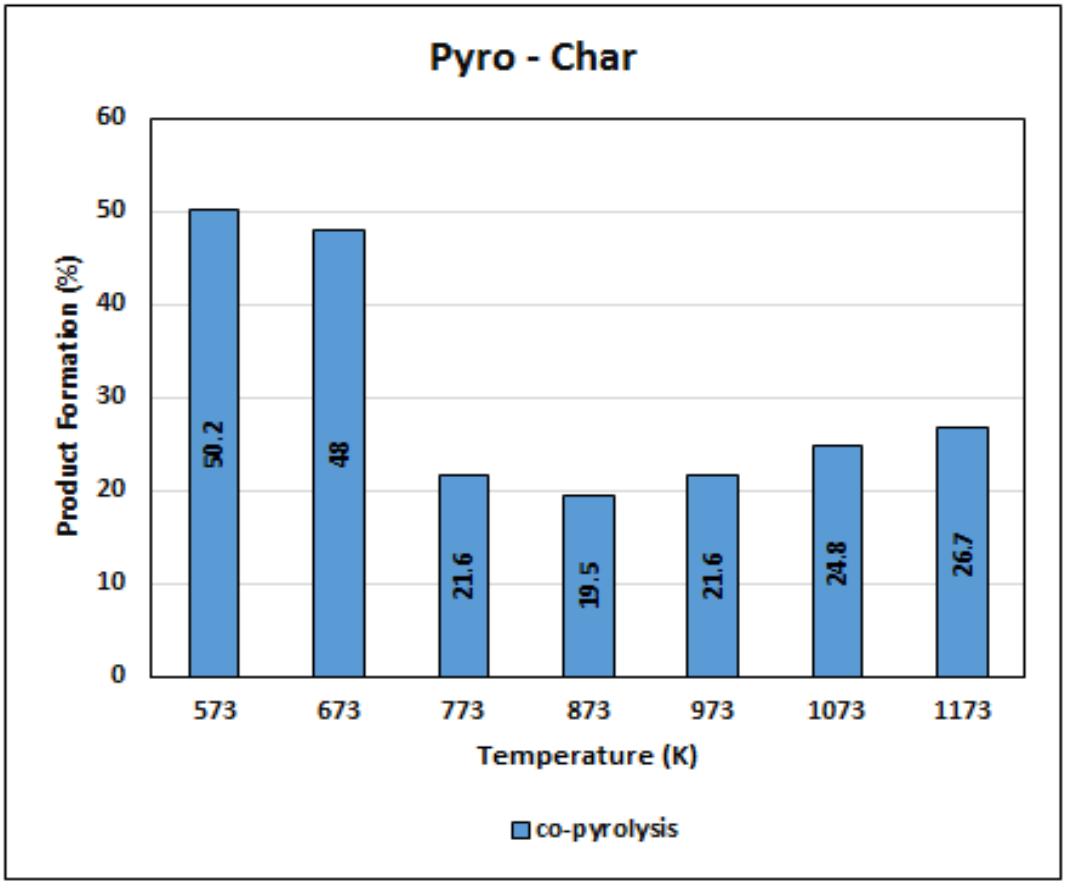

Figure 6.57. Yield of Pyro-char of co-pyrolysis of jute wastes and sesame oil cake at different temperature (K)

From figure 6.56 it is evident that the formation of pyro-char decreases in the case of non-catalytic pyrolysis of lime wastes [7,8]. In the case of non-catalytic pyrolysis of lime waste, the formation of pyro-char decreases from 38% to 24% as the temperature is increased from 573K to 1173K. In the case of catalytic pyrolysis of lime waste, the decrease in the formation of pyro-char is maximum for ZnO (28% to 17%) followed by alumina (38% to 26%), NaCl (35% to 28%), sodium Aluminosilicate (36% to 28.7%) and KCl (37% to 36%). Unlike the general trend, there is an increase in the % char at 773K in comparison to 573K in presence of ZnO. Further investigation is needed to elucidate the fact.

From figure 6.57 it is evident that in case of co-pyrolysis of lignocellulosic wastes the formation of pyro-char decreases from 50% to 20% as the temperature changes from 573K to 873K, beyond which it increases slightly with the increase in pyrolysis temperature.

For all the cases, although the decreasing trend with pyrolysis temperature of pyro-char is explainable as it is expected that the thermal decomposition of large molecular weight compounds proceeds at higher rate with the increase of temperature [40-41]. However, the increasing trend of char with temperature is against the expected behaviour and needs further investigation.

6.6.2. Pyro-oil yield of various lignocellulosic wastes

Figures 6.58 and 6.59 represent the dependence of yield of pyro-oil on pyrolysis temperature obtained through catalytic and non-catalytic pyrolysis of waste jute and lime waste respectively.

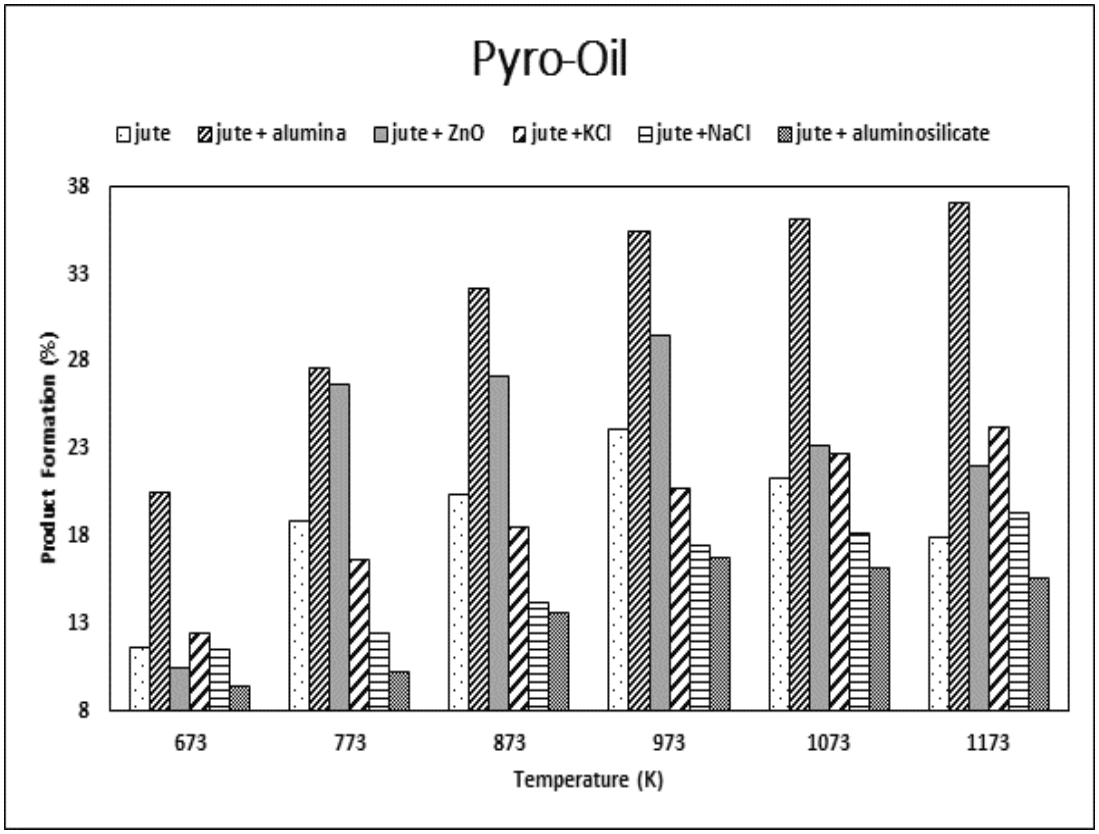

Figure 6.58. Yield of Pyro-oil of jute wastes with and without catalyst at different temperature (K).

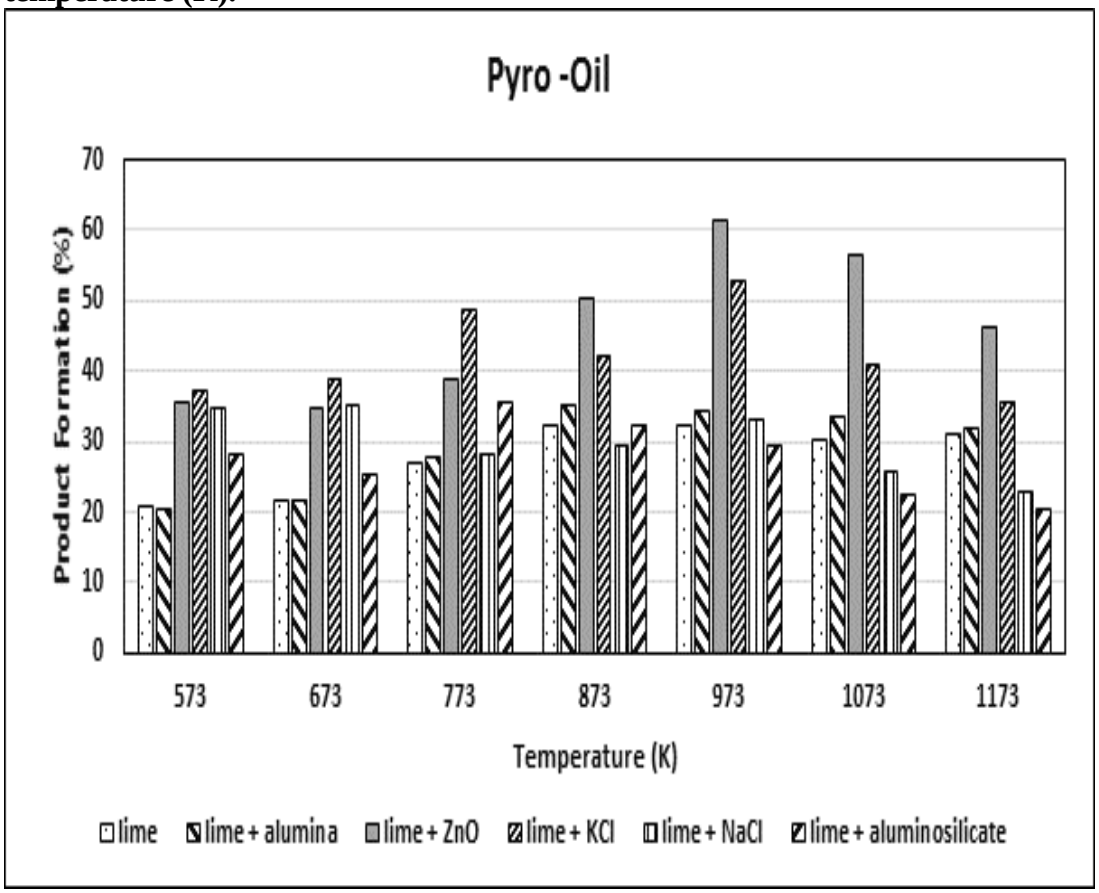

Figure 6.59. Yield of Pyro-oil of lime wastes with and without catalyst at different temperature (K)

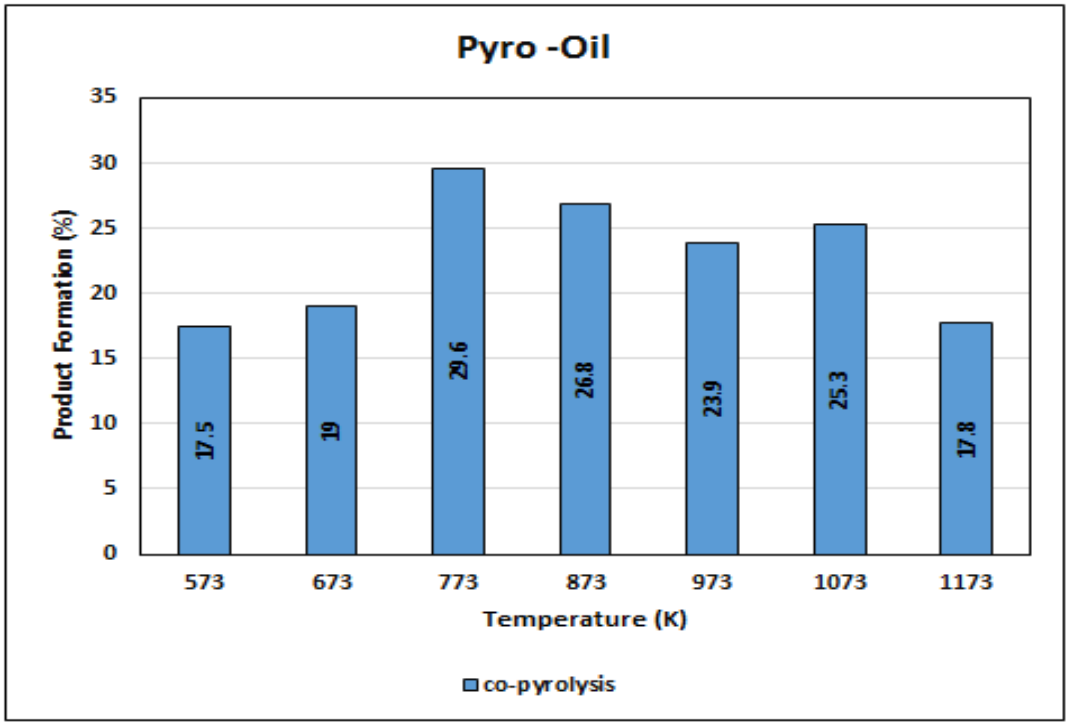

Figure 6.60. Yield of Pyro-oil of co-pyrolysis of jute wastes and sesame oil cake with and without catalyst at different temperature (K)

In figure 6.58. the yields of pyro-oil obtained through isothermal semi batch pyrolysis of jute waste with and without catalysts over 1 h have been plotted as a function of pyrolysis temperature. From the analysis of the patterns of dependence of oil yield on temperature, it appears that the catalytic effect of Al_2O_3 and ZnO are prominent. In case of non-catalytic pyrolysis of jute, the pyro-oil passes through a maximum at 973K. Same trend is observed in presence of ZnO. On the other hand, catalytic effect of alumina is very pronounced. In this case yield of pyro-oil increases monotonically even beyond 973K. Effects of NaCl and KCl on pyro-oil yield is not very significant and is almost identical. Up to 700^{o}C, the pyro-oil yield in presence of Na-K additives is a little less compared to that of jute. Similar observation has been obtained by Hoekstra et. al. during their studies on pyrolysis of pinewood in presence of Na + K catalyst [37]. Osama et al also indicated the decrease in liquid yield during the fast pyrolysis of wood and agricultural residues in presence of Na + K catalysts [34]. Sodium aluminosilicate shows inhibiting effect with respect to pyro-oil formation. This may be due to catalytic effect of sodium aluminate on cracking of pyro-oil or tar.

From figure 6.59 it is evident that the formation of pyro-oil increases in the case of catalytic and non-catalytic pyrolysis of lime waste. It is evident from the figure that in case of non-catalytic pyrolysis of lime waste the formation of pyro-oil increased from 20% to 31% with the rise of pyrolysis temperature from 573K to 1173K. In case of catalytic pyrolysis of lime waste, the presence of ZnO yields the maximum pyro-oil (35% - 61%), followed by KCl (37% to 52%), alumina (20% to 35%), NaCl (34% to 35%), sodium Aluminosilicate (28% to 35%). In the case of catalytic pyrolysis of lime waste, it is evident that the yield of pyro-oil increased till 973K after which the formation of pyro-oil is much lower than the maximum as the pyrolysis temperature is increased further [42-48]. The reason behind the decrement is need to be further investigated. The maximum yield is obtained at 973K in both the cases (catalytic and non-catalytic) of pyrolysis.

From figure 6.60 it is evident that the formation of pyro-oil increases with temperature and passes through a maximum at 773K. The decrease of pyro-oil yield beyond 773K may be due

to cracking of pyro-oil to gaseous compounds. The pattern of oil yield of co-pyrolysis is different from that of jute. This may be due to the effect of sesame oil cake on jute. The maximum oil yield is 30% for co-pyrolysis of jute waste and sesame oil cake.

6.6.3. Pyro-gas yield of various lignocellulosic wastes

Figures 6.61 -63 presents the formation of pyro-gas after catalytic and non-catalytic pyrolysis for waste jute, lime waste and co-pyrolysis of jute waste and sesame oil cake.

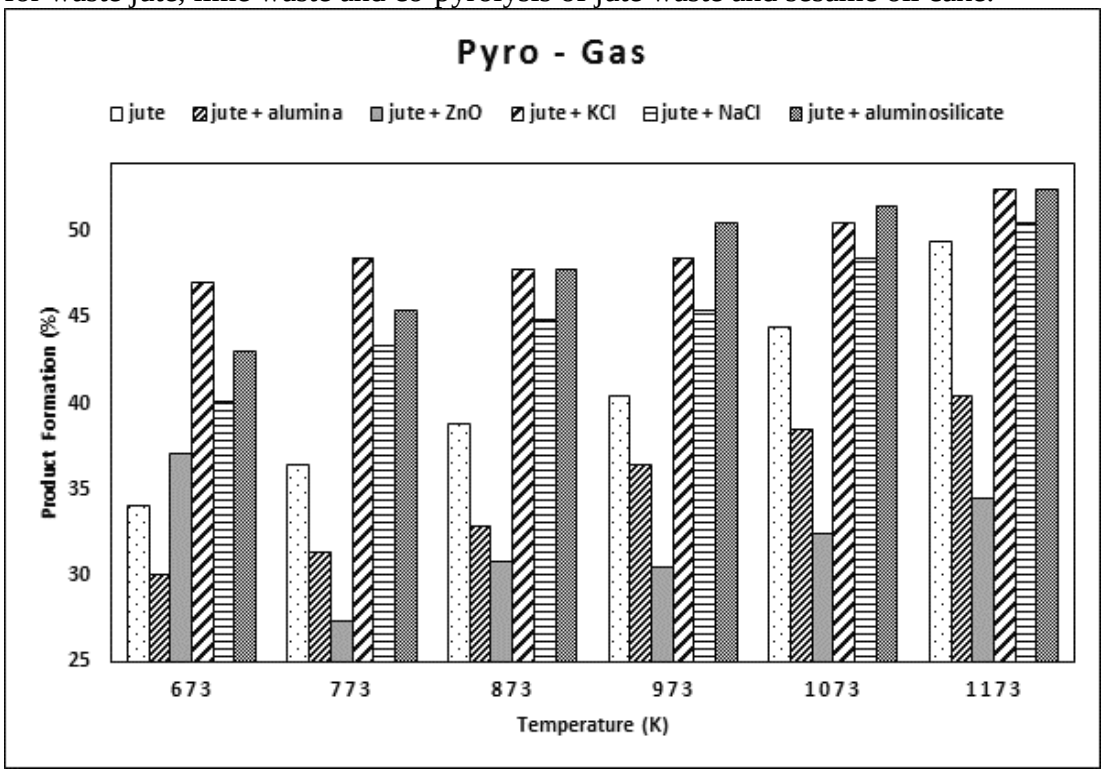

Figure 6.61. Yield of Pyro-gas of jute wastes with and without catalyst at different temperature (K).

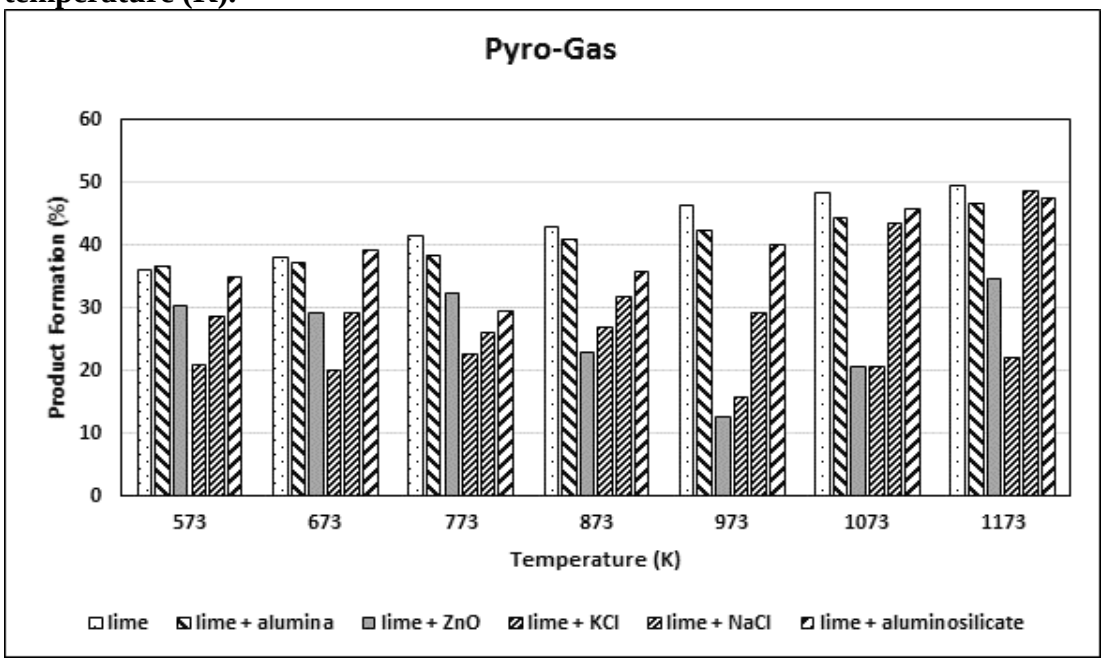

Figure 6.62. Yield of Pyro-gas of lime wastes with and without catalyst at different temperature (K)

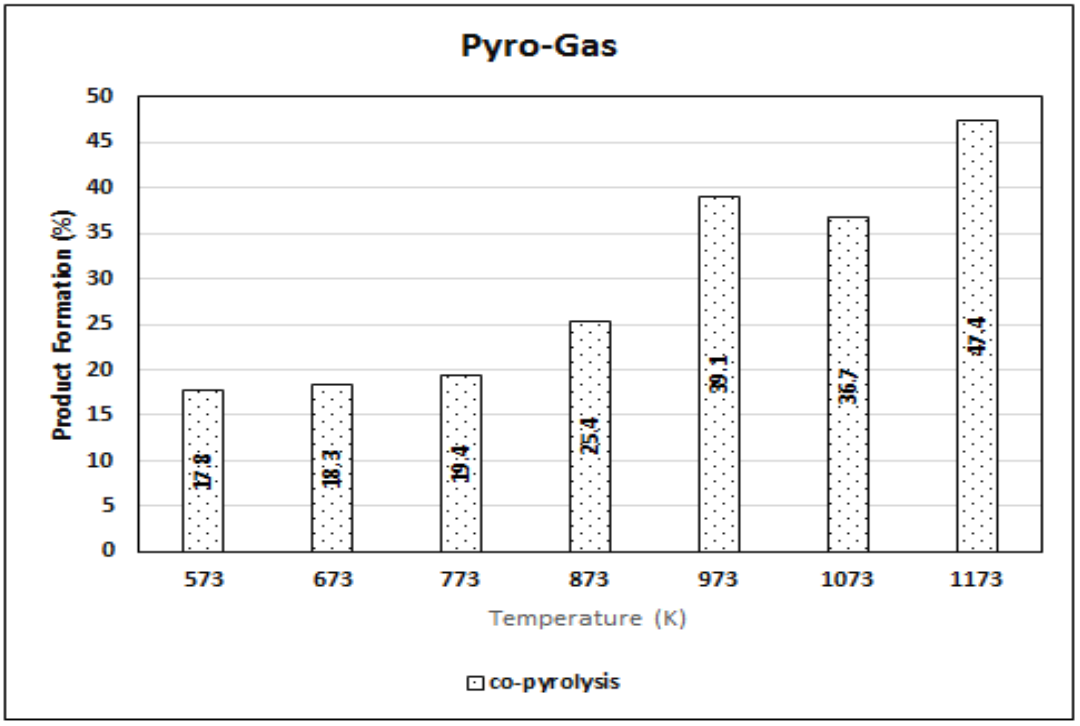

Figure 6.63. Yield of Pyro-gas of co-pyrolysis of jute wastes and sesame oil cake with and without catalyst at different temperature (K)

From figure 6.61 showing the patterns of variation of gas yield with temperature, it is evident that the yield of pyro-gas increases with temperature for both non-catalytic and catalytic pyrolysis. The catalytic effects of aluminosilicate and NaCl have been observed to be higher compared to others. This may be due to their catalytic effect on secondary tar cracking reactions.

From figure 6.62 it is evident that the formation of pyro-gas increases with temperature for catalytic and non-catalytic pyrolysis of lime waste. It is evident that in case of non-catalytic pyrolysis of lime waste the yield increases from 36% to 49%. In case of catalytic pyrolysis, the formation of pyro-gas in presence of alumina increases from 36% to 46%, followed by NaCl (28% to 48%), sodium Aluminosilicate (34% to 47%), KCl (20% to 22%). In case of catalytic pyrolysis in presence of ZnO the formation of pyro-gas decreases from 30% to 12% till 773K after which it increased to 34% as the temperature is increased. It is clear that although ZnO has positive effect on the production of pyro-oil, the effect is negative for the production of pyro-gas. All other catalysts investigated under the present study are also not effective in enhancement of pyro-gas yield.

From figure 6.63 it is evident that the yield of pyro-gas increases for co-pyrolysis of jute wastes and sesame oil cake. In case of co-pyrolysis, the formation of pyro-gas increased from 17% to 47%.

6.6.4. Elemental Analysis (C-H-O) of pyro-product

6.6.4.1. Pyro-char

The elemental, particularly C-H-O, composition of the pyro-char is a very important criterion from the perspective of its usage as a fuel. While the higher fractions of “C” and “H” in pyro-char contribute towards increase in heating value of pyro-char, higher fraction of “O” causes lowering of heating value, higher risk of polymerization etc. Figure 6.64 and 6.65 represent the C-H-O content of pyro-char of jute and lime wastes. Figure 6.66 represents the C-H-O content

of pyro-char obtained after co-pyrolysis of jute waste and sesame oil cake. From the figures, it can be inferred that while % C increases with the rise in pyrolysis temperature, %O decreases. The % H is almost insensitive to the pyrolysis temperature. The effect of alumina and zinc oxide, the best catalysts with respect to the generation of pyro oil respectively from jute and lime pyrolysis, on the C-H-O composition of pyro-char has also been depicted in Figure 6.64-6.65. Figure 6.66 represents the C-H-O composition of pyro oil obtained from co-pyrolysis of jute waste and sesame oil cake. The values of the C-H-N-S-O are provided in the table A.26-A.43 in the appendix. From the analysis of the figures, it may be generally stated that the increasing and decreasing trends of %C and %O respectively are higher in case of catalytic pyrolysis in comparison to the non-catalytic counterpart.

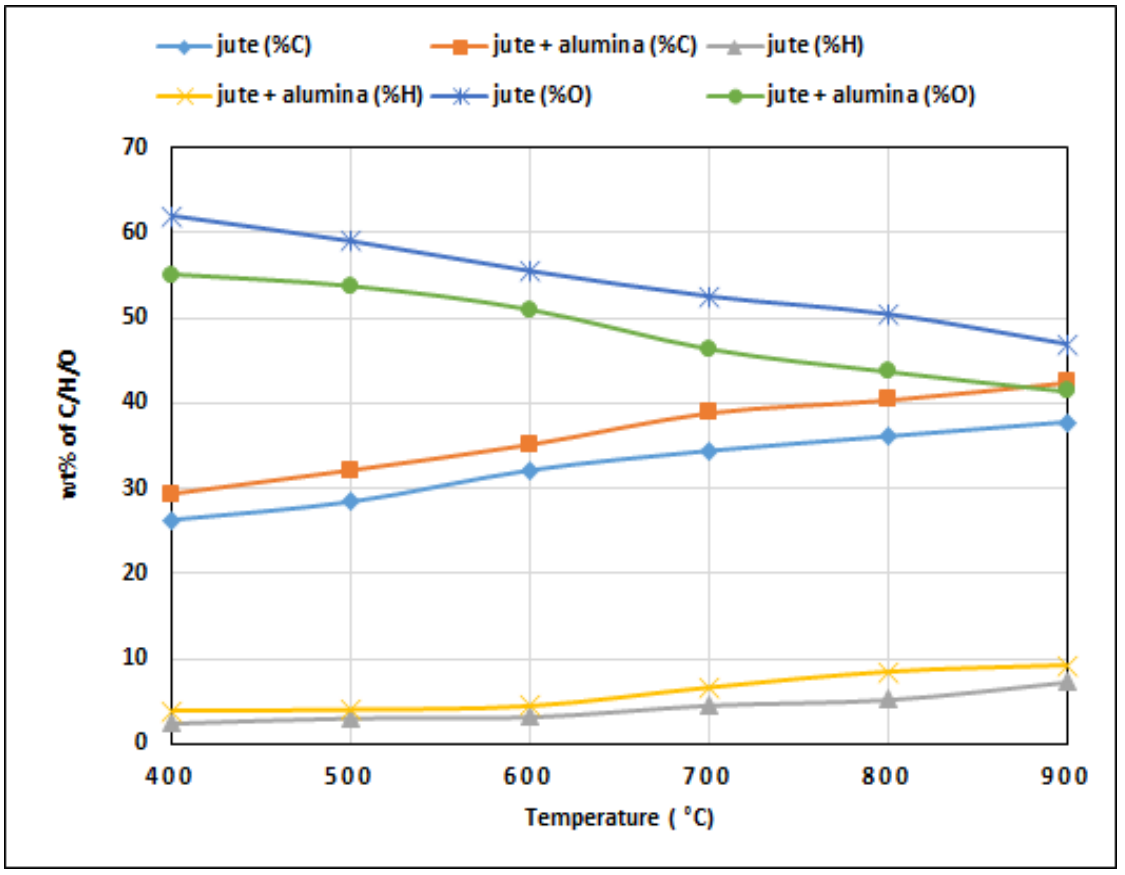

Figure 6.64. Plot of wt.% of element present in pyro-char against temperature for catalytic and non-catalytic pyrolysis of jute waste.

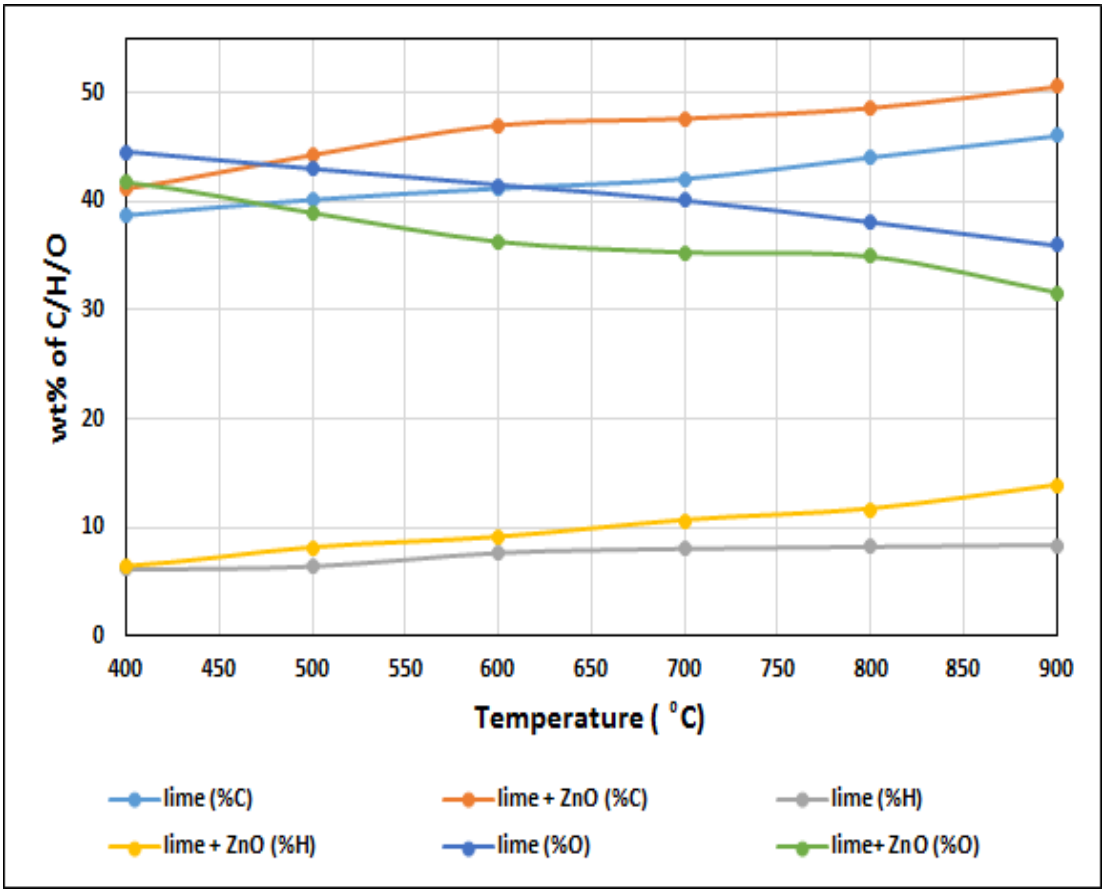

Figure 6.65. Plot of wt.% of element present in pyro-char against temperature for catalytic and non-catalytic pyrolysis of lime waste.

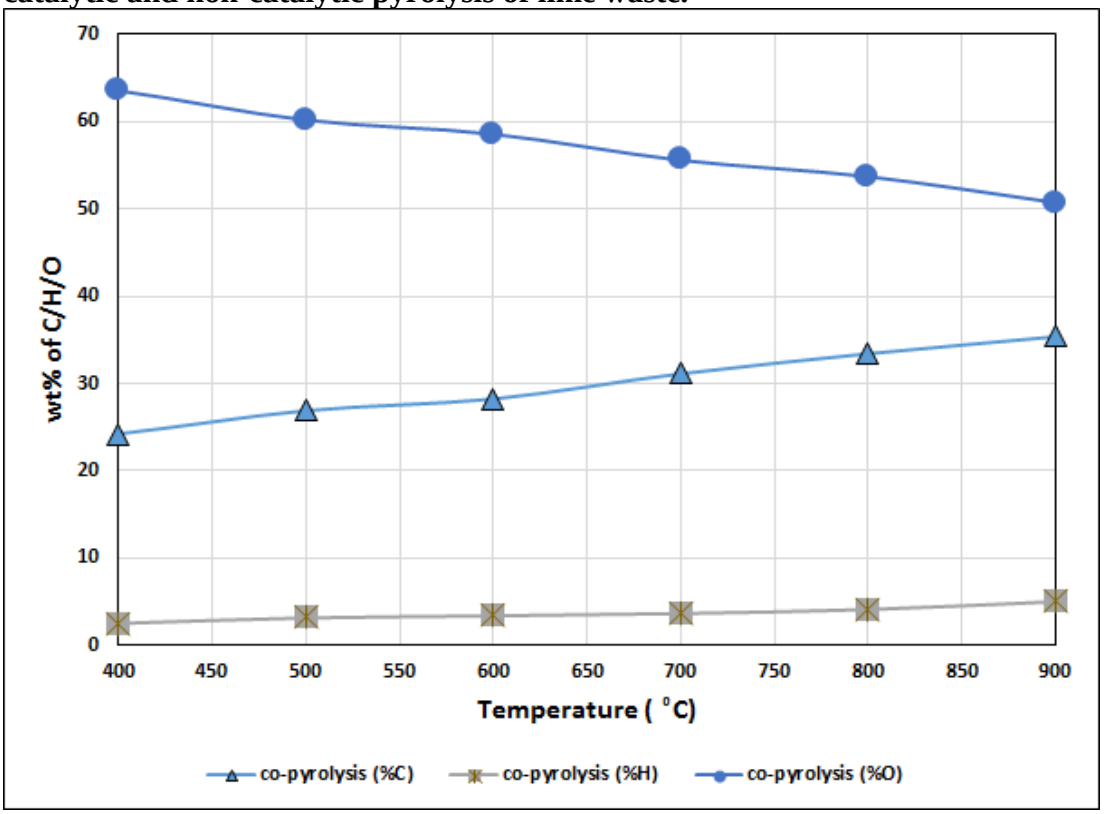

Figure 6.66. Plot of wt.% of element present in pyro-char against temperature for catalytic and non-catalytic co-pyrolysis of jute waste and sesame oil cake.

6.6.4.2. Effect of catalyst on C-H-O content of pyro-oil

Figure 6.67, 6.68 and 6.69 represent the elemental (C-H-O) composition of pyro-oil against temperature for catalytic and non-catalytic pyrolysis of waste jute, lime waste and co-pyrolysis of jute waste and sesame oil cake.

From the Figure 6.67, it is clear that carbon content of pyro-oil decreases with pyrolysis temperature for both catalytic and non-catalytic reactions. Similar observation has been reported by Yang et. al. [49] during their work on fast pyrolysis of enzymatic hydrolysis of empty fruit bunches (EHN). The content of carbon is higher for catalytic pyro-oil in comparison to non-catalytic one up to 600^{o}C. Content of hydrogen is not temperature sensitive and is not influenced by the presence of alumina. The weight fraction of oxygen in pyro-oil also decreases with pyrolysis temperature. However, up to 600^{o} C, the oxygen content in pyro-oil is lowered in presence of catalyst. Overall, alumina shows positive effect on the improvement of elemental composition of pyro-oil up to 600^{o}C. Almost similar trends of %C, %H and % O have been observed in case of pyrolysis of lime waste and co-pyrolysis of jute waste and sesame oil cake. The effect of catalyst is, however insignificant in case of pyrolysis of lime waste and co-pyrolysis of waste jute and sesame oil cake. The values of the C-H-N-S-O are provided in the table A.44-A.61 in the appendix.

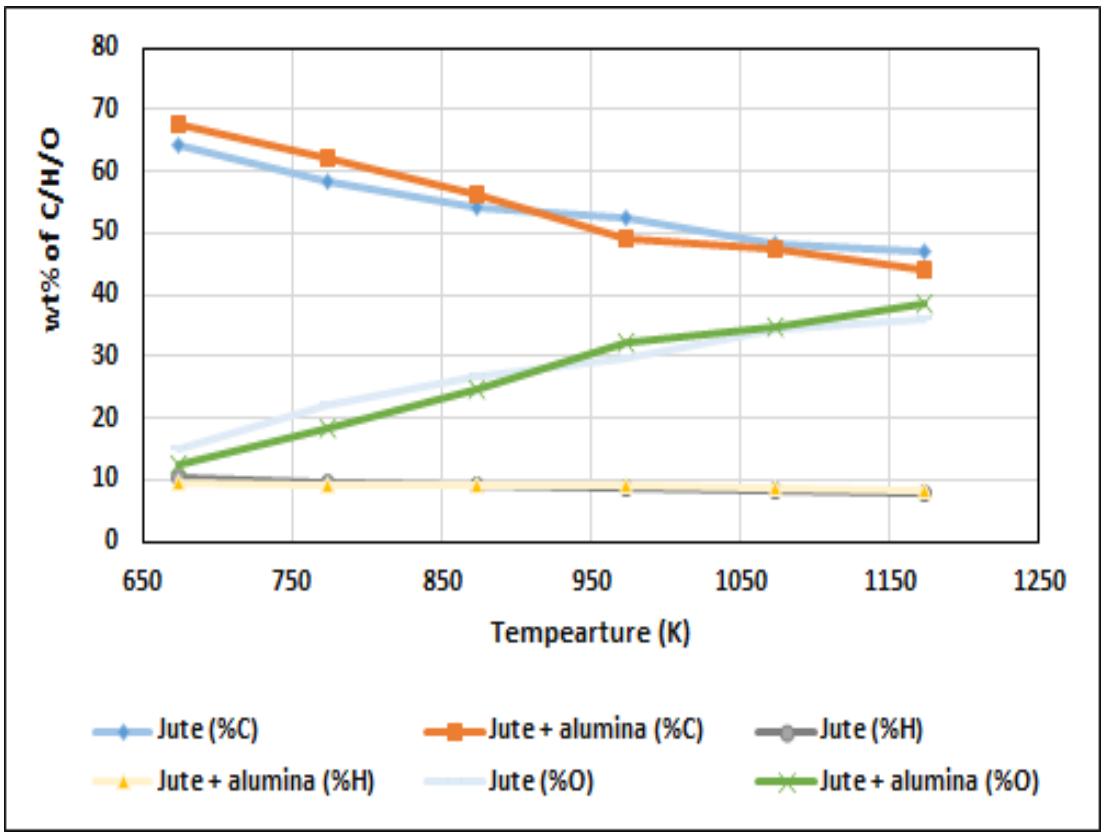

Figure 6.67. Plot of wt.% of compound present in pyro-oil against temperature for catalytic and non-catalytic pyrolysis of jute waste.

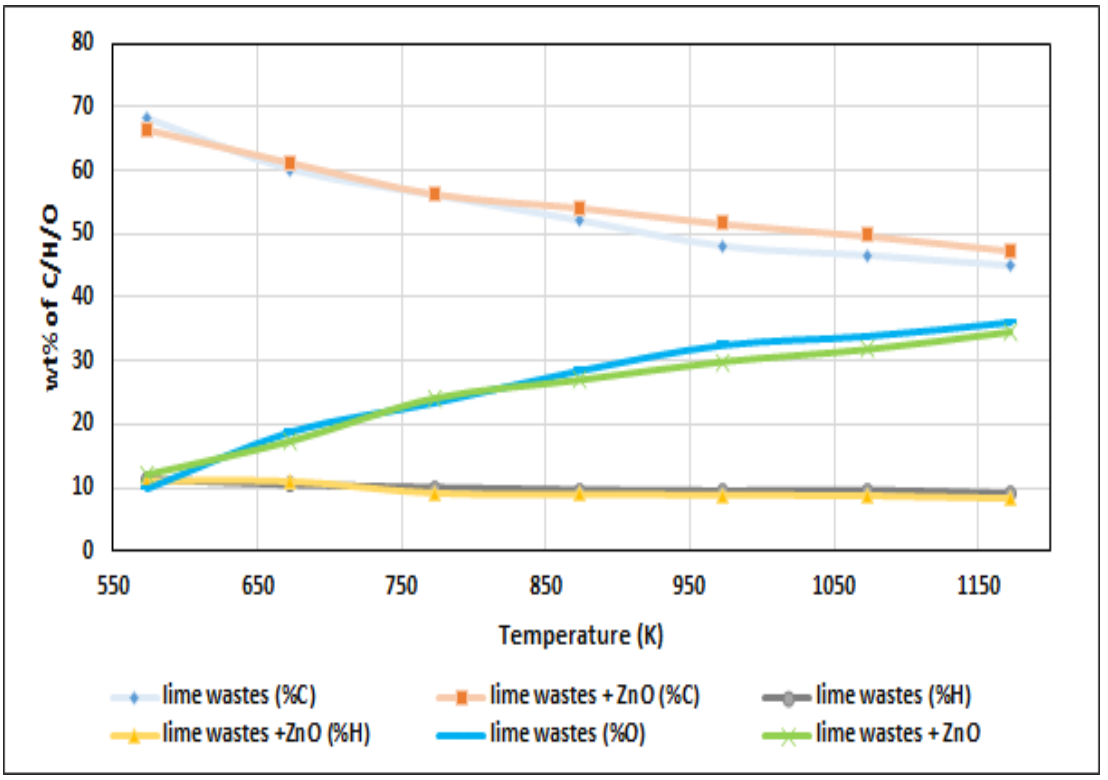

Figure 6.68. Plot of wt.% of compound present in pyro-oil against temperature for catalytic and non-catalytic pyrolysis of lime waste.

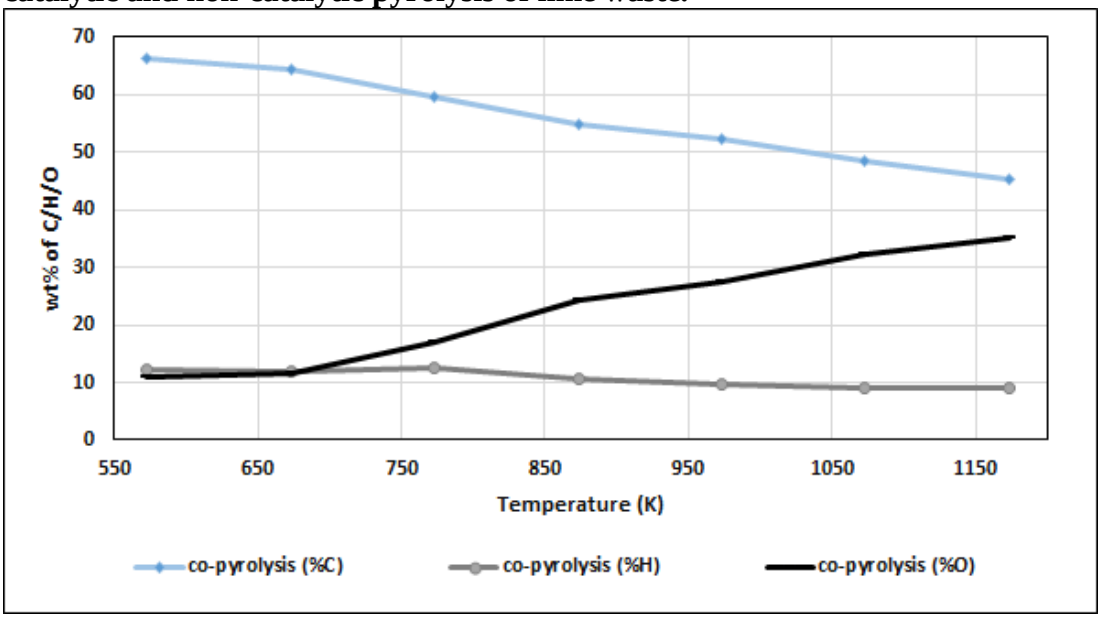

Figure 6.69. Plot of wt.% of compound present in pyro-oil against temperature for catalytic and non-catalytic co-pyrolysis of jute waste.

6.6.5. Structural Characterization of Char from Catalytic and Non-Catalytic Pyrolysis

Fig. 6.70 shows the SEM images of original jute and the solid residue obtained at 600 ^{0}C, with and without alumina. The figure distinctly shows the increase in porosity in presence of catalyst. This elucidates the proposed mechanism of catalytic activity with respect to pyro-oil yield through enhancement of surface area. The values of surface area per unit mass of bio-char obtained through pyrolysis of jute at 600 ^{0}C with and without alumina, as determined using BET method, are provided in Table 6.21. It is also ascertained that the specific surface

area of bio-char obtained through catalytic pyrolysis (5.144 $m^2 g^{-1}$) is higher than that of bio-char of non-catalytic pyrolysis (3.143 $m^2 g^{-1}$) at the same value of reaction temperature. The specific surface area of bio-char of non-catalytic pyrolysis is comparable to those observed by previous researchers during their studies on pyrolysis of saw dust, wheat and flax straws (<5 $m^2 g^{-1}$). [50] The presence of alumina on the pyrolyzing solid during catalytic pyrolysis is also established through the comparison of the XRD spectra, represented in Fig. 6.73, of solid residues of catalytic and non-catalytic pyrolysis. Close observation of the Fig. 6.64 depicting the pattern of char yield against pyrolysis temperature reveals that for both non-catalytic and catalytic process, there is a monotonous decreasing trend over the entire temperature range. The decreasing trend is sharper in case of Al_2O_3 assisted pyrolysis compared to non-catalytic process. The high catalyzing effect on pyro-oil formation may be the underlying reason to explain this observation. Similar kind of observation is obtained for lime wastes, which is shown by the figure 6.71 (SEM images) and 6.74 (XRD spectra) and for co-pyrolysis, which is shown by the figure 6.72 (SEM images) and 6.75 (XRD spectra).

Table 6.21. BET specific surface area of biochar of catalytic and non-catalytic pyrolysis of jute wastes at 600^{0}C

Pyrolysis Process	Specific surface area of char (m^2/g)
Catalytic	5.144
Non-Catalytic	3.143

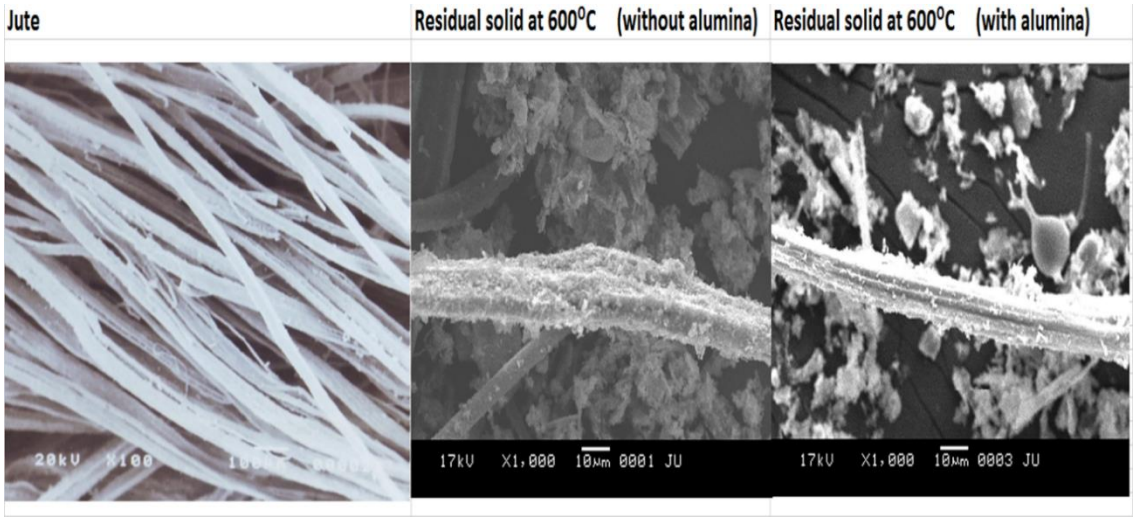

Figure 6.70. SEM images of original jute and the solid obtained at 600 ^{0}C, with and without alumina

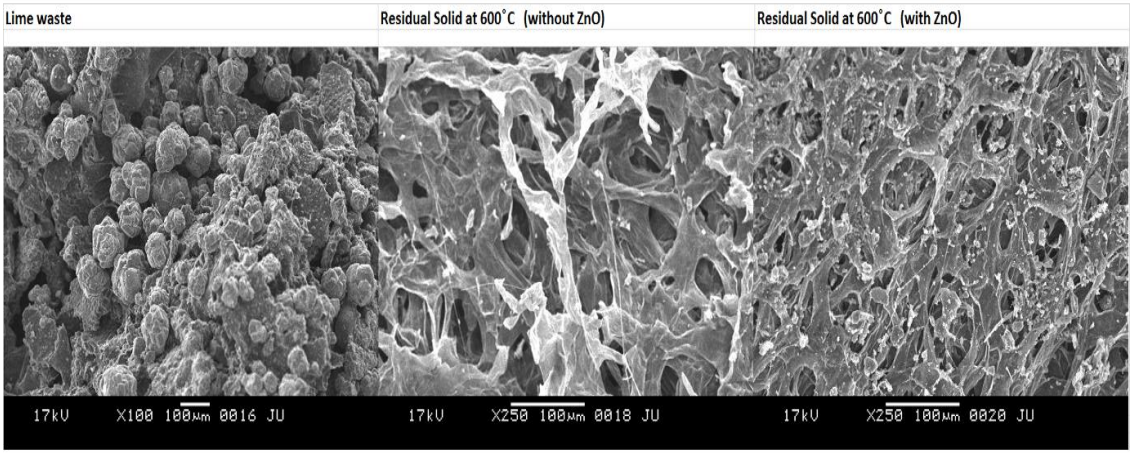

Figure 6.71. SEM images of original lime and the solid obtained at 600 ^{0}C, with and without ZnO

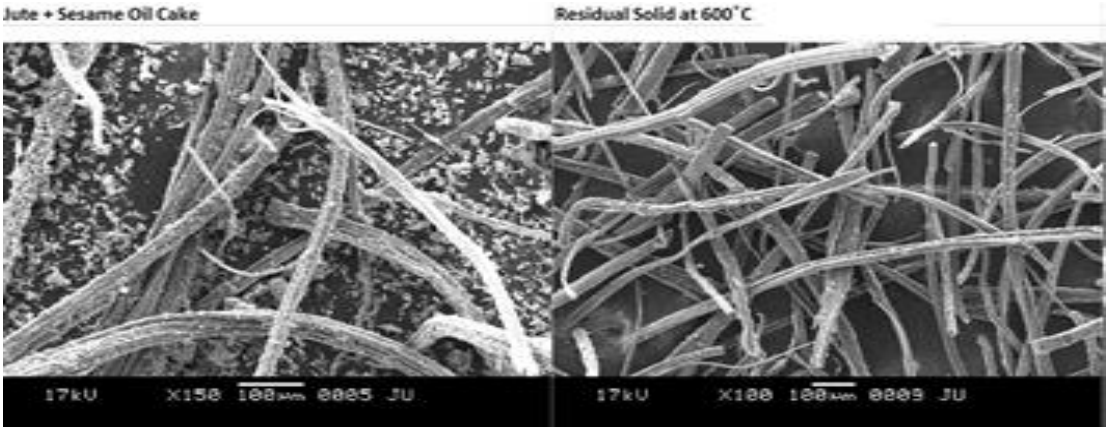

Figure 6.72. SEM images of original co-pyrolysis wastes and the solid obtained at 600 ^{0}C

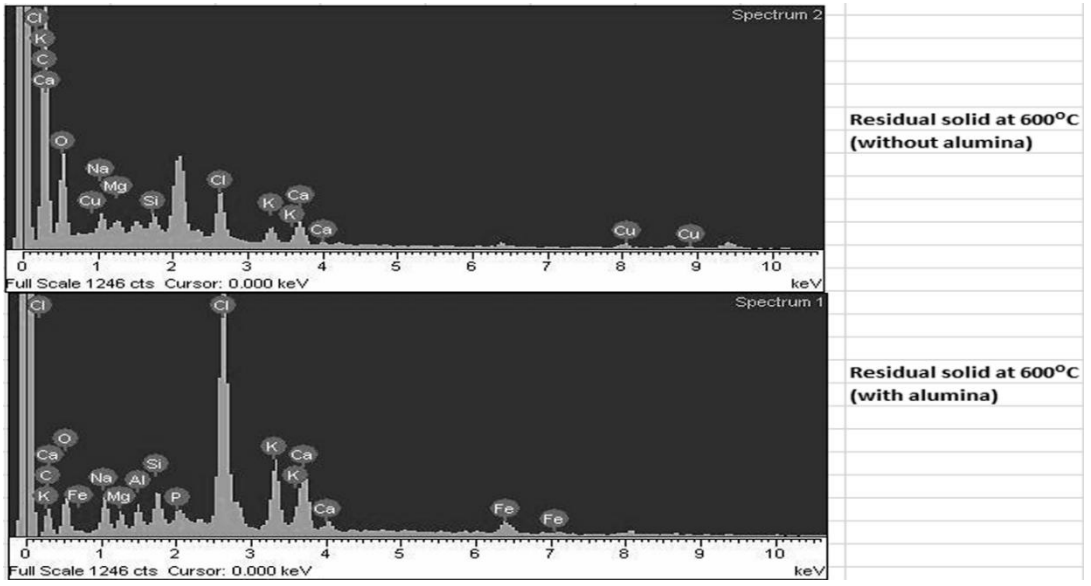

Figure 6.73. XRD spectra of solid residue obtained through non-catalytic and catalytic pyrolysis of jute at 600 ^{0}C.

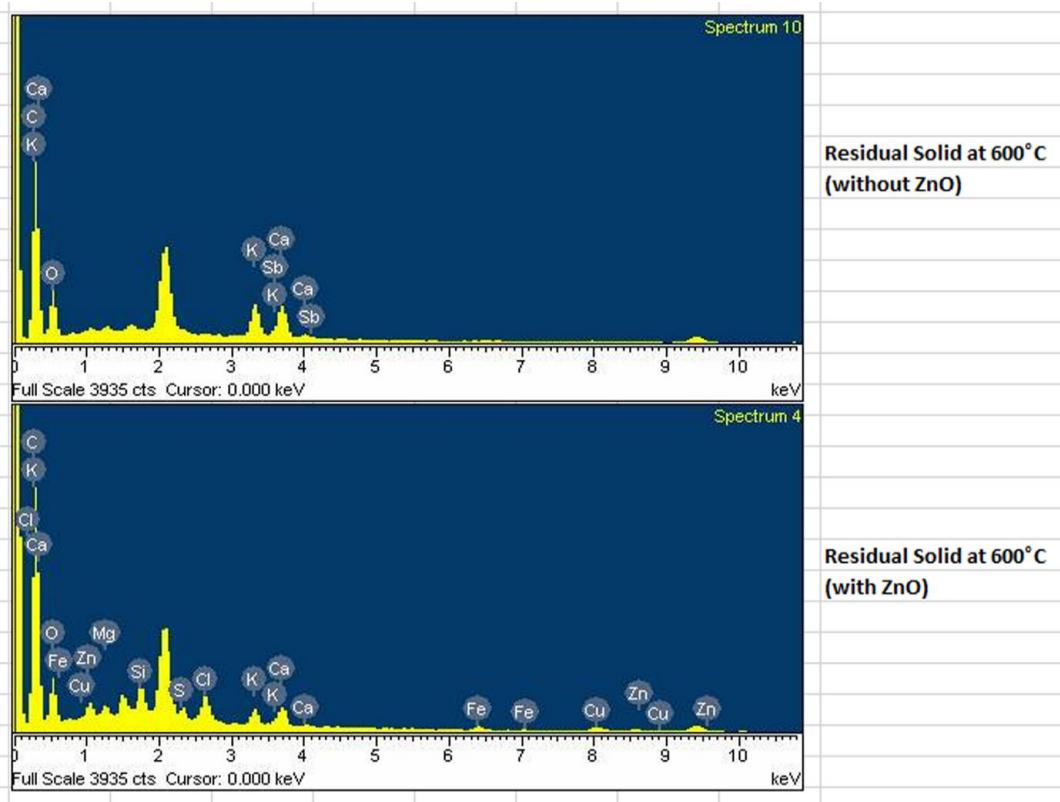

Figure 6.74. XRD spectra of solid residue obtained through non-catalytic and catalytic pyrolysis of lime at 600 ^{0}C.

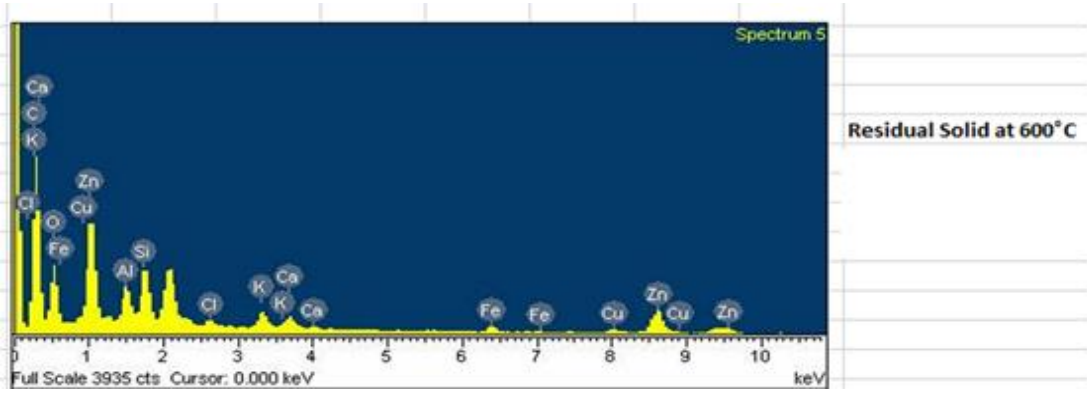

Figure 6.75. XRD spectra of solid residue obtained through non-catalytic and catalytic co-pyrolysis of jute wastes and sesame oil cake at 600 ^{0}C.

6.6.6. pH of Bio-oil

The value of pH of the pyro-oil is shown in Fig. 6.76 -6.78. For pyro-oil obtained through non-catalytic pyrolysis of jute, the pH increases with the rise in temperature till 973K beyond which it falls. In case of catalytic (Alumina) pyrolysis of jute waste, it decreases with the rise in temperature. Therefore, it may be inferred that the pyro-oil obtained through catalytic pyrolysis is, in general, more acidic in comparison to that obtained through non-catalytic process in case of jute wastes.

From the figure 6.77, which represents catalytic (ZnO) and non-catalytic pyrolysis of lime waste, it can be inferred that the pH of lime waste pyro-oil is basic in nature but the presence of catalyst makes the pyro-oil acidic. Figure 6.78 represents co-pyrolysis of jute waste and

sesame oil cake. It can be inferred from the figure that the pH of pyro-oil obtained from co-pyrolysis is acidic in nature whereas the pH of catalytic pyro-oil is basic in nature [51-54].
Since the pyro-oil obtained from non-catalytic and catalytic pyrolysis of any of the feedstocks is either acidic or basic in nature precautions should be taken during storage of the catalytic pyro-oil to avoid corrosion.

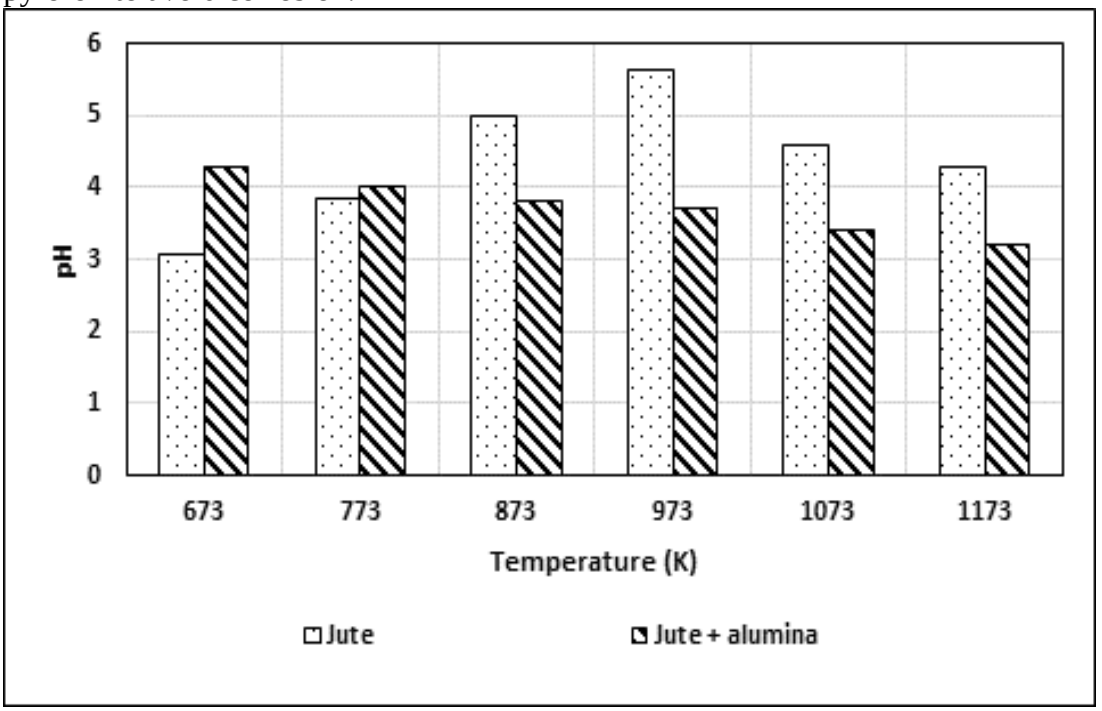

Figure 6.76. Dependence of pH of pyro-oil on the temperature of catalytic and non-catalytic pyrolysis of waste jute.

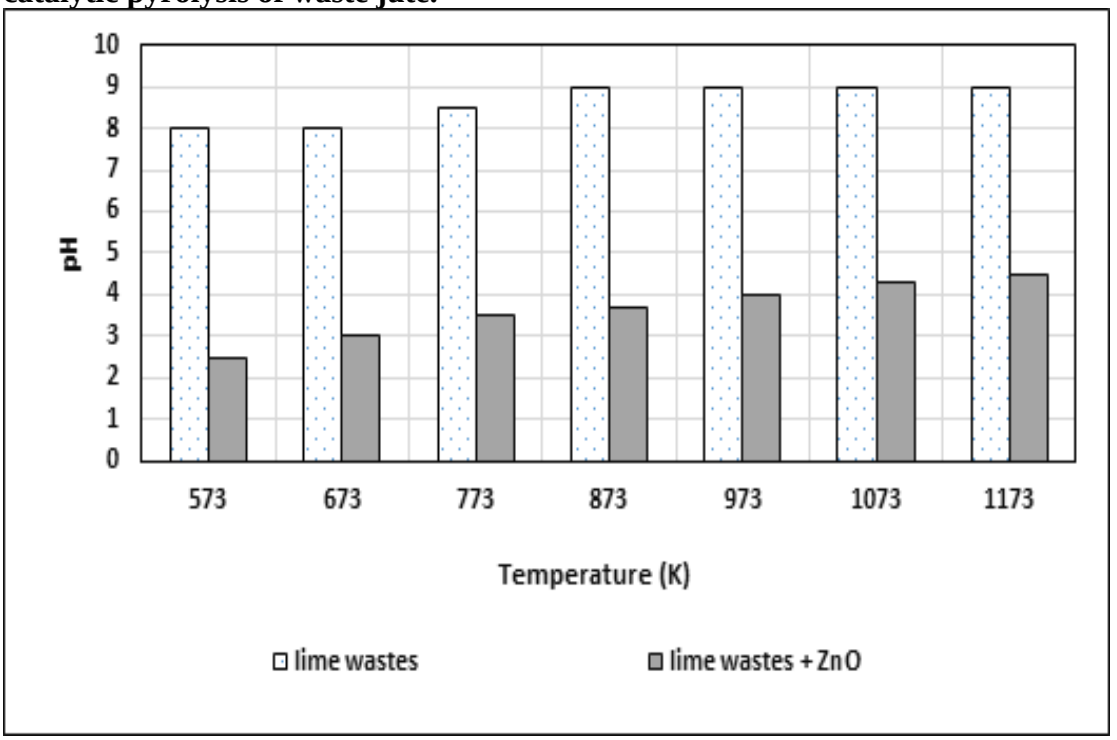

Figure 6.77. Dependence of pH of pyro-oil on the temperature of catalytic and non-catalytic pyrolysis of lime wastes

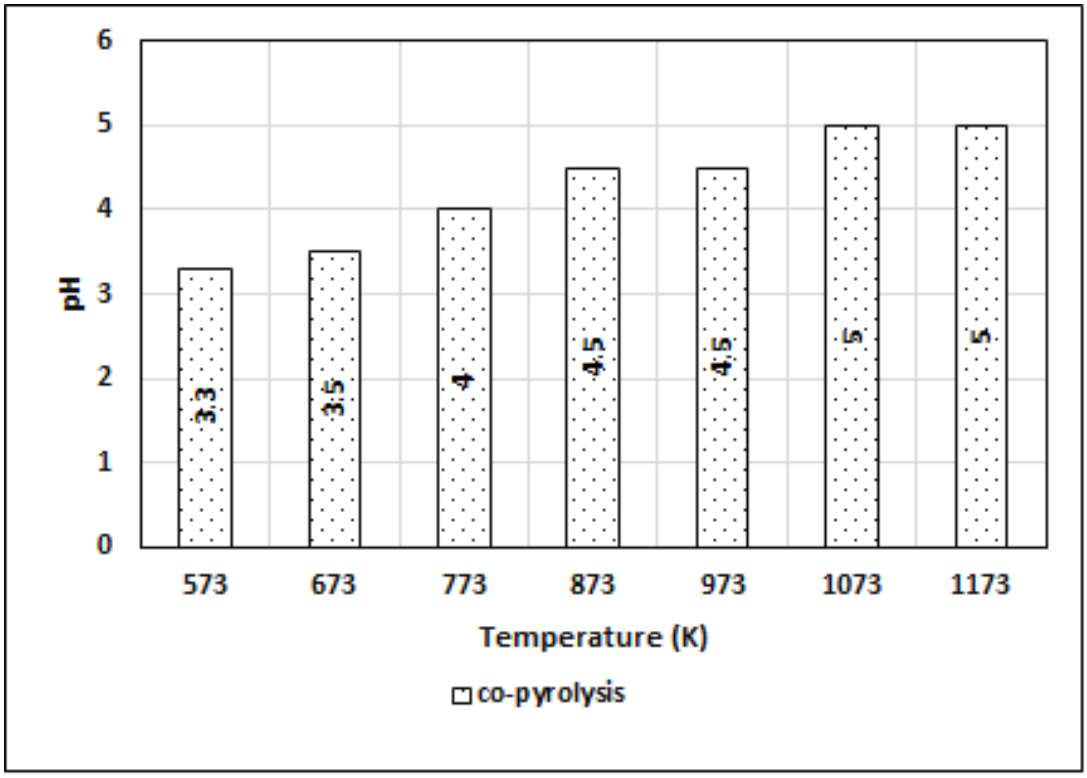

Figure 6.78. Dependence of pH of pyro-oil on the temperature of catalytic and non-catalytic co-pyrolysis of waste jute and sesame oil cake

6.6.7. Calorific value of the products

The calorific values of the pyro-char, pyro-oil are segregated into 6.6.7.1 and 6.6.7.2. respectively.

6.6.7.1. Calorific value of pyro-char

Figure 6.79, 6.80 and 6.81 depict the dependence of calorific value of pyro-char of the catalytic and non-catalytic pyrolysis of waste jute, lime wastes and co-pyrolysis of jute and sesame oil cake respectively as a function of pyrolysis temperature. From the analysis of the figures, it can be inferred that in all cases the calorific value of the pyro-char increases with the rise in pyrolysis temperature. This is due to the increase in the % C and decrease in %O in the char with the increase of pyrolysis temperature.

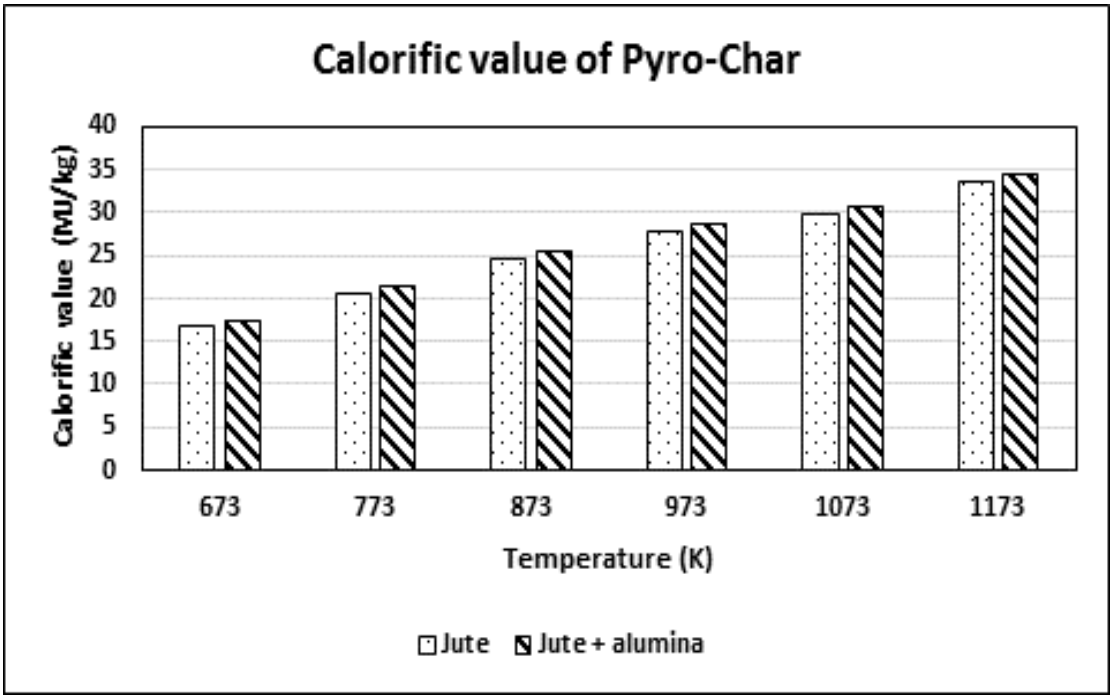

Figure 6.79. Variation of calorific values of char for both catalytic and non-catalytic pyrolysis of waste jute.

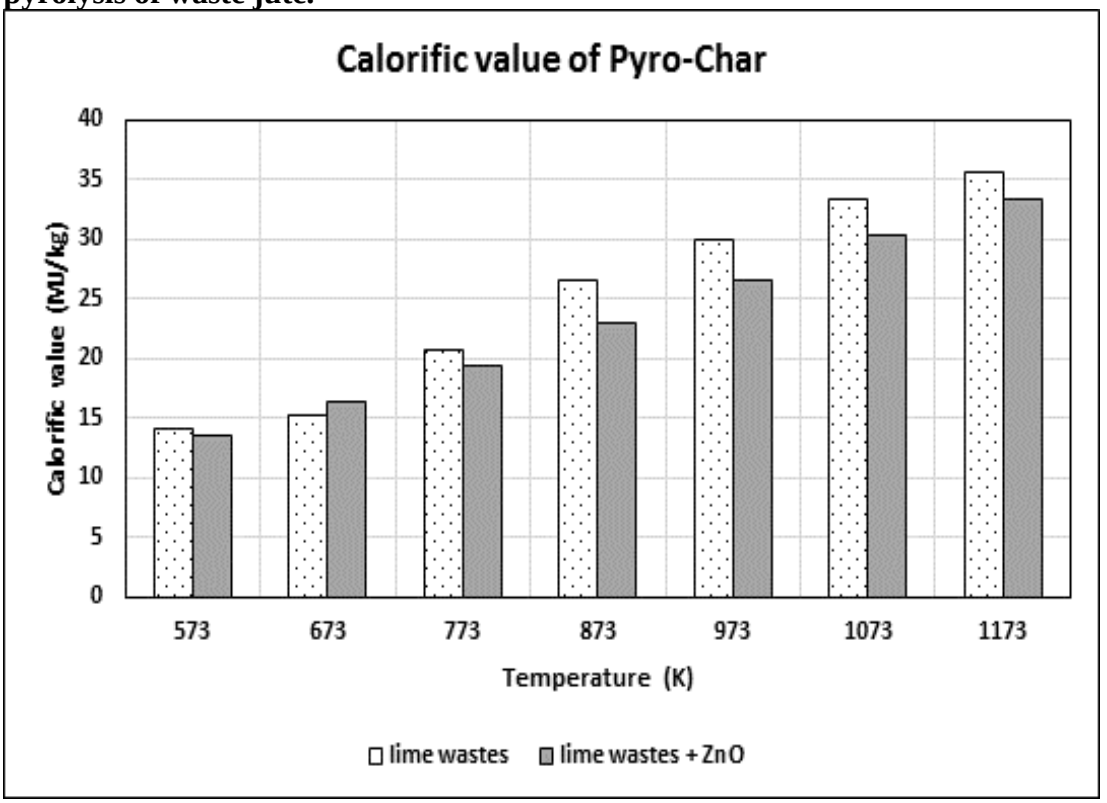

Figure 6.80. Variation of calorific values of char for both catalytic and non-catalytic pyrolysis of lime wastes

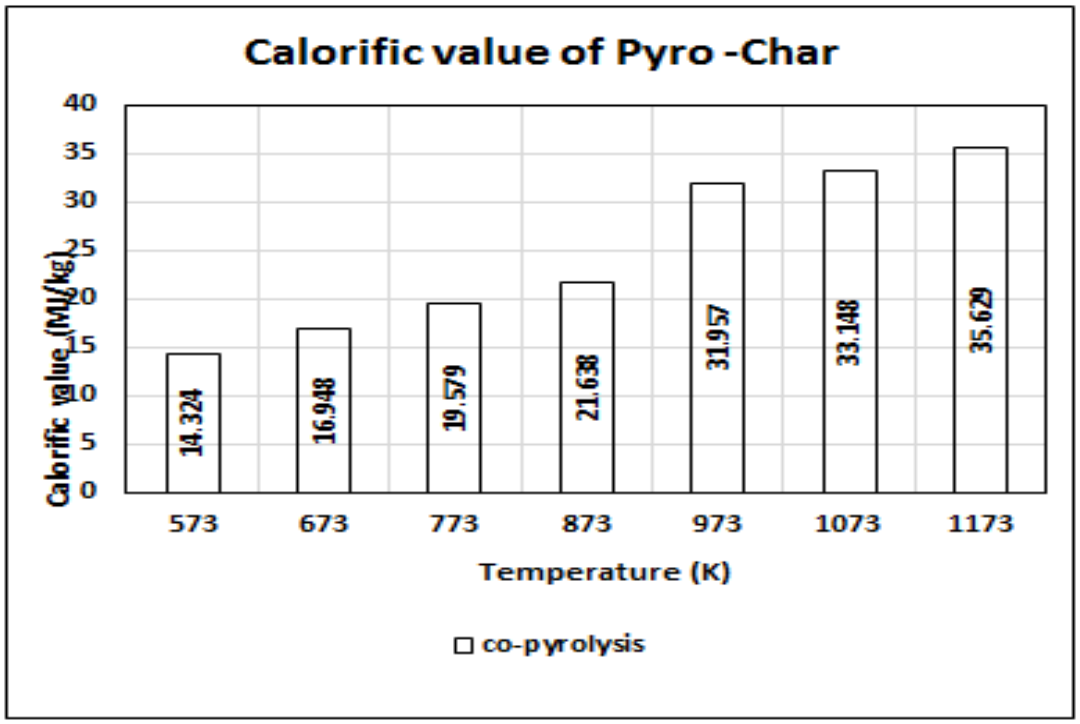

Figure 6.81. Variation of calorific values of char for both catalytic and non-catalytic co-pyrolysis of jute waste and sesame oil cake

6.6.7.2. Calorific value of pyro-oil

Figure 6.82 and 6.83 represent the calorific value of the pyro-oil of the catalytic and non-catalytic pyrolysis of waste jute and lime wastes respectively as a function of pyrolysis temperature. In Figure 6.84, the same plot has been made for the co-pyrolysis of jute wastes and sesame oil cake. In all cases the C_V of puro-oil has decreased with the increase of pyrolysis temperature. This is due to the decrease and increase in the values of %C and %O respectively with the increase of temperature.

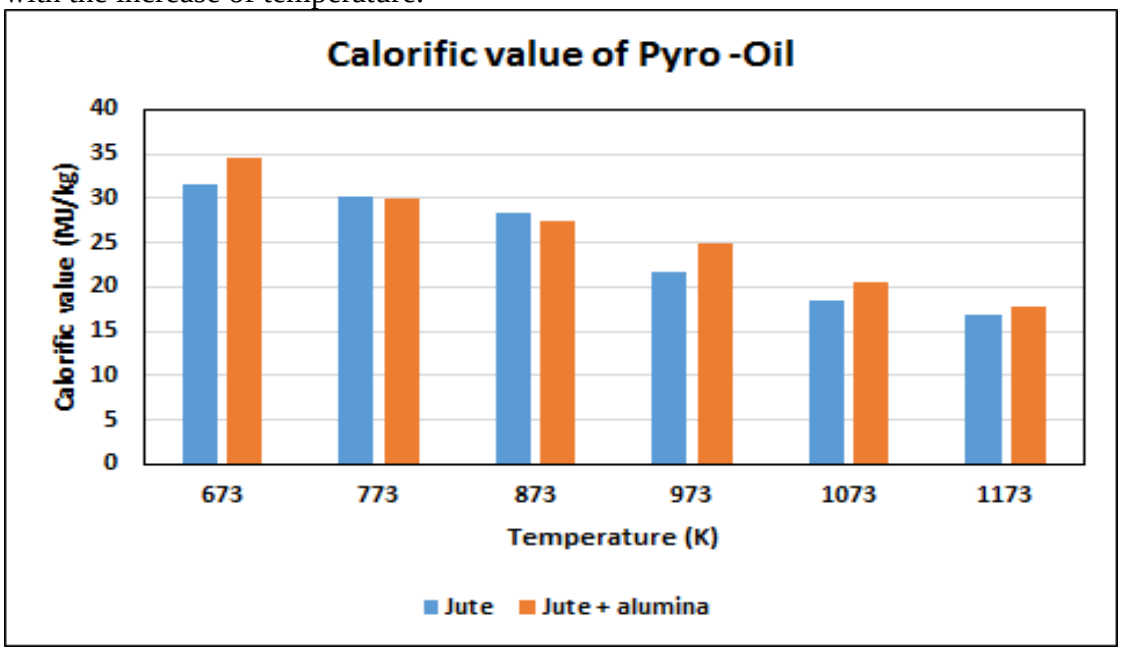

Figure 6.82. Variation of calorific values of pyro-oil for both catalytic and non-catalytic pyrolysis of waste jute.

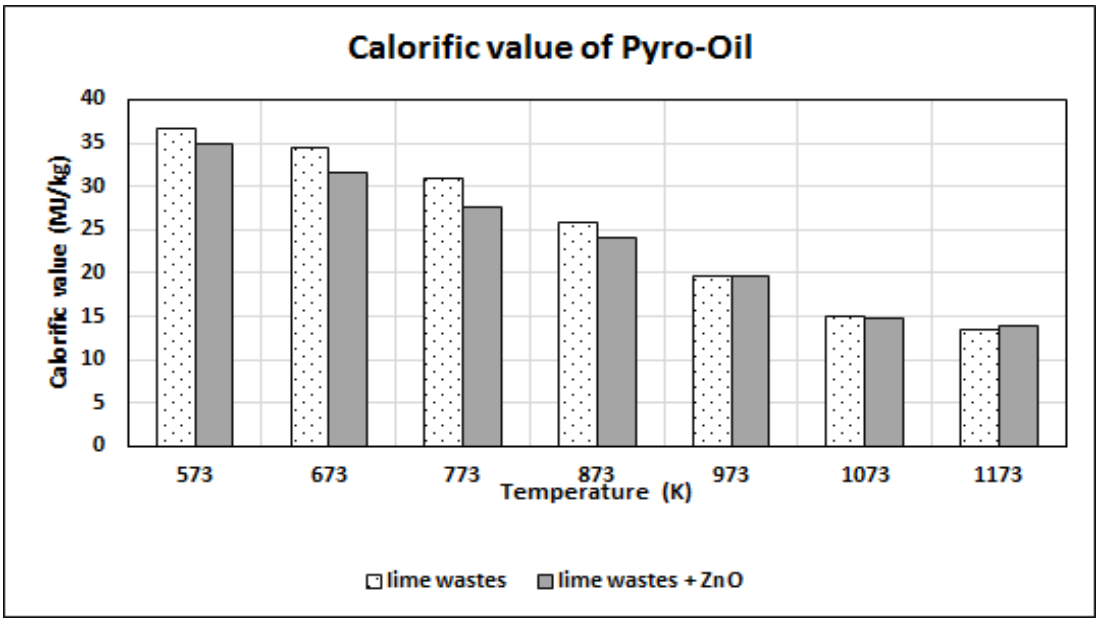

Figure 6.83. Variation of calorific values of pyro-oil for both catalytic and non-catalytic pyrolysis of lime wastes.

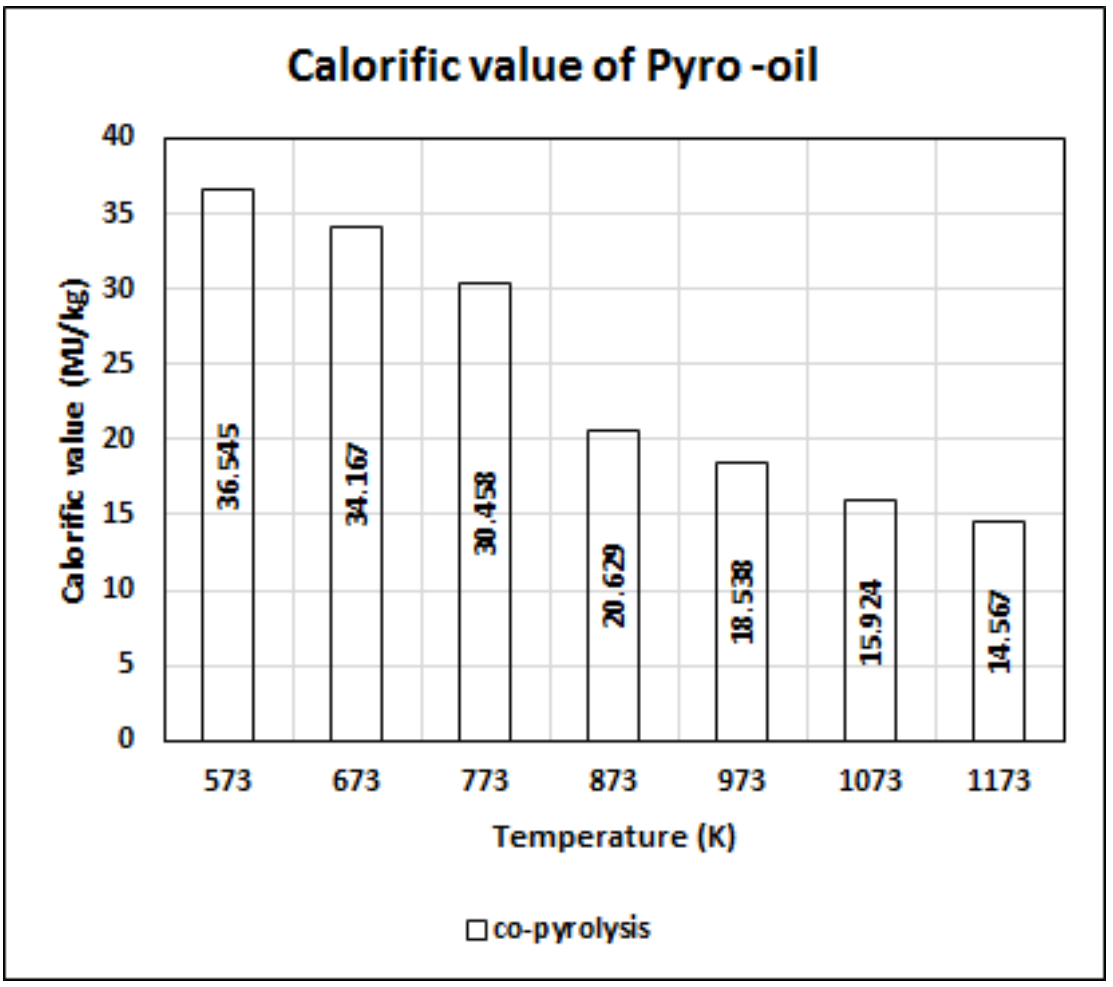

Figure 6.84. Variation of calorific values of pyro-oil for both catalytic and non-catalytic co-pyrolysis of jute wastes and sesame oil cake.

6.6.8. Distillation characterises of pyro-oil

Figure 6.85 – 6.87 represents the variation of initial boiling point (IBP) and final boiling point (FBP) of pyro-oil for non-catalytic and catalytic pyrolysis of jute wastes, lime wastes and co-pyrolysis of jute waste and sesame oil cake. Distillation characteristics of the pyro-oil obtained at different pyrolysis temperature has been determined by ASTM D86 method [55]. From the figure, it is revealed that with the use of catalysts, higher values of IBP and FBP have been obtained. This may be due to higher carbon content in the pyro-oil obtained from catalytic pyrolysis in comparison to that obtained through non-catalytic pyrolysis of the same feedstock at each pyrolysis temperature as described in section 6.6.4.2.

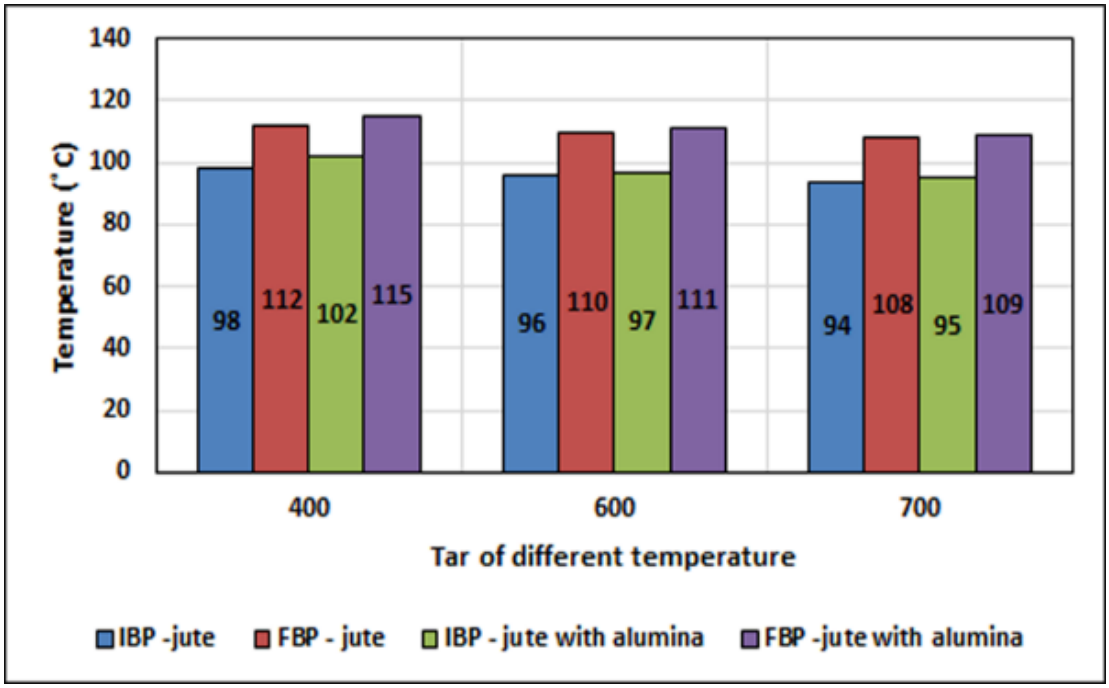

Figure. 6.85. Variation of IBP and FBP of pyro-oil for non-catalytic and catalytic pyrolysis of jute waste with temperature.

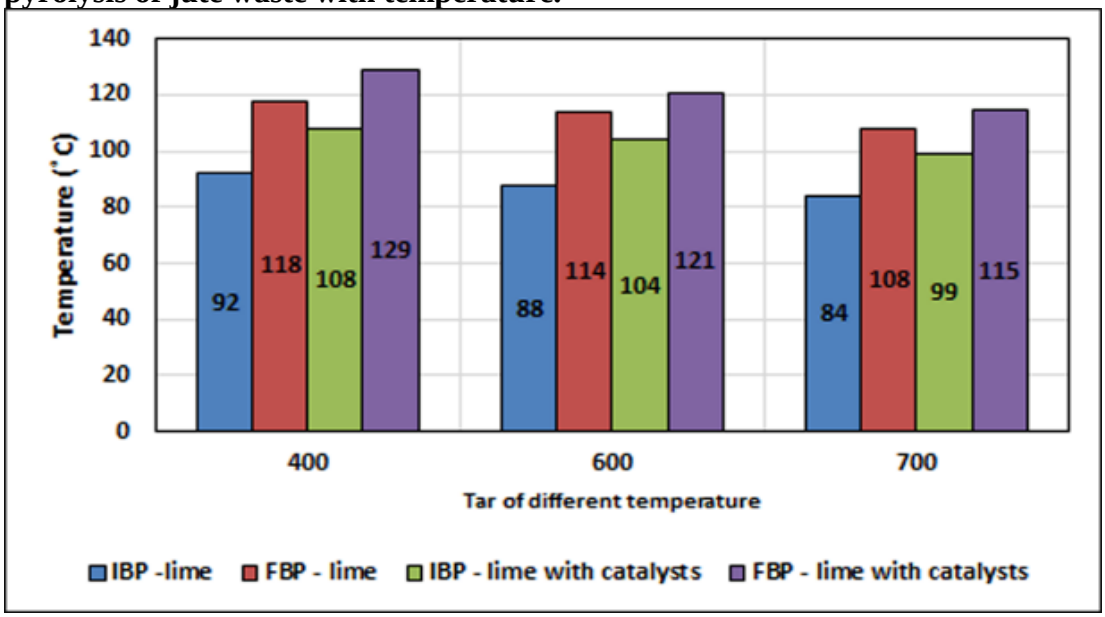

Figure. 6.86. Variation of IBP and FBP of pyro-oil for non-catalytic and catalytic pyrolysis of lime waste with temperature.

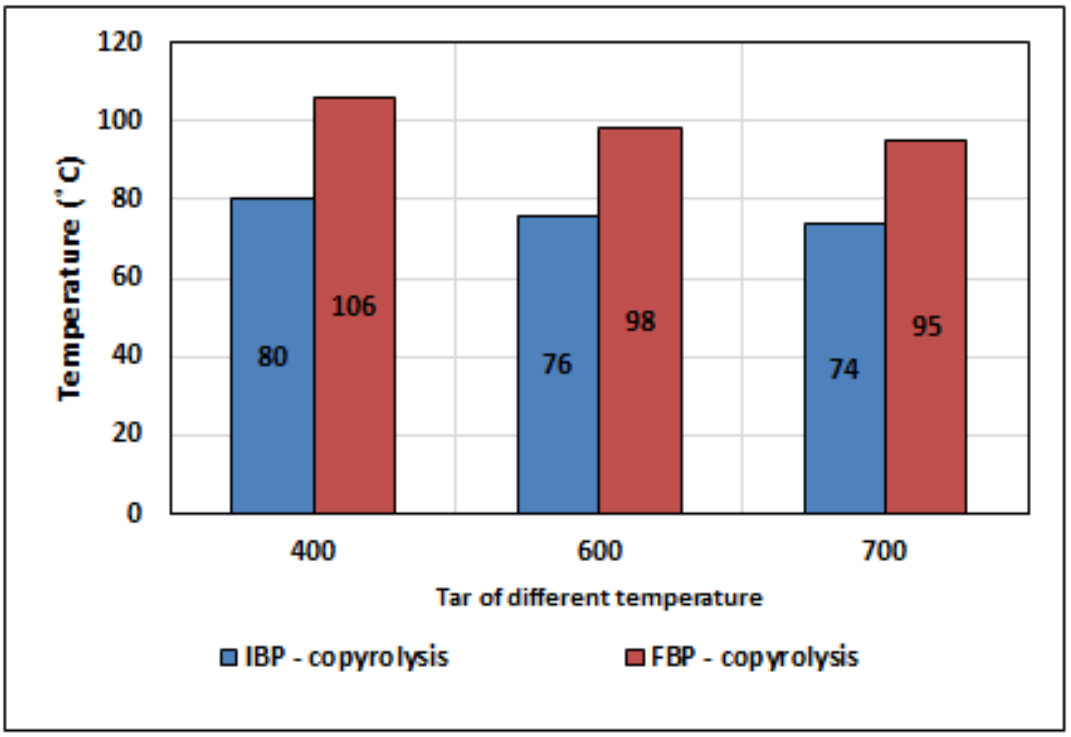

Figure. 6.87. Variation of IBP and FBP of pyro-oil for non-catalytic and catalytic co-pyrolysis of jute waste and sesame oil cake with temperature.

6.6.9. FTIR analysis of the catalytic and non-catalytic pyro-oil derived after pyrolysis of lignocellulosic feedstocks

Figure 6.88 and 6.89 represents the results of FTIR analysis of pyro-oil obtained through non-catalytic and catalytic pyrolysis of jute waste 700^{O}C. Composition of the liquid products are presented in Table 6.21. The table shows the presence of alkanes, alkenes, ketones, aldehydes and carboxylic acids, primary, secondary and tertiary alcohols, ethers and esters, single, polycyclic and substituted aromatics groups and the presence of water impurities and other polymers. The pronounced oxygenated functional groups of O – H; C = O; C – O and aromatic compounds show that the oil is highly oxygenated and therefore, very acidic, as have also been indicated by the elemental composition and the pH value. The high fraction of oxygenated compounds reduces the calorific value of the oil since C = O bonds do not release energy during combustion. Through the comparison of 6.82 and 6.83, it is difficult to effect of catalysis on the FTIR characteristics of pyro-oil The presence of hydrocarbon groups C – H; C = C; and alcohols indicate that the liquids have a potential to be used as fuel. The results of FTIR analysis is comparable to those obtained [56] and Sarkar et. al. [57] during their studies on non-catalytic and catalytic pyrolysis of jute wastes.

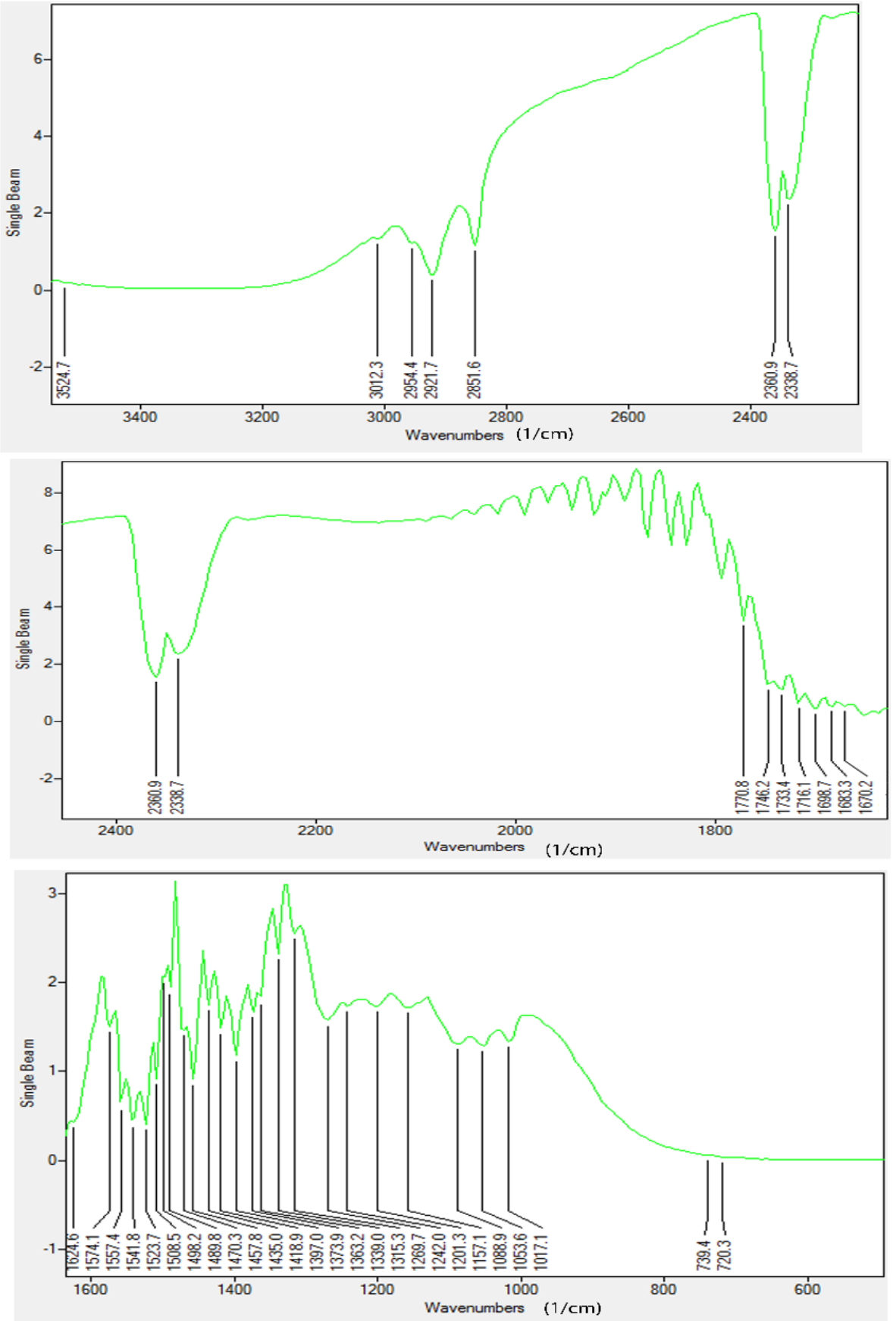

Figure 6.88. FTIR analysis of the pyro-oil of jute waste.

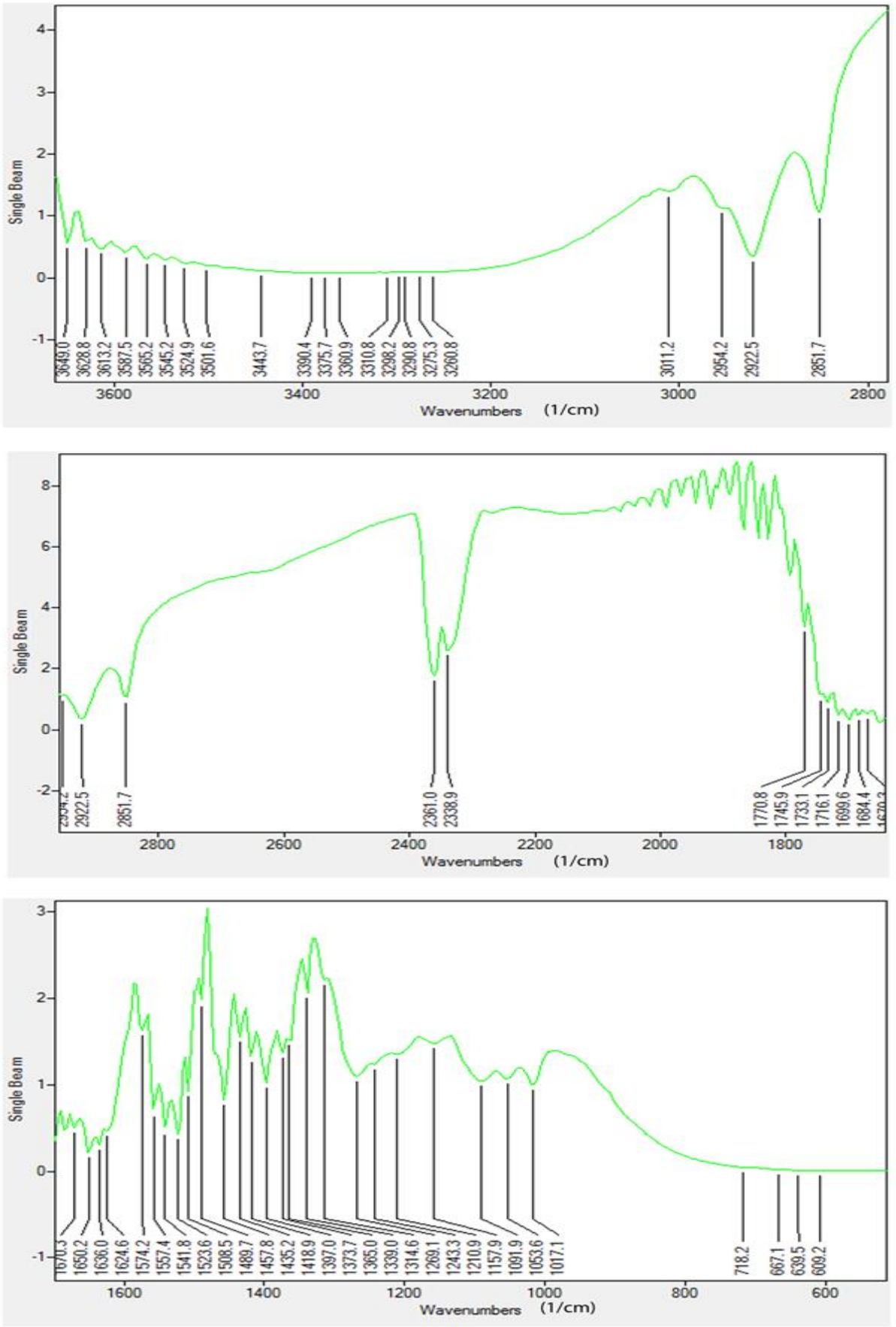

Figure 6.89. FTIR analysis of the pyro-oil of jute waste in presence of alumina.

Figure 6.90 represents the FTIR analysis of the pyro-oil obtained after co-pyrolysis of jute waste and sesame oil cake at 500^{o}C and figure 6.91 represents the analysis of the pyro-oil obtained after co-pyrolysis of jute waste and sesame oil cake with the variation in temperature (300^{o}C – 500^{o}C). Characterization with respect to chemical bonds present in the pyro-oil has been done using FTIR analysis. The functional groups of the pyro-oil obtained at temperature of 500^{o}C or 773K was analyzed by Fourier Transform Infrared (FTIR) spectroscopy to identify the basic compositional groups shown in Fig 6.90 Based on the FTIR results, the functional groups and the indicated composition of the liquid products are presented in Table 6.22. From the close analysis of the table, it appears that the bio-oil is highly oxygenated as indicated by the predominance of oxygenated functional groups namely O – H; C=O; C – O and aromatic compounds. This is also established by the elemental composition (not shown) and the acidic nature, indicated by low value of pH. The high fraction of oxygenated compounds causes the lowering of calorific value of the oil, particularly due to the presence of C=O bonds which do not release energy during combustion [192]. The presence of hydrocarbon groups C – H; C = C; and alcohols indicate that the liquids have a potential to be used as fuel. The results of FTIR analysis is comparable to those obtained by Islam and Nabi, 2005 [56] and Sarkar et. al. [57] during their studies on pyrolysis of jute wastes. The FTIR spectrum of pyro-oil obtained in the temperature range 573K have been shown in the figure 6.85, which shows a decreasing trend of compounds carrying C – O stretching and O – H bonding (1300 – 950) with the increase in temperature. This may probably be due to further cracking of these compounds above 573 K. However, the exact reason is yet to be investigated.

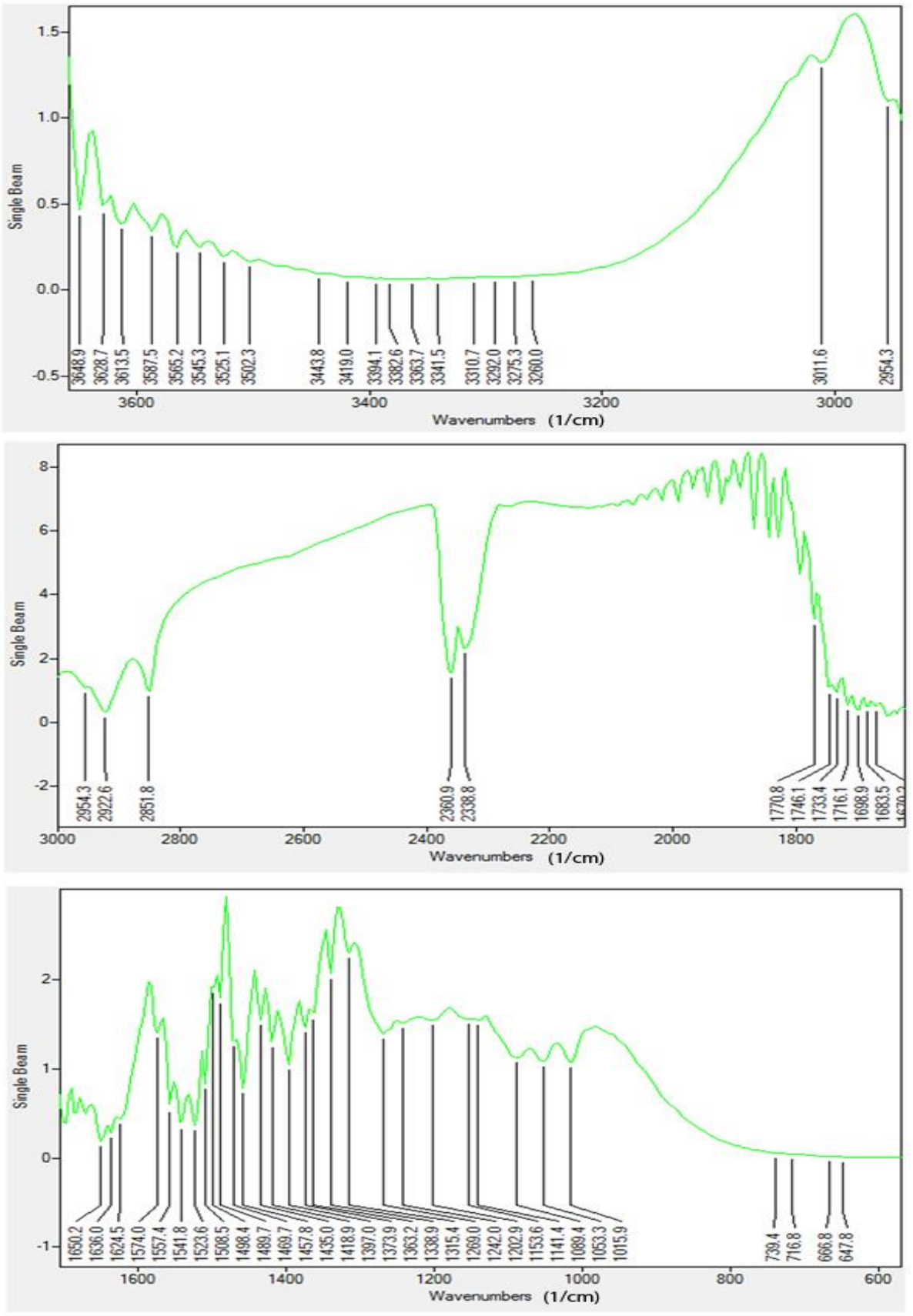

Figure 6.90. FTIR analysis of the pyro-oil obtained by co-pyrolysis at 500ºC.

Table. 6.22. FTIR functional groups and the indicated compounds of pyro-oil.

Frequency Range (cm^{-1})	Groups	Class of compounds
3600 – 3200	O – H stretching	Polymeric O – H
3050 – 2800	C – H stretching	Alkanes
1775 – 1650	C = O stretching	Ketones, Aldehydes, Carboxylic acids
1680 – 1575	C ≡ C stretching	Alkenes
1550 – 1475	$-NO_2$ stretching	Nitrogenous compounds
1490 – 1325	C – H stretching	Alkanes
1300 – 950	C – O stretching, O – H bending	Primary, Secondary and Tertiary alcohols Phenols, esters, ethers
900 – 650	-	Aromatic compounds
900 – 650	-	Aromatic compounds

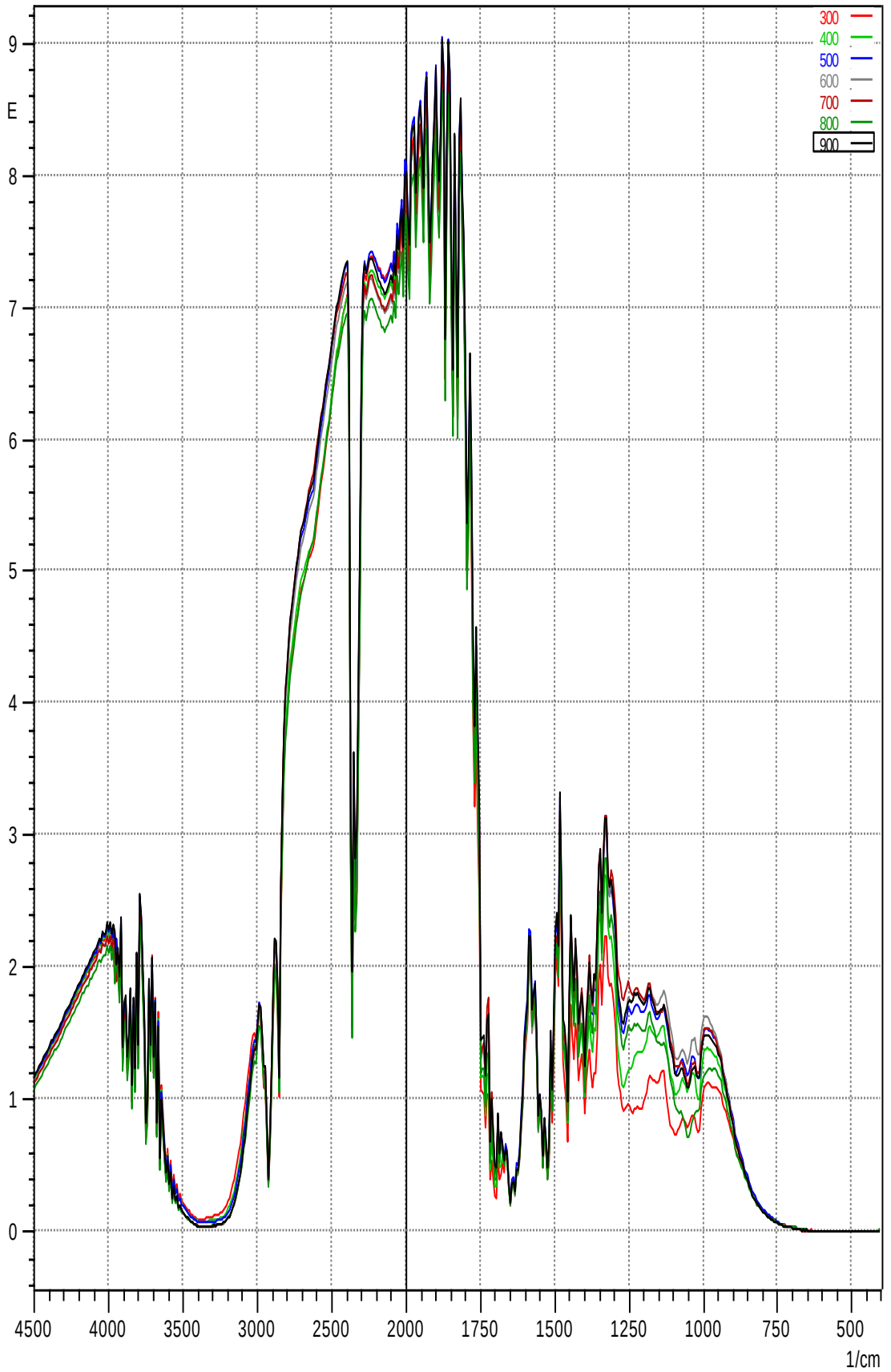

Figure 6.91. FTIR spectrum of pyro-oil obtained at different temperatures by co-pyrolysis.

6.6.10. GC/MS analysis of the pyro-oil

For the qualitative and quantitative characterization of pyro-oil obtained through non-catalytic and catalytic pyrolysis, samples were analyzed with SQ 8 Gas Chromatograph/Mass Spectrometer PerkinElmer [58], equipped with flame ionization and mass spectrometry detectors (GC-PPC-MS) The compounds present in pyro-oil obtained through non-catalytic and catalytic pyrolysis of jute at 600ºC are represented in Table 6.23, 6.24 and lime waste at 500ºC are represented in Table 6.25, 6.26. and co-pyrolysis of jute waste and sesame oil cake are represented in Table 6.27. The Tables provide the lists of compounds with their retention times and prospective uses.

Table 6.23. GC/MS analysis of the pyro-oil of waste jute

Retention time	Name of compound	Molecular Weight	Usage
3.809	1,2,3,6 – tetrahydropyridine-2-carboxylic acid ($C_6H_9NO_2$)	127	As a $GABA_A$ receptor in scientific research [59]
3.939	2-cyclopenten-1-one (C_5H_6O)	82	As a FEMA GRAS flavouring substance [60]
4.829	Oxirane, 2-ethyl-3-propyl –cis ($C_7H_{14}O$)	114	Manufacture of α-amylcinnamaldehyde and lubricant [61]
5.164	1-silacyclo-2,4-Hexadiene (C_5H_6Si)	96	Used as synthetic studies by organic chemists [62]
6.205	1-Ethylcyclopentene (C_7H_{12})	96	Useful compound in organic synthesis. [63]
6.365	1H-imidazole, 4,5 – dihydro- 2 – methyl ($C_4H_8N_2$)	84	Pharmaceutical use. [64]
7.495	Bicyclo [5,3,0] Decane ($C_{10}H_{18}$)	138	Industrial solvent [65]
7.650	2-cyclopenten-1-one,2,3-Dimethyl ($C_7H_{10}O$)	110	Building block in organic synthesis. [66] Drug for genital or sexual disorder. [67]
7.710	Cyclohexanol, 1 – Ethynyl ($C_8H_{12}O$)	124	Pharmaceutical use. [68]
8.135	Pyridine, 5 – methyl (C_6H_7N)	94	Isolated from coal tar and synthesized industrially [69]
9.021	D-Limonene ($C_{10}H_{16}$)	136	Cosmetic usage [70] Solvent for cleaning purpose /paint/biofuel. [71]
9.231	2-cyclopenten-1-one,2,3-Dimethyl [$(CH_3)_2C_5H_4(=O)$]	110	Not reported
9.616	p-cresol (C_7H_8O)	108	Antioxidant [72]

			Used as a used to capture and study the species of orchid bee [73]
10.021	Benzene methanol, 4 – hydroxyl ($C_7H_8O_2$)	124	Use as a flavorants [74], [75]
10.181	Phenol, 2 –methoxy ($C_7H_8O_2$)	124	Dermatology and radical polymerization of monomers [76]
10.406	Bicyclo-[2.2.2] Octane, 2 – methyl (C_9H_{16})	124	Not reported
11.932	5-methoxyindane ($C_{10}H_{12}O$)	148	Commercial bio-conversion of anethole to more valuable compound [77]
12.577	4-pentenoic acid, 5 – ethoxy, ethyl ester, (E)- ($C_{11}H_{12}O_2$)	172	Purification purposes. [78]
13.212	(Z)-4-methyl-5-(2-oxopropylidene)-5H-Furan-2one ($C_8H_8O_3$)	152	Use as an intermediate in the preparation of more complex compounds. [79]
13.488	(S,S,S,S)-1,1'-Bicyyclopentyl-2,2'-Dicarboxaldehyde ($C_{12}H_{18}O_2$)	194	Use as a food additive [80]
13.628	2 cyclopentene-1-acetaldehyde,2-formyl-,Alpha,3 Dimethyl ($C_{10}H_{14}O_2$)	166	Use as an antioxidant for synthetic rubber, polymer and oil derivative [81,82],
14.863	Octadecane, 1- chloro ($C_{18}H_{37}Cl$)	288	Use only in area provided with appropriate exhaust ventilation [83]
15.488	1-methoxy-2-methyl-4-(methylthio) Benzene ($C_9H_{12}OS$)	168	Therapeutic usage [84]
17.249	Phthalic acid, monoethyl ester ($C_9H_8O_4$)	194	Breakdown of glucosinate glucobrassicin[85]
17.824	2-Azetidinone, 1 – phenyl (C_9H_9NO)	147	Biomedical usage [86]
21.901	IH-1,2,3 –Triazole,4-(4-methylphenyl) ($C_3H_6N_4$)	98	For R&D use only [87]

Table 6.24. GC/MS analysis of the pyro-oil derived from catalytic pyrolysis of waste jute

Retention time	Name of compound	Molecular Weight	Usage
3.258	Hydrazine, Trimethyl- ($C_3H_{10}N_2$)	74	used in the alkyne zipper reaction [88]

3.313	Silane, Butyl Trimethyl - ($C_7H_{18}Si$)	130	use as heaters in rapid solidification [89]
3.353	Silane, Trimethyl propyl - ($C_6H_{16}Si$)	116	used under atmospheric pressure at 0 ^{0}C in dichloromethane [90]
4.999	1H –Imidazole – 4 – methanol ($C_4H_6N_2O$)	98	used in the coordination chemistry [91]
5.054	Cyclopentane, 1 – Hydroxymethyl - 1,3 – dimethyl - ($C_8H_{16}O$)	128	As air freshener [92] Froth floatation process for cleaning coal where of 95% MCHM, 4% water and 0.1% 4-methylcyclo hexamethanolmonoether. [93]
5.114	Levoglucosenone ($C_6H_6O_3$)	126	uses hydroxyquinol as a substrate with oxygen to produce 3-hydroxy-cis,cis-muconate.[94,110] Phloroglucinol is mainly used as a coupling agent in printing [95,110] It is useful for the industrial synthesis of pharmaceutical [74, 35] and explosive (TATB) [96, 110]
6.025	Trans, Trans and trans, Cis - 1,8 – Dimethyl spiro [5,5] undecane ($C_{13}H_{24}$)	180	Pharmacology [97]
6.345	2,2 – Dimethyl hex – 4 – Enylamine ($C_8H_{17}N$)	127	Not reported
7.245	Trans, Cis -1,8 – Dimethyl spiro [4,5] Decane ($C_{21}H_{27}ClO_4S$)	166	Not reported
7.620	2 – cyclopenten - 1- one, 2,3 – dimethyl ($C_7H_{10}O$)	110	Used as an antioxidant for synthetic rubber, polymer and oil derivative [98]
8.145	Pyrimidine, 5 – methyl (C_6H_7N)	94	Isolated from coal tar and synthesized industrially [99]
9.016	D – limonene ($C_{10}H_{16}$)	136	Cosmetic usage [100] Solvent for cleaning purpose /paint/biofuel. [101]
9.701	p-cresol (C_7H_8O)	108	Antioxidant [102]
10.026	Silane, Tetraethenyl ($C_8H_{12}Si$)	136	Used in plating, important material for producing catalyst, other silver compounds and paste [103]

11.952	1,3,2 – Dioxaborolane, 2 – phenyl- ($C_8H_9BO_2$)	148	Used to the myocardium [104]
12.252	(Z) – 4- Methyl – 5 – (2-oxo propylidene) – 5H – Furan – 2 – one ($C_8H_8O_3$)	152	Food preparation [105] Pyrolysis oil [106] Bio-fuel derived from woody biomass [107]
13.713	Formic acid, 2,6 – dimethoxy phenyl ester ($C_9H_{10}O_4$)	182	Not reported
14.233	Phenol, 2, 6 – Dimethoxy - ($C_8H_{10}O_3$)	154	Not reported
15.488	4-METHOXY-2-METHYL-1-METHYLSULFANYL-BENZENE ($C_9H_{12}OS$)	168	Not reported
16.709	1- acetyl – 3 – (4 – pyridyl) – pyrazoline ($C_{10}H_{11}N_3O$)	189	Not reported
17.244	N-nitrosonornicotine ($C_9H_{11}N_3O$)	177	Curing, aging, processing and smoking of tobacco [108,109]
17.824	2 - propen -1 – one, 2 – methyl – 1 – phenyl ($C_{10}H_{10}O$)	146	Not reported
19.170	2 – ethyl – 2 – phenylaziridine ($C_{10}H_{13}N$)	147	Not reported
20.946	2 – methyl benzyl phosphonic acid ($C_{12}H_{19}O_3P$)	186	Not reported
21.131	5 – phenylisoxazoline (C_9H_9NO)	147	Breakdown of glucosinate glucobrassicin [84]
21.701	Trans – 1 – cyano – 2 – phenyl cyclopropanol (C_5H_{10})	159	Not reported
22.231	2,5,6 – trimethylbenzimi	160	Not reported

		dazole ($C_{10}H_{12}N_2$)		

Table 6.25. GC/MS analysis of the pyro-oil of lime waste

No	Retention time	Name of Compound	Molecular weight	Usages
1	2.13	1,2-Dimethylbenzene (C_8H_{10})	106	1. Areas of application include the printing, rubber, and leather industries. It is a common component of ink, rubber, and adhesives [147] 2. used in the laboratory to make baths with dry ice to cool reaction vessels [148]
2	3.35	D – limonene ($C_{10}H_{16}$)	136	Cosmetic usage [140] Solvent for cleaning purpose /paint/biofuel. [141]
3	4.56	m-Ethyl methyl benzene (C_9H_{12})	120	1. Used as a common solvent, e.g. for paints, paint thinners, silicone sealants, many chemical reactants, rubber, printing ink,adhesives (glues) , lacquers, leather tanners, and disinfectants [149] 2. Used as a fuels that have recently included in jet fuel surrogate blends [150]
4	6.66	(4E,6Z)-2,6-Dimethyl-2,4,6 Octatriene ($C_{10}H_{16}$)	136	used as a perfume component [151], [152]
5	7.85	1,2,3 Trimethyl benzene (C_9H_{12})	120	It is isolated from the C_9 aromatic hydrocarbon fraction during petroleum distillation. It is also generated by methylation of toluene and xylenes [153]
6	9.45	2,6 Octadiene - 2,6-Dimethyl (E) ($C1_0H_{18}$)	138	Not found
7	9.92	Trycyclo [5.2.1.0.1,5] Decane ($C_{10}H_{17}$)	137	Not found
8	10.41	1,4 -Diethyl benzene ($C_{10}H_{14}$)	134	Not found
9	10.62	Citronellal ($C_{10}H_{18}O$)	154	Used as a strong antifungal qualifier. [154]
10	10.71	β-ionone ($C_{13}H_{20}O$)	192	used in perfumery and flavouring to recreate their scent [155], [156]
11	10.75	Octantal ($CH_3(CH_2)_6CHO$)	128	used commercially as a component in perfumes and in flavor production for the food industry [157]
12	11.40	Phenol (C_6H_6O)	94	1. used medically to help sore throat [119] 2.preparation of cosmetics including sunscreens and hair colouring [120] and skin lightening preparation [121]
13	12.51	Methyl hydroquinone ($C_6H_6O_2$)	110	used as a topical application in skin whitening to reduce the color of skin [122,123]

14	13.78	Guaiacol ($C_7H_8O_2$)	124	Guaiacol is a precursor to various flavorants, such as eugenol[124] and vanillin.[125] Its derivatives are used medicinally as an expectorant, antiseptic, and local anesthetic.
15	14.44	5-methyl-guaiacol ($C_8H_{10}O_2$)	138	Not found
16	14.62	4-propyl guaiacol ($C_{10}H_{14}O_2$)	166	Used medicinally as an expectorant, antiseptic, and local anesthetic. [124], [125]
17	15.50	Isoeugenol ($C_{10}H_{12}O_2$)	164	Not found
18	15.76	Vanillin ($C_8H_8O_3$)	152	1.used in the fragrance industry, in perfumes, and to mask unpleasant odors or tastes in medicines, livestock fodder, and cleaning products. [132] 2. used as a chemical intermediate in the production of pharmaceuticals and other fine chemicals. In 1970, more than half the world's vanillin production was used in the synthesis of other chemicals, [133] but as of 2004, this use accounts for only 13% of the market for vanillin. [133]
19	15.89	Acetovanillone ($C_9H_{10}O_3$)	166	Used in medical treatments like arthritic [158], Bowel disease [159], asthmatic [160], Atherosclerosis [160], Familial [161] and Erectile dysfunction [162], [163]
20	16.88	Homovanillyl alcohol ($C_9H_{12}O_3$)	168	Not found
21	17.15	Homovanillic acid ($C_9H_{10}O_4$)	182	used as a reagent to detect oxidative enzymes, and is associated with dopamine levels in the brain. [164]
22	17.25	Homosyringric acid ($C_{10}H_{12}O_5$)	212	Not found
23	17.67	Sringaldehyde ($C_9H_{10}O_4$)	182	Not found
24	17.86	Acetosyringone ($C_{10}H_{12}O_4$)	196	Not found
25	17.92	Butylated hydroxytoluene ($C_{15}H_{24}O$)	220	Used as food additive, household product ingredient, industrial additive, personal care product/cosmetic ingredient, pesticide ingredient, plastic/Rubber ingredient and Medical/Veterinary/Research [165]
26	18.23	m-cresol (C_7H_8O)	108	1.Used to synthetic vitamin E [166] 2. used as a solvent for dissolving polymers, e.g., polyaniline [167]
27	19.08	2,4 xylenol ($C_8H_{10}O$)	122	used in the manufacture of antioxidants [166]

28	20.34	2-allyl-p-cresol ($C_{10}H_{12}O$)	148	Used for synthetic intermediates to other compounds and materials, including plastics, pesticides, pharmaceuticals, and dyes [143]
29	21.56	3-methoxy-5-methylphenol ($C_8H_{10}O_2$)	138	Not found
30	21.99	3-methoxy-catechol ($C_7H_8O_3$)	140	Not found
31	22.49	4-methyl-catechol ($C_7H_8O_2$)	124	Not found
32	22.86	4-ethyl-catechol ($C_8H_{10}O_2$)	138	used as a precursor to fine chemicals such as perfumes and pharmaceuticals. [127]

Table 6.26. GC/MS analysis of the pyro-oil derived from catalytic pyrolysis of lime waste

No	Retention time	Name of Compound	Molecular weight	Usages
1	3.09	Hydrazine, Trimethyl – ($C_3H_{10}N_2$)	74	Not found
2	5.45	Cyclopetane, 1-hyroxymethyl-1,3-dimethyl ($C_8H_{16}O$)	128	Not found
3	6.81	2,3 Butanedione ($C_4H_6O_2$)	86	Production from glucose by fermentation [137]
4	7.52	Pyrimidine, 5-methyl ($C_4H_4N_2$)	80	Not found
5	9.05	Levoglucosenone ($C_6H_6O_3$)	126	uses hydroxyquinol as a substrate with oxygen to produce 3-hydroxy-cis,cis-muconate.[117,116]
6	10.82	2-Hydroxy-3-oxobutanal ($C_4H_6O_3$)	102	Not found
7	11.02	Succinaldehyde ($C_4H_6O_2$)	86	Used as a crosslinking agent but is less widely used than the related dialdehyde glutaraldehyde [138]
8	11.36	D – limonene ($C_{10}H_{16}$)	136	Cosmetic usage [140] Solvent for cleaning purpose /paint/biofuel. [141]

9	11.56	Citronellal ($C_{10}H_{18}O$)	154	Used as a strong antifungal qualifier. [154]
10	11.60	β-ionone ($C_{13}H_{20}O$)	192	used in perfumery and flavouring to recreate their scent [155], [156]
11	11.62	Octantal ($CH_3(CH_2)_6CHO$)	128	used commercially as a component in perfumes and in flavor production for the food industry [157]
13	11.66	β-sinensal ($C_{15}H_{22}O$)	218	Not found
14	11.70	wine lactone ($C_{10}H_{14}O_2$)	166	Not found
15	12.09	p-cresol (C_7H_8O)	108	Antioxidant [142]
16	12.71	2(5H) – Furanone ($C_4H_4O_2$)	84	used in: • synthesis of (+)-L-733,060, (+)-CP-99,994 and (2S,3R)-3-hydroxypipecolic acid [139] • synthesis of 5-substituted 2(5H) furanones (γ-butenolides) via direct aldol reaction with aromatic aldehydes catalyzed by bifunctional aminothiourea and aminosquaramide organocatalysts [139] • Michael addition reactions for synthesis of lignans [139] • three-component Michael-Aldol reactions with an aldehyde and a thiolate [139] or carbanion [139]
17	13.99	4-Hydroxy-5,6-dihydro-(2H)-pyran-2-one ($C_5H_6O_3$)	114	Not found
18	14.50	Guaiacol ($C_7H_8O_2$)	124	Guaiacol is a precursor to various flavorants, such as eugenol[124] and vanillin.[125] Its derivatives are used medicinally as an expectorant, antiseptic, and local anesthetic.
19	14.75	Cresol (C_7H_8O)	108	Used for synthetic intermediates to other compounds and materials, including plastics, pesticides, pharmaceuticals, and dyes [143]
20	15.41	5-methyl-guaiacol ($C_8H_{10}O_2$)	138	Not found
21	15.43	4-methyl-guaiacol ($C_8H_{10}O_2$)	138	Not found
22	16.00	4-Ethyl guaiacol ($C_9H_{12}O_2$)	152	Not found
23	17.34	4-vinylguaiacol ($C_9H_{10}O_2$)	150	used as a flavoring agent [144]

24	17.52	Vanillin ($C_8H_8O_3$)	152	1.used in the fragrance industry, in perfumes, and to mask unpleasant odors or tastes in medicines, livestock fodder, and cleaning products. [132] 2. used as a chemical intermediate in the production of pharmaceuticals and other fine chemicals. In 1970, more than half the world's vanillin production was used in the synthesis of other chemicals, [133] but as of 2004, this use accounts for only 13% of the market for vanillin. [133]
25	18.42	Isoeugenol ($C_{10}H_{12}O_2$)	164	Not found
26	19.08	Homovanillic acid ($C_9H_{10}O_4$)	182	used as a reagent to detect oxidative enzymes, and is associated with dopamine levels in the brain. [164]
27	19.95	Syringol ($C_8H_{10}O_3$)	154	Used as food additives and contaminants [129]
28	21.46	4-Vinylsyringol ($C_{10}H_{12}O_3$)	180	Used as an antioxidant [145]
29	21.74	4-allyl-syringol ($C_{11}H_{14}O_3$)	194	used in perfumes, flavorings, and essential oils. It is also as a local antiseptic and anaesthetic [130]
30	22.61	Sringaldehyde ($C_9H_{10}O_4$)	182	Not found
31	22.89	Acetosyringone ($C_{10}H_{12}O_4$)	196	Used as food additives and contaminants [129]
32	23.05	4-propenyl Syringol (trans) ($C_{11}H_{14}O_3$)	194	Not found
33	23.81	m-cresol (C_7H_8O)	108	1.Used to synthetic vitamin E [166] 2. used as a solvent for dissolving polymers, e.g., polyaniline [167]
34	24.01	2-allyl-p-cresol ($C_{10}H_{12}O$)	148	Used for synthetic intermediates to other compounds and materials, including plastics, pesticides, pharmaceuticals, and dyes [143]
35	24.12	3,4-dimethoxy-phenol ($C_8H_{10}O_3$)	154	Not found
36	24.26	3-hydroxy-benzaldehyde ($C_7H_6O_2$)	122	Not found
37	24.35	4-hydroxy-2-methoxyxcinamaldehyd	178	use in a study to investigate the antioxidant and antiradical activities of ferulates using a β-carotene-linoleate model system and a DPPH radical scavenging assay [168]

		e ($C_{10}H_{10}O_3$)		
38	24.56	3-methoxy-catechol ($C_7H_8O_3$)	140	Not found
39	24.62	4-methyl-catechol ($C_7H_8O_2$)	124	Not found
40	24.66	4-ethyl-catechol ($C_8H_{10}O_2$)	138	used as a precursor to fine chemicals such as perfumes and pharmaceuticals. [127]
41	24.89	5-Phenylisoox azoline (C_9H_7NO)	145	Not found

Figure. 6.27. GC/MS analysis of the pyro-oil derived from co-pyrolysis of waste jute and sesame oil cake

No	Retention time	Name of Compound	Molecular weight	Usages
1	3.35	2-octanone ($C_8H_{16}O$)	128	food additive permitted for direct addition to food for human consumption as a synthetic flavouring substance and adjuvant in accordance with the following conditions: 1) the quantity added to food does not exceed the amount reasonably required to accomplish its intended physical, nutritive, or other technical effect in food, and 2) when intended for use in or on food it is of appropriate food grade and is prepared and handled as a food ingredient. [111]
2	5.18	Decane ($C_{10}H_{22}$)	174	Used for industrial purposes [112]
3	7.02	Cyclodecane ($C_{10}H_{20}$)	140	temporary protection of sensitive surfaces [113]
4	8.16	2-dodecanone ($C_{12}H_{24}O$)	184	2-Dodecanone was used in the synthesis of brushed block copolymer by conjugating with 2-butanone, 2-hexanone, 2-octanone and 2-decanone through an acid-labile hydrazone linker to poly (ethylene glycol)-poly (aspartate hydrazide) block copolymers [114]
5	8.95	7-tridecanone ($C_{13}H_{26}O$)	198	Not found
6	9.45	8-heptadecene ($C_{17}H_{34}$)	238	Use of allogeneic, radiation-sterilised bone blocks in reconstruction of the atrophied alveolar ridge in the maxilla and mandible [115]
7	9.92	Levoglucosenone ($C_6H_6O_3$)	126	uses hydroxyquinol as a substrate with oxygen to produce 3-hydroxy-cis,cis-muconate.[117,116]

8	10.43	Phenol (C_6H_6O)	94	1. used medically to help sore throat [118] 2.preparation of cosmetics including sunscreens and hair colouring [119] and skin lightening preparation [120]
9	11.38	Methyl hydroquinone ($C_6H_6O_2$)	110	used as a topical application in skin whitening to reduce the color of skin [121,122]
10	12.62	Guaiacol ($C_7H_8O_2$)	124	Guaiacol is a precursor to various flavorants, such as eugenol[123] and vanillin.[124] Its derivatives are used medicinally as an expectorant, antiseptic, and local anesthetic
11	13.89	4-ethyl phenol ($C_8H_{10}O$)	218	used as an indicator of the yeast's presence [125]
12	14.38	Pyrocatechol ($C_6H_6O_2$)	110	used as a precursor to fine chemicals such as perfumes and pharmaceuticals. [126]
13	14.58	Phenol 2-methoxy 4 – methyl ($C_8H_{10}O_2$)	138	Used for synthetic intermediates to other compounds and materials, including plastics, pesticides, pharmaceuticals, and dyes [127]
14	15.55	3-methoxycatehol ($C_7H_8O_3$)	140	Not found
15	15.76	4-ethyl guaiacol ($C_9H_{12}O_2$)	152	Not found
16	15.91	4-methylcatechol ($C_7H_8O_2$)	124	Used as a smokeless fuel Coalite obtains homocatechol from ammoniacal liquor by solvent extraction, distillation and crystallisation.[128]
17	16.96	2,6-dimethoxyphenol ($C_8H_{10}O_3$)	154	Used as food additives and contaminants [129]
18	17.05	Eugenol ($C_{10}H_{12}O_2$)	164	used in perfumes, flavorings, and essential oils. It is also as a local antiseptic and anaesthetic [130]
19	17.20	2-methoxy-4-propylphenol ($CH_3OC_6H_3(CH_2CH_2CH_3)OH$)	166	Potential applications include the profile enhancement of smoke flavors, clove, spicy nuances for cinnamon and pepper, vanilla, and fruit nuances. [131]

20	17.94	Vanillin ($C_8H_8O_3$)	152	1.used in the fragrance industry, in perfumes, and to mask unpleasant odors or tastes in medicines, livestock fodder, and cleaning products. [132] 2. used as a chemical intermediate in the production of pharmaceuticals and other fine chemicals. In 1970, more than half the world's vanillin production was used in the synthesis of other chemicals, [133] but as of 2004, this use accounts for only 13% of the market for vanillin. [133]
21	18.78	Isoeugenol ($C_{10}H_{12}O_2$)	164	Not found
22	19.52	4'-hydroxy-3'-methoxyacetophenone ($C_9H_{10}O_3$)	166	used in the treatment of atherosclerosis in order to prevent the activity of NADPH oxidase activity, halting the production of reactive oxygen species. In effect, this inhibition stops initiation of disease in the endothelial cells [134]
23	20.31	2-propanone, 1-(-hydroxy-3-methoxyphenol) ($C_{10}H_{12}O_3$)	180	Not found
24	23.22	3,5-dimethoxy-4'-hydroxy acetophenone ($C_{10}H_{12}O_4$)	196	Not found
25	24.49	Syringaldehyde ($C_9H_{10}O_4$)	182	Not found

The Tables provide the lists of compounds with their retention times and prospective uses. The chemical composition of the pyro-oil samples is comparison to that of pyro-oils obtained by previous investigators during the studies on pyrolysis of different biomass feedstocks [51-54,169-173]. It is clear that most of the compounds are useful and thus besides the prospect of usage of pyro-oil as fuel after up-gradation through de-oxygenation etc., this may be used as a source for many valuable chemicals.

6.6.11. GC Analysis

Table. 6.28 represents the GC analysis of the pyro-gas derived from non-catalytic and catalytic pyrolysis of jute and lime waste and non-catalytic and catalytic co-pyrolysis of waste jute and sesame oil cake.

Table. 6.28. GC analysis of the pyro-gas derived from non-catalytic and catalytic pyrolysis of jute and lime waste and non-catalytic and catalytic co-pyrolysis of waste jute and sesame oil cake

	CO_2 (% of compound formed)	CO (% of compound formed)	CH_4 (% of compound formed)	H_2 (% of compound formed)
Jute waste	38.8	11.2	7.86	42.14
Jute waste in presence of alumina	44.8	6.59	5.12	43.49
Lime wastes	57.4	2.89	2.28	37.43
Lime wastes in presence of ZnO	58.2	3.27	4.18	34.35
co-pyrolysis of jute waste and sesame oil cake	52.4	4.32	4.41	38.87

From the analysis of pyro-gas obtained through non-catalytic and catalytic pyrolysis and co-pyrolysis of different biomass under study, it clear that CO_2, CO, CH_4 and H_2 are the main components present in the gaseous of pyrolysis. The composition with respect to the content of CO and H_2 is suitable to be used as energy source and as a feedstock for Fischer-Tropsch process for the conversion to liquid fuel.

6.7. Secondary cracking of pyro-oil

6.7.1. Kinetic parameters

The kinetic parameters k, k_v and k_s, as described in section 5.4, of thermal cracking of pyro-oil, obtained from non-catalytic pyrolysis of jute waste and lime waste, have been determined by plotting respectively. The values of $\frac{w_v}{w_0}$ and $\frac{w_s}{w_o}$ have been plotted against $(1-\exp[-k*t])/k$ shown in Tables A.6.-A.11. provided in the supplementary section. The corresponding values of $\frac{w_v}{w_0}$ and $\frac{w_s}{w_o}$, determined using the batch type experimental data have been shown in tables A.62-A.64 provided in the supplementary section. The kinetic parameters, k', k_v' and k_s' for thermal cracking of pyro-oil, obtained from catalytic pyrolysis of jute and lime waste using alumina and zinc oxide respectively, have been determined following the same procedure. The corresponding plots figure A.66. and table A.63-A.65. have been provided in the supplementary section. The values of k and k_v are shown in the table A.67.a and A.67.b respectively. To determine the dependence of rate constants of thermal cracking of pyro-oil obtained from non-catalytic and catalytic pyrolysis of jute and lime wastes, the logarithmic values of rate constants, k, k_v, k_s and k', k_v', k_s' respectively have been plotted

against the inverse of temperature in figures A.68.in the supplementary section. The linearity of all plots proves the validity of Arrhenius equations of temperature dependence of all rate constants. The values of activation energies and pre-exponential factors have been provided in table. In all analysis, the pyro-oil obtained at pyrolysis temperature of 500^{o}C, 700^{o}C and 900^{o}C have been used.

6.7.2. Comparison of rate constant, k

In figures 6.92.a-6.92. b the values of rate constant, k, for the thermal decomposition of pyro-oil obtained through non-catalytic and catalytic pyrolysis of waste jute have been plotted as a function of cracking temperature. Similar plots 6.93.a-6.93. b has been made for pyro-oil obtained from non-catalytic and catalytic pyrolysis of lime waste. In all cases the rate constant shows an increasing trend with the increase of cracking temperature. The rate constant k increases monotonically with temperature for thermal cracking of pyro-oil obtained through catalytic and non-catalytic pyrolysis at 500^{o}C. For waste jute, the values of rate constant, k, of pyro-oil obtained at 700^{o}C and 900^{o}C remain above that for pyro-oil obtained at 500^{o}C up to 800^{o}C and 550^{o}C respectively for non-catalytic and catalytic pyro-oil. However, for lime waste the values of rate constant, k, of thermal cracking of catalytic and non-catalytic pyro-oil at 500^{O}C always remain below those obtained at 700^{o}C and 900^{o}C. These observations may be justified by the fact that the content of high molecular weight compounds is much more in case of pyro-oil obtained at 500^{o}C in comparison to that obtained at 700^{o}C and 900^{o}C and hence the thermal cracking rate is slower in case of the former with respect to the latter ones. In case of pyro-oil obtained at 700^{o}C and 900^{o}C, the rate constant increases sharply with temperature up to 800^{o}C and saturation is observed beyond this temperature level. This may be due to the fact that the molecules present in these pyro-oil samples are no more degradable above 800^{o}C. The observation that values of thermal cracking rate constants of catalytic and non-catalytic pyro-oil from jute and lime wastes at 500^{o}C supersede those obtained at 700^{o}C and 900^{o}C cannot be explained and needs further investigation. The values of rate constant for catalytic pyro-oil are always greater than that of non-catalytic pyro-oil. This may be due to the abundance of lower molecular weight compounds in catalytic pyro-oil in comparison to that in non-catalytic ones.

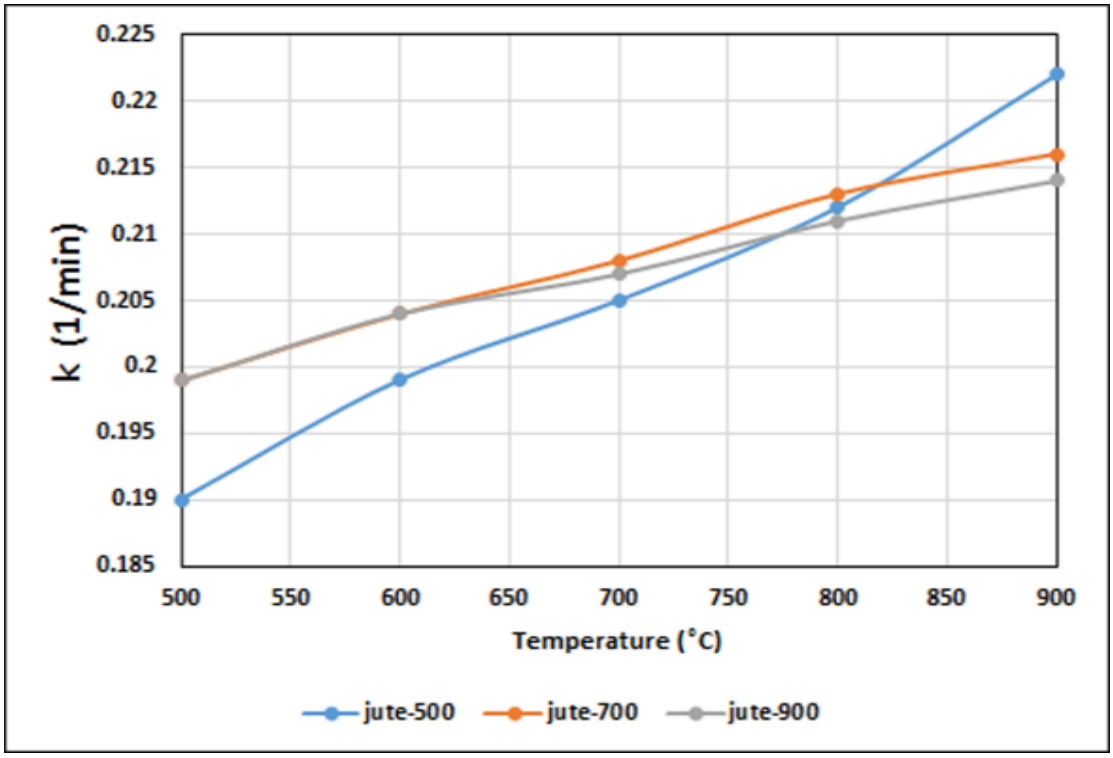

Figure 6.92.a. Variation of k of pyro-oil obtained at 500°C(773K), 700°C(973K) and 900°C(1173K) from jute waste.

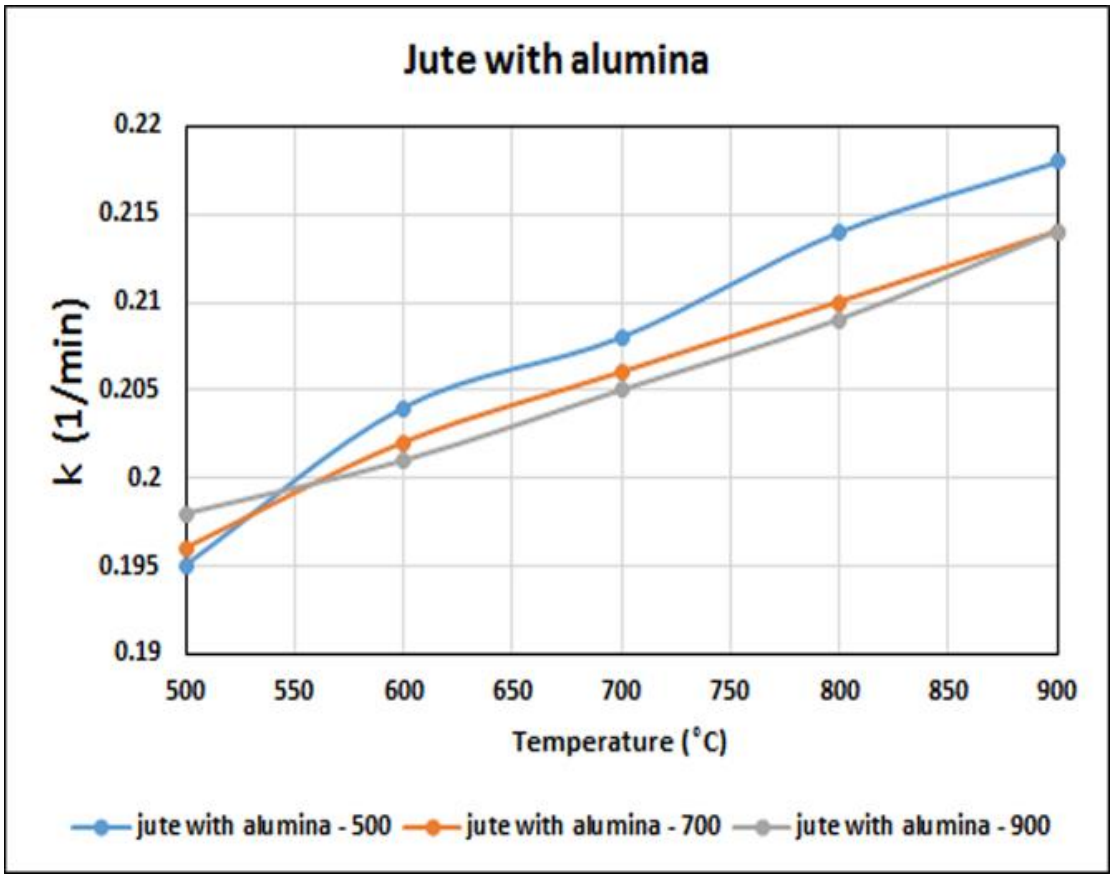

Figure 6.92.b. Variation of k of pyro-oil obtained at 500°C(773K), 700°C(973K) and 900°C(1173K) from jute waste with alumina.

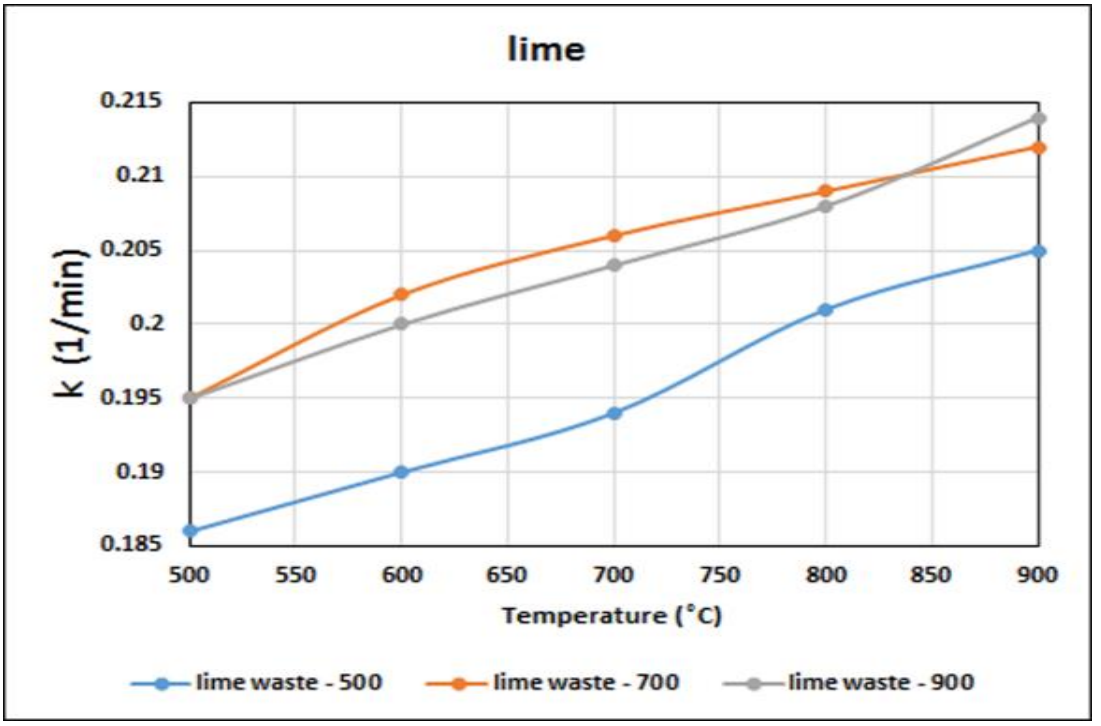

Figure 6.93.a. Variation of k of pyro-oil obtained at 500°C(773K), 700°C(973K) and 900°C(1173K) from lime waste

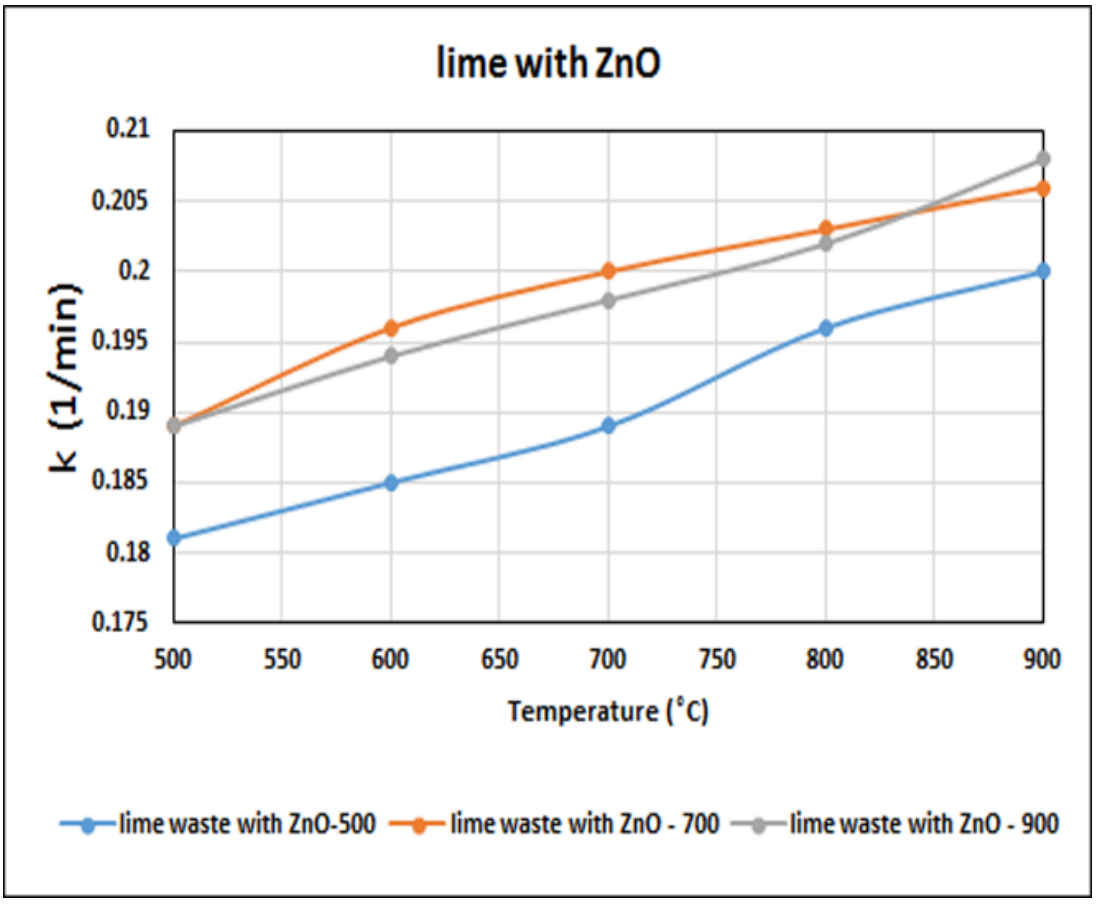

Figure 6.93.b. Variation of k of pyro-oil obtained at 500°C(773K), 700°C(973K) and 900°C(1173K) from lime waste with ZnO

6.7.3. Comparison of rate constant, k_v

From the analysis of the figures 6.94.a-6.94. b it is evident that the rate constant of generation of volatiles during thermal cracking of catalytic and non-catalytic pyro-oil increases as the pyrolysis temperature at which the pyro-oil is obtained increases i.e. $k_{900^oC} > k_{700^oC} > k_{500^oC}$ for jute. This may be explained by the fact that the content of heavy molecules in the pyro-oil increases as the pyrolysis temperature at which it is obtained decreases i.e. the higher temperature pyro-oil contains less recalcitrant molecules in comparison to lower temperature pyro-oil. Hence the formation rate of volatile is higher in case of higher temperature pyro-oil as exhibited by the trend of k_v in figure 6.95.a-6.95. b. However, in case of lime waste, the rate constant for volatile formation from pyro-oil obtained at 500°C exceeds the values corresponding to 700°C and 900°C. The values of rate constant, for volatile formation are almost equal for pyro-oil obtained at 700°C and 900°C, the values of 700°C lying slightly below. Moreover, the values of rate constant, of all pyro-oil samples obtained from lime waste are insensitive to the change in temperature. This nature of thermal decomposition of pyro-oil obtained from lime waste is not explainable and requires in-depth research investigation. For both the feedstocks the values of k_v for catalytic pyro-oil are higher than those of non-catalytic ones. This may be explained by the fact that the catalytic pyro-oil contains lower molecular weight molecules which are more prone to volatilization.

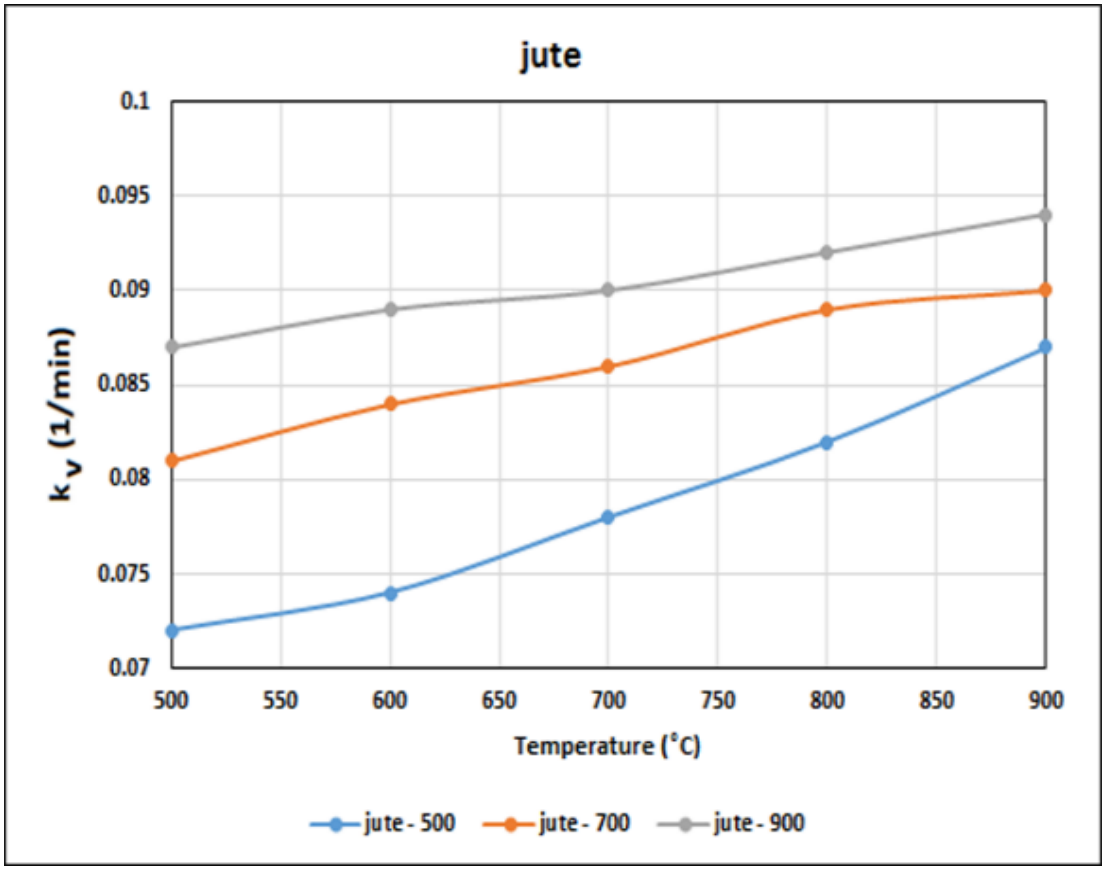

Figure 6.94.a. Variation of k_v of pyro-oil obtained at 500°C(773K), 700°C(973K) and 900°C(1173K) from jute waste

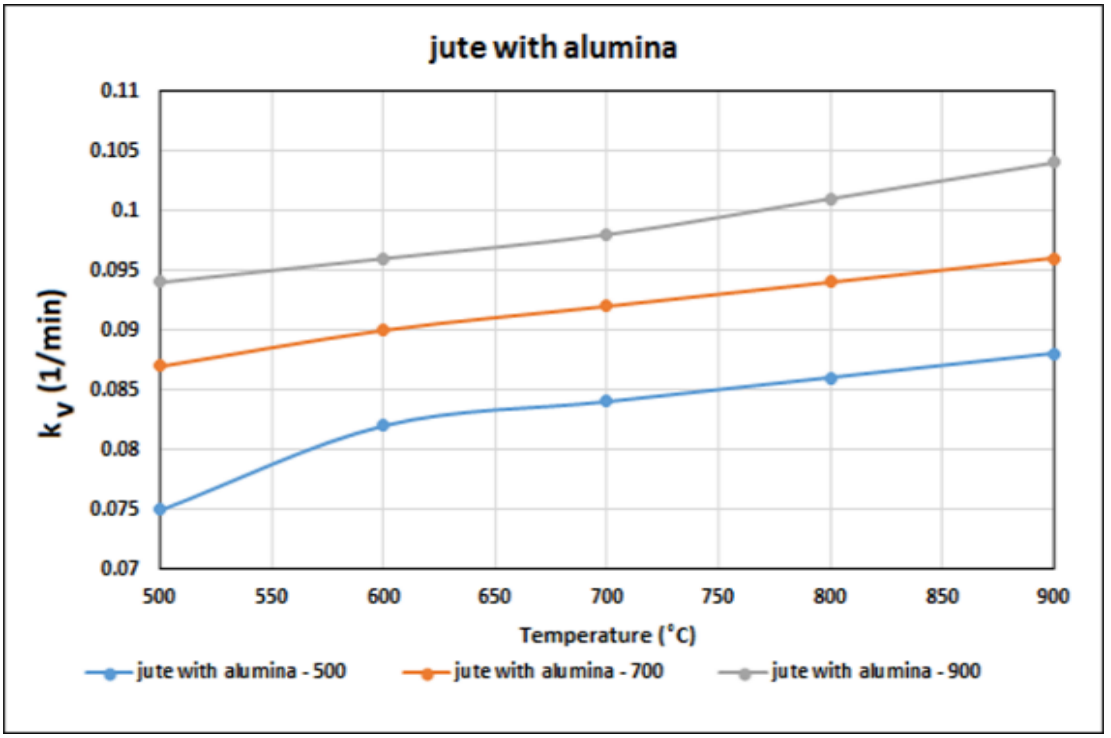

Figure 6.94.b. Variation of k_v of pyro-oil obtained at 500°C(773K), 700°C(973K) and 900°C(1173K) from jute waste with alumina.

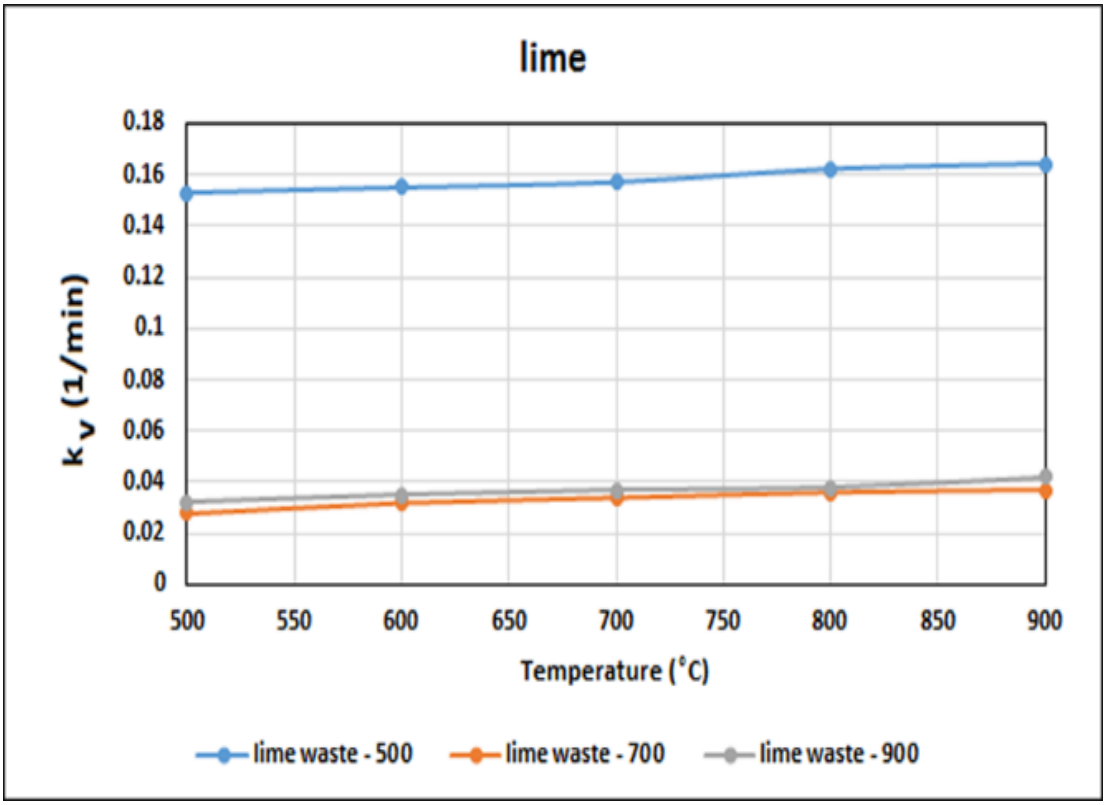

Figure 6.95.a. Variation of k_v of pyro-oil obtained at 500°C(773K), 700°C(973K) and 900°C(1173K) from lime waste

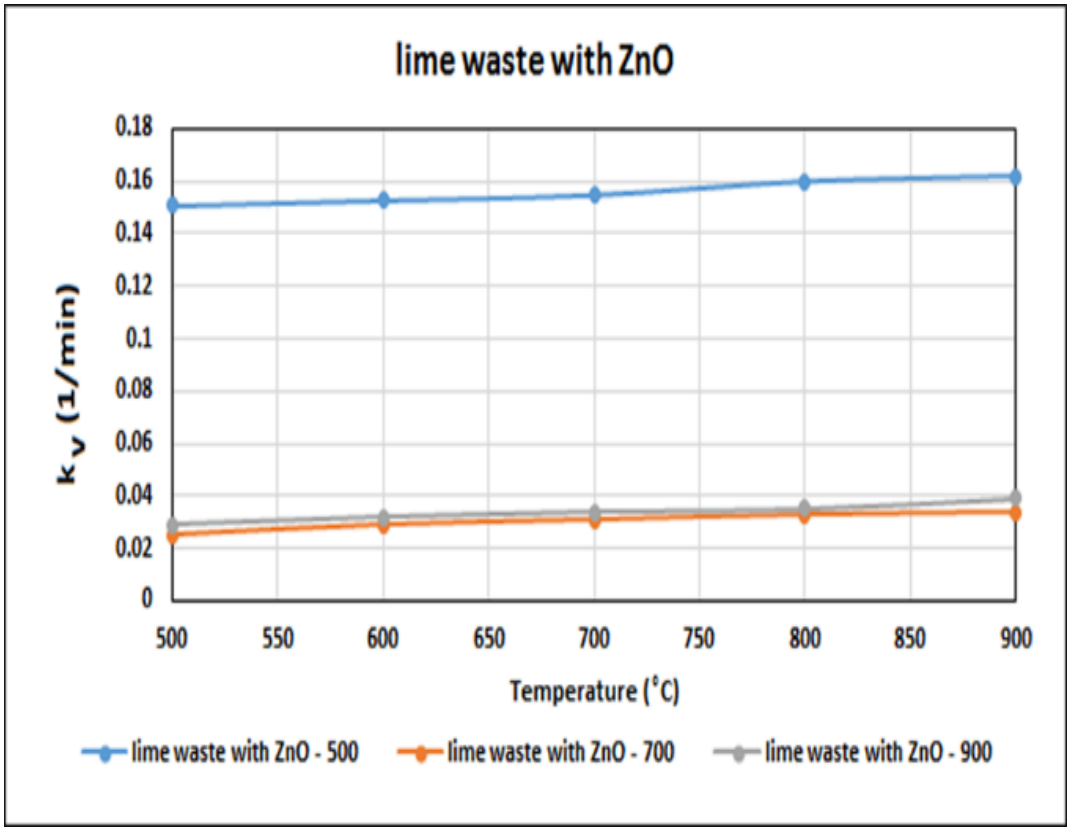

Figure 6.95.b. Variation of k_v of pyro-oil obtained at 500°C(773K), 700°C(973K) and 900°C(1173K) from lime waste with ZnO.

6.7.4. Activation energies

Figure 6.96 – 6.99 shows the variation of activation energies against temperature for various feedstocks.

From the analysis of the figures it is clear that for both waste jute and lime waste the activation energies of thermal decomposition, E and volatile formation, E_v decrease as the pyrolysis temperatures at which the pyro-oil samples are obtained increases. The array of molecules present in lower temperature pyro-oil are much heavier than that present in higher temperature pyro-oil, requiring high threshold energy for thermal cracking. Therefore, as the pyrolysis temperature increase the ease of cracking of pyro-oil also increases.

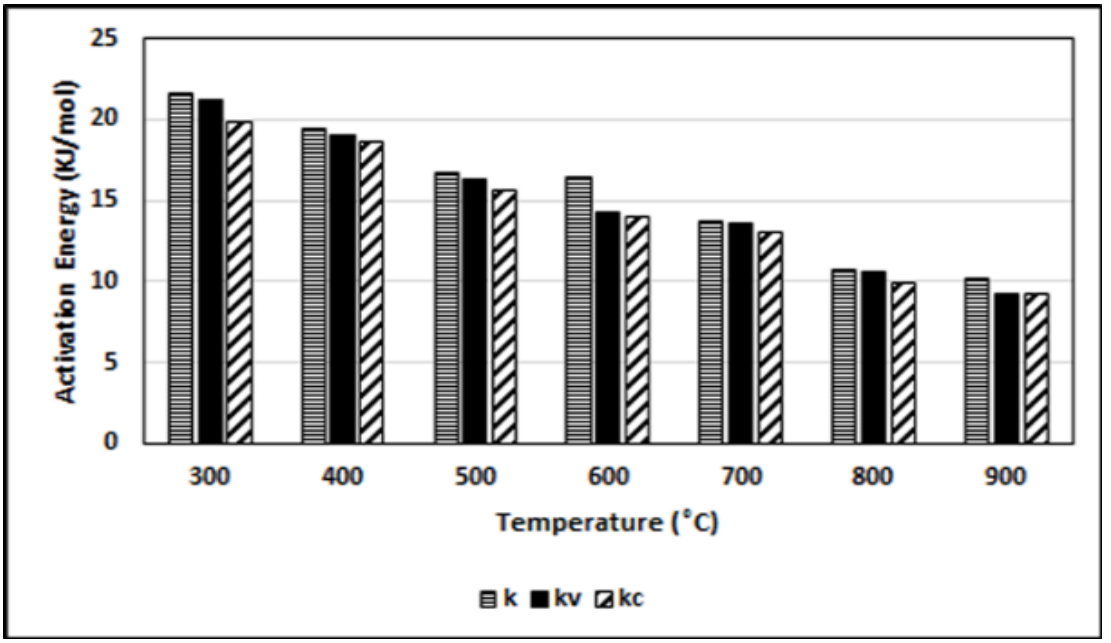

Figure 6.96. Plot of Activation energy against temperature of jute waste pyro-oil.

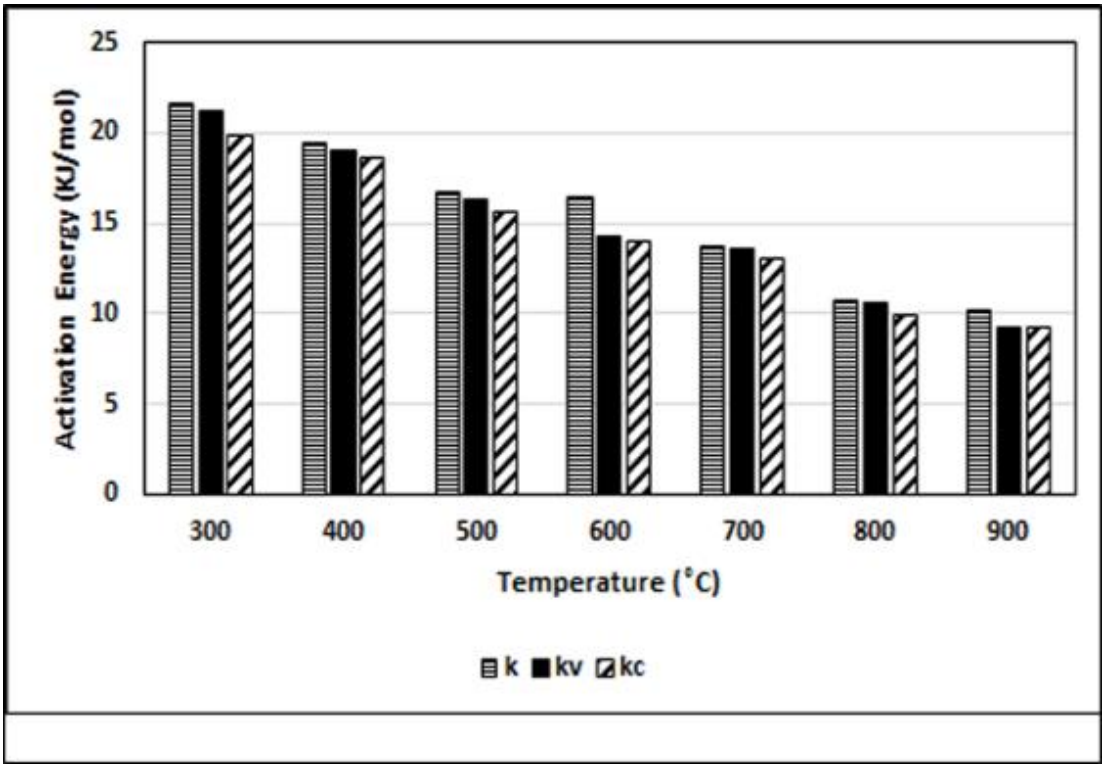

Figure 6.97. Plot of Activation energy against temperature of jute waste with alumina pyro-oil.

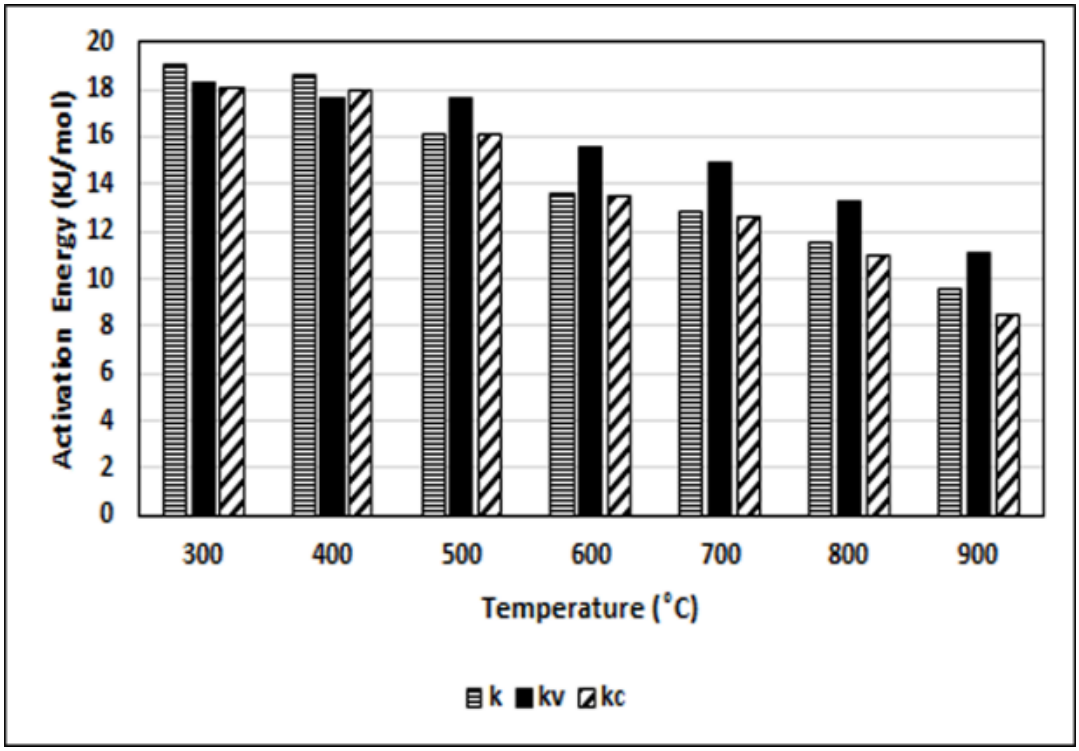

Figure 6.98. Plot of Activation energy against temperature of lime waste pyro-oil.

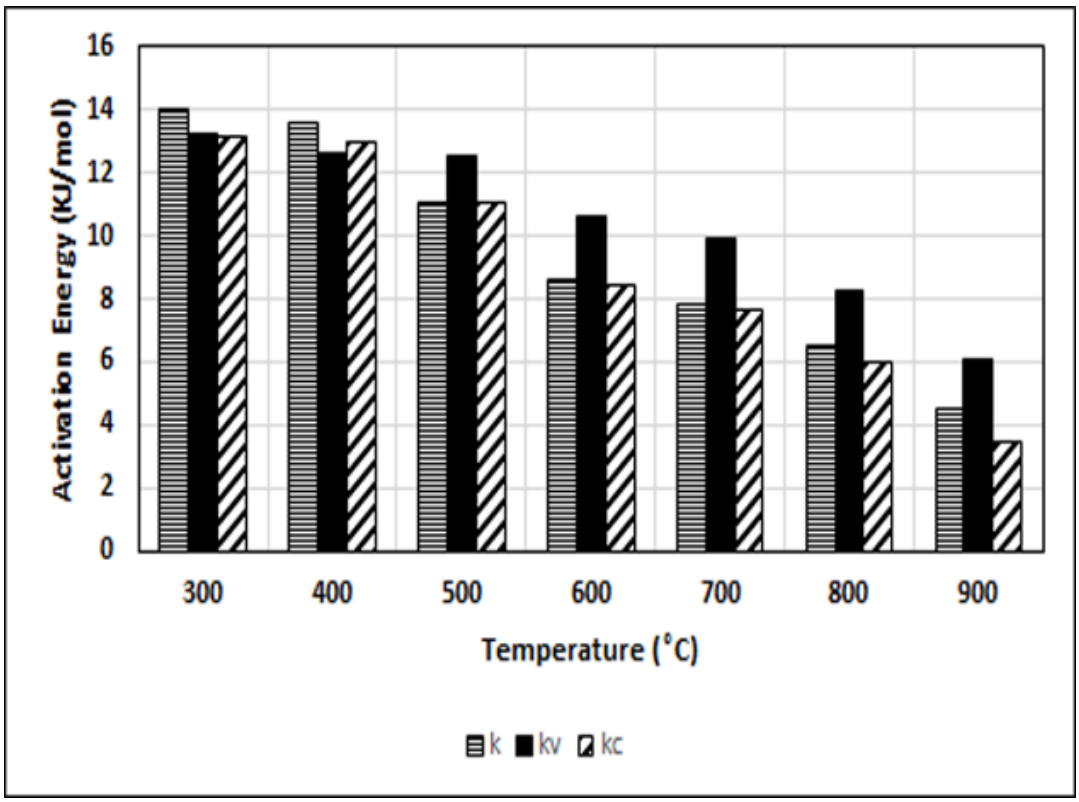

Figure 6.99. Plot of Activation energy against temperature of lime waste with ZnO pyro-oil.

6.8. Aspen Plus® Modelling

6.8.1. Selection of Aspen Plus ® Model [187]

To check the validity of *Aspen Plus*® Models [187], the experimental trends of generation of total gas and its components using the lab scale pyrolyzer have been compared with the simulated predictions using reaction scheme -I and scheme-II. Actually, the reaction schemes I and II mainly differ with respect to the occurrence of gas phase secondary reactions. While Scheme-I neglects the secondary reactions, they are accounted in scheme-II. From the analysis of figures 6.100.a. and 6.100.b., it is clear that the results of ASPEN simulation using scheme II fits the best with the experimental trends of the lab scale reactor. During this simulation, stoichiometric model based on the kinetics of primary pyrolysis, determined under the present study, has been combined with the equilibrium model for reversible secondary pyrolysis reaction. Therefore, the combination of stoichiometric and equilibrium models representing respectively the primary and secondary pyrolysis reactions in Reaction scheme-II is followed for the prediction of the performance of the 100 tpd pyrolyzer. In many pioneering studies [3,174-186] for process simulation modelling on pyrolysis of bio-wastes, mostly Requil and RGibbs *models of Aspen Plus*® have been used. However, both the models are based on the assumption of equilibrium, i.e., the condition when the change in Gibbs free energy for reaction is zero. However, the Requil and RGibbs models represent very ideal situation and is away from reality.

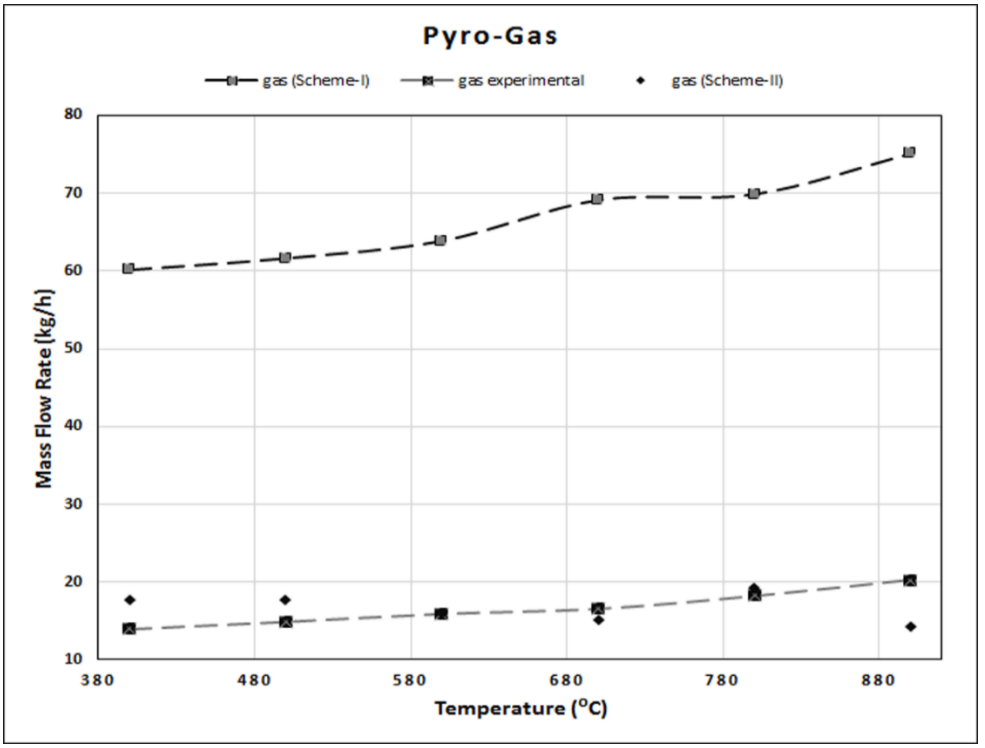

Figure 6.100.a. Prediction of production rate of pyro-gas as a function of pyrolysis temperature using Aspen Plus®

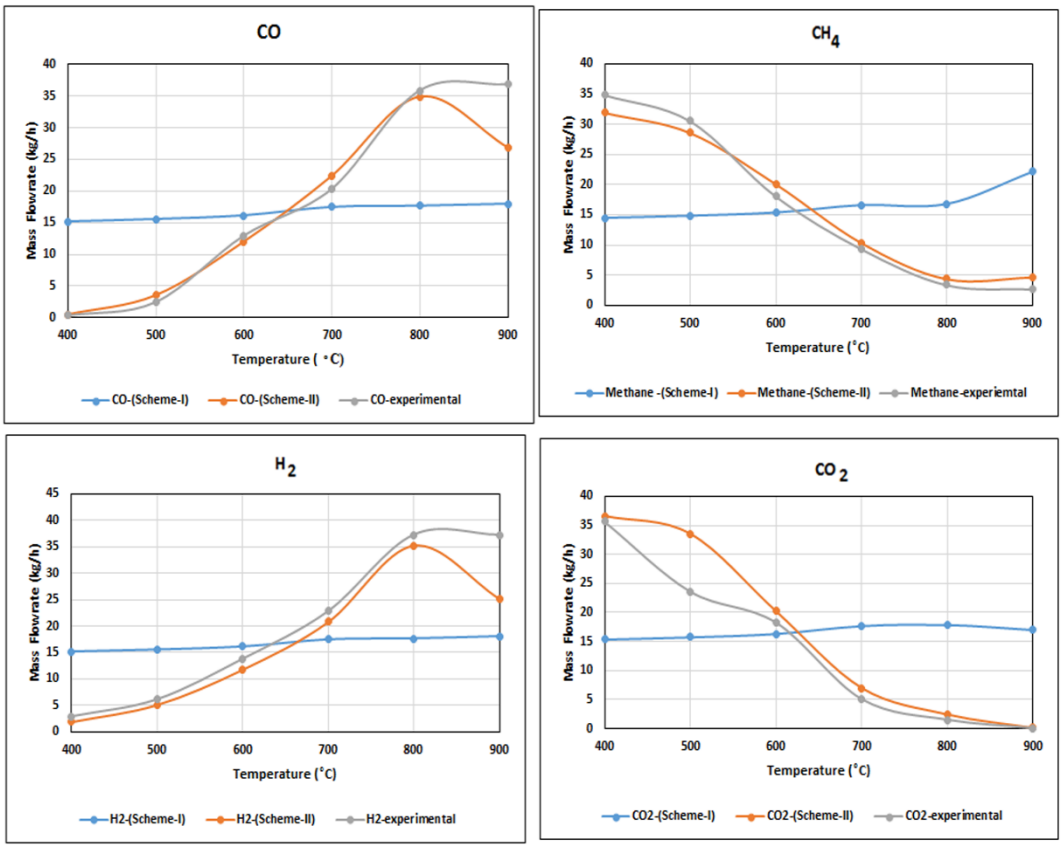

Figure 6.100.b. Prediction of production rate of gaseous components as a function of pyrolysis temperature using Aspen Plus®

Under the present investigation, the combination of both stoichiometric model for primary pyrolysis, based on exact pyrolysis kinetics of jute, already determined by semi-batch pyrolyzer by the present group, and equilibrium model based on standard data of Aspen library [187] for secondary pyrolysis has been found to be adequate. This combination may also be attempted for other pyrolysis feedstocks to represent a real situation.

6.8.2. Fischer–Tropsch [188-190] product profile

Figure 6.101 represents the production of gasoline, diesel and waxes with respect to the temperature when the CO_2 is totally recycled. It is revealed from the plot that the production of gasoline, diesel and waxes increases from 400°C to 500°C after which the increment is minimal.

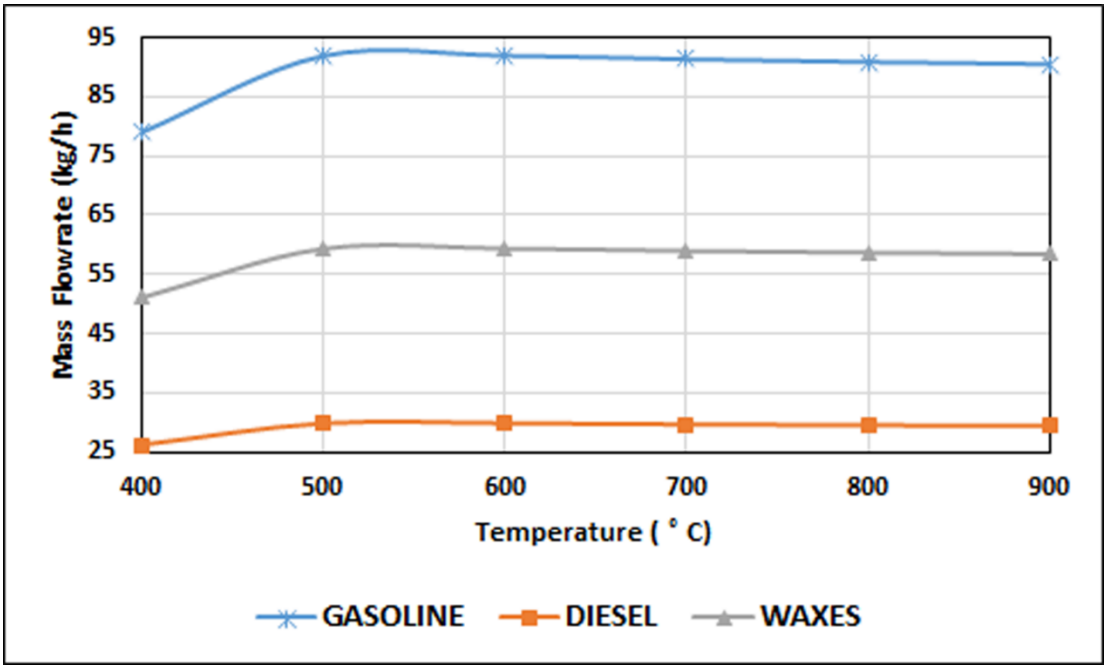

Figure. 6.101 Prediction of production rate of gasoline, diesel and waxes components as a function of pyrolysis temperature using Aspen Plus®

6.8.3. Effect of CO_2 recycle

Figures. 6.102.a, b and c show the flow rates of gasoline, diesel and waxes respectively with respect to the temperature using % CO_2 recycled as the parameter. When %CO_2 recycled is varied from 40% to 60%, the formation of gasoline, diesel and waxes shows an increasing trend with the rise in temperature. However, from 70% to 80%, the production shows an incremental trend till 800^{o}C beyond which it decreases. Thus, the recycle ratio of CO_2 plays a vital role in the formation of the products through FT process.

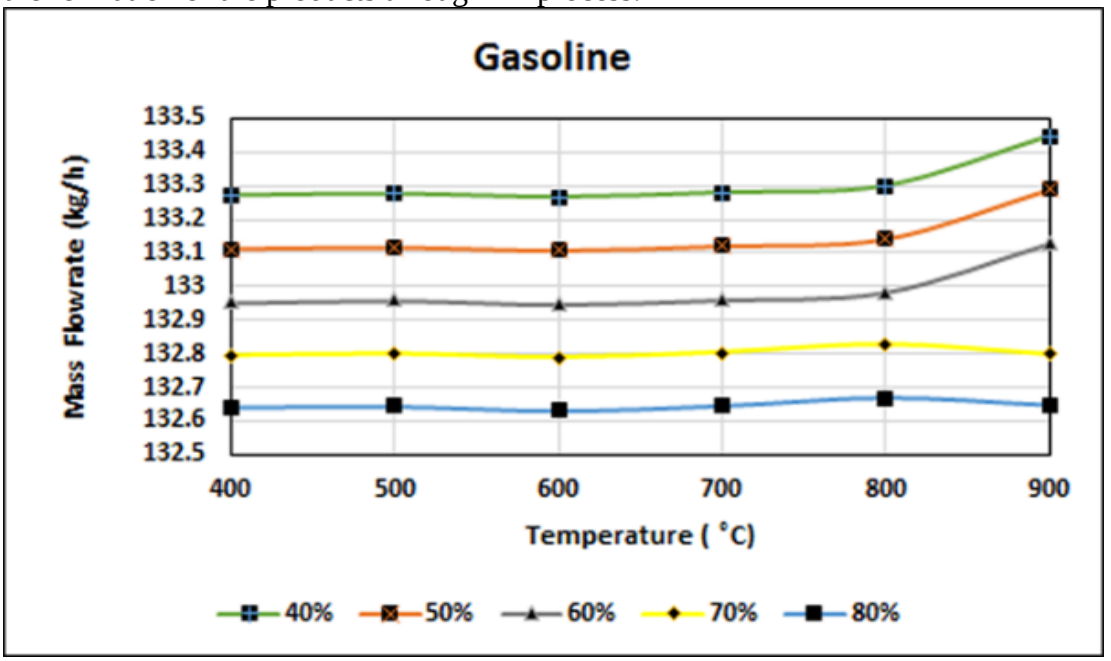

Figure 6.102.a. Prediction of production rate of gasoline components as a function of pyrolysis temperature using Aspen Plus® as CO_2 is varied.

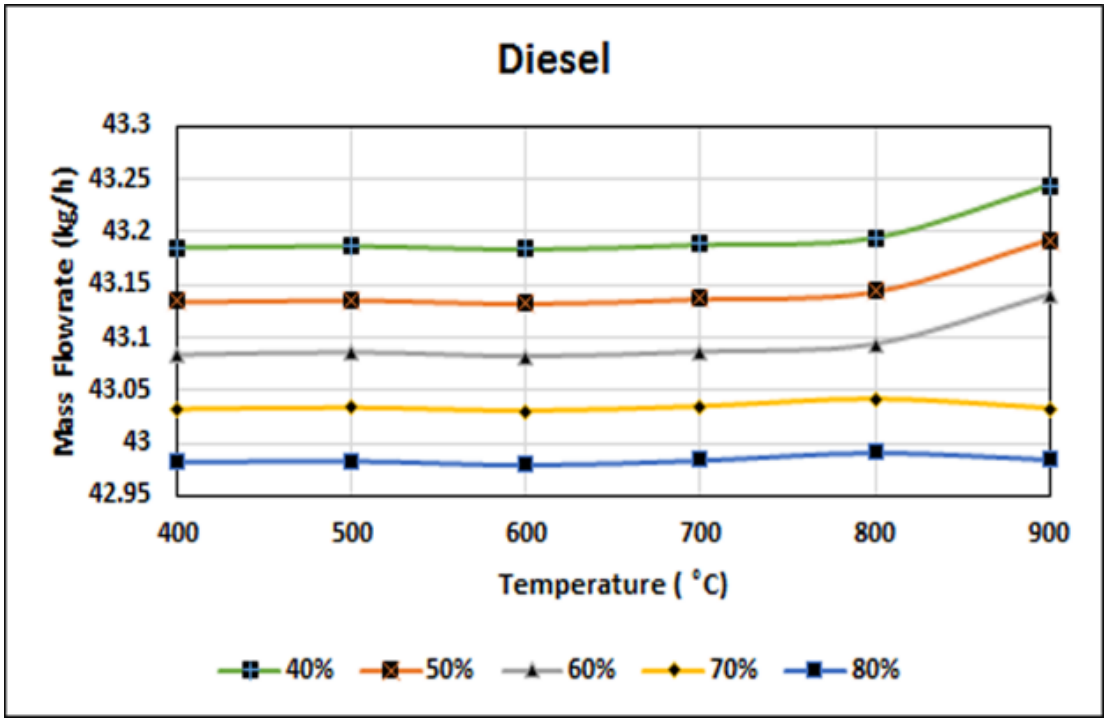

Figure 6.102.b. Prediction of production rate of diesel components as a function of pyrolysis temperature using Aspen Plus® as CO_2 is varied.

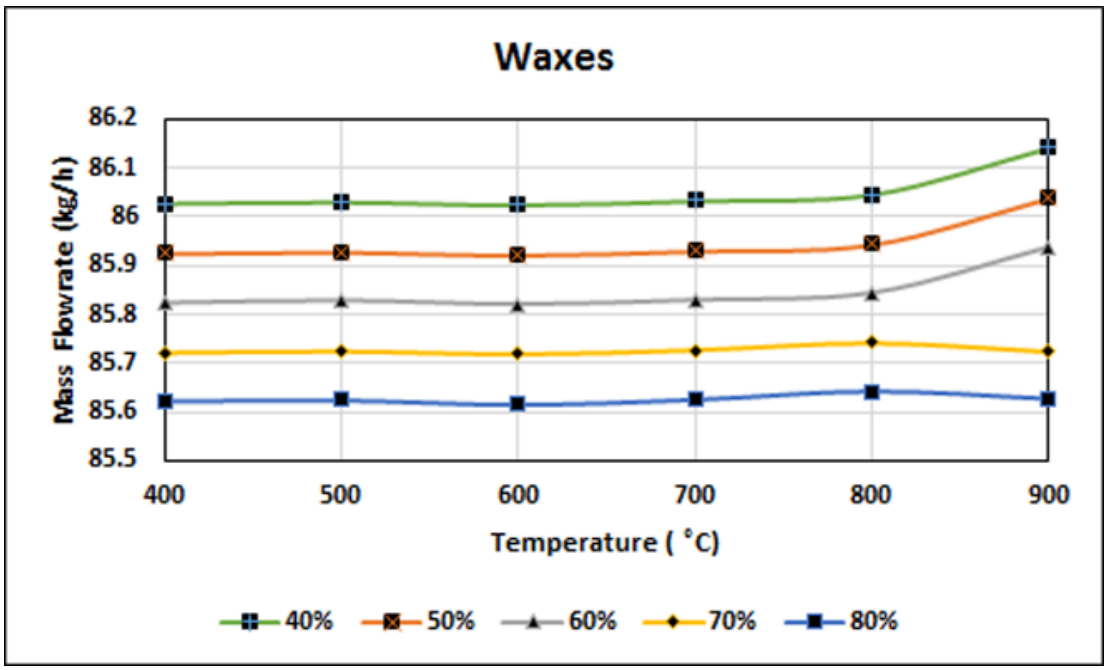

Figure 6.102.c. Prediction of production rate of waxes components as a function of pyrolysis temperature using Aspen Plus® as CO_2 is varied

6.8.4. Sensitivity of gasoline and diesel production

The flowrate of gasoline and diesel are correlated to the temperature and fraction of CO_2 recycled, in order to obtain the optimum condition using response surface methodology. Design Expert® software has been used for this purpose. The quadratic equations predicted by the statistical modelling are as follows:

$$y_i = \alpha_i + \sum_{j=1}^{2} \beta_{ij} X_j + \sum_{j=1}^{2} \sum_{\substack{u=1 \\ u \neq j}}^{2} \beta_{iuj} X_u X_j + \sum_{j=1}^{2} \beta_{ijj} X_j^2 \quad (1)$$

Figure 6.103 and figure 6.104 shows the variation of temperature with respect to the fraction of CO_2 recycled. From the ANOVA table provided in the Appendix A.69., the model equation is surface cubic type indicating large contribution of pyrolysis temperature and fraction of CO_2 recycled on this dependent variable. The model equation for optimum gasoline flowrate is

$$f_{gasoline} = 133.74286 - 0.00246(T) + 1.7848 \times R_{CO_2} + 0.013055(T)R_{CO_2} - 0.00000320311(T)^2 - 11.44147R_{CO_2}^2 \quad (2)$$

The model equation for optimum diesel flowrate is

$$f_{diesel} = 43.46582 - 0.00040583(T) - 0.52439\,R_{CO_2} + 0.00389572(T)R_{CO_2} - 0.00000144656(T)^2 - 1.68257R_{CO_2}^2 \quad (3)$$

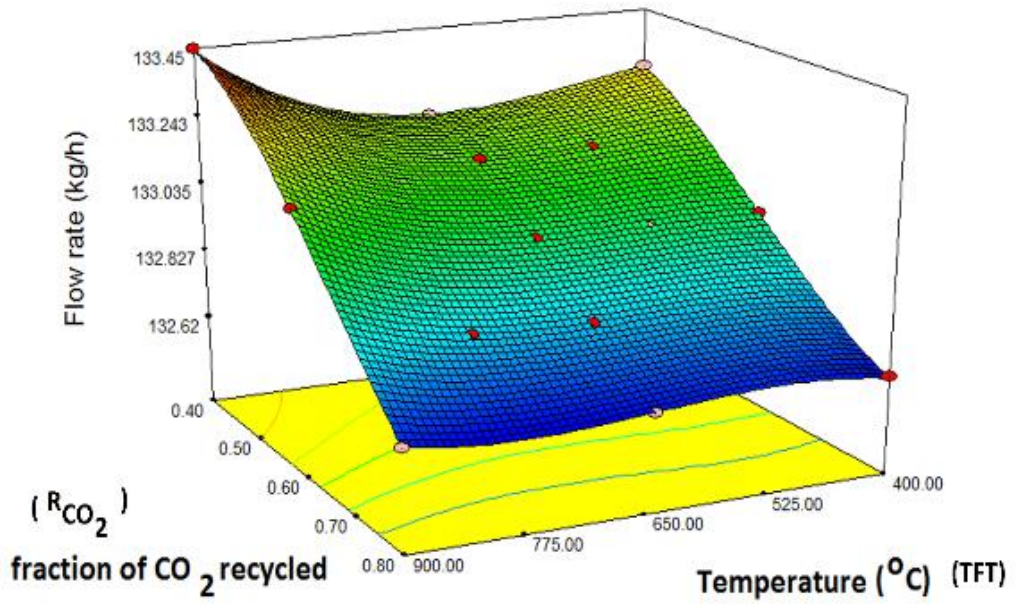

Figure 6.103. The variation of flowrate of gasoline with respect to temperature and fraction of CO_2 recycled.

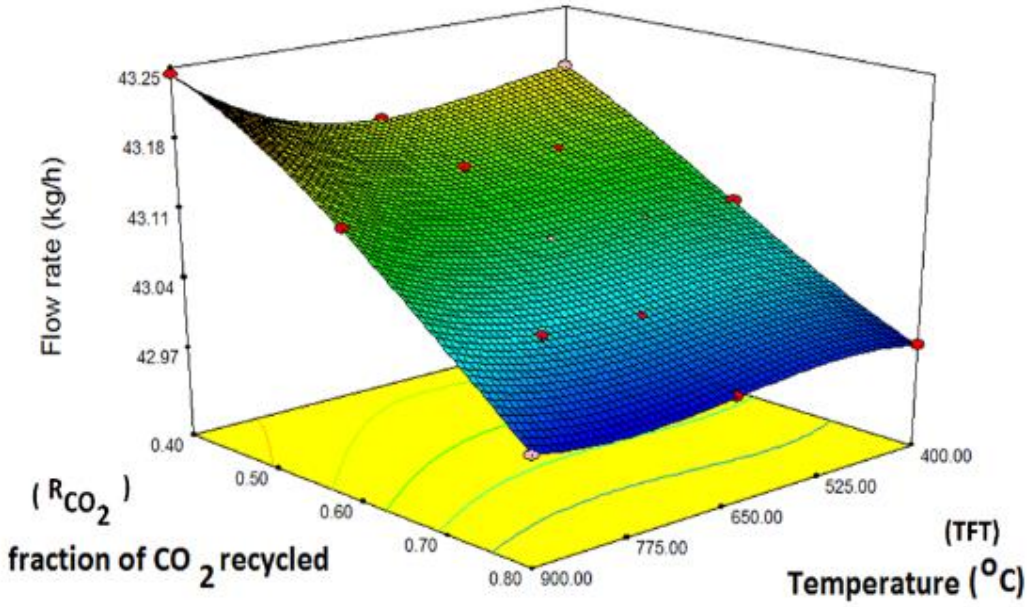

Figure 6.104. The variation of flowrate of diesel with respect to temperature and fraction of CO_2 recycled.

The maximum values of flowrates of gasoline (132.94 kg/h) and diesel (43.11 kg/h) have been obtained at T =863.7ºC and R_{CO_2} = 0.66 and T =867ºC and R_{CO_2} = 0.62 respectively. As predicted by the model equations 2, the optimum conditions of gasoline and diesel are interchangeable. As predicted by the model equation 3, the flow rate of diesel at the optimum condition of gasoline production rate (T =863.7ºC and R_{CO_2} = 0.66) is 43.08kg/h against 43.11 kg/h at its own optimum condition. For gasoline, the flow rate remains at 133kg/h when the optimum operating condition for the maximum diesel production is maintained. Therefore, either of the conditions can be maintained to obtain the maximum flow rates of both diesel and gasoline.

6.8.5. Sensitivity Analysis for Energy delivered and Environmental impact for 100 tpd plant

Sensitivity analysis has been conducted for the energy delivered and avoidance of CO_2 using pyrolysis temperature and % of char deposited for soil amendments as parameters. For each case 13 sets of conditions have been used and the values of dependent variables have been calculated using the Aspen Plus ® model already validated for semi-batch pyrolyzer. The model equation has been developed for both the cases using *Response Surface Methology*® [191] and the conditions corresponding to maximum and minimum values of EROEI and A_{CO_2} respectively have been identified.

6.8.6. Sensitivity of *EROEI*

The model equation correlating the EROEI with the pyrolysis temperature, T and % of pyro-char deposited, f, as predicted using response surface methodology is as follows:

$$EROEI = 82.2674 - 0.00577324T - 0.061404f + 0.0000490999Tf + 0.00000398516T^2 + 0.000192762f^2 \quad (4)$$

From the ANOVA table (Table.6.29), it appears that the quadratic model equation is adequate for the dependence of energy return on energy investment on T and f. From the table, it is evident that the linear temperature term is the most significant one in the quadratic equation. Hence EROEI is expected to be most sensitive with respect to the pyrolysis temperature. The contour plots showing the dependence of EROEI on T and f are shown in Figure 6.105.

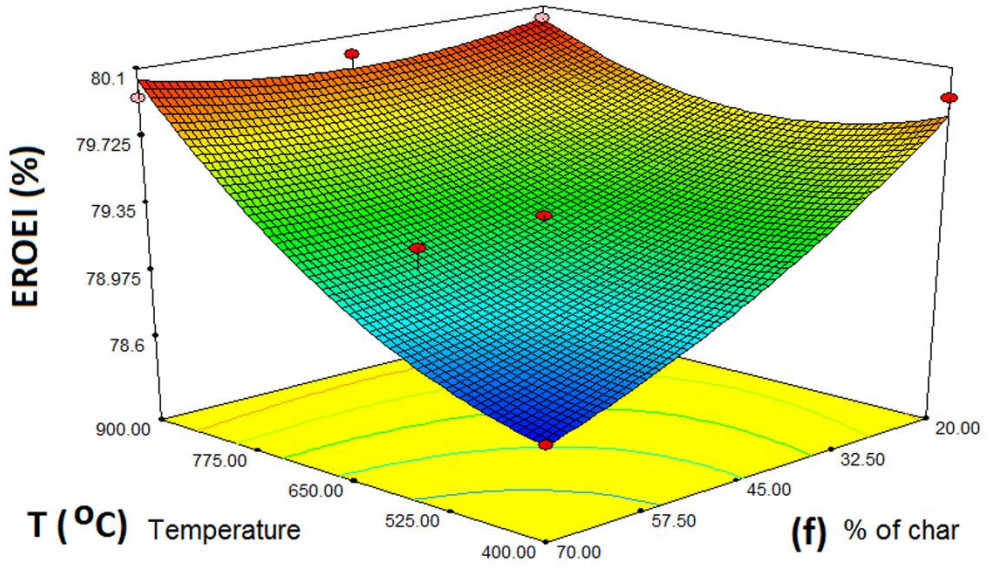

Figure 6.105. The variation of EROEI on T and f

Table. 6.29. ANOVA for response surface quadratic model for the variation of EROEI as a simultaneous function of pyrolysis temperature and % of char deposited.

Source	Sum of Squares	df	Mean Square	F Value	p-value Prob > F	
Model	2.139722	5	0.427944	23.39389	0.0003	significant
A-Temperature	0.810117	1	0.810117	44.28561	0.0003	
B-% of char	0.436571	1	0.436571	23.86548	0.0018	
AB	0.376688	1	0.376688	20.59192	0.0027	
A^2	0.073731	1	0.073731	4.030569	0.0847	
B^2	0.015391	1	0.015391	0.841338	0.3895	
Residual	0.128051	7	0.018293			

R^2= 0.9435, Adjusted R^2 = 0.9032, Predicted R^2 = 0.1793, Adeq Precision = 15.478

The maximum value of energy delivered has been obtained at pyrolysis temperature of 900^{o}C and the fraction of char deposition of 0.2. The energy generation trend may be scrutinized using Figure 6.106 and figure 6.107 where values of energy generated using gas, char and oil have been shown individually against T at f=0.2 and against f at 900^{o}C. From the figure 6.106 it is clear that energy delivered decreases with increase of pyrolysis temperature. The share of energy supplied for drying and pyrolysis is the major one at all sets of conditions. As the temperature increases, the share of thermal energy generated in the pyro-oil based power plant increases. On the other hand, it is clear from Figure 6.107 that as per expectation, the share of energy delivered using char and gas and also the overall energy delivered decrease with the increase of percentage char deposition in agricultural field. The required energy for

transportation of pyro-oil and char respectively to power plant and field always remains the same at -7776 MJ/day. The details of calculation have been provided in the Appendix. A.70 and A.72.

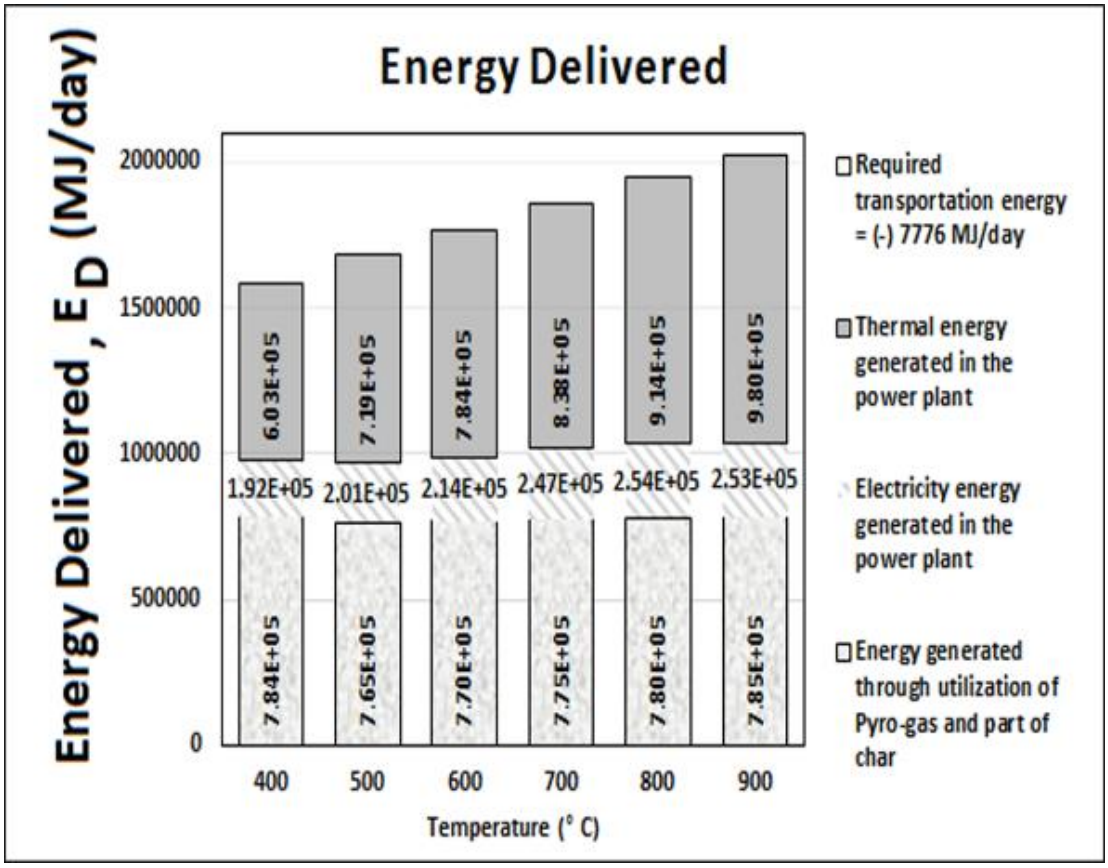

Figure 6.106. Trends of energy generation with pyrolysis temperature at 20% char deposition for soil amendment.

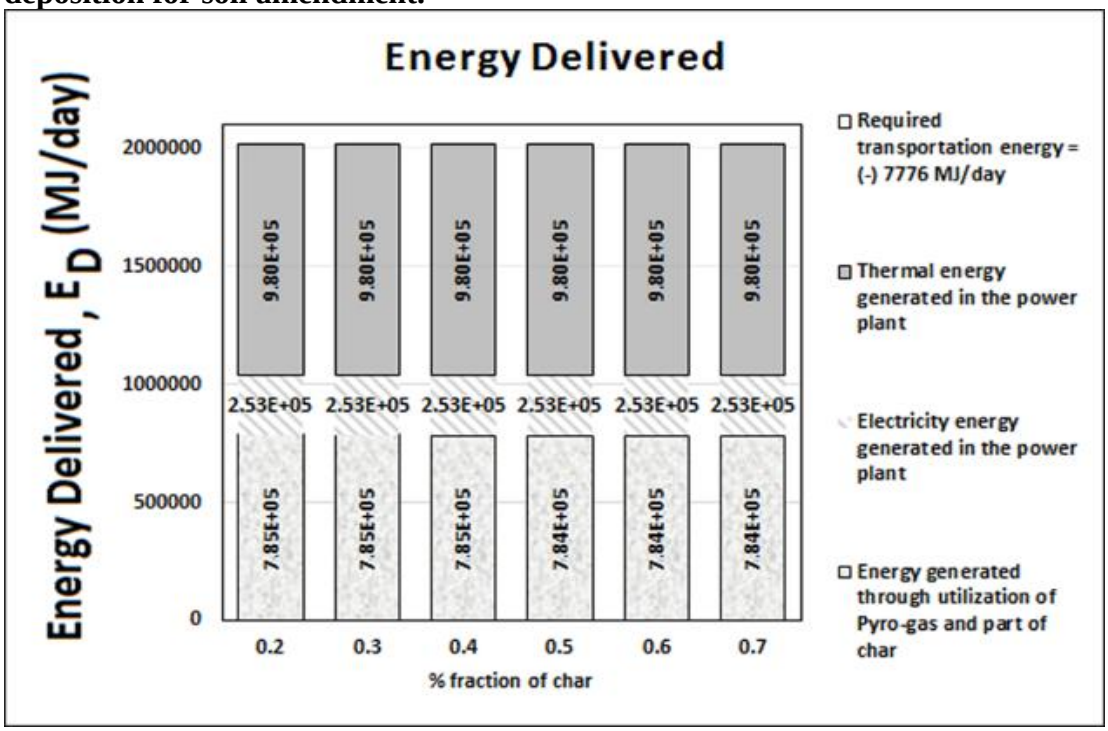

Figure 6.107 Trends of energy delivered with fraction of char deposition for soil amendment for 900ºC

6.8.7. Sensitivity of avoidance of CO_2 (A_{CO_2})

The quadratic model equation correlating avoidance of CO_2 emission with T and f is as follows:

$$A_{CO_2} = 1056.1628 - 0.1497T + 0.7927f + 0.000719372Tf + 0.000156314T^2 - 0.016002f^2 \quad \textbf{(5)}$$

From the ANOVA table (Table 6.30) also indicates that the linear temperature term is the most significant one in Eq.5 and hence A_{CO_2} is also most sensitive with respect to pyrolysis temperature.

Table 6.30. ANOVA for response surface quadratic model for the dependence of avoidance of CO_2 emission as a function of pyrolysis temperature and fraction of pyrolysis deposited for soil amendment

Source	Sum of Squares	df	Mean Square	F Value	p-value Prob > F	
Model	3152.040099	5	630.4080198	15.87070062	0.0011	significant
A-Temperature	2764.892192	1	2764.892192	69.60694475	< 0.0001	
B-% of char	95.77565419	1	95.77565419	2.411179246	0.1644	
AB	80.85882318	1	80.85882318	2.035643796	0.1967	
A^2	185.1807493	1	185.1807493	4.66197786	0.0677	
B^2	152.907795	1	152.907795	3.849497088	0.0906	
Residual	278.0504935	7	39.72149907			

R^2= 0.9189, Adjusted R^2 = 0.861, Predicted R^2 = 0.5366 and Adeq Precision = 14.463

Figure. 6.108 shows the contour plots showing the dependence of avoidance of CO_2 emission as a function of pyrolysis temperature and fraction of pyrolysis char deposited for soil amendment.

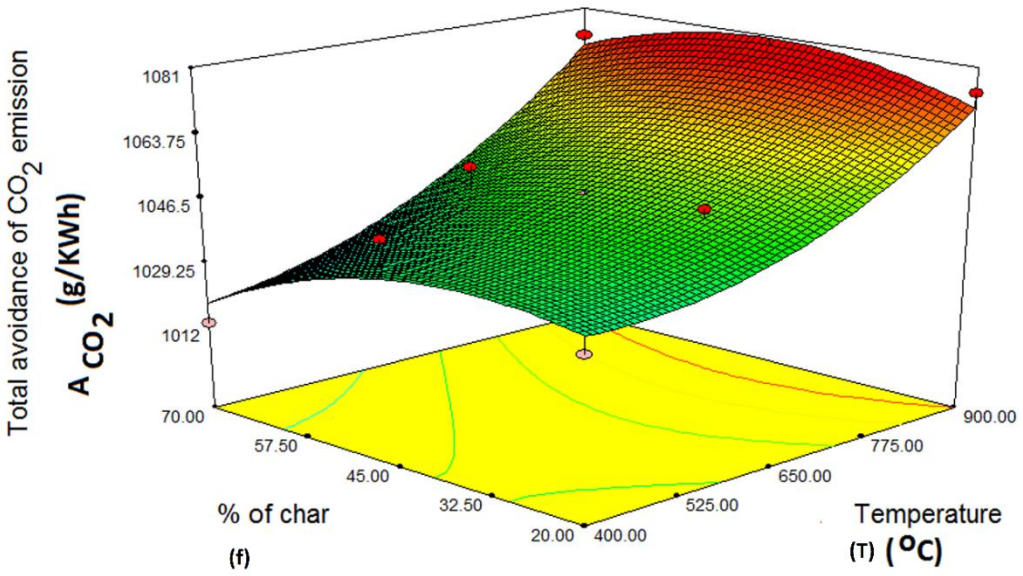

Figure 6.108 The dependence of avoidance of CO_2 emission as a function of pyrolysis temperature and fraction of pyrolysis char deposited for soil amendment.

The maximum value of avoidance of CO_2 emission of 1081 g/KWh has been obtained at T=589.4°C and f = 0.2495 respectively. In figures 6.105 and 6.106 the dependence of total avoidance of CO_2 emission respectively on T at f =0.2 and on f at T=600 °C have been shown.

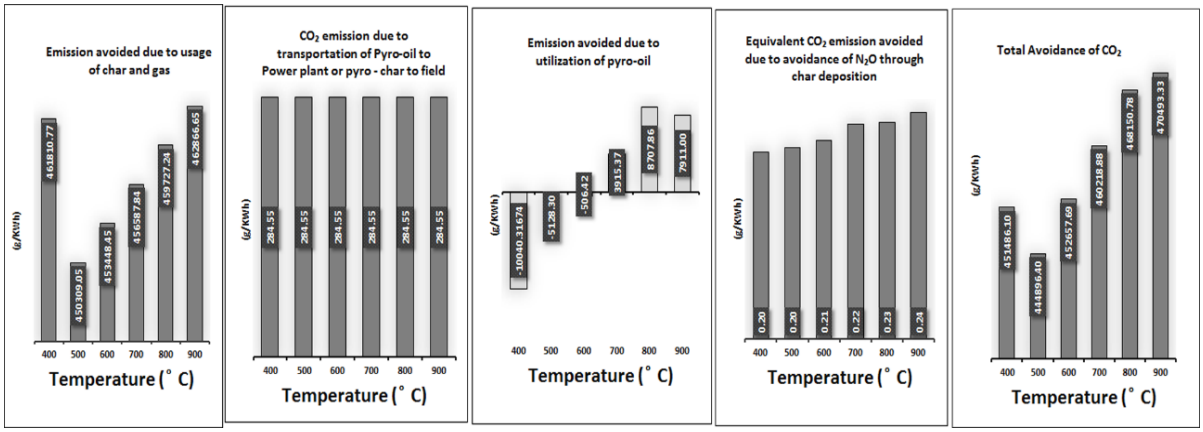

Figure 6.109. Trends of CO_2 emission and avoidance with pyrolysis temperature at 20% char deposition for soil amendment

It is clear from the figure 6.109 that the total avoidance of CO_2 emission decreases with the increase of pyrolysis temperature. Similar to the trend of total avoidance, the emission avoided due to the usage of char and gas also decreases with temperature. The emission avoided due to utilisation of pyro-oil in power plant however passes from negative to positive values as the pyrolysis temperature is increased from 400°C to 900°C. The effect of pyrolysis temperature on the avoidance of CO_2 emission due to deposition of char is insignificant. The transportation of pyro-oil and pyro-char to the power plant and agricultural field respectively creates additional CO_2 emission at a constant rate of 284.551kg/day. By scrutinizing the contribution of each component, it is apparent that the avoidance of CO_2 emission is mainly possible due to replacement of energy for pyrolysis and drying by pyro-gas and pyro-char.

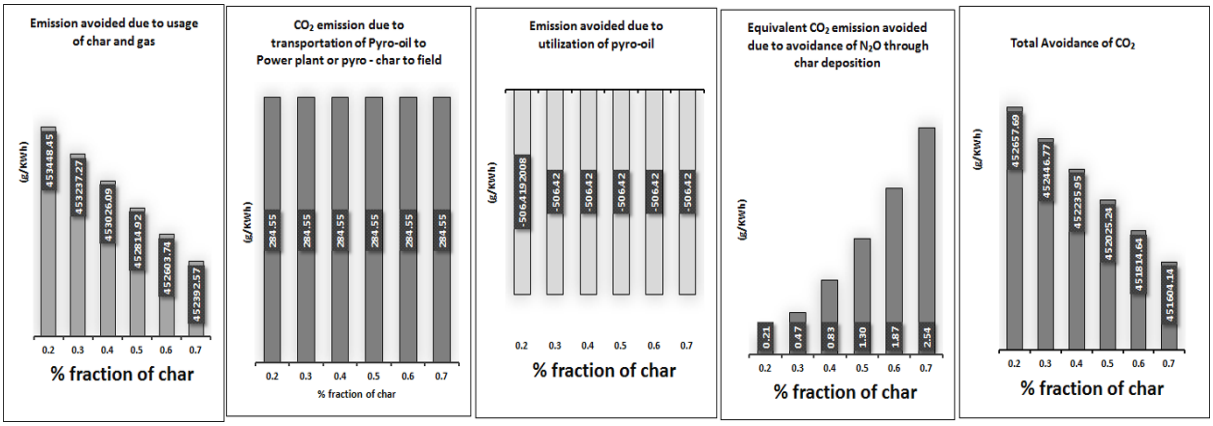

Figure 6.110. Trends of CO_2 emission and avoidance with % fraction of char deposition at 600°C char deposition for soil amendment

Figure 6.110 clearly shows that as per expectation, the overall A_{CO_2} and that due to utilization of pyro-char and gas for the supply of energy for pyrolysis and drying decreases with the increase in the fraction of char deposited for soil amendment. The details of calculation have been provided in the Appendix. A.71 and A.72

References

1. Yang, H., Yan, R., Chen, H., Lee, D. H., and Zheng, C., 2007. Characteristics of hemicellulose and lignin pyrolysis, Fuel, 86, pp. 1781-88.
2. Yang H, Yan R, Chen H, Zheng C, Lee DH, Liang DT, "Indepth investigation of biomass pyrolysis based on three major components: hemicellulose, cellulose and lignin", Energy Fuels, 20, 2006, 388–393.
3. Chowdhury, R and Sarkar, A, "Reaction Kinetics and Product Distribution of Slow Pyrolysis of Indian Textile Wastes", *International Journal of Chemical Reactor Eng.* 2012;10: 1 – 23.
4. M. Asadullah, M. Anisur Rahman, M. Mohsin Ali, M. Abdul Motin, M. Borhanus Sultan, M. Robiul Alam, M. Sahedur Rahman, "Jute stick pyrolysis for bio-oil production in fluidized bed reactor", Bioresource Technology, 99, 2008, 44–50.
5. Nabajit Dev Choudhury, Rahul Singh Chutia, Thallada Bhaskar, Rupam Kataki, "Pyrolysis of jute dust: effect of reaction parameters and analysis of products", J Mater Cycles Waste Manag, 16, 2014, 449–459.
6. Jute Commissioner. <http://www.jutecomm.gov.in/statewise%20P%20&%20R%20jute.htm.> Accessed 23 Dec 2012.
7. M.A. Lopez-Velazquez, V. Santes, J. Balmaseda, E. Torres-Garcia, "Pyrolysis of orange waste: A thermo-kinetic study", *Journal of Analytical and Applied Pyrolysis*, 99, 2013, 170 – 177.
8. B Zapata, J Balmaseda, E Fregoso-Israel, E Torres-Garcia, "Thermo-Kinetics of orange peel in air", Journal of Thermal Analysis and Calorimetry, 98, 2009, 309-315.
9. P. Grammelis, P. Basinas, A. Malliopoulou, G. Sakellaropoulos, Pyrolysis kinetics and combustion characteristics of waste recovered fuels, Fuel, 88, 2008, 195-205.
10. John E. White, Biomass pyrolysis kinetics: A comparative critical review with relevant agricultural residue case studies, Journal of Analytical and Applied Pyrolysis 91, 2011, 1–33.
11. Ruby Ray, Pinaki Bhattacharya and Ranjana Chowdhury." Simulation and Modeling of Vegetable Market Wastes Pyrolysis Under Progressive Deactivation Condition". The Canadian Journal of Chemical Engineering, 2004, 82, 566-579.
12. Ruby Ray, Ranjana Chowdhury and Pinaki Bhattacharya." Studies on pyrolysis of vegetable market wastes in presence of heat transfer resistance and deactivation", Int. J. Energy Res, 2005, 29, 811–828.
13. < http://ion.chem.usu.edu/~sbialkow/Classes/3600/Overheads/F%20Test/F%20test.html>
14. < http://www.physics.csbsju.edu/stats/t-test.html>
15. A Sarkar, "Studies on Pyrolysis of Spent Engine Oil and Lignocellulosic Part of Municipal Solid Waste (MSW)", (PhD Thesis in Chemical Engineering, No. 52/10/E), 2015.
16. W. Wu, J. Cai and R. Liu, "Isoconversional kinetic analysis of distributed activation energy model processes for pyrolysis of solid fuels", Ind. Eng. Chem.Res., 2013, 52, 14376.
17. P Tiwari, M. Deo, "Detailed kinetic analysis of oil shale pyrolysis TGA data", AIChE J, 58 (2012), pp. 505–515.
18. V. Vand, "A theory of the irreversible electric resistance changes of metallic films evaporated in vacuum", Proc Phys Soc London, A55, 1943, pp. 222–246.
19. GJ. Pitt, "The kinetics of the evolution of volatile products from coal", Fuel, 41, 1962, 267–274.
20. DB Anthony, JB. Howard, "Coal devolatilization and hydrogasification", AIChE J, 22, 1976, 625–656.
21. JM Cai, C Jin, SY Yang, Y. Chen, "Logistic distributed activation energy model—Part 1: Derivation and numerical parametric study", Bioresour Technol, 102, 2011, 1556–1561
22. JM Cai, SY Yang, T. Li, "Logistic distributed activation energy model—Part 2: Application to cellulose pyrolysis", Bioresour Technol, 102, 2011, 3642–3644.
23. L Fiori, M Valbusa, D Lorenzi, L. Fambri, "Modeling of the devolatilization kinetics during pyrolysis of grape residues", Bioresour Technol, 103, 2012, 389–397.
24. K Miura, T. Maki, "Simplified method to estimate *f*(*E*) in distributed activation energy model for analyzing coal pyrolysis reaction", J Chem Eng Jpn, 31, 1998, 228–235.

25. E Donskoi, DLS. McElwain, “Optimization of coal pyrolysis modelling”, Combust Flame, 122, 2000, 359–367.
26. AO Aboyade, M Carrier, EL Meyer, JH Knoetze, JF. Gorgens, “Model fitting kinetic analysis and characterisation of the devolatilization of coal blends with corn and sugarcane residues”, Thermochim Acta, 530, 2012, 95–106.
27. J Cai, W Wu, R. Liu, “Sensitivity analysis of three-parallel-DAEM-reaction model for describing rice straw pyrolysis”, Bioresour Technol, 132, 2013, 423–426.
28. JM Cai, WX Wu, RH Liu, GW. Huber, “A distributed activation energy model for the pyrolysis of lignocellulosic biomass”, Green Chem, 15, 2013, 1331–1340.
29. A Soria-Verdugo, N Garcia-Hernando, LM Garcia-Gutierrez, U. Ruiz-Rivas, “Analysis of biomass and sewage sludge devolatilization using the distributed activation energy model”, Energy Convers Manage, 65, 2013, 239–244.
30. H. L. Friedman, J. Polym. Sci., Part C: Polym. Symp., 1965, 50, 183–195;
31. http://hyperphysics.phy-astr.gsu.edu/hbase/math/gaufcn.html
32. Kansal, A., 2002. Solid waste management strategies for India. Indian Journal of Environmental Protection 22 (4), pp. 444–448.
33. CPCB, 2000, Status of Solid Waste Generation, Collection, Treatment and Disposal in Metro cities, Series: CUPS/46/1999–2000.
34. Oasmaa, Y. Solantausta, V. Arpiainen, E. Kuoppala and K. Sipila, Energy Fuels, 2010, 24, 1380.
35. Fonts, G. Gea, M. Azuara, J. ´Abrego and J. Arauzo, Renewable Sustainable Energy Rev., 2012, 16, 2781.
36. H.-M. Yang, S. Appari, S. Kudo, J.-ichiro Hayashi and K. Norinaga, Ind. Eng. Chem. Res., 2015, 54(27), 6855.
37. E. Hoekstra, R. J. M. Westerhof, W. Brilman, et al., AIChE J., 2012, 58, 2830.
38. Aparna Sarkar, Biswarup Mondal, and Ranjana Chowdhury, “Mathematical Modeling of a Semibatch Pyrolyser for Sesame Oil Cake”, Industrial & Engineering Chemistry Research, 2014 53(51), 19671-19680.
39. Aparna Sarkar and Ranjana Chowdhury, “Co-pyrolysis of paper waste and mustard press cake in a semi-batch pyrolyzer—optimization and bio-oil characterization”, International Journal of Green Energy, 13(4), 2016, 373-382.
40. Erta, M., and Alma, M. H., “Pyrolysis of laurel (Laurus nobilis L.) ex-traction residues in a fixed bed reactor: Characterization of bio-oil and bio-char”, J. Anal. Appl. Pyrolysis. 88, 2010, 22–29.
41. Mene´ndez, J. A., Domı´nguez, A., Inguanzo, M., Pis, J. J., “Microwave pyrolysis of sewag sludge: analysis of the gas fraction”, J. Anal. Appl. Pyrolysis, 71, 2004, 657–667.
42. Yang, Y. B., Phan, A. N., Ryu, C., Sharifi, V., Swithenbank, J., “Mathematical modelling of slow pyrolysis of segregated solid wastes in a packed-bed pyrolyzer”, Fuel, 86, 2007, 169–180.
43. Phan, A. N., Ryu, C., Sharifi, V. N., Swithenbank, Jim., “Characterisation of slow pyrolysis products from segregated wastes for energy production”, J. Anal. Appl. Pyrolysis, 81, 2008, 65–71.
44. Bhuiyan, M. N. A., Murahami, K., and Ota, M., “On thermal stability and chemical kinetics of waste newspaper by thermogravimetric and pyrolysis analysis”, Journal of environment and Engineering, 3(1), 2008, 1-12.
45. Volli, V., Singh, R. K., “Production of bio-oil from de-oiled cakes by thermal pyrolysis, Fuel, 96, 2012, 579–585.
46. Putun, A. E., Ozcan, A., and putun, E., “Pyrolysis of hazelnut shells in a fixed bed tubular reactor: yields and structural analysis of bio oil, Journal of analytical and applied pyrolysis, 52, 1999, 33-49.
47. Sensoz, S., Angin, D., and Yorgun, S., “Influence of particle size on the pyrolysis of rapeseed (Brassica napus L.): Fuel properties of bio oil”, Biomass and Bioenergy, 19, 2000, 271-279.
48. Suprabhat Seal, Achyut K. Panda, Sachin Kumar, and R.K. Singh, “Production and Characterization of Bio Oil from Cotton Seed”, Environmental Progress & Sustainable Energy, 34(2), 2015, 542-547

49. Hua-Mei Yang, Srinivas Appari, Shinji Kudo, Jun-ichiro Hayashi, and Koyo Norinaga, "Detailed chemical kinetic modelling of vapor-phase reactions of volatiles derived from fast pyrolysis of lignin ", I*nd. Eng. Chem. Res*, 2015, 54 (27), 6855.
50. R. Azargohar, S. Nanda, J. A. Kozinski, A. K. Dalai and R. Sutarto, Fuel, 2014, 125, 90–100.
51. W.Kaminsky and A.B.Kummer, "Fluidized bed pyrolysis of digested sewage sludge", Journal of Analytical and Applied Pyrolysis, 16,1989, 27-35.
52. Nisheeth P. Bahadur, David G.B. Boocock and Samir K Konar, "Liquid hydrocarbons from catalytic pyrolysis of sewage sludge lipid and canola oil: Evaluation of fuell properties", Energy and fuel, 9, 1995, 248-256.
53. A.Dominguez, J.A. Menendez, M Inguanzo, J.J.Pis, "Production of bio-fuels by high temperature pyrolysis of sewage sludge using conventional and microwave heating", Bioresource Technology, 97, 2006, 1185-1193.
54. Noemi Gil-Lalaguna, Isabel Fonts, Gloria Gea, Maria B. Murillo and Luisa Lazaro, "Reduction of water content in sewage sludge pyrolysis liquid by selective online condensation of the vapors", Energy Fuels, 24, 2010, 6555-6564.
55. http://www.astm.org/cgi-bin/resolver.cgi?D86-15
56. Islam, M.R., Nabi, M.N., Islam, M.N. "The Fuel Properties of Pyrolytic Oils Derived from Carbonaceous Solid Wastes in Bangladesh", Jurnal Teknologi 2003; 38(A):75 – 89.
57. Aparna Sarkar, Sangeeta Dutta, Ranjana Chowdhury, "Mustard Press Cake Pyrolysis and Product Yield Characterization", International Journal of Scientific & Engineering Research", Volume 4, Issue 8, August 2013.
58. Perkin Elmer Clarus 680 GC, 2013, http://global-oceans.org/site/wp-content/uploads/2013/05/Perkin%20Elmer%20Clarus%20680%20GC.pdf.
59. Wahab A, Heinemann U, Albus K, *Epilepsy Research*, 2009, 86 (2-3), 113.
60. "2-methyl furan". The Good Scents Company. Retrieved 2008, 08-26.
61. Christian Kohlpaintner, Markus Schulte, Jürgen Falbe, Peter Lappe, Jürgen Weber, Ullmann'sEncyclopedia of Industrial Chemistry, Weinheim: Wiley-VCH, 2005, doi:10.1002/14356007.
62. Santos, J; Contreras, M; Merino, *Chemical Physics Letters*, 2010, 496 (1-3), 172.
63. Squillacote, Michael E.; De Fellipis, James; Shu, Qingning, J. Am. Chem. Soc, 2005, 127 (45), 15983.
64. Kraft, M. Ya.; Kochergin, P. M.; Tsyganova, A. M.; Shlikhunova, V. S., *Pharmaceutical Chemistry Journal*, 1989, 23 (10), 861.
65. Haynes, William M, Boca Raton, Florida: CRC Press, 2010, 91 ed, 3-134, ISBN 978-1439820773.
66. Kleinfelter, Donald C.; Schleyer, Paul von R, *Org. Synth*, 1962, 42, 79.
67. Nathan B. Bennett, Allen Y. Hong, Andrew M. Harned and Brian M. Stoltz, *Org. Biomol. Chem.*, 2012, 10, 56.
68. Kania , et al, March 18, 2003, United States Patent id : 6534524.
69. Thomas Kahl, Kai-WilfridSchröder, F. R. Lawrence, W. J. Marshall, HartmutHöke, Rudolf Jäckh, *Ullmann'sEncyclopedia of Industrial Chemistry 2007, John Wiley & Sons, New York*, doi:10.1002/14356007.a02_303.
70. Banister, S. D.; Wilkinson, S. M.; Longworth, M.; Stuart, J.; Apetz, N.; English, K.; Brooker, L.; Goebel, C.; Hibbs, D. E.; Glass, M.; Connor, M.; McGregor, I. S.; Kassiou, M, *ACS Chemical Neuroscience*, 2013, 4 (7), 130403084729007, doi:10.1021/cn400035r.
71. Maugh, T, *Science*, 1979, 206 (4422), 1058.
72. Butler, Peter, *American Philatelist (American Philatelic Society)*, 2010, 124 (10), 910.
73. Wynnchuk, Maria, *Journal of Histotechnology*, 1994, (2), 143.
74. Fiege, Helmut, *Ullmann'sEncyclopedia of Industrial Chemistry*, 2000, doi:10.1002/14356007.a08_025,ISBN: 3-527-30673-0.
75. Williams, Norris H.; Whitten, W. Mark, *Biological Bulletin*, 1983, 164 (3), 355.
76. C. F. H. Allen and J. W. Gates, Jr., *Org. Synth.Coll*, 1955, 3, 418.
77. Esposito, Lawrence J.; K. Formanek; G. Kientz; F. Mauger; V. Maureaux; G. Robert; F. TruchetKirk-Othmer, *Encyclopedia of Chemical Technology, 4th edition 24. New York: John Wiley & Sons*, 1997, 812.

78. Flower, R.; Rang, H. P.; Dale, M. M.; Ritter, J. M., *Rang & Dale's Pharmacology. Edinburgh: Churchill Livingstone*, 2007, ISBN 0-443-06911-5.
79. Philip R. Ashurst, Springer, 1999, 460, ISBN : 978-0-8342-1621-1.
80. R. G. Ackman; Brown, William H.; Wright, George F, *J. Org. Chem*, 1955, 20 (9), 1147.
81. Sanae Tanaka; Hidehiko Tomokuni, *J. Heterocycl. Chem*, 1991, 28 (4), 991.
82. Wilson, Charles Welthy III, *Journal of Food Science*, 1970, 35 (6), 766.
83. De Carvalho, C. C. C. R; Da Fonseca, M. M. R., *Food Chemistry*, 2006, 95 (3), 413.
84. Qing Chena, Ting Chen, Dong Wang, Hui-Biao Liu, Yu-Liang Li, and Li-Jun Wan. *PNAS*, 2010, 107 (7), 2769.
85. <http://www.efsa.europa.eu/sites/default/files/scientific_output/files/main_documents/4066.pdf>
86. Agerbirk, Niels; Vos, Martin; Kim, Jae Hak; Jander, Georg, *Phytochemistry Reviews*, 2008, 8, 101.
87. Park, N. I.; Kim, J. K.; Park, W. T.; Cho, J. W.; Lim, Y. P.; Park, S. U., *Molecular Biology Reports*, 2010, 38 (8), 4947.
88. <http://www.bidepharmatech.com/files/document/B_COA_MSDS/MSDS-BD183791.pdf>
89. C. A. Brown and A. Yamashita, *J. Am. Chem. Soc*, 1975, 97 (4), 891.
90. Benjamin R, Dorfman, Portsdaen, Pub no: US 2006/0005900 A1, Jan 12, 2006.
91. Doyle, M. P.; Shanklin, M. S., *Organometallics*, 1993, 12, 11.
92. Marisa B. Sanders, John C. Farrokh, Joseph Hardie and Benny C. Chan, *ActaCryst*, 2013, E69, o1151.
93. Nagamura, Yusei; Satoh, Yuuichi; Tatsumi, Jun; Yamamura, Kunihiro. (European Patent Application EP1090902).
94. Richard D. Christie, Randall J. Fortin, Anthony E. Gross, published 1990, assigned to Nalco Chemical Company, US patent 4915825,
95. Mahadevan, A.; Waheeta, Hopper, *Biodegradation*, 1997, 8 (3), 159.
96. <https://en.wikipedia.org/wiki/Phloroglucinol>
97. "Intermediate Pharmaceutical Ingredients - Flopropione" , Univar Canada. Retrieved 24 April 2009
98. “Synthesis of trinitrophloroglucinol". The United States Patent and Trademark Office. 1984. Retrieved 24 April 2009
99. Vallance P, Smart TG, *British Journal of Pharmacology*, 2006, 147, Suppl 1 (S1), S304.
100. Shinkichi Shimizu, Nanao Watanabe, Toshiaki Kataoka, Takayuki Shoji, Nobuyuki Abe, SinjiMorishita, HisaoIchimura, *Ullmann'sEncyclopedia of Industrial Chemistry" 2007; John Wiley & Sons: New York.*
101. <Cyclone Power to Showcase External Combustion Engine at SAE Event, Green Car Congress, 20 September 2007>
102. <Limonene". cosmeticsinfo.org.>
103. <http://richestgroup.en.alibaba.com/product/60255540405-800893226/C8H12Si_97_.html>
104. <http://img.alfa-chemistry.com/msds/msds_4406-72-8.pdf>
105. Walton, Nicholas J.; Melinda J. Mayer; ArjanNarbad, *Phytochemistry*, 2003, 63(5), 505.
106. Van Ness, J. H, *Kirk-OthmerEncyclopedia of Chemical Technology, 3rd edition* **23**. New York: John Wiley & Sons. 1983, 704.
107. <http://ethesis.nitrkl.ac.in/5346/1/211CH1036.pdf>
108. <http://www.pnnl.gov/main/publications/external/technical_reports/PNNL-23053.pdf>
109. Siminszky, B.; Gavilano, L.; Bowen, S. W.; Dewey, R. E., *Proceedings of the National Academy of Sciences*, 2005, 102 (41), 14919.
110. Fred Shafizadeh, Peter P.S. Chin, *Carbohydrate Research*, 1977, 58(1), 79.
111. 21 CFR 172.515; U.S. National Archives and Records Administration’s Electronic Code of Federal Regulations. Available from, as of March 3, 2006: http://www.gpoaccess.gov/ecfr
112. Yaws, Carl L. (1999). Chemical Properties Handbook. New York: McGraw-Hill. pp. 159–179. ISBN 0-07-073401-1.
113. Diwakar M. Pawar; Sumona V. Smith; Hugh L. Mark; Rhonda M. Odom,; Eric A. Noe (1998). "Conformational Study of Cyclodecane and Substituted Cyclodecanes by Dynamic NMR

Spectroscopy and Computational Methods". Journal of the American Chemical Society 120 (41): 10715. doi:10.1021/ja973116c
114. http://www.sigmaaldrich.com/catalog/product/aldrich/30720?lang=en&region=IN
115. Marta Krasny, Kornel Krasny, Piotr Fiedor, Małgorzata Zadurska, Artur Kamiński, "Long-term outcomes of the use of allogeneic, radiation-sterilised bone blocks in reconstruction of the atrophied alveolar ridge in the maxilla and mandible", Cell and Tissue Banking, 16(4), 631-638 (2015)
116. Fred Shafizadeh, Peter P.S. Chin, Carbohydrate Research, 1977, 58(1), 79.
117. Richard D. Christie, Randall J. Fortin, Anthony E. Gross, published 1990, assigned to Nalco Chemical Company, US patent 4915825.
118. drugs.com. drugs.com, https://www.drugs.com/cdi/phenol-spray.html
119. A. Svobodová*, J. Psotová, and D. Walterová (2003). "Natural Phenolics in the Prevention of UV-Induced Skin Damage. A Review". Biomed. Papers 147 (2): 137–145.doi:10.5507/bp.2003.019
120. DeSelms, R. H.; UV-Active Phenol Ester Compounds; Enigen Science Publishing: Washington, DC, 2008. Archived October 3, 2011, at the Wayback Machine
121. Holmes, J.; Hagemeyer, H. (1971). Process for the production of hydroquinone US 3742071
122. Roscoe, Henry (1891). A Treatise on Chemistry, Volume 3, Part 3. London: Macmillan & Co. p. 165.
123. *C. F. H. Allen and J. W. Gates, Jr. (1955).* "o-Eugenol". Org. Synth.; *Coll. Vol. 3, p. 418*
124. Esposito, Lawrence J.; K. Formanek; G. Kientz; F. Mauger; V. Maureaux; G. Robert; F. Truchet (1997). "Vanillin". Kirk-Othmer Encyclopedia of Chemical Technology, 4th edition 24. New York: John Wiley & Sons. pp. 812–825.
125. https://en.wikipedia.org/wiki/4-Ethylphenol
126. Fiegel, Helmut et al. (2002) "Phenol Derivatives" in Ullmann's Encyclopedia of Industrial Chemistry, Wiley-VCH: Weinheim. doi:10.1002/14356007.a19_313
127. Helmut Fiegein "Cresols and Xylenols" in Ullmann's Encyclopedia of Industrial Chemistry" 2007; Wiley-VCH, Weinheim. doi:10.1002/14356007.a08_025
128. https://en.wikipedia.org/wiki/4-Methylcatechol
129. http://apps.who.int/iris/bitstream/10665/42388/1/WHO_TRS_901.pdf
130. Jadhav BK, Khandelwal KR, Ketkar AR, Pisal SS.; Khandelwal; Ketkar; Pisal (February 2004). "Formulation and evaluation of mucoadhesive tablets containing eugenol for the treatment of periodontal diseases". Drug Dev Ind Pharm. 30 (2): 195–203.doi:10.1081/DDC-120028715.
131. http://www.sigmaaldrich.com/catalog/product/aldrich/w359807?lang=en&region=IN
132. Esposito, Lawrence J.; K. Formanek; G. Kientz; F. Mauger; V. Maureaux; G. Robert; F. Truchet (1997). "Vanillin". Kirk-Othmer Encyclopedia of Chemical Technology, 4th edition 24. New York: John Wiley & Sons. pp. 812–825
133. Hocking, Martin B. (September 1997). "Vanillin: Synthetic Flavoring from Spent Sulfite Liquor" (PDF). Journal of Chemical Education 74 (9): 1055–1059.doi:10.1021/ed074p1055
134. Van den Worm E, Beukelman CJ, Van den Berg AJ, Kroes BH, Labadie RP, Van Dijk H (2001). "Effects of methoxylation of apocynin and analogs on the inhibition of reactive oxygen species production by stimulated human neutrophils". European Journal of Pharmacology 433 (2–3): 225–30. doi:10.1016/S0014-2999(01)01516-3
135. http://www.sigmaaldrich.com/catalog/product/sial/402788?lang=en&region=IN
136. https://en.wikipedia.org/wiki/Methanol
137. Ullmann's Encyclopedia of Industrial Chemistry. 6th ed.Vol 1: Federal Republic of Germany: Wiley-VCH Verlag GmbH & Co. 2003 to Present, p. V18 747 (2003)
138. Christian Kohlpaintner, Markus Schulte, Jürgen Falbe, Peter Lappe, Jürgen Weber "Aldehydes, Aliphatic" in Ullmann's Encyclopedia of Industrial Chemistry 2008, Wiley-VCH, Weinheim. doi: 10.1002/14356007.a01_321.pub2
139. http://www.sigmaaldrich.com/catalog/product/aldrich/283754?lang=en&region=IN
140. <Cyclone Power to Showcase External Combustion Engine at SAE Event, Green Car Congress, 20 September 2007>
141. Limonene". cosmeticsinfo.org
142. http://richestgroup.en.alibaba.com/product/60255540405-800893226/C8H12Si_97_.html

143. Helmut Fiegein "Cresols and Xylenols" in Ullmann's Encyclopedia of Industrial Chemistry" 2007; Wiley-VCH, Weinheim. doi:10.1002/14356007.a08_025
144. Summary of Evaluations Performed by the Joint FAO/WHO Expert Committee on Food Additives http://www.inchem.org/documents/jecfa/jeceval/jec_1395.htm
145. Antioxidant canolol production from a renewable feedstock via an engineered decarboxylase. Krista L. Morley, Stephan Grosse, Hannes Leischa and Peter C. K. Lau, Green Chem., 2013, n15, pages 3312-3317, doi:10.1039/C3GC40748A
146. Siminszky, B.; Gavilano, L.; Bowen, S. W.; Dewey, R. E., Proceedings of the National Academy of Sciences, 2005, 102 (41), 14919.
147. Bostik, Safety Data Sheet Blu-Tack, No. 13135, Bostik Corp., 2007-6. Accessed 2012-4-2. http://www.bostik-amer.com/upload/download/MSDS%20Blu%20Tack.pdf
148. "Cooling baths". UC Davis Chem Wiki. Retrieved 8 February 2015.< http://chemwiki.ucdavis.edu/Reference/Lab_Techniques/Cooling_baths>
149. "Dual cure, low-solvent silicone pressure sensitive adhesives - General Electric Company" http://www.freepatentsonline.com/6387487.html
150. Ji, C.; Egolfopoulos, F. N. (2011). "Hydrogen Flame propagation of mixtures of air with binary liquid fuel mixtures". Proc. Comb. Inst. 33: 955–961.
151. M. C. J. Enklaar, Recl. Trav. Chim. Pays-Bas Belg. 26 (1907) 157, 167.
152. M. C. J. Enklaar, Recl. Trav. Chim. Pays-Bas Belg. 26 (1907) 174; Chem. Zentrabl. 1907 II, 56; Ber. Dtsch. Chem. Ges. 41 (1908) 2084.
153. Karl Griesbaum, Arno Behr, Dieter Biedenkapp, Heinz-Werner Voges, Dorothea Garbe, Christian Paetz, Gerd Collin, Dieter Mayer, Hartmut Höke "Hydrocarbons" in Ullmann's Encyclopedia of Industrial Chemistry 2002 Wiley-VCH, Weinheim. doi:10.1002/14356007.a13_227
154. Kazuhiko NAKAHARA, Najeeb S. ALZOREKY1, Tadashi YOSHIHASHI, Huong T. T. NGUYEN and Gassinee TRAKOONTIVAKORN (2003). "Chemical Composition and Antifungal Activity of Essential Oil from Cymbopogon nardus (Citronella Grass)". JARQ 37 (4).
155. Curtis, T; Williams, DG (2001). Introduction to Perfumery (2nd ed.). Fort Washington, New York: Micelle Press. ISBN 9781870228244
156. Jensen, B (6 February 2010). "Violet". Essential Oils. Retrieved 14 January 2014
157. Christian Kohlpaintner, Markus Schulte, Jürgen Falbe, Peter Lappe, Jürgen Weber (2005), "Aldehydes, Aliphatic", Ullmann's Encyclopedia of Industrial Chemistry, Weinheim: Wiley-VCH, doi:10.1002/14356007.a01_321.pub2
158. T Hart BA, Simons JM, Knaan-Shanzer S, Bakker NP, Labadie RP (1990). "Antiarthritic activity of the newly developed neutrophil oxidative burst antagonist apocynin". Free Radical Biology & Medicine 9 (2): 127–31. doi:10.1016/0891-5849(90)90115-Y
159. Palmen, M.J.H.J.; Beukelman, C.J.; Mooij, R.G.M.; Pena A.S.; van Rees, E.P. (1995). "Anti-inflammatory effect of apocynin, a plant-derived NADPH oxidase antagonist, in acute experimental colitis". The Netherlands Journal of Medicine 47 (2): 41
160. Van den Worm E, Beukelman CJ, Van den Berg AJ, Kroes BH, Labadie RP, Van Dijk H (2001). "Effects of methoxylation of apocynin and analogs on the inhibition of reactive oxygen species production by stimulated human neutrophils". European Journal of Pharmacology 433 (2–3): 225–30. doi:10.1016/S0014-2999(01)01516-3
161. Harraz MM, Marden JJ, Zhou W, Zhang Y, Williams A, Sharov VS, Nelson K, Luo M, Paulson H, Schöneich C, Engelhardt JF (2008). "SOD1 mutations disrupt redox-sensitive Rac regulation of NADPH oxidase in a familial ALS model". The Journal of Clinical Investigation 118 (2): 659–70. doi:10.1172/JCI34060
162. Silva FH, Mónica FZ, Báu FR, Brugnerotto AF, Priviero FB, Toque HA, Antunes E (2013). "Superoxide anion production by NADPH oxidase plays a major role in erectile dysfunction in middle-aged rats: prevention by antioxidant therapy". The Journal of Sexual Medicine 10 (4): 960–71. doi:10.1111/jsm.12063
163. Silva FH, Lanaro C, Leiria LO, Rodrigues RL, Davel AP, Claudino MA, Toque HA, Antunes E (2014). "Oxidative stress associated with middle aging leads to sympathetic hyperactivity and downregulation of soluble guanylyl cyclase in corpus cavernosum". American Journal of

Physiology. Heart and Circulatory Physiology 307 (10): H1393–400. doi:10.1152/ajpheart.00708.2013
164. Lambert, G.W.; Eisenhofer, G.; Jennings, G.L.; Esler, M.D. "Regional homovanillic acid production in humans". Life Sciences 53 (1): 63–75. doi:10.1016/0024-3205(93)90612-7
165. US Dept of Health & Human Services. Household Products Database. [1].US EPA. InertFinder. [2]. US National Library of Medicine. Haz-Map. [3]. US National Library of Medicine. Hazardous Substances Data Bank. http://toxnet.nlm.nih.gov/cgi-bin/sis/htmlgen?HSDB
166. Helmut Fiegein "Cresols and Xylenols" in Ullmann's Encyclopedia of Industrial Chemistry" 2007; Wiley-VCH, Weinheim.doi:10.1002/14356007.a08_025
167. Alan G. MacDiarmid and Arthur J. Epstein. 1995. "Secondary Doping in Polyaniline" Synthetic Metals 69 (85-92)
168. M Lisa Manier, Michelle L Reyzer, Anne Goh, Veronique Dartois, Laura E Via, Clifton E Barry, Richard M Caprioli, "Reagent precoated targets for rapid in-tissue derivatization of the anti-tuberculosis drug isoniazid followed by MALDI imaging mass spectrometry." Journal of the American Society for Mass Spectrometry, 22(8), 1409-1419 (2011)
169. Nader Mahinpey, Pulikesi Murugan, Thilakavathi Mani, and Renata Raina, "Analysis of Bio-Oil, Biogas, and Biochar from Pressurized Pyrolysis of Wheat Straw Using a Tubular Reactor", *Energy & Fuels, 23, 2009,* 2736–2742.
170. T. Hassan Mohammed, Rajae Lakhmiri., Amina Azmani, "Bio-oil from Pyrolysis of Castor Seeds', International Journal of Basic & Applied Sciences IJBAS-IJENS Vol:14 No:04.
171. Peerapon Ruengvilairat, Harakhun Tanatavikorn, Tharapong Vitidsant, "Bio-Oil Production by Pyrolysis of Oil Palm Empty Fruit Bunch in Nitrogen and Steam Atmospheres", *Journal of Sustainable Bioenergy Systems*, 2, 2012,75-85
172. Puttiphon Kongnum, and Sukritthira Ratanawilai, "Catalytic Pyrolysis of Coconut Shell for Bio-oil", Int'l Journal of Advances in Chemical Engg., & Biological Sciences (IJACEBS) Vol. 1, Issue 1(2014) ISSN 2349-1507 EISSN 2349-1515
173. GUO Xiujuan, WANG Shurong, WANG Qi, GUO Zuogang and LUO Zhongyang, "Properties of Bio-oil from Fast Pyrolysis of Rice Husk", BIOTECHNOLOGY AND BIOENGINEERING *Chinese Journal of Chemical Engineering*, 19(1), 2011, 116-121.
174. Modh J K, Namjoshi S A, Channiwala S A. "Kinetics and Pyrolysis of Glossy Paper Waste". Int J Eng Res Appl (IJERA) 2012, 2(2), 2248.
175. Sarkar Aparna, Chowdhury Ranjana. "Studies on Catalytic Pyrolysis of Mustard Press Cake withNaCl", Int J Eng Sci Res Technol, 2014, 3(6), 2277-9655, 90.
176. Sarkar Aparna, Langanaki Michael, Chouwdhry Ranjana. "STUDIES ON PYROLYSIS OF SPENT ENGINE OIL IN A QUARTZ LOAD CELL". Int J Res Eng. Technol, 2014, 03(06) ISSN: 23217308; 222.
177. Asadullah M, Rahman M.N., Ali M.N, Motin M.A., Sultan, M.B, Alam, "Jute stick pyrolysis for bio-oil production in fluidized bed reactor",M.R., Rahman, *Biosource Technology*, 2008, 99, 44.
178. Minghua Zhou, Bo Zhu, Klaus Butterbach-Bahl, Tao Wang, Jessica Bergmann, Nicolas Brüggemann, Zhenhua Wang, Taikui Li, Fuhong Kuang, "Nitrate leaching, direct and indirect nitrous oxide fluxes from sloping cropland in the purple soil area, southwestern China", Environmental Pollution, 2012, 162, 361.
179. Rui Zhang, Qin H. Wang, Zhong Y. Luo, Meng X. Fang, and Ke F. Cen, "Coal Char Gasification in the Mixture of H_2O, CO_2, H_2, and CO under Pressured Conditions" , Energy Fuels, 2014, 28, 832.
180. Magnusson, H., Process simulation in Aspen Plus of an Integrated Ethanol and CHP Plant, UMEA UNIVERSITET (Master Thesis in Energy Engineering, EN0601), 2014.
181. Nicole L. Hammer, Akwasi A. Boateng, Charles A. Mullen , M. Clayton Wheeler, "Aspen Plus® and economic modeling of equine waste utilization for localized hot water heating via fast pyrolysis", Journal of Environmental Management, 2013, 128, 594.
182. Shaomin Liu, Lei Chu, Mingqiang Chen, Wentao Zhang, Wenping Xin, "Modeling and analysis of the pyrolysis of bio-oil aqueous fraction in a fixed-bed reactor", Fuel, 2014, 133, 1.

183. A.Visconti, M. Miccio, D. Juchelková, “An Aspen Plus® tool for simulation of lignocellulosic biomass pyrolysis via equilibrium and ranking of the main process variables”, INTERNATIONAL JOURNAL OF MATHEMATICAL MODELS AND METHODS IN APPLIED SCIENCES, 2015, 9, ISSN: 1998-0140.
184. Jens F. Peters, Fontina Petrakopoulou, Javier Dufour, “Exergetic analysis of a fast pyrolysis process for bio-oil production”, Fuel Processing Technology, 2014, 119, 245.
185. Qi Li, Yanan Zhang, Guiping Hu, “Techno-economic analysis of advanced biofuel production based on bio-oil gasification”, Bioresource Technology, 2015, 191 ,88.
186. Xing Xianjun, Sun ZongKang, Ma Peiyong, Yu jin, Wu Zhaobin, “Establishment of three components of biomass pyrolysis yield model”, Energy Procedia, 2015, 66, 293.
187. Aspen Tech, 2001. Aspen Physical Property System 11.1. Aspen Technology, Inc.,Cambridge, MA, USA
188. Hanaâ Er-rbib, Chakrib Bouallbou, François Werkoff, “Production of synthetic gasoline and diesel fuel from dry reforming of methane”, Energy Procedia, 29,212, 156-165.
189. Sudiro, M, Bertucco, A, “Production of synthetic gasoline and gasoil fuel by alternative processes using natural gas and coal: Process simulation and optimization”, Energy, 34,2009, 2206-2214.
190. Woo-Kyu Chae, Hak-Ju Lee, Jong-Nam Won, Jung-Sung Park and Jae-Eon Kim, “Design and Field Tests of an Inverted Based Remote MicroGrid on a Korean Island”, *Energies* 2015, *8*(8), 8193-8210.
191. Marcos Almeida Bezerra, Ricardo Erthal Santelli, Eliane Padua Oliveira, Leonardo Silveira Villar, Luciane Amélia Escaleira, “Response surface methodology (RSM) as a tool for optimization in analytical chemistry”, Talanta, 2008, 75 (5), 965 -977.
192. Mohammad Rofiqul Islam, MD. Nurun Nabi and Mohammad Nurulislam , "The fuel properties of pyrolytic oils derived from carbonaceous solid wastes in Bangladesh", Jurnal Teknologi, Volume 38, Issue A, 75-89, Jun. 2003.

Chapter. 7

CONCLUSION AND RECOMMENDATION

7. Conclusions and Recommendations

7.1. Conclusions

The pyrolysis of lignocellulosic biomass stands out as the most promising thermochemical processes to generate energy resources and chemicals from wastes. Globally, research studies are being extensively carried out to upgrade the knowledge base on pyrolysis characteristics of different lignocellulosic biomass. Before this thesis work, pyrolysis studies on Indian lignocellulosic biomass, namely rice straw, wheat straw, pith coir, soybean stalks, mustard seed, press cake, coconut shell, cashew nut shell, ground nut shell, corn cob, sesame oil cake, cotton based varieties, glossy paper cup, paper cup waste and vegetable wastes were studied. However, no research focus was given on the pyrolysis of jute packaging wastes, residues of citrus fruits and so on. The data on Catalytic pyrolysis of Indian lignocellulosic wastes was not available. The avenues of co-pyrolysis of mixture of lignocellulosic biomass of Indian origin were also rarely studied. No research attempt was reported on the further processing of pyro-products namely, pyro-oil, pyro-gas etc generated from Indian Biomass. Even under the threat of global warming, no research outcome was reported on the energy and environmental footprint of pyrolysis plant of Indian lignocellulosic biomass. Therefore, in this thesis, both experimental and theoretical approaches have been used to extensively study the pyrolysis characteristics of jute packaging wastes and lime wastes starting from the determination of non-catalytic and catalytic pyrolysis kinetics using lumped and distributed model and characterization of pyro-products to the development of mathematical model for pyrolysis reactors, studies on co-pyrolysis of jute waste with sesame oil cake, assessment of further processing of pyro-oil and pyro-gas and energy and environmental analysis of large pyrolysis plant using jute waste. The overall contributions of this thesis to the community of pyrolysis technology for lignocellulosic biomass are summarized below.

First, the process of non-catalytic and catalytic pyrolysis of Indian jute packaging wastes and lime wastes have been studied using both theoretical and experimental methodologies. Under this

i. The thermochemical properties of Indian jute packaging wastes and lime wastes have been determined using proximate [D7582 – 15] and ultimate [ASTM D5142] analyses. The higher heating values have been determined using bomb calorimeter. The feasible pyrolysis temperature range of both the feedstocks has been determined.

ii. The kinetics of the non-catalytic pyrolysis using lumped and distributed activation models have been determined for the first time.

   a. Lumped kinetics

   Reaction kinetics for the thermal decomposition of solid reactant, and the formation of total volatile, pyro-oil, pyro-gas and char have been determined using the lumped kinetic model using the experimental data obtained under isothermal condition. For both jute and lime wastes, the first order kinetics have been proved to be followed by all reactions. The Arrhenius type dependence of all rate constants on pyrolysis temperature has been determined.

   b. Distributed activated model

   DAE model using the Friedman differential isoconversional method has been followed for the determination of kinetics of nonisothermal pyrolysis for non-catalytic pyrolysis of jute and lime wastes. The TGA data of jute wastes without catalysts at different heating rates (5-25 K min^{-1}) have been used for this

purpose. It has been inferred that the activation energies and frequency factors are strongly dependent upon the pyrolytic conversion level of the samples. In case of non-catalytic pyrolysis, the activation energy has been observed to follow Gaussian distribution over a wide range of conversion..

iii. The effect of catalysts on the pyrolysis of waste jute and lime waste have been studied for the first time.
   a. Based on the maximum pyro-oil yield the most suitable catalysts for the pyrolysis of jute waste and lime waste have been selected.
   b. Similar to non-catalytic pyrolysis the first order kinetics have been proved to be valid for catalytic decomposition of solid reactant, and the formation of total volatile, pyro-oil, pyro-gas and char when the lumped kinetics have been determined using experimental data obtained under isothermal condition. The temperature dependence of all rate constants has been observed to obey the Arrhenius equation. For the most suitable catalysts, namely alumina and zinc oxide for jute and lime wastes respectively, the lower values of activation energies have been obtained for all reactions.
   c. DAE model using the Friedman differential isoconversional method has also been used for the determination of kinetics of nonisothermal pyrolysis for catalytic pyrolysis of jute and lime wastes. No Gaussian relationship is obtained between f(E) and E for catalytic pyrolysis of jute and lime waste.

iv. Products analyses for the catalytic pyrolysis of jute waste and lime waste have been done for the first time.
   a. The trends of pyro-products generated from catalytic and non-catalytic pyrolysis of jute waste and lime waste have been analyzed. While, the yields of pyro-oil have been observed to pass through a maximum at an intermediate pyrolysis temperature (around 500^{o}C), the yields of pyro-char and pyro-gas have been observed to respectively decrease and increase monotonically with pyrolysis temperature.
   b. The pyro-char has been characterized by proximate and ultimate analyses. The increasing and decreasing trends of %C and %O respectively with temperature are higher in case of catalytic pyrolysis in comparison to the non-catalytic counterpart in the case of pyro-char. The specific surface area of bio-char has been observed to increase by the catalytic effect of alumina for jute waste. The calorific values of the pyro-chars have been determined using bomb calorimeter; which has been observed to show an increasing trend with the increase of temperature.
   c. The carbon content of pyro-oil has been observed to decrease with pyrolysis temperature for both catalytic and non-catalytic reactions. The pyro-oil obtained from non-catalytic and catalytic pyrolysis of any of the feedstocks has been observed to be either acidic or basic in nature. Precautions should be taken during storage of the catalytic pyro-oil to avoid corrosion. The chemical composition of the pyro oils has been analyzed using FTIR and GC/MS. The compounds present in bio-oil from both catalytic and non-catalytic pyrolysis of waste jute and lime waste have been observed to have high potential to be used as valuable chemicals. Catalytic pyrolysis ensured the generation of bio-oil with high aromatic and aliphatic contents. The %C and %O in pyro-oil decreased and increased respectively with the increase of pyrolysis temperature. Improvement

with respect to the contents of carbon and oxygen has been observed by the use of catalysts, namely, alumina and zinc oxide respectively for the pyrolysis of jute and lime wastes. Distillation characteristics of the pyro-oil have been performed using D-86, which revealed that with the use of catalysts higher values of initial and final boiling points of pyro-oil have been obtained.

d. The composition of pyro-gases obtained from the pyrolysis of both jute and lime wastes have been analyzed using gas chromatography (GC) and the presence of CO, CO_2, H_2 and CH_4 has been detected. The gaseous composition with respect to the content of CO and H_2 has been observed to be suitable for usage as energy source and as a feedstock for Fischer-Tropsch process for the conversion to liquid fuel.

Second, a mathematical model to predict the transient behaviour of a semi batch pyrolyzer using waste jute has been developed for the first time. Differential mass balance equations have been written for unreacted biomass, pyro-oil and all gaseous components for the lab scale pyrolyzer for jute waste. Lumped kinetic parameters have been used for primary pyrolysis and kinetic data from literature have been used for the secondary pyrolysis i.e., the decomposition of pyro-oil to different gaseous components. Reactions among the gaseous components have been neglected. The set of ordinary and partial differential equations have been solved numerically using MATLAB-2014. The time trajectory of the unconverted reactant has been predicted along with the axial profiles of volatile components as a function of time. The agreement between simulated and experimental values at the pyrolyzer exit is commendable.

Third, the co-pyrolysis of Indian jute waste and sesame oil cake mixture has been studied for the first time.

a. First order kinetics is followed by the thermal decomposition, production of volatile, char, pyro-oil and pyro-gas. Arrhenius equation could explain the temperature dependence of all reaction rate constants. At all temperatures, the values of rate constants, namely, k, k_v and k_c are similar to those obtained for non-catalytic pyrolysis of jute waste.
b. Friedman type DAE model is not valid for co-pyrolysis.

Fourth, processing of the pyro-oil and pyro-gas obtained through pyrolysis of Indian jute waste and lime waste has been done for the first time.

i. Thermal cracking of the pyro-oil has been performed to study the lumped kinetic model applicable for isothermal operation. The values of activation energy for the cracking of pyro-oil obtained at different pyrolysis temperature have been obtained for both jute and lime wastes in the cracking temperature range of 300-900^oC. First order kinetics is valid for thermal decomposition of pyro-oil, formation of volatile and soot. Arrhenius type temperature dependence is again followed by all rate constants. for both waste jute and lime waste the activation energies of thermal decomposition, E and volatile formation, E_v decrease as the pyrolysis temperatures at which the pyro-oil samples are obtained increases.

ii. Sensitivity Analysis of Fischer Tropsch synthesis

ASPEN model has been developed for Fischer-Tropsch synthesis using pyro gas and the sensitivity analysis has been done to optimize the flowrates

of product diesel and gasoline using recycle ratio of CO_2 (R_{CO_2}) and pyrolysis temperature (T) as parameters.

Fifth, assessment of Energy and Environmental Footprints of a large pyrolysis unit has been done.

i. Aspen PLUS Simulation for large scale pyrolysis plant for jute waste

Two Aspen Plus® models have been developed for a lab scale (100g/h) pyrolyzer. In model-I, only primary pyrolysis has been used and in model-II combination of primary and secondary pyrolysis have been used. Rstoic has been chosen for primary pyrolysis and Requil model for secondary pyrolysis. The predictions of the two models have been compared with the results of lab-scale pyrolyzer. The model – II has been proved to be more realistic and has been used to predict the performance of the large (100 tpd) pyrolysis unit based on lignocellulosic Indian waste jute. Although the availability of jute waste in a particular locality may not always be sufficient to run a large plant of this capacity, the simulated results obtained for this scale may be utilized to set-up large plants for huge amount of lignocellulosic waste available in metro cities. In case of Kolkata the amount of lignocellulosic waste, generated per day, is as high as 8760 tpd.

ii. Assessment of Energy and Environment Footprints of a large pyrolysis unit using Process Simulation Software

The study focuses on EEA of a large scale (100 tpd) pyrolysis plant for the assessment of energy and CO_2 emission footprint by extending model –II. During EEA, all pyro-gas and a portion of pyro-char have been considered to be used to supply energy for pyrolysis and drying, pyro-oil has been used for power generation and the residual part of char has been considered to be deposited in agricultural field for soil amendment to avoid N_2O (equivalent to CO_2) emission. Distance between pyrolysis plant and power plant as well as agricultural field, each has been considered to be 20 km. Sensitivity analysis of energy efficiency and avoidance of CO_2 emission has been made with RSM techniques with pyrolysis temperature and fraction of char deposited in agricultural field as parameters. The maximum value of energy delivered has been obtained at pyrolysis temperature of 900^oC and the fraction of char deposition of 0.2. The effect of pyrolysis temperature on the avoidance of CO_2 emission due to deposition of char is insignificant. The transportation of pyro-oil and pyro-char to the power plant and agricultural field respectively creates additional CO_2 emission at a constant rate of 284.551kg/day. By scrutinizing the contribution of each component, it is apparent that the avoidance of CO_2 emission is mainly possible due to replacement of energy for pyrolysis and drying by pyro-gas and pyro-char.

7.2. Significance of Results

To the best of knowledge, the catalytic pyrolysis of this type of feedstock has been studied for the first time. The attempts of determination of distributed kinetic model parameters, process simulation modelling and energy and environmental analysis have also been done for the first time for Indian lignocellulosic biomass. Overall, the results of this research finding are expected to be useful for the generation of energy from lignocellulosic wastes of metro cities

like Kolkata. The results of Kinetic analysis will help in designing reactors for this purpose. The information on catalytic pyrolysis may be utilized for the selection of catalysts for the wastes to be handled. The analysis of the pyro-products may be utilized for the proper utilization of the products, i.e. both for the purpose of generation of energy and chemicals. The data on co-pyrolysis should facilitate the implementation of pyrolysis units using mixture of lignocellulosic feedstocks of diverse nature. Results on large scale pyrolysis plant and the Energy -environmental Analysis are expected to motivate industries and municipal authorities to set up pyrolysis units using lignocellulosic bio-wastes for the generation of energy, chemicals and for the amendment of soil of agricultural fields located in the near vicinity. The outcome of the research can be extended for the prediction of pyrolysis behaviour of other similar feedstocks like jute dust, textile waste, orange peels and so on. However, due to the specific pyrolysis behaviour of feedstocks, the data should be validated by conducting experiments with each feedstock

7.3. Recommendations for Future Work

From the Results and discussion section and the conclusions drawn above, it is clear that the results documented in this research are significant. However, there is further scope for improvement. The recommendations for future research studies are as follows:

- **Deoxygenation of pyro-oil**
  Research work should be focused on deoxygenation of pyro-oil while carrying out catalytic and non-catalytic experiments. As the oxygen content of pyro-oil is high, even with the use of catalysts. Different pre-treatment and post-treatment processes for the lowering of oxygen content in pyro-oil should be studied extensively.
- **Development of reactor Models**
  Further mathematical models should be attempted to be developed by using more realistic DAE kinetics, rather than lumped kinetics.
- **Implementations of Scale-up Technique**
  Real experimental studies have to be conducted on large scale pyrolysis plants integrated with power plants using the pyro-oil and with the scope of transportation of pyro-char to the local agricultural fields for soil amendments to validate Aspen Plus® model. Different pyrolysis feedstocks similar to jute waste and their mixtures should be attempted to be used in the large-scale units.

Nomenclature

W	weight fraction of the reactant to the basis of its initial weight
W_v	weight fraction of the volatiles to the basis of its initial weight of the reactant
W_c	weight fraction of the char to the basis of its initial weight of the reactant
W_l	weight fraction of the liquid to the basis of its initial weight of the reactant
W_g	weight fraction of the gas to the basis of its initial weight of the reactant
k_v	rate constant for volatiles formation, (min^{-1})
k_c	rate constant for char formation, (min^{-1})
k_l	rate constant for liquid formation, (min^{-1})
k_g	rate constant for gas formation, (min^{-1})
k	rate constant, (min^{-1})
E	Total activation energy, (kJ/mol)
E_v	activation energy for volatile formation, (kJ/mol)
E_c	activation energy for char formation, (kJ/mol)
E_l	activation energy for liquid formation, (kJ/mol)
E_g	activation energy for gas formation, (kJ/mol)
R	gas constant, (kJ/mol/K)
T	Pyrolysis temperature, K
t	time, (minute)
A	Pre-exponential factor
v	volatile content
v*	effective volatile
α_i	heating rate
ν_i	stoichiometric coefficients
A_{CO_2}	CO_2 avoidance
EROEI	energy return on energy investment
f	% char deposited
R_{CO_2}	recycle ratio
$W_{g.tar}\rho_g$	concentration of pyro-oil in the gas phase
$\boldsymbol{k_i}$	rate constant for pseudo-component i (units dependent on the order of the reaction)
$\boldsymbol{n_i}$	reaction order for pseudo-component i
R_T	retention time (min)
A	pre-exponential factor
E	activation energy
f(α)	function describing the biomass thermal decomposition.

Subscripts

v	volatiles
c	char
l	liquid
g	gas
0	initial condition
i	ordinal number of a non-isothermal experiment
R	residue

Response to Examiner's Queries

Query1. It is not easy to read thesis. Check the format, fonts are different size and type at different places.
Response: As per the suggestion of the thesis examiner, format and fonts of the text have been edited for better legibility. (Page No: 1-403)

Query2. Nomenclature is missing
Response: As per the suggestion of the thesis examiner, nomenclature has been included in the final version of the thesis. (Page No: 297)

Query3. Provide Abstract
Response: As per the suggestion of the thesis examiner, abstract has been included in the final version of the thesis. (Page No: 7)

Query4 Aim of the work and the hypothesis of the research should be stated clearly.
Response: As per the suggestion of the thesis examiner, the aim of the work and the hypothesis of the research have been re-written and stated properly in the final version of the thesis. (Page No: 54-57)

Query5 Conclusions should reflect the objectives
Response: As per the suggestion of the thesis examiner, conclusion has been revised to clearly reflect the objectives in the final version of the thesis. (Page No: 291-295)

Query6 The huge number of references does not demonstrate that all the papers are read enough to make the decision on the objectives of his own work. The scientific observations of the papers are not critically evaluated as to derive information applicable in the PhD work in terms of developing the methodology or modifying the existing models, methods etc.
Response: As suggested by the learned examiner, the critical analysis of the cited literature has been done in the revised version of the thesis (Literature Review Chapter). The research gap, identified through the review of literature, has been clearly stated in the revised version. The methodologies used by the previous researchers have been analyzed properly to represent their link with the experimental and theoretical strategies of the present investigations. (Page No: 32-48)

Query7 Analysis lacks proper synthesis of information that is useful in more generic terms in the processing of lignocellulosic waste.
Response: The outcome of the research has been properly analyzed to synthesize important information which has the possibility of applications in similar research studies. This has been clearly stated at the end of the "conclusion" in the final version of the thesis. (Page No: 293-295)

Query8 I fail to see a precise statement what is the most significant achievement apart of a large amount of experimental data and numerical predictions.
Response: To represent the significant achievements of the present research studies, a paragraph has been added at the end of the conclusion in the revised version of the thesis. (Page No: 293-295)

Query9 Significance of the findings: There are variety of biomass, which is similar to the ones chosen for study so the results should have wider implications. Should be discussed with

appropriate scientific justification and their implications for theory and limitations to generalization of the results.
Response: The applicability of the results of the present research in the field of pyrolysis of similar biomass feedstocks has been discussed scientifically in the last paragraph of the conclusion chapter of the final version of the thesis. The limitation of generalization has also been discussed in the conclusion. (Page No: 293-295)

Query10 Check all the figures and graph for clarity. Some figures are either too small or have too much information.
Response: As per the suggestion of the thesis examiner, all figures and graphs of the text have been edited for better clarity in the final version. (Page No: 1-403)

Query11 For example; Figure 6.88, 6.89, 6.90 FTR plot: It is not necessary to point out all peaks Frequency range beyond 3600 cm-1 is not necessary. Only point out one or two peaks they identify functional group for a particular range
Response: Figures 6.88, 6.89, 6.90 showing FTIR plots have been edited in the final version of the thesis as per the suggestion of the thesis examiner. (Page No: 245-248)

Chapter. 8

APPENDIX

Appendix.

A1. Values of W_R

(a) Jute wastes

Time (mins)	Weight fraction 673K	Weight fraction 773K	Weight fraction 873K	Weight fraction 973K	Weight fraction 1073K	Weight fraction 1173K
0	1	1	1	1	1	1
5	0.770529	0.750916	0.846008	0.815254	0.655894	0.607362
10	0.704162	0.507937	0.720532	0.59322	0.340304	0.226994
15	0.309336	0.274725	0.54943	0.383051	0.169202	0.134969
20	0.292463	0.23199	0.541825	0.372881	0.161597	0.120654
25	0.256468	0.192918	0.530418	0.345763	0.15019	0.112474
30	0.23847	0.173382	0.528517	0.322034	0.148289	0.106339
35	0.188976	0.119658	0.503802	0.29661	0.123574	0.087935
40	0.165354	0.094017	0.494297	0.29322	0.114068	0.079755
45	0.150731	0.065934	0.479087	0.286441	0.098859	0.067485
50	0.147357	0.050061	0.477186	0.277966	0.096958	0.051125
55	0.125984	0.039072	0.471483	0.271186	0.091255	0.038855
60	0.096738	0.019536	0.444867	0.271186	0.064639	0.02454

(b) lime wastes

Time (mins)	Weight fraction 573K	Weight fraction 673K	Weight fraction 773K	Weight fraction 873K	Weight fraction 973K	Weight fraction 1073K	Weight fraction 1173K
0	1	1	1	1	1	1	1
5	0.889764	0.789905	0.825746	0.67927	0.814026	0.692396	0.749755
10	0.786089	0.682128	0.525903	0.52412	0.647098	0.506912	0.655545
15	0.430446	0.585266	0.492936	0.479791	0.519382	0.394009	0.593719
20	0.410761	0.564802	0.406593	0.269883	0.473448	0.327189	0.553484
25	0.34252	0.493861	0.356358	0.25163	0.334528	0.275346	0.476938
30	0.321522	0.335607	0.189953	0.225554	0.267309	0.25	0.404318
35	0.290026	0.302865	0.152276	0.198175	0.221376	0.180876	0.378803
40	0.249344	0.260573	0.119309	0.186441	0.140713	0.125576	0.322866
45	0.232283	0.242838	0.098901	0.156454	0.13287	0.043779	0.283611
50	0.215223	0.225102	0.078493	0.142112	0.117186	0.03341	0.26104
55	0.190289	0.199181	0.048666	0.116037	0.094779	0.019585	0.241413
60	0.169291	0.177353	0.039246	0.093872	0.086937	0.010369	0.220805

A2. Values of W_V

(a) Jute wastes

Time (mins)	Volatile fraction 673K	Volatile fraction 773K	Volatile fraction 873K	Volatile fraction 973K	Volatile fraction 1073K	Volatile fraction 1173K
0	0	0	0	0	0	0
5	0.229471	0.249084	0.153992	0.184746	0.344106	0.392638
10	0.295838	0.492063	0.279468	0.40678	0.659696	0.773006
15	0.690664	0.725275	0.45057	0.616949	0.830798	0.865031
20	0.707537	0.76801	0.458175	0.627119	0.838403	0.879346
25	0.743532	0.807082	0.469582	0.654237	0.84981	0.887526
30	0.76153	0.826618	0.471483	0.677966	0.851711	0.893661

35	0.811024	0.880342	0.496198	0.70339	0.876426	0.912065
40	0.834646	0.905983	0.505703	0.70678	0.885932	0.920245
45	0.849269	0.934066	0.520913	0.713559	0.901141	0.932515
50	0.852643	0.949939	0.522814	0.722034	0.903042	0.948875
55	0.874016	0.960928	0.528517	0.728814	0.908745	0.961145
60	0.903262	0.980464	0.555133	0.728814	0.935361	0.97546

(b) lime wastes

Time (mins)	Volatile fraction 573K	Volatile fraction 673K	Volatile fraction 773K	Volatile fraction 873K	Volatile fraction 973K	Volatile fraction 1073K	Volatile fraction 1173K
0	0	0	0	0	0	0	0
5	0.110236	0.210095	0.174254	0.32073	0.185974	0.307604	0.250245
10	0.213911	0.317872	0.474097	0.47588	0.352902	0.493088	0.344455
15	0.569554	0.414734	0.507064	0.520209	0.480618	0.605991	0.406281
20	0.589239	0.435198	0.593407	0.730117	0.526552	0.672811	0.446516
25	0.65748	0.506139	0.643642	0.74837	0.665472	0.724654	0.523062
30	0.678478	0.664393	0.810047	0.774446	0.732691	0.75	0.595682
35	0.709974	0.697135	0.847724	0.801825	0.778624	0.819124	0.621197
40	0.750656	0.739427	0.880691	0.813559	0.859287	0.874424	0.677134
45	0.767717	0.757162	0.901099	0.843546	0.86713	0.956221	0.716389
50	0.784777	0.774898	0.921507	0.857888	0.882814	0.96659	0.73896
55	0.809711	0.800819	0.951334	0.883963	0.905221	0.980415	0.758587
60	0.830709	0.822647	0.960754	0.906128	0.913063	0.989631	0.779195

A3. Values of W_c

(a) Jute wastes

Time (mins)	Char fraction 673K	Char fraction 773K	Char fraction 873K	Char fraction 973K	Char fraction 1073K	Char fraction 1173K
0	0	0	0	0	0	0
5	0.024576	0.004963	0.123405	0.068743	0.02378	0.009878
10	0.031684	0.009805	0.223957	0.15136	0.045589	0.019447
15	0.073969	0.014451	0.361073	0.229562	0.057413	0.021762
20	0.075776	0.015303	0.367168	0.233346	0.057938	0.022122
25	0.079631	0.016081	0.376309	0.243437	0.058727	0.022328
30	0.081559	0.016471	0.377832	0.252266	0.058858	0.022482
35	0.086859	0.017541	0.397638	0.261726	0.060566	0.022945
40	0.089389	0.018052	0.405255	0.262988	0.061223	0.023151
45	0.090955	0.018612	0.417444	0.26551	0.062274	0.02346
50	0.091317	0.018928	0.418967	0.268664	0.062405	0.023871
55	0.093606	0.019147	0.423538	0.271186	0.062799	0.02418
60	0.096738	0.019536	0.444867	0.271186	0.064639	0.02454

(b) lime wastes

Time (mins)	Char fraction 573K	Char fraction 673K	Char fraction 773K	Char fraction 873K	Char fraction 973K	Char fraction 1073K	Char fraction 1173K
0	0	0	0	0	0	0	0
5	0.022465	0.045294	0.007118	0.033227	0.017707	0.003223	0.070913
10	0.043593	0.06853	0.019367	0.0493	0.033601	0.005166	0.09761

15	0.11607	0.089412	0.020713	0.053892	0.045762	0.006349	0.11513
20	0.120082	0.093824	0.02424	0.075638	0.050135	0.007049	0.126532
25	0.133989	0.109118	0.026293	0.077529	0.063363	0.007592	0.148223
30	0.138268	0.143236	0.03309	0.08023	0.069763	0.007858	0.168802
35	0.144687	0.150294	0.034629	0.083067	0.074136	0.008582	0.176032
40	0.152977	0.159412	0.035976	0.084282	0.081817	0.009162	0.191883
45	0.156454	0.163236	0.03681	0.087389	0.082564	0.010019	0.203007
50	0.159931	0.167059	0.037643	0.088875	0.084057	0.010127	0.209403
55	0.165012	0.172647	0.038862	0.091576	0.08619	0.010272	0.214965
60	0.169291	0.177353	0.039246	0.093872	0.086937	0.010369	0.220805

A4. t vs $\ln\left(\frac{w_o}{w}\right)$

a) jute wastes

time (mins)	$\ln\left(\frac{w_o}{w}\right)$ 673K	$\ln\left(\frac{w_o}{w}\right)$ 773K	$\ln\left(\frac{w_o}{w}\right)$ 873K	$\ln\left(\frac{w_o}{w}\right)$ 973K	$\ln\left(\frac{w_o}{w}\right)$ 1073K	$\ln\left(\frac{w_o}{w}\right)$ 1173K
0	0	0	0	0	0	0
5	0.3455	0.3455	0.3695	0.399	0.518	0.5765
10	0.691	0.691	0.739	0.798	1.036	1.153
15	1.0365	1.0365	1.1085	1.197	1.554	1.7295
20	1.382	1.382	1.478	1.596	2.072	2.306
25	1.7275	1.7275	1.8475	1.995	2.59	2.8825
30	2.073	2.073	2.217	2.394	3.108	3.459
35	2.4185	2.4185	2.5865	2.793	3.626	4.0355
40	2.764	2.764	2.956	3.192	4.144	4.612
45	3.1095	3.1095	3.3255	3.591	4.662	5.1885
50	3.455	3.455	3.695	3.99	5.18	5.765
55	3.8005	3.8005	4.0645	4.389	5.698	6.3415
60	4.146	4.146	4.434	4.788	6.216	6.918

(b) lime wastes

time (mins)	$\ln\left(\frac{w_o}{w}\right)$ 573K	$\ln\left(\frac{w_o}{w}\right)$ 673K	$\ln\left(\frac{w_o}{w}\right)$ 773K	$\ln\left(\frac{w_o}{w}\right)$ 873K	$\ln\left(\frac{w_o}{w}\right)$ 973K	$\ln\left(\frac{w_o}{w}\right)$ 1073K	$\ln\left(\frac{w_o}{w}\right)$ 1173K
0	0	0	0	0	0	0	0
5	0.2445	0.2495	0.2615	0.3095	0.3975	0.425	0.465
10	0.489	0.499	0.523	0.619	0.795	0.85	0.93
15	0.7335	0.7485	0.7845	0.9285	1.1925	1.275	1.395
20	0.978	0.998	1.046	1.238	1.59	1.7	1.86
25	1.2225	1.2475	1.3075	1.5475	1.9875	2.125	2.325
30	1.467	1.497	1.569	1.857	2.385	2.55	2.79
35	1.7115	1.7465	1.8305	2.1665	2.7825	2.975	3.255
40	1.956	1.996	2.092	2.476	3.18	3.4	3.72
45	2.2005	2.2455	2.3535	2.7855	3.5775	3.825	4.185
50	2.445	2.495	2.615	3.095	3.975	4.25	4.65
55	2.6895	2.7445	2.8765	3.4045	4.3725	4.675	5.115
60	2.934	2.994	3.138	3.714	4.77	5.1	5.58

A5. $\frac{W_V}{W_0}$ **vs** $(1-\exp[-k*t])/k$

a) jute wastes

$(1-\exp[-k*t])/k$	$\frac{W_V}{W_0}$	$\frac{W_V}{W_0}$	$\frac{W_V}{W_0}$	$\frac{W_V}{W_0}$	$\frac{W_V}{W_0}$	$\frac{W_V}{W_0}$
	400	500	600	700	800	900
0	0	0	0	0	0	0
4.227694	0.286638	0.286638	0.17139	0.239954	0.378143	0.427499
7.220337	0.489539	0.489539	0.289834	0.400961	0.603407	0.667694
9.338727	0.633166	0.633166	0.371689	0.508995	0.737599	0.80265
10.83826	0.734834	0.734834	0.428257	0.581485	0.817539	0.878477
11.89974	0.806802	0.806802	0.46735	0.630125	0.86516	0.921081
12.65112	0.857746	0.857746	0.494366	0.662762	0.893528	0.945018
13.18299	0.893807	0.893807	0.513036	0.684662	0.910427	0.958468
13.55949	0.919334	0.919334	0.525939	0.699356	0.920495	0.966025
13.826	0.937403	0.937403	0.534856	0.709215	0.926492	0.970271
14.01466	0.950194	0.950194	0.541018	0.715831	0.930064	0.972656
14.1482	0.959248	0.959248	0.545277	0.72027	0.932192	0.973997
14.24273	0.965657	0.965657	0.54822	0.723249	0.93346	0.97475

(b) lime wastes

$(1-\exp[-k*t])/k$	$\frac{W_V}{W_0}$	$\frac{W_V}{W_0}$	$\frac{W_V}{W_0}$	$\frac{W_V}{W_0}$	$\frac{W_V}{W_0}$	$\frac{W_V}{W_0}$	$\frac{W_V}{W_0}$
	300	400	500	600	700	800	900
0	0	0	0	0	0	0	0
4.435665	0.180088	0.183197	0.191827	0.226624	0.283443	0.29898	0.317885
7.909216	0.321114	0.325942	0.339513	0.392923	0.473917	0.494444	0.517559
10.62934	0.431551	0.437168	0.453217	0.514956	0.601914	0.622233	0.642981
12.75946	0.518034	0.523834	0.540756	0.604506	0.687928	0.705777	0.721764
14.42755	0.585758	0.591363	0.608153	0.670219	0.74573	0.760396	0.77125
15.73382	0.638793	0.643981	0.660041	0.718439	0.784572	0.796104	0.802333
16.75675	0.680324	0.684981	0.69999	0.753825	0.810674	0.819448	0.821858
17.55781	0.712847	0.716927	0.730746	0.779791	0.828215	0.834711	0.834123
18.18512	0.738316	0.741819	0.754425	0.798845	0.840002	0.844689	0.841826
18.67636	0.75826	0.761215	0.772656	0.812827	0.847923	0.851212	0.846665
19.06105	0.773878	0.776328	0.786691	0.823088	0.853246	0.855477	0.849705
19.36229	0.786109	0.788104	0.797497	0.830617	0.856823	0.858265	0.851614

A6. $\frac{w_c}{w_o}$ **vs** $(1-\exp[-k*t])/k$

a) jute wastes

$(1-\exp[-k*t])/k$	$\frac{w_c}{w_o}$	$\frac{w_c}{w_o}$	$\frac{w_c}{w_o}$	$\frac{w_c}{w_o}$	$\frac{w_c}{w_o}$	$\frac{w_c}{w_o}$
	400	500	600	700	800	900
0	0	0	0	0	0	0
4.227694	0.005919	0.005919	0.13753	0.089467	0.026146	0.01064
7.220337	0.010108	0.010108	0.232574	0.149499	0.041722	0.016618
9.338727	0.013074	0.013074	0.298258	0.18978	0.051	0.019977
10.83826	0.015174	0.015174	0.34365	0.216808	0.056527	0.021864
11.89974	0.01666	0.01666	0.37502	0.234944	0.05982	0.022925
12.65112	0.017712	0.017712	0.396699	0.247112	0.061782	0.02352
13.18299	0.018456	0.018456	0.41168	0.255278	0.06295	0.023855
13.55949	0.018983	0.018983	0.422034	0.260756	0.063646	0.024043
13.826	0.019356	0.019356	0.429189	0.264433	0.064061	0.024149
14.01466	0.019621	0.019621	0.434134	0.266899	0.064308	0.024208
14.1482	0.019807	0.019807	0.437551	0.268554	0.064455	0.024242
14.24273	0.01994	0.01994	0.439913	0.269665	0.064543	0.02426

(b) lime wastes

$(1-\exp[-k*t])/k$	$\frac{w_c}{w_o}$	$\frac{w_c}{w_o}$	$\frac{w_c}{w_o}$	$\frac{w_c}{w_o}$	$\frac{w_c}{w_o}$	$\frac{w_c}{w_o}$	$\frac{w_c}{w_o}$
	300	400	500	600	700	800	900
0	0	0	0	0	0	0	0
4.435665	0.036816	0.037613	0.038277	0.039562	0.044559	0.04725	0.05398
7.909216	0.065646	0.06692	0.067747	0.068594	0.074502	0.078141	0.087887
10.62934	0.088224	0.089757	0.090435	0.089898	0.094624	0.098336	0.109186
12.75946	0.105904	0.10755	0.107903	0.10553	0.108146	0.11154	0.122564
14.42755	0.119749	0.121415	0.121352	0.117002	0.117233	0.120172	0.130967
15.73382	0.130591	0.132218	0.131705	0.12542	0.123339	0.125815	0.136245
16.75675	0.139081	0.140636	0.139677	0.131597	0.127442	0.129504	0.139561
17.55781	0.14573	0.147195	0.145814	0.13613	0.1302	0.131916	0.141643
18.18512	0.150936	0.152306	0.150539	0.139457	0.132053	0.133493	0.142952
18.67636	0.155014	0.156288	0.154177	0.141898	0.133298	0.134524	0.143773
19.06105	0.158207	0.159391	0.156977	0.143689	0.134135	0.135198	0.144289
19.36229	0.160707	0.161809	0.159134	0.145003	0.134697	0.135639	0.144614

A7. $\frac{w_l}{w_o}$ **vs** $(1-\exp[-k*t])/k$

a) jute wastes

$(1-\exp[-k*t])/k$	$\frac{w_l}{w_o}$	$\frac{w_l}{w_o}$	$\frac{w_l}{w_o}$	$\frac{w_l}{w_o}$	$\frac{w_l}{w_o}$	$\frac{w_l}{w_o}$

	400	500	600	700	800	900
0	0	0	0	0	0	0
4.227694	0.145702	0.141532	0.15682	0.127758	0.226668	0.249228
7.220337	0.24884	0.236498	0.265195	0.213483	0.378761	0.416458
9.338727	0.321847	0.30022	0.34009	0.271004	0.480813	0.528668
10.83826	0.373527	0.342976	0.391849	0.309599	0.54929	0.60396
11.89974	0.410109	0.371666	0.427619	0.335497	0.595237	0.65448
12.65112	0.436004	0.390916	0.452338	0.352874	0.626067	0.688378
13.18299	0.454335	0.403833	0.469422	0.364533	0.646753	0.711124
13.55949	0.46731	0.4125	0.481228	0.372357	0.660634	0.726386
13.826	0.476495	0.418315	0.489386	0.377606	0.669947	0.736627
14.01466	0.482997	0.422217	0.495025	0.381129	0.676197	0.743498
14.1482	0.487599	0.424835	0.498921	0.383492	0.68039	0.748109
14.24273	0.490857	0.426592	0.501614	0.385078	0.683204	0.751202

b) lime wastes

$(1-\exp[-k*t])/k$	$\frac{w_l}{w_o}$	$\frac{w_l}{w_o}$	$\frac{w_l}{w_o}$	$\frac{w_l}{w_o}$	$\frac{w_l}{w_o}$	$\frac{w_l}{w_o}$	$\frac{w_l}{w_o}$
	300	400	500	600	700	800	900
0	0	0	0	0	0	0	0
4.435665	0.072538	0.072544	0.078412	0.099904	0.118061	0.11796	0.124297
7.909216	0.129343	0.12907	0.138782	0.173216	0.197397	0.195078	0.202373
10.62934	0.173826	0.173114	0.18526	0.227012	0.250711	0.245496	0.251415
12.75946	0.208661	0.207433	0.221043	0.266489	0.286538	0.278457	0.28222
14.42755	0.23594	0.234173	0.248592	0.295458	0.310613	0.300007	0.30157
15.73382	0.257302	0.25501	0.269802	0.316715	0.326792	0.314095	0.313724
16.75675	0.27403	0.271245	0.286132	0.332315	0.337664	0.323305	0.321358
17.55781	0.28713	0.283895	0.298704	0.343761	0.34497	0.329327	0.326154
18.18512	0.297389	0.293753	0.308383	0.352161	0.34988	0.333264	0.329166
18.67636	0.305422	0.301433	0.315835	0.358325	0.353179	0.335837	0.331058
19.06105	0.311713	0.307418	0.321573	0.362848	0.355396	0.33752	0.332247
19.36229	0.31664	0.312081	0.32599	0.366168	0.356886	0.33862	0.332993

A8. $\frac{w_g}{w_o}$ vs $(1-\exp[-k*t])/k$

a) jute wastes

$(1-\exp[-k*t])/k$	$\frac{w_g}{w_o}$	$\frac{w_g}{w_o}$	$\frac{w_g}{w_o}$	$\frac{w_g}{w_o}$	$\frac{w_g}{w_o}$	$\frac{w_g}{w_o}$
	400	500	600	700	800	900
0	0	0	0	0	0	0
4.227694	0.140936	0.143362	0.150015	0.112182	0.200467	0.2146
7.220337	0.240699	0.239557	0.250673	0.187455	0.334978	0.358595
9.338727	0.311319	0.304103	0.318214	0.237962	0.425233	0.455215

10.83826	0.361308	0.347413	0.363534	0.271852	0.485794	0.520045
11.89974	0.396693	0.376473	0.393942	0.294592	0.52643	0.563546
12.65112	0.421741	0.395972	0.414346	0.309851	0.553696	0.592735
13.18299	0.439472	0.409056	0.428037	0.320089	0.571991	0.61232
13.55949	0.452023	0.417835	0.437224	0.326958	0.584268	0.625461
13.826	0.460908	0.423726	0.443388	0.331568	0.592505	0.634279
14.01466	0.467197	0.427678	0.447524	0.334661	0.598032	0.640196
14.1482	0.471648	0.430331	0.450299	0.336736	0.60174	0.644166
14.24273	0.4748	0.43211	0.452161	0.338129	0.604229	0.64683

b) lime wastes

$(1-\exp[-k*t])/k$	$\frac{w_g}{w_o}$	$\frac{w_g}{w_o}$	$\frac{w_g}{w_o}$	$\frac{w_g}{w_o}$	$\frac{w_g}{w_o}$	$\frac{w_g}{w_o}$	$\frac{w_g}{w_o}$
	300	400	500	600	700	800	900
0	0	0	0	0	0	0	0
4.435665	0.10755	0.110653	0.114068	0.132256	0.165383	0.18102	0.193587
7.909216	0.191772	0.196872	0.202949	0.235308	0.27652	0.299366	0.315186
10.62934	0.257725	0.264054	0.272203	0.315606	0.351203	0.376737	0.391566
12.75946	0.309373	0.316401	0.326166	0.378173	0.401391	0.427319	0.439544
14.42755	0.349819	0.35719	0.368214	0.426925	0.435116	0.460389	0.46968
15.73382	0.381491	0.388971	0.400976	0.464911	0.45778	0.482009	0.48861
16.75675	0.406294	0.413736	0.426505	0.49451	0.47301	0.496143	0.5005
17.55781	0.425717	0.433032	0.446396	0.517574	0.483245	0.505384	0.507969
18.18512	0.440927	0.448067	0.461896	0.535544	0.490122	0.511425	0.51266
18.67636	0.452838	0.459782	0.473973	0.549547	0.494744	0.515375	0.515607
19.06105	0.462165	0.468911	0.483383	0.560457	0.49785	0.517957	0.517458
19.36229	0.46947	0.476024	0.490715	0.568959	0.499937	0.519645	0.518621

A.9. Matlab Programming

```
function pdex4
%
%   The PDEs are
%
%      D(u1)/Dt = 0.024*D^2(u1)/Dx^2 - F(u1 - u2)
%      D(u2)/Dt = 0.170*D^2(u2)/Dx^2 + F(u1 - u2)
%
%   where F(y) = exp(5.73*y) - exp(-11.46*y).
%
%   In the form expected by PDEPE, the equations are
%
%   |1|        |u1|      | 0.024*D(u1)/Dx |    |- F(u1 - u2) |
%   | | .*  D_  | | = D_ |                | + |             |
%   |1|     Dt  |u2|   Dx | 0.170*D(u2)/Dx |    |+ F(u1 - u2) |
%
%   ---         ---       ------------------    ---------------
%    c           u          f(x,t,u,Du/Dx)       s(x,t,u,Du/Dx)
%
%   The initial condition is u1(x,0) = 1 and u2(x,0) = 0 for 0 <= x <= 1.
%   The left boundary condition is D(u1)/Dx = 0, u2(0,t) = 0.  The
%   condition on the partial derivative of u1 has to be written in terms
%   of the flux.  In the form expected by PDEPE, the left bc is
%
%      |0 |       |1|     | 0.024*D(u1)/Dx |   |0|
%      | |   +   | | .*  |                | = | |
%      |u2|       |0|     | 0.170*D(u2)/Dx |   |0|
%
```

```
%     ---       ---     ------------------   ---
%    p(0,t,u)   q(0,t)    f(0,t,u,Du/Dx)      0
%
%   The right boundary condition is u1(1,t) = 1, D(u2)/Dx = 0:
%
%     |u1 - 1|       |0|     | 0.024*D(u1)/Dx |   |0|
%     |      |   +   | | .*  |                | = | |
%     |   0  |       |1|     | 0.170*D(u2)/Dx |   |0|
%
%     -------       -----    ------------------   ---
%     p(1,t,u)      q(1,t)     f(1,t,u,Du/Dx)      0
%
%   See the subfunctions PDEX4PDE, PDEX4IC, and PDEX4BC for the coding of the
%   problem definition.
%
%   The solution changes rapidly for small t.  The program selects the step
%   size in time to resolve this sharp change, but to see this behavior in
%   the plots, output times must be selected accordingly.  There are boundary
%   layers in the solution at both ends of [0,1], so mesh points must be
%   placed there to resolve these sharp changes.
%
%   [1] D03PBF, NAG Library Manual, Numerical Algorithms Group, Oxford.
%
%   See also PDEPE, @.

%   Lawrence F. Shampine and Jacek Kierzenka
%   Copyright 1984-2001 The MathWorks, Inc.
%   $Revision: 1.5 $  $Date: 2001/04/15 12:02:57 $

m = 0;
x = [0 0.005 0.01 0.05 0.1 0.2 0.5 0.7 0.9 0.95 0.99 0.995 1];
t = [0 0.005 0.01 0.05 0.1 0.5 1 1.5 2];

sol = pdepe(m,@pdex4pde,@pdex4ic,@pdex4bc,x,t);
u1 = sol(:,:,1);
u2 = sol(:,:,2);

figure;
surf(x,t,u1);
title('u1(x,t)');
xlabel('Distance x');
ylabel('Time t');

figure;
surf(x,t,u2);
title('u2(x,t)');
xlabel('Distance x');
ylabel('Time t');

% --------------------------------------------------------------------------

function [c,f,s] = pdex4pde(x,t,u,DuDx)
c = [1; 1];
f = [0.024; 0.17] .* DuDx;
y = u(1) - u(2);
F = exp(5.73*y)-exp(-11.47*y);
s = [-F; F];

% --------------------------------------------------------------------------

function u0 = pdex4ic(x);
u0 = [1; 0];

% --------------------------------------------------------------------------

function [pl,ql,pr,qr] = pdex4bc(xl,ul,xr,ur,t)
pl = [0; ul(2)];
ql = [1; 0];
pr = [ur(1)-1; 0];
qr = [0; 1];
```

A.10 Values of W_R

a) jute wastes

i) jute waste with alumina

Time (mins)	Weight fraction 673K	Weight fraction 773K	Weight fraction 873K	Weight fraction 973K	Weight fraction 1073K	Weight fraction 1173K
0	1	1	1	1	1	1
5	0.881002	0.724441	0.86744	0.826087	0.686239	0.826758
10	0.611691	0.631789	0.683513	0.741153	0.6	0.544597
15	0.565762	0.528754	0.557581	0.622851	0.547706	0.502573
20	0.517745	0.488019	0.532726	0.528817	0.489908	0.357633
25	0.419624	0.408946	0.460646	0.47725	0.394495	0.295026
30	0.374739	0.3123	0.425021	0.438827	0.316514	0.233276
35	0.210856	0.280351	0.389395	0.399393	0.244037	0.193825
40	0.195198	0.233227	0.372825	0.377149	0.205505	0.173242
45	0.15762	0.213259	0.3314	0.35996	0.162385	0.147513
50	0.140919	0.185304	0.271748	0.340748	0.13578	0.131218
55	0.124217	0.16853	0.140017	0.320526	0.108257	0.11578
60	0.106472	0.154952	0.113505	0.302326	0.100917	0.100343

ii) jute with ZnO

Time (mins)	Weight fraction 673K	Weight fraction 773K	Weight fraction 873K	Weight fraction 973K	Weight fraction 1073K	Weight fraction 1173K
0	1	1	1	1	1	1
5	0.930052	0.981633	0.921053	0.914184	0.781308	0.804721
10	0.854922	0.918367	0.892105	0.897497	0.614953	0.793991
15	0.797927	0.810204	0.692105	0.829559	0.543925	0.628755
20	0.738342	0.691837	0.652632	0.63528	0.515888	0.626609
25	0.61658	0.667347	0.538158	0.574493	0.497196	0.463519
30	0.560881	0.642857	0.481579	0.529201	0.407477	0.444206
35	0.525907	0.559184	0.425	0.506555	0.394393	0.407725
40	0.467617	0.504082	0.398684	0.432658	0.37757	0.356223
45	0.330311	0.487755	0.332895	0.388558	0.35514	0.345494
50	0.270725	0.467347	0.238158	0.342074	0.321495	0.274678
55	0.198187	0.453061	0.160526	0.294398	0.276636	0.270386
60	0.163212	0.334694	0.118421	0.272944	0.196262	0.182403

iii) jute with KCl

Time (mins)	Weight fraction 673K	Weight fraction 773K	Weight fraction 873K	Weight fraction 973K	Weight fraction 1073K	Weight fraction 1173K
0	1	1	1	1	1	1
5	0.940063	0.884034	0.948276	0.906471	0.986982	0.802277
10	0.804416	0.764706	0.756897	0.844481	0.931361	0.693582
15	0.781283	0.665546	0.625862	0.759108	0.897633	0.717391
20	0.757098	0.633613	0.6	0.670473	0.860355	0.612836
25	0.707676	0.511765	0.525	0.642741	0.798817	0.378882

30	0.685068	0.417647	0.487931	0.5677	0.748521	0.317805
35	0.602524	0.316807	0.450862	0.502991	0.678107	0.300207
40	0.542061	0.231933	0.433621	0.469277	0.64142	0.171843
45	0.48633	0.164706	0.390517	0.449157	0.560355	0.166667
50	0.462145	0.092437	0.328448	0.42795	0.537278	0.132505
55	0.380126	0.04958	0.191379	0.406199	0.454438	0.130435
60	0.371188	0.008403	0.163793	0.342034	0.443787	0.087992

iv) jute with NaCl

Time (mins)	Weight fraction 673K	Weight fraction 773K	Weight fraction 873K	Weight fraction 973K	Weight fraction 1073K	Weight fraction 1173K
0	1	1	1	1	1	1
5	0.940133	0.832094	0.753846	0.704612	0.731939	0.666364
10	0.841463	0.721573	0.677949	0.587831	0.642586	0.507706
15	0.607539	0.671626	0.575385	0.488714	0.588403	0.461469
20	0.468958	0.604676	0.50359	0.363101	0.528517	0.419764
25	0.411308	0.51966	0.434872	0.295388	0.467681	0.366274
30	0.382483	0.450584	0.411282	0.210991	0.396388	0.31913
35	0.344789	0.430393	0.367179	0.146222	0.292776	0.286491
40	0.314856	0.408077	0.346667	0.109912	0.271863	0.231188
45	0.284922	0.383634	0.315897	0.087341	0.246198	0.198549
50	0.281596	0.360255	0.283077	0.069676	0.228137	0.158658
55	0.260532	0.342189	0.26359	0.054956	0.209125	0.067996
60	0.247228	0.332625	0.230769	0.034347	0.192015	0.035358

v) jute with Aluminosilicate

Time (mins)	Weight fraction 673K	Weight fraction 773K	Weight fraction 873K	Weight fraction 973K	Weight fraction 1073K	Weight fraction 1173K
0	1	1	1	1	1	1
5	0.932065	0.875969	0.920635	0.925317	0.862797	0.821543
10	0.858016	0.760465	0.842063	0.851382	0.678628	0.787245
15	0.769022	0.736434	0.777778	0.790889	0.609499	0.719185
20	0.675272	0.629457	0.668254	0.687827	0.483905	0.653269
25	0.643342	0.593023	0.630952	0.652726	0.353562	0.615756
30	0.515625	0.524806	0.561111	0.587005	0.307124	0.601822
35	0.504755	0.512403	0.484921	0.51531	0.298681	0.562165
40	0.485054	0.489922	0.446032	0.478715	0.283377	0.490354
45	0.447011	0.446512	0.401587	0.436893	0.253826	0.462487
50	0.334239	0.317829	0.373016	0.410007	0.166227	0.404609
55	0.287364	0.264341	0.342063	0.380881	0.129815	0.344051
60	0.204484	0.216279	0.324603	0.364451	0.044327	0.324759

b) lime wastes

i) lime wastes with alumina

Time (mins)	Weight fraction 573K	Weight fraction 673K	Weight fraction 773K	Weight fraction 873K	Weight fraction 973K	Weight fraction 1073K	Weight fraction 1173K
0	1	1	1	1	1	1	1
5	0.943005	0.918919	0.776758	0.787611	0.589021	0.768325	0.830789
10	0.840674	0.825036	0.674312	0.681416	0.560831	0.609948	0.723919
15	0.489637	0.776671	0.577982	0.631268	0.502967	0.54712	0.643766
20	0.470207	0.716927	0.503058	0.59587	0.45549	0.471204	0.592875
25	0.40285	0.685633	0.477064	0.538348	0.396142	0.425393	0.552163
30	0.382124	0.634424	0.41896	0.49115	0.369436	0.383508	0.474555
35	0.338083	0.58606	0.348624	0.445428	0.335312	0.35733	0.441476
40	0.310881	0.527738	0.30581	0.402655	0.299703	0.294503	0.419847
45	0.281088	0.490754	0.279817	0.359882	0.295252	0.267016	0.396947
50	0.251295	0.462304	0.243119	0.297935	0.268546	0.242147	0.386768
55	0.213731	0.435277	0.218654	0.262537	0.255193	0.223822	0.371501
60	0.154145	0.415363	0.198777	0.256637	0.250742	0.209424	0.361323

ii) lime wastes with ZnO

Time (mins)	Weight fraction 573K	Weight fraction 673K	Weight fraction 773K	Weight fraction 873K	Weight fraction 973K	Weight fraction 1073K	Weight fraction 1173K
0	1	1	1	1	1	1	1
5	0.945026	0.852006	0.742894	0.888175	0.741222	0.81202	0.900826
10	0.802356	0.719225	0.625323	0.79563	0.663199	0.734015	0.760331
15	0.748691	0.672199	0.426357	0.72108	0.612484	0.672634	0.684573
20	0.636126	0.583679	0.381137	0.654242	0.543563	0.620205	0.614325
25	0.582461	0.518672	0.306202	0.59383	0.518856	0.558824	0.472452
30	0.53534	0.46473	0.255814	0.539846	0.477243	0.483376	0.411846
35	0.494764	0.421853	0.21447	0.494859	0.417425	0.429668	0.367769
40	0.463351	0.340249	0.113695	0.476864	0.369311	0.382353	0.320937
45	0.409686	0.295989	0.085271	0.449871	0.339402	0.355499	0.296143
50	0.376963	0.26971	0.059432	0.410026	0.308192	0.315857	0.269972
55	0.349476	0.24343	0.0323	0.383033	0.280884	0.292839	0.241047
60	0.325916	0.214385	0.020672	0.374036	0.252276	0.278772	0.22865

iii) lime wastes with KCl

Time (mins)	Weight fraction 573K	Weight fraction 673K	Weight fraction 773K	Weight fraction 873K	Weight fraction 973K	Weight fraction 1073K	Weight fraction 1173K
0	1	1	1	1	1	1	1
5	0.935288	0.856287	0.843501	0.80417	0.83187	0.807604	0.850498
10	0.85541	0.757485	0.717949	0.687217	0.779203	0.62212	0.668605
15	0.581395	0.696607	0.656057	0.629193	0.747468	0.509217	0.563123
20	0.566229	0.681637	0.595933	0.510426	0.719784	0.442396	0.420266
25	0.51365	0.639721	0.580018	0.497733	0.594193	0.390553	0.354651
30	0.497472	0.533932	0.563218	0.479601	0.572586	0.342166	0.289037
35	0.473205	0.49002	0.547303	0.460562	0.555706	0.296083	0.236711

40	0.44186	0.459082	0.523431	0.452403	0.524646	0.270737	0.20598
45	0.428716	0.446108	0.506631	0.43155	0.511816	0.239631	0.17691
50	0.415571	0.433134	0.48099	0.421578	0.500338	0.217742	0.16196
55	0.39636	0.414172	0.466844	0.403445	0.488859	0.199309	0.141196
60	0.380182	0.398204	0.44916	0.388033	0.480081	0.190092	0.123754

iv) lime wastes with NaCl

Time (mins)	Weight fraction 573K	Weight fraction 673K	Weight fraction 773K	Weight fraction 873K	Weight fraction 973K	Weight fraction 1073K	Weight fraction 1173K
0	1	1	1	1	1	1	1
5	0.900631	0.809984	0.833333	0.733427	0.642119	0.774436	0.820099
10	0.829653	0.719807	0.660767	0.562764	0.540052	0.620301	0.722084
15	0.799685	0.642512	0.501475	0.497884	0.425065	0.522556	0.583127
20	0.731861	0.565217	0.436578	0.448519	0.372093	0.424812	0.528536
25	0.706625	0.479871	0.396755	0.394922	0.267442	0.373434	0.476427
30	0.657729	0.417069	0.336283	0.349788	0.21447	0.318296	0.430521
35	0.61041	0.333333	0.281711	0.306065	0.173127	0.278195	0.398263
40	0.548896	0.293076	0.250737	0.267983	0.131783	0.260652	0.352357
45	0.5	0.26248	0.215339	0.222849	0.087855	0.229323	0.330025
50	0.463722	0.227053	0.205015	0.183357	0.046512	0.205514	0.307692
55	0.443218	0.206119	0.174041	0.146685	0.024548	0.179198	0.2866
60	0.433754	0.196457	0.157817	0.141044	0.002584	0.165414	0.282878

v) lime wastes with Aluminosilicate

Time (mins)	Weight fraction 573K	Weight fraction 673K	Weight fraction 773K	Weight fraction 873K	Weight fraction 973K	Weight fraction 1073K	Weight fraction 1173K
0	1	1	1	1	1	1	1
5	0.86114	0.84413	0.757485	0.729167	0.844371	0.762877	0.749774
10	0.779275	0.76417	0.595808	0.654356	0.756623	0.619893	0.613369
15	0.505699	0.692308	0.431138	0.59375	0.702815	0.53286	0.527552
20	0.482902	0.667004	0.374251	0.488636	0.630795	0.48135	0.415537
25	0.439378	0.624494	0.312375	0.418561	0.586921	0.441385	0.33514
30	0.422798	0.567814	0.270459	0.371212	0.555464	0.421847	0.276423
35	0.397927	0.492915	0.225549	0.351326	0.504139	0.368561	0.224029
40	0.365803	0.47166	0.163673	0.342803	0.470199	0.325933	0.173442
45	0.341969	0.448381	0.130739	0.321023	0.443709	0.262877	0.151762
50	0.328497	0.435223	0.07984	0.310606	0.403146	0.254885	0.138211
55	0.319171	0.415992	0.060878	0.291667	0.384106	0.244227	0.113821
60	0.302591	0.389676	0.03493	0.275568	0.366722	0.237123	0.106594

A.11. Values of W_v

a) jute wastes

i) jute with alumina

Time (mins)	Volatile fraction 673K	Volatile fraction 773K	Volatile fraction 873K	Volatile fraction 973K	Volatile fraction 1073K	Volatile fraction 1173K
0	0	0	0	0	0	0
5	0.118998	0.275559	0.13256	0.173913	0.313761	0.173242
10	0.388309	0.368211	0.316487	0.258847	0.4	0.455403
15	0.434238	0.471246	0.442419	0.377149	0.452294	0.497427
20	0.482255	0.511981	0.467274	0.471183	0.510092	0.642367
25	0.580376	0.591054	0.539354	0.52275	0.605505	0.704974
30	0.625261	0.6877	0.574979	0.561173	0.683486	0.766724
35	0.789144	0.719649	0.610605	0.600607	0.755963	0.806175
40	0.804802	0.766773	0.627175	0.622851	0.794495	0.826758
45	0.84238	0.786741	0.6686	0.64004	0.837615	0.852487
50	0.859081	0.814696	0.728252	0.659252	0.86422	0.868782
55	0.875783	0.83147	0.859983	0.679474	0.891743	0.88422
60	0.893528	0.845048	0.886495	0.697674	0.899083	0.899657

ii) jute with ZnO

Time (mins)	Volatile fraction 673K	Volatile fraction 773K	Volatile fraction 873K	Volatile fraction 973K	Volatile fraction 1073K	Volatile fraction 1173K
0	0	0	0	0	0	0
5	0.069948	0.018367	0.078947	0.085816	0.218692	0.195279
10	0.145078	0.081633	0.107895	0.102503	0.385047	0.206009
15	0.202073	0.189796	0.307895	0.170441	0.456075	0.371245
20	0.261658	0.308163	0.347368	0.36472	0.484112	0.373391
25	0.38342	0.332653	0.461842	0.425507	0.502804	0.536481
30	0.439119	0.357143	0.518421	0.470799	0.592523	0.555794
35	0.474093	0.440816	0.575	0.493445	0.605607	0.592275
40	0.532383	0.495918	0.601316	0.567342	0.62243	0.643777
45	0.669689	0.512245	0.667105	0.611442	0.64486	0.654506
50	0.729275	0.532653	0.761842	0.657926	0.678505	0.725322
55	0.801813	0.546939	0.839474	0.705602	0.723364	0.729614
60	0.836788	0.665306	0.881579	0.727056	0.803738	0.817597

iii) jute with KCl

Time (mins)	Volatile fraction 673K	Volatile fraction 773K	Volatile fraction 873K	Volatile fraction 973K	Volatile fraction 1073K	Volatile fraction 1173K
0	0	0	0	0	0	0
5	0.059937	0.115966	0.051724	0.093529	0.013018	0.197723
10	0.195584	0.235294	0.243103	0.155519	0.068639	0.306418
15	0.218717	0.334454	0.374138	0.240892	0.102367	0.282609
20	0.242902	0.366387	0.4	0.329527	0.139645	0.387164
25	0.292324	0.488235	0.475	0.357259	0.201183	0.621118
30	0.314932	0.582353	0.512069	0.4323	0.251479	0.682195
35	0.397476	0.683193	0.549138	0.497009	0.321893	0.699793

40	0.457939	0.768067	0.566379	0.530723	0.35858	0.828157
45	0.51367	0.835294	0.609483	0.550843	0.439645	0.833333
50	0.537855	0.907563	0.671552	0.57205	0.462722	0.867495
55	0.619874	0.95042	0.808621	0.593801	0.545562	0.869565
60	0.628812	0.991597	0.836207	0.657966	0.556213	0.912008

iv) jute with NaCl

Time (mins)	Volatile fraction 673K	Volatile fraction 773K	Volatile fraction 873K	Volatile fraction 973K	Volatile fraction 1073K	Volatile fraction 1173K
0	0	0	0	0	0	0
5	0.059867	0.167906	0.246154	0.295388	0.268061	0.333636
10	0.158537	0.278427	0.322051	0.412169	0.357414	0.492294
15	0.392461	0.328374	0.424615	0.511286	0.411597	0.538531
20	0.531042	0.395324	0.49641	0.636899	0.471483	0.580236
25	0.588692	0.48034	0.565128	0.704612	0.532319	0.633726
30	0.617517	0.549416	0.588718	0.789009	0.603612	0.68087
35	0.655211	0.569607	0.632821	0.853778	0.707224	0.713509
40	0.685144	0.591923	0.653333	0.890088	0.728137	0.768812
45	0.715078	0.616366	0.684103	0.912659	0.753802	0.801451
50	0.718404	0.639745	0.716923	0.930324	0.771863	0.841342
55	0.739468	0.657811	0.73641	0.945044	0.790875	0.932004
60	0.752772	0.667375	0.769231	0.965653	0.807985	0.964642

v) jute with Aluminosilicate

Time (mins)	Volatile fraction 673K	Volatile fraction 773K	Volatile fraction 873K	Volatile fraction 973K	Volatile fraction 1073K	Volatile fraction 1173K
0	0	0	0	0	0	0
5	0.067935	0.124031	0.079365	0.074683	0.137203	0.178457
10	0.141984	0.239535	0.157937	0.148618	0.321372	0.212755
15	0.230978	0.263566	0.222222	0.209111	0.390501	0.280815
20	0.324728	0.370543	0.331746	0.312173	0.516095	0.346731
25	0.356658	0.406977	0.369048	0.347274	0.646438	0.384244
30	0.484375	0.475194	0.438889	0.412995	0.692876	0.398178
35	0.495245	0.487597	0.515079	0.48469	0.701319	0.437835
40	0.514946	0.510078	0.553968	0.521285	0.716623	0.509646
45	0.552989	0.553488	0.598413	0.563107	0.746174	0.537513
50	0.665761	0.682171	0.626984	0.589993	0.833773	0.595391
55	0.712636	0.735659	0.657937	0.619119	0.870185	0.655949
60	0.795516	0.783721	0.675397	0.635549	0.955673	0.675241

b) lime waste

i) lime wastes with alumina

Time (mins)	Volatile fraction 573K	Volatile fraction 673K	Volatile fraction 773K	Volatile fraction 873K	Volatile fraction 973K	Volatile fraction 1073K	Volatile fraction 1173K
0	0	0	0	0	0	0	0
5	0.056995	0.081081	0.223242	0.212389	0.410979	0.231675	0.169211
10	0.159326	0.174964	0.325688	0.318584	0.439169	0.390052	0.276081
15	0.510363	0.223329	0.422018	0.368732	0.497033	0.45288	0.356234
20	0.529793	0.283073	0.496942	0.40413	0.54451	0.528796	0.407125
25	0.59715	0.314367	0.522936	0.461652	0.603858	0.574607	0.447837
30	0.617876	0.365576	0.58104	0.50885	0.630564	0.616492	0.525445
35	0.661917	0.41394	0.651376	0.554572	0.664688	0.64267	0.558524
40	0.689119	0.472262	0.69419	0.597345	0.700297	0.705497	0.580153
45	0.718912	0.509246	0.720183	0.640118	0.704748	0.732984	0.603053
50	0.748705	0.537696	0.756881	0.702065	0.731454	0.757853	0.613232
55	0.786269	0.564723	0.781346	0.737463	0.744807	0.776178	0.628499
60	0.845855	0.584637	0.801223	0.743363	0.749258	0.790576	0.638677

ii) lime wastes with ZnO

Time (mins)	Volatile fraction 573K	Volatile fraction 673K	Volatile fraction 773K	Volatile fraction 873K	Volatile fraction 973K	Volatile fraction 1073K	Volatile fraction 1173K
0	0	0	0	0	0	0	0
5	0.054974	0.147994	0.257106	0.111825	0.258778	0.18798	0.099174
10	0.197644	0.280775	0.374677	0.20437	0.336801	0.265985	0.239669
15	0.251309	0.327801	0.573643	0.27892	0.387516	0.327366	0.315427
20	0.363874	0.416321	0.618863	0.345758	0.456437	0.379795	0.385675
25	0.417539	0.481328	0.693798	0.40617	0.481144	0.441176	0.527548
30	0.46466	0.53527	0.744186	0.460154	0.522757	0.516624	0.588154
35	0.505236	0.578147	0.78553	0.505141	0.582575	0.570332	0.632231
40	0.536649	0.659751	0.886305	0.523136	0.630689	0.617647	0.679063
45	0.590314	0.704011	0.914729	0.550129	0.660598	0.644501	0.703857
50	0.623037	0.73029	0.940568	0.589974	0.691808	0.684143	0.730028
55	0.650524	0.75657	0.9677	0.616967	0.719116	0.707161	0.758953
60	0.674084	0.785615	0.979328	0.625964	0.747724	0.721228	0.77135

iii) lime wastes with KCl

Time (mins)	Volatile fraction 573K	Volatile fraction 673K	Volatile fraction 773K	Volatile fraction 873K	Volatile fraction 973K	Volatile fraction 1073K	Volatile fraction 1173K
0	0	0	0	0	0	0	0
5	0.064712	0.143713	0.156499	0.19583	0.16813	0.192396	0.149502
10	0.14459	0.242515	0.282051	0.312783	0.220797	0.37788	0.331395
15	0.418605	0.303393	0.343943	0.370807	0.252532	0.490783	0.436877
20	0.433771	0.318363	0.404067	0.489574	0.280216	0.557604	0.579734
25	0.48635	0.360279	0.419982	0.502267	0.405807	0.609447	0.645349
30	0.502528	0.466068	0.436782	0.520399	0.427414	0.657834	0.710963
35	0.526795	0.50998	0.452697	0.539438	0.444294	0.703917	0.763289

40	0.55814	0.540918	0.476569	0.547597	0.475354	0.729263	0.79402
45	0.571284	0.553892	0.493369	0.56845	0.488184	0.760369	0.82309
50	0.584429	0.566866	0.51901	0.578422	0.499662	0.782258	0.83804
55	0.60364	0.585828	0.533156	0.596555	0.511141	0.800691	0.858804
60	0.619818	0.601796	0.55084	0.611967	0.519919	0.809908	0.876246

iv) lime wastes with NaCl

Time (mins)	Volatile fraction 573K	Volatile fraction 673K	Volatile fraction 773K	Volatile fraction 873K	Volatile fraction 973K	Volatile fraction 1073K	Volatile fraction 1173K
0	0	0	0	0	0	0	0
5	0.099369	0.190016	0.166667	0.266573	0.357881	0.225564	0.179901
10	0.170347	0.280193	0.339233	0.437236	0.459948	0.379699	0.277916
15	0.200315	0.357488	0.498525	0.502116	0.574935	0.477444	0.416873
20	0.268139	0.434783	0.563422	0.551481	0.627907	0.575188	0.471464
25	0.293375	0.520129	0.603245	0.605078	0.732558	0.626566	0.523573
30	0.342271	0.582931	0.663717	0.650212	0.78553	0.681704	0.569479
35	0.38959	0.666667	0.718289	0.693935	0.826873	0.721805	0.601737
40	0.451104	0.706924	0.749263	0.732017	0.868217	0.739348	0.647643
45	0.5	0.73752	0.784661	0.777151	0.912145	0.770677	0.669975
50	0.536278	0.772947	0.794985	0.816643	0.953488	0.794486	0.692308
55	0.556782	0.793881	0.825959	0.853315	0.975452	0.820802	0.7134
60	0.566246	0.803543	0.842183	0.858956	0.997416	0.834586	0.717122

v) lime wastes with Aluminosilicate

Time (mins)	Volatile fraction 573K	Volatile fraction 673K	Volatile fraction 773K	Volatile fraction 873K	Volatile fraction 973K	Volatile fraction 1073K	Volatile fraction 1173K
0	0	0	0	0	0	0	0
5	0.13886	0.15587	0.242515	0.270833	0.155629	0.237123	0.250226
10	0.220725	0.23583	0.404192	0.345644	0.243377	0.380107	0.386631
15	0.494301	0.307692	0.568862	0.40625	0.297185	0.46714	0.472448
20	0.517098	0.332996	0.625749	0.511364	0.369205	0.51865	0.584463
25	0.560622	0.375506	0.687625	0.581439	0.413079	0.558615	0.66486
30	0.577202	0.432186	0.729541	0.628788	0.444536	0.578153	0.723577
35	0.602073	0.507085	0.774451	0.648674	0.495861	0.631439	0.775971
40	0.634197	0.52834	0.836327	0.657197	0.529801	0.674067	0.826558
45	0.658031	0.551619	0.869261	0.678977	0.556291	0.737123	0.848238
50	0.671503	0.564777	0.92016	0.689394	0.596854	0.745115	0.861789
55	0.680829	0.584008	0.939122	0.708333	0.615894	0.755773	0.886179
60	0.697409	0.610324	0.96507	0.724432	0.633278	0.762877	0.893406

A.12. Values of W_c

a) jute wastes

i) jute with alumina

Time (mins)	char fraction 673K	char fraction 773K	char fraction 873K	char fraction 973K	char fraction 1073K	char fraction 1173K
0	0	0	0	0	0	0
5	0.01418	0.050528	0.016973	0.075362	0.035218	0.019322

10	0.04627	0.067517	0.040522	0.112167	0.044898	0.050793
15	0.051743	0.08641	0.056646	0.163431	0.050768	0.05548
20	0.057465	0.093879	0.059829	0.204179	0.057255	0.071646
25	0.069157	0.108379	0.069057	0.226525	0.067965	0.078629
30	0.074505	0.1261	0.073619	0.243175	0.076718	0.085516
35	0.094034	0.131958	0.07818	0.260263	0.084853	0.089917
40	0.095899	0.140599	0.080302	0.269902	0.089178	0.092212
45	0.100377	0.144261	0.085606	0.277351	0.094018	0.095082
50	0.102367	0.149387	0.093243	0.285676	0.097004	0.096899
55	0.104357	0.152462	0.11011	0.294439	0.100094	0.098621
60	0.106472	0.154952	0.113505	0.302326	0.100917	0.100343

ii) jute with ZnO

Time (mins)	char fraction 673K	char fraction 773K	char fraction 873K	char fraction 973K	char fraction 1073K	char fraction 1173K
0	0	0	0	0	0	0
5	0.013643	0.00924	0.010605	0.032216	0.053401	0.043566
10	0.028297	0.041067	0.014493	0.038481	0.094023	0.04596
15	0.039414	0.09548	0.041359	0.063985	0.111367	0.082824
20	0.051035	0.155027	0.046661	0.136919	0.118213	0.083302
25	0.074785	0.167347	0.062038	0.159739	0.122778	0.119687
30	0.085649	0.179667	0.069639	0.176742	0.144686	0.123996
35	0.09247	0.22176	0.077239	0.185244	0.147881	0.132135
40	0.103839	0.24948	0.080774	0.212986	0.151989	0.143625
45	0.13062	0.257694	0.089611	0.229541	0.157466	0.146018
50	0.142242	0.26796	0.102337	0.246992	0.165681	0.161817
55	0.156391	0.275147	0.112765	0.26489	0.176636	0.162775
60	0.163212	0.334694	0.118421	0.272944	0.196262	0.182403

iii) jute with KCl

Time (mins)	char fraction 673K	char fraction 773K	char fraction 873K	char fraction 973K	char fraction 1073K	char fraction 1173K
0	0	0	0	0	0	0
5	0.035381	0.000983	0.010132	0.04862	0.010387	0.019077
10	0.115453	0.001994	0.047618	0.080844	0.054765	0.029564
15	0.129109	0.002834	0.073285	0.125224	0.081676	0.027266
20	0.143385	0.003105	0.078351	0.1713	0.111419	0.037354
25	0.172559	0.004138	0.093041	0.185716	0.160519	0.059926
30	0.185904	0.004935	0.100302	0.224725	0.200648	0.065819
35	0.234631	0.00579	0.107563	0.258363	0.25683	0.067517
40	0.270322	0.006509	0.11094	0.275888	0.286101	0.079902
45	0.30322	0.007079	0.119383	0.286347	0.350781	0.080401
50	0.317496	0.007691	0.131541	0.297371	0.369193	0.083697
55	0.365912	0.008054	0.15839	0.308678	0.435289	0.083897
60	0.371188	0.008403	0.163793	0.342034	0.443787	0.087992

iv) jute with NaCl

Time (mins)	char fraction 673K	char fraction 773K	char fraction 873K	char fraction 973K	char fraction 1073K	char fraction 1173K
0	0	0	0	0	0	0
5	0.019662	0.083686	0.073846	0.010507	0.063704	0.012229
10	0.052067	0.13877	0.096615	0.01466	0.084938	0.018045
15	0.128894	0.163664	0.127385	0.018186	0.097815	0.019739
20	0.174407	0.197033	0.148923	0.022654	0.112047	0.021268
25	0.193341	0.239405	0.169538	0.025062	0.126504	0.023229
30	0.202807	0.273833	0.176615	0.028064	0.143447	0.024957
35	0.215187	0.283896	0.189846	0.030368	0.16807	0.026153
40	0.225018	0.295019	0.196	0.03166	0.17304	0.02818
45	0.234849	0.307201	0.205231	0.032462	0.179139	0.029376
50	0.235941	0.318854	0.215077	0.033091	0.183431	0.030839
55	0.242859	0.327858	0.220923	0.033614	0.187949	0.034162
60	0.247228	0.332625	0.230769	0.034347	0.192015	0.035358

v) jute with aluminosilicate

Time (mins)	char fraction 673K	char fraction 773K	char fraction 873K	char fraction 973K	char fraction 1073K	char fraction 1173K
0	0	0	0	0	0	0
5	0.017462	0.034228	0.038144	0.042826	0.006364	0.085829
10	0.036496	0.066103	0.075906	0.085224	0.014906	0.102325
15	0.059372	0.072735	0.106802	0.119913	0.018113	0.135058
20	0.08347	0.102257	0.159441	0.179014	0.023938	0.166761
25	0.091677	0.112311	0.177368	0.199142	0.029984	0.184803
30	0.124506	0.131137	0.210935	0.236829	0.032138	0.191505
35	0.1273	0.134559	0.247553	0.277942	0.032529	0.210578
40	0.132364	0.140763	0.266243	0.298927	0.033239	0.245116
45	0.142143	0.152743	0.287604	0.32291	0.03461	0.258518
50	0.171131	0.188255	0.301335	0.338327	0.038673	0.286355
55	0.18318	0.203016	0.316212	0.355029	0.040362	0.31548
60	0.204484	0.216279	0.324603	0.364451	0.044327	0.324759

b) lime wastes

i) lime with alumina

Time (mins)	char fraction 573K	char fraction 673K	char fraction 773K	char fraction 873K	char fraction 973K	char fraction 1073K	char fraction 1073K
0	0	0	0	0	0	0	0
5	0.010386	0.057605	0.055384	0.073325	0.137536	0.061371	0.095729
10	0.029035	0.124306	0.0808	0.109987	0.146969	0.103325	0.156189
15	0.093006	0.158667	0.104699	0.1273	0.166334	0.119968	0.201535
20	0.096547	0.201112	0.123287	0.139521	0.182222	0.140078	0.230326
25	0.108822	0.223346	0.129736	0.15938	0.202083	0.152214	0.253358
30	0.112599	0.259728	0.144151	0.175674	0.21102	0.163309	0.297264
35	0.120625	0.294089	0.161601	0.191459	0.22244	0.170244	0.315978
40	0.125582	0.335524	0.172223	0.206226	0.234357	0.186887	0.328214

45	0.131012	0.3618	0.178671	0.220993	0.235846	0.194168	0.34117
50	0.136441	0.382012	0.187776	0.24238	0.244784	0.200756	0.346928
55	0.143286	0.401214	0.193845	0.2546	0.249252	0.20561	0.355565
60	0.154145	0.415363	0.198777	0.256637	0.250742	0.209424	0.361323

ii) lime with ZnO

Time (mins)	char fraction 573K	char fraction 673K	char fraction 773K	char fraction 873K	char fraction 973K	char fraction 1073K	char fraction 1073K
0	0	0	0	0	0	0	0
5	0.02658	0.040386	0.005427	0.06682	0.087309	0.072659	0.029398
10	0.09556	0.07662	0.007909	0.122119	0.113634	0.10281	0.071045
15	0.121507	0.089453	0.012109	0.166665	0.130745	0.126535	0.093502
20	0.175931	0.113609	0.013063	0.206603	0.153998	0.1468	0.114325
25	0.201878	0.131348	0.014645	0.242701	0.162334	0.170526	0.15638
30	0.224661	0.146068	0.015708	0.274959	0.176374	0.199688	0.174346
35	0.244279	0.157769	0.016581	0.30184	0.196556	0.220448	0.187411
40	0.259467	0.180038	0.018708	0.312593	0.212789	0.238736	0.201294
45	0.285414	0.192116	0.019308	0.328722	0.22288	0.249116	0.208643
50	0.301235	0.199287	0.019854	0.352531	0.23341	0.264438	0.216401
55	0.314525	0.206458	0.020426	0.36866	0.242623	0.273335	0.224975
60	0.325916	0.214385	0.020672	0.374036	0.252276	0.278772	0.22865

iii) lime with KCl

Time (mins)	char fraction 573K	char fraction 673K	char fraction 773K	char fraction 873K	char fraction 973K	char fraction 1073K	char fraction 1073K
0	0	0	0	0	0	0	0
5	0.039693	0.095093	0.12761	0.12417	0.155247	0.045157	0.021114
10	0.088688	0.16047	0.229987	0.198328	0.203879	0.088692	0.046804
15	0.256762	0.200753	0.280455	0.235119	0.233182	0.115191	0.061701
20	0.266065	0.210658	0.32948	0.310426	0.258745	0.130874	0.081877
25	0.298316	0.238394	0.342457	0.318474	0.374713	0.143042	0.091144
30	0.308239	0.308393	0.356156	0.329971	0.394664	0.154399	0.100411
35	0.323124	0.337449	0.369133	0.342044	0.410251	0.165215	0.107801
40	0.34235	0.357921	0.388599	0.347217	0.438931	0.171164	0.112141
45	0.350412	0.366506	0.402297	0.360439	0.450777	0.178465	0.116247
50	0.358475	0.375091	0.423205	0.366763	0.461377	0.183603	0.118358
55	0.370259	0.387638	0.434741	0.37826	0.471976	0.187929	0.121291
60	0.380182	0.398204	0.44916	0.388033	0.480081	0.190092	0.123754

iv) lime with NaCl

Time (mins)	char fraction 573K	char fraction 673K	char fraction 773K	char fraction 873K	char fraction 973K	char fraction 1073K	char fraction 1073K
0	0	0	0	0	0	0	0
5	0.076118	0.046457	0.031232	0.043772	0.000927	0.044706	0.070964
10	0.130489	0.068504	0.063569	0.071796	0.001192	0.075256	0.109628
15	0.153445	0.087402	0.093419	0.082449	0.001489	0.094628	0.164441
20	0.205399	0.1063	0.10558	0.090555	0.001627	0.114001	0.185975

25	0.22473	0.127166	0.113042	0.099356	0.001898	0.124184	0.206531
30	0.262186	0.14252	0.124374	0.106767	0.002035	0.135113	0.224639
35	0.298432	0.162993	0.134601	0.113947	0.002142	0.14306	0.237363
40	0.345553	0.172835	0.140405	0.1202	0.002249	0.146538	0.255472
45	0.383008	0.180316	0.147038	0.127611	0.002363	0.152747	0.264281
50	0.410798	0.188977	0.148973	0.134096	0.00247	0.157466	0.27309
55	0.426505	0.194095	0.154777	0.140117	0.002527	0.162681	0.28141
60	0.433754	0.196457	0.157817	0.141044	0.002584	0.165414	0.282878

v) lime with aluminosilicate

Time (mins)	char fraction 573K	char fraction 673K	char fraction 773K	char fraction 873K	char fraction 973K	char fraction 1073K	char fraction 1073K
0	0	0	0	0	0	0	0
5	0.060248	0.099519	0.008778	0.103023	0.090122	0.073704	0.029855
10	0.095768	0.150571	0.014629	0.13148	0.140936	0.118147	0.04613
15	0.214466	0.196454	0.02059	0.154534	0.172096	0.1452	0.056369
20	0.224358	0.212609	0.022649	0.194519	0.213801	0.16121	0.069734
25	0.243242	0.239751	0.024888	0.221175	0.239208	0.173632	0.079326
30	0.250435	0.27594	0.026405	0.239186	0.257424	0.179705	0.086332
35	0.261226	0.323761	0.028031	0.246751	0.287146	0.196268	0.092583
40	0.275164	0.337332	0.03027	0.249993	0.3068	0.209518	0.098619
45	0.285505	0.352195	0.031462	0.258278	0.32214	0.229117	0.101205
50	0.29135	0.360596	0.033305	0.26224	0.345629	0.231602	0.102822
55	0.295397	0.372874	0.033991	0.269444	0.356655	0.234914	0.105732
60	0.302591	0.389676	0.03493	0.275568	0.366722	0.237123	0.106594

A.13 t vs $\ln\left(\frac{w_o}{w}\right)$

a) jute waste

i) jute wastes with alumina

time (mins)	$\ln\left(\frac{w_o}{w}\right)$ 673K	$\ln\left(\frac{w_o}{w}\right)$ 773K	$\ln\left(\frac{w_o}{w}\right)$ 873K	$\ln\left(\frac{w_o}{w}\right)$ 973K	$\ln\left(\frac{w_o}{w}\right)$ 1073K	$\ln\left(\frac{w_o}{w}\right)$ 1173K
0	0	0	0	0	0	0
5	0.22	0.2865	0.29	0.31	0.32	0.34
10	0.44	0.573	0.58	0.62	0.64	0.68
15	0.66	0.8595	0.87	0.93	0.96	1.02
20	0.88	1.146	1.16	1.24	1.28	1.36
25	1.1	1.4325	1.45	1.55	1.6	1.7
30	1.32	1.719	1.74	1.86	1.92	2.04
35	1.54	2.0055	2.03	2.17	2.24	2.38
40	1.76	2.292	2.32	2.48	2.56	2.72
45	1.98	2.5785	2.61	2.79	2.88	3.06
50	2.2	2.865	2.9	3.1	3.2	3.4
55	2.42	3.1515	3.19	3.41	3.52	3.74
60	2.64	3.438	3.48	3.72	3.84	4.08

ii) jute wastes with ZnO

time (mins)	$\ln\left(\frac{w_o}{w}\right)$ 673K	$\ln\left(\frac{w_o}{w}\right)$ 773K	$\ln\left(\frac{w_o}{w}\right)$ 873K	$\ln\left(\frac{w_o}{w}\right)$ 973K	$\ln\left(\frac{w_o}{w}\right)$ 1073K	$\ln\left(\frac{w_o}{w}\right)$ 1173K
0	0	0	0	0	0	0
5	0.1265	0.5765	0.1405	0.1515	0.1515	0.1925
10	0.253	1.153	0.281	0.303	0.303	0.385
15	0.3795	1.7295	0.4215	0.4545	0.4545	0.5775
20	0.506	2.306	0.562	0.606	0.606	0.77
25	0.6325	2.8825	0.7025	0.7575	0.7575	0.9625
30	0.759	3.459	0.843	0.909	0.909	1.155
35	0.8855	4.0355	0.9835	1.0605	1.0605	1.3475
40	1.012	4.612	1.124	1.212	1.212	1.54
45	1.1385	5.1885	1.2645	1.3635	1.3635	1.7325
50	1.265	5.765	1.405	1.515	1.515	1.925
55	1.3915	6.3415	1.5455	1.6665	1.6665	2.1175
60	1.518	6.918	1.686	1.818	1.818	2.31

iii) jute wastes with KCl

time (mins)	$\ln\left(\frac{w_o}{w}\right)$ 673K	$\ln\left(\frac{w_o}{w}\right)$ 773K	$\ln\left(\frac{w_o}{w}\right)$ 873K	$\ln\left(\frac{w_o}{w}\right)$ 973K	$\ln\left(\frac{w_o}{w}\right)$ 1073K	$\ln\left(\frac{w_o}{w}\right)$ 1173K
0	0	0	0	0	0	0
5	0.15	0.1525	0.16	0.19	0.17	0.195
10	0.3	0.305	0.32	0.38	0.34	0.39
15	0.45	0.4575	0.48	0.57	0.51	0.585
20	0.6	0.61	0.64	0.76	0.68	0.78
25	0.75	0.7625	0.8	0.95	0.85	0.975
30	0.9	0.915	0.96	1.14	1.02	1.17
35	1.05	1.0675	1.12	1.33	1.19	1.365
40	1.2	1.22	1.28	1.52	1.36	1.56
45	1.35	1.3725	1.44	1.71	1.53	1.755
50	1.5	1.525	1.6	1.9	1.7	1.95
55	1.65	1.6775	1.76	2.09	1.87	2.145
60	1.8	1.83	1.92	2.28	2.04	2.34

iv) jute wastes with NaCl

time (mins)	$\ln\left(\frac{w_o}{w}\right)$ 673K	$\ln\left(\frac{w_o}{w}\right)$ 773K	$\ln\left(\frac{w_o}{w}\right)$ 873K	$\ln\left(\frac{w_o}{w}\right)$ 973K	$\ln\left(\frac{w_o}{w}\right)$ 1073K	$\ln\left(\frac{w_o}{w}\right)$ 1173K
0	0	0	0	0	0	0
5	0.2125	0.2575	0.28	0.2875	0.2875	0.272
10	0.425	0.515	0.56	0.575	0.575	0.544
15	0.6375	0.7725	0.84	0.8625	0.8625	0.816
20	0.85	1.03	1.12	1.15	1.15	1.088

25	1.0625	1.2875	1.4	1.4375	1.4375	1.36
30	1.275	1.545	1.68	1.725	1.725	1.632
35	1.4875	1.8025	1.96	2.0125	2.0125	1.904
40	1.7	2.06	2.24	2.3	2.3	2.176
45	1.9125	2.3175	2.52	2.5875	2.5875	2.448
50	2.125	2.575	2.8	2.875	2.875	2.72
55	2.3375	2.8325	3.08	3.1625	3.1625	2.992
60	2.55	3.09	3.36	3.45	3.45	3.264

v) jute wastes with Aluminosilicate

time (mins)	$\ln\left(\frac{w_o}{w}\right)$ 673K	$\ln\left(\frac{w_o}{w}\right)$ 773K	$\ln\left(\frac{w_o}{w}\right)$ 873K	$\ln\left(\frac{w_o}{w}\right)$ 973K	$\ln\left(\frac{w_o}{w}\right)$ 1073K	$\ln\left(\frac{w_o}{w}\right)$ 1173K
0	0	0	0	0	0	0
5	0.135	0.1595	0.17	0.17	0.17	0.19
10	0.27	0.319	0.34	0.34	0.34	0.38
15	0.405	0.4785	0.51	0.51	0.51	0.57
20	0.54	0.638	0.68	0.68	0.68	0.76
25	0.675	0.7975	0.85	0.85	0.85	0.95
30	0.81	0.957	1.02	1.02	1.02	1.14
35	0.945	1.1165	1.19	1.19	1.19	1.33
40	1.08	1.276	1.36	1.36	1.36	1.52
45	1.215	1.4355	1.53	1.53	1.53	1.71
50	1.35	1.595	1.7	1.7	1.7	1.9
55	1.485	1.7545	1.87	1.87	1.87	2.09
60	1.62	1.914	2.04	2.04	2.04	2.28

b) lime wastes

i) lime wastes with alumina

time (mins)	$\ln\left(\frac{w_o}{w}\right)$ 573K	$\ln\left(\frac{w_o}{w}\right)$ 673K	$\ln\left(\frac{w_o}{w}\right)$ 773K	$\ln\left(\frac{w_o}{w}\right)$ 873K	$\ln\left(\frac{w_o}{w}\right)$ 973K	$\ln\left(\frac{w_o}{w}\right)$ 1073K	$\ln\left(\frac{w_o}{w}\right)$ 1173K
0	0	0	0	0	0	0	0
5	0.196	0.2495	0.254	0.3095	0.3975	0.425	0.4665
10	0.392	0.499	0.508	0.619	0.795	0.85	0.933
15	0.588	0.7485	0.762	0.9285	1.1925	1.275	1.3995
20	0.784	0.998	1.016	1.238	1.59	1.7	1.866
25	0.98	1.2475	1.27	1.5475	1.9875	2.125	2.3325
30	1.176	1.497	1.524	1.857	2.385	2.55	2.799
35	1.372	1.7465	1.778	2.1665	2.7825	2.975	3.2655
40	1.568	1.996	2.032	2.476	3.18	3.4	3.732
45	1.764	2.2455	2.286	2.7855	3.5775	3.825	4.1985
50	1.96	2.495	2.54	3.095	3.975	4.25	4.665
55	2.156	2.7445	2.794	3.4045	4.3725	4.675	5.1315
60	2.352	2.994	3.048	3.714	4.77	5.1	5.598

ii) lime wastes with ZnO

time (mins)	$\ln\left(\frac{w_o}{w}\right)$ 573K	$\ln\left(\frac{w_o}{w}\right)$ 673K	$\ln\left(\frac{w_o}{w}\right)$ 773K	$\ln\left(\frac{w_o}{w}\right)$ 873K	$\ln\left(\frac{w_o}{w}\right)$ 973K	$\ln\left(\frac{w_o}{w}\right)$ 1073K	$\ln\left(\frac{w_o}{w}\right)$ 1173K
0	0	0	0	0	0	0	0
5	0.1795	0.2495	0.2645	0.3095	0.3975	0.425	0.4665
10	0.359	0.499	0.529	0.619	0.795	0.85	0.933
15	0.5385	0.7485	0.7935	0.9285	1.1925	1.275	1.3995
20	0.718	0.998	1.058	1.238	1.59	1.7	1.866
25	0.8975	1.2475	1.3225	1.5475	1.9875	2.125	2.3325
30	1.077	1.497	1.587	1.857	2.385	2.55	2.799
35	1.2565	1.7465	1.8515	2.1665	2.7825	2.975	3.2655
40	1.436	1.996	2.116	2.476	3.18	3.4	3.732
45	1.6155	2.2455	2.3805	2.7855	3.5775	3.825	4.1985
50	1.795	2.495	2.645	3.095	3.975	4.25	4.665
55	1.9745	2.7445	2.9095	3.4045	4.3725	4.675	5.1315
60	2.154	2.994	3.174	3.714	4.77	5.1	5.598

iii) lime wastes with KCl

time (mins)	$\ln\left(\frac{w_o}{w}\right)$ 573K	$\ln\left(\frac{w_o}{w}\right)$ 673K	$\ln\left(\frac{w_o}{w}\right)$ 773K	$\ln\left(\frac{w_o}{w}\right)$ 873K	$\ln\left(\frac{w_o}{w}\right)$ 973K	$\ln\left(\frac{w_o}{w}\right)$ 1073K	$\ln\left(\frac{w_o}{w}\right)$ 1173K
0	0	0	0	0	0	0	0
5	0.2325	0.2495	0.3155	0.3095	0.3975	0.425	0.4665
10	0.465	0.499	0.631	0.619	0.795	0.85	0.933
15	0.6975	0.7485	0.9465	0.9285	1.1925	1.275	1.3995
20	0.93	0.998	1.262	1.238	1.59	1.7	1.866
25	1.1625	1.2475	1.5775	1.5475	1.9875	2.125	2.3325
30	1.395	1.497	1.893	1.857	2.385	2.55	2.799
35	1.6275	1.7465	2.2085	2.1665	2.7825	2.975	3.2655
40	1.86	1.996	2.524	2.476	3.18	3.4	3.732
45	2.0925	2.2455	2.8395	2.7855	3.5775	3.825	4.1985
50	2.325	2.495	3.155	3.095	3.975	4.25	4.665
55	2.5575	2.7445	3.4705	3.4045	4.3725	4.675	5.1315
60	2.79	2.994	3.786	3.714	4.77	5.1	5.598

iv) lime wastes with NaCl

time (mins)	$\ln\left(\frac{w_o}{w}\right)$ 573K	$\ln\left(\frac{w_o}{w}\right)$ 673K	$\ln\left(\frac{w_o}{w}\right)$ 773K	$\ln\left(\frac{w_o}{w}\right)$ 873K	$\ln\left(\frac{w_o}{w}\right)$ 973K	$\ln\left(\frac{w_o}{w}\right)$ 1073K	$\ln\left(\frac{w_o}{w}\right)$ 1173K
0	0	0	0	0	0	0	0
5	0.1735	0.2495	0.262	0.3095	0.3975	0.425	0.4665
10	0.347	0.499	0.524	0.619	0.795	0.85	0.933
15	0.5205	0.7485	0.786	0.9285	1.1925	1.275	1.3995
20	0.694	0.998	1.048	1.238	1.59	1.7	1.866
25	0.8675	1.2475	1.31	1.5475	1.9875	2.125	2.3325

30	1.041	1.497	1.572	1.857	2.385	2.55	2.799
35	1.2145	1.7465	1.834	2.1665	2.7825	2.975	3.2655
40	1.388	1.996	2.096	2.476	3.18	3.4	3.732
45	1.5615	2.2455	2.358	2.7855	3.5775	3.825	4.1985
50	1.735	2.495	2.62	3.095	3.975	4.25	4.665
55	1.9085	2.7445	2.882	3.4045	4.3725	4.675	5.1315
60	2.082	2.994	3.144	3.714	4.77	5.1	5.598

v) lime wastes with Aluminosilicate

time (mins)	$\ln\left(\frac{w_o}{w}\right)$ 573K	$\ln\left(\frac{w_o}{w}\right)$ 673K	$\ln\left(\frac{w_o}{w}\right)$ 773K	$\ln\left(\frac{w_o}{w}\right)$ 873K	$\ln\left(\frac{w_o}{w}\right)$ 973K	$\ln\left(\frac{w_o}{w}\right)$ 1073K	$\ln\left(\frac{w_o}{w}\right)$ 1173K
0	0	0	0	0	0	0	0
5	0.277	0.2495	0.268	0.3095	0.3975	0.425	0.4665
10	0.554	0.499	0.536	0.619	0.795	0.85	0.933
15	0.831	0.7485	0.804	0.9285	1.1925	1.275	1.3995
20	1.108	0.998	1.072	1.238	1.59	1.7	1.866
25	1.385	1.2475	1.34	1.5475	1.9875	2.125	2.3325
30	1.662	1.497	1.608	1.857	2.385	2.55	2.799
35	1.939	1.7465	1.876	2.1665	2.7825	2.975	3.2655
40	2.216	1.996	2.144	2.476	3.18	3.4	3.732
45	2.493	2.2455	2.412	2.7855	3.5775	3.825	4.1985
50	2.77	2.495	2.68	3.095	3.975	4.25	4.665
55	3.047	2.7445	2.948	3.4045	4.3725	4.675	5.1315
60	3.324	2.994	3.216	3.714	4.77	5.1	5.598

A.14 $\frac{w_v}{w_o}$ vs $(1-\exp[-k*t])/k$

a) jute wastes

i) jute wastes with alumina

$(1-\exp[-k*t])/k$	$\frac{w_v}{w_0}$	$\frac{w_v}{w_0}$	$\frac{w_v}{w_0}$	$\frac{w_v}{w_0}$	$\frac{w_v}{w_0}$	$\frac{w_v}{w_0}$
	400	500	600	700	800	900
0	0	0	0	0	0	0
4.488209	0.178631	0.199986	0.203993	0.206364	0.209667	0.216172
8.090081	0.321985	0.350153	0.356634	0.35772	0.361917	0.370037
10.98065	0.43703	0.462911	0.47085	0.468733	0.472473	0.479554
13.30039	0.529355	0.54758	0.556313	0.550154	0.552753	0.557504
15.16202	0.603448	0.611157	0.620262	0.609873	0.611048	0.612987
16.65602	0.662909	0.658896	0.668113	0.653673	0.653379	0.652478
17.85497	0.710628	0.694742	0.703918	0.685798	0.684118	0.680587
18.81716	0.748923	0.721659	0.730709	0.70936	0.706439	0.700594
19.58934	0.779656	0.74187	0.750756	0.726642	0.722647	0.714834
20.20902	0.804319	0.757047	0.765757	0.739317	0.734416	0.72497
20.70633	0.824112	0.768443	0.776981	0.748613	0.742963	0.732184
21.10543	0.839996	0.777	0.78538	0.755432	0.749169	0.737319

ii) jute wastes with ZnO

$(1-\exp[-k*t])/k$	$\frac{W_v}{W_0}$	$\frac{W_v}{W_0}$	$\frac{W_v}{W_0}$	$\frac{W_v}{W_0}$	$\frac{W_v}{W_0}$	$\frac{W_v}{W_0}$
	400	500	600	700	800	900
0	0	0	0	0	0	0
4.696674	0.099569	0.082847	0.115683	0.102073	0.102073	0.143268
8.835262	0.187308	0.15534	0.216203	0.189796	0.189796	0.261449
12.48208	0.26462	0.218774	0.303547	0.265187	0.265187	0.358936
15.69556	0.332746	0.27428	0.379442	0.329979	0.329979	0.439353
18.52719	0.392777	0.32285	0.445389	0.385663	0.385663	0.505688
21.02236	0.445674	0.365349	0.502692	0.433518	0.433518	0.560407
23.22103	0.492286	0.402538	0.552484	0.474646	0.474646	0.605545
25.15845	0.533359	0.435078	0.59575	0.509992	0.509992	0.642779
26.86565	0.569552	0.463553	0.633344	0.540369	0.540369	0.673493
28.36999	0.601444	0.488468	0.666011	0.566476	0.566476	0.698829
29.69557	0.629546	0.51027	0.694395	0.588912	0.588912	0.719728
30.86365	0.654309	0.529347	0.71906	0.608195	0.608195	0.736968

iii) jute wastes with KCl

$(1-\exp[-k*t])/k$	$\frac{W_v}{W_0}$	$\frac{W_v}{W_0}$	$\frac{W_v}{W_0}$	$\frac{W_v}{W_0}$	$\frac{W_v}{W_0}$	$\frac{W_v}{W_0}$
	400	500	600	700	800	900
0	0	0	0	0	0	0
4.643067	0.086825	0.14005	0.124754	0.104735	0.103457	0.16172
8.639393	0.161557	0.260291	0.231062	0.191347	0.19074	0.294789
12.07906	0.225878	0.363525	0.321652	0.262971	0.264378	0.404283
15.03961	0.281241	0.452158	0.398847	0.322202	0.326503	0.494378
17.58778	0.328892	0.528254	0.464629	0.371183	0.378917	0.568512
19.78101	0.369905	0.593587	0.520684	0.411688	0.423136	0.629511
21.66874	0.405205	0.649679	0.568451	0.445185	0.460442	0.679704
23.29353	0.435589	0.697838	0.609156	0.472885	0.491916	0.721004
24.69199	0.46174	0.739185	0.643842	0.495792	0.518469	0.754987
25.89566	0.484249	0.774683	0.6734	0.514735	0.540871	0.78295
26.93167	0.503622	0.805161	0.698587	0.5304	0.559771	0.805958
27.82337	0.520297	0.831328	0.72005	0.543354	0.575716	0.824891

iv) jute wastes with NaCl

$(1-\exp[-k*t])/k$	$\frac{W_v}{W_0}$	$\frac{W_v}{W_0}$	$\frac{W_v}{W_0}$	$\frac{W_v}{W_0}$	$\frac{W_v}{W_0}$	$\frac{W_v}{W_0}$
	400	500	600	700	800	900
0	0	0	0	0	0	0
4.504463	0.144143	0.151639	0.187959	0.241173	0.241173	0.229828
8.146593	0.260691	0.268854	0.330016	0.422085	0.422085	0.404924
11.09148	0.354927	0.359459	0.43738	0.557794	0.557794	0.538321

13.47259	0.431123	0.429494	0.518524	0.659594	0.659594	0.63995
15.39786	0.492732	0.483631	0.579851	0.735958	0.735958	0.717377
16.95457	0.542546	0.525477	0.626201	0.793242	0.793242	0.776365
18.21325	0.582824	0.557824	0.661232	0.836212	0.836212	0.821305
19.23098	0.615391	0.582827	0.687708	0.868446	0.868446	0.855543
20.05387	0.641724	0.602154	0.707718	0.892625	0.892625	0.881627
20.71922	0.663015	0.617093	0.722841	0.910764	0.910764	0.9015
21.25721	0.680231	0.628641	0.734271	0.92437	0.92437	0.916639
21.6922	0.69415	0.637568	0.742909	0.934576	0.934576	0.928174

v) jute wastes with Aluminosilicate

$(1-\exp[-k*t])/k$	$\frac{W_V}{W_0}$	$\frac{W_V}{W_0}$	$\frac{W_V}{W_0}$	$\frac{W_V}{W_0}$	$\frac{W_V}{W_0}$	$\frac{W_V}{W_0}$
	400	500	600	700	800	900
0	0	0	0	0	0	0
4.677188	0.10056	0.115541	0.105756	0.09656	0.097939	0.115209
8.763722	0.18842	0.214047	0.194979	0.178024	0.180567	0.210482
12.33419	0.265185	0.298031	0.270253	0.246753	0.250278	0.289269
15.45377	0.332256	0.369633	0.333759	0.304737	0.30909	0.354422
18.17939	0.390857	0.430679	0.387337	0.353655	0.358708	0.408301
20.56081	0.442057	0.482725	0.432539	0.394927	0.400568	0.452857
22.6415	0.486792	0.527097	0.470674	0.429746	0.435885	0.489703
24.45942	0.525878	0.564928	0.502847	0.459121	0.46568	0.520173
26.04778	0.560027	0.597182	0.529991	0.483904	0.490817	0.545371
27.43555	0.589864	0.62468	0.552891	0.504813	0.512025	0.566208
28.64806	0.615933	0.648124	0.57221	0.522453	0.529917	0.58344
29.70746	0.63871	0.668112	0.58851	0.537335	0.545011	0.59769

c) lime wastes

i) lime wastes with alumina

$(1-\exp[-k*t])/k$	$\frac{W_V}{W_0}$	$\frac{W_V}{W_0}$	$\frac{W_V}{W_0}$	$\frac{W_V}{W_0}$	$\frac{W_V}{W_0}$	$\frac{W_V}{W_0}$	$\frac{W_V}{W_0}$
	300	400	500	600	700	800	900
0	0	0	0	0	0	0	0
4.540504	0.150291	0.183197	0.192516	0.226624	0.283443	0.29898	0.317665
8.272854	0.273831	0.325942	0.34185	0.392923	0.473917	0.494444	0.516902
11.34089	0.375384	0.437168	0.457687	0.514956	0.601914	0.622233	0.641862
13.86286	0.458861	0.523834	0.54754	0.604506	0.687928	0.705777	0.720236
15.93594	0.52748	0.591363	0.617239	0.670219	0.74573	0.760396	0.769392
17.64004	0.583885	0.643981	0.671304	0.718439	0.784572	0.796104	0.800223
19.04084	0.630252	0.684981	0.713241	0.753825	0.810674	0.819448	0.819559
20.1923	0.668365	0.716927	0.745772	0.779791	0.828215	0.834711	0.831687
21.13883	0.699695	0.741819	0.771006	0.798845	0.840002	0.844689	0.839293
21.91688	0.725449	0.761215	0.790579	0.812827	0.847923	0.851212	0.844064

22.55645	0.746618	0.776328	0.805762	0.823088	0.853246	0.855477	0.847056
23.08218	0.76402	0.788104	0.81754	0.830617	0.856823	0.858265	0.848933

ii) lime wastes with ZnO

$(1-\exp[-k*t])/k$	$\frac{W_V}{W_0}$	$\frac{W_V}{W_0}$	$\frac{W_V}{W_0}$	$\frac{W_V}{W_0}$	$\frac{W_V}{W_0}$	$\frac{W_V}{W_0}$	$\frac{W_V}{W_0}$
	300	400	500	600	700	800	900
0	0	0	0	0	0	0	0
4.576937	0.110762	0.183197	0.191552	0.226624	0.283443	0.29898	0.318863
8.401829	0.203324	0.325942	0.338585	0.392923	0.473917	0.494444	0.518852
11.59824	0.280678	0.437168	0.451446	0.514956	0.601914	0.622233	0.644284
14.26945	0.345321	0.523834	0.538077	0.604506	0.687928	0.705777	0.722954
16.50174	0.399342	0.591363	0.604574	0.670219	0.74573	0.760396	0.772296
18.36725	0.444487	0.643981	0.655617	0.718439	0.784572	0.796104	0.803242
19.92622	0.482215	0.684981	0.694797	0.753825	0.810674	0.819448	0.822652
21.22904	0.513743	0.716927	0.72487	0.779791	0.828215	0.834711	0.834825
22.31779	0.540091	0.741819	0.747955	0.798845	0.840002	0.844689	0.84246
23.22765	0.562109	0.761215	0.765674	0.812827	0.847923	0.851212	0.847249
23.988	0.58051	0.776328	0.779275	0.823088	0.853246	0.855477	0.850253
24.62342	0.595887	0.788104	0.789716	0.830617	0.856823	0.858265	0.852136

iii) lime wastes with KCl

$(1-\exp[-k*t])/k$	$\frac{W_V}{W_0}$	$\frac{W_V}{W_0}$	$\frac{W_V}{W_0}$	$\frac{W_V}{W_0}$	$\frac{W_V}{W_0}$	$\frac{W_V}{W_0}$	$\frac{W_V}{W_0}$
	300	400	500	600	700	800	900
0	0	0	0	0	0	0	0
4.461296	0.128485	0.183197	0.186959	0.226624	0.283443	0.29898	0.317665
7.997095	0.230316	0.325942	0.323331	0.392923	0.473917	0.494444	0.516902
10.79939	0.311022	0.437168	0.422805	0.514956	0.601914	0.622233	0.641862
13.02035	0.374986	0.523834	0.495363	0.604506	0.687928	0.705777	0.720236
14.78057	0.42568	0.591363	0.548289	0.670219	0.74573	0.760396	0.769392
16.17563	0.465858	0.643981	0.586894	0.718439	0.784572	0.796104	0.800223
17.28129	0.497701	0.684981	0.615053	0.753825	0.810674	0.819448	0.819559
18.15758	0.522938	0.716927	0.635594	0.779791	0.828215	0.834711	0.831687
18.85208	0.54294	0.741819	0.650576	0.798845	0.840002	0.844689	0.839293
19.40251	0.558792	0.761215	0.661505	0.812827	0.847923	0.851212	0.844064
19.83875	0.571356	0.776328	0.669477	0.823088	0.853246	0.855477	0.847056
20.18449	0.581313	0.788104	0.675291	0.830617	0.856823	0.858265	0.848933

iv) lime wastes with NaCl

$(1-\exp[-k*t])/k$	$\frac{W_V}{W_0}$	$\frac{W_V}{W_0}$	$\frac{W_V}{W_0}$	$\frac{W_V}{W_0}$	$\frac{W_V}{W_0}$	$\frac{W_V}{W_0}$	$\frac{W_V}{W_0}$
	300	400	500	600	700	800	900
0	0	0	0	0	0	0	0
4.590284	0.090429	0.183197	0.191781	0.226624	0.283443	0.29898	0.317665
8.449414	0.166453	0.325942	0.339358	0.392923	0.473917	0.494444	0.516902
11.69385	0.230369	0.437168	0.452921	0.514956	0.601914	0.622233	0.641862

14.42151	0.284104	0.523834	0.540309	0.604506	0.687928	0.705777	0.720236
16.71469	0.329279	0.591363	0.607554	0.670219	0.74573	0.760396	0.769392
18.64261	0.367259	0.643981	0.659301	0.718439	0.784572	0.796104	0.800223
20.26345	0.39919	0.684981	0.69912	0.753825	0.810674	0.819448	0.819559
21.62611	0.426034	0.716927	0.729761	0.779791	0.828215	0.834711	0.831687
22.77173	0.448603	0.741819	0.75334	0.798845	0.840002	0.844689	0.839293
23.73486	0.467577	0.761215	0.771485	0.812827	0.847923	0.851212	0.844064
24.54459	0.483528	0.776328	0.785447	0.823088	0.853246	0.855477	0.847056
25.22534	0.496939	0.788104	0.796191	0.830617	0.856823	0.858265	0.848933

v) lime wastes with Aluminosilicate

$(1-\exp[-k*t])/k$	$\frac{W_V}{W_0}$	$\frac{W_V}{W_0}$	$\frac{W_V}{W_0}$	$\frac{W_V}{W_0}$	$\frac{W_V}{W_0}$	$\frac{W_V}{W_0}$	$\frac{W_V}{W_0}$
	300	400	500	600	700	800	900
0	0	0	0	0	0	0	0
4.367247	0.168576	0.183197	0.191232	0.226624	0.283443	0.29898	0.317665
7.677859	0.296365	0.325942	0.337506	0.392923	0.473917	0.494444	0.516902
10.18748	0.393237	0.437168	0.449393	0.514956	0.601914	0.622233	0.641862
12.08991	0.466671	0.523834	0.534976	0.604506	0.687928	0.705777	0.720236
13.53206	0.522338	0.591363	0.600439	0.670219	0.74573	0.760396	0.769392
14.62529	0.564536	0.643981	0.650512	0.718439	0.784572	0.796104	0.800223
15.45401	0.596525	0.684981	0.688814	0.753825	0.810674	0.819448	0.819559
16.08223	0.620774	0.716927	0.718111	0.779791	0.828215	0.834711	0.831687
16.55845	0.639156	0.741819	0.74052	0.798845	0.840002	0.844689	0.839293
16.91946	0.653091	0.761215	0.757661	0.812827	0.847923	0.851212	0.844064
17.19312	0.663654	0.776328	0.770773	0.823088	0.853246	0.855477	0.847056
17.40057	0.671662	0.788104	0.780802	0.830617	0.856823	0.858265	0.848933

A.15. $\frac{w_c}{w_o}$ vs $(1-\exp[-k*t])/k$

a) jute wastes

i) jute wastes with alumina

$(1-\exp[-k*t])/k$	$\frac{w_c}{w_o}$	$\frac{w_c}{w_o}$	$\frac{w_c}{w_o}$	$\frac{w_c}{w_o}$	$\frac{w_c}{w_o}$	$\frac{w_c}{w_o}$
	400	500	600	700	800	900
0	0	0	0	0	0	0
4.488209	0.01885	0.049127	0.047743	0.060189	0.064184	0.072057
8.090081	0.033978	0.086016	0.083468	0.104335	0.110791	0.123346
10.98065	0.046119	0.113715	0.110199	0.136714	0.144634	0.159851
13.30039	0.055862	0.134514	0.130201	0.160462	0.16921	0.185835
15.16202	0.06368	0.150132	0.145168	0.177879	0.187056	0.204329
16.65602	0.069955	0.161859	0.156367	0.190655	0.200014	0.217493
17.85497	0.074991	0.170665	0.164747	0.200024	0.209424	0.226862
18.81716	0.079032	0.177277	0.171017	0.206897	0.216257	0.233531
19.58934	0.082275	0.182242	0.175709	0.211937	0.221218	0.238278

20.20902	0.084878	0.18597	0.17922	0.215634	0.224821	0.241657
20.70633	0.086967	0.18877	0.181847	0.218346	0.227438	0.244061
21.10543	0.088643	0.190872	0.183812	0.220334	0.229337	0.245773

ii) jute wastes with ZnO

$(1-\exp[-k*t])/k$	$\frac{w_c}{w_o}$	$\frac{w_c}{w_o}$	$\frac{w_c}{w_o}$	$\frac{w_c}{w_o}$	$\frac{w_c}{w_o}$	$\frac{w_c}{w_o}$
	400	500	600	700	800	900
0	0	0	0	0	0	0
4.696674	0.019256	0.042126	0.015393	0.038509	0.038509	0.031837
8.835262	0.036225	0.078987	0.028769	0.071605	0.071605	0.0581
12.48208	0.051177	0.111241	0.040391	0.100048	0.100048	0.079764
15.69556	0.064352	0.139465	0.05049	0.124492	0.124492	0.097634
18.52719	0.075961	0.164161	0.059265	0.1455	0.1455	0.112375
21.02236	0.086192	0.185771	0.06689	0.163555	0.163555	0.124535
23.22103	0.095206	0.20468	0.073516	0.179071	0.179071	0.134566
25.15845	0.10315	0.221226	0.079273	0.192406	0.192406	0.14284
26.86565	0.110149	0.235705	0.084276	0.203867	0.203867	0.149665
28.36999	0.116317	0.248374	0.088622	0.213716	0.213716	0.155295
29.69557	0.121752	0.259459	0.092399	0.222181	0.222181	0.15994
30.86365	0.126541	0.26916	0.095681	0.229455	0.229455	0.163771

iii) jute wastes with KCl

$(1-\exp[-k*t])/k$	$\frac{w_c}{w_o}$	$\frac{w_c}{w_o}$	$\frac{w_c}{w_o}$	$\frac{w_c}{w_o}$	$\frac{w_c}{w_o}$	$\frac{w_c}{w_o}$
	400	500	600	700	800	900
0	0	0	0	0	0	0
4.643067	0.052467	0.001391	0.023103	0.068306	0.052878	0.015445
8.639393	0.097625	0.002586	0.042789	0.124792	0.097489	0.028154
12.07906	0.136493	0.003611	0.059565	0.171503	0.135126	0.038611
15.03961	0.169948	0.004492	0.073861	0.210132	0.16688	0.047216
17.58778	0.198742	0.005248	0.086042	0.242076	0.193668	0.054296
19.78101	0.223525	0.005897	0.096423	0.268492	0.216269	0.060122
21.66874	0.244857	0.006454	0.105269	0.290338	0.235337	0.064916
23.29353	0.263217	0.006932	0.112807	0.308403	0.251424	0.06886
24.69199	0.27902	0.007343	0.11923	0.323342	0.264995	0.072106
25.89566	0.292621	0.007696	0.124704	0.335697	0.276445	0.074776
26.93167	0.304328	0.007998	0.129368	0.345913	0.286105	0.076974
27.82337	0.314404	0.008258	0.133343	0.354361	0.294255	0.078782

iv) jute wastes with NaCl

$(1-\exp[-k*t])/k$	$\frac{w_c}{w_o}$	$\frac{w_c}{w_o}$	$\frac{w_c}{w_o}$	$\frac{w_c}{w_o}$	$\frac{w_c}{w_o}$	$\frac{w_c}{w_o}$
	400	500	600	700	800	900
0	0	0	0	0	0	0

4.504463	0.047297	0.075379	0.056257	0.008691	0.008691	0.008318
8.146593	0.085539	0.133645	0.098775	0.01521	0.01521	0.014654
11.09148	0.11646	0.178684	0.13091	0.020101	0.020101	0.019482
13.47259	0.141462	0.213499	0.155196	0.023769	0.023769	0.02316
15.39786	0.161678	0.240409	0.173552	0.026521	0.026521	0.025962
16.95457	0.178023	0.261211	0.187425	0.028585	0.028585	0.028097
18.21325	0.191239	0.27729	0.197909	0.030134	0.030134	0.029723
19.23098	0.201925	0.289719	0.205834	0.031295	0.031295	0.030963
20.05387	0.210566	0.299327	0.211823	0.032167	0.032167	0.031907
20.71922	0.217552	0.306753	0.216349	0.03282	0.03282	0.032626
21.25721	0.223201	0.312493	0.21977	0.033311	0.033311	0.033174
21.6922	0.227768	0.31693	0.222356	0.033678	0.033678	0.033591

v) jute wastes with Aluminosilicate

$(1-\exp[-k*t])/k$	$\frac{w_c}{w_o}$	$\frac{w_c}{w_o}$	$\frac{w_c}{w_o}$	$\frac{w_c}{w_o}$	$\frac{w_c}{w_o}$	$\frac{w_c}{w_o}$
	400	500	600	700	800	900
0	0	0	0	0	0	0
4.677188	0.025725	0.031889	0.050579	0.059775	0.058396	0.057832
8.763722	0.0482	0.059077	0.093251	0.110205	0.107662	0.105657
12.33419	0.067838	0.082257	0.129251	0.152752	0.149227	0.145206
15.45377	0.084996	0.102019	0.159624	0.188646	0.184293	0.177911
18.17939	0.099987	0.118867	0.185248	0.21893	0.213877	0.204958
20.56081	0.113084	0.133232	0.206866	0.244478	0.238837	0.227324
22.6415	0.124528	0.145479	0.225105	0.266033	0.259894	0.245819
24.45942	0.134527	0.15592	0.240492	0.284218	0.277659	0.261115
26.04778	0.143263	0.164822	0.253474	0.29956	0.292647	0.273763
27.43555	0.150896	0.172412	0.264426	0.312503	0.305292	0.284223
28.64806	0.157564	0.178882	0.273666	0.323423	0.31596	0.292873
29.70746	0.163391	0.184399	0.281461	0.332636	0.32496	0.300026

a) lime wastes

i) lime wastes with alumina

$(1-\exp[-k*t])/k$	$\frac{w_c}{w_o}$	$\frac{w_c}{w_o}$	$\frac{w_c}{w_o}$	$\frac{w_c}{w_o}$	$\frac{w_c}{w_o}$	$\frac{w_c}{w_o}$	$\frac{w_c}{w_o}$
	300	400	500	600	700	800	900
0	0	0	0	0	0	0	0
4.540504	0.027697	0.037613	0.031792	0.039562	0.044559	0.04725	0.055142
8.272854	0.050464	0.06692	0.056452	0.068594	0.074502	0.078141	0.089726
11.34089	0.069179	0.089757	0.075581	0.089898	0.094624	0.098336	0.111418
13.86286	0.084563	0.10755	0.090419	0.10553	0.108146	0.11154	0.125022
15.93594	0.097209	0.121415	0.101929	0.117002	0.117233	0.120172	0.133555
17.64004	0.107604	0.132218	0.110857	0.12542	0.123339	0.125815	0.138907
19.04084	0.116149	0.140636	0.117783	0.131597	0.127442	0.129504	0.142263
20.1923	0.123173	0.147195	0.123155	0.13613	0.1302	0.131916	0.144368

21.13883	0.128947	0.152306	0.127322	0.139457	0.132053	0.133493	0.145689
21.91688	0.133693	0.156288	0.130554	0.141898	0.133298	0.134524	0.146517
22.55645	0.137594	0.159391	0.133062	0.143689	0.134135	0.135198	0.147036
23.08218	0.140801	0.161809	0.135007	0.145003	0.134697	0.135639	0.147362

ii) lime wastes with ZnO

$(1-\exp[-k*t])/k$	$\frac{w_c}{w_o}$	$\frac{w_c}{w_o}$	$\frac{w_c}{w_o}$	$\frac{w_c}{w_o}$	$\frac{w_c}{w_o}$	$\frac{w_c}{w_o}$	$\frac{w_c}{w_o}$
	300	400	500	600	700	800	900
0	0	0	0	0	0	0	0
4.576937	0.05355	0.037613	0.040859	0.039562	0.044559	0.04725	0.053943
8.401829	0.098301	0.06692	0.072221	0.068594	0.074502	0.078141	0.087776
11.59824	0.135699	0.089757	0.096295	0.089898	0.094624	0.098336	0.108995
14.26945	0.166953	0.10755	0.114773	0.10553	0.108146	0.11154	0.122304
16.50174	0.19307	0.121415	0.128957	0.117002	0.117233	0.120172	0.130652
18.36725	0.214897	0.132218	0.139845	0.12542	0.123339	0.125815	0.135887
19.92622	0.233137	0.140636	0.148202	0.131597	0.127442	0.129504	0.13917
21.22904	0.24838	0.147195	0.154617	0.13613	0.1302	0.131916	0.14123
22.31779	0.261118	0.152306	0.159541	0.139457	0.132053	0.133493	0.142521
23.22765	0.271763	0.156288	0.16332	0.141898	0.133298	0.134524	0.143332
23.988	0.28066	0.159391	0.166222	0.143689	0.134135	0.135198	0.14384
24.62342	0.288094	0.161809	0.168449	0.145003	0.134697	0.135639	0.144158

iii) lime wastes with KCl

$(1-\exp[-k*t])/k$	$\frac{w_c}{w_o}$	$\frac{w_c}{w_o}$	$\frac{w_c}{w_o}$	$\frac{w_c}{w_o}$	$\frac{w_c}{w_o}$	$\frac{w_c}{w_o}$	$\frac{w_c}{w_o}$
	300	400	500	600	700	800	900
0	0	0	0	0	0	0	0
4.461296	0.078965	0.037613	0.083617	0.039562	0.044559	0.04725	0.055142
7.997095	0.141549	0.06692	0.144609	0.068594	0.074502	0.078141	0.089726
10.79939	0.191149	0.089757	0.189098	0.089898	0.094624	0.098336	0.111418
13.02035	0.23046	0.10755	0.22155	0.10553	0.108146	0.11154	0.125022
14.78057	0.261616	0.121415	0.245221	0.117002	0.117233	0.120172	0.133555
16.17563	0.286309	0.132218	0.262487	0.12542	0.123339	0.125815	0.138907
17.28129	0.305879	0.140636	0.275081	0.131597	0.127442	0.129504	0.142263
18.15758	0.321389	0.147195	0.284268	0.13613	0.1302	0.131916	0.144368
18.85208	0.333682	0.152306	0.290969	0.139457	0.132053	0.133493	0.145689
19.40251	0.343424	0.156288	0.295857	0.141898	0.133298	0.134524	0.146517
19.83875	0.351146	0.159391	0.299422	0.143689	0.134135	0.135198	0.147036
20.18449	0.357265	0.161809	0.302023	0.145003	0.134697	0.135639	0.147362

iv) lime wastes with NaCl

$(1-\exp[-k*t])/k$	$\frac{w_c}{w_o}$	$\frac{w_c}{w_o}$	$\frac{w_c}{w_o}$	$\frac{w_c}{w_o}$	$\frac{w_c}{w_o}$	$\frac{w_c}{w_o}$	$\frac{w_c}{w_o}$
	300	400	500	600	700	800	900

0	0	0	0	0	0	0	0
4.590284	0.068854	0.037613	0.038708	0.039562	0.044559	0.04725	0.055142
8.449414	0.126741	0.06692	0.068494	0.068594	0.074502	0.078141	0.089726
11.69385	0.175408	0.089757	0.091415	0.089898	0.094624	0.098336	0.111418
14.42151	0.216323	0.10755	0.109053	0.10553	0.108146	0.11154	0.125022
16.71469	0.25072	0.121415	0.122626	0.117002	0.117233	0.120172	0.133555
18.64261	0.279639	0.132218	0.13307	0.12542	0.123339	0.125815	0.138907
20.26345	0.303952	0.140636	0.141107	0.131597	0.127442	0.129504	0.142263
21.62611	0.324392	0.147195	0.147291	0.13613	0.1302	0.131916	0.144368
22.77173	0.341576	0.152306	0.15205	0.139457	0.132053	0.133493	0.145689
23.73486	0.356023	0.156288	0.155712	0.141898	0.133298	0.134524	0.146517
24.54459	0.368169	0.159391	0.158531	0.143689	0.134135	0.135198	0.147036
25.22534	0.37838	0.161809	0.160699	0.145003	0.134697	0.135639	0.147362

v) lime wastes with Aluminosilicate

$(1-\exp[-k*t])/k$	$\frac{w_c}{w_o}$	$\frac{w_c}{w_o}$	$\frac{w_c}{w_o}$	$\frac{w_c}{w_o}$	$\frac{w_c}{w_o}$	$\frac{w_c}{w_o}$	$\frac{w_c}{w_o}$
	300	400	500	600	700	800	900
0	0	0	0	0	0	0	0
4.367247	0.07337	0.037613	0.04386	0.039562	0.044559	0.04725	0.055142
7.677859	0.128988	0.06692	0.07741	0.068594	0.074502	0.078141	0.089726
10.18748	0.17115	0.089757	0.103072	0.089898	0.094624	0.098336	0.111418
12.08991	0.203111	0.10755	0.122701	0.10553	0.108146	0.11154	0.125022
13.53206	0.227339	0.121415	0.137715	0.117002	0.117233	0.120172	0.133555
14.62529	0.245705	0.132218	0.1492	0.12542	0.123339	0.125815	0.138907
15.45401	0.259627	0.140636	0.157985	0.131597	0.127442	0.129504	0.142263
16.08223	0.270181	0.147195	0.164704	0.13613	0.1302	0.131916	0.144368
16.55845	0.278182	0.152306	0.169844	0.139457	0.132053	0.133493	0.145689
16.91946	0.284247	0.156288	0.173776	0.141898	0.133298	0.134524	0.146517
17.19312	0.288844	0.159391	0.176783	0.143689	0.134135	0.135198	0.147036
17.40057	0.29233	0.161809	0.179083	0.145003	0.134697	0.135639	0.147362

A.16. $\frac{w_l}{w_o}$ vs $(1-\exp[-k*t])/k$

a) jute wastes

i) jute wastes with alumina

$(1-\exp[-k*t])/k$	$\frac{w_l}{w_o}$	$\frac{w_l}{w_o}$	$\frac{w_l}{w_o}$	$\frac{w_l}{w_o}$	$\frac{w_l}{w_o}$	$\frac{w_l}{w_o}$
	400	500	600	700	800	900
0	0	0	0	0	0	0
4.488209	0.068483	0.095229	0.107644	0.092194	0.097463	0.094337
8.090081	0.123441	0.166736	0.18819	0.159813	0.168235	0.161484
10.98065	0.167547	0.220429	0.248459	0.209409	0.219626	0.209277
13.30039	0.202942	0.260747	0.293557	0.245784	0.256944	0.243294

15.16202	0.231347	0.291021	0.327302	0.272464	0.284042	0.267507
16.65602	0.254143	0.313753	0.352552	0.292032	0.30372	0.284741
17.85497	0.272437	0.330822	0.371445	0.306384	0.318008	0.297007
18.81716	0.287119	0.34364	0.385583	0.31691	0.328384	0.305738
19.58934	0.298901	0.353264	0.396161	0.324631	0.335918	0.311953
20.20902	0.308356	0.360491	0.404077	0.330294	0.341389	0.316376
20.70633	0.315944	0.365917	0.41	0.334447	0.345362	0.319524
21.10543	0.322034	0.369992	0.414432	0.337493	0.348247	0.321765

ii) jute wastes with ZnO

$(1-\exp[-k*t])/k$	$\frac{w_l}{w_o}$	$\frac{w_l}{w_o}$	$\frac{w_l}{w_o}$	$\frac{w_l}{w_o}$	$\frac{w_l}{w_o}$	$\frac{w_l}{w_o}$
	400	500	600	700	800	900
0	0	0	0	0	0	0
4.696674	0.029551	0.040874	0.054904	0.062037	0.04326	0.059602
8.835262	0.05559	0.076641	0.102612	0.115352	0.080438	0.108767
12.48208	0.078536	0.107937	0.144066	0.161172	0.112389	0.149323
15.69556	0.098755	0.135322	0.180086	0.200551	0.139849	0.182777
18.52719	0.116571	0.159285	0.211385	0.234394	0.163448	0.210374
21.02236	0.13227	0.180253	0.238582	0.263479	0.18373	0.233138
23.22103	0.146104	0.198601	0.262213	0.288475	0.201161	0.251916
25.15845	0.158294	0.214656	0.282747	0.309958	0.216141	0.267406
26.86565	0.169036	0.228704	0.30059	0.32842	0.229015	0.280183
28.36999	0.178501	0.240997	0.316094	0.344287	0.240079	0.290723
29.69557	0.186841	0.251753	0.329565	0.357923	0.249588	0.299418
30.86365	0.194191	0.261166	0.341271	0.369642	0.25776	0.30659

iii) jute wastes with KCl

$(1-\exp[-k*t])/k$	$\frac{w_l}{w_o}$	$\frac{w_l}{w_o}$	$\frac{w_l}{w_o}$	$\frac{w_l}{w_o}$	$\frac{w_l}{w_o}$	$\frac{w_l}{w_o}$
	400	500	600	700	800	900
0	0	0	0	0	0	0
4.643067	0.012046	0.039953	0.031839	0.038895	0.016986	0.039514
8.639393	0.022414	0.074254	0.05897	0.07106	0.031316	0.072028
12.07906	0.031338	0.103704	0.08209	0.09766	0.043405	0.098781
15.03961	0.039019	0.128989	0.101791	0.119656	0.053605	0.120795
17.58778	0.045629	0.150697	0.11858	0.137846	0.06221	0.138908
19.78101	0.05132	0.169335	0.132886	0.152888	0.06947	0.153813
21.66874	0.056217	0.185336	0.145077	0.165328	0.075595	0.166076
23.29353	0.060432	0.199075	0.155465	0.175615	0.080762	0.176168
24.69199	0.064061	0.21087	0.164317	0.184122	0.085122	0.184471
25.89566	0.067183	0.220997	0.171861	0.191157	0.0888	0.191303
26.93167	0.069871	0.229691	0.178289	0.196974	0.091903	0.196925
27.82337	0.072185	0.237156	0.183767	0.201785	0.094521	0.201551

iv) jute wastes with NaCl

$(1-\exp[-k*t])/k$	$\frac{w_l}{w_o}$	$\frac{w_l}{w_o}$	$\frac{w_l}{w_o}$	$\frac{w_l}{w_o}$	$\frac{w_l}{w_o}$	$\frac{w_l}{w_o}$
	400	500	600	700	800	900
0	0	0	0	0	0	0
4.504463	0.032002	0.029558	0.040024	0.049151	0.06863	0.062818
8.146593	0.057877	0.052405	0.070274	0.086021	0.120112	0.110675
11.09148	0.078799	0.070066	0.093136	0.113678	0.15873	0.147136
13.47259	0.095715	0.083718	0.110415	0.134425	0.187699	0.174914
15.39786	0.109393	0.09427	0.123474	0.149988	0.20943	0.196077
16.95457	0.120453	0.102427	0.133344	0.161662	0.225731	0.212199
18.21325	0.129395	0.108732	0.140804	0.170419	0.237959	0.224483
19.23098	0.136626	0.113606	0.146441	0.176989	0.247132	0.233841
20.05387	0.142472	0.117373	0.150702	0.181916	0.254013	0.24097
20.71922	0.147199	0.120285	0.153923	0.185613	0.259174	0.246402
21.25721	0.151021	0.122536	0.156357	0.188386	0.263046	0.25054
21.6922	0.154111	0.124276	0.158196	0.190466	0.26595	0.253692

v) jute wastes with Aluminosilicate

$(1-\exp[-k*t])/k$	$\frac{w_l}{w_o}$	$\frac{w_l}{w_o}$	$\frac{w_l}{w_o}$	$\frac{w_l}{w_o}$	$\frac{w_l}{w_o}$	$\frac{w_l}{w_o}$
	400	500	600	700	800	900
0	0	0	0	0	0	0
4.677188	0.014389	0.020501	0.0177	0.042605	0.017282	0.022061
8.763722	0.02696	0.03798	0.032633	0.078549	0.031861	0.040305
12.33419	0.037945	0.052882	0.045231	0.108874	0.044162	0.055391
15.45377	0.047542	0.065587	0.05586	0.134458	0.054539	0.067868
18.17939	0.055927	0.076418	0.064827	0.156042	0.063295	0.078185
20.56081	0.063253	0.085653	0.072392	0.174252	0.070681	0.086717
22.6415	0.069654	0.093527	0.078775	0.189615	0.076913	0.093772
24.45942	0.075246	0.100239	0.084159	0.202576	0.08217	0.099607
26.04778	0.080133	0.105962	0.088702	0.213511	0.086606	0.104432
27.43555	0.084402	0.110841	0.092535	0.222736	0.090348	0.108422
28.64806	0.088132	0.115001	0.095769	0.23052	0.093505	0.111722
29.70746	0.091391	0.118548	0.098496	0.237086	0.096168	0.11445

b) lime wastes

i) lime wastes with alumina

$(1-\exp[-k*t])/k$	$\frac{w_l}{w_o}$	$\frac{w_l}{w_o}$	$\frac{w_l}{w_o}$	$\frac{w_l}{w_o}$	$\frac{w_l}{w_o}$	$\frac{w_l}{w_o}$	$\frac{w_l}{w_o}$
	300	400	500	600	700	800	900
0	0	0	0	0	0	0	0
4.540504	0.059179	0.073706	0.083834	0.10809	0.127985	0.130152	0.131586
8.272854	0.107825	0.131137	0.148864	0.187407	0.21399	0.215241	0.214116
11.34089	0.147812	0.175887	0.199307	0.245611	0.271786	0.27087	0.265878
13.86286	0.180683	0.210756	0.238435	0.288323	0.310624	0.307239	0.298343

15.93594	0.207702	0.237925	0.268787	0.319665	0.336724	0.331016	0.318705
17.64004	0.229913	0.259095	0.29233	0.342664	0.354262	0.34656	0.331475
19.04084	0.24817	0.275591	0.310593	0.359541	0.366048	0.356722	0.339485
20.1923	0.263178	0.288444	0.324758	0.371926	0.373968	0.363366	0.344509
21.13883	0.275515	0.298459	0.335747	0.381014	0.379291	0.36771	0.34766
21.91688	0.285655	0.306263	0.344271	0.387683	0.382867	0.37055	0.349636
22.55645	0.293991	0.312343	0.350882	0.392576	0.385271	0.372406	0.350875
23.08218	0.300844	0.317081	0.356011	0.396168	0.386886	0.37362	0.351653

ii) lime wastes with ZnO

$(1-\exp[-k*t])/k$	$\frac{w_l}{w_o}$	$\frac{w_l}{w_o}$	$\frac{w_l}{w_o}$	$\frac{w_l}{w_o}$	$\frac{w_l}{w_o}$	$\frac{w_l}{w_o}$	$\frac{w_l}{w_o}$
	300	400	500	600	700	800	900
0	0	0	0	0	0	0	0
4.576937	0.060027	0.098067	0.103596	0.149288	0.222761	0.212015	0.180792
8.401829	0.110191	0.17448	0.183116	0.258838	0.372456	0.350624	0.294184
11.59824	0.152112	0.234021	0.244154	0.339227	0.473051	0.441243	0.365303
14.26945	0.187145	0.280414	0.291006	0.398217	0.54065	0.500486	0.409908
16.50174	0.216422	0.316563	0.32697	0.441505	0.586077	0.539218	0.437884
18.36725	0.240888	0.34473	0.354575	0.473271	0.616604	0.56454	0.45543
19.92622	0.261335	0.366678	0.375764	0.496581	0.637117	0.581094	0.466435
21.22904	0.278421	0.383779	0.392029	0.513686	0.650903	0.591917	0.473338
22.31779	0.2927	0.397104	0.404514	0.526238	0.660166	0.598993	0.477667
23.22765	0.304633	0.407487	0.414097	0.535449	0.666392	0.603619	0.480382
23.988	0.314605	0.415577	0.421453	0.542208	0.670575	0.606643	0.482085
24.62342	0.322939	0.421881	0.427099	0.547168	0.673386	0.60862	0.483153

iii) lime wastes with KCl

$(1-\exp[-k*t])/k$	$\frac{w_l}{w_o}$	$\frac{w_l}{w_o}$	$\frac{w_l}{w_o}$	$\frac{w_l}{w_o}$	$\frac{w_l}{w_o}$	$\frac{w_l}{w_o}$	$\frac{w_l}{w_o}$
	300	400	500	600	700	800	900
0	0	0	0	0	0	0	0
4.461296	0.082415	0.113341	0.129332	0.126748	0.202921	0.1845	0.183716
7.997095	0.147734	0.201655	0.223671	0.219758	0.339284	0.30512	0.298942
10.79939	0.199502	0.270469	0.292483	0.28801	0.430919	0.383978	0.37121
13.02035	0.24053	0.324088	0.342677	0.338094	0.492498	0.435533	0.416537
14.78057	0.273048	0.365867	0.379289	0.374846	0.533878	0.469238	0.444965
16.17563	0.298819	0.398421	0.405995	0.401816	0.561686	0.491273	0.462796
17.28129	0.319245	0.423787	0.425475	0.421606	0.580373	0.505679	0.473979
18.15758	0.335433	0.443552	0.439684	0.436129	0.59293	0.515097	0.480992
18.85208	0.348262	0.458952	0.450049	0.446786	0.601369	0.521255	0.485392
19.40251	0.358431	0.470952	0.457609	0.454606	0.60704	0.52528	0.488151
19.83875	0.36649	0.480303	0.463123	0.460344	0.610851	0.527912	0.489881
20.18449	0.372877	0.487588	0.467146	0.464555	0.613411	0.529632	0.490966

iv) lime wastes with NaCl

$(1-\exp[-k*t])/k$	$\frac{w_l}{w_o}$	$\frac{w_l}{w_o}$	$\frac{w_l}{w_o}$	$\frac{w_l}{w_o}$	$\frac{w_l}{w_o}$	$\frac{w_l}{w_o}$	$\frac{w_l}{w_o}$
	300	400	500	600	700	800	900
0	0	0	0	0	0	0	0
4.590284	0.050983	0.098813	0.098538	0.092098	0.148007	0.118486	0.110975
8.449414	0.093845	0.175807	0.174364	0.159681	0.247467	0.195949	0.180578
11.69385	0.12988	0.2358	0.232713	0.209274	0.314305	0.246592	0.224232
14.42151	0.160175	0.282546	0.277614	0.245666	0.359219	0.279701	0.251612
16.71469	0.185645	0.31897	0.312165	0.272371	0.389401	0.301347	0.268785
18.64261	0.207057	0.347351	0.338752	0.291967	0.409684	0.315498	0.279555
20.26345	0.225059	0.369465	0.359212	0.306348	0.423314	0.324749	0.28631
21.62611	0.240194	0.386697	0.374956	0.3169	0.432473	0.330798	0.290547
22.77173	0.252918	0.400123	0.387071	0.324644	0.438628	0.334752	0.293204
23.73486	0.263615	0.410585	0.396393	0.330326	0.442764	0.337337	0.294871
24.54459	0.272609	0.418736	0.403567	0.334496	0.445544	0.339027	0.295916
25.22534	0.28017	0.425088	0.409087	0.337555	0.447411	0.340132	0.296572

v) lime wastes with Aluminosilicate

$(1-\exp[-k*t])/k$	$\frac{w_l}{w_o}$	$\frac{w_l}{w_o}$	$\frac{w_l}{w_o}$	$\frac{w_l}{w_o}$	$\frac{w_l}{w_o}$	$\frac{w_l}{w_o}$	$\frac{w_l}{w_o}$
	300	400	500	600	700	800	900
0	0	0	0	0	0	0	0
4.367247	0.076256	0.075568	0.103084	0.099465	0.123985	0.109119	0.107982
7.677859	0.134063	0.134449	0.181934	0.172453	0.207303	0.180458	0.175707
10.18748	0.177883	0.180329	0.242246	0.226013	0.263293	0.227097	0.218184
12.08991	0.211102	0.216078	0.28838	0.265316	0.300918	0.257589	0.244825
13.53206	0.236283	0.243934	0.323668	0.294157	0.326201	0.277523	0.261534
14.62529	0.255372	0.265638	0.35066	0.315321	0.343192	0.290555	0.272014
15.45401	0.269842	0.28255	0.371306	0.330851	0.35461	0.299076	0.278587
16.08223	0.280812	0.295728	0.387099	0.342248	0.362282	0.304646	0.28271
16.55845	0.289127	0.305996	0.399179	0.350611	0.367438	0.308287	0.285295
16.91946	0.29543	0.313997	0.408419	0.356748	0.370903	0.310668	0.286917
17.19312	0.300209	0.320231	0.415487	0.361251	0.373232	0.312225	0.287934
17.40057	0.303831	0.325088	0.420893	0.364555	0.374796	0.313242	0.288572

A.17. $\frac{w_g}{w_o}$ vs $(1-\exp[-k*t])/k$

a) jute wastes

i) jute wastes with alumina

$(1-\exp[-k*t])/k$	$\frac{w_g}{w_o}$	$\frac{w_g}{w_o}$	$\frac{w_g}{w_o}$	$\frac{w_g}{w_o}$	$\frac{w_g}{w_o}$	$\frac{w_g}{w_o}$
	400	500	600	700	800	900
0	0	0	0	0	0	0
4.488209	0.110148	0.104757	0.09651	0.09035	0.112205	0.121835
8.090081	0.198544	0.183417	0.168978	0.158192	0.193682	0.208553

10.98065	0.269483	0.242482	0.223394	0.209134	0.252846	0.270277
13.30039	0.326413	0.286833	0.264254	0.247386	0.295809	0.31421
15.16202	0.372101	0.320136	0.294935	0.276109	0.327006	0.34548
16.65602	0.408766	0.345143	0.317973	0.297676	0.349659	0.367738
17.85497	0.438191	0.36392	0.335272	0.313871	0.366109	0.38358
18.81716	0.461804	0.378019	0.348262	0.326031	0.378055	0.394856
19.58934	0.480755	0.388606	0.358015	0.335163	0.386729	0.402882
20.20902	0.495963	0.396556	0.365339	0.342019	0.393027	0.408594
20.70633	0.508167	0.402525	0.370839	0.347167	0.397601	0.41266
21.10543	0.517962	0.407008	0.374968	0.351033	0.400922	0.415554

ii) jute wastes with ZnO

$(1-\exp[-k*t])/k$	$\frac{w_g}{w_o}$	$\frac{w_g}{w_o}$	$\frac{w_g}{w_o}$	$\frac{w_g}{w_o}$	$\frac{w_g}{w_o}$	$\frac{w_g}{w_o}$
	400	500	600	700	800	900
0	0	0	0	0	0	0
4.696674	0.070019	0.041973	0.060987	0.064206	0.058813	0.083667
8.835262	0.131717	0.0787	0.114353	0.120387	0.109358	0.152683
12.48208	0.186084	0.110837	0.161049	0.169548	0.152798	0.209614
15.69556	0.233991	0.138958	0.201909	0.212564	0.19013	0.256576
18.52719	0.276205	0.163564	0.237663	0.250205	0.222215	0.295314
21.02236	0.313404	0.185096	0.268949	0.283142	0.249788	0.32727
23.22103	0.346182	0.203936	0.296325	0.311962	0.273486	0.35363
25.15845	0.375065	0.220423	0.32028	0.337181	0.293852	0.375374
26.86565	0.400516	0.234848	0.341241	0.359248	0.311355	0.39331
28.36999	0.422943	0.247471	0.359582	0.378558	0.326397	0.408106
29.69557	0.442705	0.258517	0.375632	0.395454	0.339325	0.420311
30.86365	0.460119	0.268182	0.389675	0.410239	0.350435	0.430379

iii) jute wastes with KCl

$(1-\exp[-k*t])/k$	$\frac{w_g}{w_o}$	$\frac{w_g}{w_o}$	$\frac{w_g}{w_o}$	$\frac{w_g}{w_o}$	$\frac{w_g}{w_o}$	$\frac{w_g}{w_o}$
	400	500	600	700	800	900
0	0	0	0	0	0	0
4.643067	0.074779	0.100097	0.093255	0.107643	0.086472	0.122206
8.639393	0.139143	0.186037	0.17332	0.200061	0.159425	0.222761
12.07906	0.194541	0.259821	0.24206	0.279408	0.220973	0.305502
15.03961	0.242222	0.323169	0.301077	0.347531	0.272898	0.373584
17.58778	0.283262	0.377557	0.351748	0.40602	0.316706	0.429604
19.78101	0.318585	0.424252	0.395251	0.456235	0.353666	0.475699
21.66874	0.348988	0.464343	0.432601	0.499348	0.384847	0.513627
23.29353	0.375157	0.498763	0.464668	0.536363	0.411153	0.544836
24.69199	0.39768	0.528315	0.4922	0.568143	0.433347	0.570516
25.89566	0.417066	0.553687	0.515837	0.595427	0.452071	0.591647
26.93167	0.433751	0.57547	0.536132	0.618853	0.467868	0.609033
27.82337	0.448113	0.594172	0.553555	0.638965	0.481196	0.62334

iv) jute wastes with NaCl

$(1-\exp[-k*t])/k$	$\frac{w_g}{w_o}$	$\frac{w_g}{w_o}$	$\frac{w_g}{w_o}$	$\frac{w_g}{w_o}$	$\frac{w_g}{w_o}$	$\frac{w_g}{w_o}$
	400	500	600	700	800	900
0	0	0	0	0	0	0
4.504463	0.112141	0.122082	0.149533	0.143989	0.172543	0.167011
8.146593	0.202814	0.216448	0.26512	0.255289	0.301973	0.294248
11.09148	0.276128	0.289392	0.354466	0.341322	0.399064	0.391185
13.47259	0.335408	0.345777	0.423529	0.407824	0.471895	0.465036
15.39786	0.383338	0.389361	0.476914	0.459229	0.526528	0.5213
16.95457	0.422093	0.42305	0.518179	0.498964	0.56751	0.564166
18.21325	0.453429	0.449092	0.550076	0.529679	0.598253	0.596822
19.23098	0.478766	0.469221	0.574732	0.55342	0.621314	0.621702
20.05387	0.499252	0.484781	0.593791	0.571772	0.638613	0.640657
20.71922	0.515816	0.496808	0.608523	0.585958	0.651589	0.655098
21.25721	0.52921	0.506105	0.61991	0.596923	0.661324	0.6661
21.6922	0.540039	0.513292	0.628713	0.605399	0.668625	0.674481

v) jute wastes with Aluminosilicate

$(1-\exp[-k*t])/k$	$\frac{w_g}{w_o}$	$\frac{w_g}{w_o}$	$\frac{w_g}{w_o}$	$\frac{w_g}{w_o}$	$\frac{w_g}{w_o}$	$\frac{w_g}{w_o}$
	400	500	600	700	800	900
0	0	0	0	0	0	0
4.677188	0.086171	0.09504	0.088507	0.103616	0.080658	0.093148
8.763722	0.16146	0.176067	0.163965	0.191955	0.148706	0.170177
12.33419	0.227241	0.245149	0.228299	0.267271	0.206116	0.233877
15.45377	0.284715	0.304046	0.283148	0.331483	0.25455	0.286555
18.17939	0.33493	0.35426	0.32991	0.386228	0.295413	0.330117
20.56081	0.378805	0.397071	0.369778	0.432902	0.329887	0.366141
22.6415	0.417139	0.433571	0.403769	0.472695	0.358972	0.395931
24.45942	0.450631	0.464689	0.432748	0.506621	0.38351	0.420566
26.04778	0.479895	0.491219	0.457455	0.535546	0.404212	0.440939
27.43555	0.505462	0.513838	0.478519	0.560206	0.421677	0.457786
28.64806	0.527801	0.533123	0.496478	0.58123	0.436412	0.471718
29.70746	0.547319	0.549564	0.511789	0.599155	0.448843	0.483239

b) lime wastes

i) lime wastes with alumina

$(1-\exp[-k*t])/k$	$\frac{w_g}{w_o}$	$\frac{w_g}{w_o}$	$\frac{w_g}{w_o}$	$\frac{w_g}{w_o}$	$\frac{w_g}{w_o}$	$\frac{w_g}{w_o}$	$\frac{w_g}{w_o}$
	300	400	500	600	700	800	900
0	0	0	0	0	0	0	0
4.540504	0.091112	0.109491	0.108917	0.126641	0.155459	0.168828	0.186079
8.272854	0.166007	0.194805	0.193783	0.225318	0.259926	0.279203	0.302786
11.34089	0.227571	0.26128	0.259911	0.302206	0.330128	0.351362	0.375984

13.86286	0.278178	0.313078	0.311436	0.362117	0.377304	0.398538	0.421894
15.93594	0.319777	0.353438	0.351585	0.408799	0.409006	0.42938	0.450688
17.64004	0.353972	0.384886	0.382868	0.445173	0.43031	0.449544	0.468747
19.04084	0.382081	0.40939	0.407244	0.473515	0.444626	0.462726	0.480074
20.1923	0.405187	0.428483	0.426237	0.495599	0.454246	0.471344	0.487178
21.13883	0.42418	0.443361	0.441036	0.512807	0.460711	0.476979	0.491634
21.91688	0.439793	0.454953	0.452568	0.526215	0.465055	0.480662	0.494428
22.55645	0.452627	0.463985	0.461553	0.536662	0.467975	0.48307	0.496181
23.08218	0.463177	0.471024	0.468554	0.544803	0.469937	0.484645	0.49728

ii) lime wastes with ZnO

$(1-\exp[-k*t])/k$	$\frac{w_g}{w_o}$	$\frac{w_g}{w_o}$	$\frac{w_g}{w_o}$	$\frac{w_g}{w_o}$	$\frac{w_g}{w_o}$	$\frac{w_g}{w_o}$	$\frac{w_g}{w_o}$
	300	400	500	600	700	800	900
0	0	0	0	0	0	0	0
4.576937	0.050735	0.08513	0.088589	0.076105	0.060682	0.086965	0.136872
8.401829	0.093133	0.151462	0.157617	0.135405	0.101461	0.14382	0.222718
11.59824	0.128565	0.203147	0.211403	0.181611	0.128863	0.18099	0.276559
14.26945	0.158175	0.24342	0.253313	0.217615	0.147278	0.20529	0.310329
16.50174	0.18292	0.2748	0.285968	0.245668	0.159653	0.221177	0.331508
18.36725	0.203599	0.299251	0.311413	0.267527	0.167969	0.231564	0.344792
19.92622	0.22088	0.318303	0.331239	0.284559	0.173557	0.238354	0.353124
21.22904	0.235322	0.333148	0.346688	0.297831	0.177312	0.242794	0.358349
22.31779	0.24739	0.344715	0.358725	0.308172	0.179835	0.245696	0.361627
23.22765	0.257476	0.353728	0.368104	0.316229	0.181531	0.247593	0.363682
23.988	0.265904	0.360751	0.375413	0.322508	0.182671	0.248834	0.364972
24.62342	0.272948	0.366224	0.381107	0.3274	0.183437	0.249645	0.36578

iii) lime wastes with KCl

$(1-\exp[-k*t])/k$	$\frac{w_g}{w_o}$	$\frac{w_g}{w_o}$	$\frac{w_g}{w_o}$	$\frac{w_g}{w_o}$	$\frac{w_g}{w_o}$	$\frac{w_g}{w_o}$	$\frac{w_g}{w_o}$
	300	400	500	600	700	800	900
0	0	0	0	0	0	0	0
4.461296	0.04607	0.069856	0.059468	0.087471	0.080522	0.11448	0.133948
7.997095	0.082583	0.124287	0.105804	0.155627	0.134633	0.189324	0.21796
10.79939	0.111521	0.166699	0.141909	0.208734	0.170995	0.238255	0.270652
13.02035	0.134456	0.199746	0.170042	0.250114	0.195431	0.270244	0.303699
14.78057	0.152633	0.225496	0.191963	0.282357	0.211851	0.291158	0.324427
16.17563	0.167039	0.24556	0.209043	0.307481	0.222886	0.304831	0.337427
17.28129	0.178457	0.261194	0.222352	0.327057	0.230301	0.313769	0.34558
18.15758	0.187506	0.273375	0.232722	0.34231	0.235284	0.319613	0.350694
18.85208	0.194677	0.282867	0.240802	0.354195	0.238633	0.323434	0.353902
19.40251	0.200361	0.290263	0.247098	0.363456	0.240883	0.325932	0.355913
19.83875	0.204866	0.296026	0.252004	0.370672	0.242395	0.327565	0.357175
20.18449	0.208437	0.300516	0.255827	0.376295	0.243411	0.328632	0.357966

iv) lime wastes with NaCl

$(1-\exp[-k*t])/k$	$\frac{w_g}{w_o}$	$\frac{w_g}{w_o}$	$\frac{w_g}{w_o}$	$\frac{w_g}{w_o}$	$\frac{w_g}{w_o}$	$\frac{w_g}{w_o}$	$\frac{w_g}{w_o}$
	300	400	500	600	700	800	900
0	0	0	0	0	0	0	0
4.590284	0.039446	0.084384	0.093802	0.101228	0.135436	0.180493	0.20669
8.449414	0.072609	0.150135	0.166892	0.180103	0.226449	0.298495	0.336324
11.69385	0.100489	0.201368	0.223843	0.241563	0.28761	0.37564	0.41763
14.42151	0.123929	0.241288	0.268219	0.289451	0.328709	0.426076	0.468624
16.71469	0.143635	0.272393	0.302796	0.326765	0.356328	0.459049	0.500608
18.64261	0.160202	0.29663	0.329738	0.35584	0.374888	0.480606	0.520667
20.26345	0.17413	0.315515	0.350731	0.378495	0.38736	0.494699	0.533249
21.62611	0.18584	0.330231	0.367089	0.396147	0.395742	0.503913	0.54114
22.77173	0.195685	0.341696	0.379834	0.409902	0.401374	0.509936	0.546089
23.73486	0.203961	0.350631	0.389766	0.420619	0.405159	0.513875	0.549193
24.54459	0.21092	0.357592	0.397504	0.42897	0.407702	0.516449	0.55114
25.22534	0.21677	0.363016	0.403534	0.435477	0.409411	0.518132	0.552361

v) lime wastes with Aluminosilicate

$(1-\exp[-k*t])/k$	$\frac{w_g}{w_o}$	$\frac{w_g}{w_o}$	$\frac{w_g}{w_o}$	$\frac{w_g}{w_o}$	$\frac{w_g}{w_o}$	$\frac{w_g}{w_o}$	$\frac{w_g}{w_o}$
	300	400	500	600	700	800	900
0	0	0	0	0	0	0	0
4.367247	0.092319	0.107629	0.088932	0.112603	0.159458	0.189861	0.189861
7.677859	0.162302	0.191493	0.158226	0.200342	0.266613	0.313986	0.313986
10.18748	0.215353	0.256839	0.21222	0.268708	0.338621	0.395135	0.395135
12.08991	0.255569	0.307756	0.254291	0.321978	0.387011	0.448188	0.448188
13.53206	0.286055	0.347429	0.287073	0.363485	0.419528	0.482873	0.482873
14.62529	0.309164	0.378343	0.312616	0.395827	0.44138	0.505548	0.505548
15.45401	0.326683	0.40243	0.332519	0.421028	0.456064	0.520373	0.520373
16.08223	0.339963	0.421199	0.348027	0.440664	0.465932	0.530065	0.530065
16.55845	0.35003	0.435824	0.360111	0.455964	0.472563	0.536401	0.536401
16.91946	0.357661	0.447219	0.369526	0.467886	0.477019	0.540544	0.540544
17.19312	0.363446	0.456098	0.376863	0.477175	0.480014	0.543252	0.543252
17.40057	0.367831	0.463016	0.38258	0.484413	0.482026	0.545022	0.545022

A.18. Activation energies and Pre-exponential factor

a) jute wastes

i) jute wastes with alumina

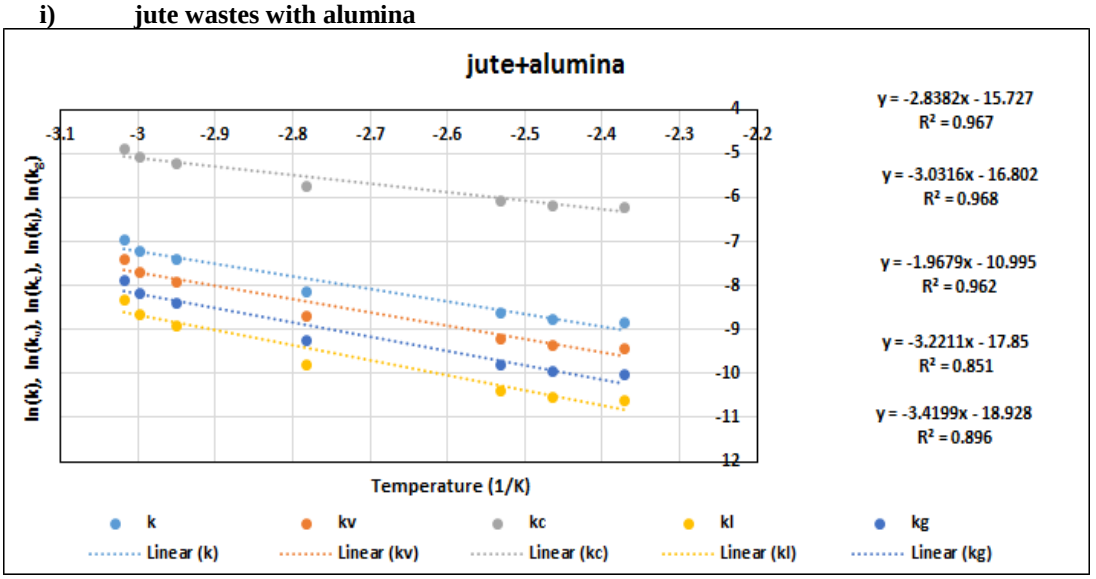

ii) jute wastes with ZnO

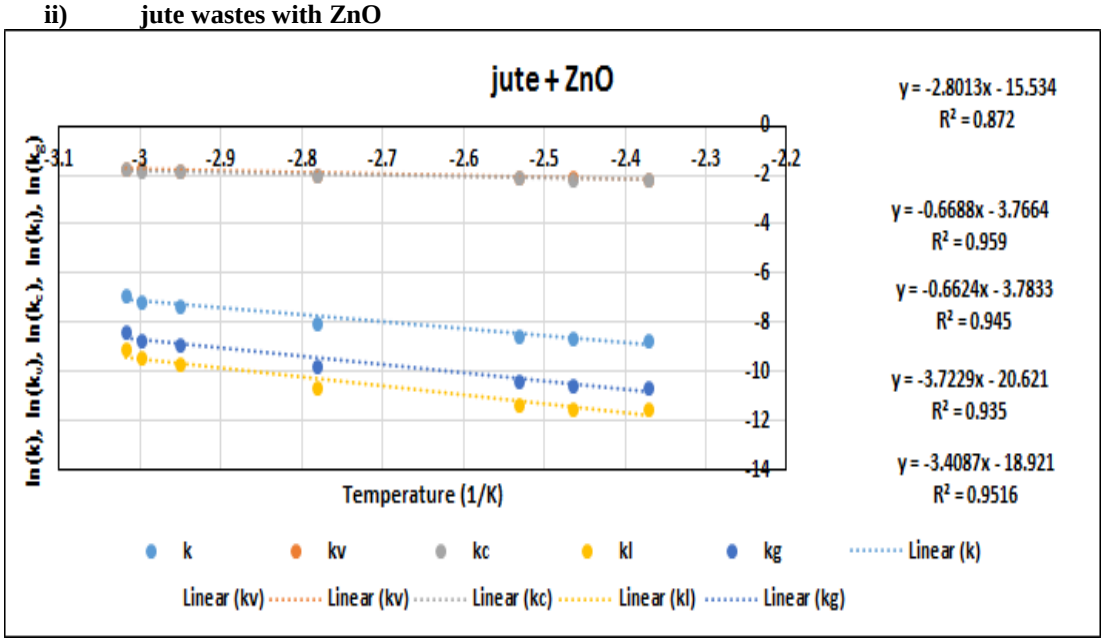

iii) jute wastes with KCl

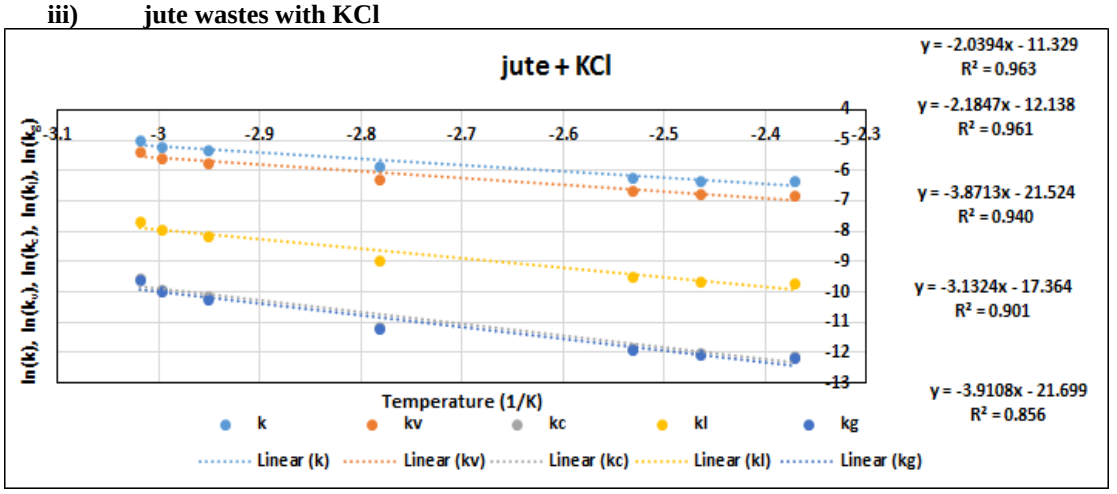

iv) jute wastes with NaCl

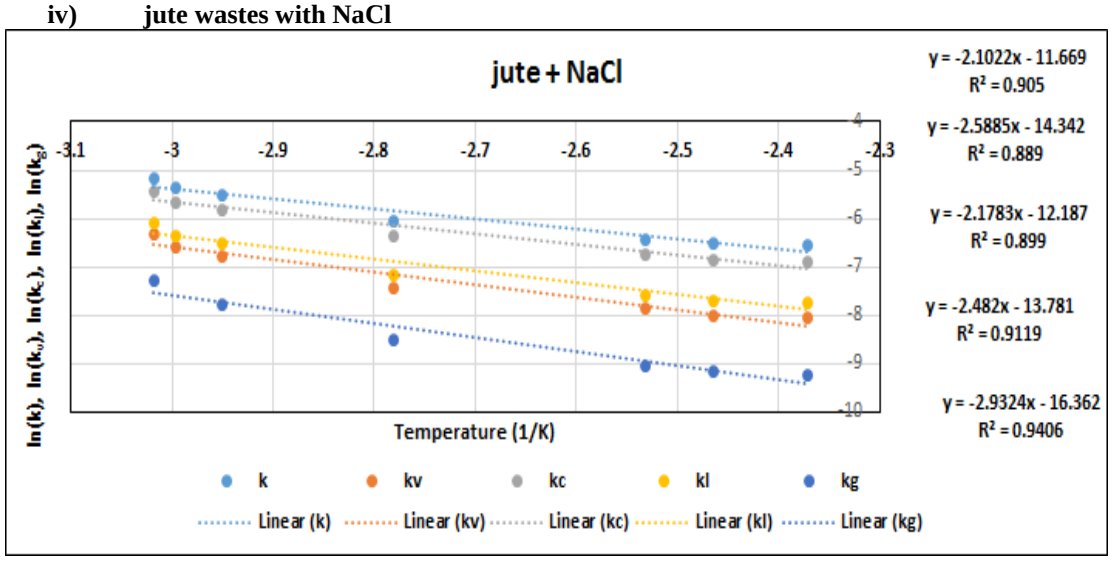

v) jute wastes with Aluminosilicate

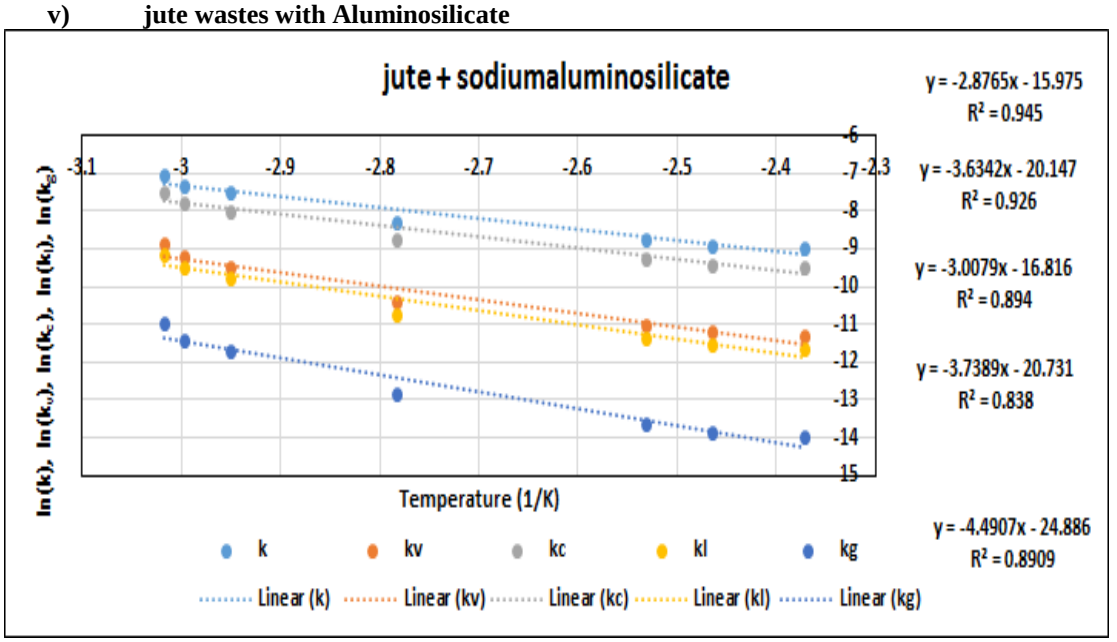

b) lime wastes

i) lime wastes with alumina

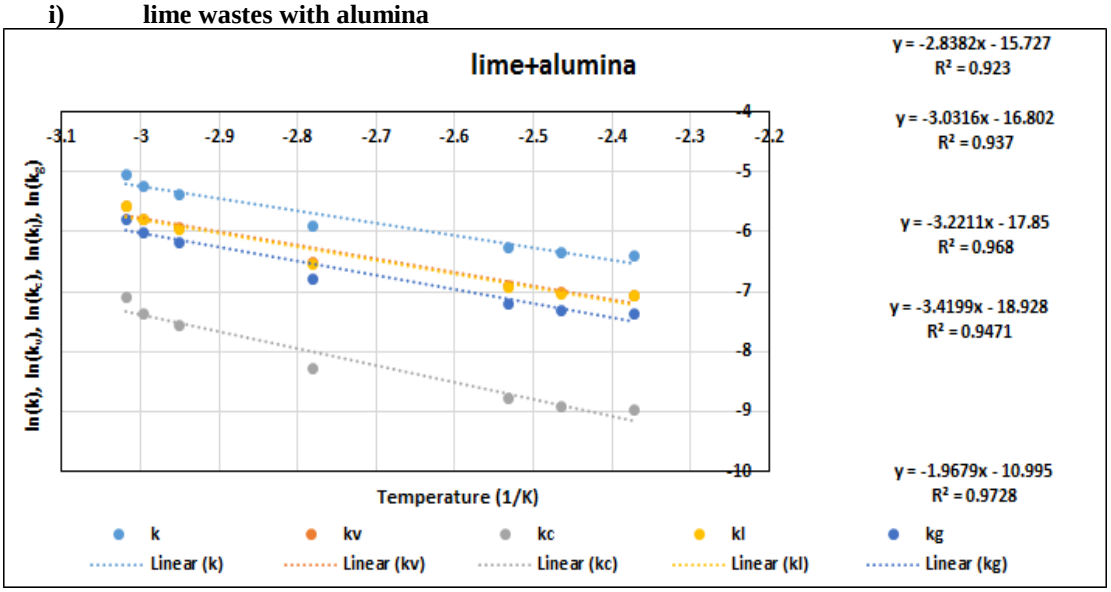

ii) lime wastes with ZnO

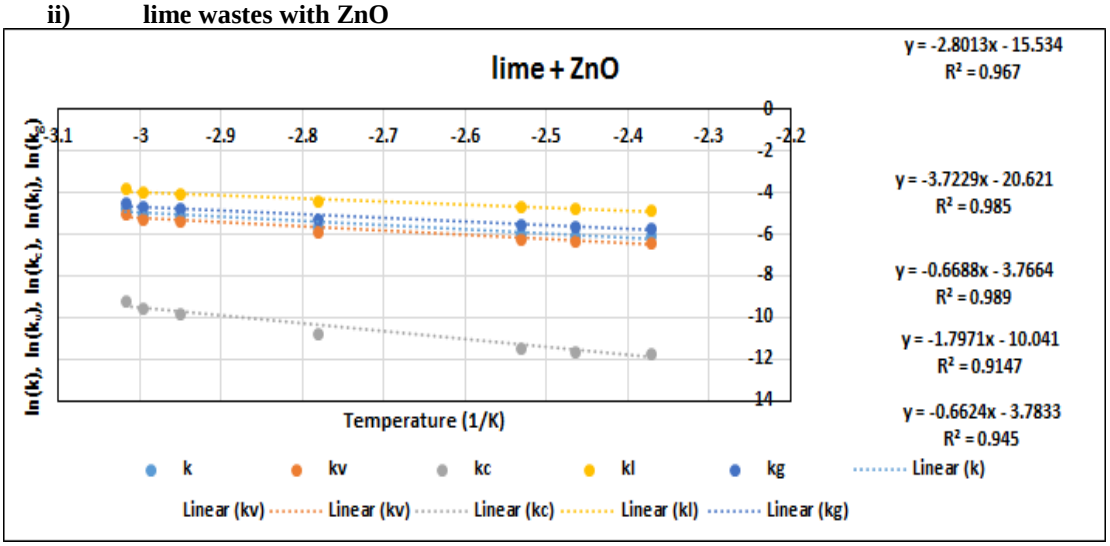

iii) lime wastes with KCl

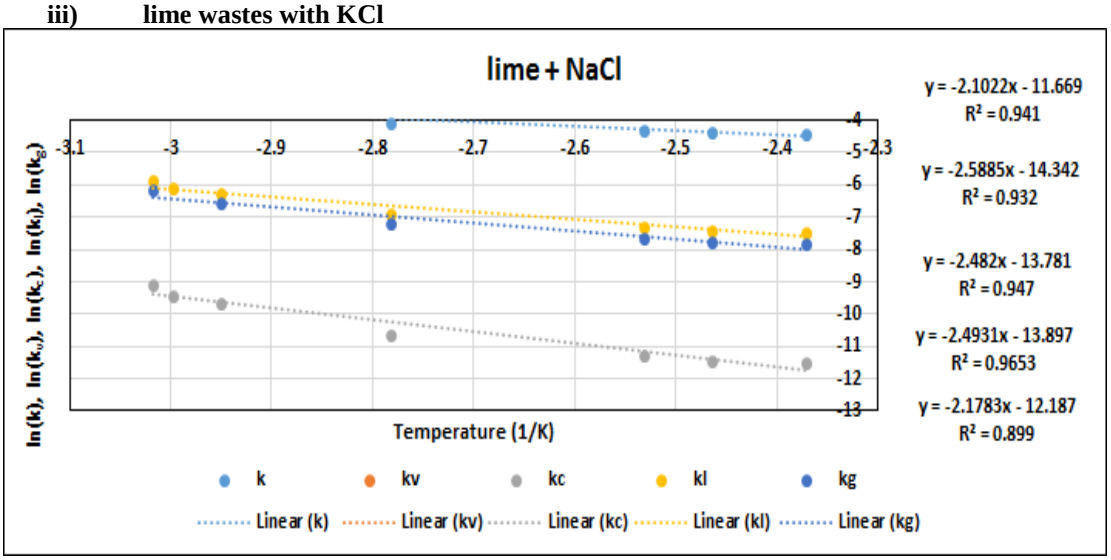

iv) lime wastes with NaCl

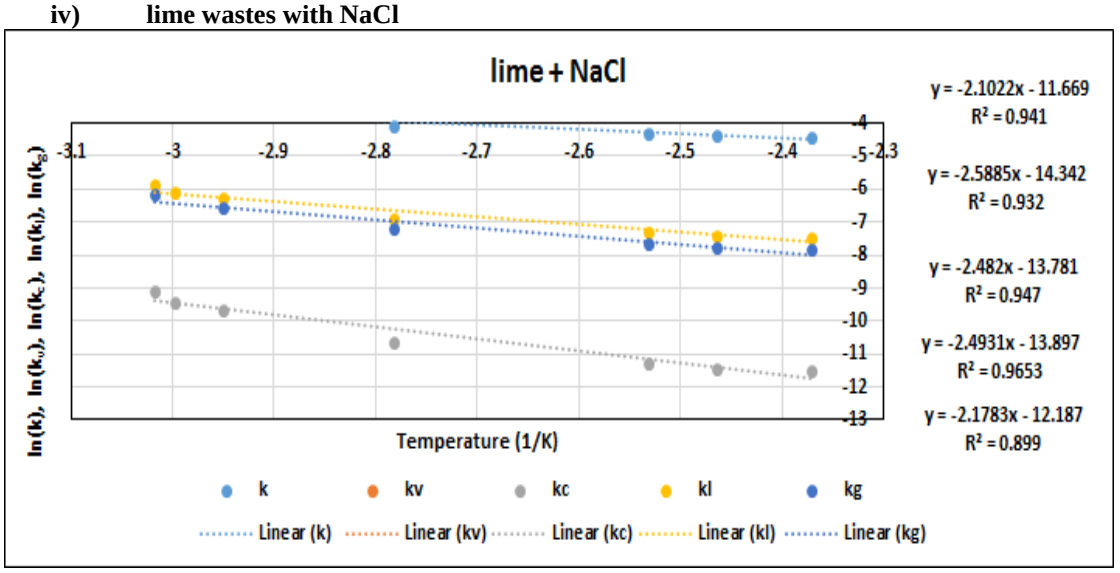

v) lime wastes with Aluminosilicate

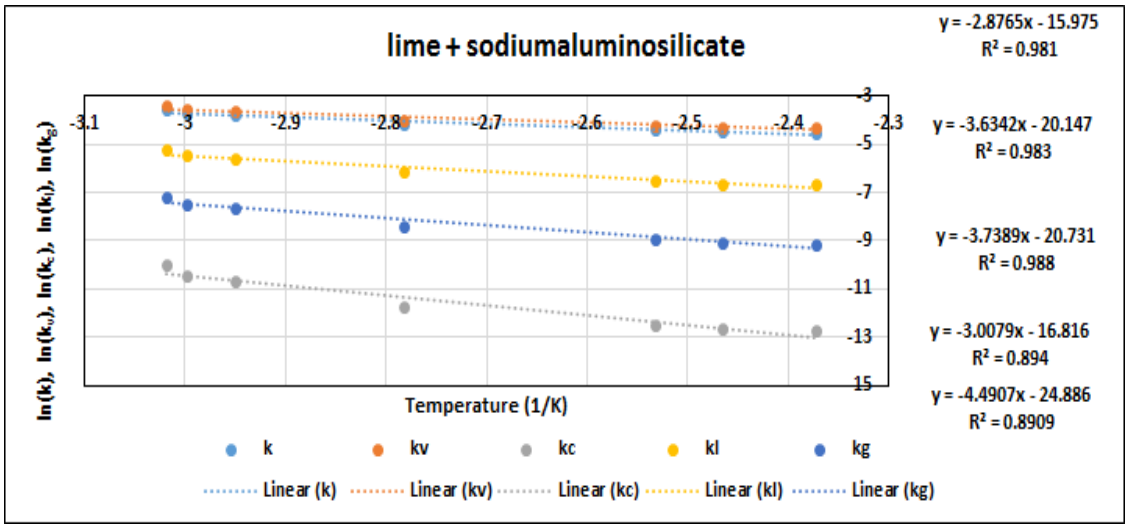

A.19. co-pyrolysis of jute wastes and sesame oil cake

a) Values of W_R

Time (mins)	Weight fraction 573K	Weight fraction 673K	Weight fraction 773K	Weight fraction 873K	Weight fraction 973K	Weight fraction 1073K	Weight fraction 1173K
0	1	1	1	1	1	1	1
5	0.889764	0.789905	0.825746	0.67927	0.803783	0.807604	0.722524
10	0.786089	0.682128	0.525903	0.52412	0.62766	0.62212	0.618063
15	0.430446	0.585266	0.492936	0.479791	0.492908	0.509217	0.54951
20	0.410761	0.564802	0.406593	0.269883	0.444444	0.442396	0.504897
25	0.34252	0.493861	0.356358	0.25163	0.297872	0.390553	0.420022
30	0.321522	0.335607	0.189953	0.225554	0.22695	0.365207	0.339499
35	0.290026	0.302865	0.152276	0.198175	0.178487	0.296083	0.311208
40	0.249344	0.260573	0.119309	0.186441	0.093381	0.240783	0.249184
45	0.232283	0.242838	0.098901	0.156454	0.085106	0.158986	0.205658
50	0.215223	0.225102	0.078493	0.142112	0.068558	0.148618	0.180631
55	0.190289	0.199181	0.048666	0.116037	0.044917	0.10023	0.158868

60	0.169291	0.177353	0.039246	0.093872	0.036643	0.056452	0.136017

b) Values of W_v

Time (mins)	Volatile fraction 573K	Volatile fraction 673K	Volatile fraction 773K	Volatile fraction 873K	Volatile fraction 973K	Volatile fraction 1073K	Volatile fraction 1173K
0	0	0	0	0	0	0	0
5	0.110236	0.210095	0.174254	0.32073	0.196217	0.192396	0.277476
10	0.213911	0.317872	0.474097	0.47588	0.37234	0.37788	0.381937
15	0.569554	0.414734	0.507064	0.520209	0.507092	0.490783	0.45049
20	0.589239	0.435198	0.593407	0.730117	0.555556	0.557604	0.495103
25	0.65748	0.506139	0.643642	0.74837	0.702128	0.609447	0.579978
30	0.678478	0.664393	0.810047	0.774446	0.77305	0.634793	0.660501
35	0.709974	0.697135	0.847724	0.801825	0.821513	0.703917	0.688792
40	0.750656	0.739427	0.880691	0.813559	0.906619	0.759217	0.750816
45	0.767717	0.757162	0.901099	0.843546	0.914894	0.841014	0.794342
50	0.784777	0.774898	0.921507	0.857888	0.931442	0.851382	0.819369
55	0.809711	0.800819	0.951334	0.883963	0.955083	0.89977	0.841132
60	0.830709	0.822647	0.960754	0.906128	0.963357	0.943548	0.863983

c) Values of W_C

Time (mins)	Char fraction 573K	Char fraction 673K	Char fraction 773K	Char fraction 873K	Char fraction 973K	Char fraction 1073K	Char fraction 1173K
0	0	0	0	0	0	0	0
5	0.022465	0.045294	0.007118	0.033227	0.007463	0.011511	0.043683
10	0.043593	0.06853	0.019367	0.0493	0.014163	0.022608	0.060129
15	0.11607	0.089412	0.020713	0.053892	0.019288	0.029363	0.070921
20	0.120082	0.093824	0.02424	0.075638	0.021132	0.033361	0.077944
25	0.133989	0.109118	0.026293	0.077529	0.026707	0.036463	0.091306
30	0.138268	0.143236	0.03309	0.08023	0.029404	0.037979	0.103983
35	0.144687	0.150294	0.034629	0.083067	0.031248	0.042115	0.108437
40	0.152977	0.159412	0.035976	0.084282	0.034485	0.045423	0.118202
45	0.156454	0.163236	0.03681	0.087389	0.0348	0.050317	0.125054
50	0.159931	0.167059	0.037643	0.088875	0.035429	0.050937	0.128994
55	0.165012	0.172647	0.038862	0.091576	0.036328	0.053832	0.13242
60	0.169291	0.177353	0.039246	0.093872	0.036643	0.056452	0.136017

A.20. t vs $\ln\left(\frac{w_o}{w}\right)$

time (mins)	$\ln\left(\frac{w_o}{w}\right)$ 573K	$\ln\left(\frac{w_o}{w}\right)$ 673K	$\ln\left(\frac{w_o}{w}\right)$ 773K	$\ln\left(\frac{w_o}{w}\right)$ 873K	$\ln\left(\frac{w_o}{w}\right)$ 973K	$\ln\left(\frac{w_o}{w}\right)$ 1073K	$\ln\left(\frac{w_o}{w}\right)$ 1173K
0	0	0	0	0	0	0	0
5	0.2445	0.2495	0.2615	0.3095	0.3975	0.425	0.4665
10	0.489	0.499	0.523	0.619	0.795	0.85	0.933
15	0.7335	0.7485	0.7845	0.9285	1.1925	1.275	1.3995
20	0.978	0.998	1.046	1.238	1.59	1.7	1.866

25	1.2225	1.2475	1.3075	1.5475	1.9875	2.125	2.3325
30	1.467	1.497	1.569	1.857	2.385	2.55	2.799
35	1.7115	1.7465	1.8305	2.1665	2.7825	2.975	3.2655
40	1.956	1.996	2.092	2.476	3.18	3.4	3.732
45	2.2005	2.2455	2.3535	2.7855	3.5775	3.825	4.1985
50	2.445	2.495	2.615	3.095	3.975	4.25	4.665
55	2.6895	2.7445	2.8765	3.4045	4.3725	4.675	5.1315
60	2.934	2.994	3.138	3.714	4.77	5.1	5.598

A.21. $\frac{w_v}{w_o}$ **vs** $(1-\exp[-k*t])/k$

$(1-\exp[-k*t])/k$	$\frac{w_v}{w_o}$	$\frac{w_v}{w_o}$	$\frac{w_v}{w_o}$	$\frac{w_v}{w_o}$	$\frac{w_v}{w_o}$	$\frac{w_v}{w_o}$	$\frac{w_v}{w_o}$
	300	400	500	600	700	800	900
0	0	0	0	0	0	0	0
4.435665	0.180088	0.183197	0.191827	0.226624	0.299947	0.31568	0.340041
7.909216	0.321114	0.325942	0.339513	0.392923	0.50151	0.522063	0.553313
10.62934	0.431551	0.437168	0.453217	0.514956	0.63696	0.656989	0.687075
12.75946	0.518034	0.523834	0.540756	0.604506	0.727982	0.7452	0.77097
14.42755	0.585758	0.591363	0.608153	0.670219	0.789149	0.80287	0.823588
15.73382	0.638793	0.643981	0.660041	0.718439	0.830253	0.840573	0.85659
16.75675	0.680324	0.684981	0.69999	0.753825	0.857875	0.865221	0.877289
17.55781	0.712847	0.716927	0.730746	0.779791	0.876437	0.881336	0.890271
18.18512	0.738316	0.741819	0.754425	0.798845	0.88891	0.891871	0.898413
18.67636	0.75826	0.761215	0.772656	0.812827	0.897292	0.898759	0.90352
19.06105	0.773878	0.776328	0.786691	0.823088	0.902925	0.903262	0.906723
19.36229	0.786109	0.788104	0.797497	0.830617	0.90671	0.906206	0.908732

A.22. $\frac{w_c}{w_o}$ **vs** $(1-\exp[-k*t])/k$

$(1-\exp[-k*t])/k$	$\frac{w_c}{w_o}$	$\frac{w_c}{w_o}$	$\frac{w_c}{w_o}$	$\frac{w_c}{w_o}$	$\frac{w_c}{w_o}$	$\frac{w_c}{w_o}$	$\frac{w_c}{w_o}$
	300	400	500	600	700	800	900
0	0	0	0	0	0	0	0
4.435665	0.036816	0.037613	0.038277	0.039562	0.028056	0.03055	0.032765
7.909216	0.065646	0.06692	0.067747	0.068594	0.046909	0.050522	0.053316
10.62934	0.088224	0.089757	0.090435	0.089898	0.059578	0.06358	0.066205
12.75946	0.105904	0.10755	0.107903	0.10553	0.068092	0.072116	0.074289
14.42755	0.119749	0.121415	0.121352	0.117002	0.073813	0.077697	0.079359
15.73382	0.130591	0.132218	0.131705	0.12542	0.077658	0.081346	0.082539
16.75675	0.139081	0.140636	0.139677	0.131597	0.080241	0.083731	0.084533
17.55781	0.14573	0.147195	0.145814	0.13613	0.081978	0.085291	0.085784
18.18512	0.150936	0.152306	0.150539	0.139457	0.083144	0.08631	0.086569
18.67636	0.155014	0.156288	0.154177	0.141898	0.083928	0.086977	0.087061
19.06105	0.158207	0.159391	0.156977	0.143689	0.084455	0.087412	0.087369

19.36229	0.160707	0.161809	0.159134	0.145003	0.084809	0.087697	0.087563

A.23. $\frac{w_l}{w_o}$ **vs** $(1-\exp[-k*t])/k$

$(1-\exp[-k*t])/k$	$\frac{w_l}{w_o}$	$\frac{w_l}{w_o}$	$\frac{w_l}{w_o}$	$\frac{w_l}{w_o}$	$\frac{w_l}{w_o}$	$\frac{w_l}{w_o}$	$\frac{w_l}{w_o}$
	300	400	500	600	700	800	900
0	0	0	0	0	0	0	0
4.435665	0.0897	0.092412	0.108181	0.084731	0.124832	0.137984	0.11464
7.909216	0.159944	0.164419	0.191469	0.146908	0.208719	0.228194	0.186541
10.62934	0.214952	0.220525	0.255592	0.192535	0.26509	0.28717	0.231638
12.75946	0.258029	0.264243	0.30496	0.226016	0.302972	0.325727	0.259922
14.42755	0.291761	0.298308	0.342968	0.250585	0.328429	0.350935	0.277661
15.73382	0.318178	0.32485	0.37223	0.268614	0.345535	0.367415	0.288787
16.75675	0.338864	0.345532	0.394759	0.281844	0.357031	0.378189	0.295765
17.55781	0.355063	0.361647	0.412104	0.291552	0.364756	0.385232	0.300142
18.18512	0.367749	0.374204	0.425458	0.298676	0.369947	0.389837	0.302887
18.67636	0.377683	0.383988	0.435739	0.303904	0.373436	0.392848	0.304609
19.06105	0.385463	0.391612	0.443654	0.30774	0.37578	0.394816	0.305689
19.36229	0.391555	0.397552	0.449748	0.310555	0.377355	0.396103	0.306366

A.24. $\frac{w_g}{w_o}$ **vs** $(1-\exp[-k*t])/k$

$(1-\exp[-k*t])/k$	$\frac{w_g}{w_o}$	$\frac{w_g}{w_o}$	$\frac{w_g}{w_o}$	$\frac{w_g}{w_o}$	$\frac{w_g}{w_o}$	$\frac{w_g}{w_o}$	$\frac{w_g}{w_o}$
	300	400	500	600	700	800	900
0	0	0	0	0	0	0	0
4.435665	0.090388	0.090785	0.084128	0.083259	0.175115	0.177696	0.225401
7.909216	0.16117	0.161523	0.14968	0.148134	0.292791	0.293869	0.366771
10.62934	0.216599	0.216642	0.200757	0.198684	0.37187	0.369819	0.455438
12.75946	0.260005	0.25959	0.240556	0.238072	0.42501	0.419473	0.511049
14.42755	0.293997	0.293055	0.271567	0.268763	0.460721	0.451935	0.545927
15.73382	0.320615	0.319131	0.29573	0.292677	0.484718	0.473158	0.567803
16.75675	0.34146	0.339448	0.314558	0.31131	0.500844	0.487033	0.581524
17.55781	0.357784	0.35528	0.329228	0.325829	0.511681	0.496104	0.590129
18.18512	0.370567	0.367615	0.34066	0.337142	0.518963	0.502034	0.595526
18.67636	0.380577	0.377227	0.349567	0.345958	0.523857	0.505911	0.598911
19.06105	0.388416	0.384717	0.356507	0.352826	0.527145	0.508446	0.601034
19.36229	0.394555	0.390552	0.361915	0.358178	0.529355	0.510103	0.602366

A.25. Activation energies and Pre-exponential factor

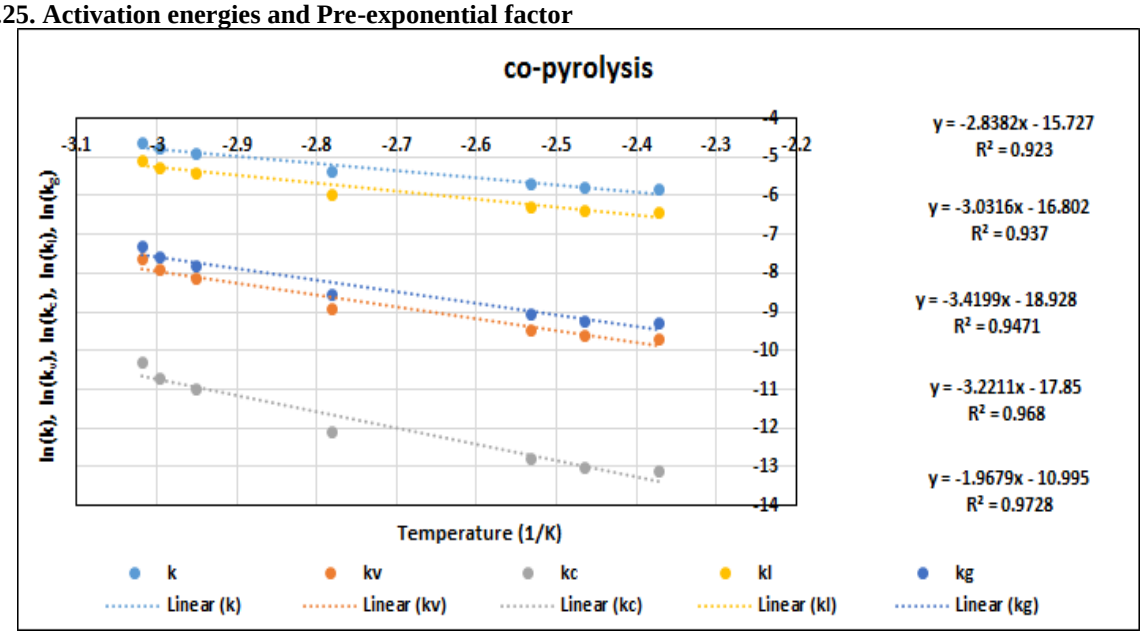

A.26. Ultimate analyses of char product obtained from pyrolysis of jute waste at different temperatures

Temperature	C	H	N	S	O (By Difference)
300°C	56.45	9.34	10.64	0.526	23.044
400°C	64.34	10.27	8.73	0.755	15.905
500°C	68.47	12.61	9.016	0.976	8.928
600°C	74.16	13.23	8.78	1.494	2.336
700°C	74.427	13.664	8.267	0.627	3.015
800°C	70.129	14.375	8.001	0.896	6.599
900°C	65.798	14.859	7.772	1.073	10.498

A.27. Ultimate analyses of char product obtained from pyrolysis of jute waste in presence of alumina at different temperatures

Temperature	C	H	N	S	O (By Difference)
300°C	50.671	10.34	10.567	0.516	27.906
400°C	57.513	9.48	9.914	0.596	22.497
500°C	60.13	9.23	9.573	0.624	20.443
600°C	63.467	9.018	9.12	0.677	17.718
700°C	69.173	8.9	8.846	0.796	12.285
800°C	57.26	8.593	8.61	0.878	24.659
900°C	54.158	8.245	8.0244	0.95	28.6226

A.28. Ultimate analyses of char product obtained from pyrolysis of jute waste in presence of ZnO at different temperatures

Temperature	C	H	N	S	O (By Difference)
300ºC	48.464	13.01	9.21	0.426	28.89
400ºC	52.5	12.183	9.009	0.614	25.694
500ºC	56.176	10.671	8.987	0.769	23.397
600ºC	64.279	9.515	8.813	0.897	16.496
700ºC	68.913	8.676	8.565	0.965	12.881
800ºC	64.274	8.349	8.416	1.234	17.727
900ºC	60.189	8.067	8.225	1.568	21.951

A.29. Ultimate analyses of char product obtained from pyrolysis of jute waste in presence of KCl at different temperatures

Temperature	C	H	N	S	O (By Difference)
300ºC	52.486	14.678	11.679	0.561	20.596
400ºC	56.684	11.596	10.545	0.694	20.481
500ºC	59.146	9.67	10.617	0.796	19.771
600ºC	60.614	8.545	9.767	0.838	20.236
700ºC	68.165	8.437	9.869	1.472	12.057
800ºC	62.325	8.067	9.272	1.129	19.207
900ºC	58.678	7.983	8.431	1.561	23.347

A.30. Ultimate analyses of char product obtained from pyrolysis of jute waste in presence of NaCl at different temperatures

Temperature	C	H	N	S	O (By Difference)
300ºC	45.123	12.634	10.675	0.492	31.076
400ºC	50.419	10.991	10.015	0.567	28.008
500ºC	56.526	10.059	9.53	0.694	23.191
600ºC	58.484	9.78	9.015	0.796	21.925
700ºC	68.569	9.945	8.545	0.927	12.014
800ºC	70.677	8.56	8.056	1.437	11.27
900ºC	76.731	5.988	5.862	0.973	10.446

A.31. Ultimate analyses of char product obtained from pyrolysis of jute waste in presence of $NaAl(SiO_3)_2$ at different temperatures

Temperature	C	H	N	S	O (By Difference)
300ºC	48.691	18.767	10.564	0.683	21.295
400ºC	54.316	15.676	12.789	0.432	16.787
500ºC	59.369	12.489	10.325	0.684	17.133
600ºC	64.104	8.016	9.416	0.789	17.675
700ºC	70.01	7.967	9.018	0.983	12.022
800ºC	68.474	7.845	9.078	0.896	13.707
900ºC	64.676	7.796	8.952	1.165	17.411

A.32. Ultimate analyses of char product obtained from pyrolysis of lime waste at different temperatures

temperature	C	H	N	S	O
300	37.147	5.961	10.416	0.293	46.183
400	38.734	6.167	10.216	0.316	44.567
500	40.19	6.432	9.913	0.467	42.998
600	41.231	7.617	9.036	0.587	41.529
700	42.134	7.989	8.97	0.796	40.111
800	44.136	8.161	8.63	0.96	38.113
900	46.14	8.313	8.534	1.034	35.979

A.33. Ultimate analyses of char product obtained from pyrolysis of lime waste in presence of alumina at different temperatures

temperature	C	H	N	S	O
300	41.08	6.95	11.85	0.982	39.138
400	42.82	7.28	10.86	0.86	38.18
500	45.91	9.02	8.97	0.753	35.347
600	48.64	9.983	8.01	0.691	32.676
700	49.25	11.548	6.94	0.58	31.682
800	50.23	12.59	5.38	0.49	31.31
900	52.17	14.78	4.67	0.402	27.978

A.34. Ultimate analyses of char product obtained from pyrolysis of lime waste in presence of ZnO at different temperatures

temperature	C	H	N	S	O
300	39.52	6.005	10.7911	0.89055	42.79335
400	41.26	6.335	9.8011	0.76855	41.83535
500	44.35	8.075	7.9111	0.66155	39.00235
600	47.08	9.038	6.9511	0.59955	36.33135
700	47.69	10.603	5.8811	0.48855	35.33735
800	48.67	11.645	4.3211	0.39855	34.96535
900	50.61	13.835	3.6111	0.31055	31.63335

A.35. Ultimate analyses of char product obtained from pyrolysis of lime waste in presence of KCl at different temperatures

temperature	C	H	N	S	O
300	38.578	5.145	8.9011	0.81455	46.56135
400	40.318	5.475	7.9111	0.69255	45.60335
500	43.408	7.215	6.0211	0.58555	42.77035
600	46.138	8.178	5.0611	0.52355	40.09935
700	46.748	9.743	3.9911	0.41255	39.10535
800	47.728	10.785	2.4311	0.32255	38.73335
900	49.668	12.975	1.7211	0.23455	35.40135

A.36. Ultimate analyses of char product obtained from pyrolysis of lime waste in presence of NaCl at different temperatures

temperature	C	H	N	S	O
300	37.678	4.945	7.9611	0.71655	48.69935
400	39.418	5.275	6.9711	0.59455	47.74135
500	42.508	7.015	5.0811	0.48755	44.90835
600	45.238	7.978	4.1211	0.42555	42.23735
700	45.848	9.543	3.0511	0.31455	41.24335
800	46.828	10.585	1.4911	0.22455	40.87135
900	48.768	12.775	0.7811	0.13655	37.53935

A.37. Ultimate analyses of char product obtained from pyrolysis of lime waste in presence of $NaAl(SiO_3)_2$ at different temperatures

temperature	C	H	N	S	O
300	36.448	4.856	6.3111	0.63825	51.74665
400	38.188	5.186	5.3211	0.51625	50.78865
500	41.278	6.926	3.4311	0.40925	47.95565
600	44.008	7.889	2.4711	0.34725	45.28465
700	44.618	9.454	1.4011	0.23625	44.29065
800	45.598	10.496	0.8411	0.21672	42.84818
900	47.538	12.686	0.1311	0.12872	39.51618

A.38. Ultimate analyses of char product obtained from pyrolysis of co-pyrolysis of jute wastes and sesame oil cake at different temperatures

temperature	C	H	N	S	O
300	22.178	2.001	9.21	0.426	66.185
400	24.224	2.546	9.009	0.61	63.611
500	26.913	3.176	8.9	0.769	60.242
600	28.269	3.41	8.816	0.89	58.615
700	31.173	3.68	8.567	0.96	55.62
800	33.5	4.123	7.416	1.23	53.731
900	35.461	5.01	7.223	1.56	50.746

A.39. Ultimate analyses of char product obtained from pyrolysis of co-pyrolysis of jute wastes and sesame oil cake in presence of alumina at different temperatures

temperature	C	H	N	S	O
300	33.7	3.48	11.45	0.88	50.49
400	35.01	3.83	10.94	0.768	49.452
500	35.845	4.086	9.64	0.65	49.779

600	36.72	4.9	8.53	0.521	49.329
700	37.91	5.12	7.36	0.462	49.148
800	38.48	6.856	6.63	0.368	47.666
900	40.12	7.91	5.14	0.301	46.529

A.40. Ultimate analyses of char product obtained from pyrolysis of co-pyrolysis of jute wastes and sesame oil cake in presence of ZnO at different temperatures

temperature	C	H	N	S	O
300	32.14	2.535	10.3911	0.78855	54.14535
400	33.45	2.885	9.8811	0.67655	53.10735
500	34.285	3.141	8.5811	0.55855	53.43435
600	35.16	3.955	7.4711	0.42955	52.98435
700	36.35	4.175	6.3011	0.37055	52.80335
800	36.92	5.911	5.5711	0.27655	51.32135
900	38.56	6.965	4.0811	0.20955	50.18435

A.41. Ultimate analyses of char product obtained from pyrolysis of co-pyrolysis of jute wastes and sesame oil cake in presence of KCl at different temperatures

temperature	C	H	N	S	O
300	31.198	1.675	8.5011	0.71255	57.91335
400	32.508	2.025	7.9911	0.60055	56.87535
500	33.343	2.281	6.6911	0.48255	57.20235
600	34.218	3.095	5.5811	0.35355	56.75235
700	35.408	3.315	4.4111	0.29455	56.57135
800	35.978	5.051	3.6811	0.20055	55.08935
900	37.618	6.105	2.1911	0.13355	53.95235

A.42. Ultimate analyses of char product obtained from pyrolysis of co-pyrolysis of jute wastes and sesame oil cake in presence of NaCl at different temperatures

temperature	C	H	N	S	O
300	30.298	1.475	7.5611	0.61455	60.05135
400	31.608	1.825	7.0511	0.50255	59.01335
500	32.443	2.081	5.7511	0.38455	59.34035
600	33.318	2.895	4.6411	0.25555	58.89035
700	34.508	3.115	3.4711	0.19655	58.70935
800	35.078	4.851	2.7411	0.10255	57.22735
900	36.718	5.905	1.2511	0.03555	56.09035

A.43. Ultimate analyses of char product obtained from pyrolysis of co-pyrolysis of jute wastes and sesame oil cake in presence of $NaAl(SiO_3)_2$ at different temperatures

temperature	C	H	N	S	O
300	29.068	1.386	5.9111	0.53625	63.09865
400	30.378	1.736	5.4011	0.42425	62.06065
500	31.213	1.992	4.1011	0.30625	62.38765
600	32.088	2.806	2.9911	0.17725	61.93765
700	33.278	3.026	1.8211	0.11825	61.75665
800	33.848	4.762	1.0911	0.09472	60.20418
900	35.488	5.816	0.4311	0.02772	58.23718

A.44. Ultimate analyses of pyro-oil product obtained from pyrolysis of jute waste at different temperatures

Temperature	C	H	N	S	O (By Difference)
300ºC	66.47	11.35	10.69	0.526	10.964
400ºC	64.24	10.27	9.73	0.637	15.123
500ºC	58.47	9.61	9.01	0.756	22.154
600ºC	54.13	9.25	8.78	0.893	26.947
700ºC	52.467	8.614	8.217	0.976	29.726
800ºC	48.123	8.345	8.001	1.079	34.452
900ºC	46.797	7.859	7.774	1.496	36.074

A.45. Ultimate analyses of pyro-oil product obtained from pyrolysis of jute waste in presence of alumina at different temperatures

Temperature	C	H	N	S	O (By Difference)
300ºC	70.671	10.34	10.56	0.516	7.913
400ºC	67.51	9.46	9.914	0.59	12.526
500ºC	62.13	9.23	9.563	0.624	18.453
600ºC	56.46	9.016	9.12	0.675	24.729
700ºC	49.123	8.9	8.84	0.796	32.341
800ºC	47.26	8.563	8.61	0.87	34.697
900ºC	44.15	8.241	8.024	0.95	38.635

A.46. Ultimate analyses of pyro-oil product obtained from pyrolysis of jute waste in presence of ZnO at different temperatures

Temperature	C	H	N	S	O (By Difference)
300ºC	68.461	15.01	9.21	0.426	6.893

400ºC	62.5	12.123	9.009	0.61	15.758
500ºC	56.173	10.6	8.9	0.769	23.558
600ºC	54.269	9.51	8.816	0.89	26.515
700ºC	48.913	8.676	8.567	0.96	32.884
800ºC	44.224	8.346	8.416	1.23	37.784
900ºC	40.1	8.001	8.223	1.56	42.116

A.47.Ultimate analyses of pyro-oil product obtained from pyrolysis of jute waste in presence of NaCl at different temperatures

Temperature	**C**	**H**	**N**	**S**	**O (By Difference)**
300ºC	65.1232	12.6	10.675	0.491	11.111
400ºC	60.416	10.991	10.015	0.567	18.011
500ºC	56.526	10.056	9.53	0.691	23.197
600ºC	50.489	9.78	9.01	0.796	29.925
700ºC	48.569	9	8.541	0.926	32.964
800ºC	44.673	8.56	8.053	1.43	37.284
900ºC	40.731	7.98	7.86	0.999	42.43

A.48.Ultimate analyses of pyro-oil product obtained from pyrolysis of jute waste in presence of KCl at different temperatures

Temperature	**C**	**H**	**N**	**S**	**O (By Difference)**
300ºC	62.486	14.678	11.679	0.561	10.596
400ºC	60.684	11.596	10.516	0.69	16.514
500ºC	55.146	9.67	10.617	0.796	23.771
600ºC	50.61	8.56	9.76	0.896	30.174

700ºC	48.1	8.432	9.813	1.436	32.219
800ºC	42.3	8.004	9.236	1.123	39.337
900ºC	38.61	7.956	8.43	1.56	43.444

A.49. Ultimate analyses of pyro-oil product obtained from pyrolysis of jute waste in presence of $NaAl(SiO_3)_2$ at different temperatures

Temperature	**C**	**H**	**N**	**S**	**O (By Difference)**
300ºC	58.691	18.76	10.569	0.613	11.367
400ºC	54.316	15.679	12.789	0.432	16.784
500ºC	49.369	12.489	10.321	0.676	27.145
600ºC	44.104	8.013	9.416	0.789	37.678
700ºC	40.01	7.967	9.014	0.989	42.02
800ºC	38.4	7.845	9.004	0.896	43.855
900ºC	34.676	7.796	8.916	1.161	47.451

A.50.Ultimate analyses of pyro-oil product obtained from pyrolysis of lime waste at different temperatures

Temperature	**C**	**H**	**N**	**S**	**O (By Difference)**
300ºC	68.14	11.313	10.416	0.393	9.738
400ºC	60.136	10.461	10.216	0.416	18.771
500ºC	56.134	9.989	9.913	0.567	23.397
600ºC	52.231	9.617	9.036	0.687	28.429
700ºC	48.19	9.432	8.97	0.896	32.512
800ºC	46.734	9.567	8.63	1.16	33.909
900ºC	45.147	8.961	8.534	1.234	36.124

A.51.Ultimate analyses of pyro-oil product obtained from pyrolysis of lime waste in presence of alumina at different temperatures

Temperature	C	H	N	S	O (By Difference)
300ºC	69.143	11.415	10.918	0.456	8.068
400ºC	64.167	10.961	10.064	0.567	14.241
500ºC	63.164	10.458	9.813	0.693	15.872
600ºC	60.216	10.064	9.013	0.891	19.816
700ºC	56.617	9.581	8.996	1.016	23.79
800ºC	54.321	9.323	8.867	1.136	26.353
900ºC	52.165	9.106	8.676	1.436	28.617

A.52.Ultimate analyses of pyro-oil product obtained from pyrolysis of lime waste in presence of ZnO at different temperatures

Temperature	C	H	N	S	O (By Difference)
300^{O}C	66.23	11.016	10.113	0.431	12.21
400ºC	61.114	10.916	9.916	0.592	17.462
500ºC	56.234	9.136	9.763	0.693	24.174
600ºC	54.123	8.96	9.021	0.893	27.003
700ºC	51.616	8.856	8.637	1.013	29.878
800ºC	49.759	8.753	8.464	1.236	31.788
900ºC	47.435	8.345	8.216	1.479	34.525

A.53.Ultimate analyses of pyro-oil product obtained from pyrolysis of lime waste in presence of NaCl at different temperatures

Temperature	C	H	N	S	O (By Difference)
300^{O}C	65.176	10.167	10.416	0.769	13.472

400ºC	63.485	10.078	9.461	0.497	16.479
500ºC	60.116	9.163	9.375	0.567	20.779
600ºC	58.486	8.964	9.021	0.798	22.731
700ºC	52.146	8.836	8.961	0.994	29.063
800ºC	56.104	8.645	8.754	1.015	25.482
900ºC	50.117	8.213	8.65	1.436	31.584

A.54. Ultimate analyses of pyro-oil product obtained from pyrolysis of lime waste in presence of KCl at different temperatures

Temperature	**C**	**H**	**N**	**S**	**O (By Difference)**
300^{O}C	67.167	10.918	10.169	0.567	11.179
400ºC	60.163	11.001	10.013	0.661	18.162
500ºC	56.216	10.013	9.29	0.761	23.72
600ºC	50.148	9.16	9.67	0.698	30.324
700ºC	48.128	9.6	9.765	0.813	31.694
800ºC	44.117	8.96	9.394	1.13	36.399
900ºC	43.264	8.92	8.9991	1.467	37.358

A.55.Ultimate analyses of pyro-oil product obtained from pyrolysis of lime waste in presence of $NaAl(SiO_3)_2$ at different temperatures

Temperature	**C**	**H**	**N**	**S**	**O (By Difference)**
300ºC	63.41	10.9	10.456	0.619	14.615
400ºC	52.146	10.875	10.567	0.569	25.843
500ºC	53.158	9.756	9.613	0.493	26.98
600ºC	50.261	9.676	9.236	0.761	30.066

700ºC	48.667	9.231	9.061	0.893	32.148
800ºC	44.285	9.879	8.934	1.013	35.889
900ºC	47.813	8.931	8.863	1.387	33.006

A.56. Ultimate analyses of pyro-oil product obtained from co-pyrolysis of jute waste and sesame oil cake at different temperatures

Temperature	**C**	**H**	**N**	**S**	**O (By Difference)**
300ºC	66.125	12.33	10.136	0.569	10.84
400ºC	64.325	11.918	11.613	0.678	11.466
500ºC	59.625	12.617	10.041	0.796	16.921
600ºC	54.749	10.516	9.616	0.916	24.203
700ºC	52.193	9.623	9.341	1.463	27.38
800ºC	48.299	9.01	9.039	1.263	32.389
900ºC	45.361	8.95	8.9	1.563	35.226

A.57. Ultimate analyses of pyro-oil product obtained from co-pyrolysis of jute waste and sesame oil cake in presence of alumina at different temperatures

Temperature	**C**	**H**	**N**	**S**	**O (By Difference)**
300ºC	68.413	13.981	12.61	0.613	4.383
400ºC	64.564	12.673	11.758	0.656	10.349
500ºC	60.126	10.567	10.117	0.796	18.394
600ºC	54.231	9.124	10.063	0.963	25.619
700ºC	52.234	8.456	9.61	1.126	28.574
800ºC	50.167	8.516	9.78	1.435	30.102
900ºC	46.168	8.2	9.56	1.613	34.459

A.58. Ultimate analyses of pyro-oil product obtained from co-pyrolysis of jute waste and sesame oil cake in presence of ZnO at different temperatures

Temperature	C	H	N	S	O (By Difference)
300^{O}C	64.111	11.617	11.514	0.5	12.258
400ºC	60.267	10.532	10.613	0.657	17.931
500ºC	56.313	10.123	9.548	0.789	23.227
600ºC	54.46	9.617	9.383	0.953	25.587
700ºC	51.07	9.423	9.016	0.993	29.498
800ºC	46.079	8.467	8.967	1.216	35.271
900ºC	44.196	8.236	8.43	1.563	37.575

A.59. Ultimate analyses of pyro-oil product obtained from co-pyrolysis of jute waste and sesame oil cake in presence of NaCl at different temperatures

Temperature	C	H	N	S	O (By Difference)
300^{O}C	60.591	10.117	10.136	0.461	18.695
400ºC	56.613	10.236	10.013	0.617	22.521
500ºC	52.667	9.454	9.176	0.567	28.136
600ºC	50.798	9.216	9.02	0.613	30.353
700ºC	51.813	8.617	8.96	0.763	29.847
800ºC	49.314	8.432	8.676	0.89	32.688
900ºC	45.669	8.015	8.43	0.949	36.937

A.60. Ultimate analyses of pyro-oil product obtained from co-pyrolysis of jute waste and sesame oil cake in presence of KCl at different temperatures

Temperature	C	H	N	S	O (By Difference)
300^{O}C	63.132	10.16	10.118	0.61	15.983

400ºC	61.667	10.078	10.006	0.59	17.659
500ºC	58.789	9.176	9.613	0.513	21.909
600ºC	54.913	9.076	9.414	0.756	25.841
700ºC	56.954	8.761	9.786	0.893	23.606
800ºC	50.126	8.432	9.618	0.965	30.859
900ºC	48.115	8.215	9.32	1.467	32.883

A.61. Ultimate analyses of pyro-oil product obtained from co-pyrolysis of jute waste and sesame oil cake in presence of $NaAl(SiO_3)_2$ at different temperatures

Temperature	**C**	**H**	**N**	**S**	**O (By Difference)**
300ºC	64.313	12.61	11.361	0.561	11.155
400ºC	56.614	10.059	10.619	0.763	21.945
500ºC	59.617	9.61	9.761	0.649	20.363
600ºC	54.222	9.517	9.816	0.893	25.552
700ºC	50.167	9.013	9.453	1.43	29.937
800ºC	46.07	8.967	9.236	1.113	34.614
900ºC	49.819	8.563	9.164	1.016	31.438

A.62.

i) Jute waste pyro-oil

a) 500ºC pyro-oil cracked at 300ºC

(1-exp(-k*t))/k	**w_v/w_o**
0	0
3.353709	0.201223
4.772871	0.286372
5.373407	0.322404

(1-exp(-k*t))/k	**w_s/w_o**
0	0
3.353709	0.375615
4.772871	0.534562
5.373407	0.601822

b) 500ºC pyro-oil cracked at 400ºC

(1-exp(-k*t))/k	**w_v/w_o**
0	0
3.261992	0.225077

(1-exp(-k*t))/k	**w_s/w_o**
0	0
3.261992	0.378391

4.555475	0.314328	4.555475	0.528435
5.068381	0.349718	5.068381	0.587932

c) 500°C pyro-oil cracked at 500°C

(1-exp(-k*t))/k	w_v/w_o	(1-exp(-k*t))/k	w_s/w_o
0	0	0	0
3.227679	0.232393	3.227679	0.380866
4.475955	0.322269	4.475955	0.528163
4.958714	0.357027	4.958714	0.585128

d) 500°C pyro-oil cracked at 600°C

(1-exp(-k*t))/k	w_v/w_o	(1-exp(-k*t))/k	w_s/w_o
0	0	0	0
3.167219	0.234374	3.167219	0.395902
4.338214	0.321028	4.338214	0.542277
4.771158	0.353066	4.771158	0.596395

e) 500°C pyro-oil cracked at 700°C

(1-exp(-k*t))/k	w_v/w_o	(1-exp(-k*t))/k	w_s/w_o
0	0	0	0
3.127822	0.24397	3.127822	0.397233
4.250074	0.331506	4.250074	0.539759
4.652734	0.362913	4.652734	0.590897

f) 500°C pyro-oil cracked at 800°C

(1-exp(-k*t))/k	w_v/w_o	(1-exp(-k*t))/k	w_s/w_o
0	0	0	0
3.082756	0.252786	3.082756	0.400758
4.150794	0.340365	4.150794	0.539603
4.520822	0.370707	4.520822	0.587707

g) 500°C pyro-oil cracked at 900°C

(1-exp(-k*t))/k	w_v/w_o	(1-exp(-k*t))/k	w_s/w_o
0	0	0	0
3.020005	0.26274	3.020005	0.407701
4.015274	0.349329	4.015274	0.542062
4.343274	0.377865	4.343274	0.586342

ii) Jute waste pyro-oil

a) 700ºC pyro-oil cracked at 300ºC

(1-exp(-k*t))/k	w_v/w_o
0	0
3.248204	0.243615
4.523403	0.339255
5.024028	0.376802

(1-exp(-k*t))/k	w_s/w_o
0	0
3.248204	0.363799
4.523403	0.506621
5.024028	0.562691

b) 700ºC pyro-oil cracked at 400ºC

(1-exp(-k*t))/k	w_v/w_o
0	0
3.200603	0.252848
4.413897	0.348698
4.873836	0.385033

(1-exp(-k*t))/k	w_s/w_o
0	0
3.200603	0.368069
4.413897	0.507598
4.873836	0.560491

c) 700ºC pyro-oil cracked at 500ºC

(1-exp(-k*t))/k	w_v/w_o
0	0
3.167219	0.256545
4.338214	0.351395
4.771158	0.386464

(1-exp(-k*t))/k	w_s/w_o
0	0
3.167219	0.373732
4.338214	0.511909
4.771158	0.562997

d) 700ºC pyro-oil cracked at 600ºC

(1-exp(-k*t))/k	w_v/w_o
0	0
3.134339	0.263284
4.264565	0.358223
4.672119	0.392458

(1-exp(-k*t))/k	w_s/w_o
0	0
3.134339	0.376121
4.264565	0.511748
4.672119	0.560654

e) 700ºC pyro-oil cracked at 700ºC

(1-exp(-k*t))/k	w_v/w_o
0	0
3.108391	0.267322
4.207066	0.361808
4.595398	0.395204

(1-exp(-k*t))/k	w_s/w_o
0	0
3.108391	0.379224
4.207066	0.513262
4.595398	0.560639

f) 700ºC pyro-oil cracked at 800ºC

(1-exp(-k*t))/k	w_v/w_o
0	0
3.076395	0.273799
4.136914	0.368185
4.502505	0.400723

(1-exp(-k*t))/k	w_s/w_o
0	0
3.076395	0.381473
4.136914	0.512977
4.502505	0.558311

g) 700ºC pyro-oil cracked at 900ºC

(1-exp(-k*t))/k	w_v/w_o
0	0
3.057428	0.275169
4.095717	0.368615
4.448315	0.400348

(1-exp(-k*t))/k	w_s/w_o
0	0
3.057428	0.385236
4.095717	0.51606
4.448315	0.560488

iii) Jute waste pyro-oil

a) 900ºC pyro-oil cracked at 300ºC

(1-exp(-k*t))/k	w_v/w_o
0	0
3.200603	0.268851
4.413897	0.370767
4.873836	0.409402

(1-exp(-k*t))/k	w_s/w_o
0	0
3.200603	0.352066
4.413897	0.485529
4.873836	0.536122

b) 900ºC pyro-oil cracked at 400ºC

(1-exp(-k*t))/k	w_v/w_o
0	0
3.187188	0.270911
4.383375	0.372587
4.832318	0.410747

(1-exp(-k*t))/k	w_s/w_o
0	0
3.187188	0.353778
4.383375	0.486555
4.832318	0.536387

c) 900ºC pyro-oil cracked at 500ºC

(1-exp(-k*t))/k	w_v/w_o
0	0
3.167219	0.275548
4.338214	0.377425
4.771158	0.415091

(1-exp(-k*t))/k	w_s/w_o
0	0
3.167219	0.354729
4.338214	0.48588
4.771158	0.53437

d) 900ºC pyro-oil cracked at 600ºC

(1-exp(-k*t))/k	w_v/w_o
0	0
3.134339	0.278956
4.264565	0.379546
4.672119	0.415819

(1-exp(-k*t))/k	w_s/w_o
0	0
3.134339	0.360449
4.264565	0.490425
4.672119	0.537294

e) 900ºC pyro-oil cracked at 700ºC

(1-exp(-k*t))/k	w_v/w_o
0	0
3.114848	0.280336
4.221325	0.379919
4.614374	0.415294

(1-exp(-k*t))/k	w_s/w_o
0	0
3.114848	0.364437
4.221325	0.493895
4.614374	0.539882

f) 900ºC pyro-oil cracked at 800ºC

(1-exp(-k*t))/k	w_v/w_o
0	0
3.089135	0.2842
4.164749	0.383157
4.539269	0.417613

(1-exp(-k*t))/k	w_s/w_o
0	0
3.089135	0.367607
4.164749	0.495605
4.539269	0.540173

g) 900ºC pyro-oil cracked at 900ºC

(1-exp(-k*t))/k	w_v/w_o
0	0
3.070054	0.288585
4.123108	0.387572
4.484315	0.421526

(1-exp(-k*t))/k	w_s/w_o
0	0
3.070054	0.368406
4.123108	0.494773
4.484315	0.538118

A.63.

I) Jute waste pyro-oil in presence of alumina

a) 500ºC pyro-oil cracked at 300ºC

(1-exp(-k*t))/k	w_v/w_o
0	0
3.296835	0.227482
4.637228	0.319969
5.182192	0.357571

(1-exp(-k*t))/k	w_s/w_o
0	0
3.296835	0.365949
4.637228	0.514732
5.182192	0.575223

b) 500ºC pyro-oil cracked at 400ºC

(1-exp(-k*t))/k	w_v/w_o
0	0
3.296835	0.365949
4.637228	0.514732
5.182192	0.575223

(1-exp(-k*t))/k	w_s/w_o
0	0
3.241341	0.379237
4.507499	0.527377
5.002096	0.585245

c) 500ºC pyro-oil cracked at 500ºC

(1-exp(-k*t))/k	w_v/w_o
0	0
3.193885	0.239541
4.398595	0.329895
4.853002	0.363975

(1-exp(-k*t))/k	w_s/w_o
0	0
3.193885	0.383266
4.398595	0.527831
4.853002	0.58236

d) 500ºC pyro-oil cracked at 600ºC

(1-exp(-k*t))/k	w_v/w_o
0	0
3.134339	0.257016

(1-exp(-k*t))/k	w_s/w_o
0	0
3.134339	0.382389
4.264565	0.520277

4.264565	0.349694
4.672119	0.383114

4.672119	0.569999

e) 500ºC pyro-oil cracked at 700ºC

(1-exp(-k*t))/k	w_v/w_o
0	0
3.108391	0.261105
4.207066	0.353394
4.595398	0.386013

(1-exp(-k*t))/k	w_s/w_o
0	0
3.108391	0.38544
4.207066	0.521676
4.595398	0.569829

f) 500ºC pyro-oil cracked at 800ºC

(1-exp(-k*t))/k	w_v/w_o
0	0
3.070054	0.264025
4.123108	0.354587
4.484315	0.385651

(1-exp(-k*t))/k	w_s/w_o
0	0
3.070054	0.392967
4.123108	0.527758
4.484315	0.573992

g) 500ºC pyro-oil cracked at 900ºC

(1-exp(-k*t))/k	w_v/w_o
0	0
3.044878	0.267949
4.068617	0.358038
4.412815	0.388328

(1-exp(-k*t))/k	w_s/w_o
0	0
3.044878	0.395834
4.068617	0.52892
4.412815	0.573666

ii) Jute waste pyro-oil in presence of alumina

a) 700ºC pyro-oil cracked at 300ºC

(1-exp(-k*t))/k	w_v/w_o
0	0
3.248204	0.269601
4.523403	0.375442
5.024028	0.416994

(1-exp(-k*t))/k	w_s/w_o
0	0
3.248204	0.337813
4.523403	0.470434
5.024028	0.522499

b) 700ºC pyro-oil cracked at 400ºC

(1-exp(-k*t))/k	w_v/w_o
0	0
3.2141	0.276413
4.444755	0.382249
4.915965	0.422773

(1-exp(-k*t))/k	w_s/w_o
0	0
3.2141	0.340695
4.444755	0.471144
4.915965	0.521092

c) 700ºC pyro-oil cracked at 500ºC

(1-exp(-k*t))/k	w_v/w_o
0	0
3.187188	0.277285
4.383375	0.381354
4.832318	0.420412

(1-exp(-k*t))/k	w_s/w_o
0	0
3.187188	0.347404
4.383375	0.477788
4.832318	0.526723

d) 700ºC pyro-oil cracked at 600ºC

(1-exp(-k*t))/k	w_v/w_o
0	0
3.147431	0.283269
4.293785	0.386441
4.711309	0.424018

(1-exp(-k*t))/k	w_s/w_o
0	0
3.147431	0.352512
4.293785	0.480904
4.711309	0.527667

e) 700ºC pyro-oil cracked at 700ºC

(1-exp(-k*t))/k	w_v/w_o
0	0
3.121325	0.287162
4.23566	0.389681
4.633486	0.426281

(1-exp(-k*t))/k	w_s/w_o
0	0
3.121325	0.355831
4.23566	0.482865
4.633486	0.528217

f) 700ºC pyro-oil cracked at 800ºC

(1-exp(-k*t))/k	w_v/w_o
0	0
3.095535	0.29098
4.178779	0.392805
4.557847	0.428438

(1-exp(-k*t))/k	w_s/w_o
0	0
3.095535	0.359082
4.178779	0.484738
4.557847	0.52871

g) 700ºC pyro-oil cracked at 900ºC

(1-exp(-k*t))/k	w_v/w_o
0	0
3.070054	0.294725
4.123108	0.395818
4.484315	0.430494

(1-exp(-k*t))/k	w_s/w_o
0	0
3.070054	0.362266
4.123108	0.486527
4.484315	0.529149

iii) Jute waste pyro-oil in presence of alumina

a) 900ºC pyro-oil cracked at 300ºC

(1-exp(-k*t))/k	w_v/w_o
0	0
3.2141	0.292483
4.444755	0.404473
4.915965	0.447353

(1-exp(-k*t))/k	w_s/w_o
0	0
3.2141	0.324624
4.444755	0.44892
4.915965	0.496512

b) 900ºC pyro-oil cracked at 400ºC

(1-exp(-k*t))/k	w_v/w_o
0	0
3.193885	0.293837
4.398595	0.404671
4.853002	0.446476

(1-exp(-k*t))/k	w_s/w_o
0	0
3.193885	0.32897
4.398595	0.453055
4.853002	0.499859

c) 900ºC pyro-oil cracked at 500ºC

(1-exp(-k*t))/k	w_v/w_o
0	0

(1-exp(-k*t))/k	w_s/w_o
0	0

3.173855	0.298342
4.353186	0.409199
4.791397	0.450391

3.173855	0.330081
4.353186	0.452731
4.791397	0.498305

d) 900°C pyro-oil cracked at 600°C

(1-exp(-k*t))/k	w_v/w_o
0	0
3.154007	0.302785
4.308514	0.413617
4.731115	0.454187

(1-exp(-k*t))/k	w_s/w_o
0	0
3.154007	0.331171
4.308514	0.452394
4.731115	0.496767

e) 900°C pyro-oil cracked at 700°C

(1-exp(-k*t))/k	w_v/w_o
0	0
3.127822	0.306527
4.250074	0.416507
4.652734	0.455968

(1-exp(-k*t))/k	w_s/w_o
0	0
3.127822	0.334677
4.250074	0.454758
4.652734	0.497842

f) 900°C pyro-oil cracked at 800°C

(1-exp(-k*t))/k	w_v/w_o
0	0
3.101953	0.313297
4.192885	0.423481
4.576556	0.462232

(1-exp(-k*t))/k	w_s/w_o
0	0
3.101953	0.335011
4.192885	0.452832
4.576556	0.494268

g) 900°C pyro-oil cracked at 900°C

(1-exp(-k*t))/k	w_v/w_o
0	0
3.070054	0.319286
4.123108	0.428803
4.484315	0.466369

(1-exp(-k*t))/k	w_s/w_o
0	0
3.070054	0.337706
4.123108	0.453542
4.484315	0.493275

A.64.

i) lime waste pyro-oil

a) 500°C pyro-oil cracked at 300°C

(1-exp(-k*t))/k	w_v/w_o
0	0
3.303868	0.49558
4.653854	0.698078
5.205468	0.78082

(1-exp(-k*t))/k	w_s/w_o
0	0
3.303868	0.095812
4.653854	0.134962
5.205468	0.150959

b) 500°C pyro-oil cracked at 400°C

(1-exp(-k*t))/k	w_v/w_o
0	0
3.282834	0.495708

(1-exp(-k*t))/k	w_s/w_o
0	0
3.282834	0.101768
4.604254	0.142732

4.604254	0.695242
5.136158	0.77556

5.136158	0.159221

c) 500°C pyro-oil cracked at 500°C

(1-exp(-k*t))/k	w_v/w_o
0	0
3.255088	0.498028
4.539394	0.694527
5.046123	0.772057

(1-exp(-k*t))/k	w_s/w_o
0	0
3.255088	0.107418
4.539394	0.1498
5.046123	0.166522

d) 500°C pyro-oil cracked at 600°C

(1-exp(-k*t))/k	w_v/w_o
0	0
3.227679	0.50029
4.475955	0.693773
4.958714	0.768601

(1-exp(-k*t))/k	w_s/w_o
0	0
3.227679	0.112969
4.475955	0.156658
4.958714	0.173555

e) 500°C pyro-oil cracked at 700°C

(1-exp(-k*t))/k	w_v/w_o
0	0
3.200603	0.502495
4.413897	0.692982
4.873836	0.765192

(1-exp(-k*t))/k	w_s/w_o
0	0
3.200603	0.118422
4.413897	0.163314
4.873836	0.180332

f) 500°C pyro-oil cracked at 800°C

(1-exp(-k*t))/k	w_v/w_o
0	0
3.154007	0.510949
4.308514	0.697979
4.731115	0.766441

(1-exp(-k*t))/k	w_s/w_o
0	0
3.154007	0.123006
4.308514	0.168032
4.731115	0.184513

g) 500°C pyro-oil cracked at 900°C

(1-exp(-k*t))/k	w_v/w_o
0	0
3.127822	0.512963
4.250074	0.697012
4.652734	0.763048

(1-exp(-k*t))/k	w_s/w_o
0	0
3.127822	0.128241
4.250074	0.174253
4.652734	0.190762

ii) Lime waste pyro-oil

a) 700°C pyro-oil cracked at 300°C

(1-exp(-k*t))/k	w_v/w_o
0	0
3.261992	0.08155

(1-exp(-k*t))/k	w_s/w_o
0	0
3.261992	0.521919

4.555475	0.113887
5.068381	0.12671

4.555475	0.728876
5.068381	0.810941

b) 700ºC pyro-oil cracked at 400ºC

(1-exp(-k*t))/k	w_v/w_o
0	0
3.227679	0.087147
4.475955	0.120851
4.958714	0.133885

(1-exp(-k*t))/k	w_s/w_o
0	0
3.227679	0.526112
4.475955	0.729581
4.958714	0.80827

c) 700ºC pyro-oil cracked at 500ºC

(1-exp(-k*t))/k	w_v/w_o
0	0
3.193885	0.089429
4.398595	0.123161
4.853002	0.135884

(1-exp(-k*t))/k	w_s/w_o
0	0
3.193885	0.533379
4.398595	0.734565
4.853002	0.810451

d) 700ºC pyro-oil cracked at 600ºC

(1-exp(-k*t))/k	w_v/w_o
0	0
3.147431	0.100718
4.293785	0.137401
4.711309	0.150762

(1-exp(-k*t))/k	w_s/w_o
0	0
3.147431	0.535063
4.293785	0.729943
4.711309	0.800922

e) 700ºC pyro-oil cracked at 700ºC

(1-exp(-k*t))/k	w_v/w_o
0	0
3.121325	0.106125
4.23566	0.144012
4.633486	0.157539

(1-exp(-k*t))/k	w_s/w_o
0	0
3.121325	0.536868
4.23566	0.728534
4.633486	0.79696

f) 700ºC pyro-oil cracked at 800ºC

(1-exp(-k*t))/k	w_v/w_o
0	0
3.101953	0.11167
4.192885	0.150944
4.576556	0.164756

(1-exp(-k*t))/k	w_s/w_o
0	0
3.101953	0.536638
4.192885	0.725369
4.576556	0.791744

g) 700ºC pyro-oil cracked at 900ºC

(1-exp(-k*t))/k	w_v/w_o
0	0
3.082756	0.114062
4.150794	0.153579
4.520822	0.16727

(1-exp(-k*t))/k	w_s/w_o
0	0
3.082756	0.539482
4.150794	0.726389
4.520822	0.791144

iii) Lime waste pyro-oil

a) 900ºC pyro-oil cracked at 300ºC

(1-exp(-k*t))/k	w_v/w_o
0	0
3.275865	0.088448
4.587904	0.123873
5.113397	0.138062

(1-exp(-k*t))/k	w_s/w_o
0	0
3.275865	0.511035
4.587904	0.715713
5.113397	0.79769

b) 900ºC pyro-oil cracked at 400ºC

(1-exp(-k*t))/k	w_v/w_o
0	0
3.248204	0.094198
4.523403	0.131179
5.024028	0.145697

(1-exp(-k*t))/k	w_s/w_o
0	0
3.248204	0.513216
4.523403	0.714698
5.024028	0.793796

c) 900ºC pyro-oil cracked at 500ºC

(1-exp(-k*t))/k	w_v/w_o
0	0
3.193885	0.102204
4.398595	0.140755
4.853002	0.155296

(1-exp(-k*t))/k	w_s/w_o
0	0
3.193885	0.520603
4.398595	0.716971
4.853002	0.791039

d) 900ºC pyro-oil cracked at 600ºC

(1-exp(-k*t))/k	w_v/w_o
0	0
3.160603	0.110621
4.323324	0.151316
4.751065	0.166287

(1-exp(-k*t))/k	w_s/w_o
0	0
3.160603	0.521499
4.323324	0.713348
4.751065	0.783926

e) 900ºC pyro-oil cracked at 700ºC

(1-exp(-k*t))/k	w_v/w_o
0	0
3.134339	0.115971
4.264565	0.157789
4.672119	0.172868

(1-exp(-k*t))/k	w_s/w_o
0	0
3.134339	0.523435
4.264565	0.712182
4.672119	0.780244

f) 900ºC pyro-oil cracked at 800ºC

(1-exp(-k*t))/k	w_v/w_o
0	0
3.108391	0.118119
4.207066	0.159869
4.595398	0.174625

(1-exp(-k*t))/k	w_s/w_o
0	0
3.108391	0.528426
4.207066	0.715201
4.595398	0.781218

g) 900ºC pyro-oil cracked at 900ºC

(1-exp(-k*t))/k	w_v/w_o
0	0

(1-exp(-k*t))/k	w_s/w_o
0	0

3.070054	0.128942
4.123108	0.173171
4.484315	0.188341

3.070054	0.528049
4.123108	0.709175
4.484315	0.771302

A.65.

i) lime waste pyro-oil in presence of ZnO

a) 500ºC pyro-oil cracked at 300ºC

(1-exp(-k*t))/k	w_v/w_o
0	0
3.339359	0.494225
4.738389	0.701281
5.324514	0.788028

(1-exp(-k*t))/k	w_s/w_o
0	0
3.339359	0.086823
4.738389	0.123198
5.324514	0.138437

b) 500ºC pyro-oil cracked at 400ºC

(1-exp(-k*t))/k	w_v/w_o
0	0
3.317999	0.494382
4.687384	0.69842
5.252549	0.78263

(1-exp(-k*t))/k	w_s/w_o
0	0
3.317999	0.092904
4.687384	0.131247
5.252549	0.147071

c) 500ºC pyro-oil cracked at 500ºC

(1-exp(-k*t))/k	w_v/w_o
0	0
3.289824	0.496763
4.620695	0.697725
5.159089	0.779022

(1-exp(-k*t))/k	w_s/w_o
0	0
3.289824	0.098695
4.620695	0.138621
5.159089	0.154773

d) 500ºC pyro-oil cracked at 600ºC

(1-exp(-k*t))/k	w_v/w_o
0	0
3.261992	0.499085
4.555475	0.696988
5.068381	0.775462

(1-exp(-k*t))/k	w_s/w_o
0	0
3.261992	0.104384
4.555475	0.145775
5.068381	0.162188

e) 500ºC pyro-oil cracked at 700ºC

(1-exp(-k*t))/k	w_v/w_o
0	0
3.2345	0.501347
4.491684	0.696211
4.980325	0.77195

(1-exp(-k*t))/k	w_s/w_o
0	0
3.2345	0.109973
4.491684	0.152717
4.980325	0.169331

f) 500ºC pyro-oil cracked at 800ºC

(1-exp(-k*t))/k	w_v/w_o
0	0
3.187188	0.50995
4.383375	0.70134
4.832318	0.773171

(1-exp(-k*t))/k	w_s/w_o
0	0
3.187188	0.114739
4.383375	0.157802
4.832318	0.173963

g) 500ºC pyro-oil cracked at 900ºC

(1-exp(-k*t))/k	w_v/w_o
0	0
3.160603	0.512018
4.323324	0.700378
4.751065	0.769672

(1-exp(-k*t))/k	w_s/w_o
0	0
3.160603	0.120103
4.323324	0.164286
4.751065	0.18054

ii) Lime waste pyro-oil in presence of ZnO

a) 700°C pyro-oil cracked at 300°C

(1-exp(-k*t))/k	w_v/w_o
0	0
3.303868	0.072685
4.653854	0.102385
5.205468	0.11452

(1-exp(-k*t))/k	w_s/w_o
0	0
3.303868	0.518707
4.653854	0.730655
5.205468	0.817259

b) 700°C pyro-oil cracked at 400°C

(1-exp(-k*t))/k	w_v/w_o
0	0
3.268918	0.078454
4.571644	0.109719
5.090806	0.122179

(1-exp(-k*t))/k	w_s/w_o
0	0
3.268918	0.523027
4.571644	0.731463
5.090806	0.814529

c) 700°C pyro-oil cracked at 500°C

(1-exp(-k*t))/k	w_v/w_o
0	0
3.2345	0.080862
4.491684	0.112292
4.980325	0.124508

(1-exp(-k*t))/k	w_s/w_o
0	0
3.2345	0.530458
4.491684	0.736636
4.980325	0.816773

d) 700°C pyro-oil cracked at 600°C

(1-exp(-k*t))/k	w_v/w_o
0	0
3.187188	0.092428
4.383375	0.127118
4.832318	0.140137

(1-exp(-k*t))/k	w_s/w_o
0	0
3.187188	0.53226
4.383375	0.732024
4.832318	0.806997

e) 700°C pyro-oil cracked at 700°C

(1-exp(-k*t))/k	w_v/w_o
0	0
3.160603	0.097979
4.323324	0.134023
4.751065	0.147283

(1-exp(-k*t))/k	w_s/w_o
0	0
3.160603	0.534142
4.323324	0.730642
4.751065	0.80293

f) 700°C pyro-oil cracked at 800°C

(1-exp(-k*t))/k	w_v/w_o
0	0

(1-exp(-k*t))/k	w_s/w_o
0	0

3.140875	0.103649
4.279135	0.141211
4.691644	0.154824

3.140875	0.533949
4.279135	0.727453
4.691644	0.797579

g) 700ºC pyro-oil cracked at 900ºC

(1-exp(-k*t))/k	w_v/w_o
0	0
3.121325	0.106125
4.23566	0.144012
4.633486	0.157539

(1-exp(-k*t))/k	w_s/w_o
0	0
3.121325	0.536868
4.23566	0.728534
4.633486	0.79696

iii) Lime waste pyro-oil in presence of ZnO

a) 900ºC pyro-oil cracked at 300ºC

(1-exp(-k*t))/k	w_v/w_o
0	0
3.317999	0.079632
4.687384	0.112497
5.252549	0.126061

(1-exp(-k*t))/k	w_s/w_o
0	0
3.317999	0.507654
4.687384	0.71717
5.252549	0.80364

b) 900ºC pyro-oil cracked at 400ºC

(1-exp(-k*t))/k	w_v/w_o
0	0
3.289824	0.085535
4.620695	0.120138
5.159089	0.134136

(1-exp(-k*t))/k	w_s/w_o
0	0
3.289824	0.509923
4.620695	0.716208
5.159089	0.799659

c) 900ºC pyro-oil cracked at 500ºC

(1-exp(-k*t))/k	w_v/w_o
0	0
3.2345	0.0938
4.491684	0.130259
4.980325	0.144429

(1-exp(-k*t))/k	w_s/w_o
0	0
3.2345	0.51752
4.491684	0.718669
4.980325	0.796852

d) 900ºC pyro-oil cracked at 600ºC

(1-exp(-k*t))/k	w_v/w_o
0	0
3.200603	0.102419
4.413897	0.141245
4.873836	0.155963

(1-exp(-k*t))/k	w_s/w_o
0	0
3.200603	0.518498
4.413897	0.715051
4.873836	0.789562

e) 900ºC pyro-oil cracked at 700ºC

(1-exp(-k*t))/k	w_v/w_o
0	0
3.173855	0.107911
4.353186	0.148008
4.791397	0.162908

(1-exp(-k*t))/k	w_s/w_o
0	0
3.173855	0.520512
4.353186	0.713922
4.791397	0.785789

f) 900ºC pyro-oil cracked at 800ºC

(1-exp(-k*t))/k	w_v/w_o

(1-exp(-k*t))/k	w_s/w_o

0	0
3.147431	0.11016
4.293785	0.150282
4.711309	0.164896

0	0
3.147431	0.525621
4.293785	0.717062
4.711309	0.786789

g) 900°C pyro-oil cracked at 900°C

(1-exp(-k*t))/k	w_v/w_o
0	0
3.108391	0.121227
4.207066	0.164076
4.595398	0.179221

(1-exp(-k*t))/k	w_s/w_o
0	0
3.108391	0.525318
4.207066	0.710994
4.595398	0.776622

A.66

a) pyro-oil of 500°C of jute waste

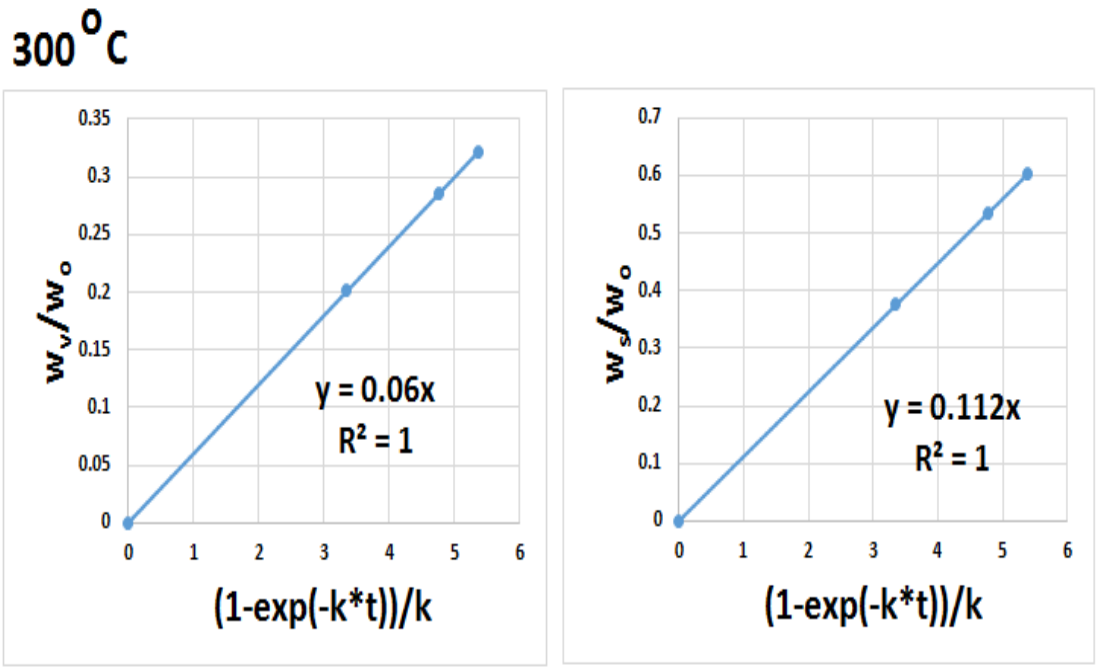

400 °C

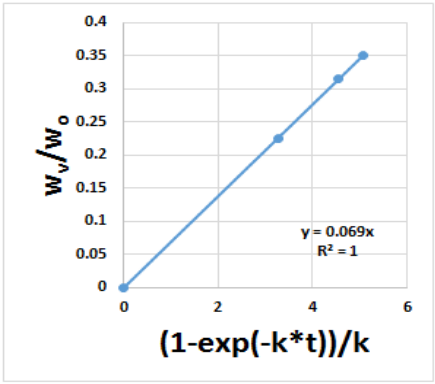

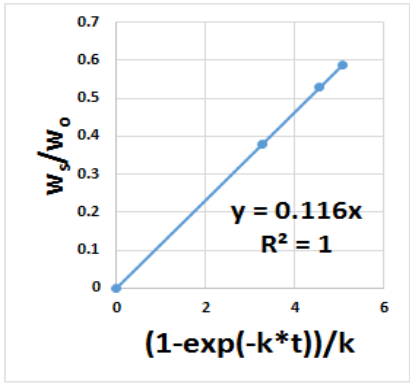

500 °C

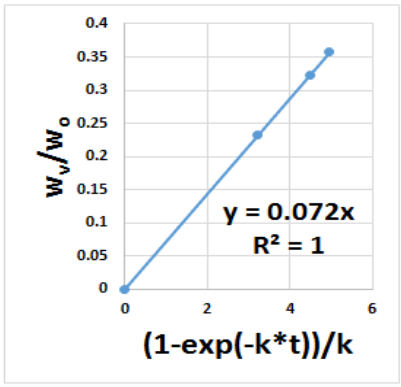

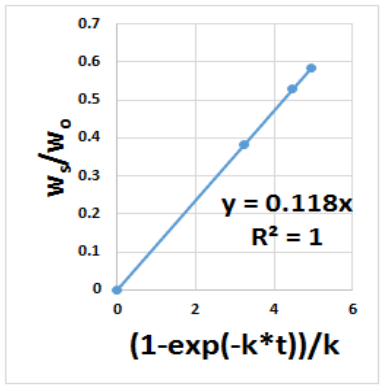

600 °C

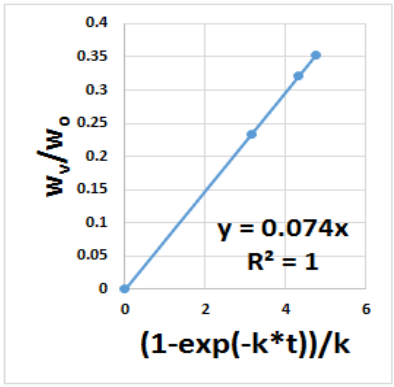

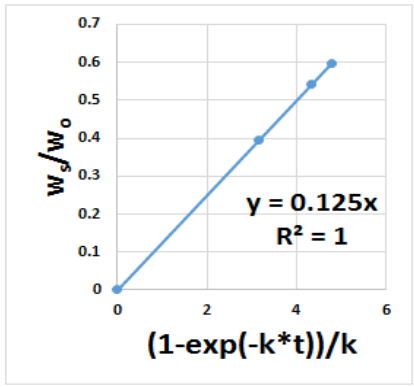

700 °C

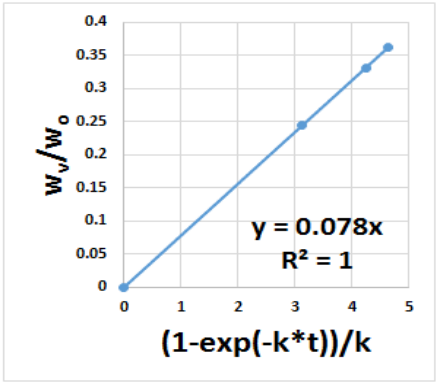

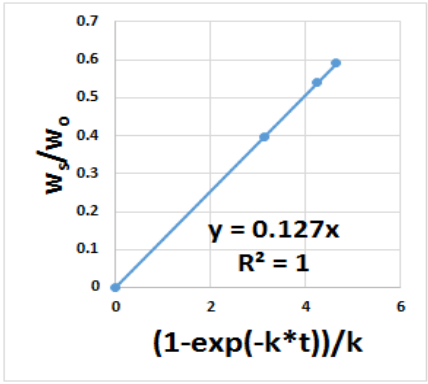

800 °C

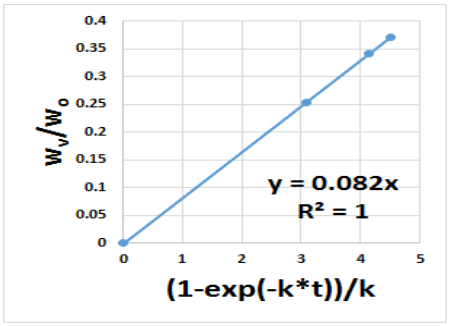

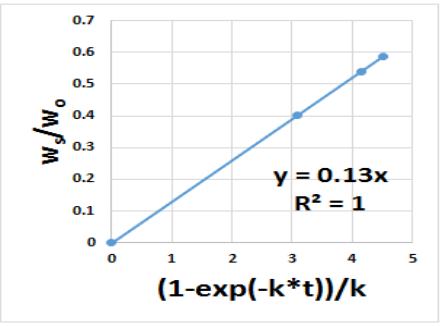

900 °C

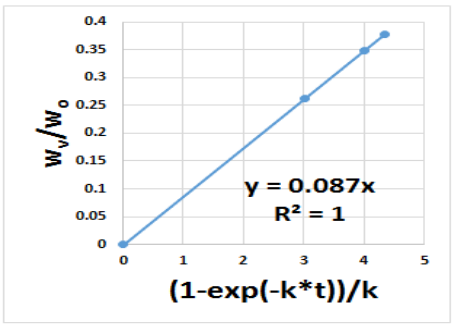

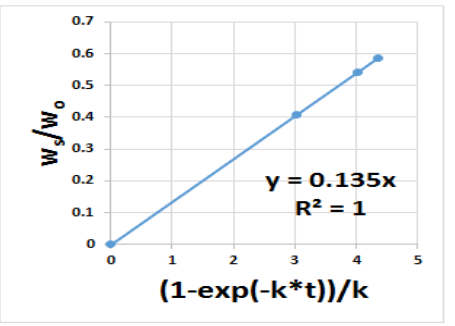

b) pyro-oil of 700ºC of jute waste

300 °C

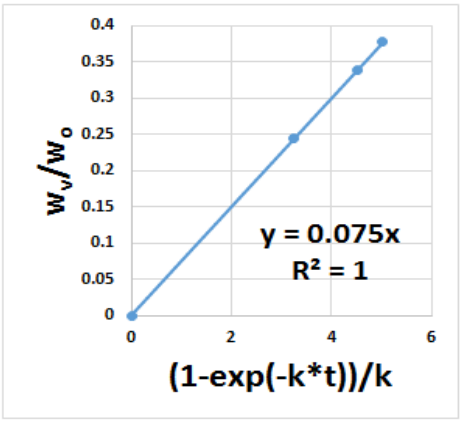

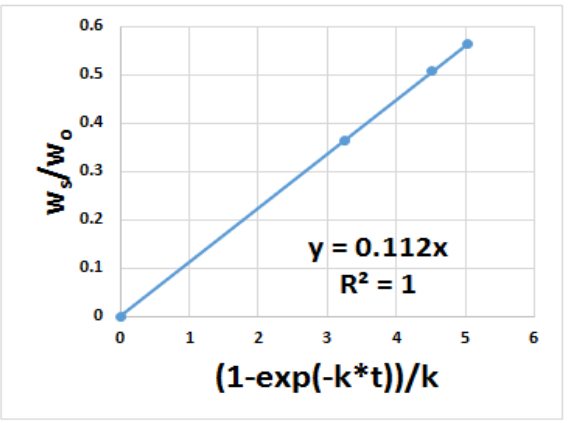

400 °C

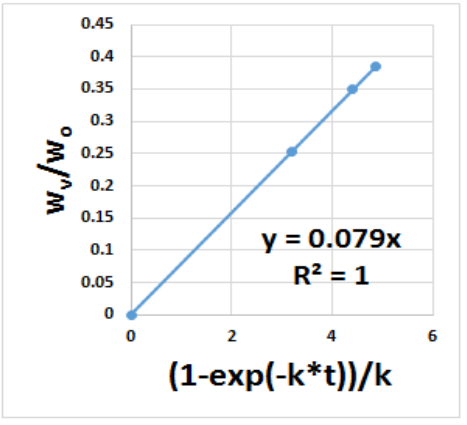

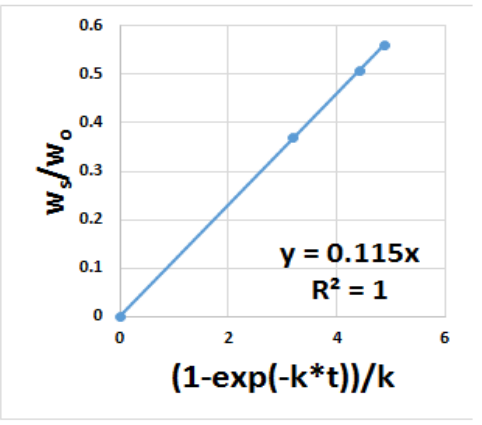

500 °C

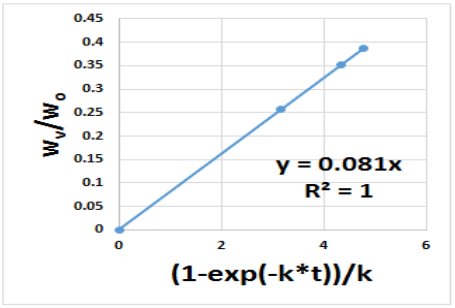

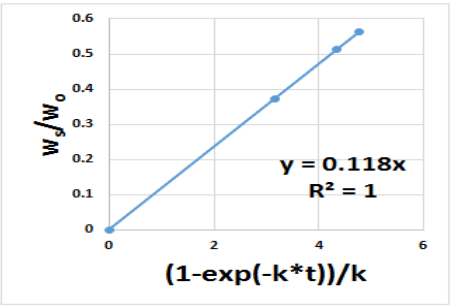

600 °C

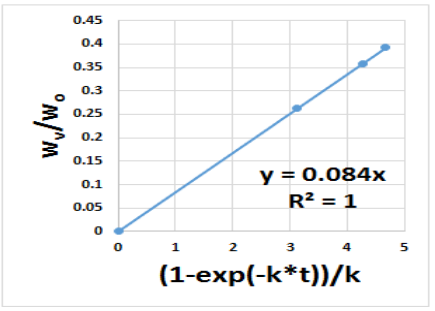

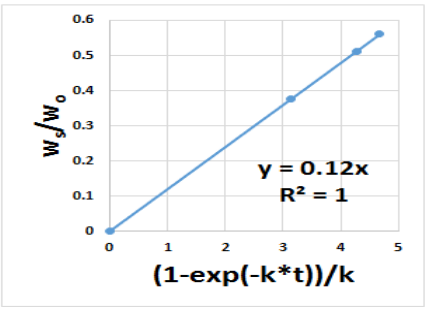

700 °C

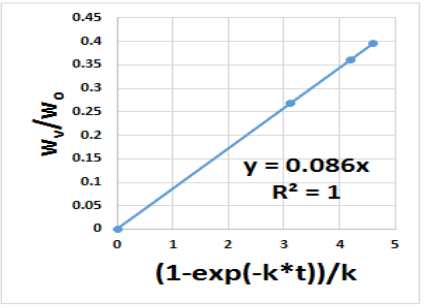

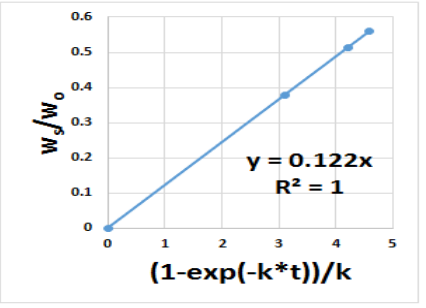

800 °C

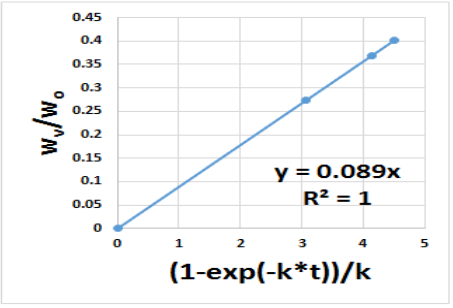

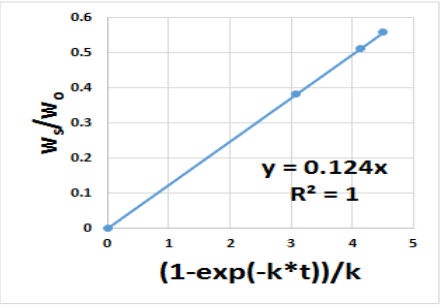

900 °C

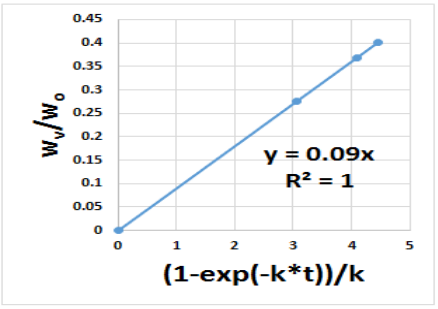

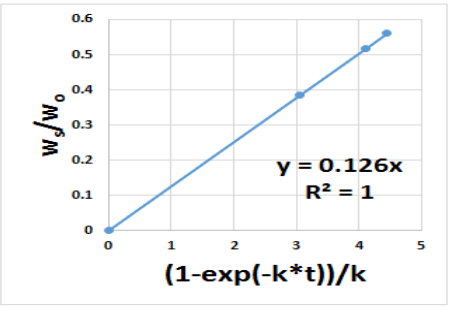

c) pyro-oil of 900°C of jute waste

300 °C

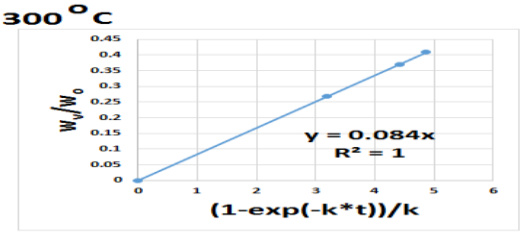

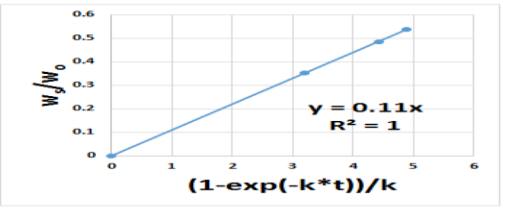

400 °C

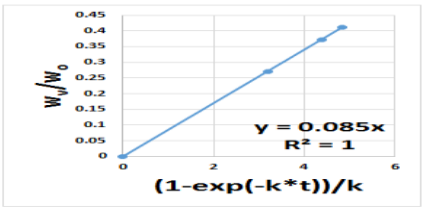

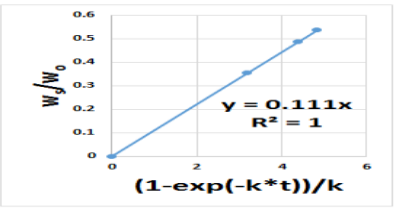

500 °C

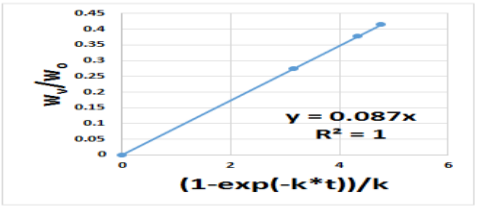

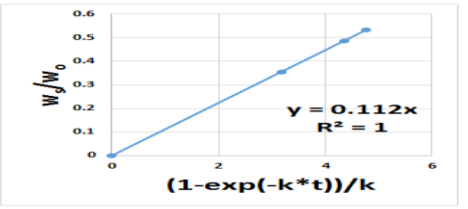

600 °C

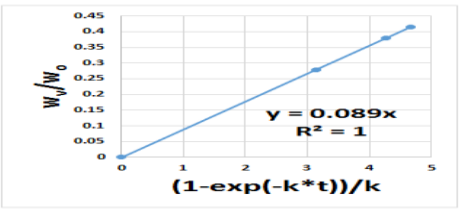

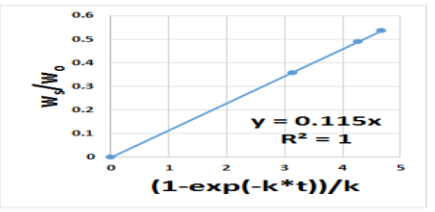

700 °C

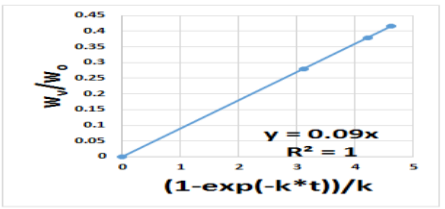

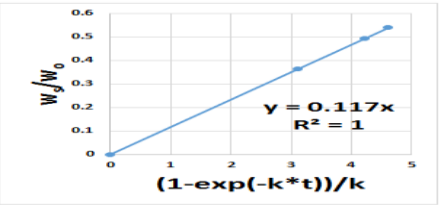

800 °C

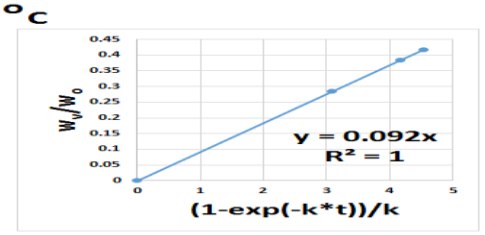

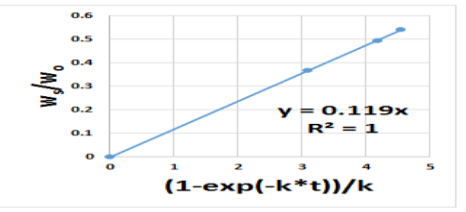

900 °C

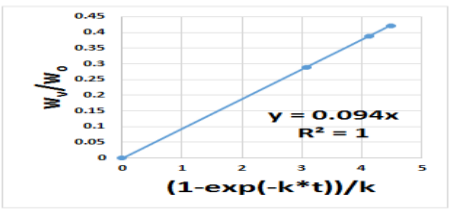

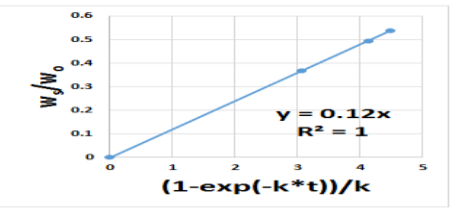

d) Pyro-oil of 500°C of jute waste in presence of alumina

300 °C

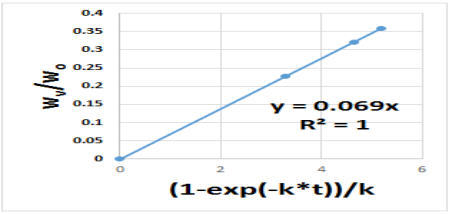

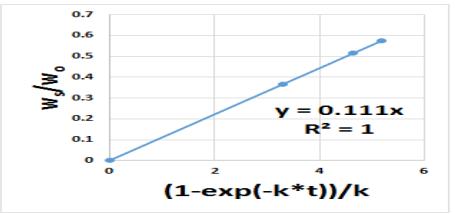

400 °C

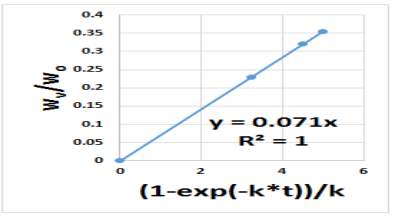

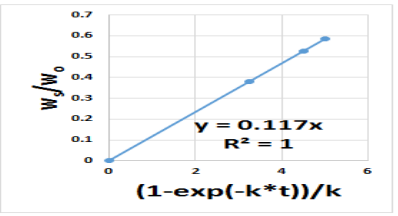

500 °C

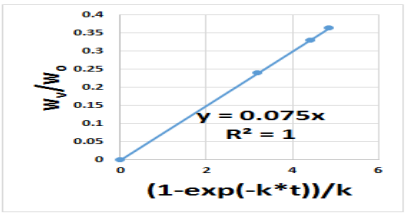

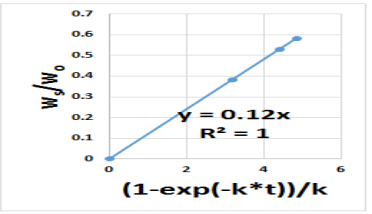

600 °C

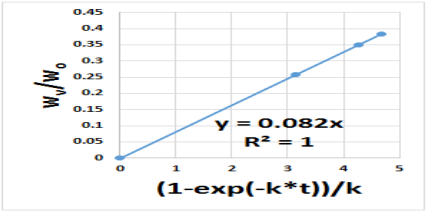

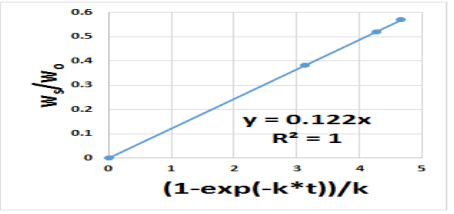

700 °C

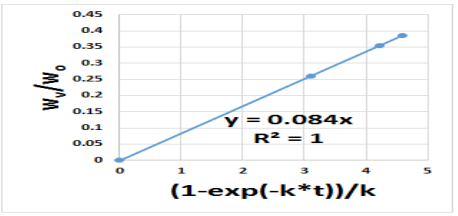

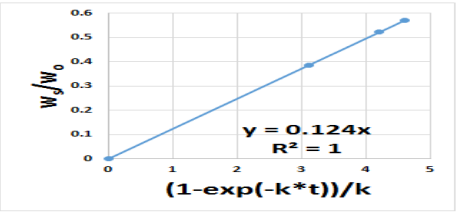

800 °C

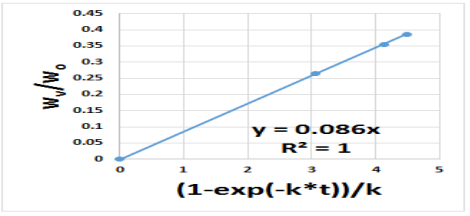

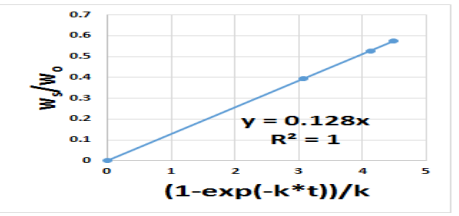

900 °C

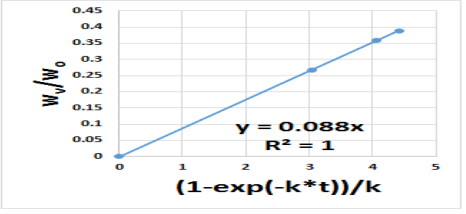

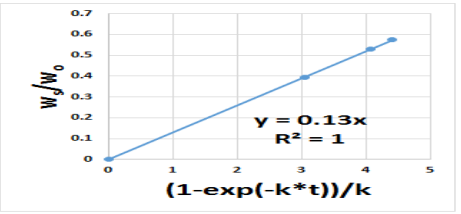

e) Pyro-oil of 700°C of jute waste in presence of alumina

300 °C

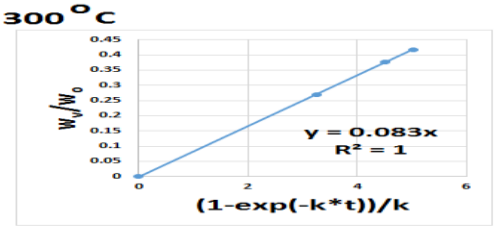

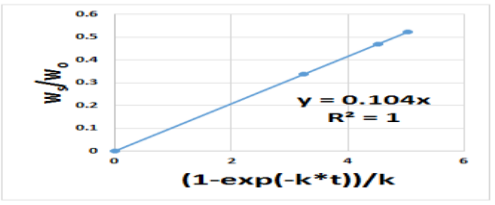

400 °C

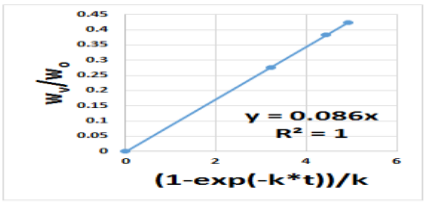

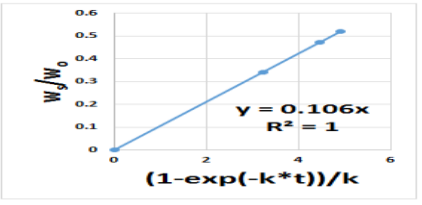

500 °C

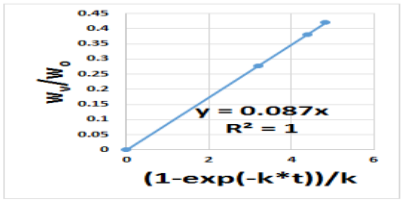

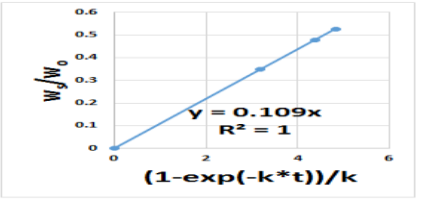

600 °C

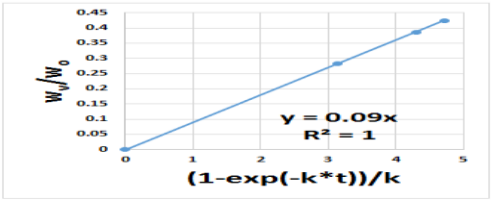

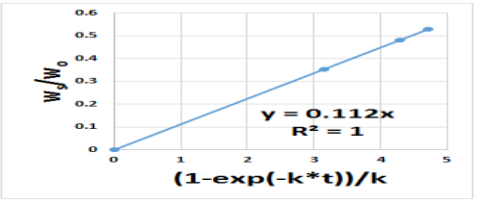

700 °C

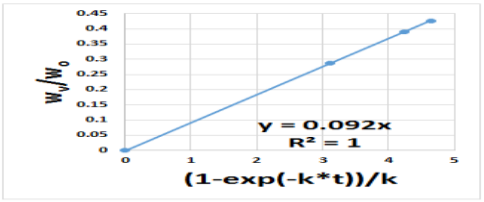

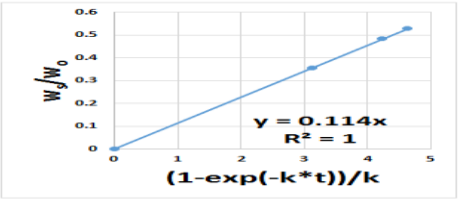

800 °C

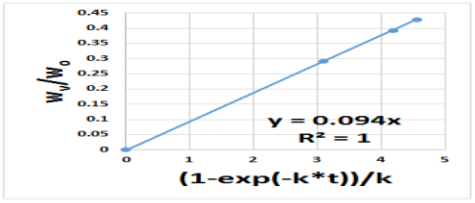

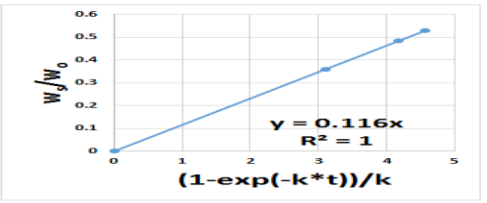

900 °C

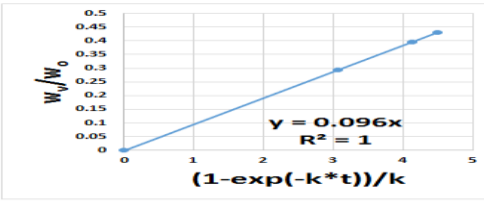

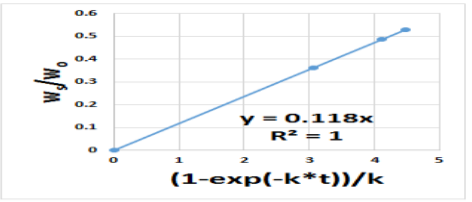

f) Pyro-oil of 700°C of jute waste in presence of alumina

300 °C

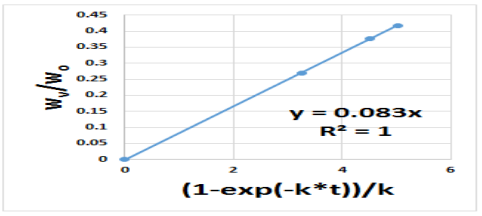

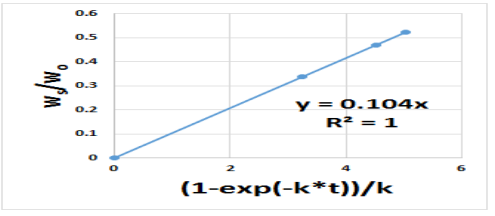

400 °C

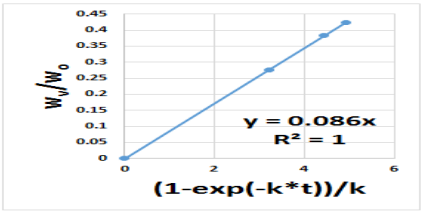

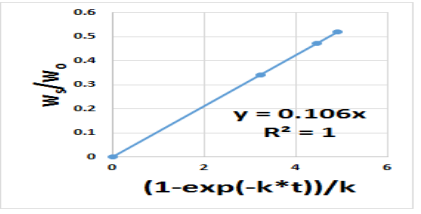

500 °C

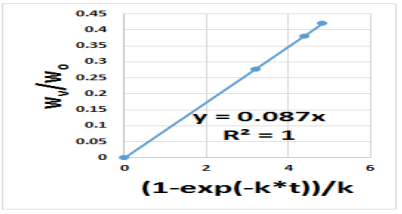

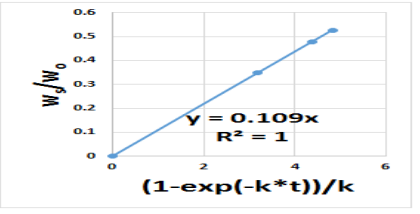

600 °C

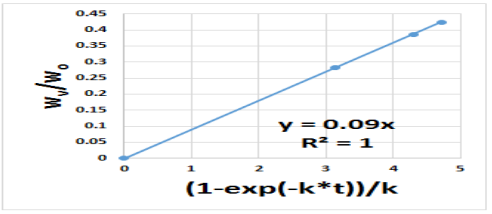

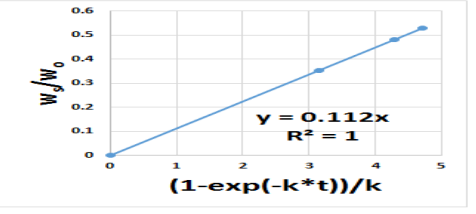

700 °C

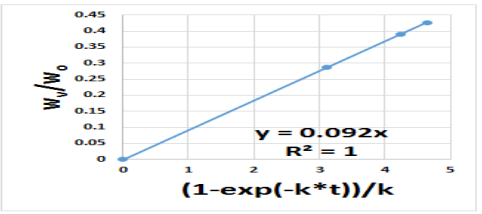

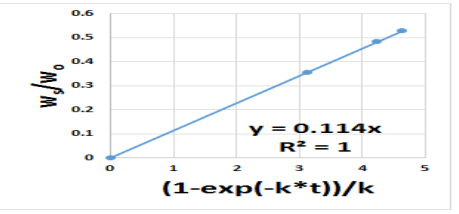

800 °C

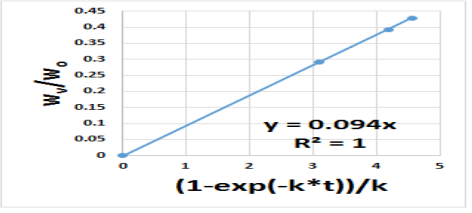

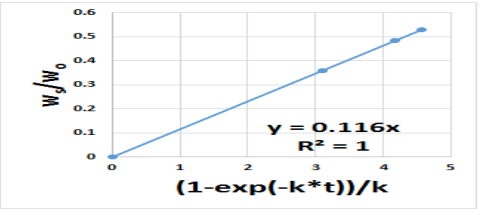

900 °C

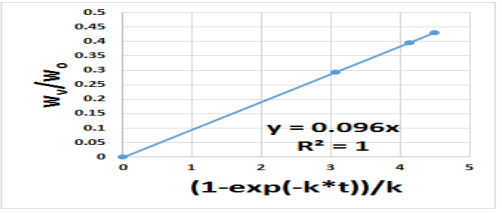

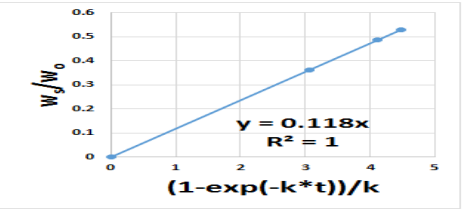

g) Pyro-oil of 900°C of jute waste in presence of alumina

300 °C

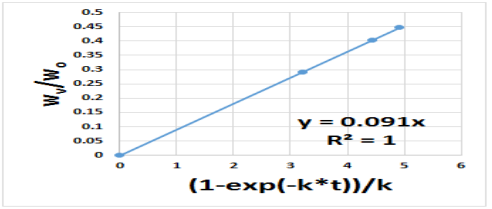

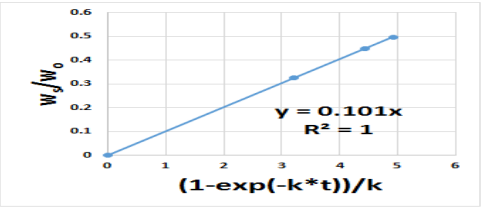

400 °C

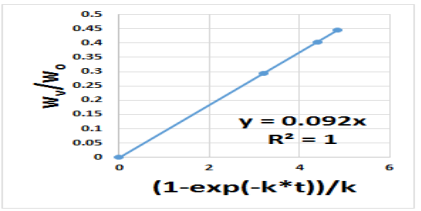

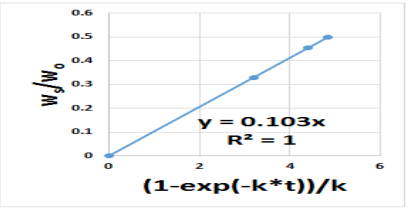

500 °C

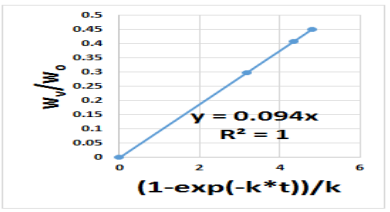

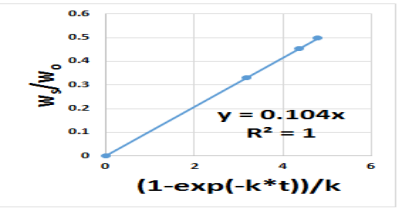

600 °C

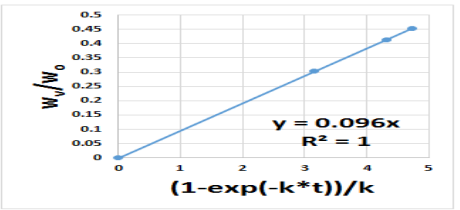

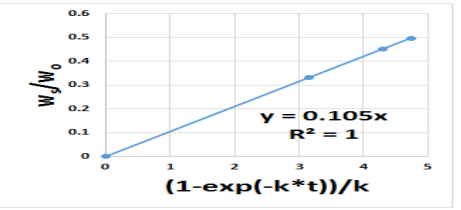

700 °C

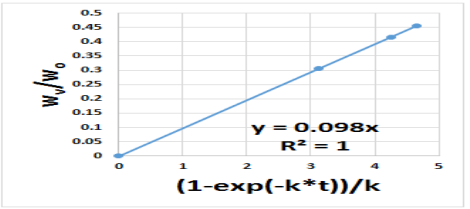

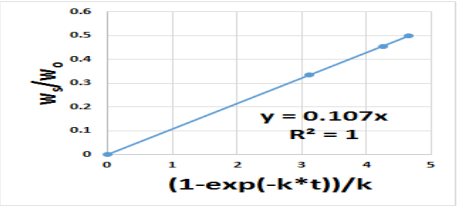

800 °C

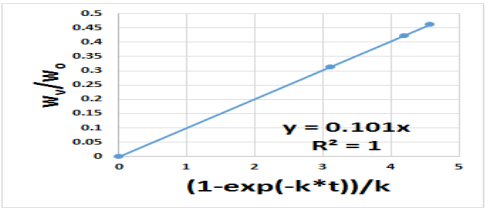

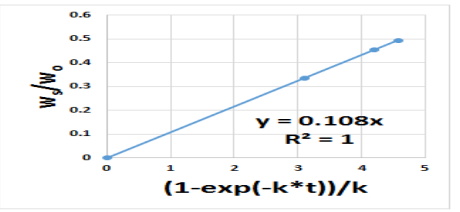

900 °C

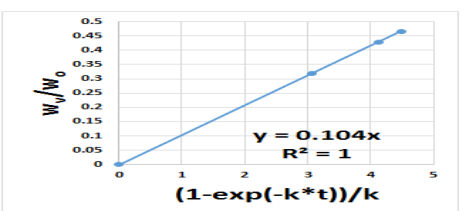

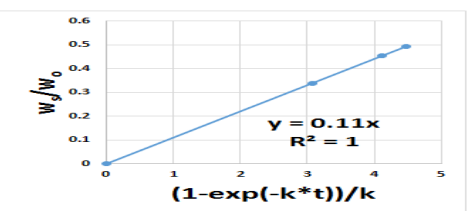

h) **pyro-oil of 500°C of lime waste**

300 °C

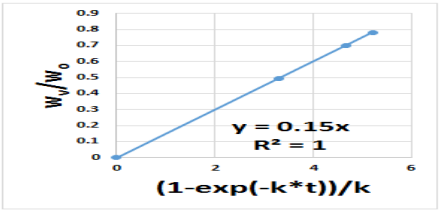

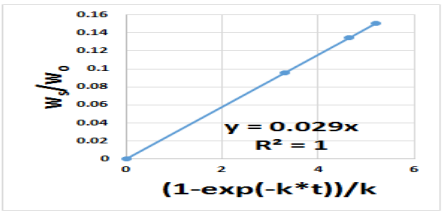

400 °C

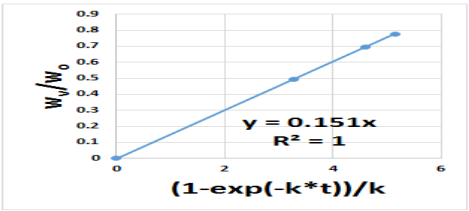

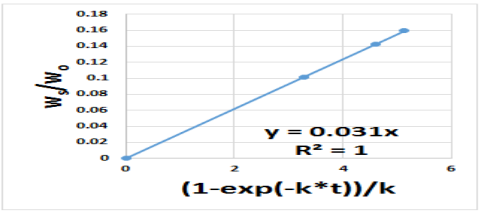

500 °C

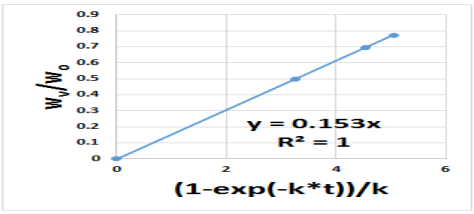

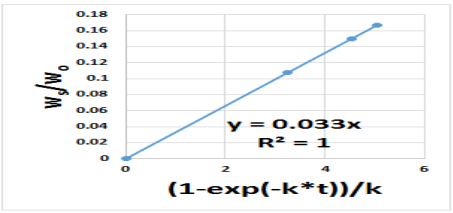

600 °C

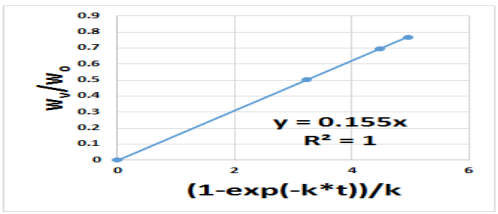

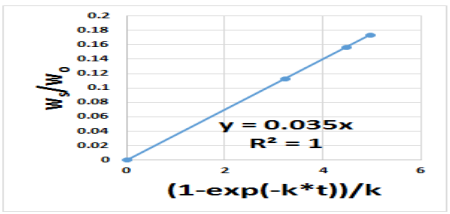

700 °C

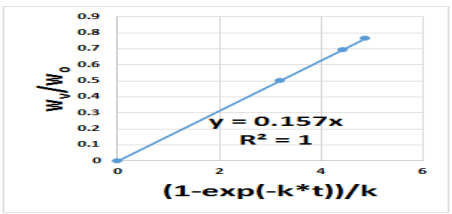

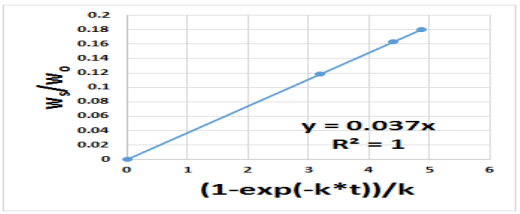

800 °C

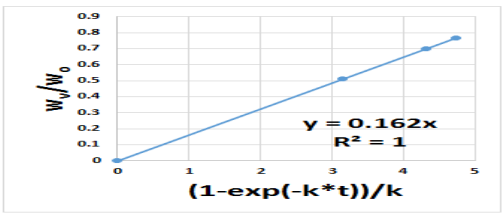

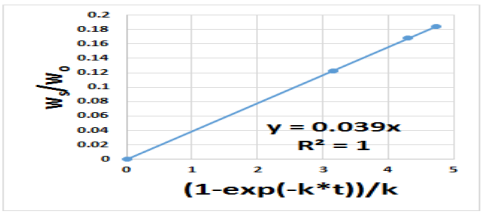

900 °C

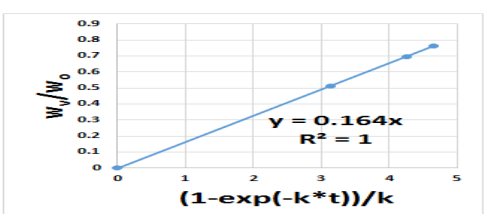

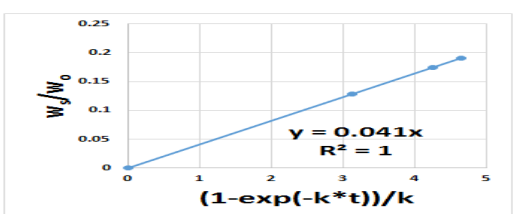

i) **pyro-oil of 700°C of lime waste**

300 °C

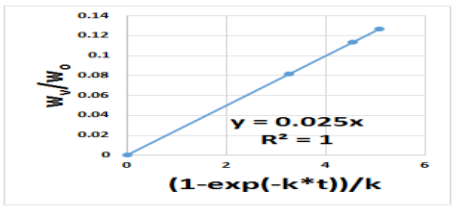

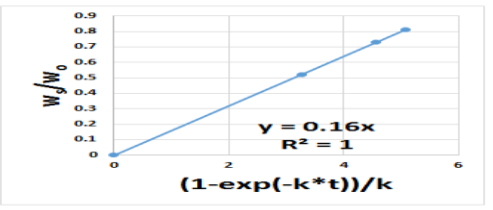

400 °C

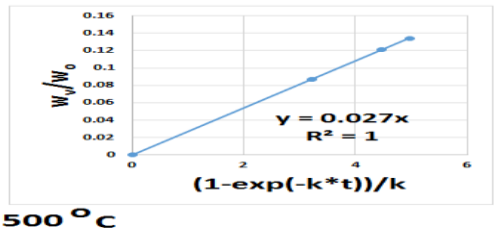

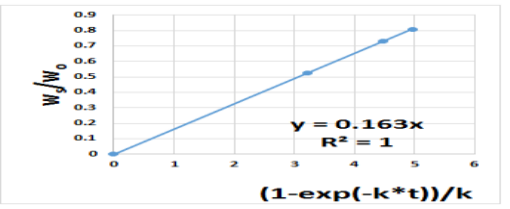

500 °C

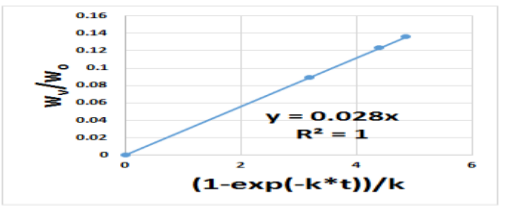

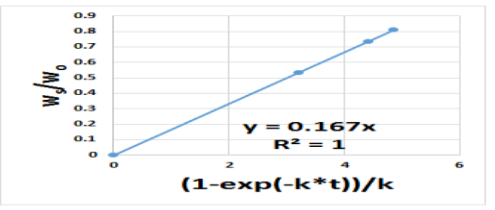

600 °C

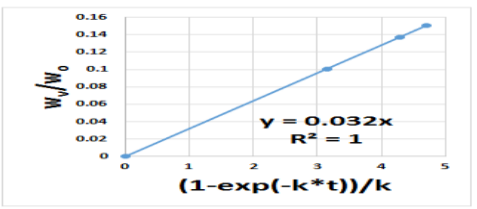

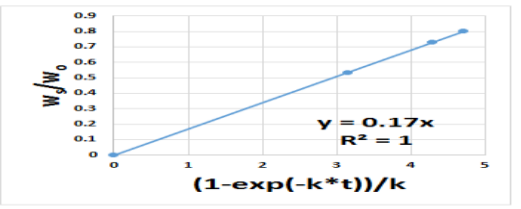

700 °C

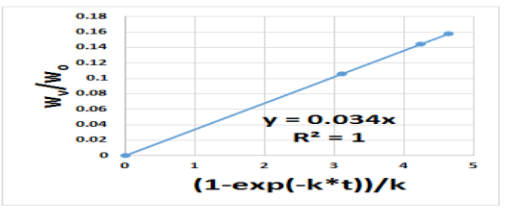

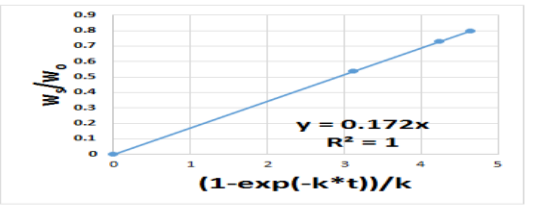

800 °C

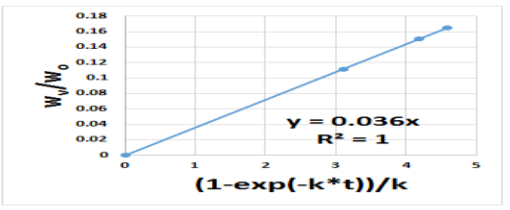

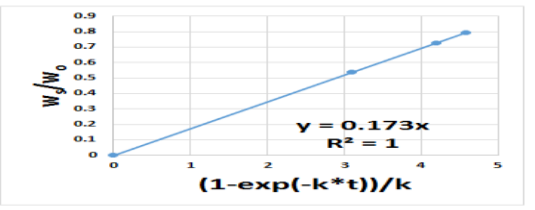

900 °C

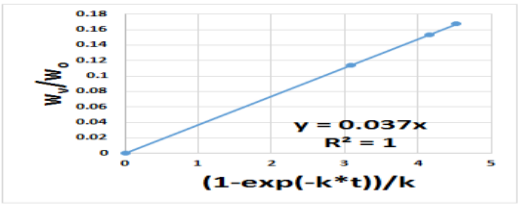

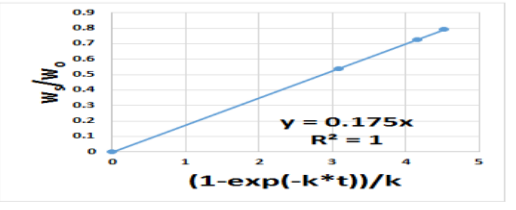

j) **pyro-oil of 900°C of lime waste**

300 °C

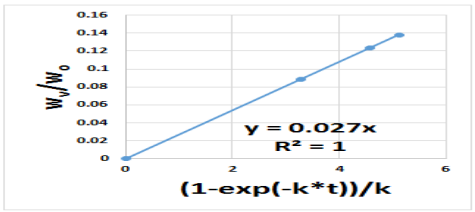

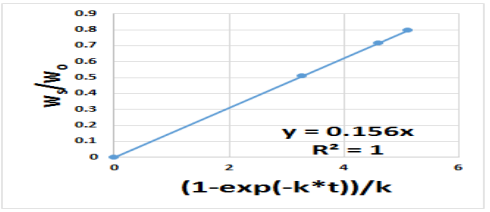

400 °C

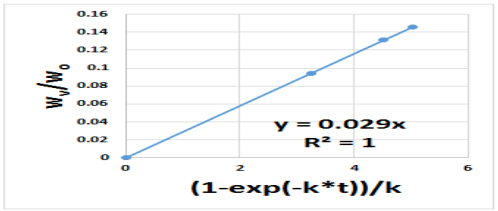

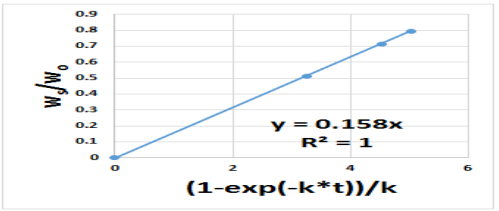

500 °C

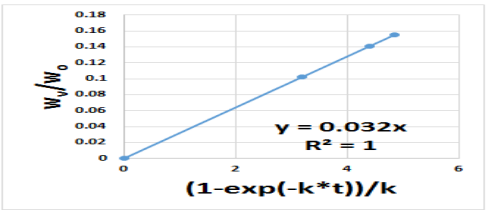

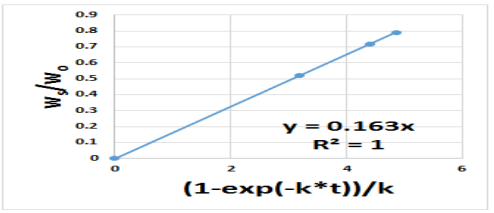

600 °C

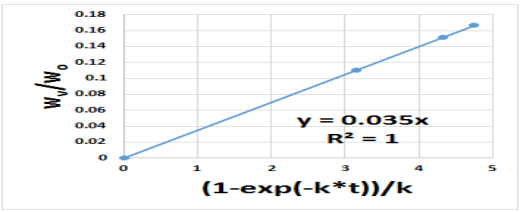

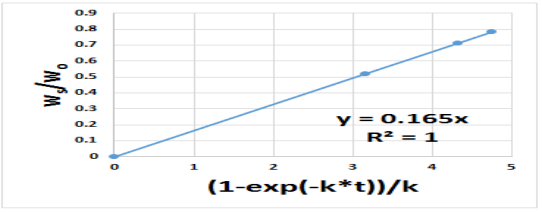

700 °C

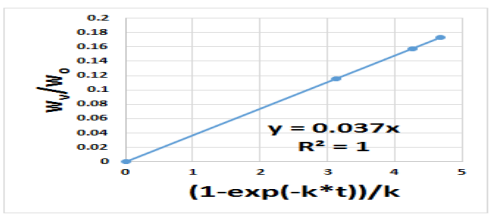

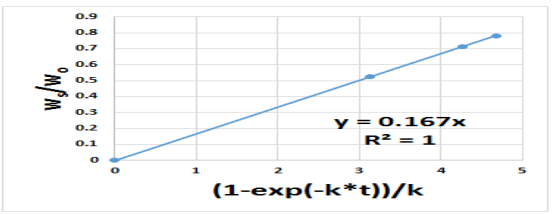

800 °C

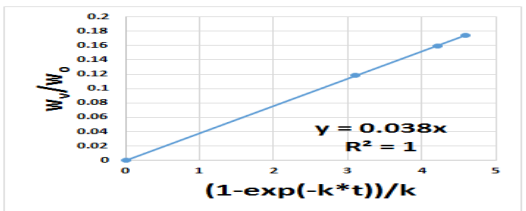

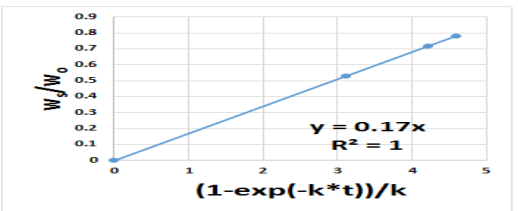

900 °C

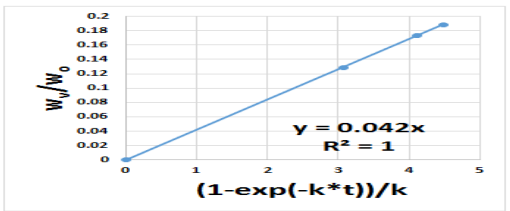

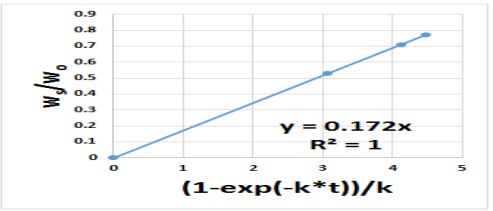

k) pyro-oil of 500ºC of lime waste in presence of ZnO

300 °C

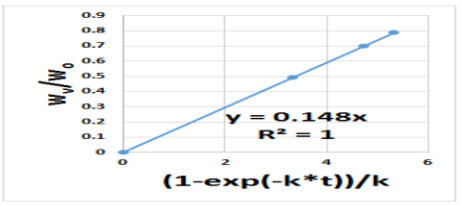

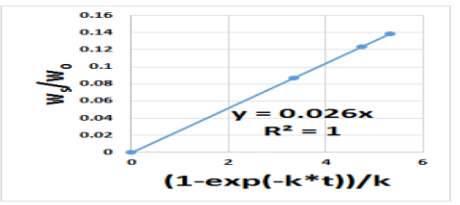

400 °C

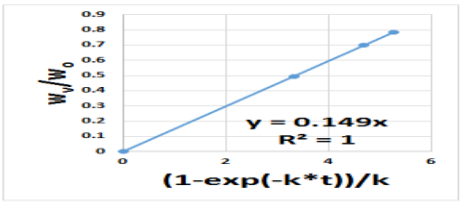

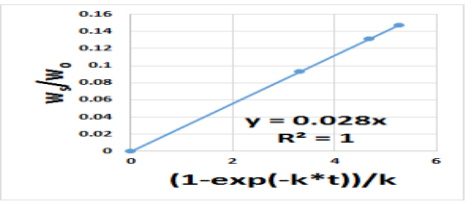

500 °C

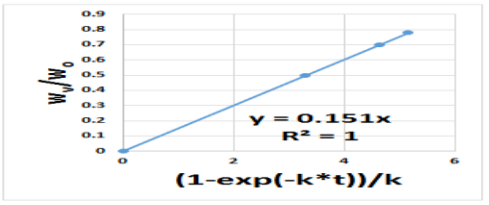

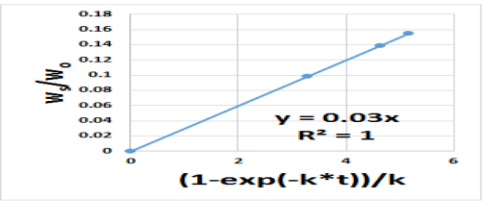

600 °C

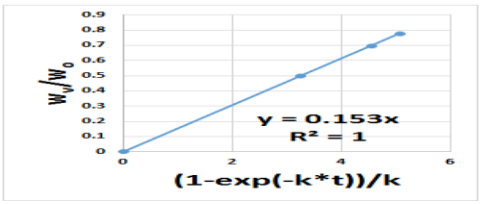

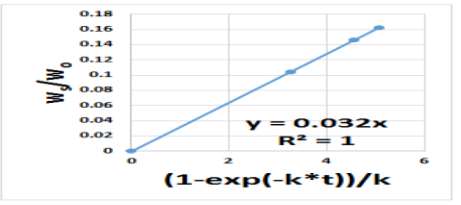

700 °C

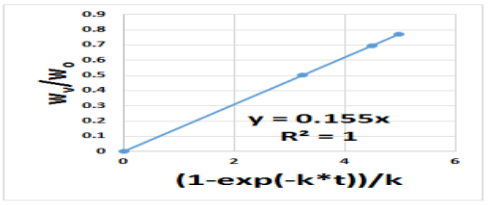

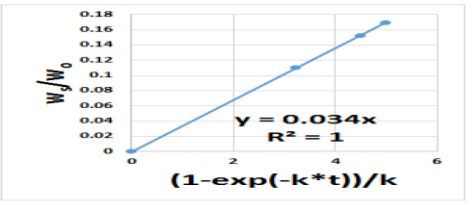

800 °C

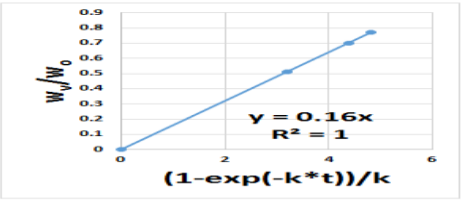

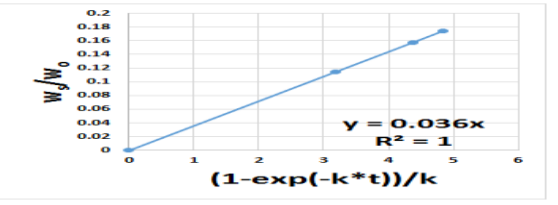

900 °C

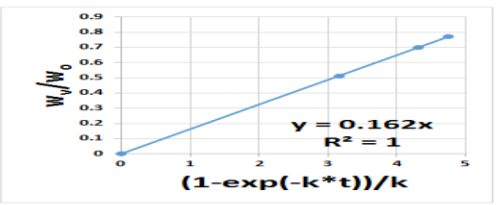

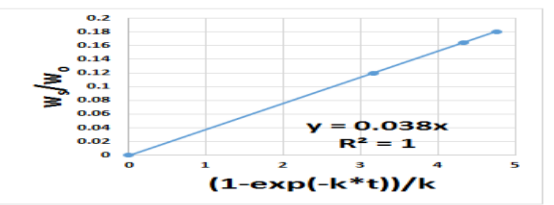

l) **pyro-oil of 700ºC of lime waste in presence of ZnO**

300 °C

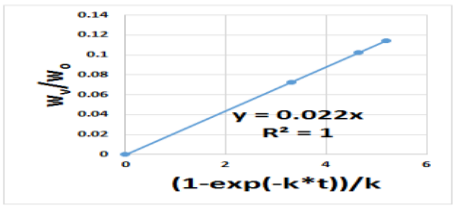

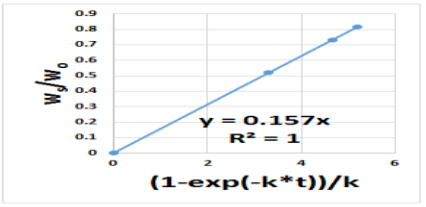

400 °C

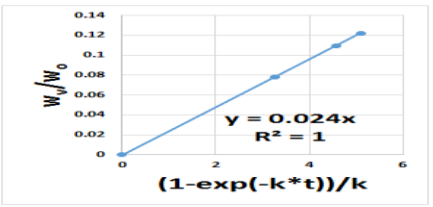

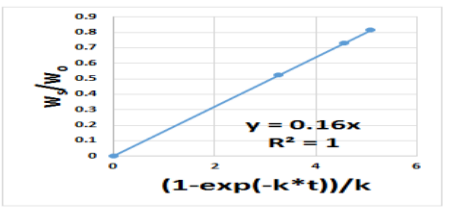

500 °C

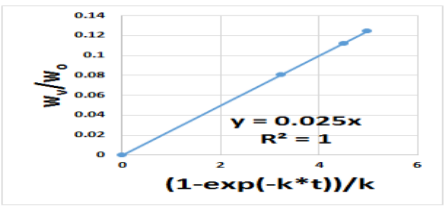

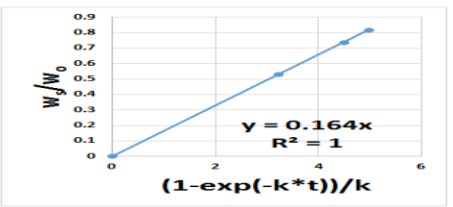

600 °C

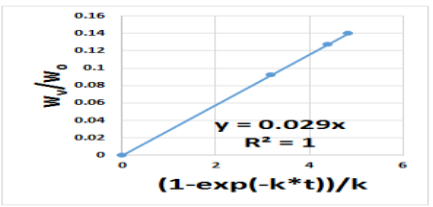

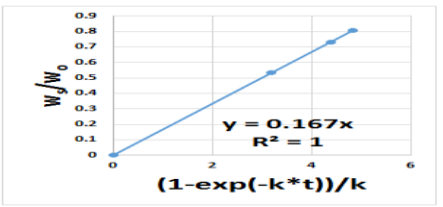

700 °C

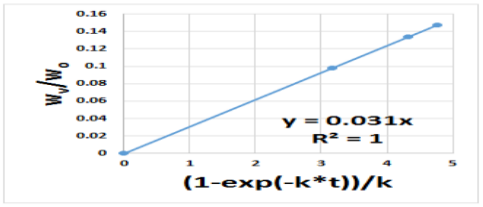

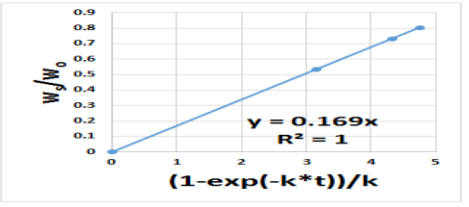

800 °C

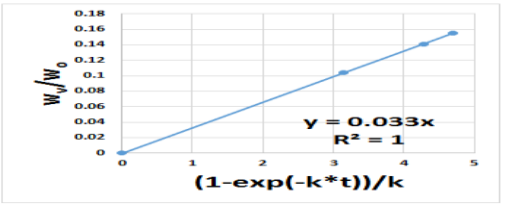

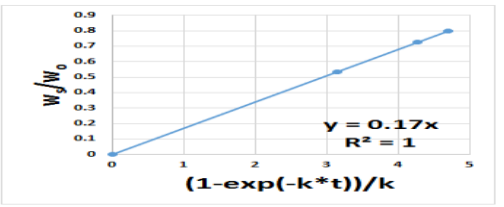

900 °C

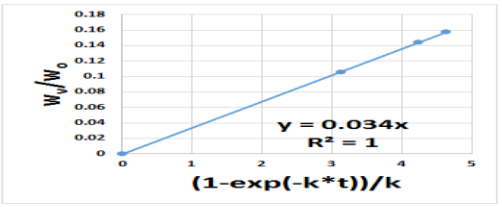

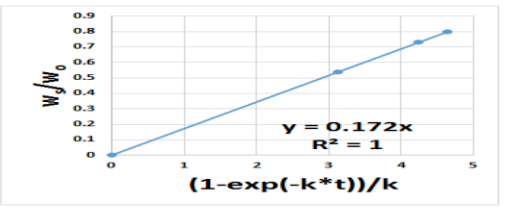

m) **pyro-oil of 900°C of lime waste in presence of ZnO**

300 °C

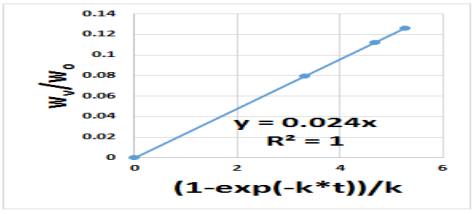

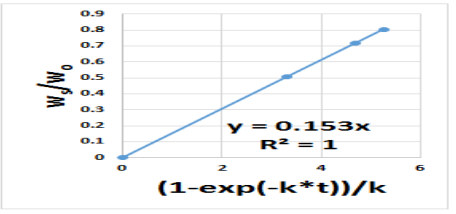

400 °C

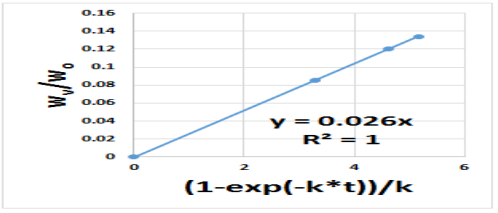

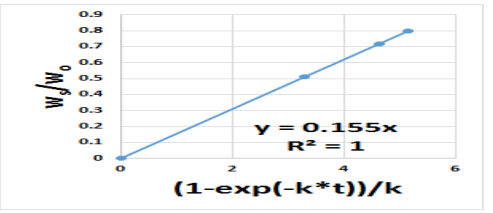

500 °C

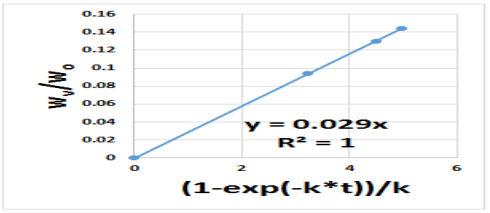

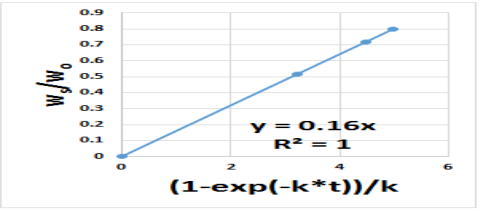

600 °C

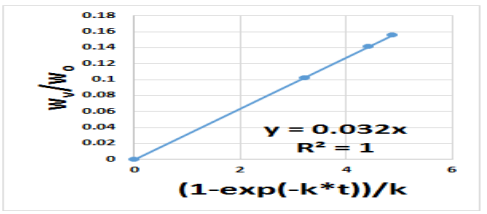

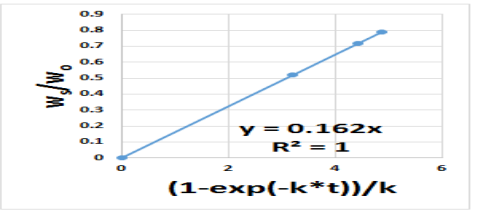

700 °C

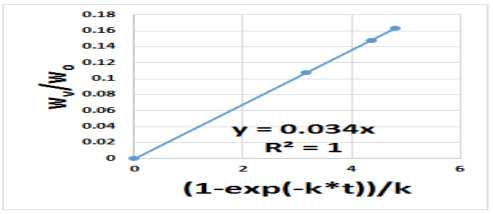

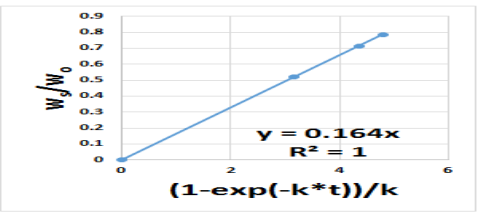

800 °C

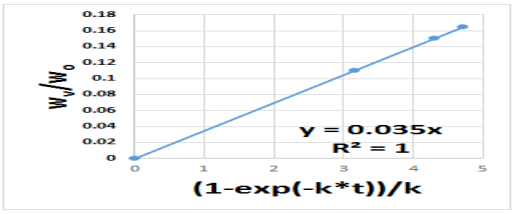

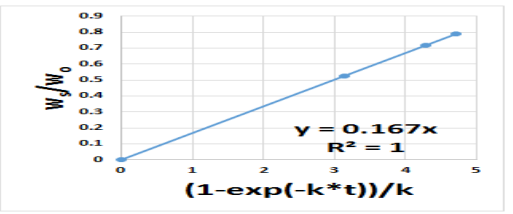

900 °C

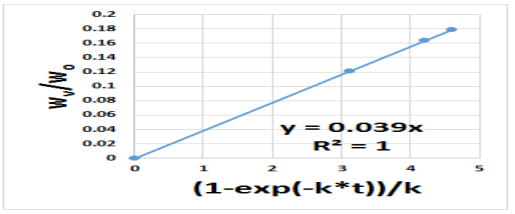

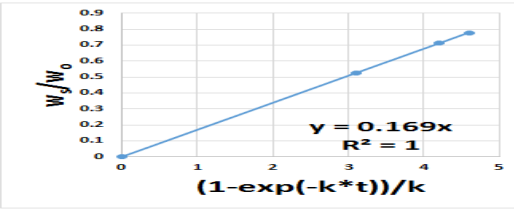

A.67. Values of k, k_v, k_s of different temperature of pyro-oil

a) values of k of pyro-oil

i) 500ºC

Temperature (K)	jute	jute+alumina	lime	lime+ZnO
573 (300 ^{O}C)	0.172	0.18	0.179	0.174
673(400 ^{O}C)	0.185	0.188	0.182	0.177
773(500 ^{O}C)	0.19	0.195	0.186	0.181
873(600 ^{O}C)	0.199	0.204	0.19	0.185
973(700 ^{O}C)	0.205	0.208	0.194	0.189
1073(800 ^{O}C)	0.212	0.214	0.201	0.196
1173(900 ^{O}C)	0.222	0.218	0.205	0.2

ii) 700 ºC

Temperature (K)	jute	jute+alumina	lime	lime+ZnO
573 (300 ^{O}C)	0.187	0.187	0.185	0.179
673(400 ^{O}C)	0.194	0.192	0.19	0.184
773(500 ^{O}C)	0.199	0.196	0.195	0.189
873(600 ^{O}C)	0.204	0.202	0.202	0.196
973(700 ^{O}C)	0.208	0.206	0.206	0.2
1073(800 ^{O}C)	0.213	0.21	0.209	0.203
1173(900 ^{O}C)	0.216	0.214	0.212	0.206

iii) 900 ºC

Temperature (K)	jute	jute+alumina	lime	lime+ZnO
573 (300 ^{O}C)	0.194	0.192	0.183	0.177
673(400 ^{O}C)	0.196	0.195	0.187	0.181
773(500 ^{O}C)	0.199	0.198	0.195	0.189
873(600 ^{O}C)	0.204	0.201	0.2	0.194
973(700 ^{O}C)	0.207	0.205	0.204	0.198
1073(800 ^{O}C)	0.211	0.209	0.208	0.202
1173(900 ^{O}C)	0.214	0.214	0.214	0.208

b) values of k_v of pyro-oil

i) 500ºC

Temperature (K)	jute	jute+alumina	lime	lime+ZnO
573 (300 ^{O}C)	0.06	0.069	0.15	0.148
673(400 ^{O}C)	0.069	0.071	0.151	0.149
773(500 ^{O}C)	0.072	0.075	0.153	0.151
873(600 ^{O}C)	0.074	0.082	0.155	0.153
973(700 ^{O}C)	0.078	0.084	0.157	0.155

1073(800 ^{O}C)	0.082	0.086	0.162	0.16
1173(900 ^{O}C)	0.087	0.088	0.164	0.162

ii) **700ºC**

Temperature (K)	jute	jute+alumina	lime	lime+ZnO
573 (300 ^{O}C)	0.075	0.083	0.025	0.022
673(400 ^{O}C)	0.079	0.086	0.027	0.024
773(500 ^{O}C)	0.081	0.087	0.028	0.025
873(600 ^{O}C)	0.084	0.09	0.032	0.029
973(700 ^{O}C)	0.086	0.092	0.034	0.031
1073(800 ^{O}C)	0.089	0.094	0.036	0.033
1173(900 ^{O}C)	0.09	0.096	0.037	0.034

iii) 900ºC

Temperature (K)	jute	jute+alumina	lime	lime+ZnO
573 (300 ^{O}C)	0.084	0.091	0.027	0.024
673(400 ^{O}C)	0.085	0.092	0.029	0.026
773(500 ^{O}C)	0.087	0.094	0.032	0.029
873(600 ^{O}C)	0.089	0.096	0.035	0.032
973(700 ^{O}C)	0.09	0.098	0.037	0.034
1073(800 ^{O}C)	0.092	0.101	0.038	0.035
1173(900 ^{O}C)	0.094	0.104	0.042	0.039

c) values of k_s of pyro-oil

i) 500ºC

Temperature (K)	jute	jute+alumina	lime	lime+ZnO
573 (300 ^{O}C)	0.112	0.111	0.029	0.026
673(400 ^{O}C)	0.116	0.117	0.031	0.028
773(500 ^{O}C)	0.118	0.12	0.033	0.03
873(600 ^{O}C)	0.125	0.122	0.035	0.032
973(700 ^{O}C)	0.127	0.124	0.037	0.034
1073(800 ^{O}C)	0.13	0.128	0.039	0.036
1173(900 ^{O}C)	0.135	0.13	0.041	0.038

ii) 700ºC

Temperature (K)	jute	jute+alumina	lime	lime+ZnO
573 (300 ^{O}C)	0.112	0.104	0.16	0.157

673(400 ^{O}C)	0.115	0.106	0.163	0.16
773(500 ^{O}C)	0.118	0.109	0.167	0.164
873(600 ^{O}C)	0.12	0.112	0.17	0.167
973(700 ^{O}C)	0.122	0.114	0.172	0.169
1073(800 ^{O}C)	0.124	0.116	0.173	0.17
1173(900 ^{O}C)	0.126	0.118	0.175	0.172

iii) 900^{o}C

Temperature (K)	jute	jute+alumina	lime	lime+ZnO
573 (300 ^{O}C)	0.11	0.101	0.156	0.153
673(400 ^{O}C)	0.111	0.103	0.158	0.155
773(500 ^{O}C)	0.112	0.104	0.163	0.16
873(600 ^{O}C)	0.115	0.105	0.165	0.162
973(700 ^{O}C)	0.117	0.107	0.167	0.164
1073(800 ^{O}C)	0.119	0.108	0.17	0.167
1173(900 ^{O}C)	0.12	0.11	0.172	0.169

A.68.

a) Activation energies and Pre-exponential factor of jute waste pyro-oil at different temperature

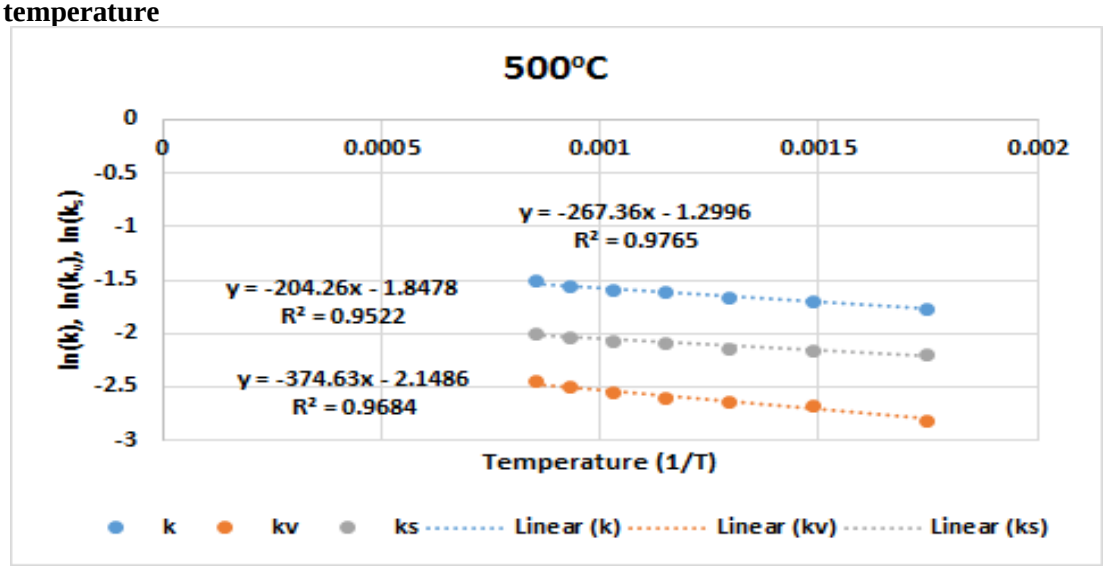

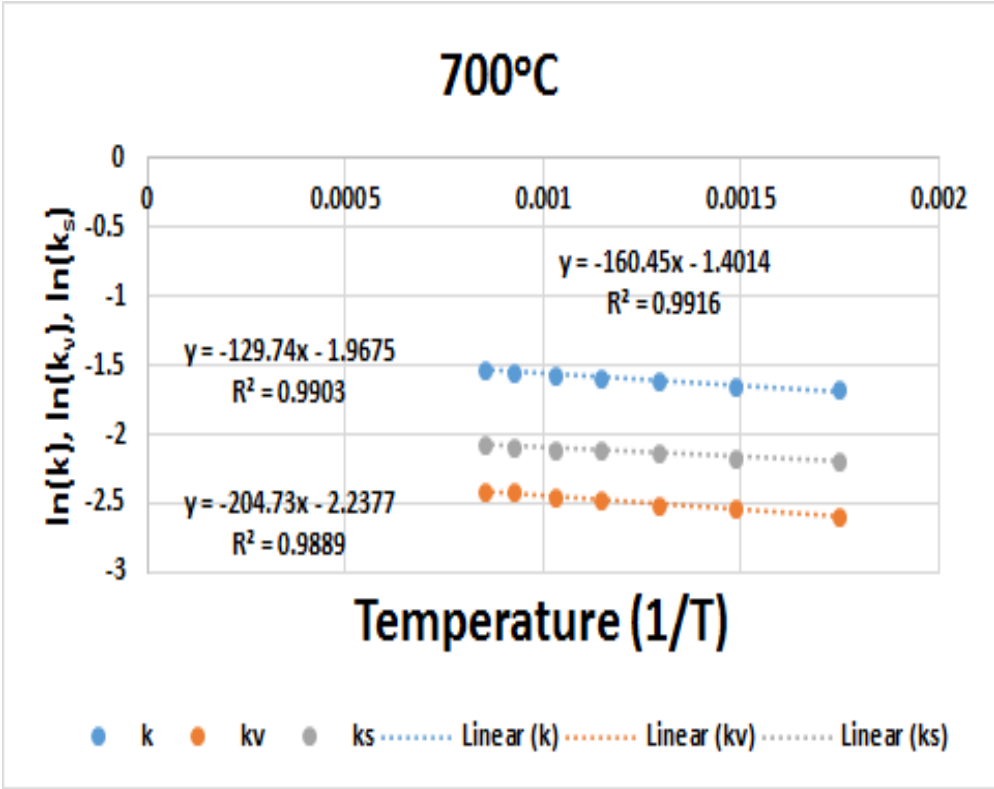
700°C
0
-0.5
-1
-1.5
-2
-2.5
-3
0
0.0005
0.001
0.0015
0.002
ln(k), ln(kv), ln(ks)
y = -160.45x - 1.4014
R² = 0.9916
y = -129.74x - 1.9675
R² = 0.9903
y = -204.73x - 2.2377
R² = 0.9889
Temperature (1/T)
k
kv
ks
Linear (k)
Linear (kv)
Linear (ks)

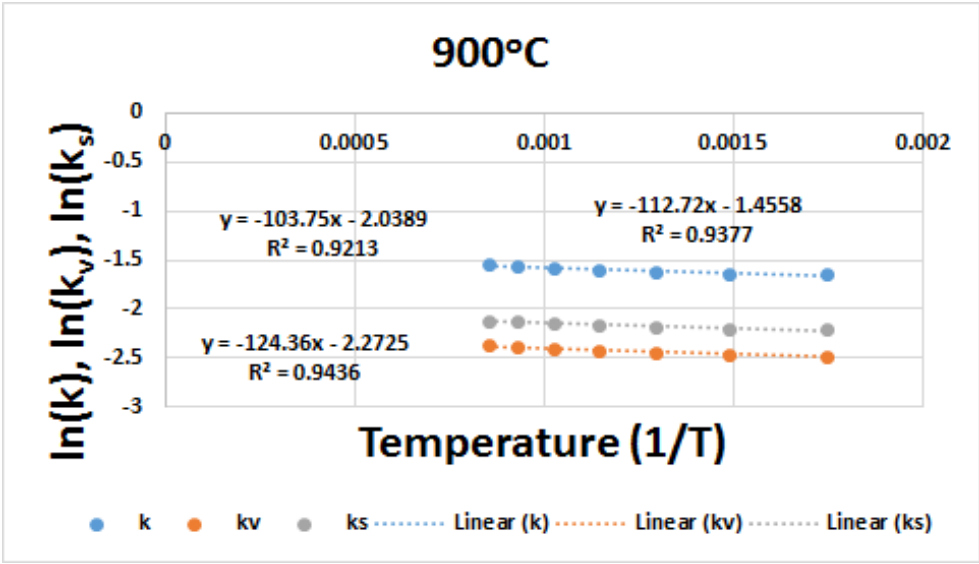
900°C
0
-0.5
-1
-1.5
-2
-2.5
-3
0
0.0005
0.001
0.0015
0.002
ln(k), ln(kv), ln(ks)
y = -103.75x - 2.0389
R² = 0.9213
y = -112.72x - 1.4558
R² = 0.9377
y = -124.36x - 2.2725
R² = 0.9436
Temperature (1/T)
k
kv
ks
Linear (k)
Linear (kv)
Linear (ks)

b) Activation energies and Pre-exponential factor of lime waste pyro-oil at different temperature

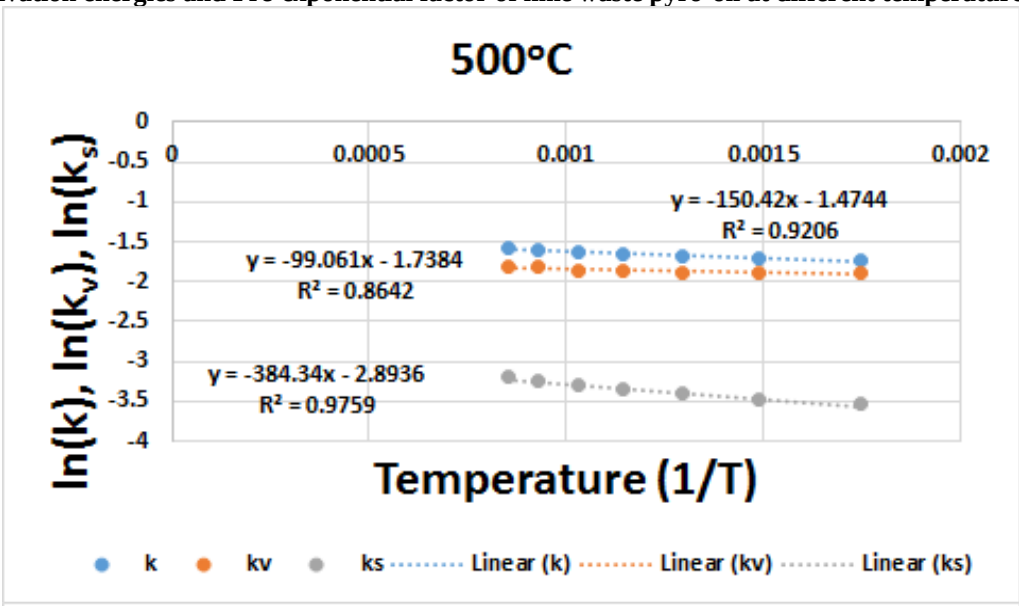

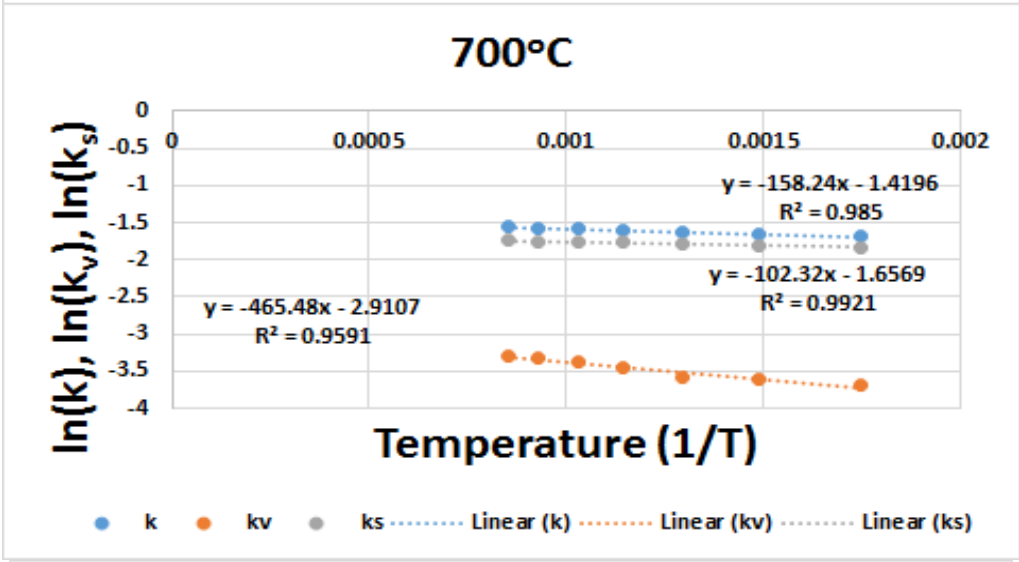

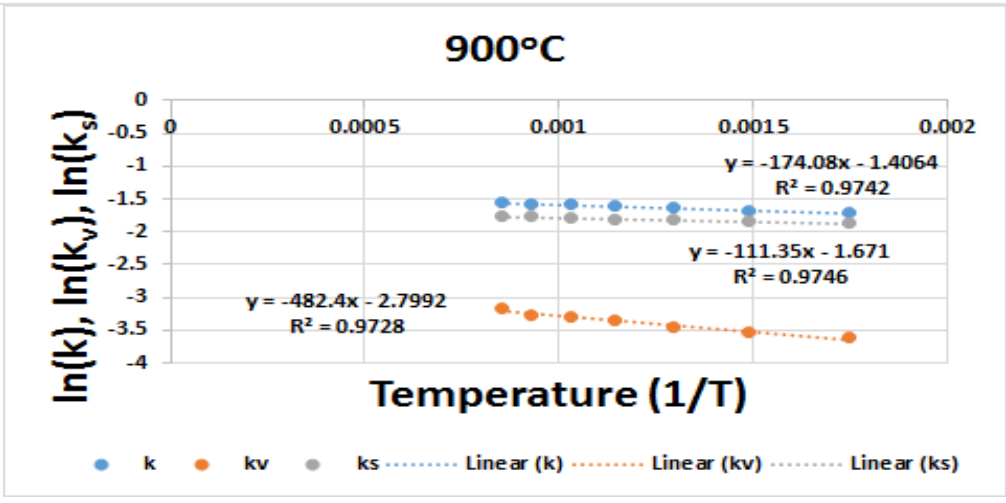

c) Activation energies and Pre-exponential factor of jute waste in presence of alumina pyro-oil at different temperature

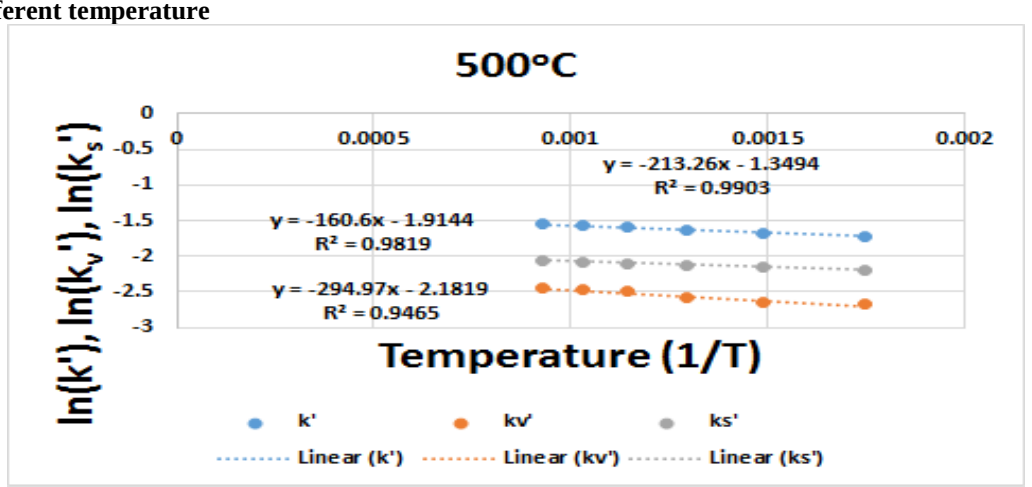

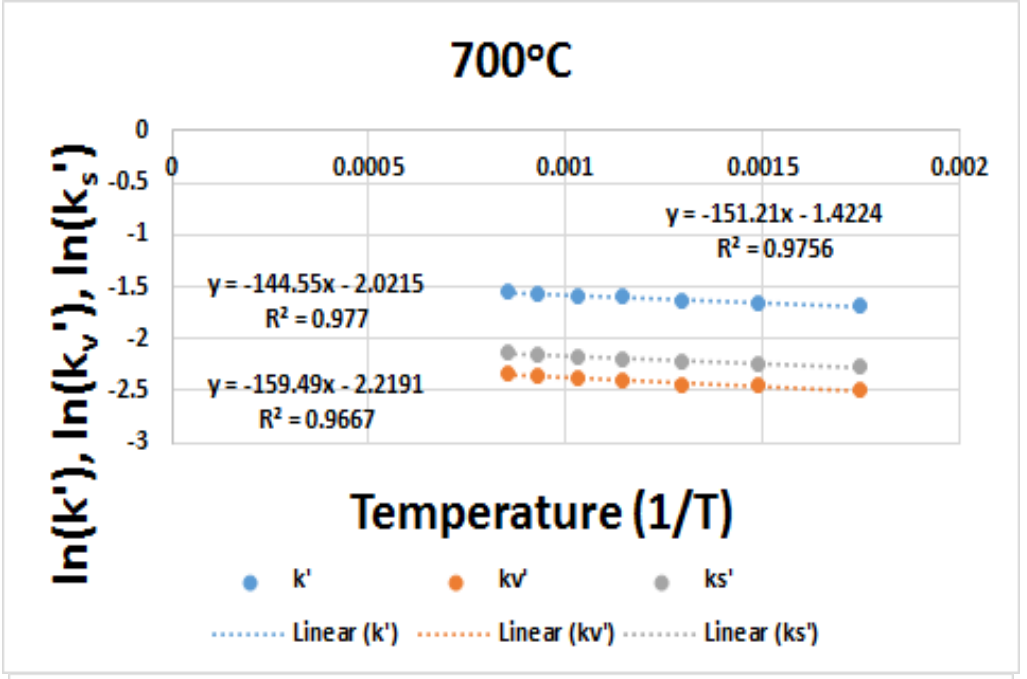

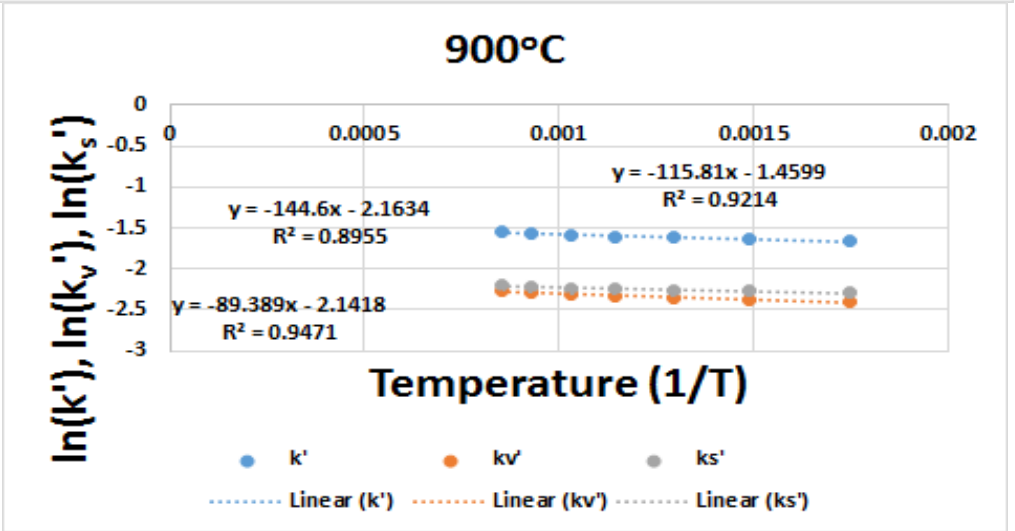

d) Activation energies and Pre-exponential factor of jute waste in presence of alumina pyro-oil at different temperature

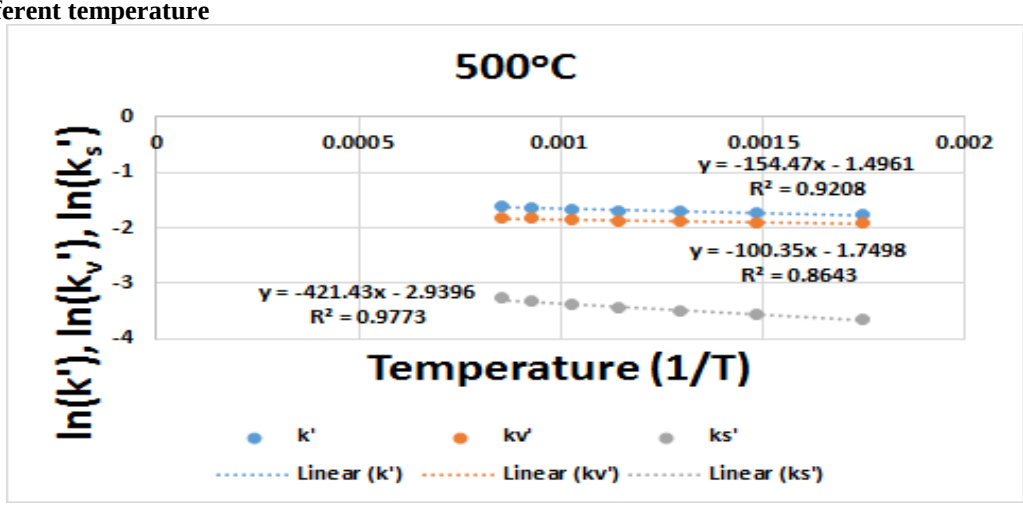

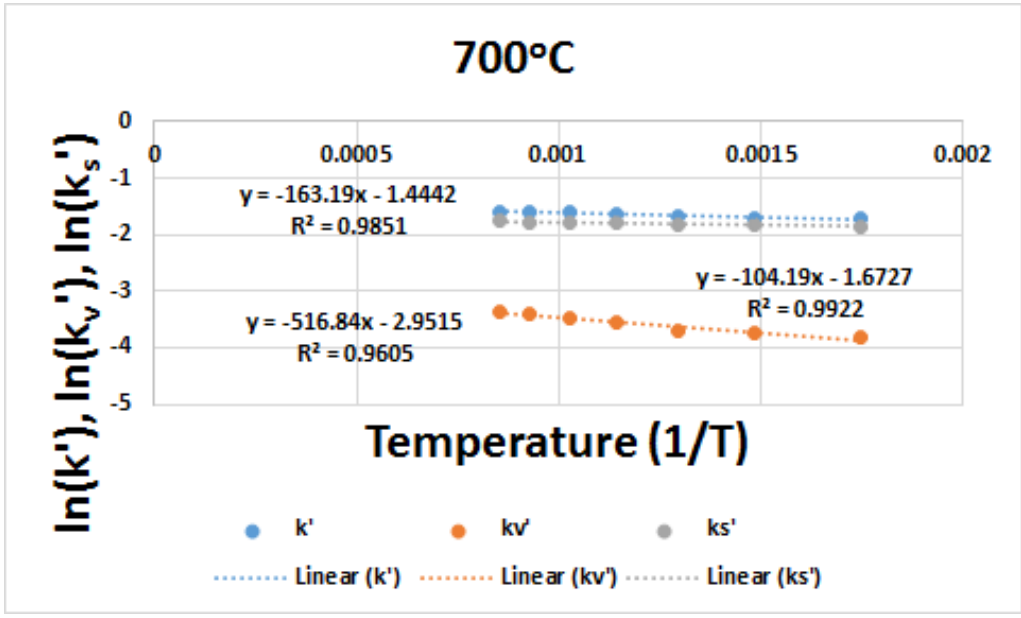

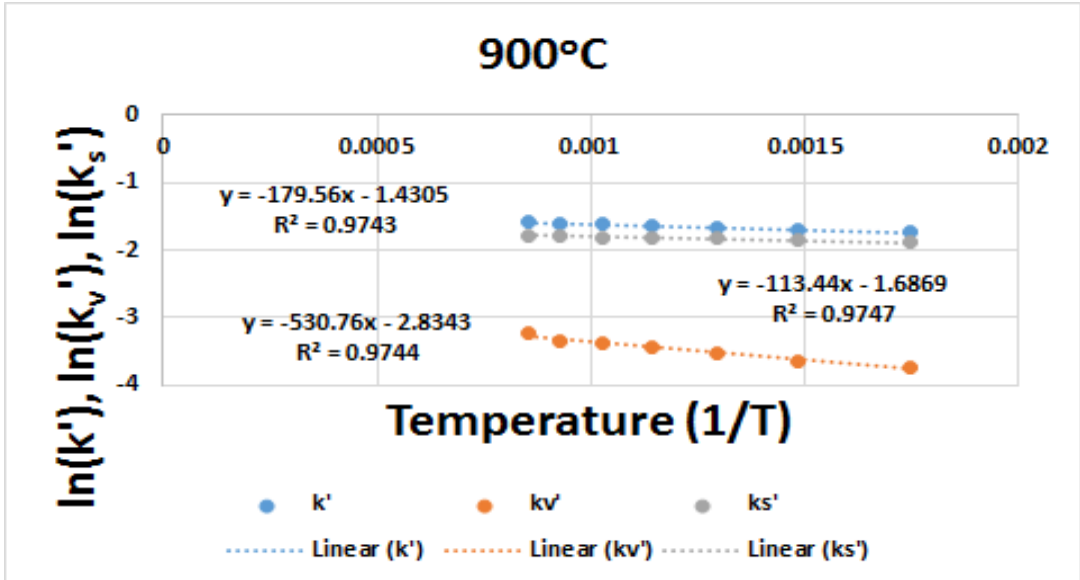

A.69.

a) ANOVA for response surface model for the variation of Diesel as a simultaneous function of pyrolysis temperature and CO_2 recycled

Source	Sum of Squares	df	Mean Square	F Value	p-value Prob > F
Model	0.87	9	0.097	254.36	< 0.0001
A-A	0.000248	1	0.000248	0.65	0.4461
B-B	0.09	1	0.09	236.35	< 0.0001
AB	0.00621	1	0.00621	16.31	0.0049
A^2	0.022	1	0.022	57.59	0.0001
B^2	0.003868	1	0.003868	10.16	0.0153
A^2B	0.01	1	0.01	26.32	0.0014
AB^2	0.002233	1	0.002233	5.86	0.046
Residual	0.002665	7	0.000381		
Cor Total	0.87	16			

R^2= 0.997, Adjusted R^2 = 0.993, Predicted R^2 = 0.9524, Adeq Precision = 53.928

b) ANOVA for response surface model for the variation of Gasoline as a simultaneous function of pyrolysis temperature and CO_2 recycled.

Source	Sum of Squares	df	Mean Square	F Value	p-value Prob > F
Model	0.091	9	0.01	556.77	< 0.0001
A-A	1.32E-05	1	1.32E-05	0.73	0.4224
B-B	0.008475	1	0.008475	467.29	< 0.0001
AB	0.00072	1	0.00072	39.72	0.0004
A^2	0.001892	1	0.001892	104.29	< 0.0001
B^2	0.000287	1	0.000287	15.84	0.0053
A^2B	0.000823	1	0.000823	45.39	0.0003
AB^2	0.000238	1	0.000238	13.14	0.0085
Residual	0.000127	7	1.81E-05		
Cor Total	0.091	16			

R^2= 0.9986, Adjusted R^2 = 0.9968, Predicted R^2 = 0.9799, Adeq Precision = 79.976

A.70. Figures for Energy delivered

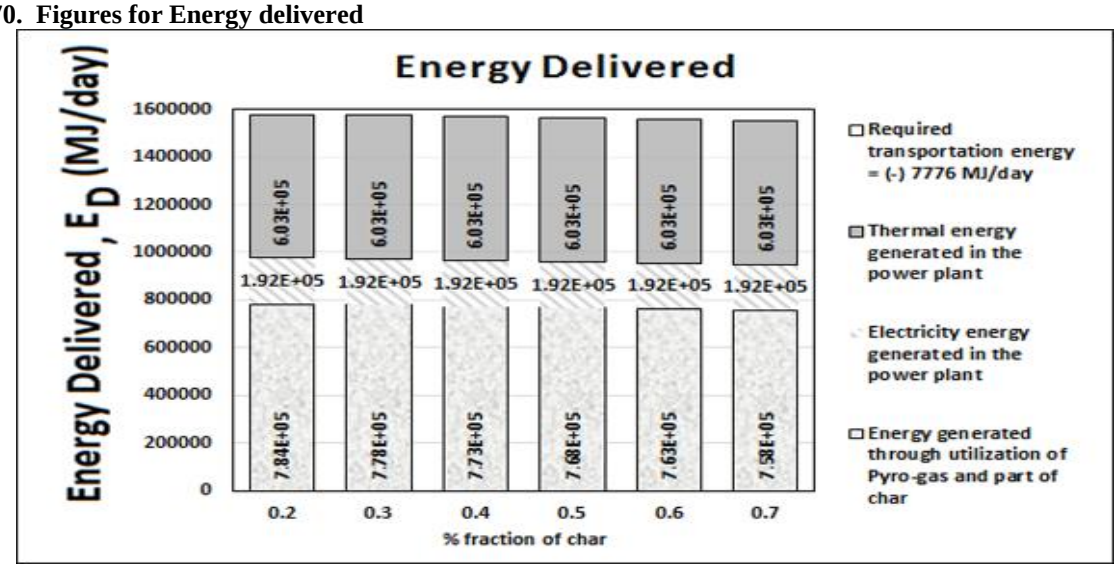

Figure A.1. Trends of energy delivered with fraction of char deposition for soil amendment for 400ºC

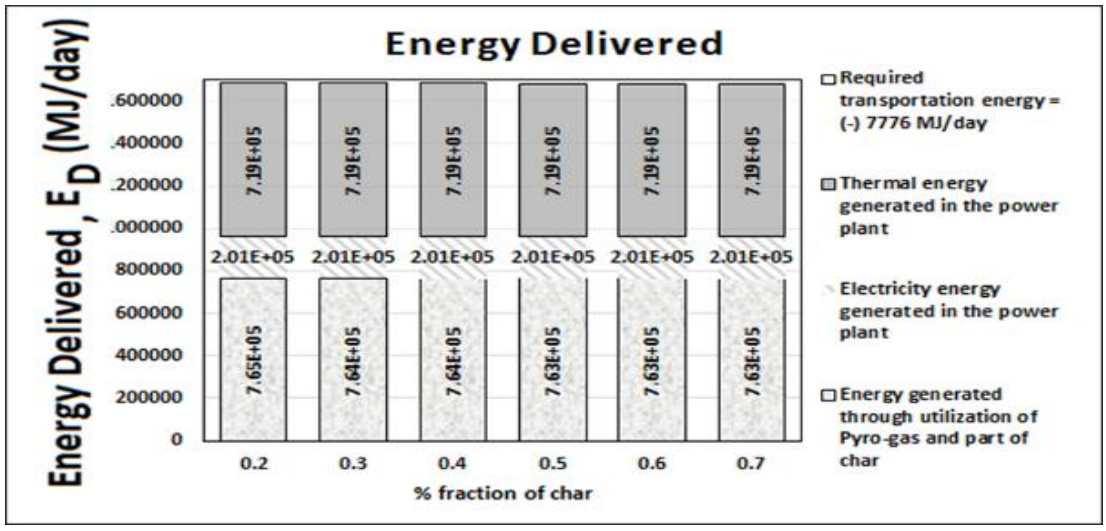

Figure A.2. Trends of energy delivered with fraction of char deposition for soil amendment for 500ºC

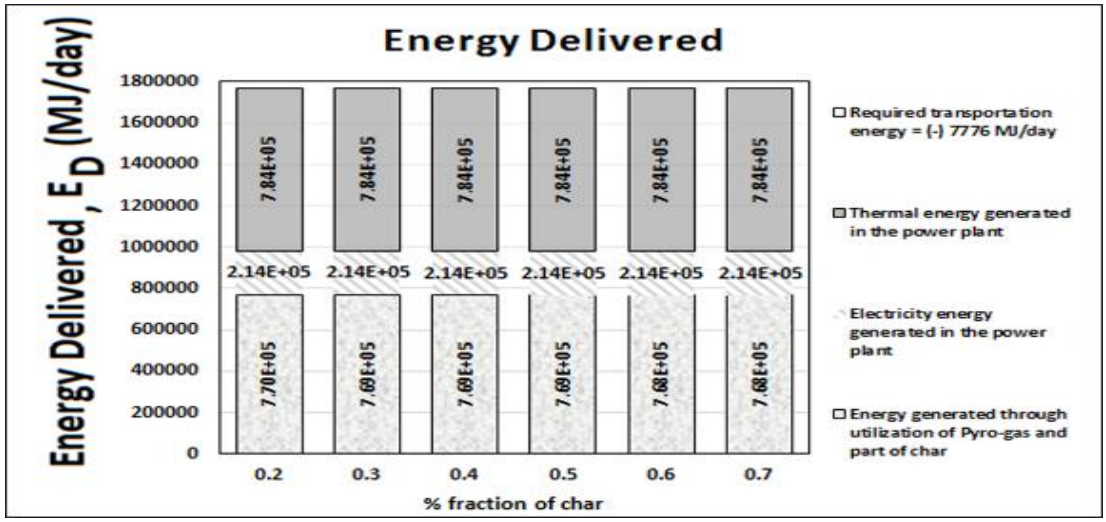

Figure A.3. Trends of energy delivered with fraction of char deposition for soil amendment for 600ºC

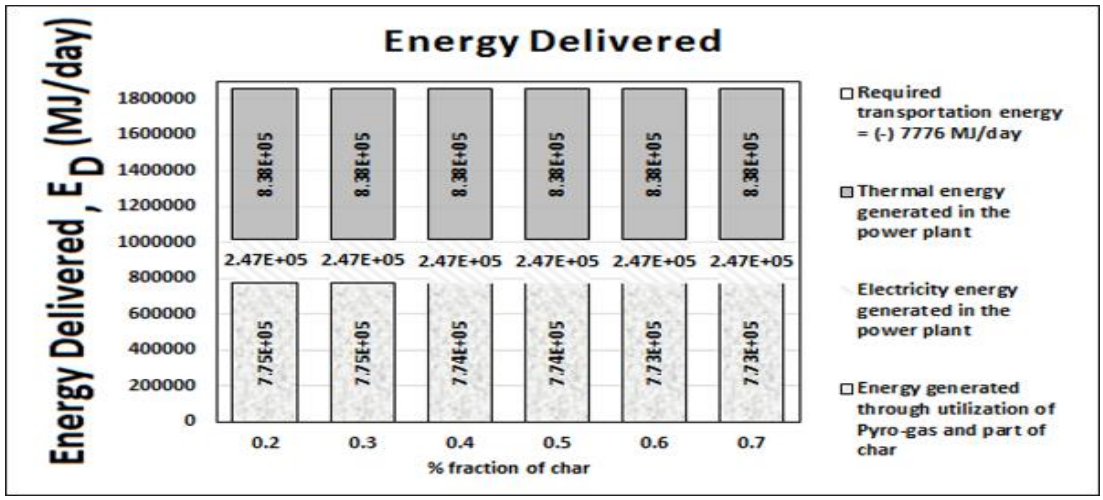

Figure A.4. Trends of energy delivered with fraction of char deposition for soil amendment for 700ºC

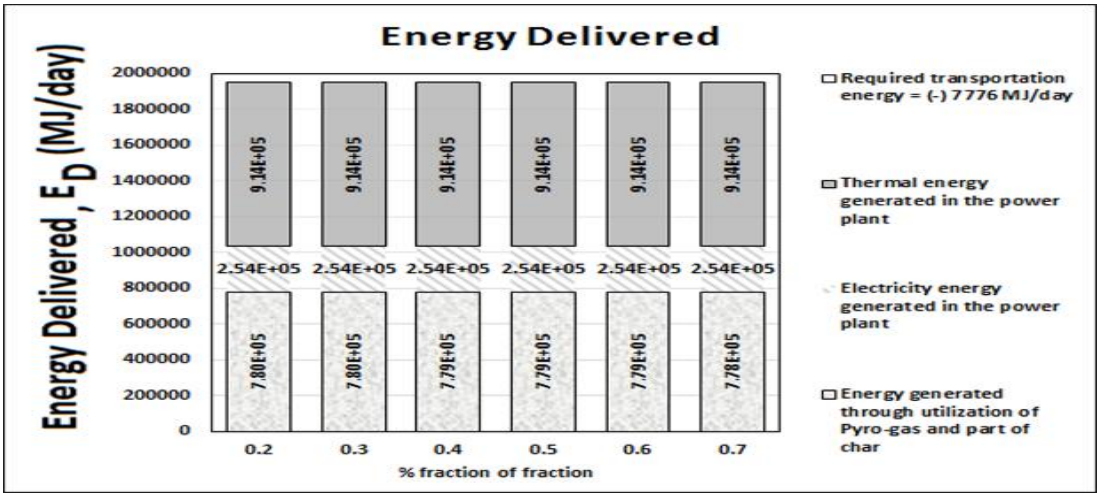

Figure A.5. Trends of energy delivered with fraction of char deposition for soil amendment for 800^{o}C

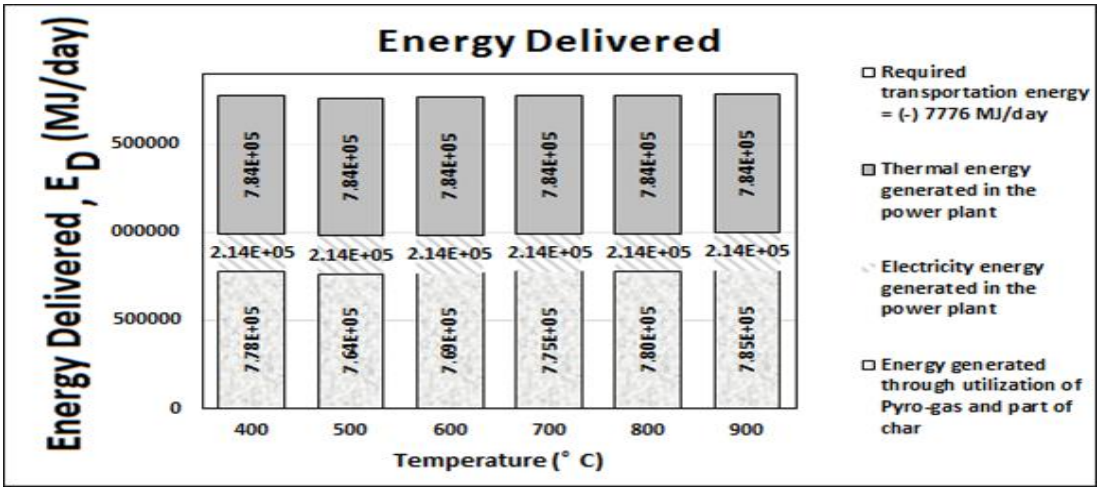

Figure A.6. Trends of energy generation with pyrolysis temperature at 30% char deposition for soil amendment.

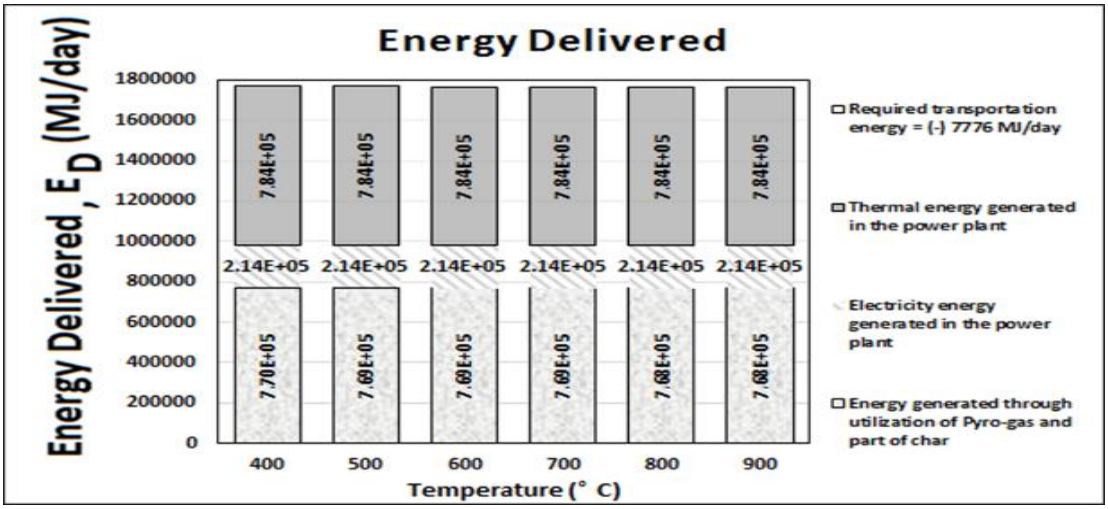

Figure A.7. Trends of energy generation with pyrolysis temperature at 40% char deposition for soil amendment.

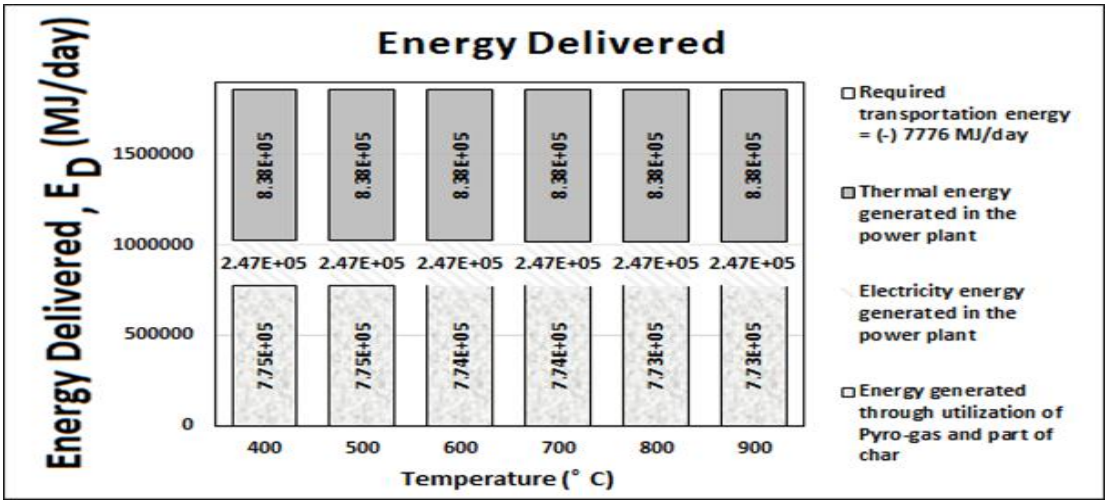

Figure A.8. Trends of energy generation with pyrolysis temperature at 50% char deposition for soil amendment.

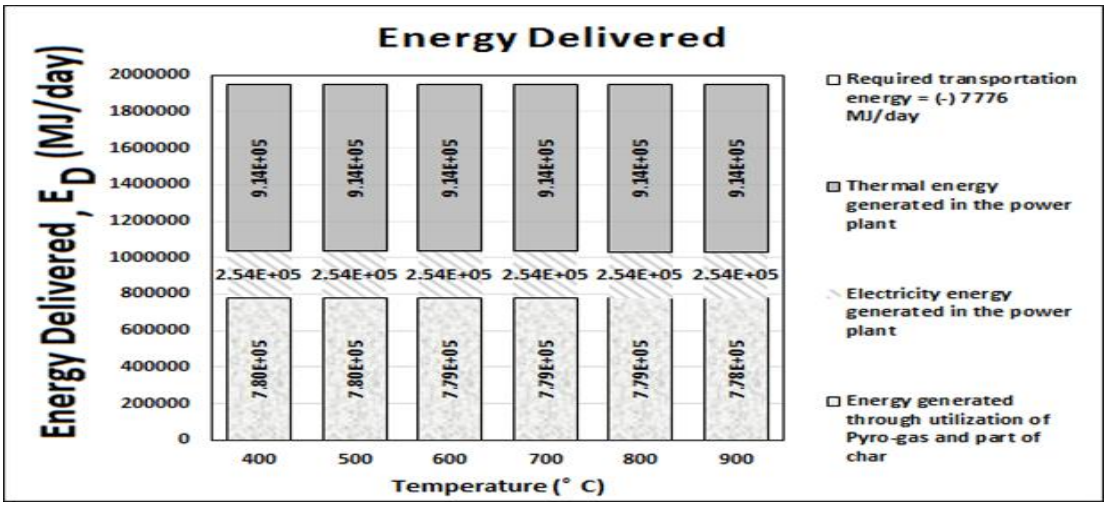

Figure A.9. Trends of energy generation with pyrolysis temperature at 60% char deposition for soil amendment.

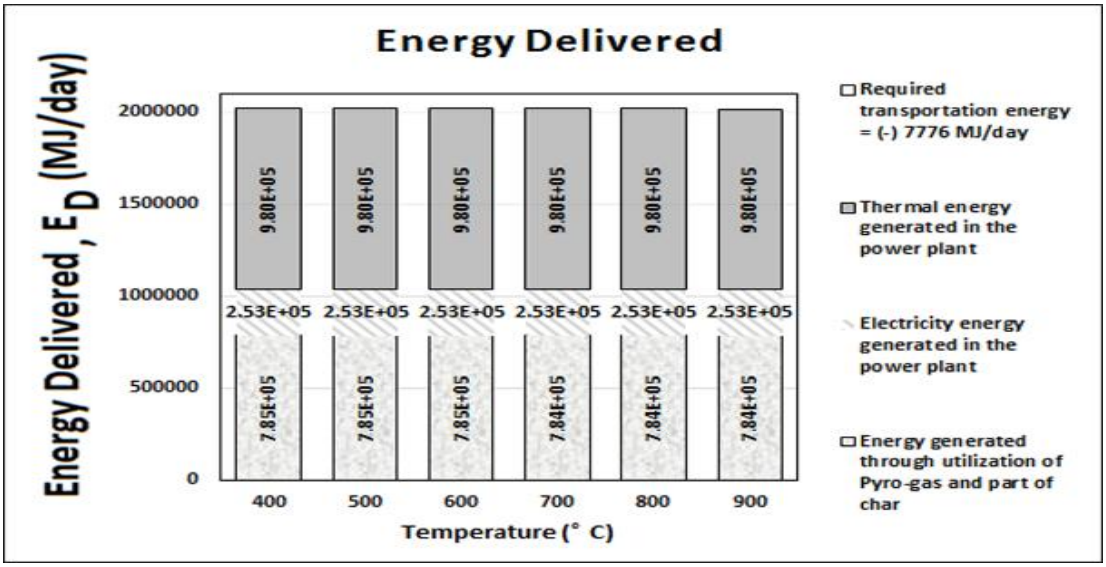

Figure A.10. Trends of energy generation with pyrolysis temperature at 70% char deposition for soil amendment.

A.71. Avoidance of CO_2

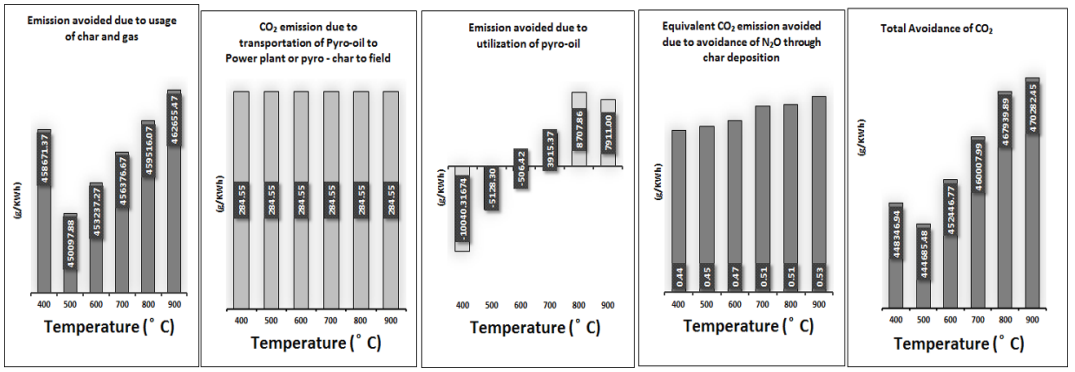

Figure A.11. Trends of CO_2 emission and avoidance with pyrolysis temperature at 30% char deposition for soil amendment

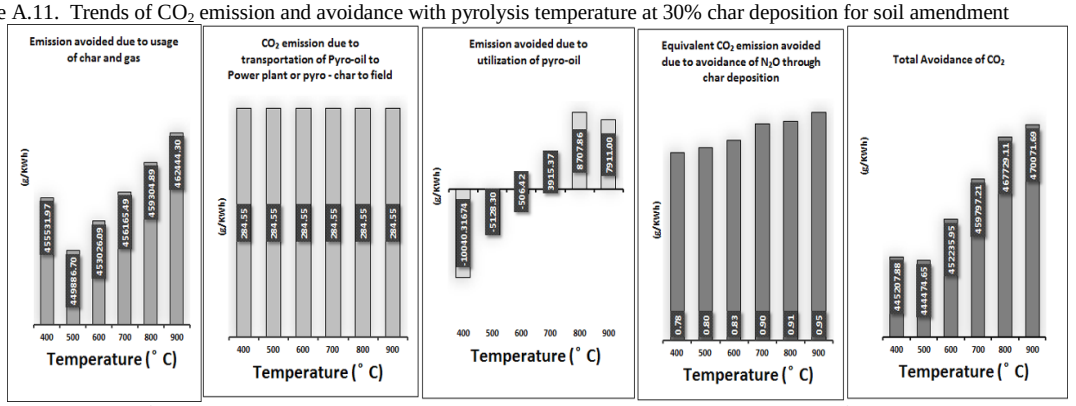

Figure A.12. Trends of CO_2 emission and avoidance with pyrolysis temperature at 40% char deposition for soil amendment

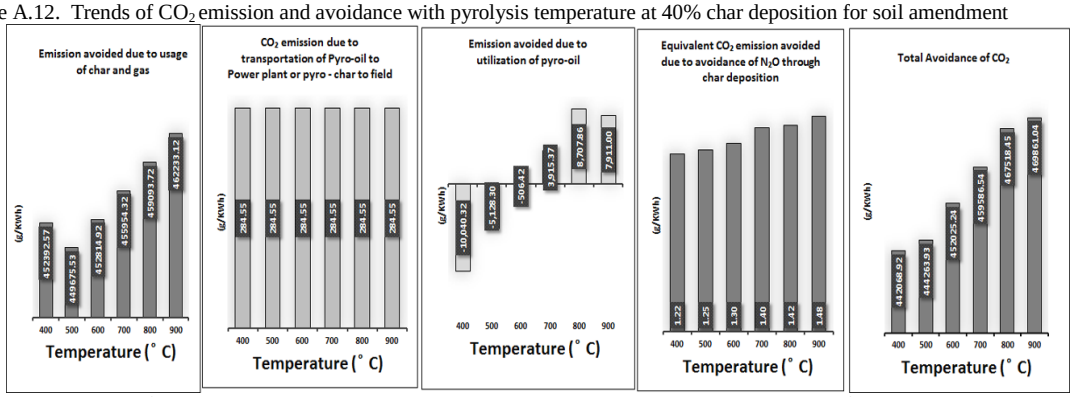

Figure A.13. Trends of CO_2 emission and avoidance with pyrolysis temperature at 50% char deposition for soil amendment

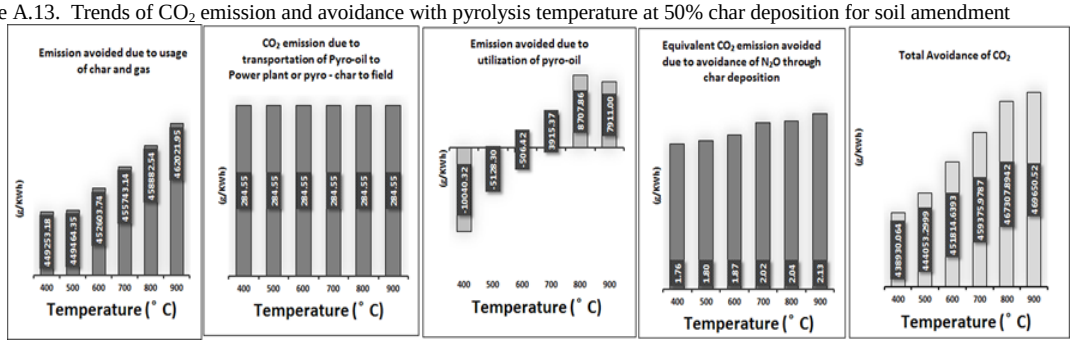

Figure A.14. Trends of CO_2 emission and avoidance with pyrolysis temperature at 60% char deposition for soil amendment

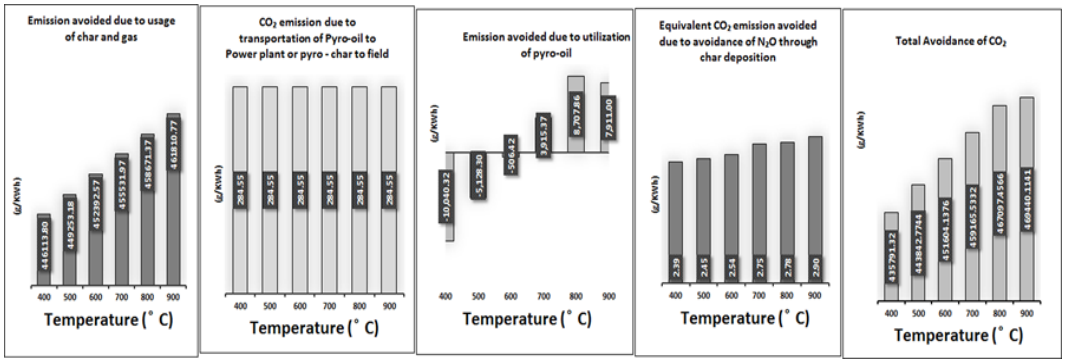

Figure A.15. Trends of CO_2 emission and avoidance with pyrolysis temperature at 70% char deposition for soil amendment

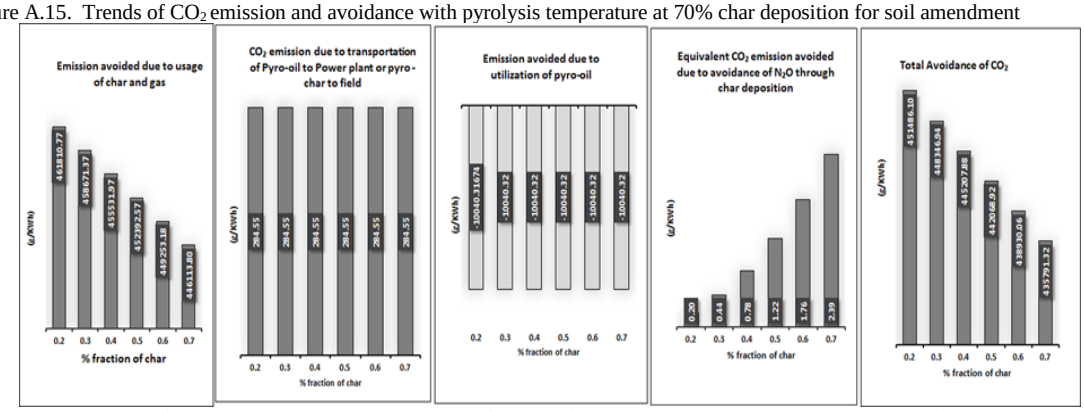

Figure A.16. Trends of CO_2 emission and avoidance with % fraction of char deposition at 400ºC char deposition for soil amendment

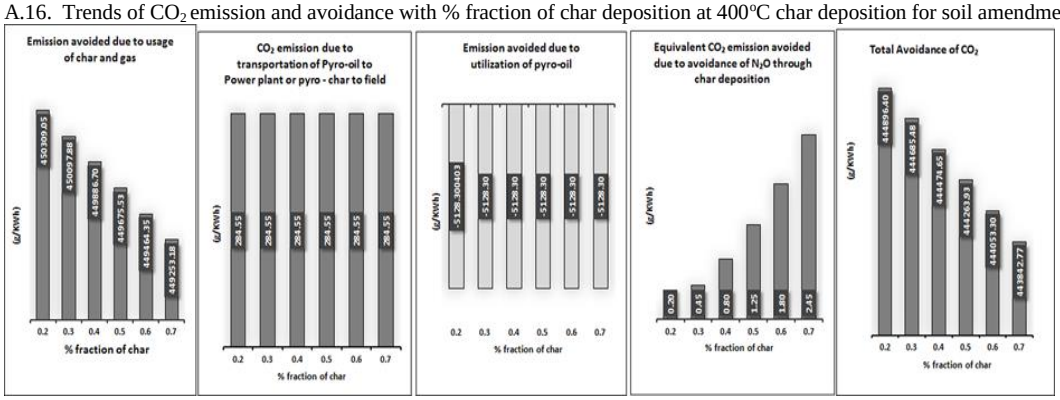

Figure A.17. Trends of CO_2 emission and avoidance with % fraction of char deposition at 500ºC char deposition for soil amendment

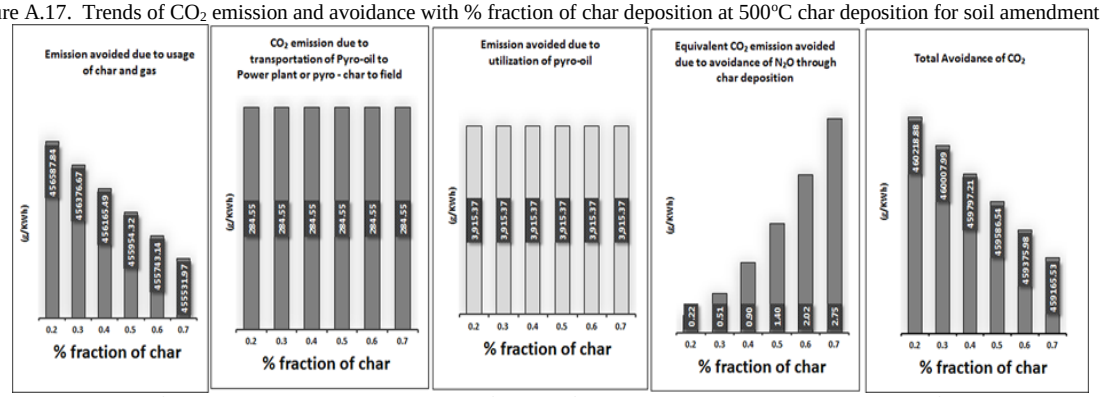

Figure A.18. Trends of CO_2 emission and avoidance with % fraction of char deposition at 700ºC char deposition for soil amendment

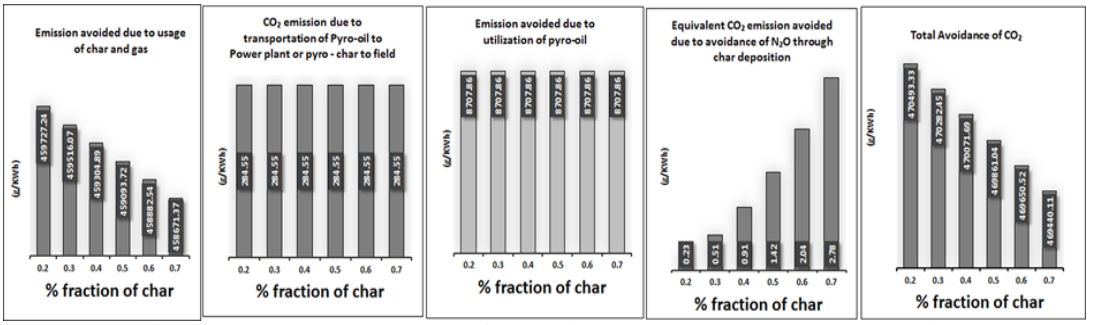

Figure A.19. Trends of CO_2 emission and avoidance with % fraction of char deposition at 800ºC char deposition for soil amendment

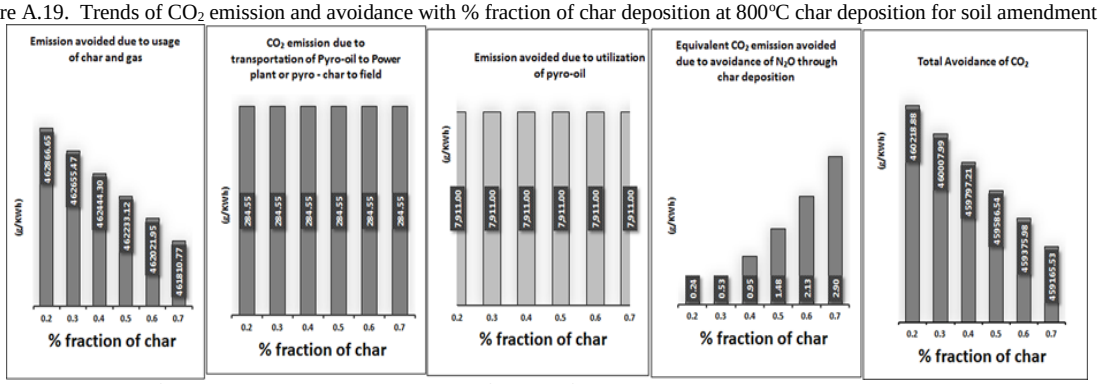

Figure A.20. Trends of CO_2 emission and avoidance with % fraction of char deposition at 900ºC char

A.72 Sample calculation of **EROEI** and A_{CO_2}

Utilization of pyro-gas and pyro-char for the supply of energy for Pyrolysis and Drying

Carbon percentage (p_1) in lignite = 71%
Average calorific value (c1) = 3767.943 kcal/kg
Coal-fired Power Plant efficiency = 30%
Electrical Grid Distribution efficiency = 91%
Mass flow rate of CO_2 due to incineration of char and gas = 524.0688 kg/h
Energy supplied due to incineration of char and gas = 7810161 kcal/h

Corresponding CO_2 emission avoided (kg) $= \dfrac{7810161 \times (\frac{71}{100})}{(\frac{91}{100}) \times \left(\frac{30}{100}\right) \times 3767.94 \times 12} \times 44 = 19766.2$ kg/h

Actual CO_2 emission avoided due to utilization of pyro-char and pyro-gas= 19766.2-524.0688= 19242.12 Kg/h

Pyro-oil used in CHP Plant

C_V of pyro-oil = 26.67 MJ/day
Percentage of carbon in pyro-oil = 64.24%
Pyro-oil produced = 858.8771 kg/h
Electrical energy generated in the CHP = 192412.5 MJ/day
Thermal energy generated in the CHP = 602856.3 MJ/day

Corresponding CO_2 emission avoided (kg) $= \dfrac{858.8771 \times \left(\frac{26.67}{100}\right)}{167} \times 12 \times 44 = 1616.57$ kg/h

Actual CO_2 emission avoided $= 1616.57 - \dfrac{858.8771 \times \left(\frac{64.24}{100}\right) \times 44}{12} = -406.49$ kg/h

Transportation of Pyro-oil to Power plant

Energy consumption for the forward journey (Pyro-unit to power plant) $= 2.5 * 2 * 44800 = 224000$ kJ

Energy consumption for the return journey $= 2*20*44800 = 1792000$ kJ

Total CO_2 emission, $= = ((4.5*12*44)/167)*20 = 284.551$ kg/day

Avoidance of N – emission due to char deposition

Mass of char produced per hour = 162.1448 kg/h

Fraction of char = 0.2

Fraction of char deposited $= \frac{162.1448 \times 0.2 \times 300 \times 24}{0.02} = 11674428$ kg/year

Amount of urea applied $= 11674428 \times 0.1 = 1167443$ kg/year

area of soil $= \frac{11674428}{1250 \times 0.00635 \times 10000} = 147.0794$ ha

N_2O emission due fertilizer $= \frac{1167443 \times 28 \times 0.0125}{604} = 6810.083$ kg/year

annual N_2O emission /ha $= \frac{6810.083}{147.0794} = 46.30208$ kg/y/ha

$N_{emission}$ avoided due to biochar application, $= 10^{(0.15+147.0794*0.0038-1.516)*46.30208} = 9.495106$

Equivalent CO_2 emission avoided, $= \frac{0.5 \times 9.495106 \times 296}{300 \times 24} = 0.195177$ kg/day

Overall E_D and A_{CO_2}

Energy delivered (E_D) by pyro-products,

$$= (\frac{7810161 \times 4.18 \times 24}{1000}) + (192412.5 + 602856.3) - 2 \times \frac{224000 + 1792000}{1000} = 1574752 \text{ MJ/day}$$

C_V of Jute = 19.7 MJ/day

Energy Efficiency, EROEI = $\frac{1574752}{19.7 \times 10{,}00{,}00{,}000} \times 100000 = 79.9367\%$

Total avoidance of CO_2 emission, A_{CO_2}

$$= (19242.1 + -406.49) \times 24 - 2 \times 284.551 + 0.19518 = 451486 \text{ kg/day}$$

$$= \left(\frac{451486}{1574752}\right) \times 3600 = 1032.13 \text{ g/KWh}$$

Chapter. 9

Publications arising from this research

RSC Advances

PAPER

View Article Online
View Journal | View Issue

Cite this: *RSC Adv.*, 2015, **5**, 98934

Catalytic pyrolysis of lignocellulosic bio-packaging (jute) waste – kinetics using lumped and DAE (distributed activation energy) models and pyro-oil characterization

S. Poddar,[a] S. De[b] and R. Chowdhury*[a]

The present study concentrates on the catalytic pyrolysis of a waste bio-packaging material, namely, jute, under iso-thermal and non-isothermal conditions using a 50 mm diameter and 164 mm long semi-batch pyrolyzer and a TGA set-up, respectively. The temperature range of pyrolysis is 673 K to 1173 K. Alumina, zinc oxide, sodium chloride, potassium chloride, and sodium aluminosilicate have been used as the catalysts. The patterns of the yields of all products of non-catalytic and catalytic pyrolysis under isothermal conditions have been compared. Lumped kinetics have been determined using the data of iso-thermal experiments. Alumina has been selected as the best performing catalyst showing the highest pyro-oil yield and lowest activation energy. The pyro-oil of catalytic pyrolysis has higher and lower contents of carbon and oxygen, respectively, and a more acidic pH in comparison to the non-catalytic counterpart. The kinetics of non-isothermal pyrolysis with and without alumina have been determined using a distributed activation energy (DAE) model. While the activation energies of non-catalytic pyrolysis follow a Gaussian distribution over a wide conversion range (0.2 to 0.8), no such pattern is obtained for catalytic (alumina) pyrolysis. The pyro-oils of both catalytic and non-catalytic pyrolysis have been analyzed using GC/MS and many components of industrial applications have been identified.

Received 9th September 2015
Accepted 25th October 2015

DOI: 10.1039/c5ra18435e

www.rsc.org/advances

Introduction

In the context of both energy security and climate change mitigation, biomass is of major interest as a renewable energy source. In recent times, agricultural residues, municipal solid wastes,[1,2] vegetable wastes like Pungam oil cakes,[3] jute waste,[4–6] soybean,[7] rapeseed,[8] sunflower oil cake,[9] cotton based textile wastes[10] and energy crops have attracted great attention as alternative energy sources. In India, jute fabric is used as an eco-friendly lignocellulosic bio-packaging material particularly for food-grains and sugar[11,12] and a large portion faces disposal problems. Although a few studies have been reported on 'waste to energy' processes[13–16] using jute wastes, more focus should be given to explore this possibility. Energy rich clean fuels may be generated from biomass through thermochemical conversion processes like pyrolysis, gasification *etc.* Pyrolysis, also known as thermolysis, is a process of thermochemical decomposition which generally leads to the generation of pyro char, pyro-oil and pyro-gas of smaller molecular weights. Pyrolysis is conducted in an oxygen deficient environment in the temperature range of 400–900 °C. The distribution of product yield may be changed by the adjustment of pyrolysis temperature. The pyro-oil obtained through pyrolysis is particularly attractive as it may be blended with petroleum crude or may be used as an automobile fuel after upgradation. Similar to coal tar, pyro-oil may also be used as a source for different valuable chemicals. Thus pyrolysis may be used as a potential process to be used in bio-refineries to generate fuel and chemicals simultaneously from biomass. One of the main shortcomings of pyro-oil is its high oxygen content.[13,17] Catalytic pyrolysis usually produce upgraded liquids.[13,18] From the literature review, it is clear that a few metal salts and oxides may serve as catalysts in pyrolysis of biomass.[19,20] From the chemical engineering view point, a catalyst usually changes the rate of a reaction by the promotion of a different molecular path leading to lowering of activation energy and hence can influence both the yield and selectivity.[21] As the catalytic reactions occur at the fluid–solid interfaces, porosity of the solid also alters the overall rates. In a pyrolysis process, an array of series–parallel reactions occur simultaneously. Although lumped kinetics are usually used for the analysis of data under isothermal conditions,[22] DAE models are usually appropriate to represent the behavior of pyrolysis of biomass under non-isothermal conditions. This model can account for difference in behavior of pyrolysis of constituent molecules like cellulose, hemicelluloses and lignin through a distribution of activation energy at different conversion levels. Therefore, DAE models should also be attempted for catalytic pyrolysis of biomass under non-isothermal condition. However,

[a]*Jadavpur University, Department of Chemical Engineering, Kolkata-700032, India. E-mail: ranjana.juchem@gmail.com*

[b]*Jadavpur University, Department of Mechanical Engineering, Kolkata-700032, India*

DAE models have not been developed for catalytic pyrolysis. No correlation has been reported on the porosity of solid residue of pyrolysis with the activity of catalysts.

Under the present research study, the catalytic effects of metal salts of Na, K, Al, Si *etc.* and metal oxides like Al_2O_3 and ZnO on pyrolysis of waste jute in the temperature range of 400 °C to 900 °C have been investigated with special reference to yields of products and characteristics of the pyro-oil and determination of kinetics using isothermal and non-isothermal data. Lumped kinetic parameters have been determined for all catalytic pyrolysis and have been compared with those of non-catalytic pyrolysis. For the best performing catalyst with respect to oil yield, the C–H–O levels in the bio-oils have been compared with those of bio-oil from non-catalytic pyrolysis. The pyrolysis kinetics under non-isothermal conditions have been determined using DAE (Distributed Activation Energy) model and the distributions of activation energies of catalytic and non-catalytic pyrolysis over conversion have been compared. The composition of pyro-oil from both catalytic and non-catalytic pyrolysis of waste jute has been compared.

Experimental

Materials

The feed material used for the catalytic and non-catalytic pyrolysis is waste jute, collected from a local market. The particle size of the feed material is 128 mm × 49 mm × 0.6 mm. The results of proximate[4] and elemental analyses of the feed material are shown along with higher heating values and bulk density in the Table 1.

Catalysts

Aluminium Oxide [Al_2O_3], zinc oxide [ZnO], sodium chloride [NaCl], potassium chloride [KCl], sodium aluminosilicate [$NaAl(SiO_3)_2$] procured from Merck, India have been used as catalysts. These chemicals are chosen because many of them have been reported[19,20,23–25] to show catalytic activity on pyrolysis of different biomass. The particle diameter of all catalysts was approximately 0.087 mm. All the catalysts were calcined for 2 h at 120 °C.[26]

Equipment

A muffle furnace (Bhattacharya & Co. India) and a Bomb calorimeter (S. C. Dey & Co. India) were used.

Table 1 The elemental analysis of jute

Proximate analysis % (w/w)	Moisture 10.025	Volatile matter 77.15		Ash 2.59	Fixed carbon 10.235	
Ultimate analysis % (w/w)	C 49.79	H 6.02	O 41.37	N 0.19	Cl 0.05	S 0.05
Heating value (MJ kg^{-1})						18.7
Bulk density (kg m^{-3})						110

Analytical instruments

A CHNSO analyzer (Perkin Elimer), a Thermogravimetric analyzer (PYRIS DIAMOND TG/DTA), SEM [Jeolmake (UK) Model JSM6360], XRD [Model Ultima-III Rigaku make (Japan) Cu target slit 10 mm], Gas Chromatograph/Mass Spectrometer (PerkinElmer SQ8) and BET surface area analyzer [Quantachrome make NOVA 4000e] were used.

Experimental procedure

The isothermal experiments were conducted in a 50 mm diameter and 164 mm long semi-batch pyrolyzer, as described in previous research articles.[4,10] For both catalytic and non-catalytic pyrolysis, the reactor was run isothermally under inert atmosphere maintained by N_2 purging in the temperature range of 673–1173 K. Each run was started with 100 g waste jute and the reactor was operated for 1 h. The volatiles coming out of the pyrolyzer was passed through a series of condensation units, as described in the previous articles.[4,10] The total weight of solid residue and char in the pyrolyzer was recorded continuously using the electronic balance attached with the pyrolyzer. The total condensate collected from all condensation units was weighed. The non-condensable gas was collected in a sampling bottle. The same process was repeated for all runs in case of both non-catalytic and catalytic pyrolysis. The pyro-oil samples were analyzed by GC/MS and the pH was determined. The pyro-char was analyzed by SEM, XRD and BET analyzers. Non-isothermal experiments were conducted with and without the best performing catalyst in the temperature range of 300–900 °C in the TGA set-up. In the thermo gravimetric analyzer, a sample was exposed to a heating program set at different heating rates of 10 °C min^{-1}, 15 °C min^{-1}, 20 °C min^{-1}, 25 °C min^{-1} and 30 °C min^{-1} and the weight loss was simultaneously recorded in a Perkin-Elmer Model. Nitrogen (150 ml min^{-1}) was used to maintain inert atmosphere. In all catalytic experiments, catalysts were thoroughly mixed with jute samples maintaining a ratio of 1 : 10.

Theoretical analysis

Lumped pyrolysis kinetics

Complex reactions in series, parallel or combination of both, occur during pyrolysis of lignocellulosic feed stocks.[4,27] The reaction pathway of non-catalytic and catalytic pyrolysis may be represented as follows:

Non-catalytic:[4]

$$\text{Jute} \rightarrow \text{active} - \text{complex} \xrightarrow[k_c]{k_v} \begin{matrix}\text{volatile}\\ \text{char}\end{matrix} \quad (1a)$$

Catalytic:

$$\text{Jute} + \text{catalyst} \rightarrow \text{active} - \text{complex} \xrightarrow[k'_c]{k'_v} \begin{matrix}\text{volatile}\\ \text{char}\end{matrix} \quad (1b)$$

Assuming the first step of catalytic and non-catalytic reactions to be instantaneous, the rate of change of mass of virgin jute waste, volatile matter and pyro-char during catalytic and non-catalytic pyrolysis are as follows:

$$\frac{dW}{dt} = -kW \quad (1c)$$

$$\frac{dW_v}{dt} = k_v W \quad (1d)$$

$$\frac{dW_c}{dt} = k_c W \quad (1e)$$

where, $k = k_v + k_c$

For catalytic pyrolysis

$$\frac{dW}{dt} = -k'W \quad (1f)$$

$$\frac{dW_v}{dt} = k'_v W \quad (1g)$$

$$\frac{dW_c}{dt} = k'_c W \quad (1h)$$

where, $k' = k'_v + k'_c$

The rate constants k, k_v and k_c and k', k'_v and k'_c have been determined through non-linear regression analysis of experimental data of semi batch pyrolyzer following the method reported by the present researchers in previous articles.[27] For the analysis of data on isothermal pyrolysis, the Arrhenius equation[87] has been attempted to describe the dependencies of rate constants k, k_v, k_c, k', k'_v and k'_c on temperature.

Pyrolysis kinetics using non-isothermal data

The distributed activation energy model (DAEM) has been used for catalytic and non-catalytic pyrolysis to examine the mechanism of reactions occurring under non-isothermal conditions.[22,28–33] As suggested by previous researchers,[22] distributions of activation energy is mainly due to the occurrence of large number of independent parallel and series reactions characterized with different activation energies.[22,28–33] The main reason behind the abnormality of activation energy may be due to the difference in bond strengths of components.[22] Under the present study the Friedman[22a,91] iso-conversional method has been used to analyze the TGA data of catalytic and non-catalytic pyrolysis of waste jute. All the reactions occurring during the experiments were assumed to be of first order irreversible type with Arrhenius type temperature dependency of the rate constants, as followed by the previous researchers.[22,25] The Friedman iso-conversional method is based on the following equation:

$$\alpha_i \left(\frac{dx}{dT}\right)_{x,i} = k_{0_x} \exp\left(-E_x/(RT_{x,i})\right) f(x) \quad (2)$$

where, $T = T_0 + \alpha t$; $x = v/v^*$; v = volatile content; and v^* = effective volatile content; i = ordinal number of a non-isothermal experiment conducted at heating rate α_i.

Using eqn (2)

$$\ln\left(\alpha_i \frac{dx}{dT}\right)_{x,i} = \ln\left(k_{0_x} f(x)\right) - \frac{E_x}{RT_{x,i}} \quad (3)$$

iso-conversion plots of $\ln\left(\alpha_i \frac{dx}{dT}\right)_{x,i}$ against $(-1000/RT)$ at different extent of conversion have been used to determine the values of activation energies and pre-exponential factors at different conversion. The distribution function of activation energies has also been determined by attempting a Gaussian pattern with mean activation energy E_0 and standard deviation σ as follows:[22]

$$f(E) = \frac{1}{\sqrt{2\pi\sigma}} \exp\left[-\frac{(E-E_0)^2}{2\sigma}\right] \quad (4)$$

Results and discussion

Pyrolysis product yield and product characteristics

In Fig. 1 the yields of pyro-oil obtained through isothermal semi batch pyrolysis of jute waste with and without catalysts over 1 h have been plotted as a function of pyrolysis temperature. From the analysis of the patterns of dependence of oil yield on temperature, it appears that the catalytic effect of Al_2O_3 and ZnO are prominent. In case of non-catalytic pyrolysis of jute, the pyro-oil passes through a maximum at 973 K. Same trend is observed in presence of ZnO. The trend of temperature-trajectories of yield of pyro-oil passing through maxima at an intermediate temperature (973 K) may be explained by the fact that although the rate of evolution of volatiles increases at higher temperature, the conversion of higher molecular weight condensable pyro-oil to lower molecular weight non-condensable gaseous components also occurs rapidly at these temperatures. This is also evident from the pattern of temperature trajectories of gas yield from the

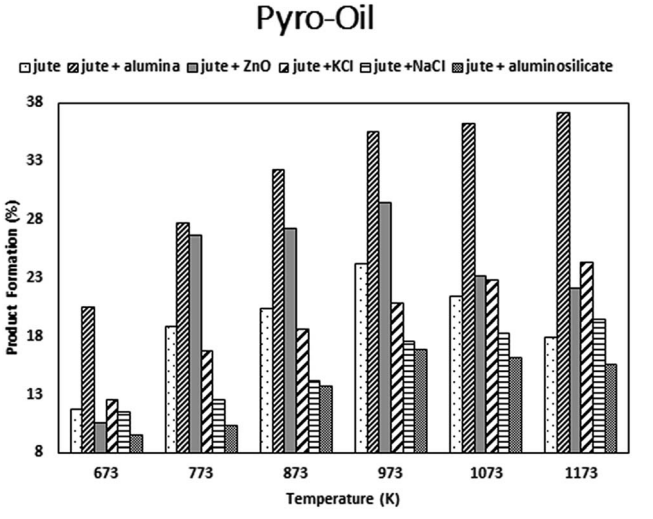

Fig. 1 Yield of pyro oil of jute without and with catalyst at different pyrolysis temperatures.

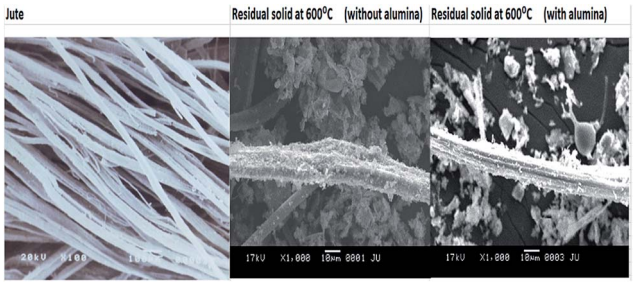

Fig. 2 SEM images of original jute and the solid obtained at 700 °C, with and without alumina.

Table 2 BET specific surface area of bio-char of catalytic and non-catalytic pyrolysis at 600 °C

Pyrolysis process	Specific surface area of char (m^2 g^{-1})
Catalytic	5.144
Non-catalytic	3.143

pyrolysis of jute with and without the same catalysts as represented in Fig. 5.

On the other hand catalytic effect of alumina is very pronounced. In this case yield of pyro-oil increases monotonically even beyond 973 K.

Effects of NaCl and KCl on pyro-oil yield is not very significant and is almost identical. Up to 700 °C, the pyro-oil yield in presence of Na–K additives is a little less compared to that of jute. Similar observation has been obtained by Hoekstra *et al.* during their studies on pyrolysis of pinewood in presence of Na + K catalyst.[24] Oasmaa *et al.* also indicated the decrease in liquid yield during the fast pyrolysis of wood and agricultural residues in presence of Na + K catalysts.[19] Sodium aluminosilicate shows inhibiting effect with respect to pyro-oil formation. This may be due to catalytic effect of sodium aluminate on cracking of pyro-oil or tar.

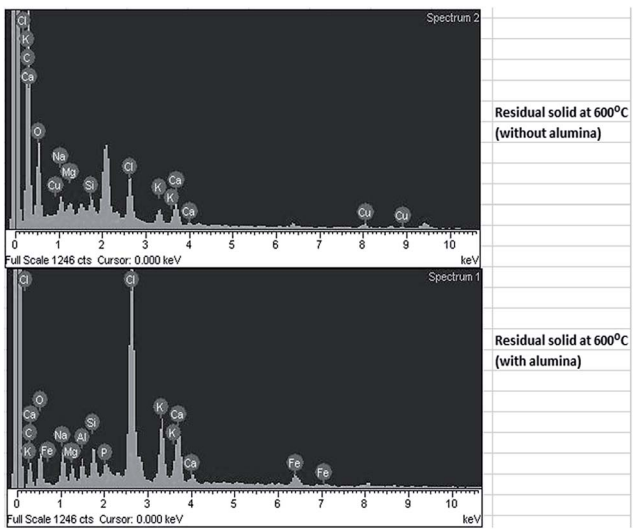

Fig. 3 XRD spectra of solid residue obtained through non-catalytic and catalytic pyrolysis of jute at 600 °C.

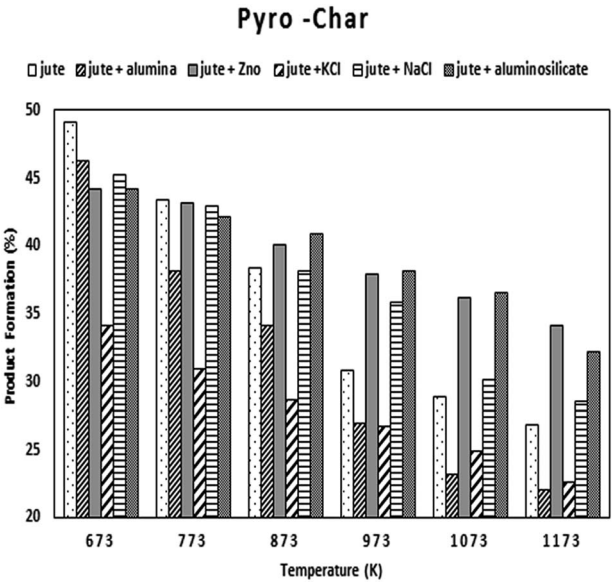

Fig. 4 Yield of pyro char of jute without and with catalyst at different pyrolysis temperatures.

Bed porosity and catalytic effect of alumina

The catalytic effect of alumina increases with the increase in pyrolysis temperature. This may be due to the increase of porosity of reacting solid with temperature, resulting in higher surface area for catalytic reaction. The SEM images of original jute and the solid obtained at 600 °C, with and without alumina, as presented in Fig. 2, distinctly show the increase in porosity in presence of catalyst, elucidating the proposed mechanism of

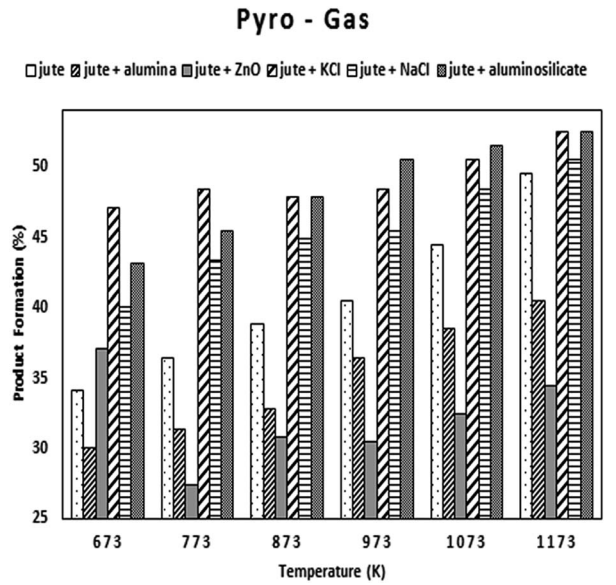

Fig. 5 Yield of pyro gas of jute without and with catalyst at different pyrolysis temperatures.

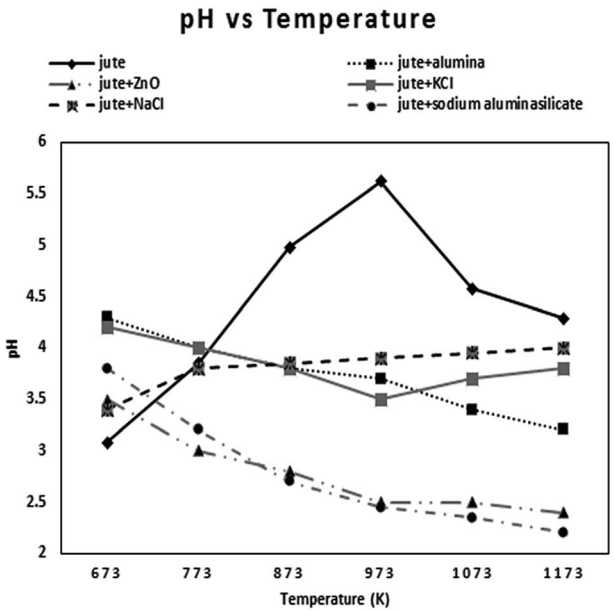

Fig. 6 Dependence of pH of pyro-oil on the temperature of catalytic and non-catalytic pyrolysis.

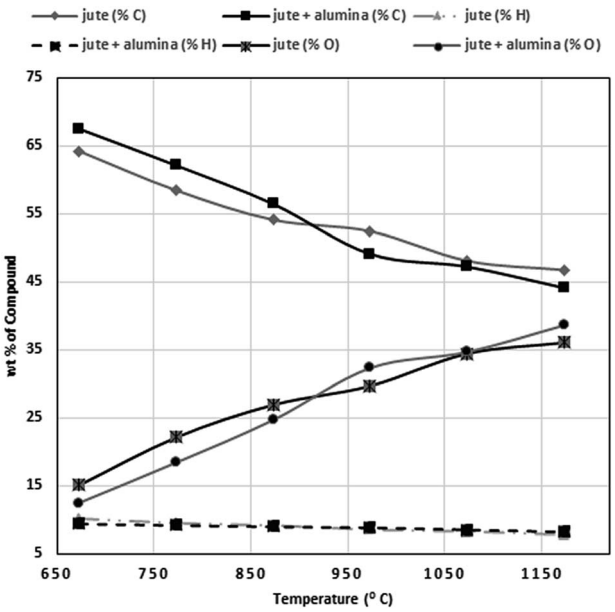

Fig. 7 Wt% of compound is plotted against temperature.

catalytic activity through enhancement of surface area. The values of surface area per unit mass of bio-char obtained through pyrolysis of jute at 600 °C with and without alumina, as determined using BET method, are provided in Table 2. It is also ascertained that the specific surface area of bio-char obtained through catalytic pyrolysis (5.144 $m^2\ g^{-1}$) is higher than that of bio-char of non-catalytic pyrolysis (3.143 $m^2\ g^{-1}$) at the same value of reaction temperature. The specific surface area of bio-char of non-catalytic pyrolysis is comparable to those observed by previous researchers during their studies on pyrolysis of saw dust, wheat and flax straws (<5 $m^2\ g^{-1}$).[88] The presence of alumina on the pyrolyzing solid during catalytic pyrolysis is also established through the comparison of the XRD spectra, represented in Fig. 3, of solid residues of catalytic and non-catalytic pyrolysis. Close observation of the Fig. 4 depicting the pattern of char yield against pyrolysis temperature reveals that for both non-catalytic and catalytic process, there is a monotonous decreasing trend over the entire temperature range. The decreasing trend is sharper in case of Al_2O_3 assisted pyrolysis compared to non-catalytic process. The high catalyzing effect on pyro-oil formation may be the underlying reason to explain this observation.

From Fig. 5 showing the patterns of variation of gas yield with temperature, it is evident that the yield of pyro-gas increases with temperature for both non-catalytic and catalytic

Table 3 Calculated activation energies and frequency factors as per Arrhenius law

Sl. No.	Feed stocks	Reaction rate constant	Activation energy (kJ mol^{-1})	Frequency factor (min^{-1})	Correlation coefficient
1	Jute	k	9.153714	0.216103	0.915
		k_v	7.201587	0.163327	0.901
		k_c	24.74246	0.156609	0.898
2	Jute + alumina	k'	3.5337	0.0545	0.967
		k'_v	4.1361	0.0447	0.968
		k'_c	13.309	0.1330	0.962
3	Jute + ZnO	k'	4.833	0.0566	0.872
		k'_v	8.129	0.5038	0.959
		k'_c	14.392	0.5071	0.945
4	Jute + KCl	k'	5.9087	0.1236	0.963
		k'_v	6.5688	0.1065	0.961
		k'_c	13.5018	0.0189	0.940
5	Jute + NaCl	k'	5.0881	0.1159	0.905
		k'_v	3.0703	0.0704	0.889
		k'_c	16.769	0.1072	0.899
6	Jute + $NaAl(SiO_3)_2$	k'	7.84737	0.0524	0.945
		k'_v	5.5672	0.0241	0.926
		k'_c	21.617	0.0458	0.894

Table 4 GC/MS analysis of the pyro-oil of waste jute

Retention time	Name of compound	Molecular weight	Usage
3.809	1,2,3,6-Tetrahydropyridine-2-carboxylic acid ($C_6H_9NO_2$)	127	As a $GABA_A$ receptor in scientific research[37]
3.939	2-Cyclopenten-1-one (C_5H_6O)	82	As a FEMA GRAS flavouring substance[38]
4.829	Oxirane, 2-ethyl-3-propyl-*cis* ($C_7H_{14}O$)	114	Manufacture of α-amylcinnamaldehyde and lubricant[39]
5.164	1-Silacyclo-2,4-hexadiene (C_5H_6Si)	96	Used as synthetic studies by organic chemists[40]
6.205	1-Ethylcyclopentene (C_7H_{12})	96	Useful compound in organic synthesis[41]
6.365	1*H*-Imidazole,4,5-dihydro-2-methyl ($C_4H_8N_2$)	84	Pharmaceutical use[42]
7.495	Bicyclo [5,3,0] decane ($C_{10}H_{18}$)	138	Industrial solvent[43]
7.650	2-Cyclopenten-1-one,2,3-dimethyl ($C_7H_{10}O$)	110	Building block in organic synthesis[44] Drug for genital or sexual disorder[45]
7.710	Cyclohexanol, 1-ethynyl ($C_8H_{12}O$)	124	Pharmaceutical use[46]
8.135	Pyridine, 5-methyl (C_6H_7N)	94	Isolated from coal tar and synthesized industrially[47]
9.021	l-Limonene ($C_{10}H_{16}$)	136	Cosmetic usage[48] Solvent for cleaning purpose/paint/biofuel[49]
9.231	2-Cyclopenten-1-one,2,3-dimethyl [$(CH_3)_2C_5H_4(=O)$]	110	Not reported
9.616	*p*-Cresol (C_7H_8O)	108	Antioxidant[50] Used as a used to capture and study the species of orchid bee[51]
10.021	Benzene methanol, 4-hydroxyl ($C_7H_8O_2$)	124	Use as a flavorants[52,53]
10.181	Phenol, 2-methoxy ($C_7H_8O_2$)	124	Dermatology and radical polymerization of monomers[54]
10.406	Bicyclo-[2.2.2] octane, 2-methyl (C_9H_{16})	124	Not reported
11.932	5-Methoxyindane ($C_{10}H_{12}O$)	148	Commercial bio-conversion of anethole to more valuable compound[55]
12.577	4-Pentenoic acid, 5-ethoxy, ethyl ester, (*E*)-($C_{11}H_{12}O_2$)	172	Purification purposes[56]
13.212	(*Z*)-4-Methyl-5-(2-oxopropylidene)-5*H*-furan-2one ($C_8H_8O_3$)	152	Use as an intermediate in the preparation of more complex compounds[57]
13.488	(*S*,*S*,*S*,*S*)-1,1′-Bicyyclopentyl-2,2′-dicarboxaldehyde ($C_{12}H_{18}O_2$)	194	Use as a food additive[58]
13.628	2-Cyclopentene-1-acetaldehyde, 2-formyl-, alpha, 3-dimethyl ($C_{10}H_{14}O_2$)	166	Use as an antioxidant for synthetic rubber, polymer and oil derivative[59,60]
14.863	Octadecane, 1-chloro ($C_{18}H_{37}Cl$)	288	Use only in area provided with appropriate exhaust ventilation[61]
15.488	1-Methoxy-2-methyl-4-(methylthio) benzene ($C_9H_{12}OS$)	168	Therapeutic usage[62]
17.249	Phthalic acid, monoethyl ester ($C_9H_8O_4$)	194	Breakdown of glucosinate glucobrassicin[63]
17.824	2-Azetidinone, 1-phenyl (C_9H_9NO)	147	Biomedical usage[64]
21.901	1*H*-1,2,3-Triazole,4-(4-methylphenyl) ($C_3H_6N_4$)	98	For R&D use only[65]

pyrolysis. The catalytic effects of aluminosilicate and NaCl have been observed to be higher compared to others. This may be due to their catalytic effect on secondary tar cracking reactions.

pH of bio-oil

The pH value of the pyro-oil is shown in Fig. 6. For pyro-oil obtained through non-catalytic pyrolysis of jute, the pH passes through a maximum of 5.7 at 973 K beyond which it drops down to 4.5 at 1173 K. Similar observation has also been reported in our previous research article on pyrolysis of jute.[36] For catalytic pyrolysis in presence of Al_2O_3, NaCl and KCl the range of variation of pH is very low (3.5–4.0). On the other hand, the pH decreases from 3.75 and 3.5 at 673 K to 2.5 at 1173 K for aluminosilicate and ZnO respectively. Therefore, it may be inferred that the pyro-oil obtained through catalytic pyrolysis is, in general, more acidic in comparison to that obtained through non-catalytic process. Further investigation should be made to elucidate the fact and precautions should be taken during storage of the catalytic pyro-oil to avoid acidic corrosion.

Lumped kinetic parameters

The lumped kinetic parameters determined using the data of isothermal experiments have been shown in Table 3.

From the analysis of the table, it is evident that the lowering of activation energy is maximum for alumina with respect to the overall pyrolysis reaction. Thus alumina is again proved to be the best performing catalyst.

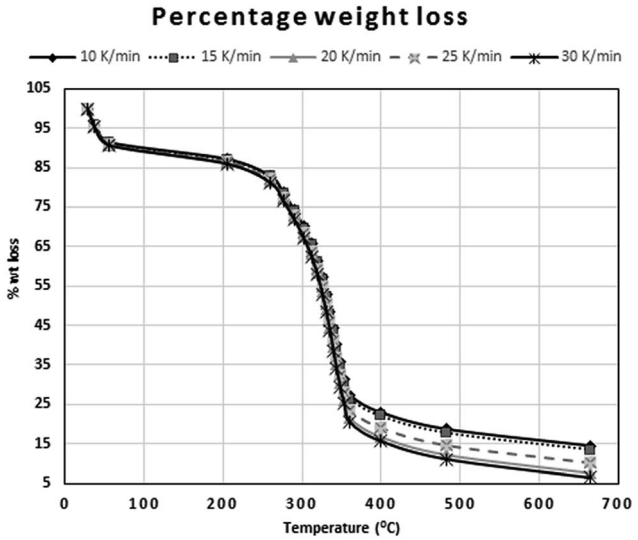

Fig. 8 Percentage of weight residue of jute waste in the temperature range of 30–900 °C at different heating rates (TGA plot).

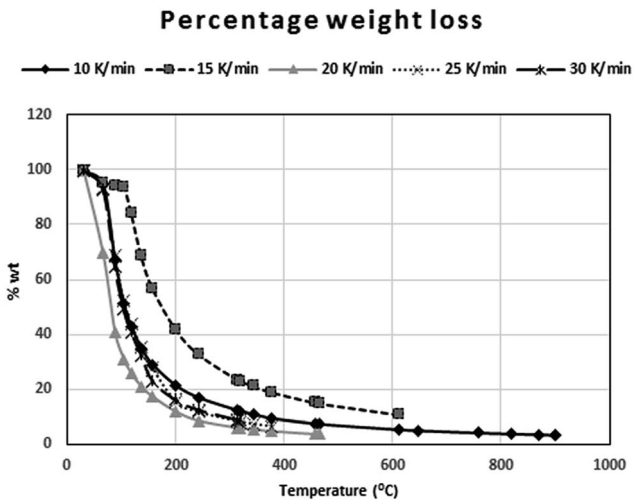

Fig. 9 Percentage of weight residue of jute waste using catalysts in the temperature range of 30–900 °C at different heating rates (TGA plot).

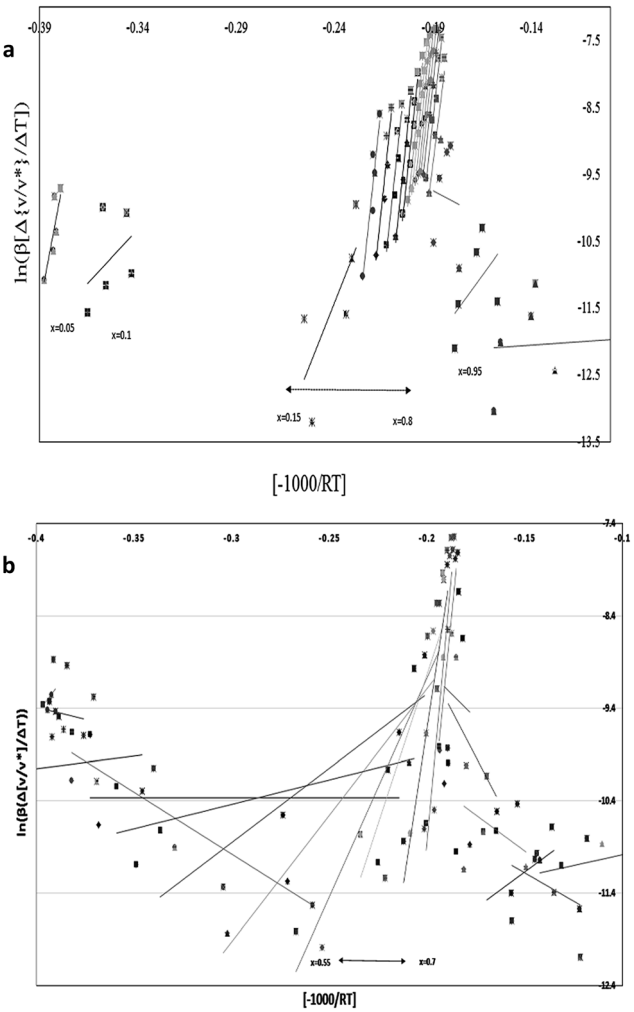

Fig. 10 (a) Plot of $\ln[\alpha_i(dx/dT)_{x,i}]$ *vs.* $(-1000/RT_i)$ at different conversion values from 0.05 to 0.95 for all the heating rates (5–25 K min^{-1}) of jute wastes. (b) Plot of $\ln[\alpha_i(dx/dT)_{x,i}]$ *vs.* $(-1000/RT_i)$ at different conversion values from 0.05 to 0.95 for all the heating rates (5–30 K min^{-1}) of jute wastes using catalysts.

Effects of alumina on C–H–O content of pyro-oil

The elemental, particularly C–H–O, composition of the pyro-oil is a very important criterion from the perspective of its usage as a fuel. While the higher fractions of "C" and "H" in pyro-oil contribute towards increase in heating value of pyro-oil, higher fraction of "O imparts" detrimental properties like low heating value, higher risk of polymerization *etc.* Therefore, the effect of alumina, the best catalyst with respect to the generation of pyro oil from jute pyrolysis, on the C–H–O composition of pyro-oil has been depicted in Fig. 7. From the Fig. 7, it is clear that carbon content of pyro-oil decreases with pyrolysis temperature for both catalytic and non-catalytic reactions. Similar observation has been reported by Yang *et al.*[23] during their work on fast pyrolysis of EHN. Other researchers have also reported similar observations[89,90] during the studies on pyrolysis of paddy husk[91] in the temperature range of 450–600 °C. This may be due to the fact that the non-condensable lower molecular weight gaseous components formed through the cracking of bio-oil at higher temperatures are rich in carbon. The content of carbon is higher for catalytic tar in comparison to non-catalytic one up to 600 °C. Content of hydrogen is not temperature sensitive and is not influenced by the presence of alumina. The weight fraction of oxygen in pyro-oil also increases with pyrolysis temperature. Raza Naqvi[91] also made similar observations during non-catalytic pyrolysis of paddy husk in the temperature range of 450–600 °C. The increase of concentration of 'O' may also be due to the carrying over of elemental carbon with the non-condensable cracked gaseous products, *i.e.*, due to decrease of %C in the bio-oil. From the results of GC/MS analysis of bio-oil at 600 °C, provided in Table 4, it is also clear that many of the constituent compounds contain oxygen in their

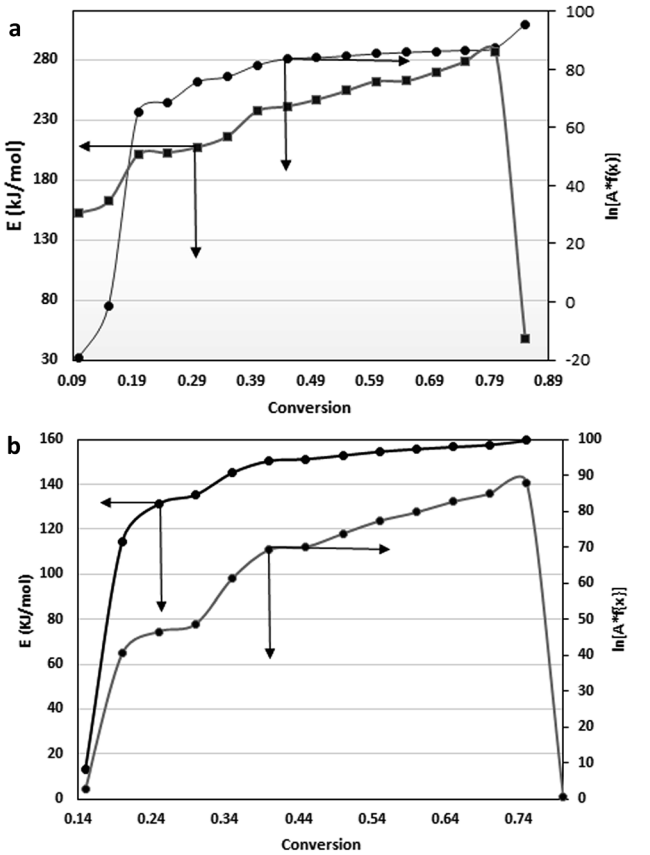

Fig. 11 (a) Plot of E and $\ln[A*f(x)]$ *vs.* conversion for jute waste. (b) Plot of E and $\ln[A*f(x)]$ *vs.* conversion for jute waste using catalyst Al_2O_3.

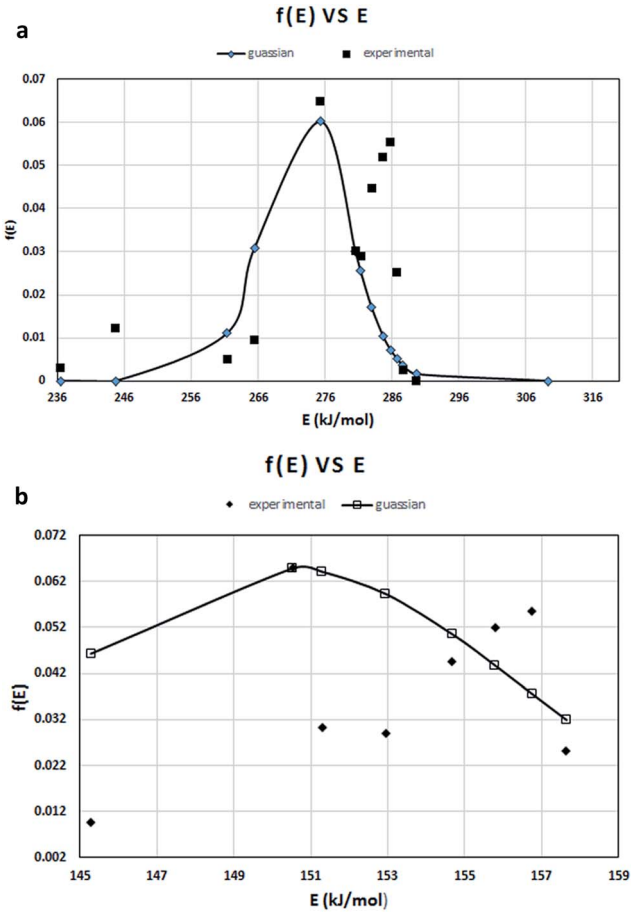

Fig. 12 (a) Plot of $f(E)$ *vs.* E obtained from Friedman differential isoconversion method and Gaussian distribution for non-catalytic pyrolysis of jute waste. (b) Comparison of plot of $f(E)$ *vs.* E obtained from Friedman differential isoconversion method and Gaussian distribution for catalytic pyrolysis of jute waste.

molecules. Further analysis of the stoichiometry of the array of reactions occurring during the primary and secondary pyrolysis may elucidate the exact underlying fact behind the decrease and increase of %C and %O respectively with pyrolysis temperature. Up to 600 °C, the oxygen content in pyro-oil is lowered in presence of catalyst. Overall, alumina shows positive effect on the improvement of elemental composition of pyro-oil up to 600 °C.

TGA plots

Fig. 8 and 9 show the time trajectory of % (w/w) of solid residue (char + unreacted jute) remaining during TGA under non-isothermal conditions using heating rate (10 K min^{-1}, 15 K min^{-1}, 20 K min^{-1}, 25 K min^{-1}, 30 K min^{-1}) as a parameter respectively with and without catalytic compound, namely alumina. From the analysis of the plots it is clearly evident that distinct patterns of weight loss are followed in different temperature ranges. This is true for both catalytic (Al_2O_3) and non-catalytic thermo gravimetric analysis. The presence of several types of components following different pyrolyzing characteristics is probably reflected by these patterns. While the cellulosic and hemi-cellulosic components of jute are thermally decomposed at less severity of temperature, the lignin present in jute is expected to react at higher temperatures corresponding to higher conversion levels.

The comparison of the plots suggests that while in case of non-catalytic process the trajectory may be divided into four zones, namely 30–100 °C, 100–275 °C, 275–350 °C and 350–700 °C, only two distinct zones, namely 30–150 °C and 150–700 °C are present in the catalytic process. The residual solid obtained at each temperature is much less in case of catalytic pyrolysis, as compared to the non-catalytic one. This may be due to pronounced catalytic effect of alumina on the pyrolysis reactions generating condensable and non-condensable volatiles.

Isoconversion plots

In Fig. 10a and b logarithm of $[\alpha_i(dx/dT)_{x,i}]$ has been plotted against $(-1000/RT_i)$ for non-catalytic and catalytic pyrolysis of waste jute respectively. A set of straight lines have been obtained at different values for conversion for both the cases validating the Friedman model with the assumptions of 1st order kinetics and Arrhenius type temperature dependence of rate constants for the pyrolytic reactions.

From the detailed analysis of the figures it is revealed that for non-catalytic pyrolysis parallel lines are obtained in the

Table 5 GC/MS analysis of the pyro-oil derived from catalytic pyrolysis of waste jute

Retention time	Name of compound	Molecular weight	Usage
3.258	Hydrazine, trimethyl- ($C_3H_{10}N_2$)	74	Used in the alkyne zipper reaction[66]
3.313	Silane, butyl trimethyl- ($C_7H_{18}Si$)	130	Use as heaters in rapid solidification[67]
3.353	Silane, trimethyl propyl- ($C_6H_{16}Si$)	116	Used under atmospheric pressure at 0 °C in dichloromethane[68]
4.999	1*H*-Imidazole-4-methanol ($C_4H_6N_2O$)	98	Used in the coordination chemistry[69]
5.054	Cyclopentane, 1-hydroxymethyl-1,3-dimethyl- ($C_8H_{16}O$)	128	As air freshener[70] Froth floatation process for cleaning coal where of 95% MCHM, 4% water and 0.1% 4-methylcyclo hexamethanolmonoether[71]
5.114	Levoglucosenone ($C_6H_6O_3$)	126	Uses hydroxyquinol as a substrate with oxygen to produce 3-hydroxy-*cis*,*cis*-muconate[35,72] Phloroglucinol is mainly used as a coupling agent in printing[35,73] It is useful for the industrial synthesis of pharmaceutical[35,74] and explosive (TATB)[35,75]
6.025	*trans*,*trans* and *trans*,*cis*-1,8-Dimethyl spiro [5,5] undecane ($C_{13}H_{24}$)	180	Pharmacology[76]
6.345	2,2-Dimethyl hex-4-enylamine ($C_8H_{17}N$)	127	Not reported
7.245	*trans*,*cis*-1,8-Dimethyl spiro [4,5] decane ($C_{21}H_{27}ClO_4S$)	166	Not reported
7.620	2-Cyclopenten-1-one, 2,3-dimethyl ($C_7H_{10}O$)	110	Used as an antioxidant for synthetic rubber, polymer and oil derivative[77]
8.145	Pyrimidine, 5-methyl (C_6H_7N)	94	Isolated from coal tar and synthesized industrially[78]
9.016	D-Limonene ($C_{10}H_{16}$)	136	Cosmetic usage Solvent for cleaning purpose/paint/biofuel[79]
9.701	*p*-Cresol (C_7H_8O)	108	Antioxidant[80]
10.026	Silane, tetraethenyl ($C_8H_{12}Si$)	136	Used in plating, important material for producing catalyst, other silver compounds and paste[81]
11.952	1,3,2-Dioxaborolane, 2-phenyl- ($C_8H_9BO_2$)	148	Used to the myocardium[82]
12.252	(*Z*)-4-Methyl-5-(2-oxo propylidene)-5*H*-furan-2-one ($C_8H_8O_3$)	152	Food preparation[83] Pyrolysis oil[84] Bio-fuel derived from woody biomass[85]
13.713	Formic acid, 2,6-dimethoxy phenyl ester ($C_9H_{10}O_4$)	182	Not reported
14.233	Phenol, 2,6-dimethoxy- ($C_8H_{10}O_3$)	154	Not reported
15.488	4-Methoxy-2-methyl-1-methylsulfanyl-benzene ($C_9H_{12}OS$)	168	Not reported
16.709	1-Acetyl-3-(4-pyridyl)-pyrazoline ($C_{10}H_{11}N_3O$)	189	Not reported
17.244	*N*-Nitrosonornicotine ($C_9H_{11}N_3O$)	177	Curing, aging, processing and smoking of tobacco[86]
17.824	2-Propen-1-one, 2-methyl-1-phenyl ($C_{10}H_{10}O$)	146	Not reported
19.170	2-Ethyl-2-phenylaziridine ($C_{10}H_{13}N$)	147	Not reported
20.946	2-Methyl benzyl phosphonic acid ($C_{12}H_{19}O_3P$)	186	Not reported
21.131	5-Phenylisoxazoline (C_9H_9NO)	147	Breakdown of glucosinate glucobrassicin[62]
21.701	*trans*-1-Cyano-2-phenyl cyclopropanol (C_5H_{10})	159	Not reported
22.231	2,5,6-Trimethylbenzimidazole ($C_{10}H_{12}N_2$)	160	Not reported

conversion range of 0.2 to 0.8. For conversion 0.05, 0.1, 0.15, 0.85, 0.9 and 0.95, the straight lines are not parallel. The parallel nature of straight lines indicates a close distribution of activation energies. On the other hand, the non-parallel relationship at lower (0.05–0.15) and higher (0.8–0.95) ranges of conversion clearly indicates the probability of occurrence of pyrolysis reactions, distinctly different from those occurring at the widely spread intermediate (0.2–0.8) conversion level. It is expected that the conversion up to 0.15 represents mostly the removal of moisture and commencement of primary pyrolysis of hemicelluloses and cellulose. On the other hand, at higher (0.8–0.95) conversion levels the pyrolysis of recalcitrant components like

lignin following a pattern, distinctly different from the primary and secondary pyrolysis of cellulosic components in the intermediate conversion ranges, is dominant. On the other hand, for catalytic pyrolysis the parallel straight lines are obtained only for conversion 0.55 to 0.7. This may be due to the random nature of catalytic effect of alumina on pyrolytic reactions of different components, namely cellulose, hemicellulose and lignin. However the catalytic effect on individual reaction may further be investigated.

In Fig. 11a and b, activation energy and $\ln[A*f(x)]$, as obtained from the iso-conversion plots, have been graphed against conversion respectively for non-catalytic and catalytic pyrolysis of waste jute. The patterns of the plots are similar to those reported by Wu *et al.*[22] during the pyrolysis of biomass feedstocks. The lower range of E for catalytic pyrolysis again establishes the positive influence of alumina on pyrolysis of waste jute. The values of the pre-exponential factors for both catalytic and non-catalytic pyrolysis are of the same order, the values of catalytic ones being slightly greater.

Distribution of activation energy

In Fig. 12a and b, $f(E)$ has been plotted against E. The analysis of the figures reveals that although $f(E)$ follows almost a Gaussian distribution where E *vs.* conversion (0.20–0.80) follow linear relationship during non-isothermal pyrolysis of jute waste, no specific distribution is followed for non-isothermal catalytic pyrolysis. While mean value of average activation energy is 276.56 kJ mol^{-1} for non-catalytic pyrolysis, it is only 150.33 kJ mol^{-1} for catalytic pyrolysis, indicating strong catalytic effect of alumina on the overall pyrolysis. When compared to the activation energies of lumped kinetics no parity is observed with those obtained through DAE modelling. Since the pyrolysis is actually a complex combination of reactions causing decomposition of different constituent molecules of a biomass, it is understandable that DAEM kinetics should represent the reality more closely.

GC/MS analysis of pyro-oil

For the qualitative and quantitative characterization of pyro-oil obtained through non-catalytic and catalytic pyrolysis, samples were analyzed with SQ 8 Gas Chromatograph/Mass Spectrometer PerkinElmer,[34] equipped with flame ionization and mass spectrometry detectors (GC-PPC-MS). The compounds present in pyro-oil obtained through non-catalytic and catalytic pyrolysis of jute at 600 °C are represented in Tables 4 and 5. The Tables provide the lists of compounds with their retention times and prospective uses.

From the consultation of the tables, it is clear that many new compounds like D-limonene, decane group, furfural group, propanol group, benzene group, phenol group, cyclopentane, 1-hydroxymethyl-1,3-dimethyl-, with aromatic and aliphatic properties are formed due to the use of alumina. It is also interesting to observe that most of the chemical compounds present in bio-oil may be utilized for different uses. This may make the pyrolysis process more attractive because even if bio-oil is not upgraded through further de-oxygenation, neutralization of acidity *etc.*, before being used as an automobile fuel, it may be used for the production of valuable chemical compounds.

Conclusion

In the present study, catalytic and non-catalytic pyrolysis of jute waste have been studied in the temperature range of 673 K to 1173 K. Alumina has been observed to be the most promising catalyst with respect to pyro-oil yield, deoxygenation and enrichment of carbon content of the oil. The presence of alumina also influences the available specific surface area of bio-char. The specific surface area of bio-char obtained at 600 °C increases from 3.143 to 5.144 $m^2 g^{-1}$ by the catalytic effect of alumina. The %C and %O in pyro-oil decreases and increases respectively with the increase of pyrolysis temperature. However, the values of %C and %O are increased and decreased respectively in presence of alumina. Reaction kinetics for the thermal decomposition of solid reactant, and the formation of volatile and char have been determined using the lumped kinetic model applicable for isothermal operation. DAE model using the Friedman differential isoconversional method has also been followed for the determination of kinetics of non-isothermal pyrolysis with and without alumina. The TGA data of jute wastes with or without catalysts at different heating rates (5–25 K min^{-1}) have been used for this purpose. It has been shown that the activation energies and frequency factors are strongly dependent upon the pyrolytic conversion level of the samples. In case of non-catalytic pyrolysis, the activation energy follows Gaussian distribution over a wide range of conversion. However, no such distribution is followed in case of catalytic pyrolysis, indicating randomness of catalytic effect of alumina. The average activation energy is much lower (150.33 kJ mol^{-1}) for catalytic pyrolysis in comparison to its non-catalytic (276.56 kJ mol^{-1}) counter-part. The chemical composition of the pyro-oil has been analyzed using GC/MS. Catalytic pyrolysis ensures the generation of bio-oil with higher aromatic and aliphatic contents. The compounds present in bio-oil from both catalytic and non-catalytic pyrolysis of waste jute have high potential to be used as valuable chemicals. It is expected that both the lumped and DAE kinetics, particularly the latter one, determined under the present study, will be of great use for design and the prediction of performance of large scale pyrolyzers for jute waste and for similar lignocellulosic wastes.

Acknowledgements

The first author acknowledges the financial support extended by University Grants Commission (UGC) in the form of BSR Fellowship. The technical assistance extended by Ms. Rima Biswas during the experimental work is highly acknowledged. All authors appreciate the co-operation rendered by Indian Association for the Cultivation of Science, Kolkata and Metallurgical and Material Engineering Department, Jadavpur University for their paid technical service for the use of GC/MS and SEM-XRD, TGA respectively. All authors appreciate the technical co-operation rendered by CSIR – CGCRI, Kolkata for

their paid technical service for the use of BET analyzer. Authors are indebted to the learned reviewers for their constructive comments for the improvement of the original manuscript.

References

1 R. Ray, P. Bhattacharya and R. Chowdhury, *Can. J. Chem. Eng.*, 2004, **82**, 566.
2 R. Ray, R. Chowdhury and P. Bhattacharya, *Int. J. Energy Res.*, 2005, **29**, 811.
3 R. S. Antony, S. D. S. Robinson, B. C. Pillai and L. R. C. Lindon, *Res. J. Chem. Sci.*, 2011, **1**(1), 70.
4 R. Chowdhury, S. Poddar and S. De, *APCBEE Proc.*, 2014, **9**, 18.
5 M. Asadullah, M. N. Rahman, M. N. Ali, M. A. Motin, M. B. Sultan, M. R. Alam and M. S. Rahman, *Bioresour. Technol.*, 2008, **99**, 44.
6 M. R. Islam, M. D. NurunNabi and M. N. Islam, *Jurnal Teknologi*, 2003, **38**(A), 75.
7 B. B. Uzun, A. E. Putun and E. Putun, *Bioresour. Technol.*, 2006, **97**(4), 569.
8 O. Onay and O. Mote Kockar, *J. Renewable Energy*, 2003, **18**(15), 2417.
9 S. Yorgun, S. Sensoz and O. M. Kockar, *J. Anal. Appl. Pyrolysis*, 2001, **60**(1), 1.
10 R. Chowdhury and A. Sarkar, *Int. J. Chem. React. Eng.*, 2012, **10**, A67.
11 Lide Cycle Assessment of Jute Products, http://www.jute.com/ecolabel.
12 http://cacp.dacnet.nic.in/ViewReports.aspx?Input=2&PageId=38&KeyId=382.
13 K. D. Maher and D. C. Bressler, *Bioresour. Technol.*, 2007, **98**, 2351–2368.
14 A. Sarkar and R. Chowdhury, *Int. J. Eng. Sci. Res. Technol.*, 2014, **3**(6), ISSN: 2277–9655.
15 D. Brown, M. Gassner, T. Fuchino and F. Marechal, *Appl. Therm. Eng.*, 2009, **29**, 2137.
16 J. van Caneghem, A. Brems, P. Lievens, C. Block, P. Billen, I. Vermeulen, R. Dewil, J. Baeyens and C. Vandecasteele, *Prog. Energy Combust. Sci.*, 2012, **38**, 551.
17 A. V. Bridgwater, *Chem. Eng. J.*, 2003, **91**, 2–3.
18 A. V. Bridgwater, *Biomass Bioenergy*, 2012, **38**, 68.
19 A. Oasmaa, Y. Solantausta, V. Arpiainen, E. Kuoppala and K. Sipila, *Energy Fuels*, 2010, **24**, 1380.
20 I. Fonts, G. Gea, M. Azuara, J. Ábrego and J. Arauzo, *Renewable Sustainable Energy Rev.*, 2012, **16**, 2781.
21 H. S. Fogler, *Elements of Chemical Engineering*, Prentice Hall of India, 1994.
22 (*a*) H. L. Friedman, *J. Polym. Sci., Part C: Polym. Symp.*, 1965, **50**, 183–195; (*b*) W. Wu, J. Cai and R. Liu, *Ind. Eng. Chem. Res.*, 2013, **52**, 14376.
23 H.-M. Yang, S. Appari, S. Kudo, J.-ichiro Hayashi and K. Norinaga, *Ind. Eng. Chem. Res.*, 2015, **54**(27), 6855.
24 E. Hoekstra, R. J. M. Westerhof, W. Brilman, *et al.*, *AIChE J.*, 2012, **58**, 2830.
25 A. Sarkar, B. Mondal and R. Chowdhury, *Ind. Eng. Chem. Res.*, 2014, **53**, 19671.
26 T. S. Nguyen, M. Zabeti, L. Lefferts, G. Brem and K. Seshan, *Bioresour. Technol.*, 2013, **142**, 353.
27 S. Bandhyopadhyay, R. Chowdhury and G. K. Biswas, *Can. J. Chem. Eng.*, 1999, **77**, 1028.
28 D. B. Anthony and J. B. Howard, *AIChE J.*, 1976, **22**, 625.
29 L. Gasparovic, J. Labovsky, J. Markos and L. Jelemensky, *Chem. Biochem. Eng. Q.*, 2012, **26**, 45.
30 T. Mani, P. Murugan and N. Mahinpey, *Ind. Eng. Chem. Res.*, 2009, **48**, 1464.
31 Z. Q. Li, C. L. Liu, Z. C. Chen, J. Qian, W. Zhao and Q. Y. Zhu, *Bioresour. Technol.*, 2009, **100**, 948.
32 J. M. Cai, S. Y. Yang and T. Li, *Bioresour. Technol.*, 2011, **102**, 3642.
33 J. Cai and Y. Chen, *Bioresour. Technol.*, 2012, **103**, 309.
34 Perkin Elmer Clarus 680 GC, 2013, http://global-oceans.org/site/wp- content/uploads/2013/05/Perkin%20Elmer%20Clarus%20680%20GC.pdf.
35 F. Shafizadeh and P. P. S. Chin, *Carbohydr. Res.*, 1977, **58**(1), 79.
36 S. Poddar, R. Biswas, S. De and R. Chowdhury, *IEEE Xplore*, 2014, DOI: 10.1109/pestse.2014.6805290.
37 A. Wahab, U. Heinemann and K. Albus, *Epilepsy Res.*, 2009, **86**(2–3), 113.
38 "2-methyl furan", The Good Scents Company, Retrieved 2008, 08–26.
39 C. Kohlpaintner, M. Schulte, J. Falbe, P. Lappe and J. Weber, *Ullmann'sEncyclopedia of Industrial Chemistry*, Wiley-VCH, Weinheim, 2005, DOI: 10.1002/14356007.
40 J. Santos, M. Contreras and G. Merino, *Chem. Phys. Lett.*, 2010, **496**(1–3), 172.
41 M. E. Squillacote, J. De Fellipis and Q. Shu, *J. Am. Chem. Soc.*, 2005, **127**(45), 15983.
42 M. Y. Kraft, P. M. Kochergin, A. M. Tsyganova and V. S. Shlikhunova, *Pharm. Chem. J.*, 1989, **23**(10), 861.
43 W. M. Haynes, *CRC Handbook of Chemistry and Physics*, ISBN 978–1439820773, CRC Press, Boca Raton, Florida, 2010, 91st edn, pp. 3–134.
44 D. C. Kleinfelter and P. V. R. Schleyer, *Org. Synth.*, 1962, **42**, 79.
45 N. B. Bennett, A. Y. Hong, A. M. Harned and B. M. Stoltz, *Org. Biomol. Chem.*, 2012, **10**, 56.
46 R. S. Kania, *et al.*, US Pat., ID: 6534524, March 18, 2003.
47 T. Kahl, K. -WilfridSchröder, F. R. Lawrence, W. J. Marshall, H. Höke and R. Jäckh, *Ullmann'sEncyclopedia of Industrial Chemistry*, John Wiley & Sons, New York, 2007, DOI: 10.1002/14356007.a02_303.
48 S. D. Banister, S. M. Wilkinson, M. Longworth, J. Stuart, N. Apetz, K. English, L. Brooker, C. Goebel, D. E. Hibbs, M. Glass, M. Connor, I. S. McGregor and M. Kassiou, *ACS Chem. Neurosci.*, 2013, **4**(7), 130403084729007, DOI: 10.1021/cn400035r.
49 T. Maugh, *Science*, 1979, **206**(4422), 1058.
50 P. Butler, *American Philatelist*, 2010, **124**(10), 910.
51 M. Wynnchuk, *J. Histotechnol.*, 1994, (2), 143.
52 H. Fiege, *Ullmann'sEncyclopedia of Industrial Chemistry*, 2000, DOI: 10.1002/14356007.a08_025, ISBN: 3-527-30673-0.

53 N. H. Williams and W. M. Whitten, *Biol. Bull.*, 1983, **164**(3), 355.
54 C. F. H. Allen and J. W. Gates Jr, *Organic Syntheses Collective*, 1955, **3**, 418.
55 L. J. Esposito, K. Formanek, G. Kientz, F. Mauger, V. Maureaux, G. Robert and F. TruchetKirk-Othmer, *Encyclopedia of Chemical Technology*, John Wiley & Sons, New York, 4th edn, 1997, vol. 24, p. 812.
56 R. Flower, H. P. Rang, M. M. Dale and J. M. Ritter, *Rang & Dale's Pharmacology*, Churchill Livingstone, Edinburgh, 2007, ISBN: 0-443-06911-5.
57 P. R. Ashurst, *Food flavourings*, Springer, 1999, p. 460, ISBN: 978-0-8342-1621-1.
58 R. G. Ackman, W. H. Brown and G. F. Wright, *J. Org. Chem.*, 1955, **20**(9), 1147.
59 S. Tanaka and H. Tomokuni, *J. Heterocycl. Chem.*, 1991, **28**(4), 991.
60 C. W. Wilson III, *J. Food Sci.*, 1970, **35**(6), 766.
61 C. C. C. R. De Carvalho and M. M. R. Da Fonseca, *Food Chem.*, 2006, **95**(3), 413.
62 Q. Chena, T. Chen, D. Wang, H.-B. Liu, Yu-L. Li and Li-J. Wan, *Proc. Natl. Acad. Sci. U. S. A.*, 2010, **107**(7), 2769.
63 http://www.efsa.europa.eu/sites/default/files/scientific_output/files/main_documents/4066.pdf.
64 N. Agerbirk, M. Vos, J. H. Kim and G. Jander, *Phytochem. Rev.*, 2008, **8**, 101.
65 N. I. Park, J. K. Kim, W. T. Park, J. W. Cho, Y. P. Lim and S. U. Park, *Mol. Biol. Rep.*, 2010, **38**(8), 4947.
66 http://www.bidepharmatech.com/files/document/B_COA_MSDS/MSDS-BD183791.pdf.
67 C. A. Brown and A. Yamashita, *J. Am. Chem. Soc.*, 1975, **97**(4), 891.
68 B. R. Dorfman and Portsdaen, *US Pat.*, Pub no: 2006/0005900 A1, Jan 12, 2006.
69 M. P. Doyle and M. S. Shanklin, *Organometallics*, 1993, **12**, 11.
70 M. B. Sanders, J. C. Farrokh, J. Hardie and B. C. Chan, *Acta Crystallogr., Sect. E: Struct. Rep. Online*, 2013, **69**, o1151.
71 Y. Nagamura, Y. Satoh, J. Tatsumi and K. Yamamura, European Patent Application EP1090902, April 11, 2001.
72 R. D. Christie, R. J. Fortin and A. E. Gross, *US pat.*, 4915825, published 1990, assigned to Nalco Chemical Company.
73 A. Mahadevan and W. Hopper, *Biodegradation*, 1997, **8**(3), 159.
74 https://en.wikipedia.org/wiki/Phloroglucinol.
75 Intermediate Pharmaceutical Ingredients – Flopropione, Univar Canada, Retrieved 24 April 2009.
76 Synthesis of trinitrophloroglucinol, The United States Patent and Trademark Office, 1984, Retrieved 24 April 2009.
77 P. Vallance and T. G. Smart, *Br. J. Pharmacol.*, 2006, **147**(1), S304.
78 S. Shimizu, N. Watanabe, T. Kataoka, T. Shoji, N. Abe, S. Morishita and H. Ichimura, *Ullmann'sEncyclopedia of Industrial Chemistry*, John Wiley & Sons, New York, 2007.
79 Limonene, http://cosmeticsinfo.org.
80 http://richestgroup.en.alibaba.com/product/60255540405-800893226/C8H12Si_97_.html.
81 http://img.alfa-chemistry.com/msds/msds_4406-72-8.pdf.
82 N. J. Walton, M. J. Mayer and A. Narbad, *Phytochemistry*, 2003, **63**(5), 505.
83 J. H. van Ness, *Kirk-OthmerEncyclopedia of Chemical Technology*, John Wiley & Sons, New York, 3rd edn, 1983, vol. 23, p. 704.
84 http://ethesis.nitrkl.ac.in/5346/1/211CH1036.pdf.
85 http://www.pnnl.gov/main/publications/external/technical_reports/PNNL-23053.pdf.
86 B. Siminszky, L. Gavilano, S. W. Bowen and R. E. Dewey, *Proc. Natl. Acad. Sci. U. S. A.*, 2005, **102**(41), 14919.
87 O. Livenspiel, *Chemical Reaction Engineering*, John Wiley & Sons, 3rd edn, 2001.
88 R. Azargohar, S. Nanda, J. A. Kozinski, A. K. Dalai and R. Sutarto, *Fuel*, 2014, **125**, 90–100.
89 T.-S. Kim, S. Oh, J.-Y. Kim, I.-G. Choi and J. W. Choi, *Energy*, 2014, **68**, 437–443.
90 H.-M. Yang, S. Appari, S. Kudo, J.-I. Hayashi and K. Norinaga, *Ind. Eng. Chem. Res.*, 2015, **54**(27), 6855–6864.
91 S. R. Naqvi, Y. Uemura and S. B. Yusup, *J. Anal. Appl. Pyrolysis*, 2014, **106**, 57614.

Journal of Advances in Mechanical Engineering and Science, Vol. 1(1) 2015, pp. 12-19

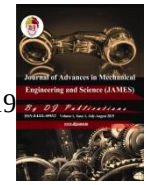

RESEARCH ARTICLE

Analysis of Tar by Catalytic Pyrolysis of Waste Jute

Sourav Poddar[1], Rima Biswas[1], Sudipto De[2] ,*Ranjana Chowdhary[1]
[1]Dept. of Chemical Engineering, Jadavpur University, Kolkata, India
[2]Dept. of Mechanical Engineering, Jadavpur University, Kolkata, India

Received-21 May 2015, Revised-25 June 2015, Accepted-8 August 2015, Published-8 August 2015

ABSTRACT

Catalytic pyrolysis involves the production of upgraded liquids in a single step within short residence times. In the present study the catalytic pyrolysis of jute has been investigated using a cylindrical semi-batch pyrolyzer made of stainless steel under both isothermal condition and within the temperature range of 400^0C to 900^0C in an inert N2 atmosphere. Aluminium Oxide (Al_2O_3) was used as the catalyst. Alumina was pre-calcined at 120ºC for 2 hr in muffle furnace before being used in the reactor. Catalyst and jute were mixed directly in the ratio of 1:10. The use of Al_2O_3 catalyst led to higher tar yield and phenolic compounds in the liquid product. The chemical composition of the pyro – oil was analyzed by Fourier Transform Infrared spectroscopy to identify the basic compositional groups and Gas Chromatography/Mass Spectrometry to quantify the components. The energy yield of the pyro-oil has been calculated.

Keywords: Aluminum oxide, Productyiel, Pyrolysis kinetic, Pyrolysis, Energy yield, FTIR, GC/MS, Jute.

1. INTRODUCTION

In recent years biomass is considered to be a major source of renewable energy and takes part in climate change mitigation and energy security context. Biomass feed stocks like agricultural residues [1], municipal solid wastes[2],vegetable wastes[3], textile disposals [4] and energy crops have attracted great attention as renewable energy sources. Pungam oil cakes [5], jute waste [6],[7], soya bean [8], rape seed [9], sunflower oil cake [10], cotton [11] are used as renewable energy sources. Energy can be engendered from biomass through thermochemical conversion processes like combustion, pyrolysis, gasification etc. Pyrolysis is the thermochemical decomposition of organic materials at elevated temperatures in the absence of oxygen to produce solid char, liquid tar, and gases. Catalytic pyrolysis involves the production of upgraded liquids in a single step within short residence times. [12] investigated spruce wood pyrolysis in presence of seven mesoporous catalysts. The increased trend of gas yield and the aqueous part of tar yield has been observed in case of each catalytic experiment, but in case of char yield not so much changes has been observed in case of catalytic and non-catalytic experiment. [13] observed that the change in the composition of the volatiles is produced by the catalytic pyrolysis of biomass.[14] investigated the effect of hydrothermal pretreatment of biomass, the product yield and composition of bio-oil which is produced from the flash pyrolysis of the biomass. They have also reported the effect of catalytic up-gradation of pyrolysis vapours derived from the biomass. In the present work catalytic pyrolysis kinetics of jute in the temperature range of 400^0C to 900^0C in an inert N2 atmosphere decreases the activation energy. The use of Al_2O_3 catalyst led to higher tar yield and phenolic compounds are increased in the liquid products compared to non-catalytic pyrolysis. The simulated results of the model were compared with the experimental results satisfactorily.

*Corresponding author. Tel.: +919830359430
Email address: mranjana.juchem@gmail.com (R.Choudhary)
Double blind peer review under responsibility of DJ Publications
http://dx.doi.org/10.18831/james.in/2015011002

2. MATERIAL AND METHODS

2.1. Materials

The feedstock used for the investigations was jute. The density and energy appease in jute [6], [7] is higher than some woods available in the world. The volatile fraction and carbon gratify in jute is higher than many agricultural biomass. Both proximate analyses and ultimate analyses of the feed material were carried out and the analytical conclusions have been shown in table 1 along with the heating value and the bulk density of the feed material.

Table 1.The attributes of jute

Proximate Analysis	Moisture	Volatile Matter	Ash	Fixed Carbon
% (W/W)	3.1	78	23	0.62

Ultimate Analysis	C	H	O	N	Cl	S
% (W/W)	49.79	6.02	41.37	0.19	0.05	0.05

Heating value (MJ /kg)	19.7
Bulk Density (gm/ml)	0.11

2.2. Catalytic materials

The catalytic material used for these experiments is Aluminium Oxide (Al_2O_3) [14]. It was previously calcined at 120ºC for 2 hrs in a muffle furnace. It has a relatively high thermal conductivity (30 Wm−1K−1).

2.3. Equipment and Experimental Set-Up

The pyrolysis of jute sample has been done by following the procedure described in [6].

3. Theoretical Analysis

3.1Pyrolysis Kinetics

Pyrolysis of lignocellulosic materials ensues by the complex reactions in series, parallel or combination of both. [15], [16]. The reaction pathway of pyrolysis has been given below:

$$Jute + Catalyst \rightarrow Active\ Complex \xrightarrow{k_v} Volatile \xrightarrow{k_c} Char \quad (3.1)$$

Therefore,

$$\frac{dW}{dt} = -kW \quad (3.2)$$

$$\frac{dW_V}{dt} = -k_v W \quad (3.3)$$

$$\frac{dW_c}{dt} = -k_c W \quad (3.4)$$

where $k = k_v + k_c$

The rate constants k, kv and kc have been determined through non-linear regression analysis of experimental data of captive sampling experiments following the methods described by [11]. The frequency factors and activation energies are given in table 2.The analysis is shown in equations (3.1),(3.2),(3.3), (3.4) and (3.5).

Table 2.The Activation energies and frequency factors of the experiment

	A	E
K	0.863898	34.77414
K_v	1.231952	40.44761
K_c	0.027223	16.8558

3.2. Energy Yield

The energy yield of pyro–oil obtained at different pyrolysis temperatures have been determined using the following correlation,

$$Energy\ Yield(\%) = \frac{w_l \times C_{V_{oil}}}{C_{V_{biomass}}} \times 100 \quad (3.5)$$

where, w_l = yield (weight fraction) of pyro – oil

CVoil= Calorific Value of pyro – oil (MJ/Kg)

CVbiomass= Calorific Value of jute (MJ/Kg)

4. RESULTS AND DISCUSSION

4.1. Trend of pyrolysis product yield and product characteristics

From the analysis of experimental data, it was observed in Figure B1 that yield of char is increased at 973 K. From 1073 K to 1173K it remained constant. The yield of tar is maximum at 1173K. On the other hand yield of gas is maximum at 873 K. From 1073 K to 1173 K it remained constant.

The use of Al_2O_3 catalyst led to higher tar forgo and phenolic compounds are increased in liquid products compared to non-catalytic pyrolysis. Catalytic pyrolysis involves the production of upgraded liquids in a single step within short residence times. The simulated results of the model were compared with the experimental eventuates satisfactorily.

4.2. Energy Yield

The values of energy yield of pyro – oil have been plotted against temperature in figure 1. From the analysis of the figure it shows that the increase in co-pyrolysis temperature results in the increase of energy yield with respect to pyro-oil. It is due to the fact that with the increase of co-pyrolysis temperature the tar becomes richer in carbon which leads to the increase in specific energy content.

4.3. Fourier Transform Infrared Spectroscopy (FTIR) Analysis of jute Tar

The functional groups of the pyro – oil obtained at temperature of 700OC or 973K was estimated by Fourier Transform Infrared (FTIR) spectroscopy to classify the basic compositional classes shown in figure B2.

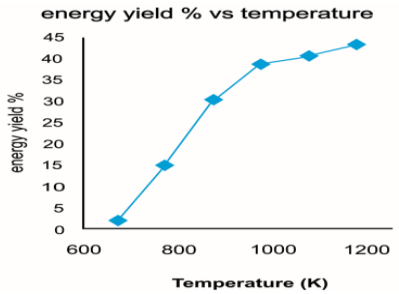

Figure 1.Energy yield variation with temperature change

Based on the FTIR results, the functional groups and the indicated composition of the liquid products are bestowed in table 3.

From the close analysis of the table, it appears that the bio-oil is highly oxygenated as indicated by the predominance of oxygenated functional groups namely O – H; C=O; C – O and aromatic compounds. This is also established by the elemental composition (not shown) and the acidic nature, indicated by low value of pH. The high fraction of oxygenated compounds causes the lowering of calorific value of the oil, particularly due to the presence of C=O bonds which do not release energy during combustion [18]. The presence of hydrocarbon groups C – H; C = C; and alcohols reveals that the liquid have a potential to be used as sustenance. The results of FTIR analysis is comparable to those obtained by [6], [17] during their studies on pyrolysis of wastes.

4.4. Pyrolysis GC/MS

The qualitative classification and quantitative computation of the pyro-oil, which embodies the volatile and semi volatile components was analyzed by SQ 8 Gas Chromatograph/Mass Spectrometer[19], equipped with flame ionization and mass spectrometry detection (GC-PPC-MS). The following figure B3 along with table A1 depicts the formation of the compounds along with the retention times.

Table 3.FTIR functional groups and the indicated compounds of jute Tar.

Frequency Range (cm^{-1})	Groups	Class of compounds
3600 – 3200	O – H stretching	Polymeric O – H
3050 – 2800	C – H stretching	Alkanes
1775 – 1650	C = O stretching	Ketones, Aldehydes, Carboxylic acids
1680 – 1575	C ≡ C stretching	Alkenes
1550 – 1475	$-NO_2$ stretching	Nitrogenous compounds
1490 – 1325	C – H stretching	Alkanes
1300 – 950	C – O stretching, O – H bending	Primary, Secondary and Tertiary alcohols Phenols, esters, ethers
900 – 650	-	Aromatic compunds
900 – 650	-	Aromatic compunds

5. CONCLUSION

In the present investigation, catalytic pyrolysis of jute has been studied in the temperature range of 400^{0}C to 900^{0}C in the presence of Aluminum Oxide (Al_2O_3). Tar yield is much higher when used with catalyst compared to using without catalyst. The fraction of oxygen decreases in the bio-oil which is also termed as pyro-oil, with the application of suitable catalysts. The chemical configuration of pyro – oil was cross checked by FTIR and GC/MS. Catalytic pyrolysis improved the production of upgraded liquids in a single step within short residence times.

REFERENCES

[1] Michael Halwache, Gerhard Kampichler, Hermann Hofbauer, Low temperature Pyrolysis of Agricultural Residues – First Result of a Pilot Plant, International Conference on Polygeneration Strategies, 2009.

[2] Michael Becidan, Experimental Studies on Municipal Solid Waste and Biomass Pyrolysis, Ph.D. Thesis, Norwegian University, May 2007.

[3] Ruby Ray, Pinaki Bhattacharya and Ranjana Chowdhury, Simulation and Modelling of Vegetable Market Wastes Pyrolysis under Progressive Deactivation Condition, The Canadian Journal of Chemical Engineering, Vol. 82, No. 3, 2004, pp. 566-579, http://dx.doi.org/10.1002/cjce.5450820317.

[4] R.Miranda, C.Sosa Blanco, D.Bustos-Martinez, C.Vasile, Pyrolysis of Textile Wastes: I Kinetics and Yields, Journal of Analytical and Applied Pyrolysis, Vol. 80, No. 2, 2007, pp. 489-495, http://dx.doi.org/10.1016/j.jaap.2007.03.008.

[5] Raja S. Antony, Smart.D.S.Robinson, B.C.Pillai and Lee Robert C.Lindon, Parametric Studies on Pyrolysis of Pungam Oil Cake in Electrically Heated Fluidized Bed Reactor, Research Journal of Chemical Science, Vol.1, No. 1, 2011, pp. 70-80.

[6] R.Chowdhury, S.Poddar, S.De, Kinetic Modelling of Non – Catalytic Pyrolysis of Waste Jute in a Fixed Bed Pyrolyzer, APCBEE Procedia, Vol. 9, 2014, pp. 18-24, http://dx.doi.org/10.1016/j.apcbee.2014.01.004.

[7] M.Asadullah, M.N.Rahman, M.N.Ali, M.A.Motin, M.B.Sultan, M.R.Alam, M.S.Rahman, Jute Stick Pyrolysis for Bio-Oil Production in Fluidized Bed Reactor, Bioresource Technology, Vol. 99, No.1, 2008, pp. 44-50, http://dx.doi.org/10.1016/j.biortech.2006.12.002.

[8] Basak Burcu Uzun, Ayse Eren Putun, Ersan Putun, Fast Pyrolysis Of Soybean Cake: Product Yield And Compositions, Bioresource Technology, Vol. 97, No. 4, 2006, pp. 569-579, pp. 569-576, http://dx.doi.org/10.1016/j.biortech.2005.03.026.

[9] Oztem Onay and O.Mote Kockar, Slow,Fast and Flash Pyrolysis of Rapeseed, Renewable Energy, Vol. 28, No. 15, 2003, pp. 2417-2433, http://dx.doi.org/10.1016/S0960-1481(03)00137-X.

[10] S.Yorgun, S.Sensoz, O.M.Kockar, Flash Pyrolysis of Sunflower Oilcake for Production of Liquid Fuels, Journal of Analytical and Applied Pyrolysis, Vol. 60, No. 1, 2001, pp.1-12, http://dx.doi.org/10.1016/S0165-2370(00)00102-9.

[11] R.Chowdhury, A.Sarkar, Reaction Kinetics and Product Distribution of Slow Pyrolysis of Indian Textile Wastes, International Journal of Chemical Reactor engineering, Vol.10, No.1, 2012, http://dx.doi.org/10.1515/1542-6580.2662.

[12] Judit Adam, Eleni Antonakou, Angelos Lappas, Michael Stöcker, Merete H. Nilsen, Aud Bouzga, Johan E. Hustad, Gisle Oye, In Situ Catalytic Upgrading of Biomass Derived Fast Pyrolysis Vapours in a Fixed Bed Reactor Using Mesoporous Materials, Microporous and Mesoporous Materials, Vol. 96, No. 1–3, 2006, pp. 93-101, http://dx.doi.org/10.1016/j.micromeso.2006.06.021.

[13] Richard French, Stefan Czernik, Catalytic Pyrolysis of Biomass for Biofuels Production, Fuel Processing

Technology, Vol. 91, No.1, 2010, pp. 25-32, http://dx.doi.org/10.1016/j.fuproc.2009.08.011.

[14] S. Stephanidis, C. Nitsos, K. Kalogiannis, E.F. Iliopoulou, A.A. Lappas, K.S. Triantafyllidis, Catalytic Upgrading of Lignocellulosic Biomass Pyrolysis Vapours: Effect of Hydrothermal Pre-Treatment of Biomass, Catalysis Today, Vol. 167, No. 1, 2011, , pp 37-45, http://dx.doi.org/10.1016/j.cattod.2010.12.049.

[15] S.Bandhyopadhyay, R.Chowdhury, G.K.Biswas, Thermal deactivation studies of coconut shell pyrolysis, The Canadian Journal of Chemical Engineering, Vol. 77, No. 5, 1999, pp. 1028-1036, http://dx.doi.org/10.1002/cjce.5450770533.

[16] Fred Shafizadeh, Peter P.S. Chin, Preparation Of 1,6-Anhydro-3,4-Dideoxy-B-D-Glycero-Hex-3-Enopyranos-2-Ulose (Levoglucosenone) and Some Derivatives Thereof, Carbohydrate Research, Vol. 58, No. 1, 1977, pp. 79-87, http://dx.doi.org/10.1016/S0008-6215(00)83406-0.

[17] Aparna Sarkar, Sangeeta Dutta, Ranjana Chowdhury, Mustard Press Cake Pyrolysis and Product Yield Characterization, International Journal of Scientific & Engineering Research, Vol. 4, No. 8, 2013.

[18] Mohammad Rofiqul Islam, MD. Nurun Nabi and Mohammad Nurul Islam, "The Fuel Properties of Pyrolytic Oils Derived from Carbonaceous Solid Wastes in Bangladesh", Jurnal Teknologi, Vol. 38, No. A, 2003, pp. 75–89, http://dx.doi.org/10.11113/jt.v38.484.

[19] PerkinElmerClarus680GC,2013.http://globaloceans.org/site/wpcontent/uploads/2013/05/Perkin%20Elmer%20Clarus%20680%20GC.pdf.

APPENDIX A

Table A1.GC/MS analysis of the bio-oil

Retention Time (min)	Name of compound	Molecular Weight (g/mol)
3.258	Hydrazine, Trimethyl-	74
3.313	Silane, Butyl Trimethyl -	130
3.353	Silane, Trimethyl propyl -	116
4.999	1H –Imidazole – 4 - methanol	98
5.054	Cyclopenteane, 1 – Hydroxymethyl - 1,3 – dimethyl -	128
5.114	Levoglucosenone	126
6.025	Trans, Trans and trans, Cis - 1,8 – Dimethyl spiro [5,5] undecane	180
6.345	2,2 – Dimethyl hex – 4 - Enylamine	127
7.245	Trans, Cis -1,8 – Dimethyl spiro [4,5] Decane	166
7.620	2 – cyclopenten -1- one, 2,3 - dimethyl	110
8.145	Pyrimidine, 5 – methyl	94
9.016	D - limonene	136
9.701	p-cresol	108
10.026	Silane, Tetraethenyl	136
11.952	1,3,2 – Dioxaborolane, 2 – phenyl-	148
12.252	(Z) – 4- Methyl – 5 – (2-oxo propylidene) – 5H – Furan – 2 – one	152
13.713	Formic acid, 2,6 – dimethoxy phenyl ester	182
14.233	Phenol, 2, 6 – Dimethoxy -	154
15.488	4-methoxy – 2-methyl – 1-(methylthio) benzene	168
16.709	1- acetyl – 3 – (4 – pyridyl) - pyrazoline	189
17.244	N-nitrosonornicotine	177
17.824	2 - propen -1 – one, 2 – methyl – 1 – phenyl	146
19.170	2 – ethyl – 2 - phenylaziridine	147
20.946	2 – methyl benzyl phosphonic acid	186
21.131	5 - phenylisoxazoline	147
21.701	Trans – 1 – cyano – 2 – phenyl cyclopropanol	159
22.231	2,5,6 - trimethylbenzimidazole	160

APPENDIX B

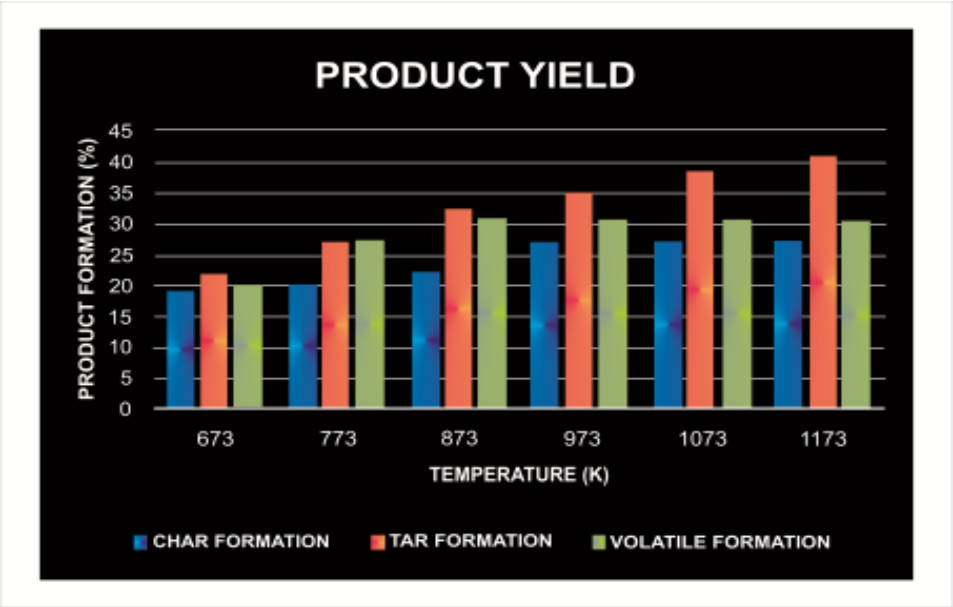

Figure B1.Catalytic Pyrolysis and product characterisation

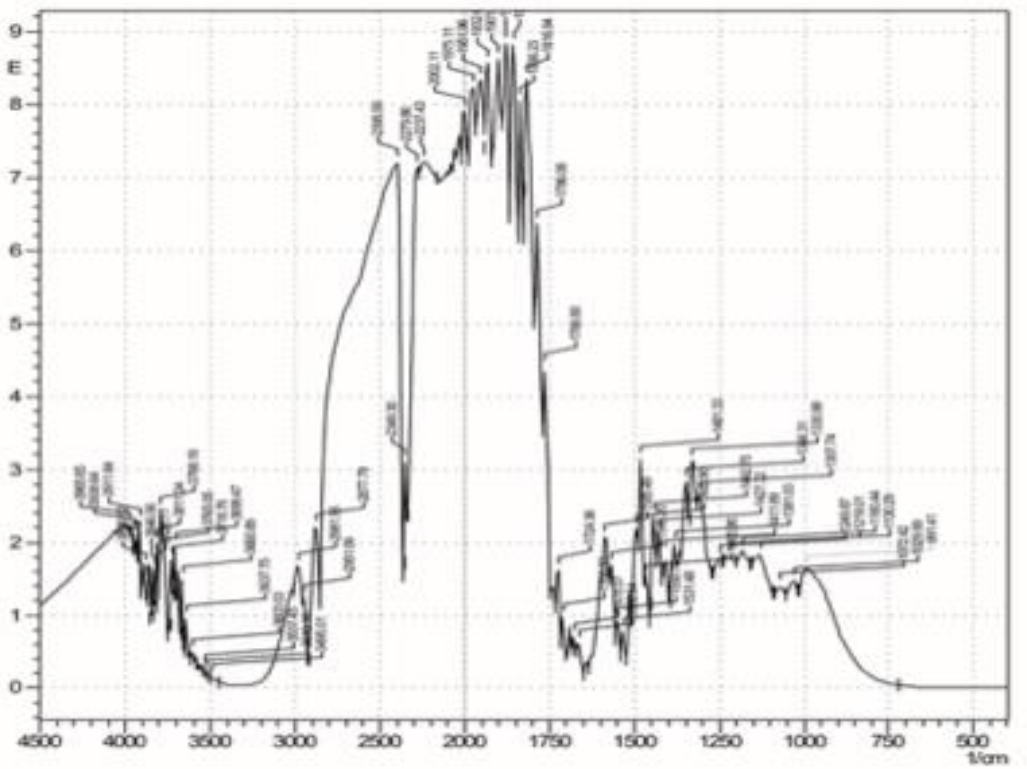

Figure B2.FTIR investigation of pyrolysis of jute at 7000C or 973K.

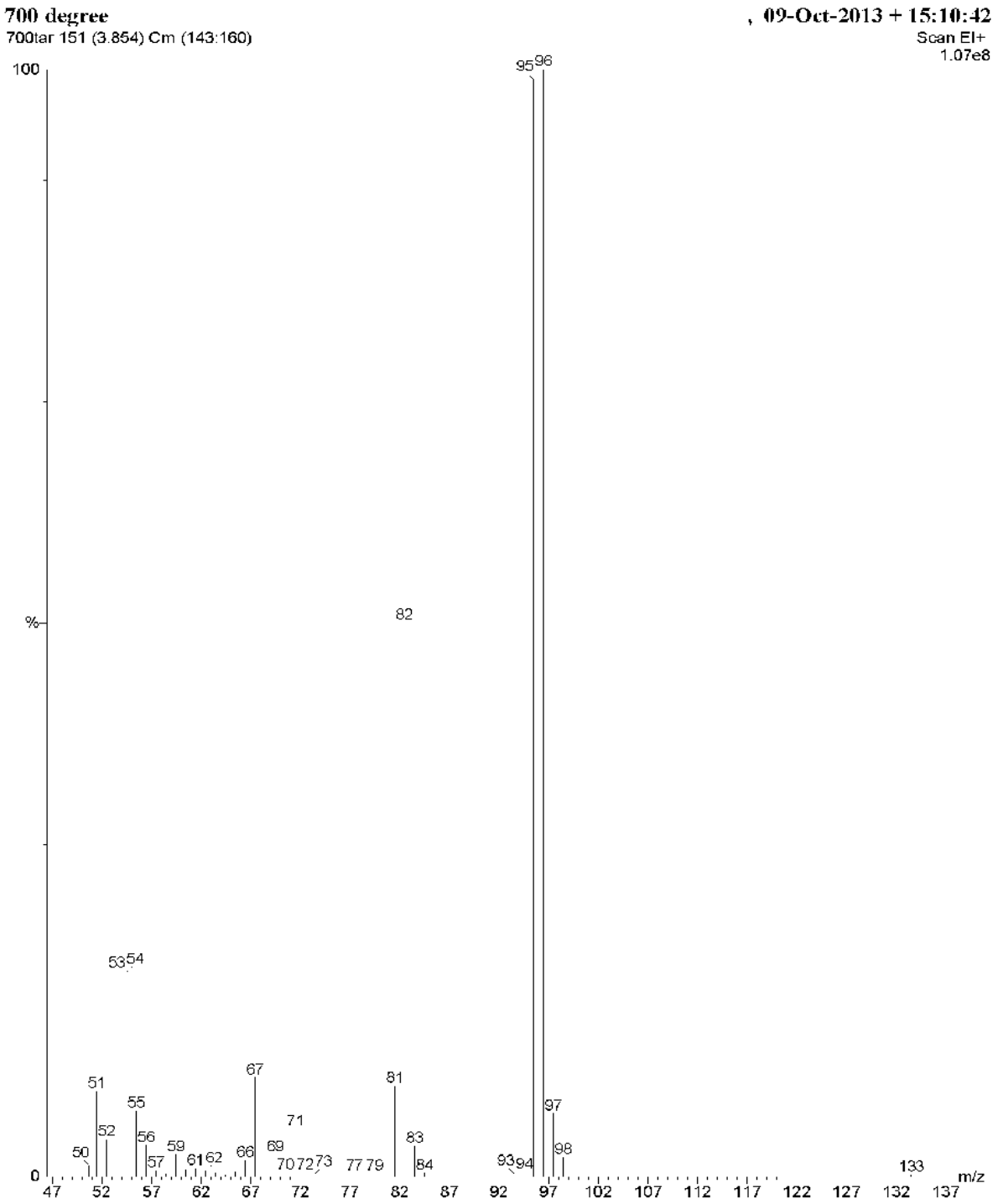

Figure B3.Chromatogram of the Product

Available online at www.sciencedirect.com

ScienceDirect

APCBEE Procedia 9 (2014) 18 – 24

Procedia APCBEE

www.elsevier.com/locate/procedia

2013 5th International Conference on Chemical, Biological and Environmental Engineering (ICBEE 2013)
2013 2nd International Conference on Civil Engineering (ICCEN 2013)

Kinetic Modelling of Non – Catalytic Pyrolysis of Waste Jute in a Fixed Bed Pyrolyzer

R. Chowdhury[a,*], S. Poddar[a] and S. De[b]

[a] *Chemical Engineering, Jadavpur University, 188, Raja Subodh Chandra Mullick Road, kolkata and 700032, India*
[b] *Mechanical Engineering, Mechanical Engineering, 188, Raja Subodh Chandra Mullick Road, kolkata and 700032, India*

Abstract

Waste jute has been investigated as an alternative feedstock for the generation of liquid and gaseous fuel through non – catalytic pyrolysis in a fixed bed reactor. Kinetic parameters for the pyrolysis of jute wastes have been determined in the temperature range of 400 – 900°C. A fixed bed reactor model has been developed using the kinetic parameters determined during the present study and the literature data on secondary tar cracking reaction.

Selection and peer review under responsibility of Asia-Pacific Chemical, Biological & Environmental Engineering Society

Keywords: pyrolysis kinetic, pyrolysis product yield, energy yield, jute.

1. Introduction

Biomass is of major interest as a renewable energy source in the context of both climate change mitigation and energy security. Among the lignocellulosic wastes generated in India jute contributes a large portion. According to the jute packing material act enacted in 1987, entire quantities of food grains and sugar have to be compulsorily packed in jute sacks. Moreover, jute sacks are also used, to some extent, in cement industries. After utilization of the packed materials many of the jute sacks face disposal problem. Therefore, suitable waste to energy technology should be utilized to generate energy from waste jute sacks. Pyrolysis is a thermal degradation process which may be utilized for the generation of non-conventional energy resources from

* Corresponding author. Tel.: +91-33-2414-6378.
E-mail address: ranjana.juchem@gmail.com.

2212-6708
Selection and peer review under responsibility of Asia-Pacific Chemical, Biological & Environmental Engineering Society
doi:10.1016/j.apcbee.2014.01.004

waste materials. The mechanism of primary pyrolysis of solid and liquid feed-stocks is as follows,

$$\text{Re}\,ac\tan t \rightarrow Char + Liquid(tar) + Gas(pyro - gas) \quad (1)$$

In recent years many works have been reported in the literature on pyrolysis of municipal solid wastes [1]-[8]. Although it is apparent that jute is one of the main contributors of lignocellulosic wastes in India, studies of pyrolysis of waste jute is however lacking. Under the present investigation, pyrolysis kinetics of waste jute sacks has been studied in the temperature range of 673K to 1173K. Lumped kinetic parameters have been determined. The yield and characteristics of pyro -oil have been determined. A mathematical model has been developed for a semi batch pyrolyser based on waste jute.

2. Experimental

Jute: Jute was collected from a local market. Table 1 summarizes the results of proximate analysis of the jute sample.

Table 1. Proximate analysis of Jute Fibres

ProximateAnalysis	Moisture	Volatile Matter	Ash	Fixed Carbon
% (W/W)	10.025	77.15	2.59	10.235

A muffle furnace (Bhattacharya & Co. India) and a Bomb calorimeter (S. C. Dey & Co. India) were used .A CHNSO analyser (Perkin Elimer) and FTIR spectroscopy (SHIMADZU FTIR 8400) were used**.** The pyrolysis of jute sample has been done by following the procedure described in [2].

3. Theoretical Analysis

3.1. Pyrolysis Kinetics

Under the present study a parallel reaction model has been attempted to describe pyrolysis kinetics of jute wastes. According to this model pyrolysis of jute has been considered to be a homogeneous solid phase reaction and the pyrolysis products have been lumped as char – the solid product and volatiles made up of tar (condensable) and gaseous products. The volatile is further assumed to crack to different gaseous components, namely, CO, CO_2, H_2, CH_4 and inert tar. The reaction pathway of pyrolysis according to the present model is as follows,

$$Jute \rightarrow active\_complex \begin{cases} \xrightarrow{k_v} volatile \\ \xrightarrow{k_c} char \end{cases} \quad (2)$$

Therefore,

$$\frac{dW}{dt} = -kW \quad (3a) \qquad \frac{dW_v}{dt} = k_v W \quad (3b) \qquad \frac{dW_c}{dt} = k_c W \quad (3c)$$

where $k = k_v + k_c$

The rate constants k, k_v and k_c have been determined through non-linear regression analysis of

experimental data of captive sampling experiments [3], [4].The frequency factors and activation energies are given in Table 2.

Table 2. Calculated Activation Energies and Frequency Factors as per Arrhenius Law

Reaction rate constant	K	k_v	k_c
Frequency Factor (min^{-1})	1.252323	23.5706	6.086054
Activation Energy (kJ/mol)	22.55588	50.6572	41.3374
Correlation coefficient	1	1	1

Among the volatile components, namely tar, CO, CO_2, H_2 and CH_4, tar generated from pyrolysis of jute is decomposed through a homogeneous tar cracking reaction. Tar cracking reaction may be represented as follows,

$$Tar \rightarrow v_{CO}CO + v_{CO_2}CO_2 + v_{H_2}H_2 + v_{CH_4}CH_4 + v_i Tar_{inert} \quad (4)$$

The stoichiometric coefficients, v_i have been reported Table 3.

The rate equation for tar cracking reaction is as follows,

$$\overset{\bullet}{r}_{j.crack} = v_j . 10^{4.98} . \exp\left(-\frac{93.37}{RT_{par}}\right).(W_{g.tar}\rho_g) \quad (5)$$

where, $(W_{g.tar}\rho_g)$ is the concentration of tar in the gas phase.

All alkanes and alkenes are lumped as methane. Secondary reactions among gaseous components are not being considered during this modelling.

3.2. Mathematical Model and Prediction

Based on the reaction kinetics [7] determined in the previous section a mathematical model has been developed to predict the gas phase composition of the pyrolysis products.
The mass balance equation for any volatile component "i" under dynamic condition is as follows,

$$\frac{\partial}{\partial t}(\varepsilon.\rho w_{vi}) = -\frac{\partial}{\partial z}(v\varepsilon\rho w_{vi}) + \varepsilon D_{gi}\rho\frac{\partial^2 w_{vi}}{\partial z^2} + \sum_{j=1}^{n} r_{ij} \quad (6)$$

Where, i = tar or CO or CO_2 or H_2 or CH_4.

The values of diffusivities, D_{gi} of all gaseous components have been provided in Table 3. The term on the left hand side of the above equation represents accumulation , 1st , 2nd and 3rd terms on the right hand side of the equation represent convective flow component, dispersive flow component and the reactive part consisting of reactions (j) of all types, namely reaction-I and II involving the component "i". The mass balance equations (6) for all components have been solved numerically using MATLAB function pdex4.

3.3. Energy Yield

The energy yield of pyro – oil obtained at different pyrolysis temperature have been determined using the following correlation,

$$Energy Yield\,(\%) = \frac{w_l X\, CV_{oil}}{CV_{jute}} X100 \qquad (7)$$

where, w_l = *yield (weight fraction) of pyro – oil ,*
CV_{oil} = *Calorific Value of pyro – oil (MJ/Kg)*
CV_{jute} = *Calorific Value of jute (MJ/Kg)*

4. Result and Discussions

4.1. Trend of pyrolysis product yield and product characteristics.

From the analysis of experimental data, it was observed (not shown) that yield of char increased upto 873K after which it remained constant. On the other hand yield of tar increased in the entire range of pyrolysis temperature from 673K to 1173K. Yield of gas was observed to increase from 673K to 973K after which it remained constant up to 1173K. The yield of volatiles again showed an increasing trend in the temperature range of 673K to 1173K. The pH values of the tar were found to be in the range of 4 – 5. The calorific values of pyro – oil varied from 16.924 to 31.545 MJ/kg as the pyrolysis temperature was increased from 673K to 1173K.

4.2. Fourier Transform Infrared Spectroscopy (FTIR) Analysis of jute Tar

The functional groups of the pyro – oil obtained at temperature of 700^{O}C was analyzed by Fourier Transform Infrared (FTIR) spectroscopy to identify the basic compositional groups. Based on the FTIR results, the functional groups and the indicated compositon of the liquid products are presented in Table 4. The table shows the presence of alkanes, alkenes, ketones, aldehydes and carboxylic acids, primary, secondary and tertiary alcohols, ethers and esters, single, polycyclic and substituted aromatics groups and the presence of water impurities and other polymers.

Table 3. Values of diffusivities of tar and components of pyro – gas

Component	Tar	Tar_{inert}	CO	CO_2	H_2	CH_4
Diffusivity (m^2/s)	10^{-6}	0	19 X 10^{-6}	14 X 10^{-6}	78 X 10^{-6}	16 X 10^{-6}
v_i	1	0.22	0.78 X 0.72222	0.78 X 0.14222	0.78 X 0.02222	0.78 X 011334

Table 4. FTIR functional groups and the indicated compounds of jute Tar

Frequency Range (cm^{-1})	3600 – 3200	3050 – 2800	1775 – 1650	1680 – 1575	1570 – 1475	1490 – 1325	1300 – 950	900 – 650
Groups	O – H stretching	C – H stretching	C = O stretching	C ≡ C stretching	-NO_2 stretching	C – H stretching	C – O stretching, O – H bending	-
Class of compounds	Polymeric O – H	Alkanes	Ketones, Aldehydes, Carboxylic acids	Alkenes	Nitrogenous compounds	Alkanes	Primary, Secondary and Tertiary alcohols Phenols, esters, ethers	Aromatic compounds

The pronounced oxygenated functional groups of O – H; C = O; C – O and aromatic compounds show that the oil is highly oxygenated and therefore, very acidic, as have also been indicated by the elemental composition and the pH value. The high fraction of oxygenated compounds reduces the calorific value of the oil since C = O bonds do not release energy during combustion. The presence of hydrocarbon groups C – H; C = C; and alcohols indicate that the liquids have a potential to be used as fuel. The results of FTIR analysis is comparable to those obtained [1] during their studies on pyrolysis of jute wastes.

4.2.1 Time Histories of Weight fraction of residue during captive sampling Experiments

Figure 2 shows the experimental weight fraction profile of pyrolysis residue with respect to time in isothermal conditions from 673K to 1173K. From close observation of the data, it appears that the pyrolysis reactions proceed considerably in the temperature range of 573K to 1173K. Below this temperature range the reactions do not occur at an appreciable rate**.**

From the plots, it is also apparent that at each temperature, a quasi – equilibrium of the reaction prevails. The rates of devolatilization reactions decline at temperatures above 673K. Therefore, the values of frequency factors and activation energies of the reactions of reactant decomposition, volatile formation and char formation are determined by regression analysis of the rate constant determined in the temperature range of 573K to 673K [3], [4]. The frequency factors and activation energies of different reactions are given in Table 3.

4.3. Results of Model Simulation

In Figure 3 the mass fraction of tar in the gas phase has been plotted against reaction time at 700^{o}C with the axial position as a parameter. It is evident that the maximum fraction of reactive tar in the gaseous phase is 31% whereas those (not shown) of CO_2, H_2, CO and CH_4 are 11, 0.1, 2, 1.75 % respectively. These are also in agreement with the experimental values.

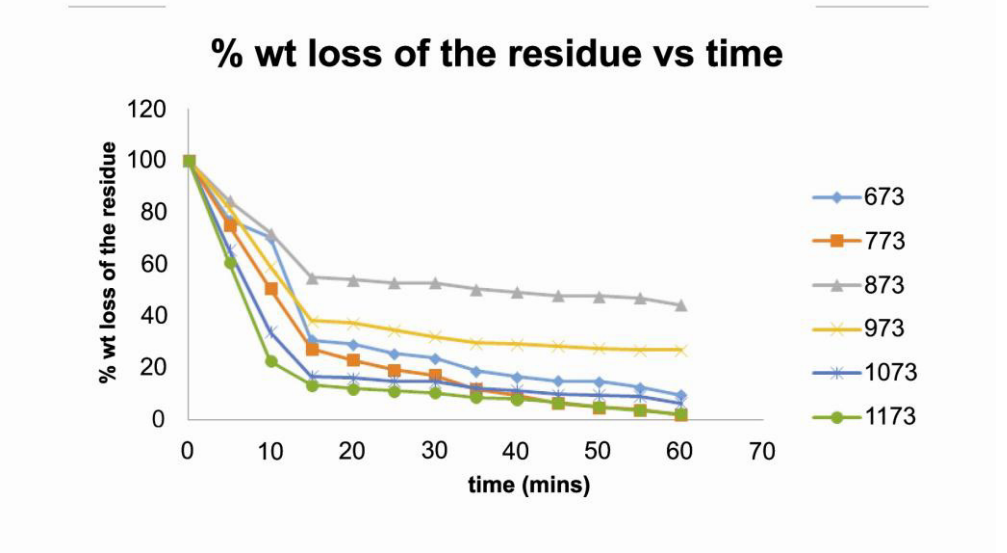

Fig. 1. Variation of percentage of weight of residue of textile wastes sample with respect to time at different pyrolysis temperature

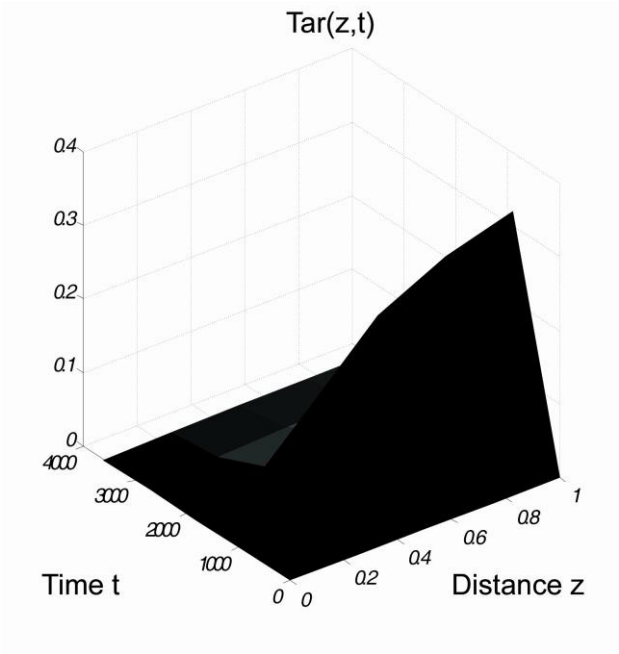

Fig. 2. The mass fraction of tar plotted against reaction time with the axial position as a parameter.

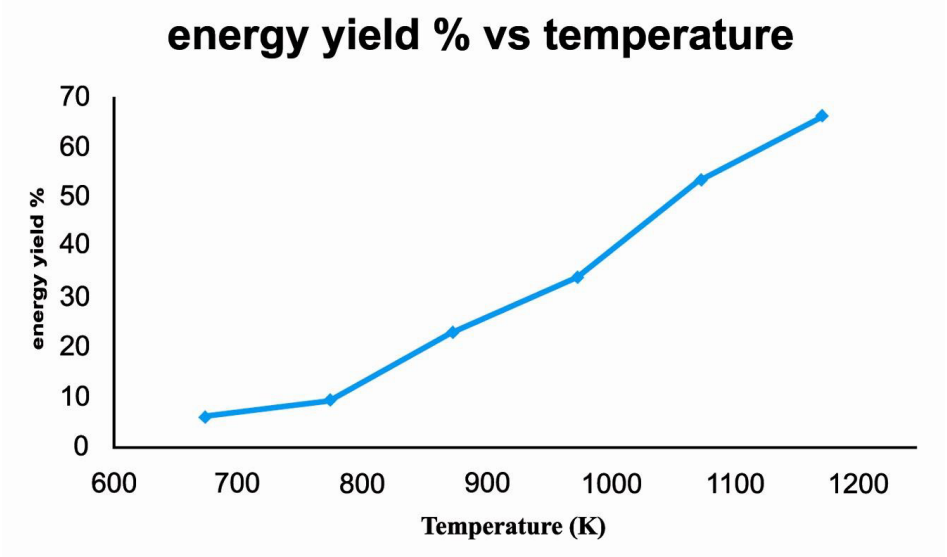

Fig. 3. Variation of energy yield (%) with temperature.

4.4. Energy Yield

The values of energy yield of pyro – oil have been plotted against pyrolysis temperature in figure 3. From

the analysis of the figure it appears that the increase in pyrolysis temperature results in the increase of energy yield with respect to pyro-oil. It may be due to the fact that with the increase of pyrolysis temperature the tar becomes richer in carbon which leads to the increase in specific energy content.

5. Conclusion

Pyrolysis kinetics of waste jute materials has been determined. A mathematical model involving partial differential equations for axial distribution of gaseous components under transient condition has been developed using the kinetic parameters determined during this study and the literature data on cracking kinetics of tar. The model can predict the behaviour of the semi- batch pyrolyzer under dynamic condition. The model may be utilized for further studies on pyrolysis using similar biomass feed stocks.

References

[1] Islam, M.R., Nabi, M.N., Islam, M.N. "The Fuel Properties of Pyrolytic oils Derived from Carbonaceous Solid Wastes in Bangladesh", *Jurnal Teknologi* 2003; 38(A):75 – 89.

[2] Chowdhury, R and Sarkar, A, "Reaction Kinetics and Product Distribution of Slow Pyrolysis of Indian TextileWastes", *International Journal of Chemical Reactor Eng.* 2012;10: 1 – 23,.

[3] Bandhyopadhyay, S., Chowdhury, R., Biswas, G.K., "Thermal deactivation studies of coconut shell pyrolysis", *Can. J. Chem. Eng.*1999; 77: 1028- 1036.

[4] Roy, R., Bhattachariya, P., Chowdhury, R., "Simulation and modeling of vegetable market wastes pyrolysis under progressive deactivation conditions".*Can. J. Chem. Eng*. 2004; 82: 566 – 579.

[5] Asadullah, M., Rahman, M.N., Ali, M.N., Motin, M.A., Sultan, M.B., Alam, M.R., Rahman, M.S "Jute stick pyrolysis for bio-oil production in fluidized bed reactor", *Biosource Technology* 2008; 99: 44 – 50.

[6] M. A. Lopez – Velazquez, V. Santes, J. Balmaseda, E. Torres – Garcia, "Pyrolysis of orange waste: A thermo – kinetic study", *Journal of Analytical and Applied Pyrolysis* 2013; 99: 170 – 177.

[7] Johann C. Wurzenberger, Susanne Wallner and Harald Raupenstrauch,"Thermal Conversion of Biomass:Comprehensive Reactor and Particle Modeling", *AIChe Journal* 2002; 48: 2398 – 2410

[8] Hang Seok Choi, Yeon Seok Choi, Hoon Chae Park, "Fast pyrolysis characterisitics of lignocellulosic biomass with varying reaction conditions", *Renewable Energy* 2012; 42: 131 – 135.

Product Characterization and Kinetic Study of Co-Pyrolysis of Waste Jute Sacks and Sesame Oil Cake

Future Energy Technologies

Sourav Poddar
Dept. of Chemical Engineering
Jadavpur University
Kolkata, India
souravpoddarsxc@gmail.com

Rima Biswas
Dept. of Chemical Engineering
Jadavpur University
Kolkata, India
biswasrima622@gmail.com

Ranjana Chowdhury*
Dept. of Chemical Engineering
Jadavpur University
Kolkata, India
ranjana.juchem@gmail.com

Sudipta De
Dept. of Mechanical Engineering
Jadavpur University
Kolkata, India
de_sudipta@rediffmail.com

***Abstract*—The co-pyrolysis of sesame oil cake and the waste jute sacks has been conducted in a long tubular type semi-batch reactor in the temperature range of 573 to 1173K in N_2 atmosphere. A reaction scheme has been proposed where two parallel reactions occur simultaneously to produce volatiles and char. Kinetic parameters, namely, rate constants, frequency factors, activation energies have been determined through nonlinear regression analysis. Effects of co-pyrolysis temperature have been observed on product yields. The pH value of the oil confirmed that the oil is acidic in nature. The functional groups of the pyro-oil have been analyzed by Fourier Transform Infrared (FTIR) spectroscopy to identify the basic functional groups. The energy yield of the pyro-oil has been calculated.**

***Index Terms*—co-pyrolysis kinetic; co-pyrolysis product yield; jute; sesame oil cake; pH value; FTIR; energy yield.**

I. Introduction

Biomass is the source of carbon that can be converted to renewable fuels and chemicals. Co-pyrolytic techniques have received much attention in recent years [1-16]. In the present investigation co-pyrolysis of waste jute and sesame oil cake has been studied. Sesame seeds contain 42-49% [13] of seed oil, whereas jute [14] contains 93 – 98% of cellulose. Every year 0.76 million tons [13] of sesame seeds are produced in India whereas 1575 thousand tons [15] of jute are produced.

V.I. Sharypov et.al (2002) (1) reported their research studies on co-pyrolysis of wood biomass and synthetic polymers and they observed high yield of light distillate fraction and benzene soluble products. Marin et.al (2002) (2) performed co-pyrolytic techniques which provide an alternative way to dispose and convert polyolefins and cellulose (or lignin) derived materials into high value feedstock and the specific benefits of this method potentially includes the reduction of the volume of waste, the recovery of chemicals and the replacement of fossil fuels. Yan-Jie Wang et. al. (2013) (3) analyzed co-pyrolysis characteristics of Torrefied pine sawdust with different rank coals. Roy et. al. (2004) (4) and Bandhopadhyay et. al. (1999) (5) studied the pyrolysis of the vegetable wastes and coconut shell respectively.

In the present work co-pyrolysis kinetics of jute and sesame oil cake in the temperature range of 573 to 1173K have been performed. Jute and sesame oil cake have been mixed in the ratio 1:1. The ratio was chosen because equal contribution of pyrolysis characteristics of each constituent is expected at 1:1 ratio. A kinetic scheme has been proposed where two parallel reactions occur simultaneously to produce volatiles and char.

II. Experimental

A. Materials

The feedstock used for these experiments was sesame oil cake and jute. Sesame seeds contain 42-49% of seed oil, whereas jute contains 20 – 35%. From 1 kg of sesame seeds 320 to 350 gm oil can be extracted by mechanical pressing and the residual part (cake) of the sesame seed are left unused. On the other hand the waste jute sacks face disposal problem after utilization of packed materials. Proximate analysis [17] and Ultimate analysis (not shown) [17] of the feed material were carried out and the analytical results for proximate analysis have been shown in Table 1.

TABLE 1. PROXIMATE ANALYSIS OF JUTE FIBRES AND SESAME OIL CAKE

Materials	Proximate Analysis	Moisture	Volatile Matter	Ash	Fixed Carbon
Jute Fibres	% (W/W)	10.025	77.15	2.59	10.235
Sesame oil cake	% (W/W)	7.41	85.72	3.80	3.07

B. Equipment

978-1-4799-3421-8/14/$31.00 ©2014 IEEE

A muffle furnace (Bhattacharya & Co. India) and a Bomb calorimeter (S. C. Dey & Co. India) were used.

C. Analytical Instruments

A CHNSO analyzer (Perkin Elimer) and FTIR spectroscopy (SHIMADZU FTIR 8400) were used.

D. Procedure

A set of experiments was carried out in a 50 mm diameter and 164 mm long tubular type semi-batch reactor [8] in the temperature range of 573 to 1173K in N_2 atmosphere. At first pyrolysis of individual feed stock, namely jute and sesame oil cake was studied independently in the temperature range of 573K to 1173K. For the study of co – pyrolysis at the same range 1:1 mixture of jute and sesame oil cake was used. The weight loss of residual biomass was recorded at the different time intervals.

III. THEORETICAL ANALYSIS

A. Pyrolysis Kinetics

In case of co–pyrolysis, a kinetic scheme has been proposed where two parallel reactions occur simultaneously to produce volatiles and char. Kinetic parameters, namely, rate constants, frequency factors, activation energies have been determined through nonlinear regression analysis. According to Shafizadeh and Chin [9], the two main competing pathways of pyrolysis of cellulosic materials are leading to the formation of char, gas and tar. In the present investigation, similar to the analysis of Bandhopadhyay et al. (1999) [5], all the volatile products have been lumped to form a single product called volatiles and solid products have been lumped to form char. The concept of an activated complex (Bradbury et al., 1979 [10]) was proposed for the reaction pathway of the co-pyrolysis of jute and sesame oilcake. This is as follows:

$$Jute + S.OilCake \rightarrow Active - Complex \begin{cases} \xrightarrow{k_v} volatile \\ \rightarrow char \\ \xrightarrow{k_c} \end{cases} \quad (1)$$

Therefore

$$\frac{dW}{dt} = -kW \quad (1a) \qquad \frac{dW_v}{dt} = k_v W \quad (1b) \qquad \frac{dW_c}{dt} = k_c W \quad (1c)$$

where $k_v + k_c = k$

Rate constants k, k_v and k_c of primary pyrolysis at different temperatures have been determined using the present experimental data. [4,5] The activation energies and frequency factors have been calculated in table 2.

B. Energy Yield

The energy yield of pyro–oil obtained at different pyrolysis temperature have been determined using the following correlation

TABLE 2. CALCULATED ACTIVATION ENERGIES AND FREQUENCY FACTORS AS PER ARRHENIUS LAW

Reaction rate constant	k	k_v	k_c
Frequency Factor (min – 1)	7.743	8.61	73.44
Activation Energy (kJ/mol)	3.86	3.72	5.45
Correlation coefficient	0.97	0.96	0.98

,

$$Energy\,Yield\,(\%) = \frac{w_l X CV_{oil}}{CV_{jute}} X100 \quad (2)$$

Where, = yield (weight fraction) of pyro – oil
= Calorific Value of pyro – oil (MJ/Kg)
= Calorific Value of jute (MJ/Kg)

IV. RESULTS AND DISCUSSION

C. Pyrolysis product yield and product characteristics

The effect of pyrolysis temperature on product yield obtained from co– pyrolysis of jute and sesame oil cake has been presented in fig.1. From the analysis of fig 1, it was observed that yield of tar increased in the range of temperature from 573K to 773 K after which it decreased. The yield of char decreased upto 873K after which it increased. On the other hand yield of gas was observed to increase from 573K to 1173K.

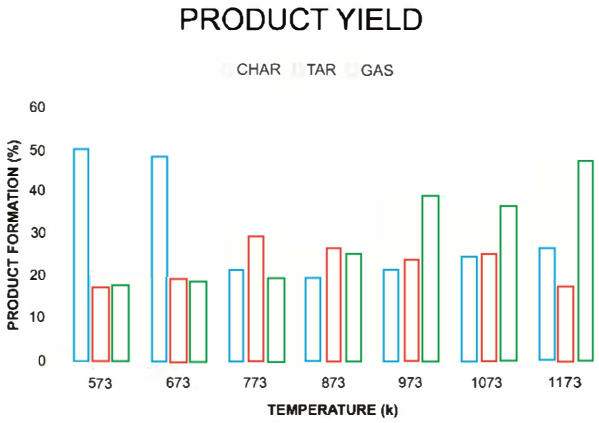

Figure1. Co-pyrolysis yield and product characterization

D. pH of Bio-oil

From the pH values of the bio-oil it is evident that it's nature is always acidic over the entire pyrolysis temperature range. The liquid products obtained from co-pyrolysis have been found to be highly viscous and high oxygen content. The pH of bio–oil generated at various temperatures has been measured and shown in figure 2.

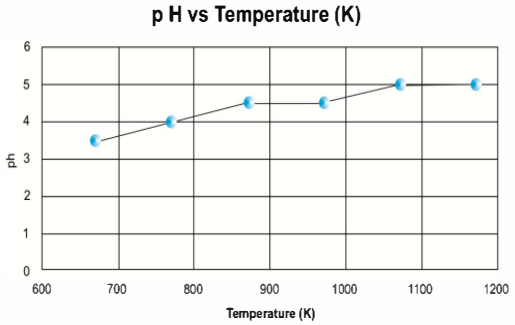

Figure 2. Variation of pH value with temperature of co-pyrolysis of pyro –oil.

It has been observed that values of pH increases with temperature after 1200K saturation is reached.

E. Fourier Transform Infrared Spectroscopy (FTIR) analysis of co-pyrolysis of jute and sesame oil cake :

Characterization with respect to chemical bonds present in the pyro-oil has been done using FTIR analysis. The functional groups of the pyro-oil obtained at temperature of 500^{O}C or 773K was analyzed by Fourier Transform Infrared (FTIR) spectroscopy to identify the basic compositional groups shown in Fig 3.

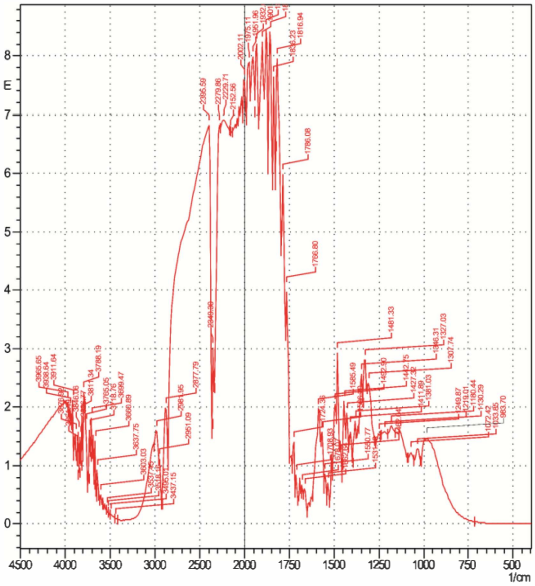

Figure 3. FTIR analysis of the pyro-oil.

Based on the FTIR results, the functional groups and the indicated composition of the liquid products are presented in Table 3.

From the close analysis of the table, it appears that the bio-oil is highly oxygenated as indicated by the predominance of oxygenated functional groups namely O – H; C=O; C – O and aromatic compounds. This is also established by the elemental composition (not shown) and the acidic nature, indicated by low value of pH. The high fraction of oxygenated compounds causes the lowering of calorific value of the oil, particularly due to the presence of C=O bonds which do not release energy during combustion [16]. The presence of hydrocarbon groups C – H; C = C; and alcohols indicate that the liquids have a potential to be used as fuel. The results of FTIR analysis is comparable to those obtained by Islam and Nabi, 2005 (11) and Sarkar et. al. (12) during their studies on pyrolysis of jute wastes.

TABLE 3. FTIR FUNCTIONAL GROUPS AND THE INDICATED COMPOUNDS OF CO-PYROLYSIS OF JUTE AND SESAME OIL CAKE TAR.

Frequency Range (cm^{-1})	Groups	Class of compounds
3900 – 3100	O – H stretching, N-H Stretch, N-H Stretch, Hydrogen-bonded O-H Stretch	Polymeric O – H, Amides (Methanamide), Amines-Primary(Ethylamine), Amines-Secondary(N-Methylethylamine), Phenols & Alcohols(Methanol)
3100-3000	C=C-H Asymmetric Stretch	Alkenes(1-Propene), Aromatic Rings(Benzene)
3050 – 2800	C – H Asymmetric & Symmetric stretching	Alkanes (Methane)
2850-2800	C-H Stretch off C=O	Aldehydes(Ethanal)
2750-2700	C-H Stretch off C=O	Aldehydes(Ethanal)
2300-2200	C≡N stretching	Nitriles (Methanenitrile)
2200-2100	C≡C Stretching	Alkynes (Propyne)
1775 – 1650	C = O stretching	Ketones(Acetone), Aldehydes(Ethanal), Carboxylic acids (Formic Acid), Esters(Methyl Formate)
1680 – 1575	C ≡ C stretching, C-C=C Symmetric stretch, N-H Bend , N=O Stretch, C=O Stretch, N-H Bend	Alkenes(1-Propene), Aromatic Rings, Amines—Primary(Ethylamine) Nitro-Groups (Nitromethane), Amides(Methanamide)
1550 – 1475	H-C-H bending, -NO_2 stretching, C-C=C Asymmetric Stretch, N-H Bend	Alkanes(Methane), Nitrogenous compounds , Aromatic Rings(Benzene), Amines—Secondary (N-Methylethylamine)
1490 – 1325	C – H stretching , N=O Bending	Alkanes, Nitro Groups(Nitromethane)
1300 – 950	C – O stretching, O – H bending	Primary, Secondary and Tertiary alcohols Phenols, esters (Methyl Formate) , ethers (Diethyl Ether)
900 – 650	-	Aromatic compounds

The FTIR spectrum of pyro-oil obtained in the temperature range 573K to 1173K have been shown in the figure 4, which shows a decreasing trend of compounds carrying C – O stretching and O – H bonding (1300 – 950) with the increase in temperature.. This may probably be due to further cracking

of these compounds above 573 K. However, the exact reason is yet to be investigated.

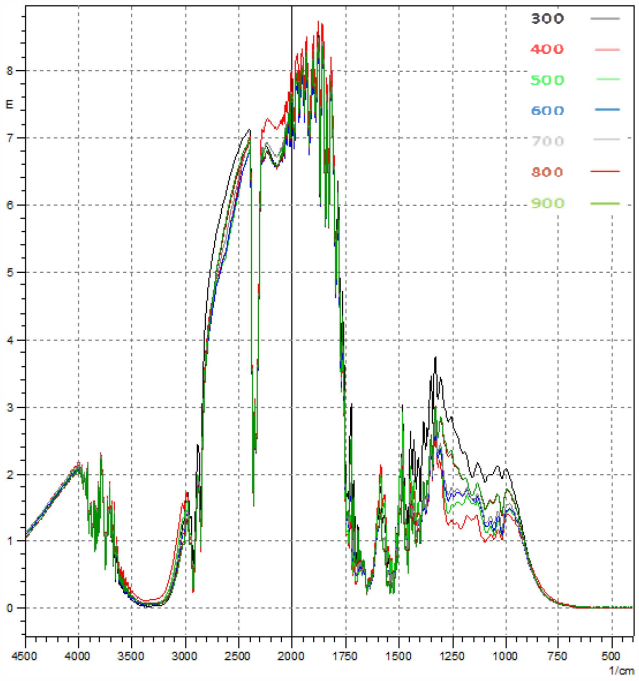

Figure 4. FTIR spectrum of pyro-oil obtained at different temperatures.

F. Energy Yield

The values of energy yield of pyro – oil have been plotted against temperature in figure 5. From the analysis of the figure it shows that the increase in co-pyrolysis temperature results in the increase of energy yield with respect to pyro-oil. It may be due to the fact that with the increase of co-pyrolysis temperature the tar becomes richer in carbon which leads to the increase in specific energy content.

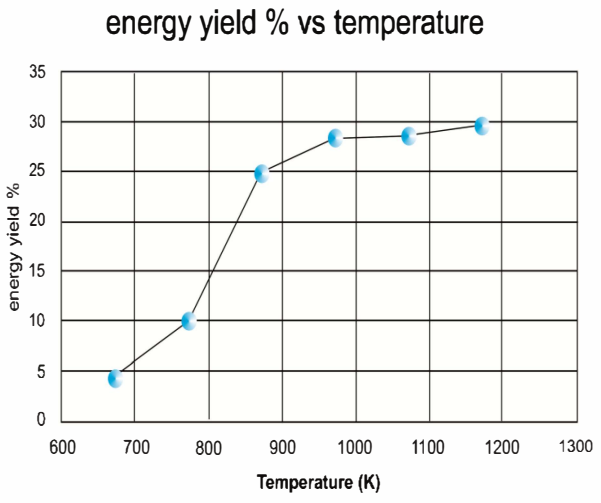

Figure 5. Variation of energy yield % with temperature.

V. Conclusion

In the present investigation, co-pyrolysis of jute and sesame oil cake has been studied at the temperature range of 573 to 1173K. In case of co – pyrolysis, a kinetic scheme has been introduced where two parallel reactions occur simultaneously to produce volatiles and char. The results of kinetic analyses show that first order reactions together with Arrhenius law account for the different subintervals of weight loss found for materials. The FTIR analysis of the pyro-oil has been shown in order to indicate the compounds present in the oil. The energy yield of the pyro-oil has been calculated to prove that the oil is good for industrial purpose. The outcome of the research study may be utilized in designing large scale pyrolyzer, which may be used in the Indian Metropolitan cities for conversion of waste to energy.

References

[1] V.I. Sharypov, N. Marin, N.G. Beregovtsova, S.V. Baryshnikov, B.N. Kuznetsov, V.L. Cebolla, J.V. Weber, "Co-pyrolysis of wood biomass and synthetic polymer mixtures. Part I: influence of experimental conditions on the evolution of solids, liquids and gases", Journal of Analytical and Applied Pyrolysis, 64, 1, 15 – 28, 2002.

[2] N Marin, S Collura, V.I Sharypov, N.G Beregovtsova, S.V Baryshnikov, B.N Kutnetzov, V Cebolla, J.V Weber, "Copyrolysis of wood biomass and synthetic polymers mixtures. Part II: characterisation of the liquid phases", Journal of Analytical and Applied Pyrolysis, volume 65(1), pg 41-55, October 2002.

[3] Yan-Jie Wang, Hao Ying, Yun-Juan Sun, Jun-Fei Jiang, Jian-Chun Jiang, Yi-Wei Gao, Wei-Jin Yu, "Co-Pyrolysis Characteristics of Torrefied Pine Sawdust with Different Rank Coals", BioResources, vol: 8(4), 5169-5183, 2013.

[4] R. Roy, P. Bhattachariya, R. Chowdhury, Simulation and modeling of vegetable market wastes pyrolysis under progressive deactivation conditions, *Canadian Journal of Chemical Engineering*, 82: 566 – 579, 2004.

[5] Bandhyopadhyay, S., Chowdhury, R., Biswas, G.K., Thermal deactivation studies of coconut shell pyrolysis, *Can. J. Chem. Eng.*1999; 77: 1028- 1036.

[6] Asadullah, M., Rahman, M.N., Ali, M.N., Motin, M.A., Sultan, M.B., Alam, M.R., Rahman, M.S "Jute stick pyrolysis for bio-oil production in fluidized bed reactor", Biosource Technology, 99, 44 – 50, 2008.

[7] R.Chowdhury, S.Poddar, S.De, "Kinetic Modelling of Non – Catalytic Pyrolysis of Waste Jute in a Fixed Bed Pyrolyzer", APCBEE Procedia, 2013.

[8] R. Chowdhury, A. Sarkar, "Reaction Kinetics and Product Distribution of Slow Pyrolysis of Indian Textile Wastes", International Journal of Chemical Reactor engineering, 2012, 10, A67.

[9] Fred Shafizadeh, Peter P.S. Chin, Preparation of 1,6-anhydro-3,4-dideoxy-β-D-*glycero*-hex-3-enopyranos-2-ulose (levoglucosenone) and some derivatives thereof, Carbohydrate Research, 58(1): 79-87, 1977.

[10] Islam, M.N., Beg, M.R.A., Islam, M.R., Pyrolytic oil from fixed bed pyrolysis of municipal solid waste and its characterization, *Renewable Energy*, 30:413-420, 2005.

[11] H. Pivcova, D. Doskočilová, E.M. Bradbury, "^{13}C and ^{1}H n.m.r. dynamic study of poly(γ-benzyl-l-glutamate) poly(β-benzyl-l-aspartate) and poly(l-alanine) in solution" Polymer, Volume 20, Issue 2, Pages 139–144, February 1979.

[12] Aparna Sarkar, Sangeeta Dutta, Ranjana Chowdhury, "Mustard Press Cake Pyrolysis and Product Yield

Characterization", International Journal of Scientific & Engineering Research", Volume 4, Issue 8, August 2013.

[13] Vikranth Volli , R.K. Singh, "Production of bio-oil from de-oiled cakes by thermal pyrolysis", Fuel, 96, 579–585, 2012.

[14] M Sarwar Jahan, Sabina Rawsan, D. A. Nasima Chowdhury and A. Al- Maruf, "Alternative pulping process for producing dissolving pulp from jute", Bioresources, Volume 3, Issue 4, 1359 – 1370.

[15] Ministry of Textiles, INDIA. 2012 < http://texmin.nic.in/sector/note_on_jute_sector.pdf>

[16] Mohammad Rofiqul Islam, MD. Nurun Nabi and Mohammad Nurul Islam , "The fuel properties of pyrolytic oils derived from carbonaceous solid wastes in Bangladesh", *Jurnal Teknologi*, Volume 38, Issue A, 75–89, Jun. 2003.

[17] Mark M. Wright, Justinus A. Satrio, Robert C. Brown, Daren E. Daugaard, David D. Hsu, "Techno-Economic Analysis of Biomass Fast Pyrolysis to Transportation Fuels", Technical Report NREL/TP-6A20-46586 , National Renewable Energy Laboratory, November 2010.

Indian Chemical Engineering Congress

65th ANNUAL SESSION OF INDIAN INSTITUTE OF CHEMICAL ENGINEERS

CHEMCON-2012

December 27-30, 2012

International Conference on
Sustainable Technologies for Energy and Environment in Process Industries
&
Indo-US Joint International Conference on Energy and Environment

Organized by

Indian Institute of Chemical Engineers Doaba Regional Centre
&
Department of Chemical Engineering
Dr. B. R. Ambedkar National Institute of Technology, Jalandhar-144011, Punjab, India

CERTIFICATE

This is to certify that Professor/ Dr./ Mr./ Ms. S. Poddar

has presented a paper (Oral) entitled Transient behaviour of a Semi-Batch Pyrolyser based on the Jute Waste - Experiments and Modelling

Co-authored with A. De, R. Chowdhury, S. De

in International Conference on "Sustainable Technologies for Energy and Environment in Process Industries" held at NIT Jalandhar during December 27-30, 2012

(Dr. Ajay Bansal)
Joint Organising Secretary

(Dr. M K Jha)
Organising Secretary

CBEES
www.cbees.org

ELSEVIER

Asia-Pacific Chemical, Biological & Environmental Engineering Society (APCBEES)

Participation and Presentation Certificate

For

2013 5th International Conference on Chemical, Biological and Environmental Engineering (ICBEE 2013)

New Delhi, India, September 14-15, 2013

Paper title: Kinetic Modelling of Non – Catalytic Pyrolysis of Waste Jute in a Fixed Bed Pyrolyzer

Presenter's name: S. Poddar(W023)

Presenter's affiliation: Jadavpur University

Conference Chair
ICBEE 2013

APCBEES

K.J's Educational Institutes

TRINITY COLLEGE OF ENGINEERING & RESEARCH, PUNE

KJ'S EDUCATIONAL INSTITUTE KJEI

ISET 2014

International Symposium on Engineering and Technology

Pune, India, January 9-10, 2014

Certificate of Participation

This certificate has been awarded to

S Poddar

from

Chemical Engineering, Jadavpur University, Kolakata, India

in recognition of the research contribution and technical presentation titled

Kinetic Modelling of Pyrolysis of Yellow Lime Waste of Fruit juice outlets

in the International Conference on Renewable Energy and Sustainable Development

held on January 09-10, 2014 in Pune, INDIA

Prof. K. D. Sapate
Convener

Dr. P. S. Dabeer
Symposium Chair

AMRITA VISHWA VIDYAPEETHAM
UNIVERSITY
Established u/s - 3 of the UGC Act 1956
BENGALURU CAMPUS
श्रद्धावान् लभते ज्ञानम्

PESTSE 2014

IEEE PES Bangalore Chapter
Power & Energy Society™

International Conference
2014 Power & Energy Systems:
Towards Sustainable Energy PESTSE 2014

Certificate of Participation

This is to certify that Prof./Dr./Mr./Ms./ Gourav Poddar
of Jadavpur University / Department of Chemical Engineering
has Presented a Paper (Oral / Poster) / Participated / Attended Tutorial Sessions titled
"Product characterization and kinetic study of co-pyrolysis of waste jute sacks & sesame oil cake future Energy Technologies"
in the International Conference 2014 Power & Energy Systems: Towards Sustainable Energy (PESTSE 2014) held at Amrita School of Engineering, Amrita Vishwa Vidyapeetham, Bengaluru from March 13th to 15th, 2014.

Ms. Anjana Jain
Convener- PESTSE 2014
Assistant Professor, EEE, ASE-B

Dr. Shikha Tripathi
General Chair- PESTSE 2014
Chairman, EEE, ASE-B

Dr. Rakesh S. G.
Patron- PESTSE 2014
Associate Dean & Head, ASE-B

AMRITA
VISHWA VIDYAPEETHAM
UNIVERSITY
Established u/s - 3 of the UGC Act 1956
BENGALURU CAMPUS
श्रद्धावान् लभते ज्ञानम्

PESTSE 2014

IEEE
IEEE PES Bangalore Chapter
Power & Energy Society™

International Conference
2014 Power & Energy Systems:
Towards Sustainable Energy PESTSE 2014

Certificate of Participation

This is to certify that Prof./Dr./Mr./Ms./ Sorav Poddar
of Dept of Chemical Engg. Jadavpur University
has Presented a Paper (Oral / Poster) / Participated / Attended Tutorial Sessions titled

in the International Conference 2014 Power & Energy Systems: Towards Sustainable Energy (PESTSE 2014) held at Amrita School of Engineering, Amrita Vishwa Vidyapeetham, Bengaluru from March 13th to 15th, 2014.

Ms. Anjana Jain	Dr. Shikha Tripathi	Dr. Rakesh S. G.
Convener- PESTSE 2014	General Chair- PESTSE 2014	Patron- PESTSE 2014
Assistant Professor, EEE, ASE-B	Chairman, EEE, ASE-B	Associate Dean & Head, ASE-B

PONJESLY COLLEGE OF ENGINEERING

(A Christian Minority and an ISO 9001 - 2008 Certified Institution)

(Approved by AICTE, New Delhi, Affiliated to Anna University, Chennai)

NAGERCOIL - 629 003

DEPARTMENT OF MECHANICAL ENGINEERING

ICRAMID'14

INTERNATIONAL CONFERENCE

ON

RECENT ADVANCES IN MECHANICAL ENGINEERING AND INTERDISCIPLINARY DEVELOPMENTS

7th & 8th March 2014

In Association With

IEEE TTP TRANS TECH PUBLICATIONS INC. SAE®

CERTIFICATE

This is to certify that Sourav Poddar.

has presented a paper entitled, Analysis of Tar By Catalytic pyrolysis of Waste Jute Alternative fuel.

held on 7th March 2014.

Co-Authors Ranjana Chowdhury.

Co-ordinator Convenor Principal

PONJESLY COLLEGE OF ENGINEERING

(A Christian Minority and an ISO 9001 - 2008 Certified Institution)

(Approved by AICTE, New Delhi, Affiliated to Anna University, Chennai)

NAGERCOIL - 629 003

DEPARTMENT OF MECHANICAL ENGINEERING

ICRAMID'14

INTERNATIONAL CONFERENCE

ON

RECENT ADVANCES IN MECHANICAL ENGINEERING AND INTERDISCIPLINARY DEVELOPMENTS

7th & 8th March 2014

In Association With

IEEE TTP TRANS TECH PUBLICATIONS INC. SAE ISTE

CERTIFICATE

This is to certify that SOURAV PODDAR

has presented a paper entitled, SHORT CONVERGING PNEUMATIC CONVEYOR USED FOR CONVEYING OF SOLIDS MODELLING, ANALYSIS AND SIMULATION OF MANUFACTURING PROCESSES held on 8th March 2014.

Co-Authors RIMA BISWAS ANIMESH SAINI

Co-ordinator

Convenor

Principal

Primary and secondary pyrolysis of Sesame oil cake --- Experiments and Kinetic Modelling

B. Mondal, A. Sarkar, S. Poddar, R. Chowdhury*

Chemical Engineering Department, Jadavpur University 700 032, India

Every year around 200 tons of sesame seeds are produced in India. Around 70 tons of sesame oils are then extracted from these seeds. The residual part is used as de-oiled cake mainly for cattle feed. There is, however, ample scope to generate energy from sesame oil cake. Under the present investigation, pyrolysis has been chosen as the thermo-chemical process to generate energy resources from sesame oil cake. The primary pyrolysis has been conducted in a 50 mm diameter and 640 mm long semi-batch pyrolyser in the temperature range of 673 - 1173K. Effects of pyrolysis temperature have been observed on product yields obtained from primary pyrolysis of sesame oil cake. CHNS analyses of tar sample obtained at different temperatures have been done. To study the morphological characteristics of char sample obtained at different temperatures, SEM analyses have been conducted. To characterise the pyro-oil with respect to chemical bonds FTIR analysis has been done. The calorific values of both char and tar samples have been determined using bomb calorimeter. Rate constants k, kv and kc of primary pyrolysis at different temperatures have been determined using the present experimental data. The activation energy and frequency factor have been calculated. The liquid products obtained from pyrolysis of sesame oil cake have been found to be highly oxygenated, viscous and prone to polymerisation during storage. It is apparent that the primary pyro-oil may be upgraded by lowering the oxygen content through secondary pyrolysis of tar. The kinetics of secondary pyrolysis of tar samples obtained through primary pyrolysis at different temperatures have been determined using captive sampling method in the temperature range of 673K to 1173K. The activation energy and frequency factor of secondary pyrolysis have been observed to vary with the temperature of primary pyrolysis through which the reactant tar is generated.

*Corresponding author: Prof. Dr. Ranjana Chowdhury; Tel: +91(033)24146378, ranjana.juchem@gmail.com

O117 (BF027)

ISOLATION OF LIGNOCELLULOSE DEGRADING FUNGI FOR IMPROVEMENT OF BIOGAS PRODUCTION FROM JATROPHA DE-OILED CAKE (JDOC)

M D Selva Pandian, Rajan Sharma, Shailey Singhal, Avinash K.Tiwari, G Sanjay Kumar

Department of Chemical Engineering, University of Petroleum and Energy Studies, Bidholi, Dehradun 248007, *Email:* gsanjay@ddn.upes.ac.in

Abstract: Lignocellulosic biomass can be used to produce biogas, a promising alternative energy source. The production of biogas from lignocellulosic biomass is currently limited by the inability of the digestion process to convert lignin and hemicelluloses. Pretreatment of the feed to remove or modify lignin and hemicelluloses can significantly enhance the biogas methane content. In the present work we investigated the effect of fungal pretreat- ment of feedstock on the production of biogas from JDOC. Five different fungi were isolated from natural JDOC inhabiting environment. These were then inoculated separately to pre-treat JDOC for 10 days in a batch mode. The JDOC pretreated by fungal isolates, were then subjected to anaerobic digestion. Biogas production was found in all pretreated JDOC substrates. An enhanced methane concentration of up to 65-86% (as compared to usual value of 60-65%) was observed.

Keywords: *Continuous Stirred Tank Reactor (CSTR), Jatropha De-oiled cake (JDOC), Pretreatment, Fungi, Biogas, Ligno-cellulosic waste*

O118 (BF036)

KINETIC STUDY AND CHARACTERIZATION OF PRODUCT YIELD OF CO-PYROLYSIS OF JUTE AND SESAME OIL

Sourav Poddar[1], Rima Biswas[1], Dr. Ranajan Chowdhury[1*], Dr. S. De[2]

[1]188, Raja Subodh Chandra Mullick Road, Jadavpur / Chemical / Jadavpur University, [2]188, Raja Subodh Chandra Mullick Road, Jadavpur / Mechanical / Jadavpur University

Email: souravpoddarsxc@gmail.com, biswasrima622@gmail.com, ranjana.juchem@gmail.com, de_supidta@rediffmail.com*

Abstract: In this present study, co-pyrolysis of sesame oil cake and the waste jute sacks was conducted in a long tubular type semi-batch reactor in the temperature range of 573 to 1173K in N2 atmosphere. At first pyrolysis of jute and sesame oil cake have been performed in the pyrolzer separately in the same temperature range. In case of co – pyrolysis, a kinetic scheme has been proposed where two parallel reactions occur simultaneously to produce volatiles and char. Kinetic parameters, namely, rate constants, frequency factors, activation energies have been determined through nonlinear regression analysis.

Keywords: *co-pyrolysis kinetic, co -pyrolysis product yield, jute, sesame oil cake.*

O119 (BF038)

GREEN CATALYTIC STEAM REFORMING PROCESS FOR CONVERSION OF BIO-OIL TO HYDROGEN USING NI/CEO$_2$-ZRO$_2$ CATALYST

Ritesh Mittal[1], K. K. Pant[2]

[1,2] Indian Institute of Technology - Delhi, Hauz Khas, New Delhi - 110016, India.

Email: r.mittal@gmail.com, kkpant@chemical.iitd.ac.in

Abstract: Bio-oil based studies for next generation renewable bio-fuels are becoming prudent area of research globally due to growing concerns for sustainable development. Reserves of fossil fuels like crude-oil, natural gas and coal etc. are scarce and their use impose great social cost of environmental & health problems. Hydrogen as a clean fuel is being considered as a good alternative energy option. Bio-oil obtained by pyrolysis of ligno-cellulosic biomass can be reformed to hydrogen and the process provides a new utilization route for bio-oil in addition to the process being carbon neutral that aids in reducing global warming. The present paper explores catalysis in steam reforming of model bio-oil using 20wt% Ni/CeO2-ZrO2 catalyst. Research results suggest that prepared catalyst effectively exhibited high activity for steam reforming of model bio-oil with high hydrogen yield and low catalyst deactivation due to reduced coke formation.

Keywords: *Bio-oil, Hydrogen, Steam Reforming.*

temperature. That is why zirconia is doped to enhance the thermal stability of the support. In this work, nickel is impregnated as nickel oxide (NiO) over the surface of CemZr1-mO2 (m = 0, 1) support and incipient wet impregnation is the process by which the catalysts are prepared. The prepared catalysts are also characterized via XRD, SEM, TEM, STEM, BET-BJH, EDS and TPR to analyze the surface morphology, extent of homogeneous nature of oxide dispersion over support, reduction conditions, etc. The foremost application of this catalyst is reduction of sooting tendency on catalyst surface during hydrocarbon reforming technology at high temperature. Prepared catalysts are found to be promising for its application in steam reforming of methane (SRM).

O141 (CAT012)

CARBONACEOUS SPECIES CHARACTERIZATION BY TEMPERATURE PROGRAMMED HYDROGENATION (TPH) ON AL_2O_3 SUPPORTED NI-FE BIMETALLIC CATALYST FOR CH_4 CRACKING REACTION

Shankar Singh[1], Kaustav Ray[2],Siddhartha Sengupta[3] Goutam Deo[4]
Department of Chemical Engineering, Indian Institute of Technology Kanpur, *Email: shankaarf@iitk.ac.in, kaustavr@iitk.ac.in, goutam@iitk.ac.in*

Abstract: Reactions involving hydrocarbon reforming and/or cracking on nickel (Ni) based catalysts generally have the problems of carbon deposition. Different types of carbonaceous species can be identified over the spent catalyst from these type of reaction Temperature Programmed Hydrogenation (TPH). In the current work To identify the different types of carbonaceous species on supported Ni catalysts 15 wt% Ni, Fe and Ni-Fe bimetallic (of various Ni:Fe ratios) catalysts, supported on γ-Al_2O_3 were prepared by the Incipient Wetness Impregnation (IWI) method. All the catalyst samples were characterized for their surface area and by X-ray diffraction (XRD). Furthermore, the different carbonaceous species deposited over these Ni based catalysts during CH_4 cracking at different times were identified by TPH. Characterization studies revealed the presence of Ni-Fe alloy and easy reduction of the bimetallic catalysts.

Keywords*: Methane cracking, TPH, TGA.*

O142 (CAT 015)

CYCLOHEXANE OXIDATION USING AG-SBA-15

Priyank Khirsariya*[a], Anand Upadyay [a], Rajubhai K Mewada [a]
Nirma University, Ahmedabad – 382 481, *Email: 12mchc10@nirmauni.ac.in,11mchc17@nirmauni.ac.in, rkmewada@nirmauni.ac.in*

Abstract: Now a days people are more interested to carry out direct oxidation of alkanes using heterogeneous catalysts. Selective oxidation of the relatively inert C- H bond of hydrocarbons is one of the most challenging reactions. Due to its commercial importance, cyclohexane oxidation is an interesting and challenging area of research for academics and industrial point of view. The commercially-practiced process suffers from very low conversions and poor selectivity for K-A oil. Cobalt and manganese salts have commonly been employed as catalysts for this reaction; however, the high activation energy of the C-H bonds in cyclohexane dictates the use of high temperatures and subsequently high pressures to carry out this reaction commercially. The existing commercial process is having only about 6% conversion and 85% selectivity. This shows the tremendous scope for improvement in conversion or selectivity for KA-oil production. This paper discusses about the air oxidation of cyclohexane. Silver was loaded in SBA-15 by in-situ preparation. Catalyst activity was tested for cyclohexane oxidation reaction using air in high pressure reactor (Nano-Mag Autoclave reactor). The reactions were carried out at 160 0C and 15 kg/cm2 air pressure. Samples were analyzed using Shimadzu 2010 GC with RTXWax 30 m capillary column. Ag-SBA-15 catalyst has shown about 10.5 % conversion with 86 % selectivity for KA-oil. The catalyst was characterized to correlate with its activity for cyclohexane oxidation. The reaction parameters to be optimized.

Keywords*: Selective oxidation of cyclohexane, K-A oil, Ag/SBA-15,*

O143 (CAT016)

CATALYTIC PYROLYSIS OF WASTE JUTE – EXPERIMENT & KINETIC MODELLING

Rima Biswas[1], Sourav Poddar[1], Dr. Ranjana Chowdhury[1], Dr. S. De[2]
[1&2]188, Raja Subodh Chandra Mullick Road, Jadavpur / Chemical / Jadavpur University,
Email: biswasrima622@gmail.com, souravpoddarsxc@gmail.com, ranjana.juchem@gmail.com, de_supidta@rediffmail.com*

Abstract: In the present study the catalytic pyrolysis of jute has been investigated using a cylindrical semi-batch pyrolyzer made of stainless steel under both isothermal and condition within the temperature range of 400°C to 900°C in an inert N_2 atmosphere. Aluminium Oxide (Al_2O_3) was used as the catalyst. Alumina was pre-calcined at 120°C for 2 hr in muffle furnace before being used in the reactor. Catalyst and jute were mixed directly at the ratio of 1:10. Non-catalytic pyrolysis of jute sample was conducted in the pyrolser in using the same temperature range. The use of Al_2O_3 catalyst led to higher tar yield and phenolic compounds are increased in liquid products, compared to non-catalytic pyrolysis. Catalytic pyrolysis involves the production of upgraded liquids in a single step within short residence times. The simulated results of the model were compared with the experimental results satisfactorily.

Keywords: *pyrolysis kinetic, pyrolysis product yield, jute, Aluminum Oxide.*

ICRESD 88

Kinetic Modelling of Pyrolysis of Yellow Lime Waste of Fruit juice outlets

S Poddar[a], R Biswas[b],R Chowdhury[c], S De[d]

[a,b,c,d] *Jadavpur University, Kolakata, India*
ranjana.jschem@gmail.com

Pyrolysis is a thermo-chemical process to generate energy resources from bio waste. Under the present investigation, the pyrolysis of yellow lime wastes has been conducted in a 50 mm diameter and 640 mm long semi-batch pyrolyzer in the temperature range of 573 - 1173K. Effects of pyrolysis temperature have been observed on product yields obtained from primary pyrolysis of lime waste. The liquid products obtained from pyrolysis of lime waste have been found to be highly viscous and prone to polymerization during storage. Kinetic parameters of the pyrolysis material have been evaluated with the experimental data. The pH value of the lime waste oil confirmed that the oil is alkaline in nature.
Keywords: pyrolysis kinetic, pyrolysis product yield, pH value, lime waste.

ICRESD 89

Influence of Fly Ash to Improve the Shear Strength of Commercial and Natural Soil

Suresh Murugan[a], Murugaiyan Vijayarangam[b]

[a,b] *Pondicherry Engineering College, Puducherry*
suresh.biotel@gmail.com

Industrial waste materials are utilized to improve the problematic soils is a cost efficient and eco friendly method. The present paper evaluated the influence of fly ash on the commercial and natural soil to improve its geotechnical properties. In this experiment, Atterberg's limit, maximum dry density (MDD), optimum moisture content (OMC) of the samples with various fly ash proportion i.e. at 10%, 20%, 30% and 40% were analyzed. The main objective of this study is to investigate the improvement of shear strength on soils were evaluated using unconfined compression strength (UCS) test. The test results showed a significant change in the geotechnical properties of samples with fly ash. The UCS values improved by using fly ash from 108.4 kPa to 171.5 kPa for natural soil. The commercial soil obtained the optimum strength about 228 kPa at 10% of fly ash on the soil.

Keywords: Waste utilization, Fly ash, Shear strength, UCS test

Gmail **sourav poddar <souravpoddarsxc@gmail.com>**

imp

1 message

Ranjana Chowdhury <ranjana.juchem@gmail.com> Mon, Dec 23, 2013 at 5:38 PM
To: sourav poddar <souravpoddarsxc@gmail.com>

hemcon 2013 Secretariat <ictchemcon2013@gmail.com> Nov 17

to me

Dear Ranjana Chowdhury,

Thank you for your recent submission of the full paper for possible presentation at Chemcon 2013. The Full papers were further screened by the technical committee and based on the recommendations, I am pleased to inform you that your abstract reference number CRE010 entitled "Primary and Secondary Semi-batch Pyrolysis of Yell------" has been **accepted** for the **Poster presentation** in Chemcon 2013. Please also make sure that one of the authors must register for the program with payment of required fees and if we find that none of the authors mentioned in the paper have registered by December 1, 2013, we will remove the paper from the program. Pls. also note that registration is mandatory for authors attending the conference.

With best regards

Dr. Virendra K. Rathod

Department of Chemical Engineering,

Institute of Chemical Technology,

Matunga, Mumbai – 400019

Website: www.chemcon2013.com

Nov 17